Technical University of Košice

Faculty of Electrical Engineering and Informatics

SCYR

24th Scientific Conference of Young Researchers
Proceedings from Conference

ISBN 978-80-553-3474-5

2024

Sponsors & Organizers

SCYR 2024: 24th Scientific Conference of Young Researchers
Proceedings from Conference

Published: Faculty of Electrical Engineering and Informatics
Technical University of Košice
Edition I, 182 pages, number of CD Proceedings: 50 pieces

Editors: Assoc. Prof. Ing. Karol Kyslan, PhD.
Assoc. Prof. Ing. Emília Pietriková, PhD.
Ing. Lukáš Pancurák

ISBN 978-80-553-3474-5

Scientific Committee of SCYR 2024

General chair: Prof. Ing. Liberios Vokorokos, PhD.

Editorial board chairman: Assoc. Prof. Ing. Karol Kyslan, PhD.

Committee Members & Reviewers:
Ing. Tibor Gujdan, Fpt Slovakia s.r.o.
Ing. Juraj Bujňák, PhD., Siemens Healthineers
Assoc. Prof. Ing. Jaroslav Džmura, PhD.
Prof. RNDr. Vladimír Lisý, DrSc.
Prof. Ing. Alena Pietriková, CSc.
Assoc. Prof. Ing. Marek Pástor, PhD.
Assoc. Prof. Ing. František Babič, PhD.
Assoc. Prof. Ing. Eva Chovancová, PhD.
Assoc. Prof. Ing. Emília Pietriková, PhD.
Assoc. Prof. Ing. Peter Feciľak, PhD.
Assoc. Prof. Ing. Peter Papcun, PhD.
Assoc. Prof. Ing. Matúš Pleva, PhD.
Assoc. Prof. Ing. Ján Papaj, PhD.
Assoc. Prof. Ing. Stanislav Ondáš, PhD.

Organizing Committee of SCYR 2024

Members: Assoc. Prof. Ing. Karol Kyslan PhD.
Assoc. Prof. Ing. Emília Pietriková, PhD.
Ing. Ivana Olšiakova
Ing. Peter Provázek
Ing. Lukáš Pancurák
Ing. Simona Saparová
Ing. Šimon Gans
Ing. Matúš Dopiriak
Ing. Kristián Mičko

Contact address: Faculty of Electrical Engineering and Informatics
Technical University of Košice
Letná 9
040 01 Košice
Slovak Republic

Foreword

Dear Colleagues,

SCYR (Scientific Conference of Young Researchers) is a scientific event focused on exchange of information among young researchers from Faculty of Electrical Engineering and Informatics at the Technical University of Košice – series of annual events that was founded in 2000. Since 2000, the conference has been hosted by FEEI TUKE with rising technical level and unique multicultural atmosphere. The 24th Scientific Conference of Young Researchers (SCYR 2024) was held on April 19, 2024 at University Conference Centre, Technical University of Košice. The mission of the conference, to provide a forum for dissemination of information and scientific results relating to research and development activities at the Faculty of Electrical Engineering and Informatics, has been achieved. Approx. 60 participants, mostly by doctoral categories, were active in the conference.

Faculty of Electrical Engineering and Informatics has a long tradition of students participating in skilled labor where they have to apply their theoretical knowledge. SCYR is an opportunity for doctoral and graduating students to train their scientific knowledge exchange. Nevertheless, the original goal is still to represent a forum for the exchange of information between young scientists from academic communities on topics related to their experimental and theoretical works in the very wide spread field of a wide spectrum of scientific disciplines like informatics sciences and computer networks, cybernetics and intelligent systems, electrical and electric power engineering and electronics.

Traditionally, contributions can be divided in 2 categories:

- Electrical & Electronics Engineering
- Computer Science

with approx. 60 technical papers dealing with research results obtained mainly in the University environment. This day was filled with a lot of interesting scientific discussions among the junior researchers and graduate students, and the representatives of the Faculty of Electrical Engineering and Informatics. This Scientific Network included various research problems and education, communication between young scientists and students, between students and professors. Conference was also a platform for student exchange and a potential starting point for scientific cooperation. The results presented in papers demonstrated that the investigations being conducted by young scientists are making a valuable contribution to the fulfillment of the tasks set for science and technology at the Faculty of Electrical Engineering and Informatics at the Technical University of Košice.

We want to thank all participants for contributing to these proceedings with their high quality manuscripts. We hope that conference constitutes a platform for a continual dialogue among young scientists.

It is our pleasure and honor to express our gratitude to our sponsors and to all friends, colleagues and committee members who contributed with their ideas, discussions, and sedulous hard work to the success of this event. We also want to thank our session chairs for their cooperation and dedication throughout the entire conference.

Finally, we want to thank all the attendees of the conference for fruitful discussions and a pleasant stay in our event.

Liberios VOKOROKOS
Dean of FEEI TUKE

April 19, 2024, Košice

Contents

Crossover of Encryption Algorithms

[1]*Peter PEKARČÍK (2nd year),*
Supervisor: [2]*Eva CHOVANCOVÁ*

[1,2]Dept. of Computers and Informatics, FEI TU of Košice, Slovak Republic

[1]peter.pekarcik@tuke.sk, [2]eva.chovancova@tuke.sk

***Abstract*—Our work focuses on the creation of new encryption algorithms using genetic algorithms. We created an initial population of encryption algorithms and evaluated their properties. After that, we implement the first model of the crossover genetic algorithm and compare its properties with algorithms on the input to the process. The results of the measurements are presented below.**

***Keywords*—crossover, cryptography, encryption algorithms, fitness score, genetic algorithms, initial population, selection**

I. Introduction

Data security has become a critical and impressive issue. Different algorithms are used to achieve the highest security. According to [1], the most used encryption algorithms were invented between 1976 and 1998. Significant progress has been made in computer systems since then. Today's most used encryption algorithms are based on operations like shifts, permutations, substitutions, or transpositions. Our work uses the crossover operation to select specific parts of encryption algorithms and combine them to produce new algorithms.

II. Initial state of problem

According to [2], dozens of different encryption algorithms exist today. They can be generally divided into:

- **Symmetric-key algorithms** use the same key for encryption and decryption. They can be divided into:
  - **Block ciphers** working on blocks of fixed length;
  - **Stream ciphers** working on a continuous stream of symbols;
- **Asymmetric-key algorithms** use different but mathematically related keys - *public* and *private*.

According to [3], *DES*, *3DES*, *Blowfish*, and *AES* are the most used *symmetric algorithms* and the most used *public key* are *RSA, Diffie-Hellman, ElGammal*, and *Rabin encryption*.

Some were modified to improve their properties. The results are the *Modified Cesar cipher* [4], *Modified Playfair cipher* [5], *Modified Substitution cipher* [6], *S-DES* [7], *Modified RSA* [8] or *H-Rabin* [9].

From [10], we also know that there are *genetic algorithms*. They aim to imitate the natural changes in living ecosystems, which are social systems, evaluate the psychological consequences, and model the variable methods. They are based on evolutionary theory. In our solution, we decide to combine these two disciplines.

III. Task solved during last year

The standard genetic algorithm mentioned in the previous cheaper, contains processes of:

- *creation of an initial population of chromosomes*;
- *computation of fitness score*;
- *selection*;
- *crossover* of results of selection;
- *mutation*.

We focused on the *creation of the initial population*, the *computation of the fitness score* and the *crossover*.

A. Creation of initial population

The initial population entails the possible solution. We used algorithms used in the practice of modern cryptography:

- RSA Algorithm;
- Rabin Encryption;
- ElGamal Public-key Encryption;
- Data Encryption Standard;
- Advanced Encryption Standard;
- Elliptic Curve Cryptography;
- Triple Data Encryption Standard;
- Blowfish;
- Twofish.

B. Computation of fitness score

The following solved process was the *calculation of the fitness score*. We decided to use metrics for the evaluation of encryption algorithms that, according to [11], are:

- encryption time;
- decryption time;
- throughput of encryption;
- throughput of decryption;
- CPU process time;
- memory utilization.

We create a database of measurement results. After that, data was loaded and followed computation according to the following rules:

- algorithm with a minimum value had a fitness score of 100;
- algorithm with a maximum value had a fitness score of 1;
- the difference between maximum and minimum was divided by 100, and other algorithms assigned fitness score as multiple its value by divided value;
- the result value was multiplied by constant values of `percentages_distribution`.

The results of the computation of the fitness score are in the *TABLE I*. The same results were reached for different parameters; here is an example:

TABLE I
RESULTS OF MEASURMENTS OF FITNESS SCORE

Algorithm	Fitness score	Example of parameters
DES	5.954108	50, 0, 0, 0, 50, 0
AES	31.602354	50, 0, 50, 0, 0, 0
Blowfish	40.072414	50, 0, 50, 0, 0, 0
ECC	60.968311	50, 0, 0, 50, 0, 0
ElGamal	14.558933	50, 0, 0, 0, 50, 0
IDEA	5.327043	50, 0, 50, 0, 0, 0
RSA	53.868454	50, 50, 0, 0, 0, 0

C. Crossover

For the initial testing of crossover, we used *Cesar* and *Vignere encryption*. The goal was to implement a module that could create a source code of the new algorithm with better metrics values. We perform measurements of properties from *Chapter III.B*. They are introduced in the tables *TABLE II*, *TABLE III* and *TABLE IV*:

TABLE II
RESULTS OF CROSSOVER I

Algorithm	Speed of encryption [s]			Speed of decryption[s]		
	32 B	64 B	128 B	32 B	64 B	128 B
Cesar	4 e^-14	4 e^-14	4 e^-14	1 e^-14	1 e^-14	1 e^-14
Vigener	2 e^-14	2 e^-14	1 e^-14	2 e^-14	1 e^-14	1 e^-14
Crossover result	7 e^-14	4 e^-14	6 e^-14	4 e^-14	5 e^-14	6 e^-14

TABLE III
RESULTS OF CROSSOVER II

Algorithm	Throughput of encryption [s]			Throughput of decryption[s]		
	32 B	64 B	128 B	32 B	64 B	128 B
Cesar	8 e^17	1.6 e^18	3.2 e^18	3.2 e^18	6.4 e^18	1.28 e^19
Vigener	1.6 e^18	3.2 e^18	1.28 e^19	1.6 e^18	6.4 e^18	1.28 e^19
Crossover result	4.57 e^17	2.13 e^18	2.13 e^18	8 e^17	1.28 e^18	2.13 e^18

TABLE IV
RESULTS OF CROSSOVER III

Algorithm	Memory utilization [MB]			Processor time[s]		
	32 B	64 B	128 B	32 B	64 B	128 B
Cesar	2.17418	2.1643	2.17418	0.000005	0.000005	0.000006
Vigener	2.33391	2.33457	2.33484	0.000001	0.000002	0.000002
Crossover result	2.50543	2.41363	2.41780	0.000004	0.000007	0.000007

As you can see, there was no improvement when evaluating the metrics. However, the key aspect of encryption algorithms is security. This is why we created a series of tests of resistance against attacks - *Bruteforce attack* and *Dictionary attack*. The results of these tests are presented in *TABLE V* and *TABLE VI*.

TABLE V
RESISTANCE AGAINST ATTACKS I

Algorithm	Bruteforce attack on key - all possibilities [s]	Bruteforce attack on key - random search[s]
Cesar	2.17418	2.1643
Vigener	2.33391	2.33457
Crossover	2.50543	2.41363

TABLE VI
RESISTANCE AGAINST ATTACKS II

Algorithm	Dictionary attack on key - all possibilities[s]	Dictionary attack on key - random search[s]
Cesar	0.000001	0.000004
Vigener	0.000035	0.000037
Crossover	0.000058	0.000088

In measurements of resistance against attack, created algorithms show better results than original algorithms.

IV. CONCLUSION

In our work, we devoted two typical operations for genetic algorithms - *computation of fitness score* and *crossover*. In the *computation of the fitness score*, we use the most critical metric for encryption algorithms and compute the fitness score for all algorithms from the set. In the *crossove*r, we create the first crossovered algorithm developed from the *Caesar cipher* and *Vigener cipher*. This procedure will probably be applicable for more complicated ciphers, but the question is whether it will be further improved. Based on the discussion, we, therefore, decided to abandon this procedure. The current direction of cryptography is towards *post-quantum cryptography*, which we will also address in our following research.

REFERENCES

[1] R.Rivest, A.Shamir, and L.Adleman, "A method for obtaining digital signatures and public-key cryptosystems," *Communications of the ACM*, vol. 21, pp. 120–126, 1978.
[2] A. Menezes, P. van Oorchot, and S. Vanstone, *Handbook of Applied Cryptography*. CRC Press, 2001, vol. 5.
[3] M. F. Mushtaq, S. Jamel, A. H. Disina, Z. A. Pindar, N. S. A. Shakir, and M. M. Deris, *(IJACSA) International Journal of Advanced Computer Science and Applications*, vol. 8, no. 11, 2017.
[4] B. Purnama and H. Rohayani, "A new modified caesar cipher cryptography method with legible ciphertext from a message to be encrypted," *Procedia Computer Science*, vol. 59, pp. 195–204, 2015.
[5] M. S. Mohammed, "Novel method using crossover (genetic algorithms) with matrix technique to modifying by using playfair," *Diyala Journal of Engineering Sciences*, vol. 6, no. 3, pp. 97–106, 2013.
[6] S. K. Mahata and M. Dey, "A novel approach for cryptography using modified substitution cipher and triangulation," *International Research Journal of Computer Science (IRJCS)*, vol. 3, no. 4.
[7] K. Raj, B. Sharma, N. Kumar, and D. Kaur, "Differential cryptanalysis on s-des," *International Journal of Management and Information Technologiy*, vol. 1, no. 2, pp. 42 – 45, 2012.
[8] A. Niverha, S. M. Preethy, and J. K. Sanrosh, "Modified rsa encryption algorithm using four keys," *International Journal of Engineering Research and Technologies (IJERT)*, vol. 3, no. 07, pp. 1 – 5, 2015.
[9] H. R. Hashim, "H-rabin cryptiosystem," *Journal of Mathematics and Statistics*, vol. 10, no. 3, pp. 304 – 308, 2014.
[10] M. Michell, "An introduction to genetic algorithms," 1998.
[11] B. Bharathi, G. Manivasagam, and K. Anand, "Metrics for performance evaluation of encryption algorithms," *International Conference on Emerging Trends in Engineering, Science and Management*.

War of the Worlds: Lossless encoding vs. Compressed sensing

[1]*Jozef KROMKA (3rd year),*
Supervisor: [2]*Ján ŠALIGA*

[1,2]Dept. of Electronics and Multimedia Communications, FEI TU of Košice, Slovak Republic

[1]jozef.kromka@tuke.sk, [2]jan.saliga@tuke.sk

***Abstract*—The article provides a comprehensive overview of the author's accomplishments and contributions over the past year. It primarily outlines a novel memory-efficient lossless real-time encoding algorithm and presents preliminary results for Electrocardiogram (ECG) signals. Furthermore, supplementary findings related to previously developed compressed sensing (CS) methods applied to cardiovascular signals are provided.**

***Keywords*—Cardiovascular signals, Compressed sensing, Lossless encoding, Signal processing**

I. Introduction

Signal and data compression stand out as extensively studied topics in the field of signal processing. Every day, we encounter various forms of compression, whether consciously or not. When discussing signal compression, there are two primary categories: lossless compression, which preserves data in its exact form, and lossy compression, where some information is sacrificed for increased compression. Recently, one specific type of lossy compression has garnered global attention, namely CS [1].

The significance of cardiovascular (CV) sensing systems has grown markedly over the past years in the context of CV disease prevention. Among the foremost indicators providing valuable insights into an individual's CV system status are the ECG and blood pressure (BP) measurements.

In recent years, several lossless encoding algorithms for ECG signals have been introduced [2], [3], [4], demonstrating the capability to achieve compression ratios (CR) of up to 2.9. Nevertheless, these algorithms commonly rely on the device's memory and computational resources, employing a combination of dictionary-based encoding and Adaptive linear prediction (ALP). Hence, a novel encoding algorithm was developed [5] that is not only memory-efficient but also swift, requiring minimal computational power.

In the context of CS, were also proposed various methods for ECG [6], [7] and BP [8], [9] sensing. However, these proposed methods use some form of additional steps and components to achieve compression or to sense the data. The methods that were introduced last year [10], [11] aimed to address certain limitations associated with some of these existing approaches. The additional results obtained while working on the extended version of these works will be presented.

The article is structured as follows: In the second section, a novel lossless encoding algorithm for memory-efficient and real-time compression is introduced and preliminary results are presented. In the third section, supplementary findings regarding methods for ECG compressed sensing and pulse wave sensing are provided. The last section concludes the article and outlines the future work of the author.

II. Real-time lossless encoding of cardiovascular signals

The flowchart of the proposed encoding algorithm is shown in Fig. 1.

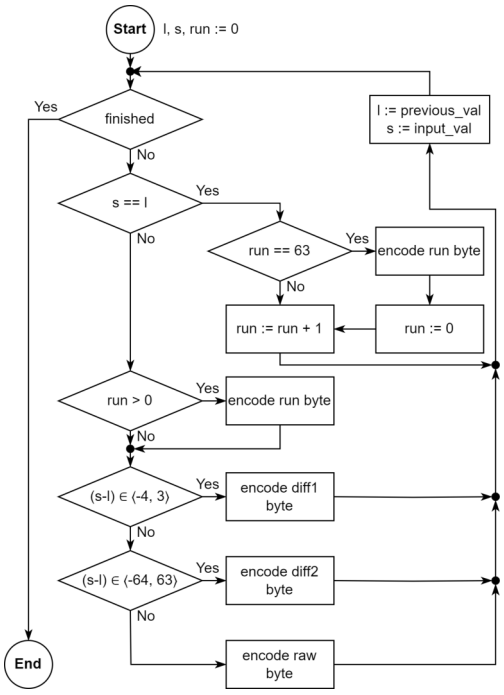

Fig. 1. The proposed encoding algorithm.

The encoding method utilizes three variables in its process. The first variable, denoted by s, stores the current two-channel sample, while the second variable, l, holds the previous two-channel sample. The third variable, run is employed for storing run-length data. These variables are initialized to zero at the start of the encoding process. Subsequently, the first two-channel sample is loaded, initiating the encoding procedure. The encoding process entails comparing the two-channel sample to the previous sample, leading to four possible outcomes. Specifically, the samples may have the same value, or the difference between them may fall within the interval of

-4 to 3. Alternatively, the difference may lie within the interval of -64 to 63, or none of these cases may occur. Each of the cases is then encoded into packets with a unique header and stored or sent.

The method was evaluated in terms of achieved CR. MIT ECG database was used and achieved CR was compared with some of the previously developed methods. The results are shown in the Table. I below.

TABLE I
COMPARISON WITH OTHER METHODS IN THE MIT-BIH DATABASE.

Encoding technique	Average CR
Peak detection + backward difference Huffman coding [2]	2.64
ALP + content adaptive Golomb-Rice coding [3]	2.77
ALP + Golomb-Rice coding [4]	2.89
The proposed method	1.98

From the obtained results, it can be concluded that the proposed method yielded an average CR approximately 25-45% lower than other recent methods. While the proposed method achieves a lower CR than other recent methods, its primary advantage lies in the algorithm's simplicity of implementation and memory efficiency. The speed and memory usage evaluation will be performed and published in the extended version of the article [12].

III. COMPRESSED SENSING OF CARDIOVASCULAR SIGNALS

Over the past year, We have focused on developing extended versions of algorithms for ECG CS [10] and Pulse Wave CS [11]. In this section, only additional results related to these methods will be presented, as the underlying techniques were previously presented during last year's SCYR conference.

Regarding the method for Multiwavelet CS of ECG signals, the original article introduced a linear quantization method for signal quantization. In the extended version, simulations with non-linear quantization were conducted. The results indicated that the resulting CR remained approximately the same, while the Percentage Root-Mean-Square Difference (PRD) was lower, signifying better performance for non-linear quantization. The detailed comparison is presented in Fig. 2.

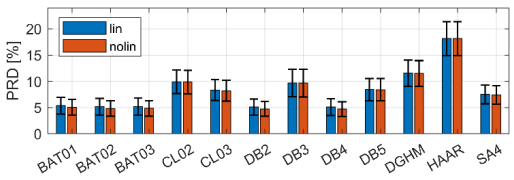

Fig. 2. Evaluation of PRD for linear and nonlinear quantization.

In the context of the CS-based measurement method for Pulse Wave estimation, simulations with varying distances of electrodes were conducted. Our evaluation focused on assessing how the amplitude of the pulse wave would change with different spacing of the electrodes. These results are shown in Fig. 3. Based on the results, was inferred that a more accurate estimation of the pulse wave can be achieved with larger spacing between the electrodes. It is important to note, however, that for measuring BP, two pairs of electrodes are required. Building a wearable device with electrodes positioned too far apart may pose challenges. Therefore, in the development of such devices, a balance must be struck between achieving optimal reconstruction and maintaining a manageable device size.

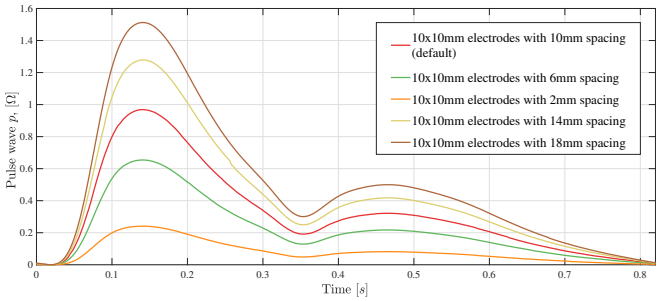

Fig. 3. Comparison of electrodes spacing against constant size.

IV. CONCLUSION AND QUO VADIS

This article briefly showcased my work in the past year. In summary, I published 4 papers [5], [10], [11], [13] from which 2 are published in high impact factor (Q1) journal.

My next steps regarding PhD study will be to finish two articles [12], [14] of which one is an extended version of [5]. Furthermore, as a 3rd year PhD student, I need to work on and complete my dissertation thesis.

ACKNOWLEDGMENT

The work is a part of the project supported by the Science Grant Agency of the Slovak Republic (No. 1/0413/22).

REFERENCES

[1] D. Donoho, "Compressed sensing," *IEEE Transactions on Information Theory*, vol. 52, no. 4, pp. 1289–1306, 2006.
[2] S.-C. Lai, P.-C. Tail, M.-K. Lee, S.-F. Lei, and C.-H. Luo, "Prototype system design of ECG signal acquisition with lossless data compression algorithm applied for smart devices," in *2018 IEEE International Conference on Consumer Electronics-Taiwan (ICCE-TW)*, 2018, pp. 1–2.
[3] T.-H. Tsai and W.-T. Kuo, "An efficient ECG lossless compression system for embedded platforms with telemedicine applications," *IEEE Access*, vol. 6, pp. 42 207–42 215, 2018.
[4] T.-H. Tsai and F.-L. Tsai, "Efficient lossless compression scheme for Multi-channel ECG signal," in *ICASSP 2019 - 2019 IEEE International Conference on Acoustics, Speech and Signal Processing (ICASSP)*, 2019, pp. 1289–1292.
[5] **J. Kromka**, O. Kovac, and J. Saliga, "Lossless real-time signal encoding for two-channel signals: A case study on ECG," *26th IMEKO TC4 International Symposium and 24th International Workshop on ADC/DAC Modelling and Testing*, p. 26 – 29, 2023.
[6] L. De Vito, E. Picariello, F. Picariello, S. Rapuano, and I. Tudosa, "A dictionary optimization method for reconstruction of ECG signals after compressed sensing," *Sensors*, vol. 21, no. 16, 2021.
[7] J. Šaliga, I. Andráš, P. Dolinský, L. Michaeli, O. Kováč, and **J. Kromka**, "ECG compressed sensing method with high compression ratio and dynamic model reconstruction," *Measurement*, vol. 183, Oct. 2021.
[8] T. Panula, J.-P. Sirkiä, D. Wong, and M. Kaisti, "Advances in non-invasive blood pressure measurement techniques," *IEEE Reviews in Biomedical Engineering*, vol. 16, pp. 424–438, 2023.
[9] Y. Yu, G. Anand, A. Lowe, H. Zhang, and A. Kalra, "Towards estimating arterial diameter using bioimpedance spectroscopy: A computational simulation and tissue phantom analysis," *Sensors*, vol. 22, no. 13, 2022.
[10] O. Kováč, **J. Kromka**, J. Šaliga, and A. Jusková, "Multiwavelet-based ECG compressed sensing," *Measurement*, vol. 220, p. 113393, 2023.
[11] **J. Kromka**, J. Saliga, O. Kovac, L. De Vito, F. Picariello, and I. Tudosa, "Radial artery pulse wave estimation by compressed sensing measurements of wrist bio-impedance," *Measurement*, vol. 219, p. 113174, 2023.
[12] **J. Kromka**, O. Kováč, A. Jusková, and J. Šaliga, "QOE - Universal lossless real-time multichannel signal encoding algorithm," manuscript submitted for publication in Measurement.
[13] **J. Kromka**, L. Fekete, and J. Saliga, "Case study of NI G Web technology application for remote educational laboratory," *26th IMEKO TC4 International Symposium and 24th International Workshop on ADC/DAC Modelling and Testing*, p. 140 – 143, 2023.
[14] **J. Kromka**, J. Šaliga, O. Kováč, A. Jusková, L. De Vito, F. Picariello, S. Rapuano, and I. Tudosa, "Online impedance estimation of induction motor coils using a CS-based measurement method," manuscript submitted for conference IMEKO 2024.

Radiance Fields Empowering Vehicular Metaverse

[1]*Matúš DOPIRIAK (2nd year),*
Supervisor: [2]*Juraj GAZDA*

[1,2]Dept. of Computers and Informatics, FEI TU of Košice, Slovak Republic

[1]matus.dopiriak@tuke.sk, [2]juraj.gazda@tuke.sk

***Abstract*—Metaverse merges physical and digital realms, enabling advanced autonomous mobility features through edge computing and digital twins (DTs). DTs, created via 3D reconstruction, enhance virtual prototyping and prediction. However, real-time DT updates from connected autonomous vehicles (CAVs) to edge servers can strain networks. We propose a novel solution utilizing distributed radiance fields (RFs) and multi-access edge computing (MEC) for efficient video compression and DT updates. Our RF-based encoder and decoder significantly compress data, achieving up to 75% savings for H.264 frame pairs with minimal loss in image quality, as evidenced by high peak signal-to-noise ratio (PSNR) and structural similarity index measure (SSIM) scores in tests using CARLA simulator data.**

***Keywords*—Digital twin, radiance fields, vehicular metaverse, video compression.**

I. Introduction

Multi-access edge computing (MEC) enhances data traffic management by redistributing computational tasks and data from connected autonomous vehicles (CAVs) to MEC servers. Metaverse, benefiting from this offloaded data, reconstructs the physical world in a dynamic, real-time simulation, relying on vast data from sensors as cameras, LiDAR, and radar. MEC's hierarchical architecture and localized data offloading strategy minimize excessive data transfer, reducing the need for extensive data transmission to centralized unit. Nevertheless, it remains imperative to employ advanced data compression techniques to further enhance transmission latency optimization. According to the scholarly research conducted by Hirlay Alves et al. [1], the successful realization of the digital twin (DT) concept within smart city environments hinges upon the attainment of a network latency window ranging from 5 ms to 10 ms, accompanied by a reliability level of $1 - 10^{-5}\%$. Contemporary studies [1], [2], [3], [4], [5] additionally emphasize the significance of metaverse and DTs adoption in the context of constructing alternative digital environments that alleviate the reliance on sophisticated sensor data such as LiDARs.

II. Related Work

Deep learning video compression enhances efficiency and quality over H.264, using neural networks for optimization, yet requires significant computation and large datasets. Zhang et al. [6] present a novel video compression strategy utilizing implicit neural representations. Unlike traditional codecs, it streamlines the process by foregoing pretrained networks, interpolation-based warping, and dedicated training datasets. Chen et al. [7] present an investigation into two innovative compression mechanisms, i.e., motion residual compression (MRC) and disparity residual compression (DRC) in binocular automotive video data. These approaches harness both geometric and temporal correlations to efficiently encode motion and disparity offsets. Comprehensive analyses of various deep learning methodologies applied to video compression are documented in [8] and [9]. Birman et al. [9] classify the predominant methodologies identified in the literature into four categories: end-to-end schemes, next video frame prediction, generative models, and autoencoder schemes. However, current literature lacks approaches that incorporate encoder and decoder frameworks predicated on radiance fields (RFs).

RFs, as Instant neural graphics primitives (INGP) [10] or 3D Gaussian Splatting (3DGS) [11], denote a technique for photorealistic approximation of the radiance of 3D scenes, facilitating the reconstruction of views from arbitrary locations and angles. This technique allows for the creation of digital replicas of real-world environments, known as DTs. Liu et al. [12] explored distributed visual data collection for the generation of RF-based DTs to assess the update speed from real-world to DT under varying DT qualities and network conditions. However, the research does not address the potential application of RFs for rapid compression to enhance latency reduction further. Byravan et al. [13] demonstrated the effectiveness of RF-based simulators where a robot trained in a RF environment successfully transferred learned policies to real-world scenarios. These studies not only validate the potential for large-scale RF-based metaverse environments capable of real-time state transfer from the real world into the metaverse but also highlight the knowledge gap our research aims to address.

III. Experimental Results

Our approach integrates RF encoder and RF decoder with a data encoding scheme that merges camera pose and H.264 encoded discrepancies between actual and RF rendered frames. The encoder uses camera pose from CAVs to generate a RF-rendered frame and encode differences into a *P-frame* delta. This data is sent to a roadside unit (RSU), a communication device located alongside roads, with a MEC server for decoding, enabling the reconstruction of the original scene by combining the camera pose and *P-frame* delta to accurately render the RF view and its deviations from reality. A dataset for the RFs was created by rendering an urban 3D scene with CARLA simulation, using 18 cameras on a car moving in both street directions. Compression efficiency was evaluated by analyzing compression gains from 144 frames captured by cameras along the vehicle's trajectory.

TABLE I
AVERAGE MEAN VALUES OF RF MODELS

Metrics	**PSNR ↑**		**SSIM ↑**		**LPIPS ↓**	
Scenario	INGP	3DGS	INGP	3DGS	INGP	3DGS
Empty	26.33	29.41	0.75	0.85	0.38	0.24
Vehicles	21.33	21.78	0.68	0.71	0.44	0.30

Compression efficiency is measured against H.264 codec compression of *I-frame* and *P-frame* pairs, across resolutions from 300x168 to 1920x1080 (full HD) suitable for subsequent computer vision tasks. Using presets 'veryslow', 'medium', 'veryfast', and constant rate factors (CRFs) of 18, 23, and 28. We averaged encoded image pair values for final analysis. Notably, our method generates the *I-frame* using RFs, avoiding its network transmission. Compression savings are calculated as $100 * I_{size}/(I_{size} + P_{size})$, indicating the percentage reduction in data size by omitting the *I-frame*.

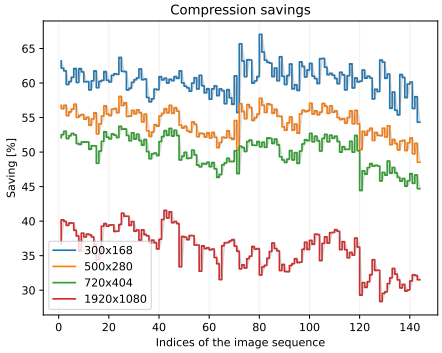

Fig. 1. Encoder setting-averaged compression savings relative to H.264 achieved for individual images with vehicles in the scene scenario using INGP.

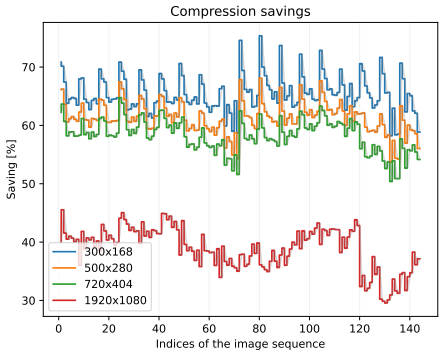

Fig. 2. Encoder setting-averaged compression savings relative to H.264 achieved for individual images with vehicles in the scene scenario using 3DGS.

Table I provides an assessment of the RF models through the employment of peak signal-to-noise ratio (PSNR), structural similarity index measure (SSIM), and learned perceptual image patch similarity (LPIPS) metrics. In the scenario adding vehicles to the 3D scene, absent from RF models, a performance drop in metrics was observed for both models. The difference in performance was subtle, as indicated by the LPIPS metric in Table I, which showed consistent variance with the empty scenario. Fig. 1 and Fig. 2 reveal compression savings of 28%-68% for INGP and 30%-75% for 3DGS. The vehicular scenario demonstrates increased compression efficiency at lower resolutions, attributable to the encoding of a reduced amount of information, encompassing disparities and artifacts between frames.

IV. Conclusion

In this study, we present a novel compression technique with RF-based encoder and decoder to enable a low-latency, photorealistic metaverse for CAVs. Dataset generated with CARLA simulator demonstrates significant compression and reconstruction quality, indicating the potential for scalable, realistic vehicular metaverse applications. Future research endeavors are primarily directed towards harnessing temporal data across frames to enhance compression efficiency through motion estimation methodologies such as optical flow. Subsequent research objectives concentrate on forecasting future traffic patterns on MEC server side, with the aim of utilizing RF variants.

Acknowledgment

This work was supported by The Slovak Research and Development Agency project no. APVV-18-0214, no. APVV SK-CZ-RD-21-0028, and the Slovak Academy of Sciences under Grant VEGA 1/0685/23.

References

[1] H. Alves, G. D. Jo, J. Shin, C. Yeh, N. H. Mahmood, C. H. M. de Lima, C. Yoon, G. Park, N. Rahatheva, O.-S. Park, and et al., "Beyond 5G urllc evolution: New service modes and practical considerations," *ITU Journal on Future and Evolving Technologies*, vol. 3, no. 3, p. 545–554, 2022.

[2] S. Mihai, M. Yaqoob, D. V. Hung, W. Davis, P. Towakel, M. Raza, M. Karamanoglu, B. Barn, D. Shetve, R. V. Prasad, H. Venkataraman, R. Trestian, and H. X. Nguyen, "Digital Twins: A Survey on Enabling Technologies, Challenges, Trends and Future Prospects," *IEEE Communications Surveys and Tutorials*, vol. 24, no. 4, pp. 2255–2291, 2022.

[3] M. Xu, W. C. Ng, W. Y. B. Lim, J. Kang, Z. Xiong, D. Niyato, Q. Yang, X. Shen, and C. Miao, "A Full Dive Into Realizing the Edge-Enabled Metaverse: Visions, Enabling Technologies, and Challenges," *IEEE Communications Surveys and Tutorials*, vol. 25, no. 1, pp. 656–700, 2023.

[4] Y. Ren, R. Xie, F. R. Yu, T. Huang, and Y. Liu, "Quantum Collective Learning and Many-to-Many Matching Game in the Metaverse for Connected and Autonomous Vehicles," *IEEE Transactions on Vehicular Technology*, vol. 71, no. 11, pp. 12 128–12 139, 2022.

[5] M. Xu, D. Niyato, H. Zhang, J. Kang, Z. Xiong, S. Mao, and Z. Han, "Generative ai-empowered effective physical-virtual synchronization in the vehicular metaverse," in *2023 IEEE International Conference on Metaverse Computing, Networking and Applications (MetaCom)*, 2023, pp. 607–611.

[6] Y. Zhang, T. van Rozendaal, J. Brehmer, M. Nagel, and T. Cohen, "Implicit neural video compression," *arXiv preprint arXiv:2112.11312*, 2021.

[7] Z. Chen, G. Lu, Z. Hu, S. Liu, W. Jiang, and D. Xu, "LSVC: A learning-based stereo video compression framework," in *Proceedings of the IEEE/CVF Conference on Computer Vision and Pattern Recognition*, 2022, pp. 6073–6082.

[8] D. Ding, Z. Ma, D. Chen, Q. Chen, Z. Liu, and F. Zhu, "Advances in video compression system using deep neural network: A review and case studies," *Proceedings of the IEEE*, vol. 109, no. 9, pp. 1494–1520, 2021.

[9] R. Birman, Y. Segal, and O. Hadar, "Overview of research in the field of video compression using deep neural networks," *Multimedia Tools and Applications*, vol. 79, pp. 11 699–11 722, 2020.

[10] T. Müller, A. Evans, C. Schied, and A. Keller, "Instant neural graphics primitives with a multiresolution hash encoding," *ACM Transactions on Graphics (ToG)*, vol. 41, no. 4, pp. 1–15, 2022.

[11] B. Kerbl, G. Kopanas, T. Leimkühler, and G. Drettakis, "3D Gaussian Splatting for Real-Time Radiance Field Rendering," 2023.

[12] Y. Liu, X. Tu, D. Chen, K. Han, O. Altintas, H. Wang, and J. Xie, "Visualization of Mobility Digital Twin: Framework Design, Case Study, and Future Challenges," in *2023 IEEE 20th International Conference on Mobile Ad Hoc and Smart Systems (MASS)*. IEEE, 2023, pp. 170–177.

[13] A. Byravan, J. Humplik, L. Hasenclever, A. Brussee, F. Nori, T. Haarnoja, B. Moran, S. Bohez, F. Sadeghi, B. Vujatovic *et al.*, "Nerf2real: Sim2real transfer of vision-guided bipedal motion skills using neural radiance fields," in *2023 IEEE International Conference on Robotics and Automation (ICRA)*. IEEE, 2023, pp. 9362–9369.

Physical model of continuous processing line

[1]*Pavol SMOLEŇ (5th year)*
Supervisor: [2]František ĎUROVSKÝ

[1,2]Dept. of Electrical Engineering and Mechatronics, FEI TU of Košice, Slovak Republic

[1]pavol.smolen@student.tuke.sk, [2]frantisek.durovsky@tuke.sk

***Abstract* – The paper presents a physical model of a material processing line intended for education of complex mechatronic systems control. The mechanical part of model consists of uncoiler, coiler, bridle, tension roll and horizontal web accumulator. The control of physical model is done by a PLC-based technological controller and the motors are powered by frequency converters. The model allows set up different configurations of the processing line. The article is supplemented with a simple example of processing line configuration with corresponding control structure and time responses of important line variables.**

***Keywords* - control of material processing lines, tension control, technological controller**

I. Introduction

Material processing lines (MPL) are used in various types of industries: metallurgical, paper, wood, chemical, printing, etc. These lines are usually divided into input (entry) section (IS), processing or technological section (PS) and output (exit) section (OS). The material is fed to the line at the entry from the coil on uncoiler, proceeds through the PS and after treatment is wound on the line output on the coiler. If the line includes a cross cutting of material, where the strip is cut into sheets, there is a packaging section at the line output [1].

At simpler lines, the strip is loaded into the line at each coil. In more complex technology, where the loading of material into the PS is complicated, the strip from the new coil at the line entry is welded to the previous strip end, so that the passage of the material through the PS is smooth and does not require the strip re-loading. In this case, the term "endless strip" is usually used. Such lines are also called continuous material processing lines (CMPL) [2].

II. Physical model of material processing line

The concept of MPL physical model was chosen to include basic components of MPL and to test different line structures. The resulting concept of MPL arrangement is shown in Fig. 1. The model contains six drives that represent the basic components of continuous processing lines: uncoiler (1), bridle (2), horizontal web accumulator (4) and coiler (7). Two force sensors (3) and (6) are included in the assembly, which can be used to direct tension control [3]. In addition, another driven tension roll with a large belt contact (5) is included in the line, which enables the realization of tension control structures [4], [5]. The structure of the line can be changed as needed. The construction of the model from aluminium profiles is deliberately robust to withstand the unintentional but often rough handling that can occur during practical exercises.

Table 1 Parameters of MPL physical model

Parameter	Value	Unit
Line max speed	10,0	m/min
Acceleration and deceleration time	5,0	s
Max strip tension	200,0	N
Accumulator length	0,6	m
Accumulator max. speed	5,0	m/min
Rolls diameter	80,0	mm
Uncoiler / Coiler min. diameter	100,0	mm
Uncolier / Coiler max. diameter	195,0	mm

Based on the motors and sensors attachment, the basic line parameters were defined (Table 1). The material that is wound in the line is a 35 mm wide celluloid film strip. The speed of the line is limited by the size of web accumulator and the maximum speed of its linear drive.

III. Experimental results

The control structure according to Fig. 2 was tested in the following mode: the line was started at speed of 5,0 m/min. At 18:55:09 the speed was increased to 10,0 m/min and then reduced to 5,0 m/min and at 18:55:25 to 2,0 m/min. The measured responses are shown in Fig. 3. The upper graph shows the logic signals that indicate the operation mode of the line (log. 1, i.e. line is running), the generator mode of uncoiler (log. 1, i.e. the uncoiler is breaking the strip) and motor mode

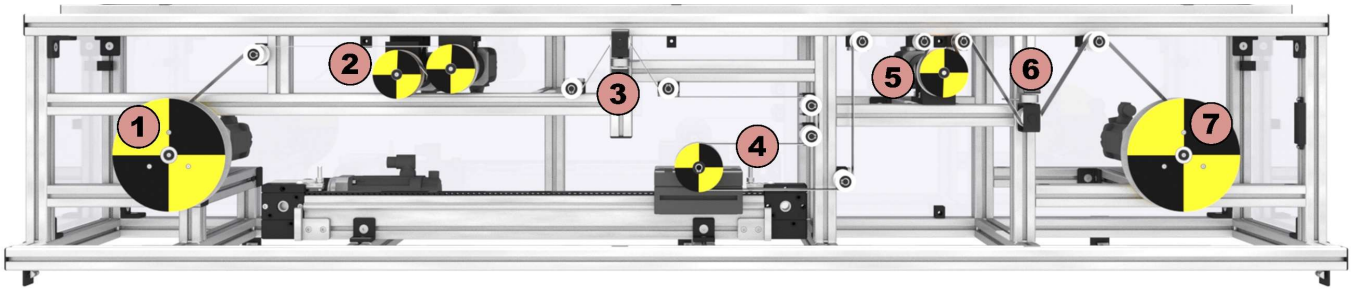

Fig. 1. Physical model of MPL: 1 - Uncoiler; 2 - Bridle 1; 3 – Pressure sensor 1; 4 – Web accumulator; 5 – Tension roll, 6 - Pressure sensor 2; 7 - Coiler

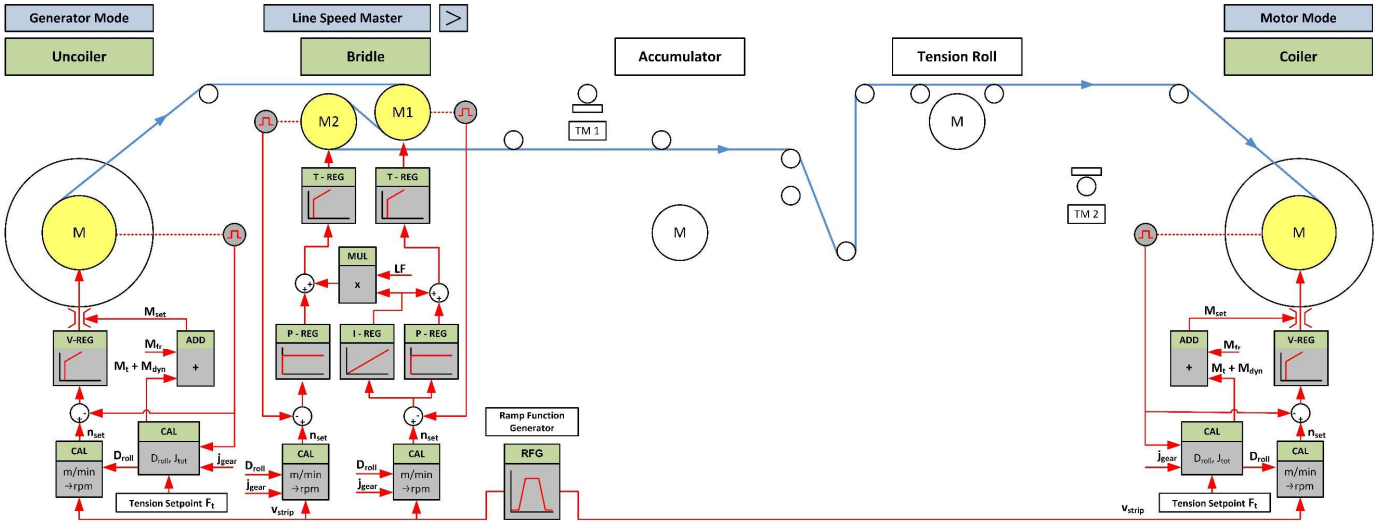

Fig. 2. Experimental control structure

of coiler (log. 0, i.e. the coiler is pulling the strip). Both drives work in tension control mode. The next graph shows the actual circumferential speeds of individual drives. The graphs below show the tension between uncoiler and bridle and between bridle and coiler. Since an indirect tension control was applied on coiler and uncoiler, the tension in sections were calculated from the torque of motors.

The response of actual tension shows in individual sections overshoots strip tension during acceleration and deceleration. These overshoots represent approximately 2,5 % of the tension setpoint. They may be caused by an inaccurate setting of dynamic torque compensation.

At time 18:55:34 tension setpoint between uncoiler and bridle was changed from 20 N to 30 N and at time 18:55:37 the same change was done between bridle and coiler. The actual tensions follow the reference.

IV. Conclusion

The physical model of material processing line presented in this paper contains the basic components that occur on real lines in industry. These components can be arranged in several configurations to test different types of processing lines. Used software as well as the methods of controlling and monitoring of the model are commonly applied in industry.

References

[1] BWG Duisburg, "BWG Bergwerk und Walzwerk Maschinenbau GmbH Anniversary Book", Duisburg, Germany, 2015

[2] J. Jadlovský, M. Čopík, P. Papcun, "Distribuované systémy riadenia", Elfa Košice, 2013, ISBN 978-80-8086-227-5.

[3] Siemens AG, "SIMOTION Line Tension Control": Siemens application example. Entry-ID: 56293754, V2.2.1, 01/2019. [Online]. Available: https://support.industry.siemens.com/cs/ww/en/view/56293754. [Accessed: June 20, 2023].

[4] Magura, D.; Kyslan, K.; Padmanaban, S.; Fedák, V. Distribution of the Strip Tensions with Slip Control in Strip Processing Lines. Energies 2019, 12, 3010. https://doi.org/10.3390/en12153010

[5] Magura, D.; Fedák, V.; Sanjeevikumar, P.; Kyslan, K. Tension Controllers for a Strip Tension Levelling Line. In Proceedings of the Advances in Systems, Control and Automation. Lecture Notes in Electrical Engineering; Springer: Singapore, 2018; Vol. 42, pp. 33–44

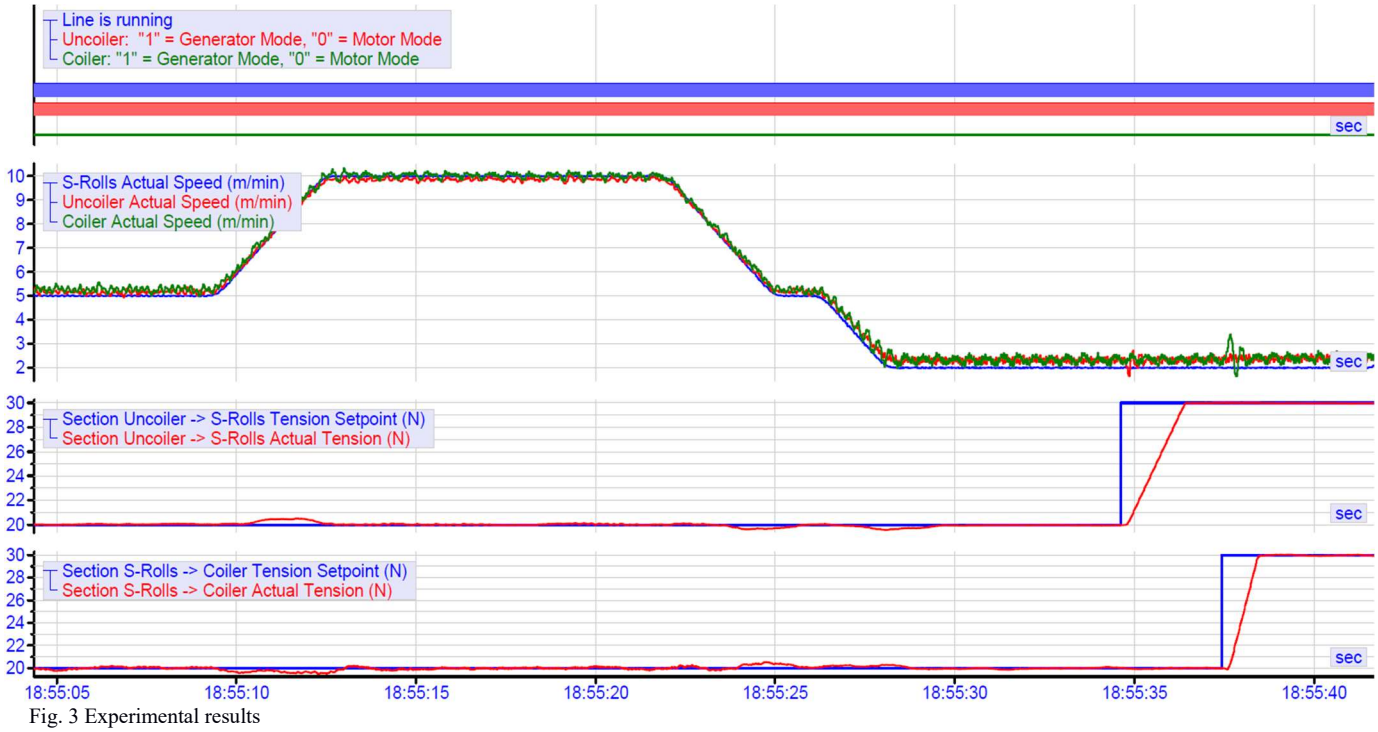

Fig. 3 Experimental results

DMA and XRD study of TPS-based materials

[1]*Leoš ONDRIŠ (2nd year)*
Supervisor: [2]Oľga FRIČOVÁ

[1,2]Dept. of Physics, FEI TU of Košice, Slovak Republic

[1]leos.ondris@tuke.sk, [2]olga.fricova@tuke.sk

***Abstract*—Starch is a natural semi-crystalline polysaccharide that is mainly used in the food industry. Plasticization of starch yields thermoplastic starch (TPS) with properties suitable for the use in other industries. TPS can be also blended with other biodegradable polymers (e.g. PBAT) or reinforced by nanofillers (e.g. montmorillonite – MMT). The effect of MMT and PBAT on relaxation transitions in TPS and TPS/PBAT blends was investigated by dynamic-mechanical analysis (DMA) and X-ray diffractometry (XRD), respectively.**

***Keywords*—thermoplastic starch, nanocomposites, blends, X-ray diffractometry, dynamic-mechanical analysis**

I. Introduction

New biodegradable polymeric materials from renewable sources are being developed to replace conventional plastics derived from fossil sources. One of the most promising materials is thermoplastic starch (TPS). Native starch is a semi-crystalline carbohydrate polymer consisting of two types of polysaccharides – (predominantly) linear amylose and (highly) branched amylopectin. Starch is mainly used in the food industry, for the use in other industries it has to be modified so that it can be processed by procedures common to conventional plastics [1]. The most common treatment is thermomechanical processing with water and other low-molecular-weight compounds (e.g. polyols, amides) which results in thermoplastic starch (TPS) [2][3]. The choice of plasticizers depends on TPS desired properties and applications. However, TPS has poor thermal stability, it is prone to absorb moisture and retrogradation process occurring during storage leads to its embrittlement. Thus, the TPS properties need to be further adjusted. Common TPS modifications include adding reinforcing (nano)fillers and blending with other (biodegradable) polymers [1][2]. Experimental methods such as dynamic-mechanical analysis (DMA) and X-ray diffractometry (XRD) provide information about relaxation transitions and structure of starch-based materials.
In this paper, DMA and XRD techniques were used to study the effect of montmorillonite (MMT) nanofiller on TPS matrix and the effect of PBAT polymer on properties of TPS/PBAT blends as part of basic research of these materials.

II. Samples preparation

The examined samples were prepared at the Polymer Institute, Slovak Academy of Sciences in Bratislava using a procedure described in detail in [4].
To prepare TPS, native corn starch was mixed with distilled water and glycerol with weight ratio 1:2.3:0.5, respectively. In the case of TPS nanocomposites (TPS5M), MMT nanoparticles (0.05 weight parts to 1 part of dry starch) were dispersed in distilled water before the preparation of the suspensions mentioned above. The suspensions were dried and then processed in a laboratory mixer. To prepare TPS/PBAT blends, TPS or TPS5M materials were mixed with PBAT (already processed in laboratory mixer) in the ratio of 30/70. Compression moulding was used for sample slabs preparation (approx. 1mm thick). The studied samples are denoted TPS, TPS5M, PBAT, TPS/PBAT and TPS5M/PBAT.

III. Experimental methods

DMA measurements were performed on a TA Instruments DMA Q800. The samples were cut into 3 x 0.6 cm^2 strips. The measurements were carried out in tensile mode. In all measurements, the harmonic strain frequency was set to 5 Hz, the harmonic strain amplitude to 5 μm, and the heating rate to 2°C/min.

XRD diffractograms were detected on a Rigaku MiniFlex600 XRD analyser. The XRD was operated at a voltage of 40 kV and a current of 15 mA. Cu K_α X-rays with a wavelength of λ=0.154 nm were used. The sample and the detector were rotated at 2.5°/min and 5°/min, respectively. The method theta-2theta was used for XRD measurements.

IV. Experimental

A. DMA measurements

During DMA measurements, the response of the studied material to an applied harmonic force over a certain temperature range is detected. The loss factor $\tan\delta$, which is determined by the ratio of dissipated and stored energy in one cycle of sample deformation, reaches local maxima when temperature-induced relaxation transitions occur in particular temperature intervals. An important transition is the so-called glass transition, in which the mechanical properties of polymeric materials change significantly due to the fact that the motion of the chain segments is restricted below the glass transition temperature T_g and released above T_g.
Two pronounced maxima can be observed in the temperature dependences of loss factor $\tan\delta$ for the TPS (Fig. 1, black curve) and TPS5M (Fig. 1, red curve) samples. This is ascribed to the non-uniform distribution of plasticizer molecules in the sample volume, leading to the formation of plasticizer-rich and starch-rich domains. The maximum below 0°C which corresponds to the glass transition in plasticizer-rich domains and the broad maximum above 0°C appears to consist of two maxima can be assigned to the release of segmental motion of linear amylose chains (at approx. 40°C) and the branched amylopectin chains (at 63°C) in starch-rich domains [5]. In the case of the TPS5M sample, only one maximum at 58.2°C can

be observed because of similar segmental mobility of both amylose and amylopectin chains in starch-rich domains [6]. The presence of MMT particles in TPS caused a small restriction of the mobility of amylose chains and a slight increase of the mobility of amylopectin chains. The glass transition for the plasticizer-rich domains in the TPS sample is observed at -46°C, while in the TPS5M sample at a slightly higher temperature of -43.8°C. This difference is due to a slight mobility restriction of starch chains in these domains, probably due to the interaction of glycerol with MMT particles.

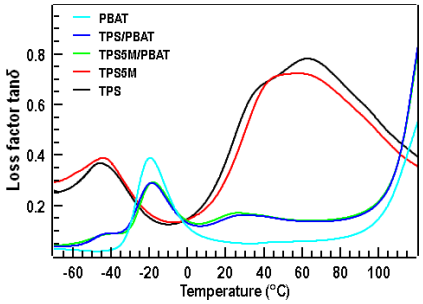

Fig. 1 Temperature dependence of loss factor tanδ of studied samples

In the temperature dependence for the PBAT sample (Fig. 1, cyan curve), one maximum can be seen at -19.6°C, corresponding to a glass transition in the amorphous PBAT domains. Another relaxation transition is observed above 120°C when overall chain mobility is enhanced due to melting of PBAT crystalline domains [7].

TPS and PBAT are immiscible polymers, so domain formation of individual components can be expected. In the temperature dependence of the loss factor tanδ of the TPS/PBAT blend (Fig. 1, blue curve), a maximum corresponding to the glass transition in the PBAT component is observed at -18.8°C, close to that one for pure PBAT, and two maxima for TPS component, at -41°C and 30°C for plasticizer-rich and for starch-rich domains, respectively. Comparing the mobility of starch chains in the TPS/PBAT blend and pure TPS, it is slightly restricted in the plasticizer-rich and enhanced in starch-rich domains. The significant decrease in T_g (increase in chain mobility) for the starch-rich domains is probably due to the restriction of the crystallization of the starch chains in the small TPS domains in the PBAT matrix. Temperature dependence of the TPS5M/PBAT blend is almost identical to that one for TPS/PBAT.

B. XRD measurements

In the diffractogram of the TPS sample (Fig. 2, black curve), a pronounced maximum at 2theta ≈ 20.6° and a less pronounced one at 2theta ≈ 13.3° can be seen. These maxima correspond to crystalline structure of V_A-type of starch. This crystalline structure can transform into V_H-type over time [1].

Diffraction maximum at 2theta ≈ 7.6° in MMT diffractogram (not shown) corresponding to the distance d_{001}=1.17 nm shifts to lower 2theta values if interlayer space is intercalated [8] as we can see in the diffractogram for TPS5M (Fig. 2, red curve) where the maximum at 2theta ≈ 4.8° is observed. Diffraction maximum at 2theta ≈ 20.6° related to V_A-type starch structure is less pronounced than for the TPS sample. It can be a consequence of the intercalation of some amount of water and glycerol molecules into MMT particles which lowered the starch chain mobility and suppressed ordering of starch chains into crystalline structures. Maximum at 2theta ≈ 19.8° probably belongs to MMT [8].

PBAT diffractogram (Fig. 1, cyan curve) shows five diffraction maxima at 2theta ≈ 16°, 17.1°, 20.1°, 22.8° and 24.5° corresponding to the crystalline domains of PBAT [7].

Based on diffractogram shape, crystalline structures are present also in the PBAT component of both studied blends (Fig. 2, blue and green curves).

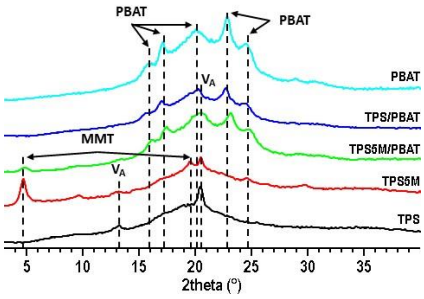

Fig. 2 XRD diffractograms of studied samples

The main difference between diffractograms of the studied blends consists in the presence of maximum at 2theta ≈ 4.8° corresponding to the intercalated MMT structure in the TPS component of TPS5M/PBAT blend.

V. Conclusion

The addition of MMT nanoparticles to the TPS matrix restricted motion of starch chains. XRD measurements confirmed an intercalated structure of MMT in TPS. In the studied blends PBAT and TPS domains with different mobility were formed. The effect of MMT on the structure and molecular mobility in the TPS5M/PBAT blend is almost negligible probably due to a small TPS content in the blend.

The thermograms of TPS(5M/PBAT blends show minimal changes in the temperature range 0-80°C therefore they can be considered as the best candidates for practical applications, e. g. in food packaging [1][2]. Further research will be focused on the stability of these blends during storage.

Acknowledgment

The research presented was supported by the Scientific Grant Agency of the Ministry of Education of Slovak Republic through grant VEGA No. 1/0751/21. We would like to thank prof. I. Chodák and Dr. H. Peidayesh for providing samples.

References

[1] M. N. Belgacem, A. Gandini, *Monomers polymers and composites from renewable resources: Starch: Major sources, properties, and applications as thermoplastic materials*, Kidlington: Elsevier Ltd., 2008, ch. 15.

[2] J. H. Han, *Innovations in Food Packaging: Thermoplastic Starch*, Elsevier Ltd, 2014, ch. 16.

[3] S. Krejíčková, A. Ostafinska, M. Šlouf, "Termoplastifikovaný škrob a jeho aplikace," in *Chemické listy*, vol. 112, pp. 531-537.

[4] H. Peidayesh, et al. "Biodegradable nanocomposites based on blends of poly(butylene adipate-co-terephthalate) (PBAT) and thermoplastic starch filled with montmorillonite (MMT): Physico-mechanical properties," in *Materials*, vol. 17, 2024, pp. 540.

[5] H. Schmitt, et al. "Studies on the effect of storage time and plasticizers on the structural variations in thermoplastic starch," in *Carbohydrate Polymers*, vol. 115, 2015, pp. 364-372.

[6] O. Fričová, M. Hutníková, "Viscoelastic behavior of starch plasticized with urea and glycerol.," in *AIP Conference Proceedings*, vol. 2131, 2019, pp. 020011.

[7] M. Lackner, F. Ivanič, M. Kováčová, I. Chodák, "Mechanical properties and structure of mixtures of poly(butylene-adipate-co-terephthalate) (PBAT) witch thermoplastic starch (TPS)," in *International Journal of Biobased Plastics*, vol. 3, 2021, pp. 126-138.

[8] L. Ondriš, M. Hutníková, Ľ. Popovič, H. Peidayesh, O. Fričová, "XRD and DMA study of thermoplastic starch-based nanocomposites," in *AIP Conference Proceedings*, vol. 3054, 2024, pp. 030010.

Modeling of Bidirectional Buck-Boost DC/DC Converter for Hybrid Energy Storage System

[1]*Dávid BODNÁR (3rd year)*
Supervisor: [2]František ĎUROVSKÝ

[1,2]Dept. of Electrical Engineering and Mechatronics, FEI TU of Košice, Slovak Republic

[1]david.bodnar@tuke.sk, [2]frantisek.durovsky@tuke.sk

***Abstract*—Hybrid energy storage systems (HESS) are becoming more common in dynamic and stationary applications. To exploit the maximum potential of hybrid energy storage systems, they are equipped with DC/DC converters, which provide efficient cooperation between two or more components with different voltage levels within one energy storage. Despite the high efficiency of DC/DC converter, it plays an important role in the overall system's efficiency. In this paper, a model of a bidirectional buck-boost converter for battery-ultracapacitor energy storage systems was created in the PLECS Blockset environment. The model was designed to estimate the energy efficiency of the converter across a wide power and voltage range. The created model can be used especially for designing energy storage systems.**

***Keywords*—DC/DC converter, modeling, PLECS.**

I. Introduction

In electric vehicle applications, the high efficiency of HESS and the whole powertrain is important for HESS component size optimization because the vehicle range is directly affected by the efficiency of the traction chain. In this paper, we assume an application of HESS in a 7-ton electric midibus, which should be one of the most convenient applications for HESS due to frequent energy regeneration under vehicle braking. To make HESS viable over battery energy storage systems (BESS), the energy efficiency of the overall HESS system must be the same or better compared to BESS. If the efficiency of the HESS were lower, the vehicle range would decrease, and the same battery capacity would not be sufficient. Moreover, the higher weight of HESS affects the energy consumption of the vehicle too. Battery capacity would need to be increased, which has a negative impact on costs. Therefore, HESS efficiency must be carefully studied to determine the impact of HESS on the vehicle range.

There are many factors influencing the efficiency of HESS. HESS consists of 3 main components, a battery pack, ultracapacitor modules (UC), and a DC/DC converter. All of them have different efficiencies which depend on different factors. The energy efficiency of a Li-ion battery depends on the current profile [1] and on the internal impedance of the cell too [2], which is affected by temperature, battery State of Charge, and battery State of Health [3]. The energy efficiency of UC is a function of the maximum and minimum working voltages, the working current, and the internal resistance [4]. The energy efficiency of UC decreases with increasing working current and internal resistance and increases with working UC voltages. In addition, in the cycles with rest, energy efficiency also depended on the self-discharge and self-charge voltages. The efficiency of a DC/DC converter depends on several factors such as the converter's topology, switching frequency, and choice of semiconductor components. However, the efficiency significantly varies during the operation, where the input and the output voltages have a significant influence, and the actual power plays a major role in the converter's efficiency [5][6]. The efficiency increases with increasing power until it reaches the peak and then drops slowly with further increasing power due to ohmic resistance [6].

The goal of this paper is to create a model of a bidirectional DC/DC converter in PLECS Blockset, which would be able to calculate the energy efficiency of the converter for different scenarios, namely different UC voltages and input powers. From the simulation results, a look-up table describing the converter's energy efficiency was created to enhance the speed of the HESS simulations maintaining high accuracy for the HESS designing process.

The paper is organized as follows. Section II describes the modeling of the DC/DC converter, section III deals with simulation results of the converter's efficiency, and section IV concludes the paper.

II. UC model of DC/DC Converter in PLECS Blockset

The battery pack and the UC pack operate in different voltage ranges, therefore a DC/DC converter is used in the HESS, which allows the control of the energy flow and maximizes the use of the UC.

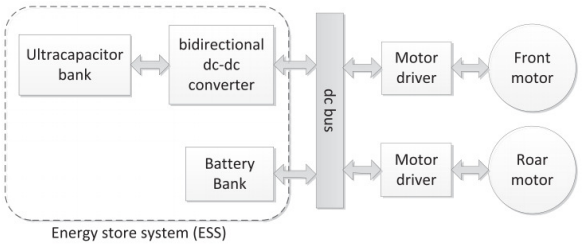

Fig. 1 Schematic representation of hybrid energy storage system with a bidirectional DC/DC converter [7]

For our application, the ultracapacitor semi-active topology is shown in Fig. 1. From the HESS simulation point of view, we are mainly interested in the losses in the converter, as they can significantly affect the range of the vehicle. Therefore, we created a model of a bidirectional DC/DC converter (Fig. 2) in the PLECS Blockset program, which allows a simulation of power semiconductor systems. We used SCT4013DR SiC

MOSFETs, connecting 5 in parallel to handle the current requirements, which is the maximum current of 500 A. The transistor model for the PLECS software is available on the manufacturer's website. PLECS allows relatively accurate calculations of switching and conduction losses. Summing up all power losses of the converter, the converter's efficiency can be calculated as:

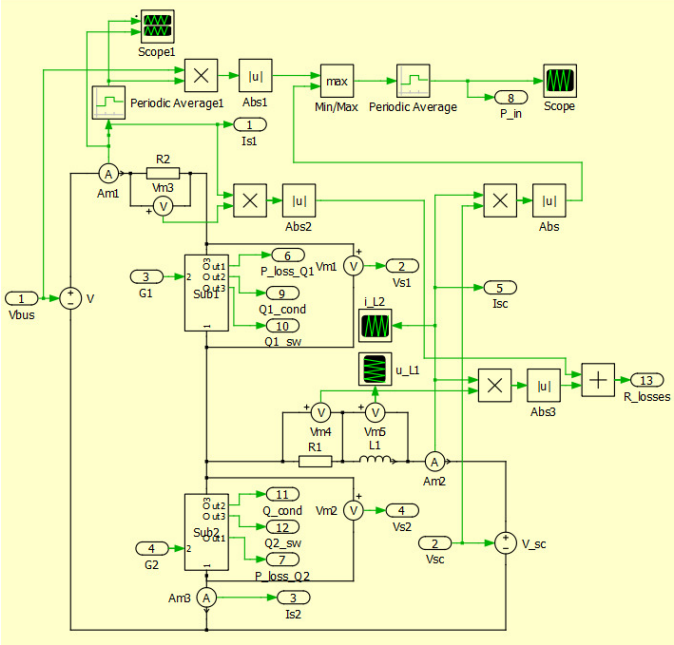

Fig. 2 Scheme of a bidirectional DC/DC converter in PLECS with loss calculation

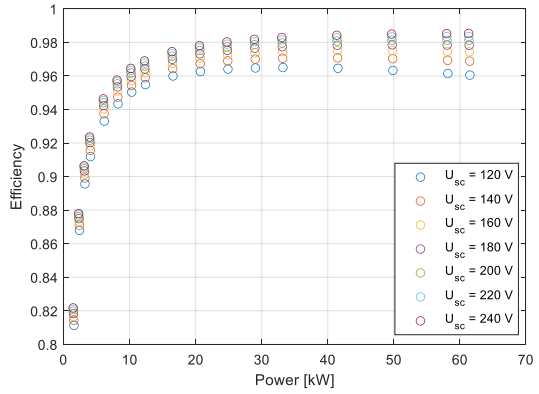

Fig. 3 Efficiency of DC/DC converter in the buck mode

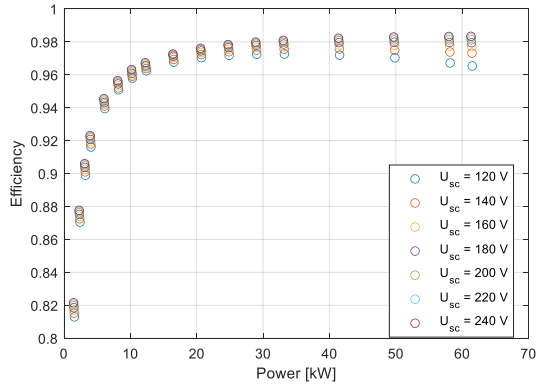

Fig. 4 Efficiency of DC/DC converter in the boost mode

$$\eta_{conv} = 1 - \frac{P_{loss}}{P_{in}}, \quad (1)$$

where P_{loss} stands for power losses, and P_{in} is the input power.

III. Efficiency Results of UC Model

The results for the buck mode are shown in Fig. 3, for the boost mode in Fig. 4. Simulations of the efficiency of the DC/DC converter were performed for a battery voltage of 400 V and the UC voltage ranged from 120-240 V with a step of 20 V. The output current was controlled to maintain the constant output power, which ranged from 1 to 60 kW. The switching frequency of the converter was 50 kHz. In Fig. 3 and Fig. 4, the efficiency is displayed as a function of output power for different levels of UC voltages. From the simulations' results, we can observe low efficiency at low powers, which is caused by losses in the iron of the coil. The efficiency stabilized at approximately 96-98% at higher powers and only slightly decreased with further increasing power.

IV. Conclusion

In this paper, a model of a bidirectional buck-boost DC/DC converter was created in PLECS Blockset. The calculated energy efficiency of the converter during its operation depends mainly on the input power, which is significantly lower at lower input powers. Therefore, it is recommended to enable the ultracapacitor's power flow from a certain threshold power level in battery-ultracapacitor HESS to reduce losses.

In future research, the proposed model will be used to model HESS in an electric midibus. The simulation results should show the impact of HESS on the vehicle range, which will help to assess the impact and viability of HESS in these applications.

Acknowledgment

This work was supported by Slovak Research and Development Agency on the basis of Contract no. APVV-18-0436. This work was supported by the Scientific Grant Agency of the Ministry of Education of the Slovak Republic under the project VEGA 1/0363/23.

References

[1] K. Li and K. J. Tseng, "Energy efficiency of lithium-ion battery used as energy storage devices in micro-grid," in *IECON 2015 - 41st Annual Conference of the IEEE Industrial Electronics Society*, Institute of Electrical and Electronics Engineers Inc., 2015, pp. 5235–5240. doi: 10.1109/IECON.2015.7392923.

[2] D. Anseán, M. González, J. C. Viera, V. M. García, J. C. Álvarez, and C. Blanco, "Electric vehicle Li-ion battery evaluation based on internal resistance analysis," in *2014 IEEE Vehicle Power and Propulsion Conference, VPPC 2014*, Institute of Electrical and Electronics Engineers Inc., 2014. doi: 10.1109/VPPC.2014.7007058.

[3] L. Lam and P. Bauer, "Practical capacity fading model for Li-ion battery cells in electric vehicles," *IEEE Trans Power Electron*, vol. 28, no. 12, pp. 5910–5918, 2013, doi: 10.1109/TPEL.2012.2235083.

[4] J. J. Quintana, A. Ramos, M. Diaz, and I. Nuez, "Energy efficiency analysis as a function of the working voltages in supercapacitors," *Energy*, vol. 230, Sep. 2021, doi: 10.1016/j.energy.2021.120689.

[5] C. Riczu, S. Habibi, and J. Bauman, "Design and Optimization of An Electric Vehicle with Two Battery Cell Chemistries," in *2018 IEEE Transportation and Electrification Conference and Expo, ITEC 2018*, Institute of Electrical and Electronics Engineers Inc., Aug. 2018, pp. 788–794. doi: 10.1109/ITEC.2018.8450156.

[6] M. Li *et al.*, "The structure and control method of hybrid power source for electric vehicle," *Energy*, vol. 112, pp. 1273–1285, Oct. 2016, doi: 10.1016/j.energy.2016.06.009.

[7] J. Armenta, C. Núñez, N. Visairo, and I. Lázaro, "An advanced energy management system for controlling the ultracapacitor discharge and improving the electric vehicle range," *J Power Sources*, vol. 284, pp. 452–458, Jun. 2015, doi: 10.1016/j.jpowsour.2015.03.056.

Polymer Paste Production Based on Modified Ag_2O Particles to Form Conductive Ag Layers

[1]*Peter PROVÁZEK (3rd year)*
Supervisor: [2]Alena PIETRIKOVÁ

[1,2]Dept. of Technologies in Electronics, FEI TU of Kosice, Slovak Republic

[1]peter.provazek@tuke.sk, [2]alena.pietrikova@tuke.sk

***Abstract*— This paper is focused on the tasks and obtained results in the previous year of the postgraduate study. It provides the possibility of using wet planetary ball milling to modify silver oxide (Ag_2O) particles. In addition, the formulation, and production of Ag_2O-based self-reducing polymer paste are presented. It examines the effect of the thermal process (vacuum, temperatures) and the number of printed layers on the sheet resistance of Ag layers. The findings from the experiments suggest that wet planetary ball milling is suitable for modifying Ag_2O particles for their use in self-reducing polymer paste.**

***Keywords*—Ag_2O, polymer conductive paste, wet planetary ball milling.**

I. Introduction

The most important part of the electronic structures are the conductive layers. Metal particles such as Au, Cu, and Ag, as well as their oxides, are the base components of the conductive pastes [1]. Silver emerges as the major choice due to its advantages such as high chemical stability, reasonable price, and high electrical conductivity [2]. One of the challenges in the field of flexible electronics is the development and production of new low-temperature polymer conductive pastes [3]. These pastes require fine metal powders because the particle size, morphology, purity, and distribution affect electrical conductivity [4]

The electrical and mechanical properties of conductive paste can be modified by adding metal oxides like Ag_2O particles. These particles are reduced to Ag by a specific solvent at low temperatures [5]. According to the literature, Ag_2O particle modification for polymer paste production has not been studied. Scientific papers on Ag_2O particle milling by planetary ball milling led to its selection for experiments [6], [7]. Particle size and distribution are subject to change by the planetary ball milling. Additionally, milling reduces Ag_2O particles to Ag.

The goal of this paper is to produce fine Ag_2O powders with a homogenous particle size distribution and a diameter below 5 µm for screen printing by wet planetary ball milling [8]. Furthermore, to avoid milling contamination and Ag_2O particle reduction to Ag. In general, the reactivity of the particles could be increased by changing their size [9]. At a lower processing temperature (120 °C), Ag_2O particles can be reduced to Ag. In addition, the size and distribution of particles can affect their electrical conductivity [4]. Particles prepared in this way are used to produce Ag_2O-based paste. Finally, the paste is screen-printed on 50 µm PET Mylar A substrate (polymer foil) and sintered at 120-160 °C for 10 minutes. The effect of vacuum and the number of printed layers (1, 2, 3) on sheet resistance is observed.

II. Initial Status

During the third year of my Ph.D. study, I focused on the production of a polymer conductive paste based on silver oxide particles. The possibility of size reduction of the particles by wet planetary ball milling to create fine and pure Ag_2O powder has been investigated in the first step of paste production. Moreover, the milling had to be carried out without reducing Ag_2O particles to Ag, since this process takes place only during thermal processing. Particle size, purity, and distribution were analyzed depending on the screen printing technology. Finally, when the paste has been produced the effect of processing temperature, vacuum, and the number of printed layers on the sheet resistance was investigated. The 4-point probe test method was used to measure the sheet resistance of each sintered layer.

III. Solved Tasks in the Previous Year

Tasks which are summarized in the following section were solved in the last year of postgraduate study.

A. Modifying of Ag_2O particles by planetary ball milling

This task aimed to modify the size of the Ag_2O particles as well as their particle distribution concerning screen printing technology. Furthermore, to ensure that Ag_2O does not reduce to Ag by milling. For this purpose, wet planetary ball milling was chosen. The Ag_2O particles were milled for 5 hours in methanol. Selected milling parameters: milling ball filling ratio 0.2, ball-to-powder ratio 8:1, ratio balls, methanol, and Ag_2O 8:1:1 (10 g of particles are used in the milling process). The balls and jars are made of agate. In a count of 17/5, balls with diameters of 10/20 mm were used for milling.

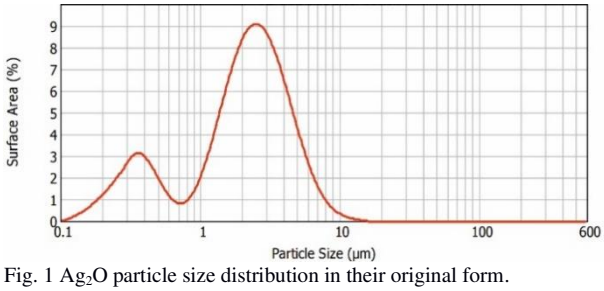

Fig. 1 Ag_2O particle size distribution in their original form.

The sun wheel and jars spin at 120 rpm, while the jars spin around their own axis and in the opposite direction of the sun wheel. In the Fig. 1 the laser diffraction analysis results of the particle size in their origin form and in the Fig. 2 after 5 hours of milling using the Mastersizer 2000 are presented.

The results of particles in their origin form have two main groups of particles size around 0.35 µm and 2.16 µm.

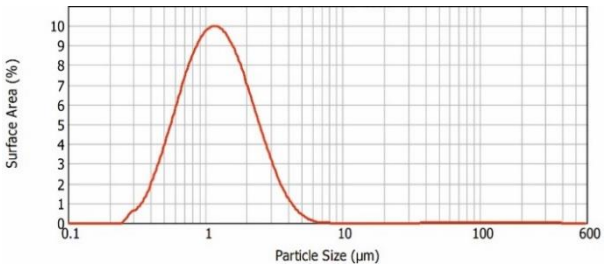

Fig. 2 Ag_2O particle size distribution after 5 hours of milling.

The particle size of Ag_2O particles after 5 hours of milling have more homogenous particle distribution. In addition, milling has decreased the particle size in median from 2.167 µm to 1.183 µm.

In addition, the powders were analyzed for purity, the XRD patterns presents that the peaks of the original particles were reduced (in some cases disappeared) during milling as shown in the Fig. 3. These phenomena can be attributed to the reduction in the crystallite size of the Ag_2O crystalline phase.

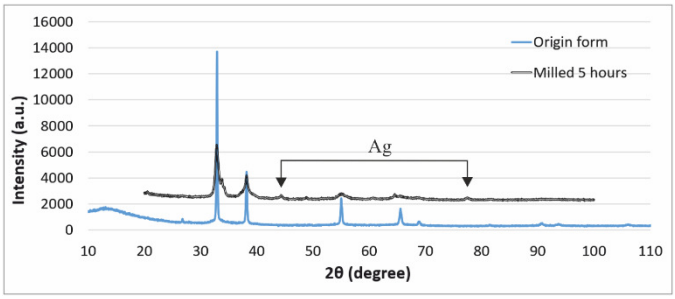

Fig. 3 XRD patterns of Ag2O particles.

Simultaneously, the cubic Ag phase, is crystallized from Ag_2O through the milling process, as shown in Fig. 3 in 3% of the total composition.

B. Sheet resistance of printed layers by Ag_2O-based paste

The sheet resistance of printed layers is important indicator for assessing Ag_2O to Ag thermal self-reduction efficiency. The effect of vacuum, processing temperature, and number of printed layers to sheet resistance is shown in the Fig. 4.

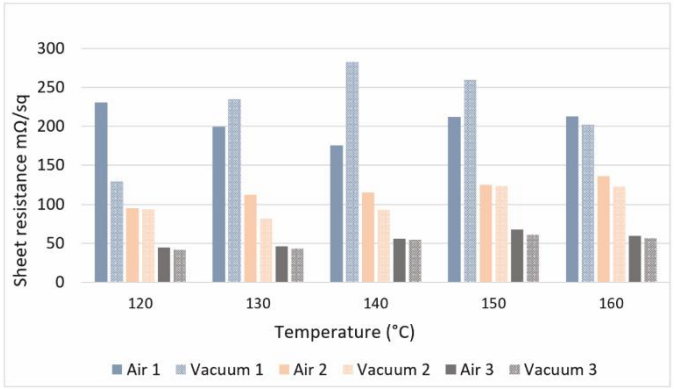

Fig. 4 The effect of processing condition of printed layers to sheet resistance.

At 140 °C under vacuum, the minimum sheet resistance for a single layer is measured to be 129.24 mΩ/sq. The minimum sheet resistance for two layers is measured to be 81.61 mΩ/sq at the temperature of 130 °C under vacuum. In total, three layers processed under vacuum achieve the lowest sheet resistance of 41.44 mΩ/sq at 120 °C.

IV. Conclusion

This paper deals with the modifying of Ag_2O particles by wet planetary ball milling for their use in formulation of self-reducing polymer paste. The result indicates that this method is appropriate for modifying particles size distribution as well as to produce fine metal Ag_2O powders with median 1.183 µm indicating a 45.4% decrease from the original size. In addition, the particle size distribution became more homogeneous. The Ag_2O paste has been screen printed and thermal processed and self-reduce to conductive Ag layers. Results show that self-reducing paste may create highly conductive layers with 41.44 mΩ/sq sheet resistance after 10 minutes of thermal processing at 120 °C under vacuum. Printing three layers of Ag_2O paste is necessary to achieve the mentioned sheet resistance.

Our experiments show that wet planetary ball milling of Ag_2O particles modifies their size and distribution, making them appropriate for polymer conductive self-reducing paste used to create Ag conductive layers.

Acknowledgment

This paper was supported by the projects KEGA 011TUKE-4/2023 and APVV 22-0289.

References

[1] S. Chandrasekaran, A. Jayakumar, and R. Velu, ‘A Comprehensive Review on Printed Electronics: A Technology Drift towards a Sustainable Future’, *Nanomaterials*, vol. 12, no. 23, p. 4251, Nov. 2022, doi: 10.3390/nano12234251.

[2] N. Ibrahim, J. O. Akindoyo, and M. Mariatti, ‘Recent development in silver-based ink for flexible electronics’, *Journal of Science: Advanced Materials and Devices*, vol. 7, no. 1, p. 100395, Mar. 2022, doi: 10.1016/j.jsamd.2021.09.002.

[3] D. Corzo, G. Tostado-Blázquez, and D. Baran, ‘Flexible Electronics: Status, Challenges and Opportunities’, *Front.Electron.*, vol. 1, p. 594003, Sep. 2020, doi: 10.3389/felec.2020.594003.

[4] N. Li *et al.*, ‘Preparation of Micro-Size Spherical Silver Particles and Their Application in Conductive Silver Paste’, *Materials*, vol. 16, no. 4, p. 1733, Feb. 2023, doi: 10.3390/ma16041733.

[5] H. Zhang, Y. Gao, J. Jiu, and K. Suganuma, ‘In situ bridging effect of Ag2O on pressureless and low-temperature sintering of micron-scale silver paste’, *Journal of Alloys and Compounds*, vol. 696, pp. 123–129, Mar. 2017, doi: 10.1016/j.jallcom.2016.11.225.

[6] G. R. Khayati and K. Janghorban, ‘The nanostructure evolution of Ag powder synthesized by high energy ball milling’, *Advanced Powder Technology*, vol. 23, no. 3, pp. 393–397, May 2012, doi: 10.1016/j.apt.2011.05.005.

[7] G. R. Khayati and K. Janghorban, ‘Preparation of nanostructure silver powders by mechanical decomposing and mechanochemical reduction of silver oxide’, *Transactions of Nonferrous Metals Society of China*, vol. 23, no. 5, pp. 1520–1524, May 2013, doi: 10.1016/S1003-6326(13)62625-4.

[8] C. W. Foster, R. O. Kadara, and C. E. Banks, ‘Fundamentals of Screen-Printing Electrochemical Architectures’, in *Screen-Printing Electrochemical Architectures*, in SpringerBriefs in Applied Sciences and Technology. , Cham: Springer International Publishing, 2016, pp. 13–23. doi: 10.1007/978-3-319-25193-6_2.

[9] G. Schimo, A. M. Kreuzer, and A. W. Hassel, ‘Morphology and size effects on the reduction of silver oxide by hydrogen’, *Physica Status Solidi (a)*, vol. 212, no. 6, pp. 1202–1209, Jun. 2015, doi: 10.1002/pssa.201431669.

Usability of a ML-based application for medical experts

[1]*Oliver LOHAJ (3rd year)*
Supervisor: [2]Ján PARALIČ

[1,2]Dept. of Cybernetics and Artificial Intelligence, FEEI TU of Košice, Slovak Republic

[1]oliver.lohaj@tuke.sk, [2]jan.paralic@tuke.sk

***Abstract*—The aim of this article is to create a predictive model for diagnosing COVID-19. In the theoretical part of the article, we focused on analyzing the COVID-19, explainability and usability of ML methods. In the practical part, we analyzed and used data from the Brazilian Albert Einstein Israelite Hospital. We created a total of 4 models using CRISP-DM methodology on different data modifications and trained the models using LightGBM, XGBoost, random forests and linear regression algorithms. We then integrated the best model into a dashboard application focused on the explainability of the model. We then tested the resulting dashboard usability with doctors and students of medicine.**

***Keywords*—COVID-19, dashboard, explainability, usability**

I. Introduction

The world has faced an extraordinary challenge in the form of the COVID-19 pandemic during years 2020-2023, which had significant health, social and economic consequences. The increased incidence of the disease and the consequent need for rapid and more accurate diagnosis and treatment have created a need for new tools and approaches. In this work, we will address the use of machine learning in COVID-19 diagnostics. We will firstly go through definitions of usability, explainability and motivation – why is ML approach to COVID-19 important. We have integrated the most accurate model into an educational dashboard focused on explainability, which includes explanations of attributes, performance metrics and predictions for selected patients from the dataset. We will describe how we measured its usability. In the end, we will draw conclusions from testing the dashboard.

II. State of the art analysis

A. COVID-19 diagnostics and classification

COVID-19, also known as the coronavirus disease, has become a dominant topic of global debate and has led to restrictions on free movement, schools, and business closures, significantly affecting the daily lives of millions of people [1].

Currently, COVID-19 diagnosis relies on symptom monitoring, antigen tests, and RT-PCR tests. Antigen tests have minimal false positives but lower sensitivity than RT-PCR tests, potentially missing early-stage infections. RT-PCR tests are highly sensitive and accurate but are costly and confined to healthcare settings, limiting accessibility.

The presence of COVID-19 can be predicted based on known symptoms. In the study [2] a model was created that predicted COVID-19 based on eight parameters. The dataset originated in Israel and contained information on patients with suspected COVID-19. They achieved a specificity of 71.98% and a sensitivity of 87.3%. In the study, they tried to eliminate biased symptoms like headache, but this did not help improve the accuracy of the model.

In different research [3], 1980 COVID-19 patients were enrolled for the aim of prediction of mechanical ventilation. 1036 patients' data were collected for training and 674 patients were enrolled for validation using XGBoost algorithm. For the second aim to predict in-hospital mortality, 3491 hospitalized patients via ER were enrolled. CatBoost was applied for training and validation of the cohort. Attributes, like older age, higher temperature, increased respiratory rate and a lower oxygen saturation SpO_2 from the first set of vital signs were associated with an increased risk of mechanical ventilation amongst the 1980 patients in the ER. The model had a high accuracy of 86.2% and a negative predictive value of 87.8%. While patients who required mechanical ventilation, had a higher respiratory rate, Body mass index (BMI) and longer length of stay in the hospital were the major features associated with in-hospital mortality. The second model had a high accuracy of 80% with negative predictive value of 81.6%.

Our experiments showed that adding information about the COVID-19 variant did not influence the performance of the resulting ML model [1]. It also turned out that medical experts were much more precise in the identification of significant attributes than Forward Stepwise Selection (FSS). Explainability methods identified almost the same attributes as a medical expert and interesting interactions among them, which the expert discussed from a medical point of view. This provides very good evidence, that ML models derived from given data can be trusted by the doctors.

B. Explainability of ML models

Artificial intelligence methods could contribute to eliminating human error and to obtaining faster and more accurate diagnoses. Indeed, several models of artificial intelligence, especially deep neural networks, have produced significant results in solving various challenging tasks, including medical diagnostics [4]. However, these complex models have the character of a "black box", meaning that, as a rule, they cannot provide a comprehensible explanation of the proposed decision for the doctor to assess [5] Therefore, in order to increase the credibility of these black-box models in the eyes of doctors, it is necessary to focus on their explainability. This is why we focused on explainability of the most successful model in our research and we deployed it in the dashboard form.

C. Usability in general

Usability refers to the effectiveness, efficiency and satisfaction with which users can interact with a product or a system to achieve their goals [6]. It encompasses aspects such as user interface design, task efficiency and learnability [7]. Explainability, particularly relevant in complex environments like machine learning, ensures that users can understand the reasoning behind system outputs, fostering trust and facilitating informed decision-making and with that, the level of usability goes up. Usability can be measured in many ways, one of the most used methods is the SUS (System Usability Scale) questionnaire containing 10 statements focused on the usability of the system [8]. The task of the users was to indicate the degree of agreement or disagreement with the given statement on the Likert scale. Each answer is then assigned a value that is used to calculate the SUS score.

III. MODELLING

In the modelling part, we followed the CRISP-DM methodology. We wanted to see the difference in models' statistics with using different type of data preprocessing. That is why in each iteration of different data preprocessing we used 4 different ML algorithms, namely XGBoost, LightGBM, Random Forest and logistic regression to create models. In each iteration, we focused on sensitivity and specificity values for each model.

A. Dataset

To create our models, we used a dataset from the Albert Einstein Hospital in Brazil. The dataset contains 5644 records and a total of 119 attributes about age group, need for hospitalization, blood and urine tests, and tests for other respiratory diseases. The dataset contains a large amount of missing data, and during data preprocessing, we removed attributes where more than 90% of values were missing. In addition, we converted categorical attributes to numerical attributes in the dataset. As we mentioned before, we trained 4 models (Model 1-4) in all 4 iterations using different data preprocessing, as follows. In the sections

B. Iteration 1 – data completion

In the first iteration, we tried to fill in the missing values with both the average value within the attribute and the k–nearest neighbors' method, which uses broader information from other records. The results were disappointing, as sensitivity ranged from 5% to 10%. The specificity was almost 100%, but in this case, it is not a relevant result because the model labeled almost all patients as negative, which in medicine a false negative is the result we try to minimize.

C. Iteration 2 – removal of patients with large amount of missing data

In second iteration, we tried to remove patients where more than 50% of the data were missing. Sensitivity of all 4 models ranged from 10% to 18%, which were also disappointing results. The specificity was again, almost 100% for all 4 models.

D. Iteration 3 – random oversampling

For 3rd iteration, we adjusted the data using a random minority class oversampling method to balance the ratio of positive to negative patients. In this model, we began to observe the first significant improvement, but the results were not very satisfactory, namely specificity around 50% and sensitivity 80% for all 4 models.

E. Iteration 4 – combining the best data preprocessing techniques

We created Iteration 4 by combining conditions applied in Iteration 2 and 3, eliminating patients where more than 50% of values were missing and oversampling a minority class. The models achieved much better results, the best model – XGBoost – achieved sensitivity of 95.8% and specificity of 82.15%.

F. Modelling conclusion

Our experiments with data pre-processing have shown that with such a high number of missing values, in some cases over 90%, data imputation on whole dataset was ineffective and it distorted the dataset. On the contrary, in our research, the elimination of records where more than 50% of data were missing proved beneficial, and the method of random oversampling of positive patients, which balanced the ratio of positive and negative patients, proved to be beneficial as well.

The XGBoost gradient boosting algorithm turned out to be the most accurate algorithm. However, very similar results were achieved by LightGBM algorithm and random forest. The logistic regression in this case lagged further behind.

IV. DASHBOARD

A. Dashboard focused on model explainability

By implementing the XGBoost model from Iteration 4, we created a dashboard focused on model explainability. The dashboard consists of three pages, where the first contains information about the work and its goals and authors. The second is devoted to explaining attributes and introducing performance metrics. The third page (see example screenshot in Fig. 1) is dedicated to predictions. With the "Random Index" button, the user can select a random patient, and then the patient's ID and the actual result of the COVID-19 test, which is used to check the model, are displayed. User can then observe patients actual test result and percentage-expressed prediction of the model. In addition, the user sees graphically and textually displayed the model, that predicts the COVID-19 disease, and shows the sorted attributes that had an impact on the model's decision.

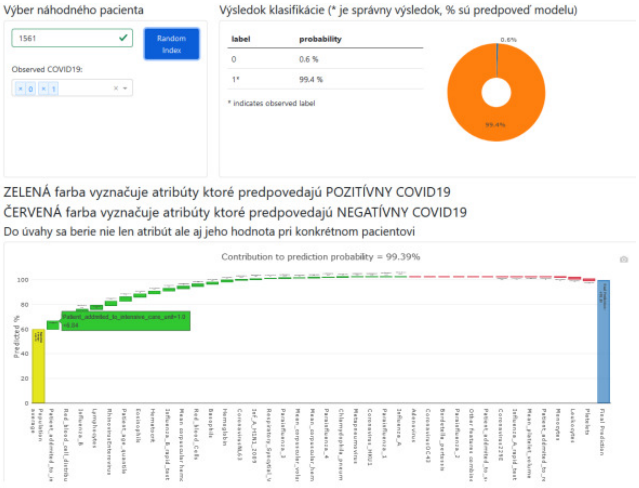

Fig. 1 Dashboard - a patient prediction page

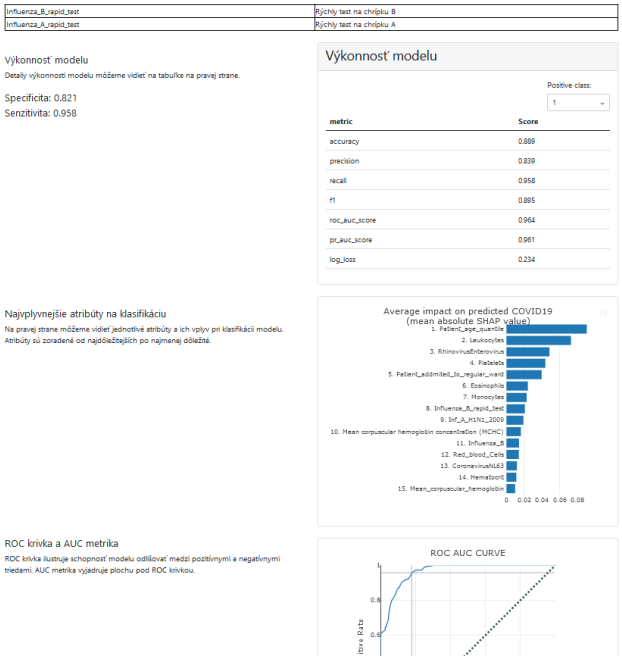

Fig. 2 Dashboard – model explanation

The page "dashboard – model explanation" as seen in Fig. 2 is devoted to presenting all the attributes with which the model works. Individual attributes are displayed on top of the screen, in the table together with a translation or explanation. In addition to the attributes, the user learns the model's performance statistics, such as accuracy, precision, recall etc. under the description table. Users can also see the model's ROC curve (on the bottom of the screen), and the most influential attributes for model decision-making (see the bar graph in the middle section of Fig. 2.

B. Testing developed dashboard

We tested the dashboard app with four respondents from the target users' group of medical experts, two of whom were doctors and two students of medicine. The testing took the form of a presentation of the work, assignment of a short task in the dashboard application, which all participants solved correctly, and then a standardized SUS questionnaire [7], which consisted of 11 questions. In the last question, respondents could give a free answer. The app's usability score (SUS) has reached 71.25%, which can be interpreted as good, but there is room for improvement. Specifically, respondents would like to see the possibility of predicting their own patient and removing tests for other respiratory diseases from the dataset.

V. Conclusion

To improve the usability of the application dashboard, it would be advisable to obtain the used dataset in its original form without standardized values and then train the model on this data. The model itself would retain the same performance metrics, but it would add the ability to predict someone's own patient in the dashboard.

Another option to improve the dashboard is to create a fifth model that could not only classify COVID-19, but also differentiate between other respiratory diseases.

Acknowledgment

This work was supported by the Slovak Research and Development Agency under the contract No. APVV-22-0414 and contract No. APVV-20-0232, and by the Scientific Grant Agency of the Ministry of Education, Research, Development and Youth of the Slovak Republic and the Slovak Academy of Sciences under grant No. 1/0685/21.

References

[1] Lohaj, O., Paralič, J., Bednár, P., Paraličová, Z., Huba, M.: Unraveling COVID-19 Dynamics via Machine Learning and XAI: Investigating Variant Influence and Prognostic Classification. Mach. Learn. Knowl. Extr. 2023, 5, 1266-1281. https://doi.org/10.3390/make5040064

[2] Zoabi, Y., Deri-Rozov, S. & Shomron, N. Machine learning-based prediction of COVID-19 diagnosis based on symptoms. npj Digit. Med. 4, 3 (2021). https://doi.org/10.1038/s41746-020-00372-6

[3] Yu, L., Halalau, A., Dalal, B., Abbas, A. E., Ivascu, F., Amin, M., & Nair, G. B. (2021). Machine learning methods to predict mechanical ventilation and mortality in patients with COVID-19. PLoS One, 16(4), e0249285.

[4] Paralič, J., Kolárik, M., Paraličová, Z., Lohaj, O., Jozefík, A.: Perturbation-Based Explainable AI for ECG Sensor Data. Appl. Sci. 2023, 13, 1805. https://doi.org/10.3390/app13031805

[5] Riccardo Guidotti, Anna Monreale, Salvatore Ruggieri, Franco Turini, Fosca Giannotti, and Dino Pedreschi. 2018. A Survey of Methods for Explaining Black Box Models. ACM Comput. Surv. 51, 5, Article 93 (September 2019), 42 pages. https://doi.org/10.1145/3236009

[6] Lohaj, O., Paralič, J., Jevčák, J.: Meranie aspektov použiteľnosti systémov pre podporu rozhodovania lekárov. In: Electrical Engineering and Informatics 14 : Proceedings of the Faculty of Electrical Engineering and Informatics of the Technical University of Košice. - Košice (Slovensko) : Technická univerzita v Košiciach s. 96-101 [CD-ROM]. - ISBN 978-80-553-4407-2

[7] Lohaj, O., Paralič, J., Kushnir, D., Vanko, J. I.: Usability of a synthetically generated dataset for decision support. 2024 IEEE 22nd World Symposium on Applied Machine Intelligence and Informatics (SAMI), Stará Lesná, Slovakia, 2024, pp. 000435-000440, doi: 10.1109/SAMI60510.2024.10432913.

[8] Pavlusová, M., Lohaj, O., Pella, Z., Paralič, J.: Modeling the influence of factors associated with atherosclerosis. 2023 IEEE 21st World Symposium on Applied Machine Intelligence and Informatics (SAMI), Herl'any, Slovakia, 2023, pp. 000063-000068, doi: 10.1109/SAMI58000.2023.10044481.

Big data research in the electricity distribution network for increasing the reliability and efficiency of electricity distribution

[1]*Ardian HYSENI (1st year)*
Supervisor: [2]Jaroslav PETRÁŠ

[1,2]Dept. of Electric Power Engineering, FEI TU of Košice, Slovak Republic

[1]ardian.hyseni@tuke.sk, [2]jaroslav.petras@tuke.sk

***Abstract*— Big data research is revolutionizing the electricity distribution network by significantly enhancing its reliability and efficiency. This transformative approach leverages vast volumes of data collected from various sources within the grid, including smart meters, sensors, and IoT devices. Through advanced analytics and machine learning algorithms, utilities are now able to predict and preemptively address potential system failures, reduce energy wastage, and optimize the flow of electricity based on real-time demand and supply conditions. The integration of renewable energy sources into the distribution network is further facilitated by big data, enabling a smoother transition to green energy while maintaining grid stability. This abstract outlines the key breakthroughs achieved in this field, the ongoing challenges, and the potential future directions for research and application. By improving data-driven decision-making, big data research is setting the stage for more resilient, efficient, and sustainable electricity distribution networks, promising a significant impact on global energy management practices.**

***Keywords*— Big data, Electricity distribution network, Grid reliability and efficiency, Predictive analytics, Machine learning algorithms.**

I. INTRODUCTION

Integrating big data analytics into electricity distribution networks represents a significant advancement in efforts to improve the reliability and efficiency of power systems. The focus on leveraging the extensive data generated by smart grids, which include inputs from electricity meters, distribution stations, and external factors like weather conditions and market trends, is pivotal in enhancing decision-making processes. This integration is aimed at optimizing power plant scheduling, subsystem operations, and maintenance activities, contributing to the overall performance enhancement of the grid.[1][2]

Smart grids are at the heart of this initiative, employing modern communication and information technologies to refine energy production, distribution, and storage processes. The reduction in costs and management efforts, alongside improved planning capabilities through advanced data management techniques, illustrates the benefits of this integration. Communication systems within smart grids, such as Home Area Networks (HANs), Business Area Networks (BANs), and Neighborhood Area Networks (NANs), facilitate data transmission across different technologies, playing a critical role in this ecosystem. Information systems, including Supervisory Control and Data Acquisition (SCADA) systems, Advanced Metering Infrastructure (AMI), and Outage Management Systems (OMS), are essential in managing and leveraging the collected data to achieve a grid that is more flexible, scalable, and efficient.[3][4]

An innovative aspect of enhancing distribution network reliability involves the strategic placement of Distributed Generation (DG), which aims to bring generation capabilities closer to load centers. This approach has been shown to significantly improve system reliability, as evidenced by reductions in key reliability indicators such as the System Average Interruption Frequency Index (SAIFI), System Average Interruption Duration Index (SAIDI), and Expected Energy Not Supplied (EENS).[5][6]

Furthermore, the application of big data analytics within the nuclear sector highlights the potential for cost savings while maintaining or improving safety standards. This involves addressing the diversity in data types and volumes present in nuclear power plants to garner insights into equipment performance, thereby facilitating optimized operation and maintenance.[7][8]

For those interested in a deeper dive into these topics, resources such as articles from Energy Informatics, the Journal of Big Data, MDPI's Sustainability journal, and technical reports on OSTI.GOV provide a wealth of information on the current research landscape, challenges, and future directions in the field of big data analytics for electricity distribution network enhancement.[9][10]

Regarding the application of Benford's Law in this context, it offers an intriguing perspective. Benford's Law, which predicts the frequency distribution of leading digits in numerical data sets, could potentially be applied to detect anomalies or irregularities within the vast amounts of data processed by smart grids. This could include identifying fraudulent activities, optimizing the allocation of resources, or improving the accuracy of consumption forecasts. The utilization of Benford's Law within the framework of big data analytics in electricity distribution networks underscores the innovative approaches being explored to further enhance grid reliability and efficiency.[11]

II. THE THEORY BEHIND BENFORD'S LAW

Simon Newcomb was the first to notice the peculiar patterns of number distribution in 1881, a phenomenon later revisited and more thoroughly explored by Frank Benford in 1938, who named it the "Law of Anomalous Numbers." Their discovery

stemmed from the observation that the initial pages of logarithmic, square root, and trigonometric tables showed more wear than later pages, suggesting that numbers starting with lower digits (1, 2, etc.) were consulted more frequently. This led to the formulation of a probability distribution for the first significant digit, which Benford found to be uneven across various datasets, favoring smaller leading digits, contrary to the intuitive expectation of uniform distribution among all digits.[12]

To understand this phenomenon, it's essential to clarify what constitutes a "significant number": it's any real number except zero, labeled as x, where the foremost significant decimal number of x, denoted as D1(x), is the distinct integer j within the range of 1 to 9 that meets specified conditions. This sets the groundwork for analyzing datasets according to Benford's Law (BL), revealing that not all datasets align equally with BL's predictions, particularly those exhibiting a disproportionate inclination towards numbers starting with lower digits.[13]

$$10k\ j \leq |x| < 10k\ (j + 1) \quad (1)$$

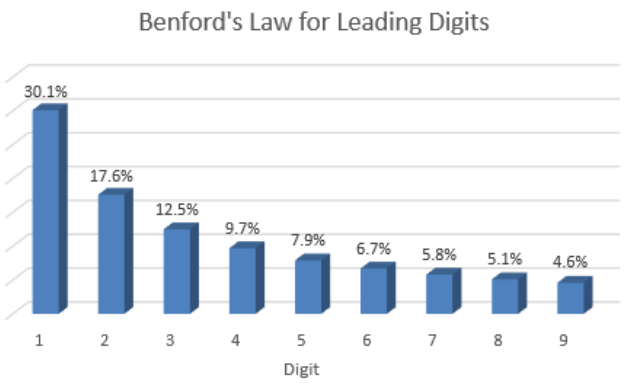

Figure 1 Benford's Law first digit probability distribution

Assuming you're dealing with a payment amount that has three digits, one might initially think that the probability of the first digit being any number from 1 through 9 is equally likely, essentially a 1 in 9 chance. However, Benford's Law challenges this intuition by suggesting that numbers don't appear as uniformly as one might expect. Specifically, according to Benford's Law, there's a 12.5% chance the first digit will be 3, contrasting with a higher likelihood of 30.1% for the digit 1. This discrepancy highlights the non-random distribution of first digits in real-world data.[14]

In the context of fraud detection, Benford's Law is a valuable tool for auditors and fraud examiners. It's based on the premise that in datasets of natural numbers, like payment amounts, the distribution of first digits follows a predictable pattern. Fraudulent activities, such as submitting inflated invoices, tend to deviate from this pattern. For instance, if an unusually high number of payments begin with the digit 9, exceeding Benford's Law prediction of 4.6%, it may indicate potential fraud, as fraudsters might prefer larger amounts to maximize their gain, thereby disrupting the expected numerical distribution.[15]

III. Advancing Grid Modernization through Big Data: Challenges, Innovations, and Collaborative Pathways

In the domain of big data research within electricity distribution networks, significant strides have been made toward enhancing grid reliability and efficiency, as well as integrating renewable energy sources more effectively. The solved problems include the development of advanced predictive analytics for anticipating system failures and demand spikes, the implementation of demand response strategies to manage consumption patterns, and the improvement of grid operations through real-time data monitoring and management. These advancements have significantly contributed to the stability and sustainability of electricity distribution systems.[16]

However, several unsolved problems persist, presenting both solvable and unsolvable challenges at this juncture. Solvable problems include improving the scalability of big data solutions to accommodate the growing complexity and size of electricity networks, enhancing data privacy and security measures to protect sensitive information, and further optimizing the integration of distributed energy resources (DERs) to maximize efficiency and minimize disruptions. These issues are within reach of current technological advancements and ongoing research efforts.[17]

On the other hand, some challenges might be currently viewed as unsolvable due to existing technological, regulatory, or economic constraints. These include completely eliminating the vulnerability of power grids to cyber-attacks given the ever-evolving nature of cybersecurity threats, achieving full grid autonomy with 100% reliability in all conditions, and completely overcoming the intermittency issues associated with certain renewable energy sources without any form of backup or energy storage solutions.[18] The next direction of work in this field involves several key areas: further advancing big data analytics and machine learning algorithms to enhance predictive capabilities, developing more robust cybersecurity measures tailored to the unique needs of electricity distribution networks, and innovating in energy storage and grid management technologies to better integrate renewable energy sources. Additionally, there is a growing emphasis on creating flexible market mechanisms that can accommodate the dynamic nature of electricity generation and consumption, fostering greater participation from prosumers, and leveraging blockchain and other decentralized technologies for energy trading.[19]

Addressing these unsolved problems and exploring these next steps require a multidisciplinary approach, combining efforts from electrical engineering, data science, cybersecurity, and energy policy. Collaboration among academia, industry, and government entities will be crucial in navigating these challenges and unlocking new opportunities for the evolution of electricity distribution networks.[20]

IV. Benford Law in Electric Power Engineering

Electricity theft significantly contributes to non-technical losses within distribution networks, posing challenges for energy providers. In networks equipped with smart technology, smart meters facilitate detailed monitoring of electricity usage across various points and levels, enhancing the ability to track consumption and losses in specific areas [11].

Benford's Law (BL) emerges as a valuable tool for detecting electricity theft by analyzing consumption patterns. It also finds application in predicting and monitoring electricity usage, where it can highlight discrepancies in expected consumption patterns influenced by external factors like weather conditions and holidays. This capability of BL to identify anomalies aids in forecasting future consumption, thereby optimizing the planning and management of electricity production [11]. Furthermore, BL supports the monitoring of electricity production processes, identifying inconsistencies or disruptions. By comparing actual production data with the expected BL distribution, energy companies can pinpoint areas needing analysis and data improvement, helping to reduce energy losses [11]. However, applying BL in electric power engineering faces certain limitations, including the challenge of working with small datasets that lack statistical significance, the potential failure of BL distribution in cases of symmetrically distributed data or evenly distributed first digit probabilities, the impact of intentional data manipulation by companies for operational reasons, and deviations caused by unusual events like supply dropouts [11]. Limited research has been conducted on datasets from electricity distribution networks. Unique factors, such as the seasonal nature of electricity consumption and the physical or digital means of electricity theft, necessitate tailored approaches that may not directly align with methods designed for other types of datasets [11]. In essence, while Benford's Law offers promising ways for addressing issues within electric power engineering, its application must be carefully considered in light of these constraints and the specific characteristics of electricity distribution data.

Addressing these unsolved problems and exploring these next steps require a multidisciplinary approach, combining efforts from electrical engineering, data science, cybersecurity, and energy policy. Collaboration among academia, industry, and government entities will be crucial in navigating these challenges and unlocking new opportunities for the evolution of electricity distribution networks [11].

V. Application

We developed a C# application using Visual Studio Code designed to process large datasets for Benford's Law analysis. This application efficiently extracts the first digit from each data point, calculates the distribution according to Benford's Law, and then generates both a graphical representation and a detailed table of the results. This enhances the analysis by providing a clear visual and numerical comparison of the actual data distribution against the expected Benford's Law distribution, facilitating easier identification of deviations or anomalies within the dataset. In the fig.2 we input our real-world dataset, sourced from electrical meter readings, into our custom-developed software. This step is crucial for ensuring that the analysis is grounded in actual consumption patterns, providing a solid foundation for our investigation into Benford's Law adherence. By leveraging authentic data, we enhance the validity and applicability of our findings, offering insights that are directly relevant to the field of electrical data analysis.

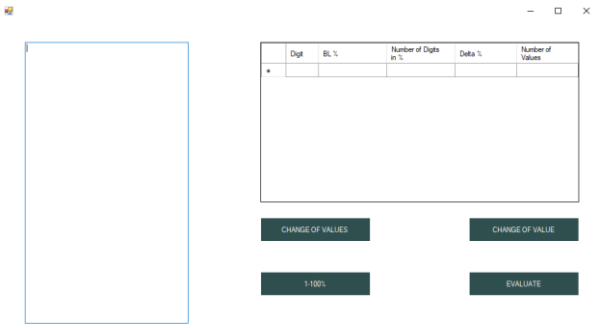

Figure 2 Program for calculating Benford's law.

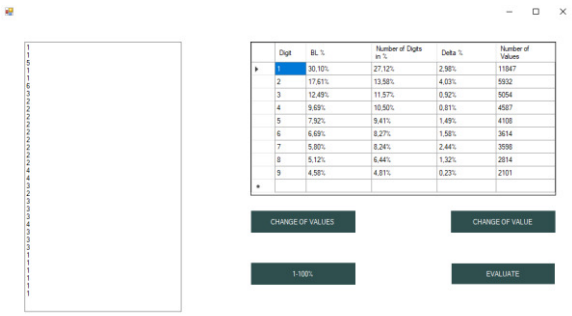

Figure 3 Program using calculation according to Benford's law

The software generates an insightful visualization in the form of a graph, which is derived from the dataset analysis. This graphical representation is an integral part of the output, offering a clear and immediate understanding of the data's adherence to Benford's Law, alongside any identified deviations. This feature complements the numerical data, providing a comprehensive overview that enhances the interpretability of the results.

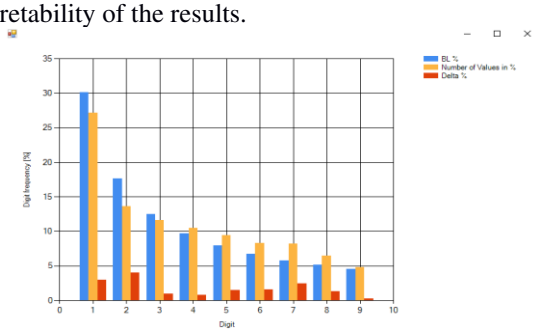

Figure 4 Graph from the program.

Our software, beyond analyzing datasets for Benford's Law compliance, features versatile functionality for data manipulation and detailed analysis. It allows for precise adjustments to the dataset by a specified percentage, ranging from 1% to 100%, according to user-defined parameters. Additionally, it includes a unique capability to selectively modify specific data points based on certain criteria, enabling users to experiment with the impact of these changes on the overall dataset's statistical properties. This functionality is particularly useful for exploring how various modifications influence the observed distribution patterns, offering insights into the dataset's structural integrity and susceptibility to irregularities.

VI. Experimental Methodology

The methodology starts with collecting electricity usage data from smart meters. Initially, the dataset's adherence to

Benford's Law (BL) is assessed by calculating deviations from BL's expected distribution. Only datasets with minimal deviations proceed, indicating compatibility with BL. Next, the dataset undergoes simulated interventions, altering specific portions of the data, followed by re-evaluation of BL deviations. Comparing deviations between original and modified datasets helps identify successful detection of these interventions, demonstrating BL's applicability in spotting falsified data within similar datasets [11].

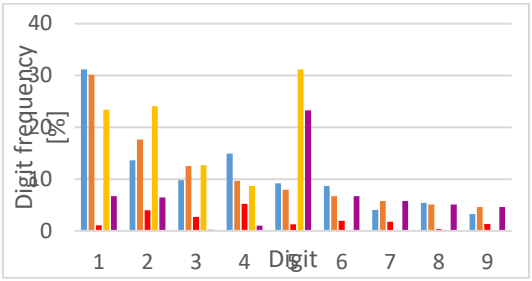

Figure 5 Analyzing the change in the probability distribution before and after implementing a specific manipulation, namely dividing the dataset by two, to observe its impact on the distribution pattern according to Benford's Law

In the electricity distribution network at measuring node No. 1, the original data aligns closely with Benford's Law (BL), with observed deviations from BL's expected first digit probability distribution being minimal, notably around 4-5% for the digits 2 and 4 [11].

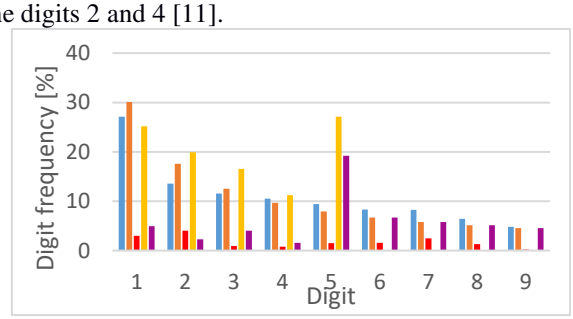

Figure 6 Evaluating changes in the probability distribution before and after modifying the dataset by adding an integer number. This process assesses how such alterations impact the adherence to expected statistical patterns.

VII. Conclusion

Big data's role in enhancing electricity distribution networks has proven crucial for improving grid reliability and efficiency. By leveraging vast amounts of data through smart meters and analytics, utilities can now anticipate and manage system demands more effectively, reducing costs and energy waste. This has also facilitated a smoother integration of renewable resources, contributing to a more sustainable energy system. Yet, challenges like data security and the need for advanced analytics persist. Moving forward, the focus on big data will intensify, promising further advancements in energy distribution and grid management, highlighting the importance of innovation and collaboration across the sector for a sustainable energy future. Presented method and results could be exploited by electricity distribution companies when detecting non-technical losses.

Acknowledgment

This research was funded by the the Ministry of Education, Science, Research and Sport of the SlovakRepublic and the Slovak Academy of Sciences [VEGA 2/0029/24].

References

[1] E. Kabir, M. A. A. Hannan, M. S. Hossain, and H. R. Pota, "Leveraging Big Data Analytics for Smart Grid Optimization and Reliability Enhancement," in IEEE Access, vol. 8, pp. 175729-175742, 2020, doi: 10.1109/ACCESS.2020.3027875.

[2] P. Siano, "Big Data Analytics in Smart Grids: A Review of Opportunities and Challenges," in Energies, vol. 16, no. 16, p. 6016, 2023, doi: 10.3390/en16166016.

[3] J. M. Guerrero, P. C. Loh, T. L. Lee, and M. Chandorkar, "Smart Grid: Integration of Renewable Energy Sources," 2nd ed., Cham: Springer International Publishing, 2020, doi: 10.1007/978-3-030-41033-1.

[4] M. H. Albadi and E. F. El-Saadany, "The Role of Data Management in Smart Grids," CIGRE, 2012, [Online]. Available: https://www.cigre.org/userfiles/files/Publications/Reference_papers/CIGRE_WG_Net.

[5] M. E. Khodayar, M. Shafie-khah, and J. P. S. Catalão, "Distributed Generation Integration: Impacts on Power Distribution Network Reliability," in Electric Power Systems Research, vol. 203, p. 107613, 2022, doi: 10.1016/j.epsr.2022.107613.

[6]] A. A. El-Zoughby and M. M. A. Salama, "The Impact of Distributed Generation on Power Distribution System Reliability," in International Journal of Electrical Engineering, vol. 8, no. 1, pp. 25-42, 2014, doi: 10.1115/1.4027154.

[7] A. S. K. Reddy, R. Ranjan, and P. K. Dash, "Big Data Analytics for Nuclear Power Plant Operation Optimization," in IEEE Transactions on Nuclear Science, vol. 66, no. 1, pp. 25-34, 2019, doi: 10.1109/TNS.2018.2871225.

[8] J. H. Park, J. W. Park, S. H. Hong, and Y. S. Lee, "Nuclear Power Plant Big Data Analytics: A Survey of Technologies and Applications," in Progress in Nuclear Energy, vol. 154, p. 105211, 2023, doi: 10.1016/j.pnucene.2022.105211.

[9] M. A. A. Hannan, E. Kabir, M. S. Hossain, and H. R. Pota, "A Survey of Big Data Analytics in Smart Grids: Applications and Challenges," IEEE Xplore, 2020, doi: 10.1109/ACCESS.2020.3027875.

[10] The World Bank, "Big Data: Revolutionizing the Electricity Sector," 2015, [Online]. Available: https://openknowledge.worldbank.org/server/api/core/bitstreams/d6f9cef3-12b0-5af8-9af6-15677d1ad141/content.

[11] Petráš, J., Pavlík, M., Zbojovský, J., Hyseni, A. and Dudiak, J. Benford's Law in Electric Distribution Network. Mathematics 2023, 11, 3863. https://doi.org/10.3390/math11183863.

[12] David Hand, "Measuring the Universe: The Role of Measurement in Modern Science," Oxford University Press, 2004, pp. 152-153. (Provides a historical context for Benford's Law and its early applications).

[13] Mark J. Nigrini, "A Beginner's Guide to Benford's Law," International Journal of Mathematics and Computer Science, vol. 8, no. 3, pp. 10-18, 2018, doi:10.5923/j.ijmcs.2018.08.03.02. (Explains the concept of significant digits and their role in Benford's Law).

[14] M. A. A. Hannan, M. S. Hossain, E. Kabir, and A. Wasik, "Benford's Law-Based Anomaly Detection in Payment Data for Fraud Identification," IEEE Transactions on Industrial Informatics, vol. 13, no. 3, pp. 1232-1243, Jun. 2017, doi: 10.1109/TII.2016.2643024. (Provides a more detailed explanation of how Benford's Law is used in fraud detection).

[15] Mark J. Nigrini, "Data Forensics: Investigating Fraud, Errors, and Data Anomalies," John Wiley & Sons, 2014, pp. 245-257.

[16] IEEE Smart Grid Coordination Center, "Big Data Analytics for Smart Grids: A Survey," IEEE Xplore, 2018, doi: 10.1109/ACCESS.2018.8527407.

[17] P. Siano, "Big Data Analytics in Smart Grids: A Review of Opportunities and Challenges," in Energies, vol. 16, no. 16, p. 6016, 2023, doi: 10.3390/en16166016.

[18] S. R. Sanders, "Cybersecurity of Smart Grids," Proceedings of the IEEE, vol. 104, no. 11, pp. 1747-1755, Nov. 2016, doi: 10.1109/JPROC.2016.2597422.

[19] F. Yılmaz and M. H. Çetin, "Big Data Analytics for Smart Grids: A Survey," IEEE Access, vol. 8, pp. 44487-44505, 2020, doi: 10.1109/ACCESS.2020.2983245.

[20] F. Amin, M. A. Khan, M. U. Farooq, A. Hussain, Y. S. Alfattah, and Z. A. Khan, "A Survey of Advanced Machine Learning Techniques for Smart Grids," arXiv preprint arXiv:2203.06665, 2022

Federated Learning for Edge Computing in Transport

[1]*Alexander BRECKO (3rd year),*
Supervisor: [2]Iveta ZOLOTOVÁ Consultant: [3]Erik KAJÁTI

[1,2,3]Dept. of Cybernetics and Artificial Intelligence, FEEI TU of Košice, Slovak Republic

[1]alexander.brecko@tuke.sk, [2]iveta.zolotova@tuke.sk, [3]erik.kajati@tuke.sk

***Abstract*—As the Internet of Things continues to expand, there is a significant increase in the number of devices and the data they produce. To handle this growth, computing processes are moving from centralized cloud systems to edge computing, closer to where data is generated. Nevertheless, it is common to find limited computing resources at the edge of the network. This paper presents an overview of methodologies that can facilitate the distribution of data among numerous edge devices. Together, these devices contribute to the development of a complex model by using federated learning that uses different data sources. The article describes the experiments and results that were carried out during the last year of the study with the help of federated learning and edge devices.**

***Keywords*—Edge AI, edge computing, federated learning, Internet of Things**

I. Introduction

The Internet of Things (IoT) has grown quickly in recent years, allowing for connecting numerous devices to the network and facilitating computing and sensing [1]. Although cloud services have been used for more complex computer tasks, edge computing has recently received more attention. Owing to the capabilities of these edge devices, basic machine learning (ML)and artificial intelligence (AI) tasks, as well as computation and processing, can be moved from the cloud to the network's edge. ML is undoubtedly becoming increasingly popular, but there is a privacy issue. The primary problem is the central collection of millions of photos, movies, or other types of data on a server. Our research mainly focuses on training models at the network's edge and the closely related federated learning (FL). In FL [2], clients handle computations rather than a single central server. The FL concept gained popularity in 2016 and 2017, coinciding with the launch of Gboard by Google.

II. The initial status

Two years ago, we provided an overview of edge devices that can collect data from sensors and actuators at the conference. We also analyzed edge devices in paper [3], focusing on devices that can deploy AI at the network's edge and train AI at the network's edge. In this case, we focused primarily on ARM architecture devices that are commercially available and have a maximum power consumption of up to 40 W. We reviewed several devices such as NVIDIA Jetson Family, Coral Family, and other boards.

At last year's conference [4], we presented the first results of deploying AI at the edge of the network, where we created a couple of experiments with the YOLOv5 (You Only Look Once version 5) model, as well as the first experiments where we started to train simple AI models for vehicle classification on edge devices. In this section, we looked closely at FL and the possibility of deploying FL at the network's edge.

Using data dispersed across multiple devices, including smartphones, computers, and smart home devices, FL is a method to create ML models without the need to share data with a central server. Instead of centralizing all the data in one place, FL aims to train a model using data stored locally in each device. Here, devices train their local models, transferring their weights to the server for aggregate processing. Thus, a global model is created without sending private data to the server.

III. The tasks solved in the previous year

We focused on FL techniques that can be used for edge computing in our study. A review paper [5], which focuses specifically on FL approaches with calculations at the network's edge, has been published as part of our research.

Considering that the previous years of the study were spent exploring the potential of edge devices, this year, we have already embarked on the actual training of the models using FL and edge devices. Our primary focus has been on convolutional neural networks and vehicle classification using cameras at toll gates. Based on the features, dimensions, and existence of vehicle trailers, we have identified 10 classes into which we will classify the vehicles.

The first step was to create a dataset large enough to train a neural network (NN) model and simulate the FL process. In creating the dataset, we created just over 20000 images of different types of vehicles. However, this dataset is unweighted and, therefore, needs to be taken into consideration when training the model. The CNN model extracts the features of each image of a given object. It is a complex and computationally intensive depth model used for object classification. The model is designed and trained as a classical depth classification model with the output of classification probabilities in ten classes. In our cases, we used the Tensorflow and Keras libraries. From these libraries, we tested different models offered by these libraries, such as Mobile-Net, ResNet, or EfficientNet. Of course, each of these NNs has different versions of complexity and computational complexity, and our goal was to see what the edge device itself can handle. First of all, it was necessary to adjust our unweighted data set by weighting the entire dataset.

Our first training and subsequent evaluation of the models showed unsatisfactory results. Simpler and less complex models such as EfficientNetB2 achieved accuracies of about 50-55% and loss over 1,5. More complex models, which are somewhat more computationally intensive, had to be used in our case. Here, we encountered further problems related to the memory of our edge devices, which have 4GB of RAM. When trying to train the ResNet101 and EfficientNetB6 models, we ran into the problem that training could not even be done due to insufficient memory. Attempts to mitigate memory limitations for both ResNet101 and EfficientNetB6 by reducing the batch size were unsuccessful, ultimately leading to persistent out-of-memory errors despite these adjustments. In our case, we decided to use the EfficientNetB4 model, which we successfully trained on our NVIDIA Jetson NX Xavier. Among the models evaluated, EfficientNetB4 emerged as the most suitable choice for our solution, offering the optimal balance between efficiency and power consumption within the constraints of our edge devices. However, training this model on an NVIDIA device took a lot of work for the data we had on stored devices. In this case, we decided to use a smaller sample of data, namely 11500 data for training and 2500 data for model validation. Using this amount of data, we successfully completed the model's training with a result of approximately 69% accuracy and 0.87 loss on the validation set.

To enhance our dataset, we employed a range of data augmentation strategies. This involved horizontally flipping images, making slight adjustments to brightness and color saturation, modifying contrast, rotating images by up to 24 degrees, introducing noise, and adding externally sourced data from the internet. These measures enabled us to significantly expand our dataset to a total of 49,630 images.

We allocated 4630 of the original images for validation, stored on the server side. This allows us to test the model with data that none of the clients have seen. The rest of the data was divided among three clients, giving each around 15000 images (12500 for training and 2500 for validation). This data distribution and the overall system architecture are illustrated in Fig. 1.

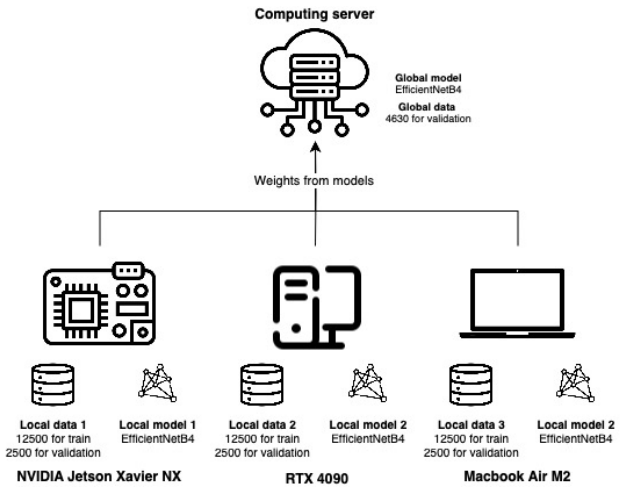

Fig. 1. FL architecture of the presented experiments

Utilizing FL in our study provided us with the advantage of accessing a more extensive dataset while ensuring the privacy and integrity of the data remained intact. This was particularly crucial, as the data was distributed uniformly across all participating devices, ensuring that each class was represented equally. This equitable distribution made it possible to implement the FedAvg strategy, a method that calculates the average of local models from various devices at the server level to construct a comprehensive global model. Through this approach, we attained a notable success rate of 86% and a loss rate of 0,52, affirming the efficiency of our FL methodology in leveraging edge devices. This achievement is significant as it demonstrates FL's capability to facilitate high-performance model training without transmitting sensitive data to centralized servers, bolstering data security. We summarized the experiments that we successfully completed with the results in a Table I.

Of course, we also tried other ways to get the best results from the available dataset. When using more complex models where edge devices do not play an important role, it is possible to arrive at more accurate validation results [6]. These models can no longer be run on edge devices. These results are currently submitted to a peer-reviewed journal.

TABLE I
CLASSIFICATION MODEL EXPERIMENTS

Architecture	Model	Acc	Loss	Data
Centralized	EfficientNetB2	50-55%	>1,5	20000 images
Centralized	EfficientNetB4	69%	0,87	14000 images
FL	EfficientNetB4	86%	0,52	49630 images

IV. Future work

In the near future, we would also like to evaluate the latest experiments based on centralized and federated learning in a newly prepared article. We aim to develop a method for applying FL in Industry 4.0 and transportation, using edge AI devices. Our focus will be on enabling these devices to fully utilize their processing capabilities (including GPU usage) and optimizing overall communication and training processes (like the number of FL rounds, epochs, and local model complexity) for practical model deployment. This approach will ensure efficient use of both GPU and CPU in each device, maximizing their performance.

Acknowledgment

This publication was supported by the APVV grant ENISaC - Edge-eNabled Intelligent Sensing and Computing (APVV-20-0247)

References

[1] S. Madakam, V. Lake, V. Lake, V. Lake *et al.*, "Internet of things (iot): A literature review," *Journal of Computer and Communications*, vol. 3, no. 05, p. 164, 2015.

[2] C. Zhang, Y. Xie, H. Bai, B. Yu, W. Li, and Y. Gao, "A survey on federated learning," *Knowledge-Based Systems*, vol. 216, p. 106775, 2021.

[3] L. Pomšár, A. Brecko, and I. Zolotová, "Brief overview of edge ai accelerators for energy-constrained edge," in *2022 IEEE 20th Jubilee World Symposium on Applied Machine Intelligence and Informatics (SAMI)*. IEEE, 2022, pp. 000 461–000 466.

[4] A. Brecko, "Federated learning for edge computing for industry 4.0," 2023, pp. 152–154. [Online]. Available: http://scyr.kpi.fei.tuke.sk/wp-content/scyr-files/proceedings/SCYR_2023_Proceedings.pdf

[5] A. Brecko, E. Kajati, J. Koziorek, and I. Zolotova, "Federated learning for edge computing: A survey," *Applied Sciences*, vol. 12, no. 18, 2022. [Online]. Available: https://www.mdpi.com/2076-3417/12/18/9124

[6] A. Brecko, J. Čamaj, P. Papcun, and I. Zolotová, "Vehicle detection and classification based on image data acquired by highway gate," *In review*.

Effect of liquid isoprene rubber on molecular mobility of thermoplastic starch/PBAT blends

[1]*Simona SAPAROVÁ (2nd year)*
Supervisor: [2]Mária KOVAĽAKOVÁ

[1,2]Department of Physics, FEI TU of Košice, Slovak Republic

[1]simona.saparova@tuke.sk, [2]maria.kovalakova@tuke.sk

***Abstract*— In this paper, the effect of liquid isoprene rubber (LIR) as a compatibilizer on molecular mobility of thermoplastic starch/PBAT blend was studied using NMR techniques. The changes in ^{1}H BL and ^{1}H MAS NMR spectra indicate that with increasing LIR content, an increase in molecular mobility of glycerol molecules occurs in the studied samples. From ^{13}C CP/MAS NMR spectra can be inferred that, LIR influences recrystallization of starch chains.**

***Keywords*— thermoplastic starch, PBAT, isoprene rubber, nuclear magnetic resonance**

I. Introduction

Biodegradable polymers (BDP) made from synthetic or renewable resources are very promising materials since they can be used as environmentally friendly alternatives to the traditional plastics made from fossil sources. Thermoplastic starch (TPS) is one of the most intensely studied BDP made from natural source. TPS can be obtained by the thermomechanical processing – plastification, which requires the presence of plasticizer (water, glycerol, urea, sorbitol etc.). The properties of TPS depend on the used plasticizers and the conditions of plastification, in which semicrystalline native starch is transformed into amorphous material. [1]

Poly(butylene adipate-co-terephthalate) (PBAT) is an example of synthetic BDP. PBAT is produced by polycondensation reaction of butanediol, adipic and terephthalic acids. PBAT is semicrystalline polymer, which is fully biodegradable and compostable. Mechanical properties of PBAT are like those of low-density polyethylene. To enhance mechanical properties and reduce the price of resulting material, PBAT/TPS blends began to be produced. [2]

TPS is hydrophilic and PBAT is hydrophobic material. To improve compatibility of those immiscible polymers, a compatibilizer like liquid isoprene rubber (LIR) can be used. LIR is almost odorless, transparent, colorless and synthetically made viscous liquid rubber, which is like natural rubber. [3]

To determine the area of application for which TPS/PBAT blends are suitable, it is important to know their structure and molecular mobility. These properties can be investigated by nuclear magnetic resonance (NMR). NMR is based on the interaction of nuclei possessing magnetic moment with an external homogenous and oscillating radiofrequency magnetic fields. Solid state NMR is a frequently used experimental method in polymer research. [4] In this paper, the effect of LIR on molecular mobility of TPS/PBAT blends was studied using NMR techniques.

II. Materials and methods

The studied samples were prepared at the Polymer Institute, SAS in Bratislava. Native corn starch Meritena® 100 from Brenntag (Bratislava, Slovakia) and glycerol (purity 99%) from CentralChem Ltd. (Bratislava, Slovakia) and liquid isoprene rubber (LIR-410) were used for TPS preparation. In the first step of sample preparation, LIR was dissolved in glycerol by mechanical mixing for 5 min at ambient temperature. The next step was a continuous mechanical mixing of the components consisted of starch (S) and the mixture of LIR and glycerol (G) for 5 minutes by a glass rod. Then TPS-LIR materials were processed in a laboratory mixer Plastograph Brabender PLE 331 for 10 min at 130 °C and 100 rpm. The mass ratio w_S:w_G:w_{LIR} was 1:0.5:X, where X is 0.05 for TPSL05/PBAT sample, 0.1 for TPSL1/PBAT sample. For the preparation of TPS without LIR, a mixture of native starch (S), glycerol (G) water (W) was prepared. The mass ratio w_S:w_G:w_W was 1:0.5:2.3. The mixture was heated at a temperature of 100°C for 5 hours and then left overnight at 60°C to prevent moisture absorption by the sample. PBAT was blended with TPS mixture in mass ratio 75:25 for 10 minutes at a temperature of 130°C at 100 revolutions per minute. Slabs of circular shape with thickness of 1 mm were formed by two-step compression molding at a temperature of 180°C using 2 minutes preheating without pressure and additional 4 min at a pressure of 2.65 MPa followed by cooling down to the temperature around 80 °C under pressure.

NMR spectra were measured on a 400 MHz Varian spectrometer. ^{1}H NMR spectra were obtained for static samples (so-called broad line – BL ^{1}H NMR spectra) and using magic angle spinning (MAS) technique with MAS rate of 10 kHz. ^{13}C NMR spectra were measured using the cross polarization (CP) and MAS techniques. The detailed information on the parameters of NMR measurements can be found in [5]. All measurements were performed at room temperature two days after samples preparation. The measured spectra were processed using Mestrelab Research Mnova 9.0 software.

III. Results and discussion

^{1}H MAS NMR spectra for studied samples consist of 4 resolved signals (Fig. 1) with chemical shift values of 7.9 (^{1}H nuclei in terephthalate unit), 5.1 (OH groups of glycerol), 3.7 (CH_2/CH groups of glycerol and OCH_2 groups in PBAT) and 1.6 ppm (CH_2 groups in PBAT) superimposed on a broad signal of other ^{1}H nuclei with lower mobility in PBAT crystalline phase, starch molecules and bound molecules of glycerol (and water). Signals from ^{1}H nuclei in LIR are not observed because

they overlap with signals from PBAT and glycerol. The signal with chemical shift of 4.8 ppm observed in ^{1}H MAS NMR spectrum for TPS/PBAT sample originates from ^{1}H nuclei in water not bound to starch. With increasing LIR content in the studied samples, a decrease in linewidth of signal from ^{1}H nuclei in glycerol is observed indicating an increase in its molecular mobility. [6][7]

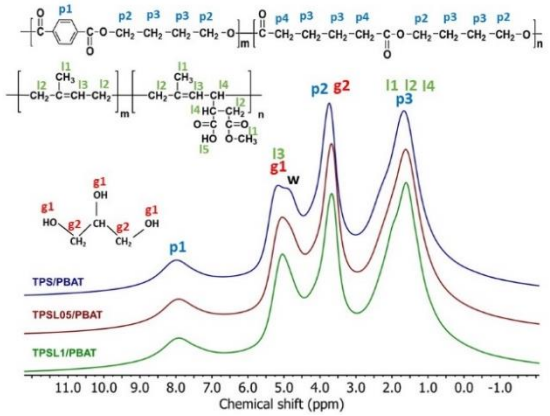

Fig. 1 ^{1}H MAS NMR spectra for studied samples and chemical structure of PBAT, glycerol and LIR

^{1}H BL NMR spectra for studied samples (Fig. 2) consist of one narrow signal from ^{1}H nuclei in mobile LIR, glycerol and starch molecules, PBAT chains in amorphous phase and one broad signal (BS) from ^{1}H nuclei in rigid starch chains, less mobile glycerol molecules and PBAT chains in ordered phase. By the deconvolution of these spectra, it is possible to obtain more detailed information (Fig. 1, Tab. 1). The obtained data shows that narrow signal is the superposition of signals from ^{1}H nuclei in LIR and glycerol OH groups (4.9 ppm), glycerol CH_2, PBAT OCH_2 groups and mobile starch chains (3.6 ppm), and PBAT CH_2 groups (1.6 ppm). [8]

Addition of LIR to the studied samples caused changes in their molecular mobility. With increasing LIR content, a decrease in linewidth of signal with chemical shift of 3.6 ppm is observed which indicates increase in molecular mobility of glycerol molecules. The increase in relative intensity of broad signal (Tab. 1) indicates a decrease in molecular mobility in the studied samples, which is probably caused by starch recrystallization.

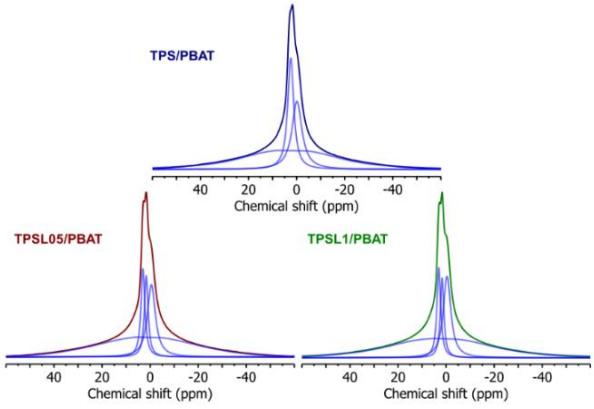

Fig. 2 ^{1}H BL NMR spectra for studied samples

Tab. 1 Linewidths (lw) and relative intensities (I_r) of signals obtained from the deconvolution of ^{1}H BL NMR spectra for studied samples

Sample	4.9 ppm		3.6 ppm		1.6 ppm		3.5 ppm	
	lw (kHz)	I_r (%)	lw (kHz)	I_r (%)	lw (kHz)	I_r (%)	lw (kHz)	I_r (%)
TPS/PBAT	-	-	1.2	22.9	2.0	23.3	18.5	53.8
TPSL05/PBAT	0.7	8.8	0.8	12.8	1.7	23.0	19.5	55.4
TPSL1/PBAT	0.7	9.2	0.7	11.1	1.6	22.3	20.0	57.5

^{13}C CP/MAS NMR spectra for studied samples depicted in Fig. 3 consist of 10 signals originating from ^{13}C nuclei in starch, glycerol, LIR and PBAT. Starch chains in the TPS/PBAT sample are disordered because the resonance of C1 starch carbons (103 ppm) shows only one broad signal with the shape typical for disordered chains. The signal from C6 carbons is not observed. The reason is its larger line width and low intensity. With increasing LIR content, changes in the shape of C1 signal are observed which indicates formation of regions with ordered starch chains. The most distinct change is observed for the sample with the highest LIR content. [6][7]

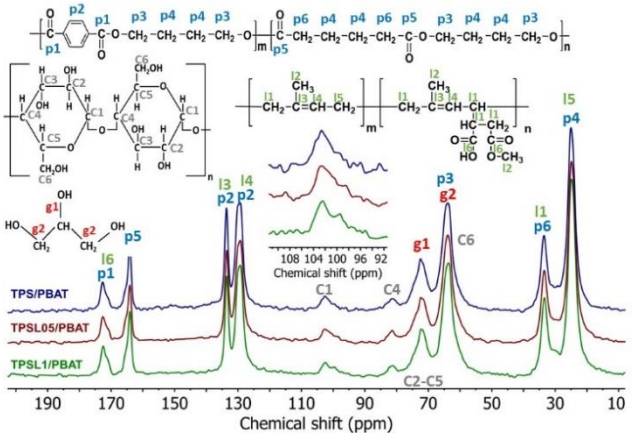

Fig. 3 ^{13}C CP/MAS NMR spectra for studied samples and chemical structure of PBAT, starch, glycerol and LIR

IV. Conclusion

The increasing LIR content in the studied samples results in

- the increase in molecular mobility of glycerol molecules inferred from the changes in ^{1}H MAS NMR spectra,
- the decrease in starch chain mobility, deduced from the changes in ^{1}H BL NMR spectra, are caused by the formation of ordered structures confirmed by ^{13}C CP/MAS NMR spectra.

The effect of other compatibilizers, their content and storage on the structure and molecular mobility of TPS/PBAT blends is planned to be studied in near future.

Acknowledgment

This work was supported by the Slovak Grant Agency through VEGA project no. 1/0751/21. We would like to thank prof. I. Chodák and Dr. H. Peidayesh for providing samples.

References

[1] R. Shanks, I. Kong, *Thermoplastic starch.* IntechOpen: Melbourne, 2012.
[2] M. Lackner et al., "Mechanical properties and structure of mixtures of poly(butylene-adipate-co-terephthalate) (PBAT) with thermoplastic starch (TPS)," in *Int. J. of Biobased Plastics,* vol. 3, 2021, 126-138.
[3] P. Wang et al., "Solvent-free synthesis, plasticization and compatibilization of cardanol grafted onto liquid isoprene rubber," in *Composites Science and Technology,* vol. 215, 2021, 109027.
[4] F. A. Bovey, P. A. Mirau, *NMR of Polymers.* San Diego: Academic Press, Inc. 1996.
[5] A. Baran et al., "Effects of urea and glycerol mixture on morphology and molecular mobility in thermoplastic starch/montmorillonite-type nanofiller composites studied using XRD and NMR," in *J. of Polym. Res.*, vol. 29, 2022, 257.
[6] O. Fričová et al., "Influence of aging on molecular motion in PBAT-thermoplastic starch blends studied using solid-state NMR," in *Int. J. of. Polym. Anal. and Charac.,* vol. 25, 2020, 275-282.
[7] O. Fričová, M. Hutníková, "Solid-State NMR Study of Poly(3-Hydroxybutyrate) and Ecoflex® Blends," in *Acta Physica Polonica A,* vol. 129, 2016, 388-393.
[8] N. Šmídová et al., "Structural characterization of poly(butylene-adipate-co-terephthalate) (PBAT)/thermoplastic starch blends," in *AIP Conf. Proc.,* vol. 2778, 2023, 040026.

The Use of Wireless Sensor Network in the Long-Term Measurement and Correlation Analysis of PM and Meteorological Factors

[1]*Simona KIREŠOVÁ (3rd year)*
Supervisor: [2]Milan GUZAN

[1,2]Dept. of Theoretical and Industrial Electrical Engineering, FEI TU of Košice, Slovak Republic

[1]simona.kiresova@tuke.sk, [2]milan.guzan@tuke.sk

***Abstract*—This paper deals with the use of Wireless Sensor Networks in the long-term measurement and monitoring of particulate matter (PM) and meteorological factors. The network consists of 14 sensor nodes, the time-series database InfluxDB, and the Grafana tool used for the analysis and the visualization of the measured data. In addition, a correlation analysis between PM and meteorological factors is performed.**

***Keywords*—correlation analysis, measurement, meteorological factors, particulate matter, wireless sensor networks.**

I. Introduction

The motivation to study Wireless Sensor Networks (WSNs) is driven by their unique characteristics and potential applications. Unlike centralized systems, WSNs operate in a decentralized manner. Sensor nodes, equipped with microprocessors, memory, and various sensors, function independently and communicate wirelessly to collect and transmit data from the physical environment. This decentralized approach offers advantages such as improved signal-to-noise ratio, energy efficiency, robustness, and scalability compared to centralized systems, making WSN highly relevant in various applications including environmental monitoring, industrial sensing, infrastructure protection, and smart home technology [1].

A significant application of WSN is environmental monitoring, particularly in the assessment of air quality. The author's previous work has addressed PM, its sources, composition, the negative impact on human health, methods of measurement, and types of PM sensors [2], [3]. Furthermore, specialized prototypes of measurement devices have been created for outdoor environmental measurements at several locations in eastern Slovakia, focusing on PM concentrations [4], AQI [5], the sample period [6], and the correlation between PM and meteorological factors [7], [8] from a short-term perspective, testing the viability of this approach before moving on to long-term monitoring in this paper. Another environment of PM measurement was carried out in an industrial setting [9], where the importance of monitoring PM concentrations is paramount due to the requirement for maintaining a level of cleanliness.

However, the need for deployment of long-term outdoor measurements of PM concentration remained. Creating a WSN that consists of several measurement stations spanning a large area is a viable approach for long-term measurement and monitoring.

II. Measuring and Monitoring PM in the Outdoor Environment

A. The Wireless Sensor Network

At the core of our WSN are sensor nodes, which are individual measuring devices, connected to the Internet via Wi-Fi. The measuring devices are based on the ESP8266 microcontroller (the block diagram is shown in Fig. 1).

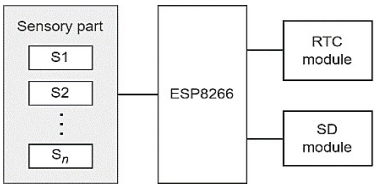

Fig. 1. The block diagram of the sensor node.

The data is measured by the sensor nodes every 5 seconds and stored in a **.csv* file on an SD card, which is interfaced with the microcontroller via the SD module. The RTC module is used to timestamp each measurement. An important part of the sensor node is the sensory part of the device, which depends on the physical quantities measured by a given node.

The WSN is made up from 14 nodes, whose geographical location is marked in Fig. 2. 13 nodes are located in the eastern Slovakia, except for 1 node in Füzérkomlós (Hungarian village near the Slovak border). The nodes measure PM, VOC, NOx, CO2, temperature (T), RH, pressure (P) and wind speed (WS).

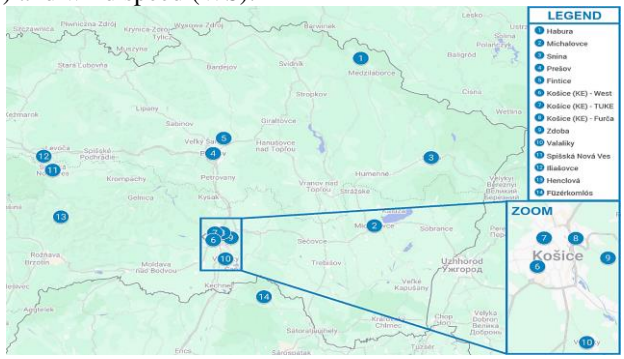

Fig. 2. The geographical location of the sensor nodes in the WSN.

Sensor nodes in the WSN produce large amounts of time series data, managed efficiently using InfluxDB, a time series database. Each sensor node connects to the internet via Wi-Fi

and sends the measured data to the time-series database InfluxDB, which facilitates data visualization through customizable dashboards. Additionally, InfluxDB supports data analysis and modification through scheduled tasks, where Flux scripts perform calculations and write modified data back to the database. We used tasks in InfluxDB to calculate Pearson's correlation coefficient between pollutant concentrations and other variables over 24 hours [10]. For visualization using static and dynamic dashboards, Grafana is used. Grafana presents users with a user-friendly home screen featuring tabs for accessing created dashboards, real-time alerts for sensor nodes experiencing measurement interruptions, and an interactive map displaying the locations and information about the sensor nodes in the network. The dashboards consist of line, bar graphs, calendar heatmaps and state timelines, that show the measured values at a given location, as well as hourly and daily averages [11], [12].

B. Correlation Analysis

The process of analysis in terms of correlation will be demonstrated for one sensor node: Košice-TUKE. The node is located on the university campus, on the 1st floor on the windowsill, oriented to the north. In front of the building, there is a side road with very little traffic.

As mentioned previously, correlation analysis is calculated by the database [10]. First, hourly averages are calculated, as previous experience [13] has shown that using hourly averages is more appropriate than using raw data because the dynamics of many of the measured variables can obscure the real trends and relationships between variables and calculating averages helps reduce the noise in the measured data. Next, the averaged data was divided into one-day intervals and Pearson's correlation coefficients (r) were calculated between all variables for these intervals, as well as p-values for testing the null hypothesis (that there is no relationship between the observed phenomena) [14]. If $p \leq 0.05$, then the null hypothesis can be rejected, and it can be said that the results are statistically significant [15].

We will focus on the correlation between PM10 and meteorological factors (T, RH, P, WS). As can be seen in Fig. 3, there was a prevalence of a negative correlation between PM10 and temperature and a positive correlation between PM10 and humidity. The presence of humidity in the atmosphere induces the adhesion of water molecules to particulate matter, leading to the growth of PM. As these particles grow, both their mass and number increase. This is particularly notable for ultrafine PM, which, being the most abundant, would typically remain undetectable below the detection limits of the sensor (< 0.3 µm) until their expansion in size renders them detectable. Pressure correlated positively with PM10 on some days and negatively on others, but the positive correlation was more prevalent than the negative correlation, especially in the spring and summer. It is possible that the high pressure hindered the upward movement of PM, which contributed to the higher PM concentration and a positive correlation. A slight negative correlation was found between PM10 and wind speed. The strength of this correlation is influenced by the fact that PM cannot correlate in the absence of wind, but PM concentration decreases in the presence of wind, showing that wind has an important effect on pollutant dispersal.

III. Conclusion

WSNs serve as effective instruments for collecting data across vast geographical areas over extended periods. Time-series databases play a pivotal role, serving not only as repositories for data storage but also for calculations and detailed data analysis. Complementing databases with tools like Grafana are indispensable for data visualization, which provides a clear understanding of trends and relationships within the measured data.

Correlation analysis for yielded the following results (but it is important to note that they cannot be generalized until measurements from other locations are analyzed). Significant negative correlation between PM/temperature and PM/wind speed as well as a positive correlation between PM/humidity was found. The correlation between PM/pressure also tended to be more positive than negative, but there were more irregularities. The presence of irregularities in the correlations, especially in autumn and winter months, indicates the influence of other factors (e.g. heating season or other human activities). Even though PM in urban areas is more influenced by industrial production and traffic, the primary sources of urban PM are all year round, while the secondary influence of household heating is seasonal, which is reflected in the correlation inconsistencies. Additionally, due to pressure being less prone to dynamic changes than temperature, RH, and wind speed, it may be worthwhile to investigate the PM/pressure correlation from a longer standpoint.

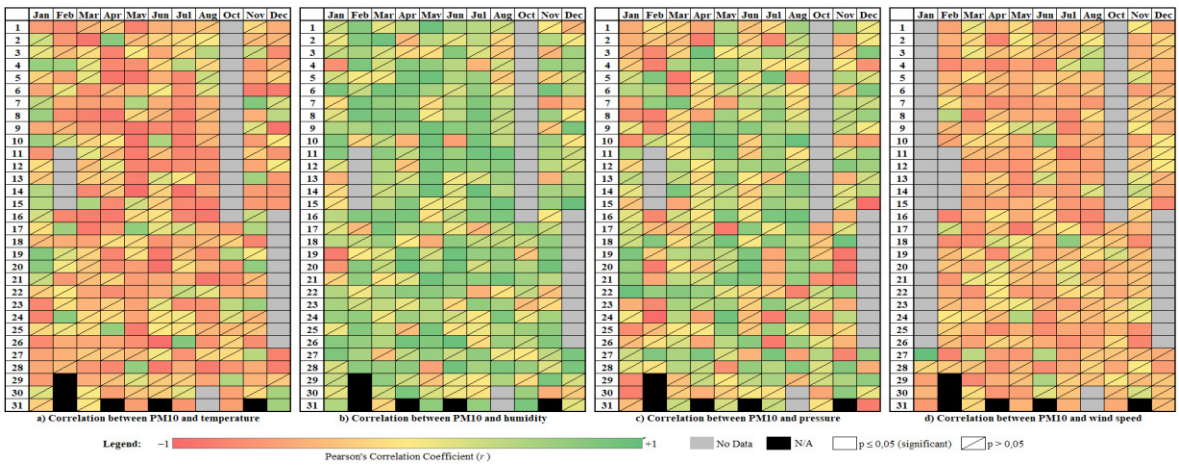

Fig. 3. The visualization of Pearson's Correlation Coefficient (r) between PM10 and meteorological factors, using a red-yellow-green color scale (see legend). Cells containing r that were not statistically significant ($p > 0.05$) were crossed out, while cells with statistically significant r ($p \leq 0.05$) were left uncrossed.

REFERENCES

[1] F. Zhao and L. Guibas, “Wireless Sensor Networks: An Information Processing Approach,” Morgan Kaufmann Publishers, Massachusetts, 2004. ISBN 1-88560-914-8.

[2] S. Kirešová: “Particulate Matter and the Methods of Its Measurement: An Overview,” In SCYR 2022: 22nd Scientific Conference of Young Researchers, Proceedings from Conference, pp 43-47, Apr 2022.

[3] S. Kirešová, M. Guzan: “Measurement of Particulate Matter: Principles and Options of Measurement at Present,” Acta Electrotechnica et Informatica, vol. 22, no. 2, pp. 8-18, Jun 2022.

[4] S. Kirešová, M. Guzan: “Concentration of Particulate Matter in the Air: A Comparison of Measurements,” Electrical Engineering and Informatics 13, pp. 301-306, Jul 2022. (In Slovak).

[5] S. Kirešová, M. Guzan, V. Rusyn: “Particulate Matter PM2.5 and PM10 and Its Impact on Air Quality in Urban or Rural Areas,” In 2nd International Workshop on Information Technologies: Theoretical and Applied Problems. Ternopil, Ukraine, Nov 2022.

[6] S. Kirešová, M. Guzan: “Analyzing the Sample Period of Particle Mass Concentration Measurements,” In Proceeding of scientific and student’s works in the field of Industrial Electrical Engineering 11, pp. 210-214. Košice, Slovakia, Jul 2022.

[7] S. Kirešová, M. Guzan, P. Galajda: “Measuring Particulate Matter (PM) Using SPS30,” In 32nd International Conference Radioelektronika, pp 160–165. Košice, Slovakia, Apr 2022.

[8] S. Kirešová, M. Guzan: “Determining the Correlation between Particulate Matter PM10 and Meteorological Factors,” Eng, vol. 3, no. 3, pp. 343-363, Aug 2022.

[9] S. Kirešová: “Measuring and Monitoring Particulate Matter in an Industrial Environment,” In SCYR 2023: 23rd Scientific Conference of Young Researchers, Proceedings from Conference, pp 84-87, Apr 2023.

[10] S. Kirešová, M. Guzan, B. Sobota, V. Fedák, R. Bača, and D. Bakši, "The Use of Time Series Database in Measurements," 2023 International Conference on Electrical Drives and Power Electronics (EDPE), The High Tatras, Slovakia, 2023, pp. 1-8.

[11] S. Kirešová, M. Guzan, B. Fecko, O. Somka, V. Rusyn, R. Yatsiuk, “Grafana as a Visualization Tool for Measurements”, 2023 IEEE 5th International Conference on Modern Electrical and Energy System (MEES), Kremenchuk, Ukraine (2023).

[12] S. Kirešová, V. Rusyn, M. Guzan, G. Vorobets, B. Sobota, O. Vorobets, "Utilizing low-cost optical sensor for the measurement of particulate matter and calculating Pearson's correlation coefficient," Proc. SPIE 12938, Sixteenth International Conference on Correlation Optics, 2024.

[13] S. Kirešová, M. Guzan: “Determining the Correlation Between Particulate Matter and Wind Speed,” In Proceeding of scientific and student’s works in the field of Industrial Electrical Engineering 12, pp. 170-173. Košice, Slovakia, Jul 2023.

[14] MathWorks, “Correlation coefficients – MATLAB,” Available: <https://mathworks.com/help/matlab/ref/corrcoef.html>. (Accessed: 2024-1-28).

[15] M. Munk, “Computer Data Analysis,” Constantine the Philosopher University in Nitra, 2011. ISBN 978-80.8094-895-5.

Diversity in Extended Reality and Unified Environment

[1]*Miriama MATTOVÁ (3rd year)*
Supervisor: [2]Branislav SOBOTA

[1,2]Dept. of Computers and Informatics, FEI TU of Košice, Slovak Republic

[1]Miriama.Mattova@tuke.sk, [2]Branislav.Sobota@tuke.sk

***Abstract*— This paper presents an analysis of the diversity within extended reality technology implementation, along with a proposal for a unified environment capable of hosting avatars from extended reality subdivisions. Environment implementation solves some of the diversities analysed in introduction such as multidevice support as well as hosting avatars from mentioned subdivisions. A unified environment was implemented based on the proposed concept.**

***Keywords*—diversity, extended reality, unification, multidevice**

I. Introduction

Extended reality (XR) technology encompasses three primary subdivisions: Virtual Reality (VR), Augmented Reality (AR), and Mixed Reality (MR). There is a notable rise in scientific interest regarding these technologies. With increasing interest and adoption of these technologies, it could be said that there is a corresponding linear increase in the diversity. Diversity – in a sense of device support and implementation - may result in increased complexity in implementation. Therefore, an analysis of the current state of the issue was conducted. Following Tab. I present used queries as well as article occurrences.

TABLE I
USED QUERIES FOR ANALYZING CURRENT STATE OF THE ISSUE AS WELL AS NUMBER OF ARTICLES OCCURENCES

Library	Occurrence Q1	Occurrence Q2
Web of science	389	1
Scopus	6 491	65
IEEE Digital Library	34	0
ACM Digital Library	1677	68
Q1: ("XR" OR "VR" OR "AR" OR "MR") AND ("multidevice") AND ("support" OR "implementation")		
Q2: ("XR" OR "VR" OR "AR" OR "MR") AND ("Unification" OR "multidevice")		

Authors Cárdenas-Robledo et al. [1] conducted a systematic literature review focusing on practical XR implementation techniques within the context of Industry 4.0. This review effectively highlights the diversity of XR technologies, which, as previously mentioned, introduces implementation challenges. One such challenge is addressed by Belo et al. [2], who propose the use of adaptive interfaces. The scarcity of sufficiently developed tools for realistic XR settings is noted by Cárdenas-Robledo et al. [1], a sentiment echoed by Ashtari et al. [3], who present a table illustrating the diversity and barriers faced by developers working on AR/VR environments. These findings are further supported by Krauß et al. [4], who discuss individual development challenges encountered by developers within the same sample. From the perspective of directly unifying XR technologies, several aspects warrant attention. One primary unification process involves avatar synchronization, as explored by Guan et al. [5], who reviewed and implemented supplements to extended body components in conjunction with the work of [6]. Key outcomes of this collaboration include opportunities for new forms of interface between the virtual and physical body, along with a taxonomy for concepts related to the extended body. In terms of interaction with the environment, Matteo et al. [7] propose the pattern to define a set of input events that abstract from specific input devices. They argue that this approach allows events to be mapped across modalities for interaction, thereby facilitating the reconfiguration of basic interaction according to available devices without necessitating modifications across different sections of the source code.

It is evident that efforts are underway to address the given problem; however, these solutions often remain partial. For instance, works [8], [9], and [10] do not assess the collaboration between XR avatars or the interaction issues of multiple users, as addressed in work [5]. Similarly, while work [6] proposes an environment template for hybrid systems, its emphasis is primarily on MR. Consequently, the aforementioned works either do not fully address or only partially tackle the challenges outlined in the tables referenced in [3] and [4]. Therefore, this brief article will concentrate on the concept for a unified XR environment, along with the experiments conducted thus far.

II. Concept of unified XR environment

The primary challenge lies in the diverse array of hardware devices entering the XR environment. Thus, it is posited that minimizing the impact of data structures from external devices will result in a more unified space. To achieve this, the concept proposes a server-side solution where processed images are sent based on displayer parameters. Interaction with the environment would be facilitated through an external multimodal application, which configures inputs and outputs of devices such as haptic suits, gloves, controllers, or other sensors. However, as the multimodal interaction application is currently in the process of being developed, this chapter will concentrate on the unified environment itself. The primary objective is not only to unify the diverse devices but also to harmonize the coexistence of VR, AR, and MR avatars within the same space.

A. VR space

Each XR subdivision includes a VR space where digital objects are positioned, defined by a coordinate system such as Cartesian coordinates. However, the distant scenery, often referred to as the skybox, varies across subdivisions. In VR technologies, the skybox consists of simulated virtual scenery, whereas in AR, the skybox is replaced by a captured reality via a camera. In MR, it can be considered that the skybox is non-existent or transparent, as users perceive reality without it being processed.

B. VR objects

Objects can be categorized into static objects (SO), local interactive objects (LIO), and shared interactive objects (SIO). Regarding collaboration across avatars, SIOs are visible to every avatar and can be interacted with collectively. LIOs, such as menus, are visible to specific avatars and are intended for individual interaction by that particular avatar. SIOs are regarded as scenery objects, visible only to VR avatars, given that in AR and MR, the scenery is replaced by reality. When defining objects in an environment processed on a server, server performance depends on the complexity of the objects to ensure efficient operation. From the perspective of object complexity, it is possible to define $C_{oi} = f(B_i, P_i, C_{Mi})$, where C_o is object komplexity, B is number of vertices, P is number of polygons, C_M is komplexity of material and i is object iteration. Complexity of the environment then can be defined as sum of object complexities $C_p = \sum_{i=1}^{N} C_{oi}$ where $C_p$is environment complexity. Therefore, with the rising of C_p, effectivity of image processing decreases.

C. Unified Avatar

Since the unified environment operates on a server-based model, avatars can be constructed based on the parameters of the user's display device. A template of an avatar can be created with default parameters applicable to every avatar, such as body collider, head component, and controller components. Dynamic parameters such as field of view (FOV), resolution, number of cameras (stereoscopic, monoscopic), screen layout with multiple cameras (fullscreen, side-by-side, up-down), and type (VR, AR, MR) need to be applied when a user enters the environment. Based on the given parameters and the selected type, objects are displayed or removed from the view of the avatar accordingly. Avatar will then process the image and send final frame to the user displayer. This raises the question of whether the server can effectively manage data overload. As it is assumed, that avatars may move around the environment and C_o variable, effect on GPU (Grafic processing unit) will be non-linear. Therefore it is possible to define following relation $I_{GPU} = f(C_p, C_{avatar}, \mathrm{N}, \mathrm{FPS})$ where I_{GPU} is complexity effect on GPU, C_{avatar} is the complexity of avatar based on the object complexity relation, N is a number of avatars and FPS is the frame per second value from environment. Example can be applied on $I_{GPU} = C_p + a \cdot C_{avatar} \cdot N^2 \cdot FPS$ where a is a coefficient, which capture non-linear effect with the addition of a new avatar in the environment.

D. Spatial data

When dealing with a unified and collaborative environment, it is essential to consider three scenarios regarding real space objects (RSO) and avatar spatial dimensions (SD_A). If the unified virtual space hosts an avatar that is based on:

S1 – VR subdivision

S2 – AR and/or MR subdivision where $(SO \approx \mathrm{RSO} \vee \mathrm{SO} = \mathrm{RSO}) \wedge (PD_{A_1} \approx PD_{A_n} \vee PD_{A_1} = PD_{A_n})$

S3 – AR and/or MR subdivision where $\mathrm{SO} \neq \mathrm{RSO} \wedge PD_{A_1} \neq PD_{A_n}$

III. IMPLEMENTATION OF UNIFIED XR ENVIRONMENT

A collaborative environment was created, accessible to users via a web browser. User can select from predefined avatars (VR - Desktop, Stereoscopic mobile, Meta Quest, Digital twin of Lirkis Cave, AR – Desktop webcam, Mobile camera, Meta Quest passthrough, MR – one side hologram, fours side hologram, MS Hololens) or set up custom avatar for each type based on the parameter mentioned in previous chapter. Instance of the avatar will be created in the environment and web will continuously present pictures generated from server. Avatars were tested with a representation on Fig. 1-4.

Fig. 1. VR, monoscopic – desktop, mobile

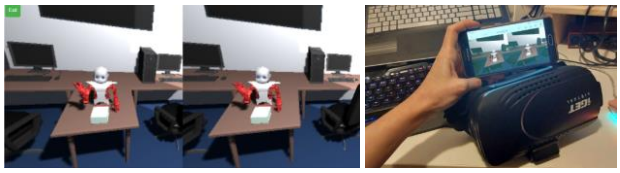

Fig. 2. VR, stereoscopic, side-by-side view – Mobile, Head mounted displays

Fig. 3. AR, monoscopic – desktop, mobile

Fig. 4. MR, holograms 1side, 4side

As mentioned previously, spatial information synchronization is not yet implemented, as the multimodal controller is still in development. Consequently, in the AR and MR views, SIOs may appear to be in 2D, although they are in 3D, with synchronization missing from reality. Unified solution currently does not support stereoscopic view for MR, MS Hololens model in a picture were placed from the library.

Avatars can exist in environment simultaneously. However further optimization on an image creation and transfer must be done as with the rising number of the avatars, I_{GPU} is not parallelized which results in data overload and network communication is still in a process of empirical testing for optimal architecture, as today, some of the images are being skipped based on the I_{GPU} value. It is planned to use more

powerful GPU as well as parallelize the image creation for a more optimal results as today it is being tested on Intel(R) Core(TM), i7-6700HQ CPU 2.60GHz.

IV. Conclusion

The paper presents an analysis of XR diversity and the current state of the issue. A concept for a unified environment was proposed and implemented, facilitating avatar collaboration and image streaming on various XR devices. However, further implementation of a multimodal controller for interaction and parallelization of image creation is required and will be pursued in future work.

Acknowledgment

This work has been supported by Slovak KEGA Agency under grant no. 048TUKE-4/2022: „Collaborative virtual reality technologies in the educational process“ and the APVV grant no. APVV-21-0105 “Trustworthy human–robot and therapist–patient interaction in virtual reality”.

References

[1] Leonor Adriana Cárdenas-Robledo, Óscar Hernández-Uribe, Carolina Reta, Jose Antonio Cantoral-Ceballos, Extended reality applications in industry 4.0. – A systematic literature review, Telematics and Informatics, Volume 73, 2022, 101863, ISSN 0736-5853,W.-K. Chen, *Linear Networks and Systems* (Book style). Belmont, CA: Wadsworth, 1993, pp. 123–135.

[2] João Marcelo Evangelista Belo, Mathias N. Lystbæk, Anna Maria Feit, Ken Pfeuffer, Peter Kán, Antti Oulasvirta, and Kaj Grønbæk. 2022. AUIT – the Adaptive User Interfaces

[3] Narges Ashtari, Andrea Bunt, Joanna McGrenere, Michael Nebeling, and Parmit K. Chilana. 2020. Creating Augmented and Virtual Reality Applications: Current Practices, Challenges, and Opportunities. Association for Computing Machinery, New York, NY, USA, 1–13. https://doi.org/10.1145/3313831.3376722

[4] Krauß, Veronika, Alexander Boden, Leif Oppermann and René Reiners. “Current Practices, Challenges, and Design Implications for Collaborative AR/VR Application Development.” Proceedings of the 2021 CHI Conference on Human Factors in Computing Systems (2021): n. pag.

[5] J. Guan and A. Morris, "Extended-XRI Body Interfaces for Hyper-Connected Metaverse Environments," 2022 IEEE Games, Entertainment, Media Conference (GEM), St. Michael, Barbados, 2022, pp. 1-6, doi: 10.1109/GEM56474.2022.10017701.

[6] R. Pathak, A. A. Simiscuka and G. -M. Muntean, "An Adaptive Resolution Scheme for Performance Enhancement of a Web-based Multi-User VR Application," 2021 IEEE International Symposium on Broadband Multimedia Systems and Broadcasting (BMSB), Chengdu, China, 2021, pp. 1-6, doi: 10.1109/BMSB53066.2021.9547069.

[7] Serpi, Matteo & Carcangiu, Alessandro & Murru, Alessio & Spano, Lucio. (2018). Web5VR: A Flexible Framework for Integrating Virtual Reality Input and Output Devices on the Web. Proceedings of the ACM on Human-Computer Interaction. 2. 1-19. 10.1145/3179429.

[8] Wong, E.S.; Wahab, N.H.A.; Saeed, F.; Alharbi, N. 360-Degree Video Bandwidth Reduction: Technique and Approaches Comprehensive Review. Appl. Sci. 2022, 12, 7581. https://doi.org/10.3390/app12157581

[9] S. Lee, J. -B. Jeong and E. -S. Ryu, "Group-Based Adaptive Rendering System for 6DoF Immersive Video Streaming," in IEEE Access, vol. 10, pp. 102691-102700, 2022, doi: 10.1109/ACCESS.2022.3208599.

[10] X. Xu, X. Tan, S. Wang, Z. Liu and Q. Zheng, "Multi-Features Fusion based Viewport Prediction with GNN for 360-Degree Video Streaming," 2023 IEEE International Conference on Metaverse Computing, Networking and Applications (MetaCom), Kyoto, Japan, 2023, pp. 57-64, doi: 10.1109/MetaCom57706.2023.00023.

Automated Knowledge Evaluation in Software Engineering Disciplines

[1]*Tomáš BUČEK (1st year),*
Supervisor: [2]*Ján GENČI*

[1,2]Dept. of Computers and Informatics, FEI TU of Košice, Slovak Republic

[1]tomas.bucek@tuke.sk, [2]jan.genci@tuke.sk

***Abstract*—Manual evaluation of students' knowledge is a time-consuming process. Automation of students' knowledge evaluation can be achieved by using automatically evaluated tests and practical assignments. A reliable and well-balanced educational test can be developed using classical test theory or item response theory. This paper describes the actual state in the area of educational test development as well as systems used for automated evaluation of software engineering practical assignments.**

***Keywords*—Classical Test Theory, Item Response Theory, Programming Assignment Evaluation**

I. Introduction

With the increasing number of students at universities, it is increasingly difficult to manually evaluate students' knowledge. At the same time, it is important to ensure the evaluation of knowledge at different levels, an example of which is the consideration of Bloom's taxonomy. According to Bloom's taxonomy, student should be able to not only remember knowledge presented during lectures, but should be able to apply the knowledge as well as evaluate any information based on this type of knowledge. As Britto and Usman [5] present, the use of Bloom's taxonomy in course design increases the level of students' knowledge. The solution to the problem of manual evaluation is the use of automated approaches, such as the creation of well-balanced tests and the automated evaluation of student assignments.

The most common tools for automatic knowledge evaluation are tests and practical assignments. Creating a well-balanced test able to differentiate between students with different levels of knowledge is a crucial requirement for applying any automatically evaluated tests. Also, question present in the test should be of reasonable difficulty. In the case of too easy questions, even students who did not prepare enough for the test could get a high rating. We also want to minimize the effect of random guessing and produce final score which almost exactly reflects students' knowledge. This can be achieved by one of the most popular approaches today, either Classical Test Theory or Item Response Theory.

However, the use of tests may not be sufficient to verify knowledge at all levels of Bloom's taxonomy. The main problem is the verification of the ability to apply the acquired knowledge and skills in the field of software engineering. Therefore, it is advisable to use practical assignments in the design of the course, which students must work out in order to successfully complete the course. Apart from the creation of the assignment itself, however, its evaluation is a problem. Evaluating each assignment manually can be time-consuming, so it is necessary to apply the correct methods of automated evaluation so that, similar to the use of tests, the resulting score corresponds as closely as possible to the student's knowledge.

II. Test Theory

An educational test is a tool for obtaining a numerical result representing the level of student's knowledge. It is therefore necessary that a well-balanced and reliable test is used. Otherwise, the resulting score would not correspond to the student's knowledge. Developing such test can be achieved by employing a test development theory. At the moment, there are 2 most effecient test theory models, Classical Test Theory and Item Response Theory.

In the last 30 years, 22221 papers based on Classical Test theory and 17955 papers about Item Response Theory were published. However, in the last 10 years, approximately the same amount of papers has been published regarding Item Response Theory (11115) as for Classical Test Theory (12359), which indicates that area of Item Response Theory is growing.

A. Classical Test Theory

As Lord [14] presents, classical test theory is based on three concepts. True score, test score, and error score. Test score, denoted as X, is the total score observed in a test. True score, denoted as T, is the total score which would student achieve on a perfectly balanced test. Error score, denoted as E, is a measurement error. True score can be calculated according to equation (1). We can reformulate equation (1) into equation (2) to get a formula for the observed score.

$$T = X + E \tag{1}$$

$$X = T - E \tag{2}$$

It follows from equation (2) that a student can get a low score in two situations. In the first case, because he did not prepare enough for the test and therefore got a low score legitimately. In the second case, student prepared enough for the test, but the measurement error was too high, which indicates that unreliable test was used, or, as Sherbeck [12] describes, some external factors were applied, such as room temperature.

An important feature in test development is its reliability. As Sherbeck [12] describes, there are 3 types of reliability, stability, equivalence, and internal consistency. Stability is the retention of approximately the same score when the same test is repeated over a period of time. Equivalence is a property determined with respect to another variant of the test, and it expresses how much the results correspond to each other when both tests are performed. Internal consistency represents the homogeneity of test items.

On the other hand, reliability is not the only important feature of an educational test. As Engelhardt [8] describes, there are other characteristics important as much as reliability:

- Validity
- Discrimination
- Good comparative data
- Tailored to population

Validity is a characteristic that indicates that the test really measures the level of knowledge of the student in the given area. If the test was not valid enough, the results would not be correct because they would not be related to what the students were learning.

Discrimination is a property that determines how well the test can differentiate between a student who has prepared and a student who has not prepared for the test. In the case of a low level of discrimination, there could be situations where students who did not prepare for the test end up with a final score very similar to those who did not prepare. In such a case, the test does not provide reliable results because it is not possible to reliably identify smart students.

At the same time, it is necessary to have good comparative data to verify the properties of the test and also to adapt the questions in the test to the target group so that they reflect the expected level of knowledge, example of which can be parallel tests introduced by Hambleton and Jones [11]. As mentioned earlier, test developers want to evaluate students' knowledge at different levels of Bloom's taxonomy.

Engelhardt describes a distribution of item types used in the test as following:

- Interpret (60%)
- Apply (30%)
- Recall (10%)

It is also important to know the target group when developing a test. Different students have different levels of knowledge, therefore we must design a test to reflect the abilities of students in target group.

B. Item Response Theory

As Baker [3] explains, item response theory is based on equation (3), where P is defined as the probability of a correct response to an item, b is the difficulty parameter, c is the random-guessing parameter, a is the discrimination parameter, and i is the index of individual item. The person parameter θ represents the magnitude of latent trait of the individual, which is the attribute measured by the test. It might be a cognitive ability, physical ability, skill, knowledge, attitude, or personality characteristic.

$$P(\theta) = c_i + \frac{1 - c_i}{1 + e^{-a_i(\theta - b_i)}} \tag{3}$$

According to Hambleton, Swaminathan, and Rogers [10], depending on the use of parameters a and c, one-parameter and two-parameter models can be obtained.

As Bichi, Hafiz, and Bello [4] describe, two important characteristics of an Item response model are unidimensionality and local independence of individual test items. Unidimensionality means, that each test item is used for evaluating only one area of knowledge. Local independce means, that answers for individual items in test cannot be found in other items or guessed on the basis of other questions. Evaluating the test characteristics can help in identifying the deficiencies in existing tests and areas that need to be improved as it was found in [4].

Yilmaz [20] emphasizes that the use of open-ended questions together with multiple-choice questions in one test can lead to inaccurate values. However, applying a combination of two models, can handle both open-ended and multiple-choice questions. As presented in [20], multiple combinations of 1,2, and 3-Parameter logistic model and graded response model or partial credit model. As a result, 3-Parameter logistic model in a combination of graded response model produces the best results and the final reliability value of 0.82. However the reliability value is not indicating a high reliable test, author proved that there is a way of dealing with a combination of different item types in the same test using a combination of different item response theory models.

C. Comparison of Item Response Theory and Classical Test Theory

Major difference between classical test theory and item response theory is introduced by Hambleton and Jones [11]. Classical test theory mostly works with test-level score, while item response theory focuses on item-level score and links the true score to individual items present in the educational test.

There is, however, a possibility to observe similarities, or even a possible to way to transform a classical test theory model to item response model, as it is presented by Raykov and Marcoulides [17], where authors presented two approaches of converting a classical test theory model to an equivalent item response theory model, as well as creating a classical test theory model based on an existing item response theory model.

Cakan and Mutluer [16] described a comparison of item response theory and classical test theory methods used for computing a test score equating value for a PISA (Programme for International Student Assessment) 2012 Mathematics test. The authors examined twelve variants of both classical test theory and item response theory models. They found the LevineTS equating method as the worst equating method, while the Tucker equating method as the best equating method with the least error among the models of classical test theory. However, the TS item response model was found to be the best equating method, with error score of 0.0111, among all of the examined models.

In [18], Stage described a switch from classical test theory to item response theory for evaluation of norm-referenced test used for selection to higher education in Sweden. The test is split up into five sub-tests carried out separately. The author emphasizes other disadvantages of classical test theory, such as item difficulty and item discrimination indices being dependent on the group of examinees in which they have been obtained. A three-parameter model was chosen. However, item response theory is not applicable on all of the sub-tests, because in some of them, there is a direct connection between individual

test items, which violates the local independence restriction of item response theory models and made it difficult to fit an item response model on the data.

III. Automated Knowledge Evaluation

Basic concepts of classical test theory and item response theory, as well as current state of research, were presented in previous section. There are some similarities and differences between item response theory and classical test theory, which are presented in II-C.

As mentioned earlier, use of tests may not be sufficient to verify knowledge at all levels of Bloom's taxonomy, therefore existing systems capable of automated evaluation of practical assignments is presented in this section as well.

Item response theory, as well as classical test theory, can be applied in order to solve various educational problems. This is described in III-B.

A. Systems for automatic evaluation of programming assignments

As it was mentioned above, if we want to evaluate students' abilities to apply learned knowledge in the field of software engineering, it is appropriate to use a practical assignment. Using a system which evaluates students' assignments automatically can help teachers focus on more important topics. Also, it is important to provide students with a constant feedback, as Galan et al. describe in [9].

As Mekterović, Brkić, and Horvat [15] mention, most of the modern programming assessment systems are implemented as web application able to provide a student with a feedback on demand. Evaluation system is able to perform a static and dynamic analysis of uploaded code, store the results and display them to the user using a graphical user interface. It is also important to execute the students' untrusted code in a sandbox environment, in order to prevent any system corruption in case of unexpected events. Authors used normalized Levenshtein distance for detecting the plagiarism and set the acceptable similarity limit to 70 percent.

Galan et al. describe an AA framework [9] able to test software engineering projects with a very high granularity. This is enabled by creating every possible combination of inputs for the students' program, and verification that program is still working correctly, which is definitely of the requirements for a modern reliable software.

A challenging task is how to determine the final score of individual students in team tasks, while at the same time taking into account how individual students worked on the project. Thus, a student who did not participate in the team project should not receive a high score despite the fact that the project is evaluated very well overall. A solution for this problem is presented by Chen, Nguyen, and Dow [7]. Authors created a system capable of evaluation individual students' work on team projects. Authors were using Gitlab to store students' projects and track their activity. Gitlab was connected to continuous integration and assessment server, which is responsible for static analysis and evaluation of the source code. Log extractor was collecting logs from Gitlab and assessment server, and passed them to the contribution analyzer. Contribution analyzer measured the impact of changes introduced each team member and their code quality. Overall, presented system has the ability to identify students not participating in team

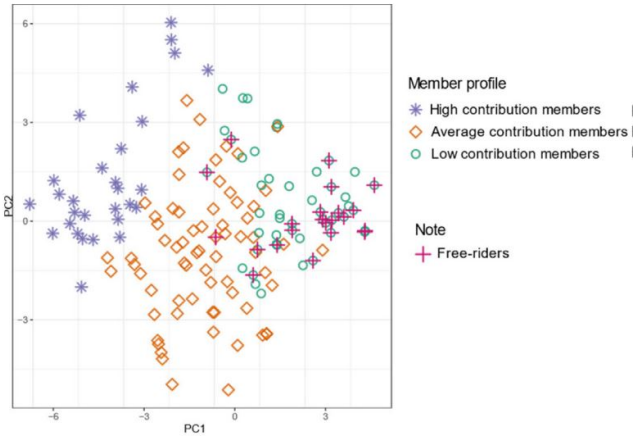

Fig. 1. Identification of free-riders [7]

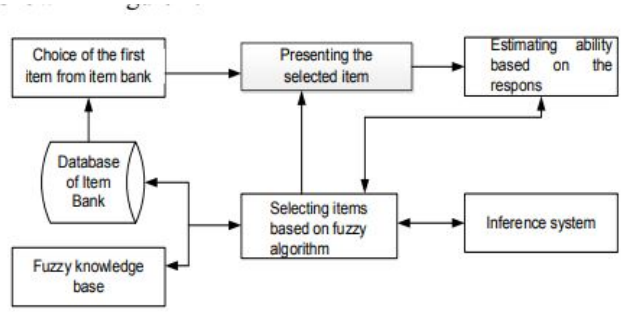

Fig. 2. Process of generating items [19]

projects actively, so-called free-riders, which is a significant advantage. Authors also decided to use peer evaluations as well as to apply machine learning models on collected data in order to identify free-riders. They performed a crosscheck to validate the data and identified students suspected of not working on the project, which is documented in Fig. 1.

B. Application of Item Response Theory

As Chang and Ying present [6], a different approach is to create an individual test for each examinee. The authors claim that the use of a personalized test for each examinee increases the accuracy of the final score, because the given test is tailored to the abilities of each examinee. However, creating a completely different test for each student violates the concept of standardised tests, because the same requirement is not applied for each student. From our perspective, maximal acceptable difference in individual test can be achieved by using different variants of each question, while each variant of the question checks the same area of the student's knowledge.

Similar approach is presented by Wulandari, Hadi, Haryanto [19]. Authors describe a system capable of selecting questions for the student based on his previous answers. The process of generating individual items is presented in Fig. 2. Process of selecting test items starts by selecting the first item from the question bank. After participants respond to the item, the level of the participant's ability is estimated again. Based on the input of item difficulty, item differentiator power, and the response of test participants' answers, next items are chosen. As mentioned above, such approach violates the concept of standardised tests. There is a possibility to make such approach

work by adjusting the maximum achievable score or total score after each incorrect question, because it is assumed, that after an incorrect answer is submitted, items with lower difficulty will be chosen for the next iteration and student might be able to answer them easily. On the other hand, such concept might be working very well in the area of formative assessments. As formative assessments are focused on learning instead of evaluating students' knowledge, such test could help students focus on areas in which they have gaps.

Al-Musawi [2] describes a practical usage of item response theory while developing a criterion-referenced test to measure student's achievement in educational evaluation. After several questions and students' samples were removed, the final model was applied successfully. Four items with high difficulty and low discrimination values were removed. As a result, item difficulty range changed from 0.17-0.95 to 0.11-0.84. Author used Alpha-Cronbach value to measure test reliability, which was estimated at 0.92. Alpha-Cronbach value 0.92 represents a high reliability of a test.

B. Kartowagiran, Sugiman, and V. Pandra [13] present the application of item response theory during a mathematical test development. Authors claim, that develop test does not violate the unidimensionality restriction, because test measures only one skill. Also, authors proved the local independence by measuring a covariant value close to zero. As the final model, a 2-Parameter model with discrimination value and difficulty value was chosen.

Abed, Al-Absi, and Abu shindi [1] described an application of item response theory while developing a numerical ability test. 3-Parameter model was used to develop a test. The individual item difficulty values are in range [-1.12, 0.65], which are acceptable values. Authors achieved a test reliability of 0.91, which indicates a high reliable test.

IV. Future research directions

There is no known information about the use of item response theory or classical test theory in the creation of tests focused on the field of software engineering at the Technical University in Košice. The further continuation of the research will be focused on the automated evaluation of student knowledge using the creation of tests based on the theory of testing, as well as the automated evaluation of students' practical skills using automated evaluation system.

We will primarily focus on Operating Systems course, where a mix of various item types is used. However, open-ended questions are mostly used in tests used as a final exam.

Starting with evaluating state of tests currently being used from the perspective of item response theory, we will calculate the actual test reliability and identify items which do not work correctly. We will also need to ensure local independence and unidimensionality of individual test items. The process of test development and maintenance can be also automated using some software solutions. After modifying existing tests, we will obtain the statistics and evaluate the total progress in test development.

V. Conclusion

The main concepts of and current state in the area of item response theory and classical test theory was presented in this paper. Existing guidelines for creating a well-balanced test with the ability to differentiate between students with different knowledge levels and measure correct areas of students' knowledge were identified. A possible solution of fitting an item response theory model on a test containing different item types by using a combination of item response theory models was observed, as well as existing tools for evaluating individual students' work on a team projects in order to identify free-riders.

References

[1] E. R. Abed, M. M. Al-Absi, and Y. A. Abu shindi. Developing a numerical ability test for students of education in jordan: An application of item response theory. *International education studies*, 9(1):161, 2015. ISSN 1913-9020.

[2] N. Al-Musawi. Using item response models to develop a criterion-referenced test to measure the students' achievement in educational evaluation. *Journal of Educational and Psychological Studies [JEPS]*, 10:727, 12 2016.

[3] F. Baker. *The Basics of Item Response Theory*. ERIC Clearinghouse on Assessment and Evaluation, 2001. ISBN 1-886047-03-0.

[4] A. A. Bichi, H. Hafiz, and S. A. Bello. Evaluation of northwest university, kano post-utme test items using item response theory. *International journal of evaluation and research in education*, 5(4):261, 2016. ISSN 2252-8822.

[5] R. Britto and M. Usman. Bloom's taxonomy in software engineering education: A systematic mapping study. In *2015 IEEE Frontiers in Education Conference (FIE)*, pages 1–8. IEEE, 2015. ISBN 9781479984541.

[6] H.-H. Chang and Z. Ying. A global information approach to computerized adaptive testing. *Applied Psychological Measurement*, 20:213–229, 09 1996.

[7] H.-M. Chen, B. Nguyen, and C.-R. Dow. Code-quality evaluation scheme for assessment of student contributions to programming projects. *Journal of Systems and Software*, 188, 02 2022.

[8] P. Engelhardt. An introduction to classical test theory as applied to conceptual multiple-choice tests. In C. Henderson and K. Harper, editors, *Getting Started in PER*, volume 2. American Association of Physics Teachers, College Park, April 2009.

[9] D. Galan, R. Heradio, H. Vargas, I. Abad, and J. A. Cerrada. Automated assessment of computer programming practices: The 8-years uned experience. *IEEE Access*, 7:130113–130119, 2019.

[10] R. K. Hambleton. *Fundamentals of Item Response Theory*. Sage Publications, 1991. ISBN 0-8093-3646-X.

[11] R. K. Hambleton and R. W. Jones. Comparison of classical test theory and item response theory and their application to test development. *Instructional Topics in Educational Measurement*.

[12] L. S. Helms. Tests aren't reliable, the nature of alpha, and reliability generalization as a meta-analytic method. In *Basic Concepts in Classical Test Theory*. ERIC Clearinghouse, 1999. URL `https://eric.ed.gov/?id=ED427083`.

[13] B. Kartowagiran, Sugiman, and V. Pandra. Mathematics test development by item response theory approach and its measrument on elementary school students. *Turkish journal of computer and mathematics education*, 12(5):464–483, 2021. ISSN 1309-4653.

[14] F. M. Lord. *Applications of Item Response Theory To Practical Testing Problems*. Routledge, Nov. 2012. ISBN 9781136557248. URL `http://dx.doi.org/10.4324/9780203056615`.

[15] I. Mekterović, L. Brkić, and M. Horvat. Scaling automated programming assessment systems. *Electronics*, 12(4), 2023. ISSN 2079-9292. URL `https://www.mdpi.com/2079-9292/12/4/942`.

[16] C. Mutluer and M. Cakan. Comparison of test equating methods based on classical test theory and item response theory. *Journal of Uludag University Faculty of Education*, 2023. ISSN 2667-6788.

[17] T. Raykov and G. A. Marcoulides. On the relationship between classical test theory and item response theory: From one to the other and back. 76(2):325–338, 2016. ISSN 0013-1644.

[18] C. Stage. Classical test theory or item response theory: The swedish experience. *Journal of Uludag University Faculty of Education*, 2003. ISSN 1100-696X.

[19] F. Wulandari, S. Hadi, and H. Haryanto. Computer-based adaptive test development using fuzzy item response theory to estimate student ability. *Computer Science and Information Technology*, 8(3):66–73, 2020. ISSN 2331-6063.

[20] H. Yilmaz. A comparison of irt model combinations for assessing fit in a mixed format elementary school science test. *International Electronic Journal of Elementary Education*, 11:539–545, 06 2019.

Enhancing venous leg ulcer images via style mixing generation

[1]*Dávid Jozef Hreško (3rd year),*
Supervisor: [2]*Peter Drotár*

[1,2]IISLab, FEI TU of Košice, Slovak Republic

[1]david.jozef.hresko@tuke.sk, [2]peter.drotar@tuke.sk

***Abstract*—Leg ulcers resulting from impaired venous blood return are a prevalent type of chronic wound, significantly impacting the quality of life for affected individuals. Therefore, timely assessment and appropriate treatment are crucial to facilitate their healing process. Collecting high-quality wound data is vital for effective clinical management, allowing for the monitoring of healing progress and potentially training machine learning models to predict healing outcomes. However, obtaining a sufficient volume of quality data from individuals with leg ulcers is challenging. To address this, we propose using a generative adversarial network based on the StyleGAN architecture to synthesize new images from existing samples. These synthesized images were then validated by two clinicians.**

***Keywords*—leg ulcers, generative networks, style mixing, medical imaging**

I. Introduction

Venous leg ulcers represent the most prevalent form of chronic wounds [1]. These wounds exert a substantial adverse influence on the well-being of individuals affected by them, leading to heightened healthcare utilization and imposing significant economic burdens [2], [3]. Timely evaluation and intervention for such wounds could enhance treatment outcomes. In a prior investigation, we utilized 64 thermal images of venous leg ulcers obtained during initial assessments to illustrate that healing status could be forecasted with a sensitivity of 78.57% and a specificity of 60% through the utilization of an optimized Bayesian neural network [4]. To refine the performance of the healing prediction model, additional samples for training are imperative. However, gathering data on venous leg ulcers necessitates the involvement of trained personnel, rendering data acquisition costlier and often time-consuming.

In our context, we employed the StyleGAN architecture [5] due to its status as the current state-of-the-art in generative models, capable of delivering impressive outcomes across various domains. From a medical standpoint, this architecture has previously been adeptly adapted to generate diverse 3D medical images across different modalities, including MRI and CT scans [6]. Additionally, StyleGAN has been effectively utilized to produce realistic high-resolution samples of retina images [7]. Drawing from our understanding, we introduced a novel approach primarily focused on VLU data and its synthetic counterpart.

II. Methodology

A. Dataset

This study is part of a longitudinal observational study of venous leg ulcers [4], [8]. RGB images of the leg ulcers from 56 older patients were used. The participants were recruited from metropolitan Melbourne, Australia with informed consent. The images were collected by a trained person at the initial visit and at weeks 1, 2, and 4 using a DSLR camera. Some participants had multiple wounds. The image resolution was 3264×1836 pixels. In the present study, 264 images were used as input for the synthesizing process.

B. Preprocessing

We initiated our experiments by implementing preprocessing procedures. Initially, we standardized the orientation of the original images to ensure horizontal alignment. Subsequently, we resized the images to dimensions of 256x256 pixels.

C. GAN architecture

To create synthetic images, we employed a generative adversarial network (GAN) based on the StyleGAN architecture [5], as illustrated in Fig. 1. Specifically, we utilized the latest iteration of StyleGAN, known as StyleGAN v3 [9]. A key element of StyleGAN is its generator architecture, called Progressive GAN, which facilitates the generation of high-resolution images by initially producing lower-resolution images and progressively enhancing their resolution. Another enhancement is the incorporation of a generative technique called style-mixing, enabling the manipulation of specific visual attributes. Furthermore, StyleGAN introduces a method called style-modulation, allowing for the adjustment of style strength in the generated images, thereby enhancing their realism.

D. Training details

For our training regimen, we opted for the translation variant of StyleGAN, known as StyleGAN-T, primarily because the translation operation was more suited to our dataset's natural characteristics. The batch size was set to 32, with a regularization weight γ of 2, a per-GPU batch size of 16, and a snapshot frequency of 10. Although optional augmentation with random x-flips was disabled during training, we retained other augmentation techniques such as scaling, rotation, and other visual modifications. The training process spanned 15000

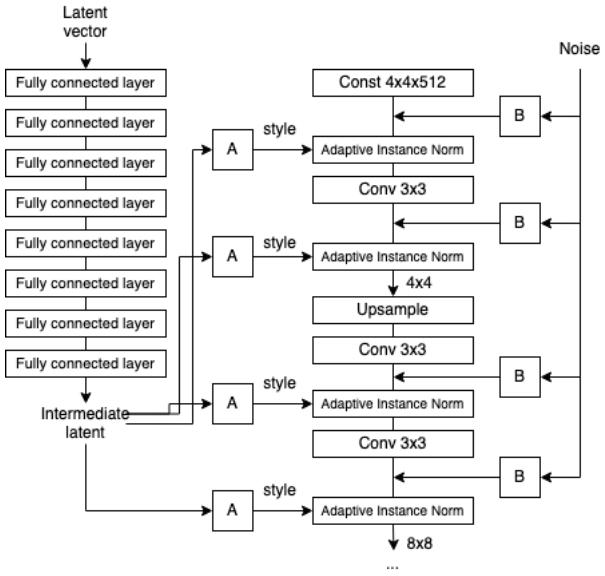

Fig. 1: Overview of the StyleGAN concept. Here "A" refers to the learned affine transform, and "B" represents learned per-channel scaling factors to the noise input.

Fig. 2: Examples of synthetic VLU images

epochs. We employed the Adam optimizer for both networks, with beta values set to 0 and 0.99. The initial learning rate was configured at 0.0025, with an ϵ value of $1e-08$. For the loss function, we utilized the standard implementation used in the second version of StyleGAN, with the R1 regularization parameter set to 2.

III. Results

A. Qualitative results

Two clinicians were asked to evaluate the quality of the synthetic images. The initial clinician accurately identified seven synthetic images, misclassifying one genuine image, and expressed uncertainty regarding two images (one original and one synthetic). Meanwhile, the second clinician correctly identified seven synthetic images but misclassified three genuine images. Notably, both clinicians provided identical feedback for the six synthetic images.

B. Quantitative results

Throughout the entire training process, we calculated the Frechet Inception Distance (FID) [10]. The initial metric value stood at 590.16, with the lowest recorded value being 95.49, achieved after 8000 epochs. The average FID value amounted to 116.89. These findings suggest that the model's performance progressively improved over time, resulting in the generation of increasingly realistic images. Example images can be seen in figure 2

IV. Conclusion

In this study, we introduced a GAN based on the StyleGAN v3 architecture to generate synthetic VLU images. Two clinicians evaluated the synthetic images, and although they could correctly identify seven out of ten images, their feedback varied. This underscores the importance of meticulously validating synthetic data by experts before integrating it into training datasets. One major limitation is that the GAN was trained solely on data from a single source, potentially resulting in bias towards our dataset in the synthesized images. To mitigate this limitation, we intend to expand our dataset by acquiring additional data for GAN training. Our future research will focus on optimizing network parameters to produce higher-quality synthetic images, which can serve as training samples for automated wound segmentation algorithms.

References

[1] L. Martinengo, M. Olsson, R. Bajpai, M. Soljak, Z. Upton, A. Schmidtchen, J. Car, and K. Järbrink, "Prevalence of chronic wounds in the general population: systematic review and meta-analysis of observational studies," *Annals of epidemiology*, vol. 29, pp. 8–15, 2019.

[2] F. L. Joaquim, R. M. C. R. A. Silva, M. P. Garcia-Caro, F. Cruz-Quintana, and E. R. Pereira, "Impact of venous ulcers on patients' quality of life: an integrative review," *Revista brasileira de enfermagem*, vol. 71, pp. 2021–2029, 2018.

[3] N. Graves, C. Phillips, and K. Harding, "A narrative review of the epidemiology and economics of chronic wounds," *British Journal of Dermatology*, vol. 187, no. 2, pp. 141–148, 2022.

[4] Q. C. Ngo, R. Ogrin, and D. K. Kumar, "Computerised prediction of healing for venous leg ulcers," *Scientific Reports*, vol. 12, no. 1, p. 17962, 2022.

[5] T. Karras, S. Laine, and T. Aila, "A style-based generator architecture for generative adversarial networks," in *Proceedings of the IEEE/CVF conference on computer vision and pattern recognition*, 2019, pp. 4401–4410.

[6] L. Fetty, M. Bylund, P. Kuess, G. Heilemann, T. Nyholm, D. Georg, and T. Löfstedt, "Latent space manipulation for high-resolution medical image synthesis via the stylegan," *Zeitschrift für Medizinische Physik*, vol. 30, no. 4, pp. 305–314, 2020.

[7] M. Kim, Y. N. Kim, M. Jang, J. Hwang, H.-K. Kim, S. C. Yoon, Y. J. Kim, and N. Kim, "Synthesizing realistic high-resolution retina image by style-based generative adversarial network and its utilization," *Scientific Reports*, vol. 12, no. 1, p. 17307, 2022.

[8] M. Monshipouri, B. Aliahmad, R. Ogrin, K. Elder, J. Anderson, B. Polus, and D. Kumar, "Thermal imaging potential and limitations to predict healing of venous leg ulcers," *Scientific Reports*, vol. 11, no. 1, p. 13239, 2021.

[9] T. Karras, M. Aittala, S. Laine, E. Härkönen, J. Hellsten, J. Lehtinen, and T. Aila, "Alias-free generative adversarial networks," *Advances in Neural Information Processing Systems*, vol. 34, pp. 852–863, 2021.

[10] M. Heusel, H. Ramsauer, T. Unterthiner, B. Nessler, and S. Hochreiter, "Gans trained by a two time-scale update rule converge to a local nash equilibrium," *Advances in neural information processing systems*, vol. 30, 2017.

Digital Twin and Human-Machine Collaboration in Industry 5.0

[1]*Maroš KRUPÁŠ (2nd year),*
Supervisor: [2]*Iveta ZOLOTOVÁ, Consultant:* [3]*Erik KAJÁTI*

[1,2,3]Dept. of Cybernetics and Artificial Intelligence, FEEI TU of Košice, Slovak Republic

[1]maros.krupas@tuke.sk, [2]iveta.zolotova@tuke.sk, [3]erik.kajati@tuke.sk

***Abstract*—With the intent to further increase production efficiency while making human the centre of the processes, human-centric manufacturing focuses on concepts such as digital twins and human-machine collaboration. This paper presents summary of our research on these concepts, mainly including our conceptual framework and also analyzed enabling technologies and methods to facilitate the creation of human-centric applications in Industry 5.0. Finally, it presents expected future works of our research in this area.**

***Keywords*—digital twin, human-centric, human-machine collaboration, Industry 5.0**

I. Introduction

The emergence of the Digital Twin (DT) concept amidst industrial revolutions has reshaped industries, transforming approaches to design, monitoring, and maintenance. A DT, essentially a virtual replica of physical entities fueled by real-time data integration from sensors and IoT (Internet of Things) devices, serves as a dynamic tool for analysis and decision-making across their lifecycles. Concurrently, human-centric manufacturing seeks to prioritize human involvement in systems and processes, with Human-Machine Collaboration (HMC) aiming to combine human and machine strengths. Yet, existing HMC applications often prioritize productivity over human-centricity. This paper addresses the necessity of leveraging DTs to develop more human-centric HMC solutions. By examining current research and identifying enabling technologies and methods, it aims to pave the way for a systematic approach to creating human-centered applications in Industry 5.0.

II. Initial status

Previous year publication [1] presented the concept of Industry 5.0, its enabling technologies, and its three core values - human-centric, resilient and sustainable [2]. In regard to this concept and its human-centric value, the paper's main focus was also to provide an overview of the human-machine collaboration concept, which aims to enhance the working capabilities of humans and machines. In this case, new challenges for researchers and scientists arise when designing human-machine collaborative applications that put humans at the center of production while maintaining the flexibility and effectiveness of different applications. Last publication identified and presented these challenges based on recent literature and identified research gaps in this area. From the identified research gaps we chose to focus our research on identifying and implementing technologies and methods suitable for the different types of human-centered solutions. This included improving enabling technologies to their full potential when designing DT of HMC and utilize them together in a synergistic manner.

III. Objectives solved in previous year

We started with the development of a systematic approach for designing human-centric applications. Based on identified research challenges and enabling technologies, we proposed a reference framework in our paper [3] to enable the development of the human-centric human-machine collaboration workspace, involving various heterogeneous robots, including UGVs (Unmanned Ground Vehicles) and UAVs (Unmanned Aerial Vehicles). To further develop this framework, we aimed to explore how DTs can be utilized to foster more human-centric solutions in the realm of HMC and therefore we delved into the current state of research on human-centric applications that involve DTs in HMC settings. Our focus shifted on comprehensive identification of the enabling technologies and methodologies that support the development of human-centric applications combining DTs with HMC.

We focused on several key enabling technologies highlighted in the official Industry 5.0 document [4] and the literature identified. Selecting appropriate DT tools is crucial for implementing key HMC technologies like AI (Artificial Intelligence) and HMI (Human-Machine Interaction) methods. The variety of methods and techniques can make selecting the right ones challenging. Identifying common and uncommon use cases for DT technologies in the HMC domain aids organizations in leveraging this technology for operational and process improvement, focusing on human-centered applications. In our review paper [5], we divided the identified technologies into 4 categories and found multiple examples in literature for each category.

First category is *DT and simulation*, where crucial tools like simulation platforms, software, and communication frameworks are pivotal. A five-dimension DT model serves as a reference for applying DT technology across different domains. HMC DT applications include safety, ergonomics, maintenance, task planning, optimization, testing, and training. Various methods utilize DTs for tasks like safe robot-human interactions, ergonomic optimization, decision support, and human action recognition. Simulation technologies aid in designing and testing safe HMC workspaces. Some of the

most common tools for HMC include Unity, Robot Operating System, Matlab, V-REP and Tecnomatix Process Simulate.

Second category is *AI*, which is particularly emphasized for its integration into DTs. Specific AI methods and tasks tailored for various HMC challenges were identified, focusing on safety, ergonomics, efficiency improvements, and more. Notably, artificial neural networks are frequently used for tasks like computer vision, while traditional AI methods and Deep Learning offer distinct advantages. Reinforcement Learning and Generative AI present innovative approaches, while Multimodal and Composite AI push the boundaries of AI research, enhancing performance and capabilities across diverse applications.

Third category of technologies includes *human-machine interaction* technologies, particularly in bridging interactions between the physical and virtual worlds. These technologies play a crucial role in enhancing human-centric aspects of DTs, aiding in various HMC applications by offering intuitive data visualization and interaction methods. Interactive digital interfaces, such as touch interfaces and web interfaces, provide efficient ways for humans to engage with technological systems, while immersive interfaces like Augmented Reality (AR) and Virtual Reality (VR) blend the physical and digital worlds, offering unique modes of immersion and interaction. Natural Interaction Interfaces (NUIs) and multimodal interfaces enable more intuitive interaction, incorporating gestures, voice commands, motion, and gaze tracking. Human-focused sensors, including localization sensors and physiological sensors, gather digital data from humans and physical systems, crucial for enhancing user experience and safety in various applications. These sensors play a vital role in understanding human behavior and intentions during interactions with machines, offering valuable insights for HMC systems.

Fourth category covers *data transmission, storage, and analysis technologies*, facilitating a constant flow of data between physical and digital entities. Data transmission, often facilitated by advanced IoT devices and sensors, continuously gathers data from the physical counterpart and transmits it to the digital model for real-time updates. Cloud-based storage solutions securely store vast amounts of data, enabling scalability, accessibility, and redundancy. Leveraging AI and machine learning algorithms, digital twins process and analyze incoming data, predicting future states and simulating scenarios for optimization. Cloud computing offers scalable resources, while fog computing brings cloud capabilities closer to the data source. Edge computing processes data near its source, enhancing security, reliability, and privacy, crucial in scenarios like healthcare and human safety. Task offloading, using innovative solutions like deep reinforcement learning, addresses challenges in scenarios requiring low latency and limited computation hardware. Edge-based digital twins offer superior value with reduced latency, facilitated by ongoing advancements in Edge AI and AI-enabled hardware. Integration of big data analytics with human-machine collaboration driven by digital twin technology enhances management approaches, promoting efficiency and precision in various industrial scenarios.

IV. Future work and conclusion

Our research aims to provide analysis of suitable technologies and methods for developing human-centered human-machine collaboration applications, enhancing the understanding of human-centric design in Industry 5.0. By analyzing the impact and significance of these identified enabling technologies and methods in the implementation of digital twins across various human-machine collaboration applications, we can offer new insights into the role of digital twins, contributing to the knowledge on digital twin technology and its applications in various industrial contexts. Next step will be to propose an updated version of the framework for the integration of diverse enabling technologies in Industry 5.0, providing a systematic approach to technology selection and integration. The goal of the framework is to be applied to various industrial scenarios to test its effectiveness in achieving synergistic technology integration.

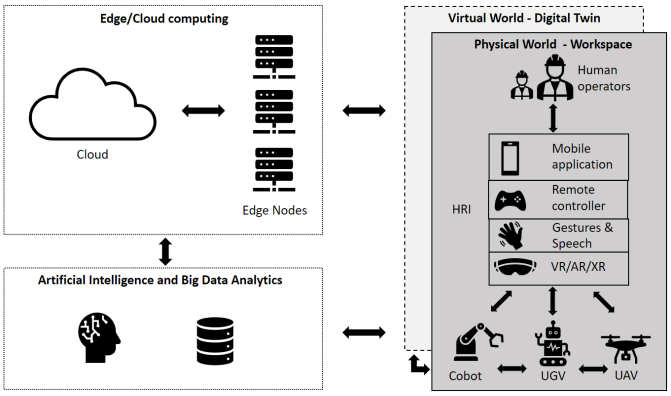

Fig. 1. Human-centric human-robot collaboration conceptual framework

Furthermore, we define criteria, metrics, and guidelines for selecting appropriate technology combinations for different use cases, considering factors like efficiency cost-effectiveness, user-friendliness, ease of implementation and human-centricity. We will design and create prototype case studies or experiment applications based on our framework, focusing on user experience and efficiency in digital twin-driven human-machine collaboration to understand the practical implications, limitations, and benefits of these technologies in different industry contexts. In the final steps we evaluate the performance, scalability, and adaptability of these applications based on our defined criteria and metrics in simulated or real-world settings using devices such as UAVs or UGVs.

Acknowledgment

This publication was supported by the VEGA grant EDEN: EDge-Enabled intelligeNt systems (1/0480/22).

References

[1] M. Krupas, *23rd Scientific Conference of Young Researchers Proceedings from Conference*. Kosice: Faculty of Electrical Engineering and Informatics, Technical University of Košice, 4 2023, p. 80–83.

[2] E. Commission, D.-G. for Research, Innovation, M. Breque, L. De Nul, and A. Petridis, *Industry 5.0 – Towards a sustainable, human-centric and resilient European industry*. Publications Office of the European Union, 2021.

[3] M. Krupas, S. Chand, Y. Lu, X. Xu, E. Kajati, and I. Zolotova, "Human-centric uav-ugv collaboration," in *2023 IEEE 19th International Conference on Automation Science and Engineering (CASE)*. IEEE, 2023, pp. 1–6.

[4] E. Commission, D.-G. for Research, Innovation, and J. Müller, *Enabling Technologies for Industry 5.0 – Results of a workshop with Europe's technology leaders*. Publications Office, 2020.

[5] M. Krupas, C. Liu, E. Kajati, and I. Zolotova, "Towards human-centric digital twin for human-machine collaboration: A review on enabling technologies and methods," *Sensors*, 2024. [in review process].

Simplified analytical model of a magnetoelastic Pressductor sensor for initial value setting of an optimization process

[1]*Šimon GANS (3rd year)*
Supervisor: [2]Ján MOLNÁR

[1,2]Dept. of Theoretical and Industrial Electrical Engineering, FEI TU of Košice, Slovak Republic

[1]simon.gans@tuke.sk, [2]jan.molnar@tuke.sk

***Abstract*—The work addresses the development of a mathematical model of the Pressductor type sensor. The knowledge obtained from the model is used to guess an geometric configuration that maximizes its sensitivity. The model is verified via FEM simulations. The optimal geometry guess is used as an initial state in an optimization problem to find the optimum when additional factors are considered. The results show that the initial guess was reasonable and the model is usable.**

***Keywords*— Magnetoelasticity, Model, Pressductor, Simulation.**

I. Introduction

Mathematical models of magnetoelastic sensors are a powerful tool for analyzing their operation without laborious experimental preparation of samples [1]. However, creating analytical models is mathematically challenging and usually FEM models [2] or direct experimentation [3] are used. Various non-linear and hysteretic behaviors which are typical for magnetic materials make derivations impossible [4]. Therefore nearly all mathematical models work with simplified physics that still yield information about the workings of the system [5].

In optimization problems a set of parameters is introduced that affects the system in various ways. A cost function for determining the performance. is required. An optimum is found by either minimizing or maximizing the function using various algorithms [4]. Optimization problems with many parameters tend to be time-consuming, because of the search space size so finding the optimum can be a problematic [6].

Additional knowledge in the form of a simple analytical model can cut down the search space size by ruling out some obviously non-optimal parameter combinations.

II. Model Simplifications

The proposed model assumes material isotropy and linearity. Demagnetizing fields due to the shape anisotropy are neglected since they cannot be solved for analytically [7].

Because the sensors are made of thin silicon steel sheets, the effect of eddy currents is surpressed to some extent. Under a certain magnetizing frequency value the eddy current effect can be neglected entirely [8].

When a mechanical force is applied internal stresses exist. Holes make the mechanical field around them inhomogeneous [9]. The effect of holes can be neglected if they are relatively small and far apart.

III. Stress vectors

The action of force is modeled with a homogeneous mechanical stress field that is defined by a $\boldsymbol{\sigma}$ vector with the same direction as the force by eq. (1),

$$\vec{\sigma} = \sigma(\cos(\beta)\,\vec{\imath} + \sin(\beta)\vec{\jmath}) \tag{1}$$

where σ is the size of the stress and β is the angle between the $\boldsymbol{\sigma}$ vector and the positive direction of the x-axis as shown in Fig. 1. The change of magnetic properties of the medium due to stress is described in literature [8] by equation (2),

$$\Delta\mu = \frac{2\lambda_{ms}}{B_S^2}\mu^2\sigma \tag{2}$$

in which $\Delta\mu$ is the change of permeability, λ_{ms} is the coefficient of magnetostriction at saturation, B_s is the magnetic flux density at saturation and μ is the permeability of the unstressed material [8]. The magnetic flux vectors $\boldsymbol{B^F}$ have components defined by equation (3),

$$\overrightarrow{B^F} = \vec{B} + \overrightarrow{\Delta B^F} \tag{3}$$

where $\boldsymbol{B^F}$ is a superposition of the field with no action of stress $\boldsymbol{B}$ and its change due to the action of stress $\boldsymbol{\Delta B^F}$. which can be expressed by eq. (4).

$$\overrightarrow{\Delta B^F} = k\mu(\vec{B}\cdot\vec{\sigma})\frac{\vec{\sigma}}{|\vec{\sigma}|} \tag{4}$$

IV. Flux computation

The magnetic flux flowing through the sensing coil Φ is given by eq. (5), where S is the area of the sensing coil and $\boldsymbol{dS}$ is the normal vector to the area element.

$$\phi = \int_S \overrightarrow{B^F}\cdot\overrightarrow{dS} \tag{5}$$

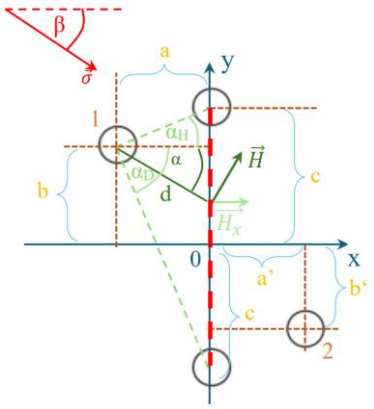

Fig. 1: The schematic of the system. The two magnetizing coil conductors have been labeled "1" and "2" and the numbers will be used as indexes in the further equations.

Without the action of force the magnetic flux equation (6) was derived.

$$\phi^0 = \frac{hc\mu N_1 I}{2\pi}\left(\frac{\cos^2(\alpha_D)-\cos^2(\alpha_H)}{a} - \frac{\cos^2(\alpha'_D)-\cos^2(\alpha'_H)}{a'}\right) \quad (6)$$

The evaluation of the flux in the stressed state Φ^F was derived as a superposition of fluxes $\Phi_1{}^F$ and $\Phi_2{}^F$ from eq. (7), (8) and (9).

$$\phi_1^F = \frac{hcN_1 Ik\sigma\mu^2}{4\pi a}\cos(\beta)\left((\cos(2\alpha_D - \beta) - \cos(2\alpha_H - \beta)) + 2\sin(\beta)(\alpha_D - \alpha_H)\right) \quad (7)$$

$$\beta' = \pi - \beta \quad (8)$$

$$\phi_2^F = -\frac{hcN_1 Ik\sigma\mu^2}{4\pi a'}\cos(\beta')\left((\cos(2\alpha'_D - \beta') - \cos(2\alpha'_H - \beta')) + 2\sin(\beta')(\alpha'_D - \alpha'_H)\right) \quad (9)$$

The total flux Φ through the secondary coil is expressed by eq. (10).

$$\phi = \phi^0 + \phi_1^F + \phi_2^F \quad (10)$$

V. Induced Voltage Evaluation

When we consider the applied force to be static, then the only time-dependent variable is the magnetizing current. Assuming that the current is harmonic, then the induced voltage is defined by equation (11),

$$u(t) = -(C_1 + k_1\sigma\mu C_2)N_1 N_2 \mu I_m \omega\cos(\omega t + \varphi) \quad (11)$$

in which C_1 and C_2 are constants entirely dependent on the coil placement and force direction. For sensing purposes the value of C_2 is important which defines the stress sensitivity.

VI. Optimization of a Finite Sensor Geometry

To optimize the coil placement of a real sensor a rectangular ferromagnetic sheet with dimensions of 48 mm x 16 mm x 0.3 mm was modeled via FEM software. The rules from the mathematical model have been followed to guess the optimal geometry (**Fig. *2***). The positions of the coils have been parametrized optimized to maximize the flux change due to force. The cost function was defined by equation (31),

$$cost = -|\phi_{1N} - \phi_{0N}| \quad (31)$$

where Φ_{1N} and Φ_{0N} are fluxes flowing through the secondary coil when a force of 1 N and 0 N respectively. The minus sign ensures that optimum occurs when the cost function is minimized.

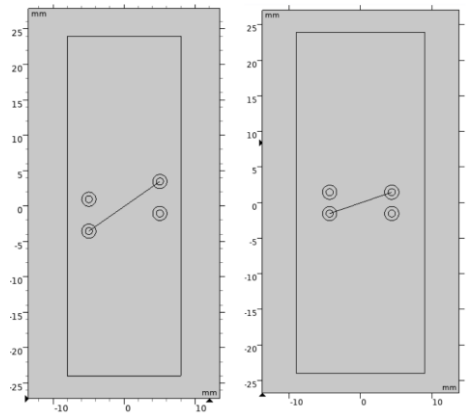

Fig. 2: The initial geometry of the sensor due to knowledge obtained from the simplified model - left and the optimized geometry when additional factors were considered – right.

VII. Conclusion

The initial parameter values selected by the model were used for further optimization where more physical phenomena are considered (finite sensor dimensions, stress inhomogeneities around holes, etc.) which the analytical model neglected.

Giving the material a specific shape affects the distribution of the magnetic field. Tests have shown that the agreement of the model with FEM simulations when the simplifications hold true is very good. The optimization problem took approximately 10 minutes on an Intel i5-8300H CPU with 16 GB of RAM via a MATLAB script [10].

For further work an analytical model for anisotropic materials is being developed.

References

[1] Dapino M., Calkins T., Smith R., Flatau A., A Magnetoelastic Model For Magnetostrictive Sensors, North Carolina State University, Center for Research in Scientific Computation, Raleigh, 2002. Available on the internet at: https://www.researchgate.net/publication/228601359_A_magnetoelastic_model_for_Villari-effect_magnetostrictive_sensors?_tp=eyJjb250ZXh0Ijp7InBhZ2UiOiJwdWJsaWNhdGlvbiIsInByZXZpb3VzUGFnZSI6bnVsbH19

[2] Nowicki M., Tensductor – Amorphous Alloy Based Magnetoelastic Tensile Force Sensor, Sensors, 2018, 18(12), 4420., doi: 10.3390/s18124420

[3] Gans Š., Molnár J., Kováč D., Kováčová I., Fecko B., Bereš M., Jacko P., Dziak J., Vince T., Driving Signal and Geometry Analysis of a Magnetoelastic Bending Mode Pressductor Type Sensor, Sensors, 23(20), 8393, doi: 10.339/s23208393

[4] Gans Š., Molnár J., Kováč D., Estimation of Jiles-Atherton Parameters of Toroid Cores Using MATLAB/Simulink, Acta Physica Polonica A, 2023, Vol. 143, No. 5, pp. 345-414, doi: 10.12693/APhsyPolA.143.389

[5] Zhang Q., Su Y., Zhang L., Luo J., Magnetoelastic Effect-Based Transmissive Stress Detection for Steel Strips: Theory and Experiment, Sensors, 2016, 16(9), 1382, doi: 10.3390/s16091382.

[6] Marion R., Scorretti R., Siauve N., Raulet M., Krähenbühl, Identification of Jiles-Atherton model parameters using Particle Swarm Optimization, IEEE Transactions on Magnetics, 2008, Vol.44, Issue 6, pages 894-897, doi: 10.1109/TMAG.2007.914867

[7] Tu Y.O, Calculation of demagnetizing field by means of FFT, Mathematics and Computers in Simulation, 1978, Vol. 20, Issue 4, pages 271-284, doi: 10.1016/0378-4754(78)90019-8.

[8] Tomčíková I., Modeling of Magnetic Field Distribution in Magnetoelastic Force Sensor, 2018, 1(41). Available on the internet at: https://www.researchgate.net/publication/266292425_MODELING_OF_MAGNETIC_FIELD_DISTRIBUTION_IN_MAGNETOELASTIC_FORCE_SENSOR

[9] Tomčíková, I., Kováč D., Kováčová I., Stress Field Distribution in Magnetoelastic Pressure Force Sensor, Communications – Scientific Letters of the University of Žilina, 2010, 12(1), pages 16-19, doi: 10.26552/com.C.2010.1.16-19

[10] MathWorks MATLAB documentation, fminsearch. Documentation for MATLAB version R2023b. Available on the internet at: https://www.mathworks.com/help/matlab/ref/fminsearch.htm

Utilizing WAMPAC and Artificial Intelligence for real-time control in power

[1]*Marek BOBČEK (1st year)*
Supervisor: [2]Zsolt ČONKA

[1,2]Dept. of Electric Power Engineering, FEI TU of Košice, Slovak Republic

[1]marek.bobcek@tuke.sk, [2]zsolt.conka@tuke.sk

***Abstract*—This article explores the transformative impact of integrating deep learning into electrical power systems, energy management and grid optimization. Focusing on applications such as load forecasting, fault detection, and distributed energy resource integration.**

***Keywords*—WAMPAC, PHASOR, GRID, AI, PROTECTION**

I. WIDE AREA MEASUREMENTS PROTECTION AND CONTROL

Wide Area Measurement Protection and Control (WAMPAC) is a vital framework in electrical power engineering designed to revolutionize the monitoring, protection, and control of power systems across extensive geographic regions. The implementation of WAMPAC involves the integration of synchronized measurements from multiple locations within a power grid, allowing for real-time decision-making and enhancing the reliability and stability of the electrical network [1]. At the heart of WAMPAC lies the crucial technology of synchrophasors. Synchrophasors are precise measurements of voltage and current phasors, providing a comprehensive view of the power system's dynamic behavior [2]. Phasor Measurement Units (PMUs) are employed to capture these synchronized measurements at different locations in the power system [3]. These PMUs sample the waveforms at high frequencies, typically ranging from 30 to 60 samples per second, ensuring accurate and real-time data acquisition [2].The synchronization of phasor measurements is a key feature, allowing for a coherent representation of the system's instantaneous characteristics. This synchronization is essential for making informed decisions and gaining insights into the grid's overall health and performance [4].To enable the effective operation of WAMPAC, a robust communication infrastructure is imperative. The real-time synchronized measurements collected by PMUs need to be transmitted from various locations to a central control center for analysis and decision-making [5]. High-speed communication networks play a crucial role in facilitating rapid data exchange between the monitoring devices and the control center [5]. The implementation of WAMPAC's communication infrastructure ensures that the collected data is not only accurate but also timely. This is essential for the successful application of advanced analytics and algorithms in the central control center [5]. The synchronized phasor data from PMUs is sent to a central control center where sophisticated analytics and algorithms are applied for monitoring and analysis [6]. This centralized approach enhances the capabilities of power system operators to assess the overall health of the grid, detect anomalies, and make informed decisions in real-time [6].The use of advanced analytics allows for the identification of potential issues before they escalate, contributing to the overall reliability of the power system [6]. By leveraging a centralized monitoring and analysis framework, WAMPAC empowers operators to respond proactively to evolving grid conditions. WAMPAC goes beyond traditional protection mechanisms by enabling the development of wide-area protection schemes. These schemes are designed to respond to disturbances or faults over a large geographical area [7]. The analysis of synchronized data from PMUs allows protective relays to make faster and more accurate decisions, isolating faulty equipment and preventing cascading failures [7]. Wide-area protection capabilities of WAMPAC enhance the resilience of power systems, reducing the likelihood and impact of disruptions [7]. This is particularly crucial in the context of the increasing complexity and interconnectivity of modern power grids. In addition to protection, WAMPAC facilitates wide-area control strategies aimed at improving the stability of the power grid [8]. These strategies may involve adjusting generator setpoints, controlling power flow on transmission lines, or implementing remedial actions to address vulnerabilities within the system^[8^].Wide-area control strategies are essential for maintaining the balance and stability of the power grid, especially during dynamic events or disturbances [8]. The real-time data provided by WAMPAC allows for swift and coordinated actions to ensure the continued reliable operation of the electrical network. WAMPAC significantly enhances situational awareness for power system operators by providing a comprehensive and synchronized view of the entire grid [6]. The real-time and synchronized nature of synchrophasor data enables operators to detect and analyze disturbances, faults, or abnormal conditions promptly [6]. This enhanced situational awareness is a critical component of effective grid management. Operators can make timely decisions, implement appropriate control actions, and mitigate potential issues before they escalate, contributing to the overall resilience and reliability of the power system [6]. The implementation of WAMPAC is driven by several factors. The increasing complexity and interconnectivity of modern power systems pose challenges that traditional monitoring and control systems may struggle to address [9]. WAMPAC, with its emphasis on synchronized measurements and advanced control strategies,

offers a solution to these challenges [9]. Moreover, the need for improved reliability and resilience in power systems, coupled with advancements in technology, has propelled the adoption of WAMPAC [9]. The ability to make real-time decisions based on synchronized and accurate data positions WAMPAC as a key enabler for the efficient and stable operation of electrical power networks. Wide Area Measurement Protection and Control (WAMPAC) is a transformative framework in electrical power engineering [6]. Synchrophasors, with their synchronized and high-frequency measurements, form the backbone of WAMPAC, providing a coherent view of the power system's dynamic behavior [2]. The integration of advanced communication infrastructure, centralized monitoring, and analysis, as well as wide-area protection and control strategies, collectively contribute to the enhanced reliability, stability, and resilience of electrical power networks. As power systems continue to evolve, WAMPAC stands as a critical technology that not only addresses current challenges but also prepares the grid for the demands of the future. The centralized approach to monitoring and control, coupled with the real-time capabilities enabled by WAMPAC, positions it as a cornerstone in the ongoing efforts to modernize and optimize electrical power systems.

II. DEEP LEARNING IN ELECTRICAL POWER SYSTEMS

In recent years, the fusion of deep learning techniques with electrical power systems and distributions has sparked a transformative revolution, reshaping the landscape of energy management and grid optimization [15]. Deep learning, a subset of machine learning that involves neural networks with multiple layers, has demonstrated unprecedented capabilities in deciphering intricate patterns within vast datasets [10]. This intersection of deep learning and power systems holds immense promise for addressing the evolving challenges faced by modern electrical grids, such as load forecasting, fault detection, and the integration of renewable energy sources. Traditional methods in power systems, while effective, often struggle to cope with the increasing complexity arising from the integration of diverse energy resources and the dynamic nature of modern power grids. Deep learning, with its ability to autonomously learn and adapt to complex patterns, presents a compelling alternative for addressing these challenges [17].

Load Forecasting: Load forecasting is a pivotal aspect of power system operation, influencing resource allocation, energy production planning, and overall grid reliability. Deep learning models, particularly recurrent neural networks (RNNs) and long short-term memory networks (LSTMs), have demonstrated exceptional capabilities in capturing temporal dependencies and non-linear patterns within historical load data [11]. The deep learning approach allows for more accurate and dynamic load forecasts, contributing to enhanced grid stability and efficiency. Research by Brownlee [11] highlights the application of deep learning models for multi-step time series forecasting in power usage. By leveraging Python-based frameworks, researchers and practitioners can harness the power of deep learning to predict future load demand with improved precision and efficiency.

Fault Detection: The reliable and timely detection of faults in power systems is crucial for maintaining grid resilience and minimizing downtime. Deep learning techniques, including convolutional neural networks (CNNs) and recurrent neural networks (RNNs), have proven effective in automating fault detection processes. Zeiler and Fergus [12] delve into the visualization and understanding of convolutional networks, shedding light on how these architectures can be applied to identify and classify faults in power systems. The ability of CNNs to recognize spatial patterns within data and RNNs to capture temporal dependencies makes them valuable tools in fault detection, ensuring a rapid response to mitigate potential disruptions.

Integration of Distributed Energy Resources: The integration of distributed energy resources, such as solar panels and wind turbines, into power grids introduces new challenges and opportunities. Deep learning models offer a robust framework for managing the uncertainties associated with these distributed sources and optimizing power flow in smart grids. Zhang and Hines [13] explore the role of deep learning in power systems, emphasizing its potential in addressing challenges related to distributed energy resources. The adaptive nature of deep neural networks enables them to learn from real-time data, facilitating optimal power flow management and contributing to the efficient utilization of renewable energy sources.

State Estimation and Energy Management: Deep learning techniques play a pivotal role in state estimation, a process critical for maintaining the stability and reliability of power systems. State estimation involves estimating the current operating state of the power grid based on available measurements. Deep learning models, with their ability to capture complex relationships in high-dimensional data, offer advantages in improving the accuracy of state estimation algorithms. Research by Wang et al. [14] explores the application of deep learning in power system state estimation. By incorporating neural network models into traditional state estimation frameworks, researchers have achieved notable improvements in estimation accuracy, particularly in scenarios with high penetration of renewable energy sources.

Challenges and Considerations: While the integration of deep learning into electrical power systems holds tremendous promise, several challenges and considerations must be addressed. One primary concern is the reliability and interpretability of deep learning models, especially in safety-critical applications. The "black-box" nature of deep neural networks raises questions about their trustworthiness and the ability to explain decisions made in critical scenarios [18]. Data quality and security also emerge as significant considerations. Deep learning models heavily rely on large and diverse datasets for training, and the quality of these datasets directly influences the performance of the models [16]. Ensuring the security of data and the robustness of deep learning models against adversarial attacks is paramount, especially in the context of critical infrastructure like power grids. Additionally, ethical considerations must be taken into account when deploying deep learning models in power systems. The potential biases embedded in training data and the implications of algorithmic decisions on different demographic groups or regions require careful examination [21]. A comprehensive and responsible approach to deploying deep learning in power systems necessitates a thorough understanding of the ethical implications and a commitment to addressing them.

The integration of deep learning into electrical power systems marks a paradigm shift in how we approach energy management, load forecasting, and grid optimization [19]. The ability of deep neural networks to autonomously learn and adapt to complex patterns positions them as valuable tools in addressing the evolving challenges of modern power grids. As research in this field progresses, it is crucial to strike a balance

between technological advancements and the ethical, security, and interpretability considerations necessary for the reliable operation of power grids in the deep learning era.

III.CONCEPT OF FAULT DETECTION AI

Algorithm phase 1:

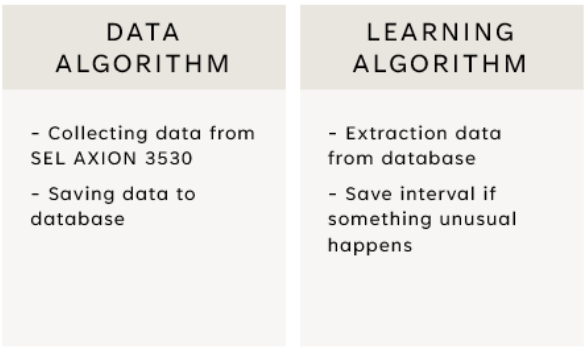

Fig. 1. First phase of algorithm

DATA ALGORITHM:

- Initialize connection to SEL AXION 3530.Set up data collection parameters (e.g., sampling frequency, data types).
- Begin data collection from SEL AXION 3530.
- Receive and store collected data in a temporary buffer.
- Periodically transfer the accumulated data to the database.
- Verify the integrity of the stored data.
- Log any errors or issues encountered during data collection.
- Repeat the data collection process based on the defined schedule or trigger events.

LEARNING ALGORITHM

- Extract data from the database.
- Analyze the data to identify patterns and trends.
- Utilize machine learning or statistical methods to learn normal system behavior.
- Establish a baseline for the collected data.
- Monitor for unusual events or anomalies in the system.
- If an anomaly is detected, save relevant information and timestamp to the database.
- Adjust the learning model based on new data and experiences.
- Periodically update the learned model to adapt to system changes.

Algorithm phase 2:

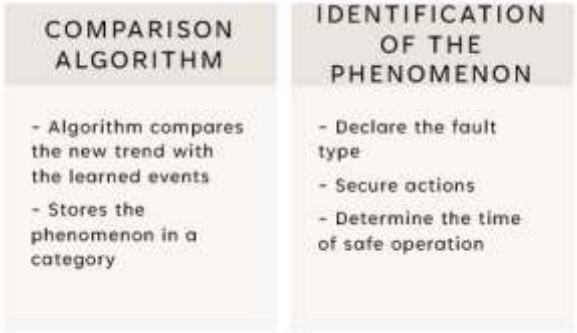

Fig. 2. Second phase of algorithm

COMPARISON ALGORITHM:

- Retrieve the latest trend or data from the system.
- Compare the new data with the learned events and baseline.
- Identify any deviations or anomalies in the current system behavior.
- Categorize the identified phenomenon based on predefined categories.
- Store the categorized information in the database for further analysis.
- Log any errors or issues encountered during the comparison process.

IDENTIF. OF THE PHENOMENON:

- Declare the fault type based on the categorized phenomenon.
- Secure actions by implementing predefined safety measures.
- Determine the time required for safe operation and fault resolution.
- Log the identified fault type, performed actions, and the estimated time for resolution.
- Communicate the identified fault type and recommended actions to relevant personnel or systems.

Final phase of algorithm:

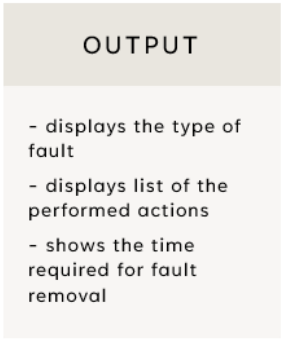

Fig. 3. Output from AI for Fault detection

The output of the system includes:

- Type of fault identified (e.g., voltage fluctuation, abnormal frequency).
- List of performed actions in response to the identified fault.
- Time required for fault resolution and restoration of normal operation.
- This information is presented in a format that is easily accessible to operators or monitoring systems, allowing for timely response and efficient management of system issues.

IV. CONCLUSION

Artificial Intelligence (AI) has emerged as a transformative force across various industries, revolutionizing the way we collect, analyze, and interpret data. The described set of algorithms showcases a sophisticated system designed for monitoring and managing complex systems, with a particular focus on the SEL AXION 3530 and fault detection. In this conclusion, we will delve into the broader implications, use cases, and potential of such AI applications. The Collecting Algorithm (Algorithm 1) serves as the foundational step in the entire process. By efficiently gathering data from the SEL

AXION 3530, it lays the groundwork for subsequent analysis and decision-making. This algorithm not only ensures the systematic collection of information but also highlights the importance of real-time data acquisition in industrial settings. The ability to seamlessly integrate with sensors and devices, such as the SEL AXION 3530, positions AI as a critical enabler for predictive maintenance and proactive fault detection. Moving to the Learning Algorithm (Algorithm 2), we see the emphasis on data extraction and anomaly detection. This step reflects the evolving landscape of machine learning, where algorithms can autonomously learn patterns and identify anomalies. The system's ability to save intervals when unusual events occur not only aids in troubleshooting but also contributes to the continuous improvement of the AI model. As datasets grow and the system learns from diverse scenarios, its predictive capabilities become more robust, providing a dynamic and adaptive solution for industrial operations. The Comparison Algorithm (Algorithm 3) takes the learned events and compares them with new trends, categorizing phenomena based on predefined patterns. This step demonstrates the power of AI in recognizing patterns that may not be apparent to human operators. By automating the comparison process, the system can swiftly identify deviations from normal behavior, enabling timely intervention and minimizing the risk of system failures. This algorithm serves as a testament to the efficiency gains and improved accuracy that AI brings to the field of fault detection and management. The Identification of the Phenomenon Algorithm (Algorithm 4) represents the culmination of the AI system's capabilities. By declaring the fault type, securing actions, and determining the time of safe operation, this algorithm provides a comprehensive solution for incident response. The ability to autonomously diagnose faults and prescribe corrective actions showcases the potential for AI to enhance the efficiency and reliability of industrial processes. This not only minimizes downtime but also contributes to the overall safety and longevity of critical infrastructure. The outputs generated by this AI system are tailored to meet the specific needs of industrial operators. Displaying the type of fault allows for quick identification and targeted responses. The list of performed actions provides transparency and accountability, aiding in post-incident analysis and continuous improvement. Additionally, the time required for fault removal serves as a crucial metric for evaluating system performance and optimizing maintenance schedules. The broader use of such AI applications extends beyond the specific example outlined here. In industrial settings, where the complexity of systems often surpasses human capacity for real-time monitoring, AI becomes an invaluable ally. Predictive maintenance, fault detection, and incident response are just a few areas where AI can significantly impact efficiency, reliability, and safety. One notable application is in the field of smart grids, where AI can optimize energy distribution, anticipate faults, and adapt to changing demand patterns. In healthcare, AI-driven diagnostic tools can enhance the accuracy and speed of disease identification, leading to more effective treatments. In finance, AI algorithms can analyze market trends, detect fraudulent activities, and optimize investment portfolios. The potential applications are vast, spanning across sectors and domains. However, as with any transformative technology, the widespread adoption of AI also raises ethical and societal considerations. Issues related to data privacy, algorithmic bias, and job displacement require careful attention and thoughtful regulation. The described AI system exemplifies the remarkable advancements in machine learning and data analytics, particularly in the context of industrial fault detection and management. The ability to collect, learn, compare, and identify phenomena in real-time showcases the transformative potential of AI in optimizing operations, improving safety, and reducing downtime.

ACKNOWLEDGMENT

This work was supported by the Ministry of Education, Science, Research and Sport of the Slovak Republic and the Slovak Academy of Sciences under the contract no. VEGA 1/0627/24

REFERENCES

[1] A. G. Phadke and J. S. Thorp, Synchronized Phasor Measurements and Their Applications, Springer Science & Business Media, 2008
[2] B. Gou, Y. Liu, and F. Wu, High-speed Synchrophasor Technology: Architectures and Applications, CRC Press, 2015
[3] P. K. Dash and D. Thukaram, Synchrophasor Applications in Power Systems, CRC Press, 2016
[4] Y. Zhang, Y. Li, and Y. Zhong, "Phasor Measurement Unit Placement in Power Systems for State Estimation," IEEE Transactions on Power Systems, vol. 31, no. 5, pp. 3541–3551, 2016
[5] P. Hines, S. Blumsack, and E. Cotilla-Sanchez, "Do we need a power grid 'Apollo program'?," IEEE Power and Energy Magazine, vol. 7, no. 2, pp. 52–59, 2009
[6] A. G. Phadke and J. S. Thorp, "Wide-area measurement systems in power systems," IEEE Transactions on Power Systems, vol. 25, no. 1, pp. 97–104, 2010
[7] Y. Gu, Y. Tang, and B. F. Wollenberg, "Wide-area monitoring, protection and control in power systems," Proceedings of the IEEE, vol. 99, no. 1, pp. 80–93, 2009
[8] Y. Zhang, X. Fu, and Y. Liu, "Wide-Area Control in Power Systems with Real-Time Communication: A Review," IET Cyber-Physical Systems: Theory & Applications, vol. 1, no. 1, pp. 13–27, 2013
[9] L. Mili and Q. Chen, Smart Grids: Advanced Technologies and Solutions (2nd ed.), CRC Press, 2017
[10] Wang, C., Huang, J., & Wang, J. (2018). "A Comprehensive Review on Load Forecasting Methods." Energies, 11(5), 1194
[11] Brownlee, J. (2018). "How to Develop Multi-Step Time Series Forecasting Models for Power Usage with Python." Machine Learning Mastery
[12] Zeiler, M. D., & Fergus, R. (2014). "Visualizing and Understanding Convolutional Networks." In European Conference on Computer Vision (ECCV)
[13] Zhang, Y., & Hines, P. D. (2017). "Deep Learning in Power Systems." Proceedings of the IEEE, 105(11), 2011-2015
[14] Wang, B., Li, C., & Zeng, P. (2019). "Deep Learning-Based Power System State Estimation." IEEE Transactions on Power Systems, 34(1), 735-746
[15] Khojasteh, Y., & Abedinia, O. (2020). "Deep Learning Applications in Power Systems: A Comprehensive Review." Energies, 13(14), 3519.
[16] Huang, J., Wang, C., & Wang, J. (2020). "Deep Learning for Short-Term Load Forecasting in Distribution Systems." Energies, 13(7), 1614
[17] Taylor, J., Rodriguez, D., & Marzband, M. (2021). "Deep Learning Techniques for Fault Detection and Classification in Power Systems: A Review." IEEE Access, 9, 15868-15887
[18] Liu, Z., Wu, Y., & Wu, D. (2019). "Deep Learning Applications in Power System State Estimation: A Review and Comparative Study." Energies, 12(24), 4693
[19] Mishra, S., & Saxena, A. (2018). "Applications of Deep Learning Techniques in Load Forecasting: A Review." In 2018 IEEE Calcutta Conference (CALCON)
[20] Chen, Y., & Zhang, X. (2019). "Deep Learning Applications in Power Systems Fault Diagnosis." In 2019 8th International Conference on Renewable Energy Research and Applications (ICRERA)
[21] Gao, W., Li, Q., & Cai, Z. (2020). "Deep Learning-Based Short-Term Load Forecasting: A Review and Future Directions." Energies, 13(20), 5412

Effect of dopant on Ag_2S properties

[1]*Gabriela HRICKOVA (3rd year)*
Supervisor: [2] Peter Lukacs

[1,2] Department of Technologies in Electronics, Faculty of Electrical Engineering and Informatics, TUKE, Slovakia

[1]gabriela.hrickova@tuke.sk, [2]peter.lukacs@tuke.sk

***Abstract*— Thermoelectric materials are a group of materials that can generate small amounts of energy at the temperature difference between the environment and the application itself. Wearable electronics are one application in which these materials could be used as an energy alternative. Silver sulfide, a ductile semiconducting material, is one of the promising compounds for thermoelectric use. We can enhance the properties of the Ag_2S material by selecting the appropriate dopants. This paper examines the influence of Ge on the thermoelectric properties of Ag_2S samples.**

***Keywords*—Ag_2S, Ge, thermoelectric properties**

I. Introduction

The thermoelectric effect is the direct transformation of temperature difference into electric voltage, or vice versa, in a thermoelectric couple. The generation of electric voltage occurs when a temperature difference is applied to a thermoelectric material. This effect is also reversible, meaning that when electric voltage is applied to the opposite ends of a thermoelectric material, heat is transferred from one end to the other, creating a temperature difference between the ends. There are three thermoelectric effects: the Seebeck effect, the Peltier effect, and the Thomson effect [1], [2], [3], [4]. Thermoelectric effects have served as the base for the development of a variety of industrial, medical, and military applications over the past decade. Many possibilities exist for the most excellent thermoelectric materials [5], [6], [7], [8]. Ag_2S is a promising material applicable to thermoelectric generators. It is a ductile material [9], [10], [11], [12], so it can be used as a base for thermoelectric devices that will be subjected to a mechanical load.

II. Samples' preparation and measurement

A. Samples' preparation

Pure Ag, S, and Ge powders were used to create the Ag_2S-based samples. The pure powders were mixed in respective proportions to produce the following powder mixtures: Ag_2S, $Ag_2Ge_{0.05}S_{0.95}$, $Ag_2Ge_{0.1}S_{0.9}$, $Ag_2Ge_{0.2}S_{0.8}$ and $Ag_2Ge_{0.3}S_{0.7}$ (at. ratio). Next, the powder mixtures were annealed for 10 hours at 160°C in a steel container under an argon atmosphere to produce homogenous α-Ag_2S-based powders. The temperature of annealing was chosen to prevent the formation of β-Ag_2S in the powders. Annealing powders have been produced into 4-millimeter-diameter rods via cold extrusion.

B. Chemical composition and microscopy analysis of microstructure

Two scanning electron microscopes (SEM): Tescan Vega 3 LMU and JEOL JSM 7000F, were used to analyse the chemical composition and microstructure of the samples. Each microscope was equipped with an elemental energy dispersive X-ray (EDX) analyser. The JEOL JSM 7000F was used to verify the chemical composition, while the Tescan Vega 3 LMU was used to map the elemental composition using EDX (Fig. 1). Prior to each SEM examination, the rod specimens were cut into 10-millimeter-long parts.

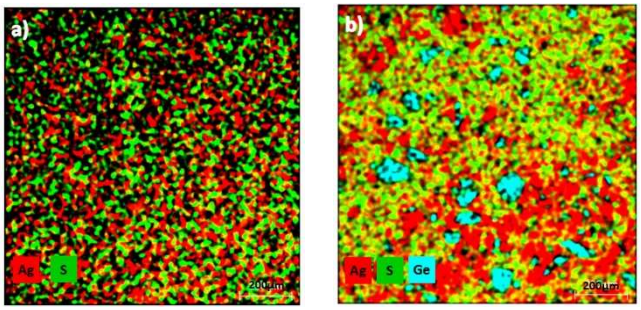

Fig. 1 Composite elemental distribution from TESCAN EDX mapping a) Ag_2S, b) $Ag_2Ge_{0.3}S_{0.7}$.

C. X-ray diffraction analysis of microstructure

Powder samples were measured by X-ray diffraction to define phase composition and unit cell parameters for α-Ag_2S using Philips X'Pert Pro Diffractometer (Cu X-ray tube, $\lambda = 1.5418$ Å). Fig. 2 represent X-ray diffraction analysis of Ag_2S-based doped Ge. Purple vertical lines represents position of diffraction peaks from the COD database [13], black line represent Ag_2S, navy line represent $Ag_2Ge_{0.05}S_{0.95}$, green line represent $Ag_2Ge_{0.1}S_{0.9}$, light magenta represent $Ag_2Ge_{0.2}S_{0.8}$, and light blue represent $Ag_2Ge_{0.3}S_{0.7}$.

D. Thermoelectric properties

The aim of the measurement of selected thermoelectric parameters was to determine the impact of doping on the properties of the Ag_2S-based material. The Seebeck coefficient, and conductivity were measured with a laboratory developed apparatus. Power factor (PF) has been calculated using the following equation:

$$PF = \alpha^2.\sigma \qquad (1)$$

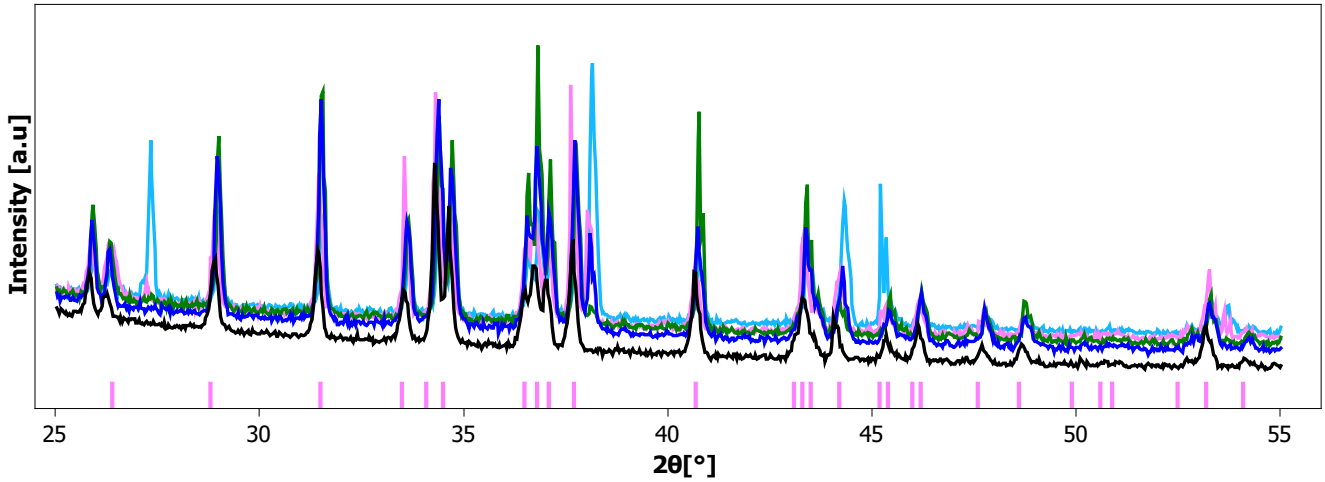

Fig. 2 X-ray diffraction analysis of $Ag_2Ge_xS_{(1-x)}$

Tab. 1 Thermoelectric properties of $Ag_2Ge_xS_{(1-x)}$

	Ag_2S	$Ag_2Ge_{0.05}S_{0.95}$	$Ag_2Ge_{0.1}S_{0.9}$	$Ag_2Ge_{0.2}S_{0.8}$	$Ag_2Ge_{0.3}S_{0.7}$
σ [S.m^{-1}]	0.102	2.35	14.24	58.23	5106.23
α [μV.K^{-1}]	-1051	-408	-397	-243	-87
PF [mV^2.S.m.K^{-2}]	113	393	2239	3428	38725

III. Conclusion

The incorporation of Ge doping significantly improves the thermoelectric characteristics of materials based on Ag_2S. Pure Ag_2S has a PF value that is nearly zero, whereas the addition of Ge doping substantially scale up the Seebeck coefficient. The sample consisting of $Ag_2Ge_{0.3}S_{0.7}$ has the greatest PF. The results indicate that the prepared material consists of two phases: Ag_2S and unincorporated Ge. The basic cell has the same dimensions as previously reported, and X-ray diffraction shows that each dopant has been partially incorporated into the Ag_2S structure. It is possible to argue that the dopant's incorporation into the Ag_2S compound was only partial. An alternate homogenization technique is required to achieve a more efficient synthesis between the dopant and the material. Bragg diffraction peaks exhibit a crystalline character, which is consistent with the available data. The absence of Ge in the base material is supported by elemental analysis and SEM EDX, which may be the result of synthesis errors. A different material synthesis method is necessary to achieve more effective integration.

The experiments' outcome suggests the potential application of materials in wearable electronic devices and sensors.

References

[1] M. Lundstrom and C. Jeong, *Near-equilibrium transport: fundamentals and applications*. in Lessons from nanoscience, no. v. 2. Singapore ; Hackensack, NJ: World Scientific, 2013.

[2] H. J. Goldsmid, *Introduction to Thermoelectricity*, vol. 121. in Springer Series in Materials Science, vol. 121. Berlin, Heidelberg: Springer Berlin Heidelberg, 2016. doi: 10.1007/978-3-662-49256-7.

[3] H. J. Goldsmid, 'The Thermoelectric and Related Effects', in *Introduction to Thermoelectricity*, vol. 121, in Springer Series in Materials Science, vol. 121. , Berlin, Heidelberg: Springer Berlin Heidelberg, 2016, pp. 1–7. doi: 10.1007/978-3-662-49256-7_1.

[4] H. J. Goldsmid, *The Physics of Thermoelectric Energy Conversion*. IOP Publishing, 2017. doi: 10.1088/978-1-6817-4641-8.

[5] J. Wei *et al.*, 'Review of current high-ZT thermoelectric materials', *J Mater Sci*, vol. 55, no. 27, pp. 12642–12704, Sep. 2020, doi: 10.1007/s10853-020-04949-0.

[6] W. A. D. M. Jayathilaka *et al.*, 'Significance of Nanomaterials in Wearables: A Review on Wearable Actuators and Sensors', *Adv. Mater.*, vol. 31, no. 7, p. 1805921, Feb. 2019, doi: 10.1002/adma.201805921.

[7] R. He, G. Schierning, and K. Nielsch, 'Thermoelectric Devices: A Review of Devices, Architectures, and Contact Optimization', *Adv. Mater. Technol.*, vol. 3, no. 4, p. 1700256, Apr. 2018, doi: 10.1002/admt.201700256.

[8] S. Yang, P. Qiu, L. Chen, and X. Shi, 'Recent Developments in Flexible Thermoelectric Devices', *Small Science*, vol. 1, no. 7, p. 2100005, Jul. 2021, doi: 10.1002/smsc.202100005.

[9] W.-X. Zhou, D. Wu, G. Xie, K.-Q. Chen, and G. Zhang, 'α-Ag $_2$ S: A Ductile Thermoelectric Material with High *ZT*', *ACS Omega*, vol. 5, no. 11, pp. 5796–5804, Mar. 2020, doi: 10.1021/acsomega.9b03929.

[10] M. Zhu, X.-L. Shi, H. Wu, Q. Liu, and Z.-G. Chen, 'Advances in Ag2S-based thermoelectrics for wearable electronics: progress and perspective', *Chemical Engineering Journal*, vol. 473, p. 145236, Oct. 2023, doi: 10.1016/j.cej.2023.145236.

[11] T. Wei, P. Qiu, K. Zhao, X. Shi, and L. Chen, 'Ag $_2$ Q-Based (Q = S, Se, Te) Silver Chalcogenide Thermoelectric Materials', *Advanced Materials*, vol. 35, no. 1, p. 2110236, Jan. 2023, doi: 10.1002/adma.202110236.

[12] H. Chen *et al.*, 'Room-temperature plastic inorganic semiconductors for flexible and deformable electronics', *InfoMat*, vol. 3, no. 1, pp. 22–35, Jan. 2021, doi: 10.1002/inf2.12149.

[13] S. Gražulis *et al.*, 'Crystallography Open Database (COD): an open-access collection of crystal structures and platform for world-wide collaboration', *Nucleic Acids Research*, vol. 40, no. D1, pp. D420–D427, Jan. 2012, doi: 10.1093/nar/gkr900.

The human aspect of explainable machine learning models

[1]*Miroslava MATEJOVÁ (2nd year)*
Supervisor: [2]Ján PARALIČ

[1,2]Dept. of Cybernetics and Artificial Intelligence, FEI TU of Košice, Slovak Republic

[1]miroslava.matejova@tuke.sk, [2]jan.paralic@tuke.sk

***Abstract*— The idea of explainability states that a machine learning model and its results can be sufficiently explained to a human being to be deemed acceptable. Including people in the process of developing explainable machine learning models is essential. But there are very few articles, which address the problem of specific explainability requirements of particular user types and how to address them. Therefore, requirements of the various stakeholder types are outlined in the article. When assessing explainable models using different metrics acquired through surveys or reviews, humans play a crucial role as well.**

***Keywords*—Explainability, explainable artificial intelligence, machine learning, user perspective**

I. Introduction

The swift development and application of Artificial Intelligence (AI) and Machine Learning (ML) technologies, specifically utilizing opaque deep neural networks, has generated significant curiosity regarding explainability - the ability to make AI algorithms comprehensible to humans. Artificial intelligence has impacted our lives in a variety of ways. Such systems can produce decisions that directly impact individuals, such as in the fields of security, transportation, and medicine. The risk comes from producing and applying results that are illogical, illegitimate, or that prevent a thorough explanation of their behavior from being obtained [1]. It is necessary to gain a deeper comprehension of how these models operate and what they produce. Enhancing the comprehension of models can also result in the fixing of any potential flaws in them. There is a large body of algorithmic work on explainable AI (XAI) due to the recent spike in interest in the field. As we identified in previous research [2], the user aspect is one of the most important factors in this area. Even though many people agree that explainability features are essential for AI systems, it's still unclear how to meet the needs of actual users who need to understand AI.

II. Types of stakeholders

The reasons for wanting to understand black box ML models vary. Everyone wants to look inside, but they want to do it for different reasons. Examples of high-level usage include e.g. debugging models, detecting bias and building trust [3]. This suggests that there are different groups of people with different interests in the explainability of AI systems: people who operate the systems, seek to improve them; other people are influenced by decisions based on the AI outputs; other deploy the systems for everyday tasks, or establish the regulatory framework for their use. These people with different roles are commonly called stakeholders.

Previous research has discussed different classes of stakeholders in the context of XAI. For example, Preece et al. [4] distinguish four main groups of stakeholders: developers, theorists, ethicists and users. Arrieta et al. [5] categorize the main classes of stakeholders into domain experts/users, data scientists/developers/product owners, users affected by model decisions, managers/executive board members, and regulatory entities. Fig. 1 describes the types of stakeholders as defined in [5] along with the reason for the need for explainability of artificial intelligence models.

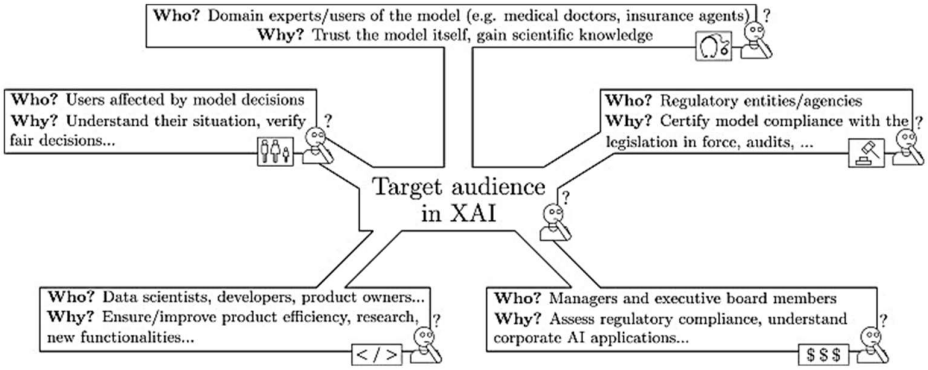

Fig. 1 Diagram illustrating the various goals of explainability in machine learning models as desired by various audience types [5].

III. STAKEHOLDERS' DESIDERATA

Stakeholder desiderata are one of the reasons for XAI's growing popularity. As stakeholders, combined with their particular requirements, influence the explanation process, it is important that they are taken into account when selecting, developing and evaluating explainability methods in a given context. A number of studies [5], [6] have been created to examine the needs of stakeholders.

A. Domain experts/users of the model

Doctors, loan officers, and hiring managers are a few examples of this type of stakeholders. Most users are neither technical specialists, nor are they familiar with the inner workings of the systems they use. The two most crucial things they need are *trust* and *usability*.

B. Data scientists/developers/product owners

Developers are well knowledgeable about the systems and driven to make them better. Developers place a high value on *verification*—that is, determining whether a system functions as intended. *Performance* is a major need for developers.

C. Users affected by model decisions

Affected parties are such persons within the scope of the system's influence. Patients, applicants for work or credit are typical examples of this class. The decisive requirements of the parties concerned are *fairness* and *morality/ethics*. The aim is to prevent discrimination against individuals, not on the basis of their own actions or characteristics, but on the basis of the actions or characteristics of the social groups to which they belong (e.g. women, ethnic minorities, older people).

D. Managers/executive board members

The decision-makers who choose which systems to implement want those systems to be widely *accepted*. The worst-case scenario in terms of adoption is that users reject well-functioning systems, so the systems end up never being used. Their next requirement is the *compliance of the system with legal regulations*. They are responsible for ensuring system compliance with regulations.

E. Regulatory entities

Regulators are establishing moral and legal guidelines for the creation, application, and general usage of systems. This class comprises legislators, attorneys, and ethicists. *Trustworthy* and *accountability* are crucial requirements for regulators. Holding the responsible person accountable is essential for accountability. Regulators wish to stay away from circumstances where the law is difficult to implement or when mistakes are not held accountable.

IV. HUMAN-CENTERED EVALUATION

Explainable systems can be compared from the point of view of several levels. Doshi-Velez and Kim [7] propose three main levels of explainability assessment: application-grounded, human-grounded, and functionally-grounded. Application-grounded evaluation involves testing on a real-world task by conducting end-user experiments. Human-grounded evaluation also tests in practice, the difference is that these experiments are conducted with lay people. Functionally-grounded level does not require assessment of people, but it uses a formal definition of explainability as a model of explanatory quality. Application-grounded evaluation and human-grounded evaluation can be combined into one group of human-centered evaluations.

Qualitative human-centered metrics include asking about the usefulness of, satisfaction with, and trust in the explanations provided through interviews or questionnaires [8], [9]. Holzinger et al. [9] presented in their work the System Causability Scale, which is inspired by the System Usability Scale [10], but is aimed at measuring the extent to which an explanation helps an expert understand the cause.

V. CONCLUSION

Different types of stakeholders are an important aspect in creating explainable machine learning models. Important elements that must be taken into account while putting them into practice are determined by their requirements. In addition, human testing plays a significant role in the evaluation of explainability techniques.

In the coming period, we plan to conduct several experiments and user studies as part of our research. One of the planned studies will be to compare different explainability methods within different medical stakeholder groups. The goal will be to investigate whether any of the parties has a preference for a certain type or form of explanation and to what extent the explanation is useful for them.

ACKNOWLEDGMENT

This work was supported by the Slovak Research and Development Agency under the contract No. APVV-22-0414 and contract No. APVV-20-0232, and by the Scientific Grant Agency of the Ministry of Education, Research, Development and Youth of the Slovak Republic under grant no. 1/0685/21.

REFERENCES

[1] D. Gunning, “Explainable Artificial Intelligence (XAI),” Defense Advanced Research Projects Agency (DARPA), 2017.

[2] M. Pavlusová, “The way to the methodological choice of explainability and interpretability methods,” in SCYR 2023: 23rd Scientific Conference of Young Researchers, Košice: Faculty of Electrical Engineering and Informatics, 2023, pp. 185–188.

[3] A. Brennen, “What do people really want when they say they want ‘explainable AI?’ we asked 60 stakeholders,” Conference on Human Factors in Computing Systems - Proceedings, Apr. 2020, doi: 10.1145/3334480.3383047

[4] A. Preece, D. Harborne, D. Braines, R. Tomsett, and S. Chakraborty, “Stakeholders in Explainable AI,” Sep. 2018, Accessed: Feb. 21, 2024. [Online]. Available: http://arxiv.org/abs/1810.00184

[5] A. Barredo Arrieta *et al.*, “Explainable Artificial Intelligence (XAI): Concepts, taxonomies, opportunities and challenges toward responsible AI,” *Information Fusion*, vol. 58, pp. 82–115, Jun. 2020, doi: 10.1016/J.INFFUS.2019.12.012.

[6] M. Langer *et al.*, “What do we want from Explainable Artificial Intelligence (XAI)? – A stakeholder perspective on XAI and a conceptual model guiding interdisciplinary XAI research,” *Artif Intell*, vol. 296, p. 103473, Jul. 2021, doi: 10.1016/J.ARTINT.2021.103473.

[7] F. Doshi-Velez and B. Kim, “Towards A Rigorous Science of Interpretable Machine Learning,” Feb. 2017, doi: 10.48550/arxiv.1702.08608.

[8] F. Poursabzi-Sangdeh, D. G. Goldstein, and J. M. Hofman, “Manipulating and measuring model interpretability,” Conference on Human Factors in Computing Systems - Proceedings, May 2021, doi: 10.1145/3411764.3445315.

[9] Holzinger, A. Carrington, and H. Müller, “Measuring the Quality of Explanations: The System Causability Scale (SCS): Comparing Human and Machine Explanations,” KI - Kunstliche Intelligenz, vol. 34, no. 2, pp. 193–198, Jun. 2020, doi: 10.1007/S13218-020-00636-Z/TABLES/1

[10] J. Brooke, “SUS: A quick and dirty usability scale,” in *Usability evaluation in industry*, USA: CRC Press: Boca Raton, 1996.

Parameter Mismatch in Finite Control Set Model Predictive Direct Speed Control

[1]*Lukáš PANCURÁK (2nd year),*
Supervisor: [2]*Karol KYSLAN*

[1,2]Dept. of Electrical Engineering and Mechatronics, FEI TU of Košice, Slovak Republic

[1]lukas.pancurak@tuke.sk, [2]karol.kyslan@tuke.sk

***Abstract*—Finite Control Set Model Predictive Control (FCS-MPC) is a highly regarded strategy known for its superior dynamic behavior and flexible control objective definition. This study systematically analyzes parameter mismatches and their impact on FCS-MPDSC for Permanent Magnet Synchronous Motors (PMSM). Variations in resistance, inductances, and inertia are assessed using RMSE metrics, providing insights into control performance and addressing parameter mismatch challenges. The control algorithm operates in the *dq* coordinate system, utilizing a linear Kalman filter (LKF) for load torque estimation.**

***Keywords*—model predictive control, sensitivity analysis, speed control**

I. Introduction

MPC is increasingly used in power electronics and motor control, relying on mathematical models for system prediction [1]. It employs a cost function for optimization, offering flexibility but facing challenges such as high-frequency ripples and sensitivity to parameter mismatch. However, accurate parameters are crucial for high-quality motor control, and parameter mismatch remains a significant challenge, impacting control performance [2]. This paper aims to analyze parameter mismatch and its impact on control quality. The proposed FCS-MPDSC method utilizes a linear Kalman filter for load torque estimation and a novel cost function design.

II. Finite Control Set Model Predictive Direct Speed Controller

The load torque value is estimated using linear Kalman Filter (LKF). Estimated load torque will be further denoted as T_{LKF}. Predictive model and model for LKF was discretized using Taylor series expansion. More detailed explanation of LKF employed in this paper can be found in [3].

The control algorithm consists of several steps, starting with measurement of current and position, estimation of load torque, calculation of predictions, optimization algorithm in form of a cost function, and lastly selection and application of optimal actuation. The speed control is represented in the cost function given by (1) as the error between the reference and predicted value. Similarly, currents i_d and i_q are controlled concerning their references. Lastly, vector sum of currents is also controlled. Weighting factors have been selected by trial and error method. Constraints to limit maximum current was also implemented. Implemented constraints, as well as the detailed description of the cost function can be found in [3]. The cost function is designed as [3]:

$$\begin{aligned} J(k) = {} & \lambda_1(\omega^* - \omega^p(k+1))^2 + \lambda_2(i_d^P(k+1))^2 + \\ & + \lambda_3(i_q^*(k+1) - i_q^P(k+1))^2 + \\ & + \lambda_4(i_{vect}(k+1))^2, \end{aligned} \tag{1}$$

III. Parameter mismatch in model predictive control

Parameter variations in PMSM during operation can stem from several factors. In surface-mounted PMSMs (SM-PMSMs), common sources of parameter mismatch include phase inductance (L_{ph}) and phase resistance (R_{ph}), arising from operational variations, inaccurately set nominal values, or modeling errors. Load torque and friction are notable parameters affected by external disturbances, while inertia, if inaccurately set or observed, can also impact the controller significantly. To analyse the impact of parameter mismatch, a simulation model in MATLAB Simulink, designed in [3] was used. Model parameters of PMSM itself was changed to simulate parameter mismatch in the control loop. For clear comprehension of analysed parameters, we will establish auxiliary variables, as given in 2, where R_0, L_0, J_0 are initial values, R, L, J are actual values, and η represent a ratio.

$$\eta_R = \frac{R}{R_0};\ \eta_L = \frac{L}{L_0};\ \eta_J = \frac{J}{J_0}; \tag{2}$$

To evaluate results of simulations, root mean square error for phase current and for angular speed was calculated. In following equation i_a, ω and i_a^*, ω^* are measured and reference values, n is total number of sample and j is current sample:

$$RMSE(i_a, \omega) = \sqrt{\sum_{j=1}^{n} \frac{(i_a, \omega(j) - i_a^*, \omega^*(j))^2}{n}}, \tag{3}$$

IV. Simulation results

Weighting factors of simulated controller was set as $\lambda_1 = 1200$, $\lambda_2 = \lambda_3 = 1$ and $\lambda_4 = 0.05$. Nominal

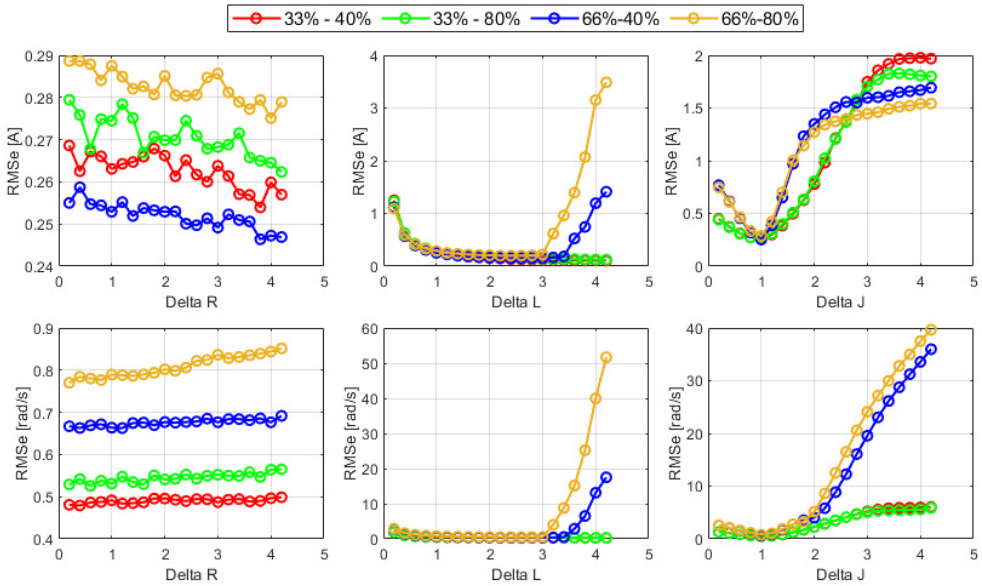

Fig. 1: RMSE values for test configuration 1-4, for each varied parameter

TABLE I: Test configuration settings

	T_L [% of T_N]	ω [% of ω_N]
Test configuration 1	33	40
Test configuration 2	33	80
Test configuration 3	66	40
Test configuration 4	66	80

values of PMSM are $n_n = 3000rpm$, $I_n = 2.6A$, $R_{2ph} = 7.5\Omega$, $L_{2ph} = 22.7mH$, $k_t = 1.7Nm/A$ and $J_M = 0.00015kgm^2$. The simulated inverter model includes ideal switches. The control performance of FCS-MPC under parameter mismatch is quantified in terms of RMSE for four test configurations, as shown in the Table I. In each simulation, specific test configurations varied parameters like resistance (R), inductances (L_d and L_q), and inertia (J) individually. RMSE was computed for each variation, focusing on steady-state performance and evaluating phase current (i_a) and angular speed (ω).

The impact of varying resistance values is shown in Fig.1, where the upper part illustrates RMSE values for phase current and the bottom part shows RMSE values for angular speed. Despite higher parameter mismatch, simulations reveal a subtle decrease in RMSE values in both cases. This trend, which is consistent with prior experimental analyses [4], suggests that resistance changes affect control quality very minimally. For inductance variation a noticeable rise in RMSE occurs when L is lower than L_0, with negligible changes observed at higher values of L until significant differences emerge. The influence of varying inertia J shows that deviations from the nominal value lead to prominent changes in RMSE, particularly affecting speed control. It is worth noting that majority of sensitivity analyses focus on current control in FCS-MPC or PI speed control in the outer loop, not particularly on FCS-MPDSC. These results are supported by findings from studies such as [5], [6], reinforcing the validity of this analyses.

V. Conclusion

The simulations tested FCS-MPDSC's sensitivity to parameter mismatch in PMSM models, finding robust control with resistance changes but decreased quality with lower inductance. Higher inductance had minimal impact until significant differences occurred. Inertia variations significantly affected control, emphasizing the need for accurate values. This highlights the importance of enhancing FCS-MPDSC's robustness in future research.

Acknowledgment

This work was supported by the Scientific Grant Agency of the Ministry of Education, Science, Research and Sport of the Slovak Republic and Slovak Academy of Sciences (VEGA) under the project VEGA 1/0363/23.

References

[1] S. Kouro, M. A. Perez, J. Rodriguez *et al.*, "Model predictive control: Mpc's role in the evolution of power electronics," *IEEE Industrial Electronics Magazine*, vol. 9, no. 4, pp. 8–21, 2015.

[2] H. A. Young, M. A. Perez, and J. Rodriguez, "Analysis of finite-control-set model predictive current control with model parameter mismatch in a three-phase inverter," *IEEE Transactions on Industrial Electronics*, vol. 63, no. 5, pp. 3100–3107, 2016.

[3] L. Pancurák, T. Jure, and K. Kyslan, "Finite control set model predictive direct speed control of pmsm," in *2023 International Conference on Electrical Drives and Power Electronics (EDPE)*, 2023, pp. 1–6.

[4] C. Martín, M. Bermúdez, F. Barrero, M. R. Arahal, X. Kestelyn, and M. J. Durán, "Sensitivity of predictive controllers to parameter variation in five-phase induction motor drives," *Control Engineering Practice*, vol. 68, pp. 23–31, 2017.

[5] P. F. C. Gonçalves, S. M. A. Cruz, and A. M. S. Mendes, "Sensitivity to parameter mismatch in a bi-subspace predictive current control strategy for six-phase pmsm drives," in *IECON 2020 The 46th Annual Conference of the IEEE Industrial Electronics Society*, 2020, pp. 4875–4880.

[6] J. Yang, Y. Liu, and R. Yan, "A comparison of finite control set and continuous control set model predictive control schemes for model parameter mismatch in three-phase apf," *Frontiers in Energy Research*, vol. 9, p. 727364, 08 2021.

Memory effect in 5CB liquid crystal based composites

[1]*Dmytro Miakota (3rd year)*
Supervisor: [1]Natália TOMAŠOVIČOVÁ

[1]Institute of Experimental Physics of the Slovak Academy of Sciences, Košice, Slovak Republic

[1]dmytro.miakota@tuke.sk, [2]nhudak@saske.sk

***Abstract*— Liquid crystal doped with aerosil (SiO_2) nanoparticles is recognized for demonstrating an electromechanical memory effect. Following exposure to an electric field, the induced state persists due to the presence of aerosil nanoparticles. This study investigates the memory effect induced by both electric and magnetic fields. We examine liquid crystal 4-cyano-4′-pentylbiphenyl (5CB) doped with non-magnetic aerosil nanoparticles, as well as a combination of aerosil nanoparticles with elongated magnetic goethite nanoparticles and spherical Fe_3O_4, using capacitance measurements. Studied systems exhibited hysteresis in capacitance-voltage and capacitance-magnetic field dependencies. The measurements reveal a significant influence of temperature. The observed electromechanical and magnetomechanical memory effects suggest the potential utilization of the system in voltage-driven or magnetic field-driven non-volatile memory devices.**

***Keywords*— liquid crystal, magnetic nanoparticles, liquid crystal composites.**

I. Introduction

Liquid crystals (LCs) are predominantly recognized for their usage in flat panel displays, where they can be easily manipulated by an electric field. Even a small electric field, typically in the range of volts or millivolts, can induce changes in their optical characteristics, causing them to transition from opaque to transparent states. Apart from their responsiveness to electric fields, liquid crystals also react to various other stimuli such as magnetic fields, pressure, temperature, and light, making them suitable for a wide range of applications. Interest in non-display applications began to flourish in the 1980s [1]. Over the past decades, researchers have unveiled numerous potential uses for liquid crystals, including biosensors, light valves, filters, switches, tunable lenses, adaptive contact lenses, tunable lasers, smart windows, and more. [2–4]

The objective of the research is to experimentally investigate the changes of physical properties of liquid crystal composites doped with aerosil nanoparticles and goethite nanorods and spherical Fe_3O_4 nanoparticles under the influence of magnetic and electric fields. To attain the objective, the capacitance measurements were employed as primary experimental method.

II. Liquid Crystals

Liquid crystal materials in the isotropic phase act similarly to any other liquid. However, upon cooling, these materials go through one or more mesophases before reaching the crystalline phase (thermotropic liquid crystals). Mesophases are intermediate states in which the material exhibits properties of both liquids and solids. Within the mesophase, liquid crystal molecules can be ordered in various ways, such as the nematic phase, in which the elongated molecules of the liquid crystal all point in the same direction. This direction is represented by a director $\vec{n}$ [5].

The response of a liquid crystal to an external electric or magnetic field is typically observed using a cell consisting of two separated glasses with a polymer layer in between. The overall design of the liquid crystal cell is depicted in Fig. 1. In this work the alignment of LC molecules was planar, long axes of molecules are parallel with the cell surface.

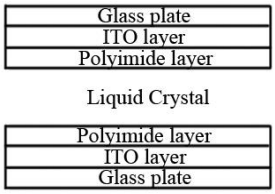

Fig. 1. Liquid crystal cell for optical and dielectric measurements. ITO layer on glass plates serves as electrode and polyimide layer provides required alignment.

When a sufficiently large field, known as the critical or threshold field, is applied to the material, the liquid crystal molecules will begin to reorient. This effect is called the Fréedericksz transition [6].

III. Memory Effect

The memory effect, i. e. the increase in capacitance after applying voltage: the increasing voltage causes an increase in the capacitance, decreasing of voltage causes decreasing of capacitance, but in case of these composites a hysteresis is present and the final capacitance at $U = 0$ V is higher than the initial capacitance. The memory effect has been studied in a 5CB (4-cyano-4'-pentylbiphenyl) liquid crystal doped with non-magnetic SiO_2 nanoparticles [7]. It was found that even a small quantity of NPs has a strong influence on the memory effect.

The explanation of the memory effect is that a weak network is created among the SiO_2 nanoparticles and the LC (Fig. 2). By application of electric field composite changed its arrangement and follow the alignment of nematic domains. Moreover, the LC composite stays stabilized even after the electric field is turned off [8].

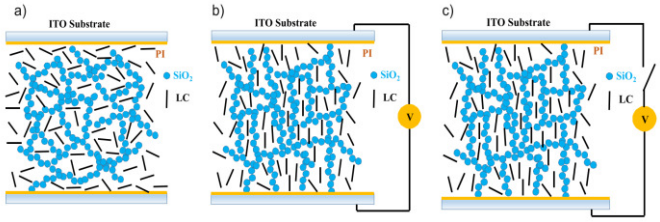

Fig. 2. A schematic of creation a SiO_2 NPs network in the nematic phase. The spheres represent the NPs and the lines represent the LC molecules. (a) Initial orientation with no electric field; (b) the electric field is turned on; and (c) the electric field is turned off.

IV. Materials and Methods

A. 5CB Liquid Crystal

4-Cyano-4'-pentylbiphenyl (5CB) is a thermotropic nematic liquid crystal with nematic to isotropic transition temperature at $T_{NI} \approx 33.7$ °C and a glass transition temperature at $T_g \approx 20.0$ °C.

B. Fe_3O_4 Nanoparticles

For those experiments the magnetite (Fe_3O_4) nanoparticles with mean diameter of 10 nm were purchased from Ocean NanoTech. The size of Fe_3O_4 nanoparticles was verified by transmission electron microscope (TEM).

C. Goethite nanorods

The goethite nanorods were synthesized following a recipe in [9]. The microstructural characterization of the nanopowders was performed using a transmission electron microscopy (TEM). The average length, width, and thickness of the goethite nanorods were estimated to be 350 ± 100 nm, 25 ± 7 nm and 10 ± 5 nm respectively.

D. Methods

The transition from the isotropic to the nematic phase was studied using dielectric measurements. The samples, consisting of either undoped 5CB or 5CB doped with SiO_2, Fe_3O_4 NPs or goethite nanorods, were filled into capacitors for the measurement of memory effect.

V. Conclusions and Results

In liquid crystal 5CB doped with aerosil nanoparticles, the memory effect manifests following the application of voltage and magnetic fields. These electromechanical and magnetomechanical memory effects arise from the network formed by the aerosil nanoparticles. This network effectively maintains the reoriented position of the liquid crystal molecules induced by the voltage and magnetic field. When the composite is heated and subsequently cooled to its operational temperature, the composite's response is altered, contingent upon the heating temperature. This phenomenon can be elucidated by the breaking and reformation of the network. The memory effect exhibits either enhancement or attenuation based on the heating temperature (Fig. 3 (a), (b), (c)).

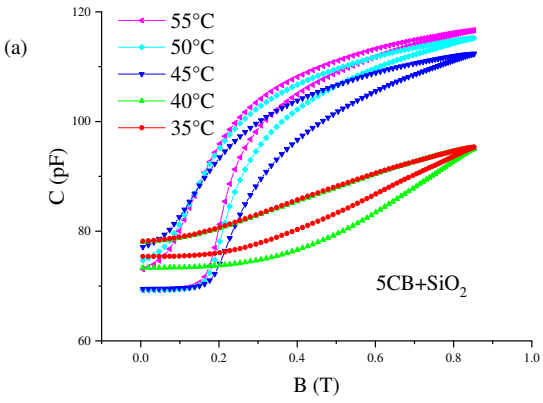

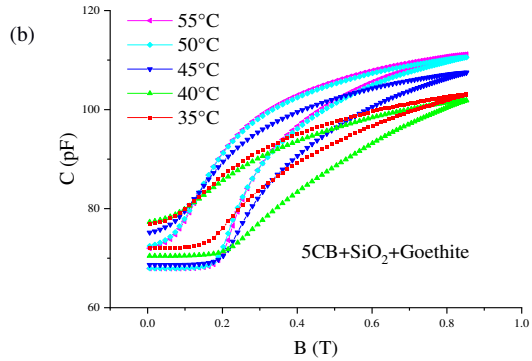

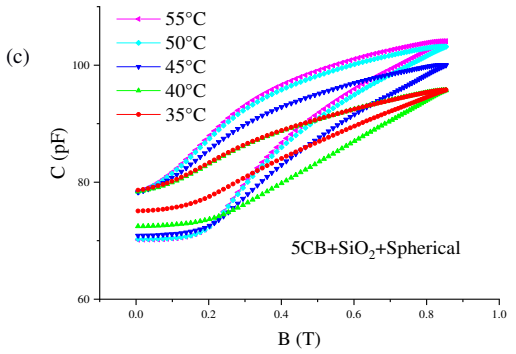

Fig. 3. Temperature effect on magnetomechanical memory effect in the composite of 5CB LC doped with aerosil (a); goethite nanorodes (b) and magnetite NPs (c)

VI. Next Steps

The plan for further research is to study the influence of different parameters, such as heating/cooling rates, intensity of electric or magnetic fields, NPs concentration that may influence the memory effect in liquid crystals composites with nanoparticles. Studying the effect of nanoparticle doping on properties of liquid crystal composites is important for the discovery of new properties and effects.

References

[1] T. Geelhaar, K. Griesar, B. Reckmann, "125 years of liquid crystals—a scientific revolution in the home", *Angew. Chem.*, vol. 52, pp. 8798-8809, 2013.

[2] C. Luan, H. Luan, D. Luo, "Application and technique of liquid crystal-based biosensors", *Micromachines*, vol. 11, no.2, p. 176, 2020.

[3] J. Beeckman, K. Neyts, P.J.M. Vanbrabant, "Liquid-crystal photonic applications", *Opt. Eng.*, vol. 50, no. 8, p. 081202, 2011.

[4] J. Bailey, P.B. Morgan, H.F. Gleeson, J.C. Jones, "Switchable liquid crystal contact lenses for the correction of presbyopia", *Crystals*, vol. 8, no. 1, p. 29, 2018.

[5] P.G. de Gennes, J. Prost, "The Physics of Liquid Crystals", *Oxford Scholarship Online*, 1993.

[6] I. W. Stewart, "The Static and Dynamic Continuum Theory of Liquid Crystals: A Mathematical Introduction", *Liquid Crystals Book Series 2*, New York, Taylor & Francis, p. 360, 2004.

[7] V. Gdovinová, N. Tomašovičová, S.-C. Jeng, K. Zakutanská, P. Kula, P. Kopčanský, "Memory effect in nematic phase of liquid crystal doped with magnetic and non-magnetic nanoparticles", *Journal of Molecular Liquids*, vol. 282, pp. 286-291, 2019.

[8] K. Zakutanská, D. Miakota, V. Lacková, S.-C. Jeng, D. Węgłowska, F. Agresti, M. Jarošová, P. Kopčanský, N. Tomašovičová, "Effect of temperature on memory effect in nematic phase of liquid crystal and their composites with aerosil and geothite nanoparticles", *Journal of Molecular Liquids*, vol. 391, p. 123357, 2023

[9] P. Kopčanský, V. Gdovinová, S. Burylov, N. Burylova, A. Voroshilov, J. Majorošová, F. Agresti, V. Zin, S. Barison, J. Jadzyn and N. Tomašovičová, "The influence of goethite nanorods on structural transitions in liquid," *Journal of Magnetism and Magnetic Materials*, vol. 459, pp. 26-32, 2017.

Cybersecurity threats from phishing to AI-generated deepfakes

[1]*Miroslav Murin (1st year),*
Supervisor: [2]*Miroslav Michalko*

[1,2]Dept. of Computers and Informatics, FEI TU of Košice, Slovak Republic

[1]miroslav.murin@tuke.sk, [2]miroslav.michalko@tuke.sk

***Abstract*—In the digital era, organizations face escalating cyber threats, including sophisticated phishing attacks and AI-generated disinformation. This article explores area of of cyber threats, with a particular focus on hoaxes, phishing, and AI-generated content such as images, videos, and audio recordings. It highlights the critical role of advanced detection technologies, including machine learning and artificial intelligence, in identifying and mitigating these threats before they inflict significant damage. Furthermore, the paper emphasizes the importance of cybersecurity education and awareness among employees as a crucial line of defense against cyber attacks. Through a comprehensive analysis of current threats such as phishing, AI-generated fraud, and a detailed examination of various detection and prevention strategies, the paper presents a multi-dimensional approach to increasing an organization's resilience.**

***Keywords*—Generative Adversarial Networks, Hoaxes, Machine learning, Phishing**

I. Introduction

In today's digital era, organisations are constantly facing the growing threat of cyber attacks, which are becoming more sophisticated and complex. Some of the most prevalent and devastating forms of these attacks include hoaxes, phishing emails, as well as fake generated images and videos. These methods are often used by attackers to deceive individuals and organisations, putting their sensitive data at risk and, in many cases, even gaining unauthorised access to important information systems. In this context, cybersecurity is becoming not only a technological but also a social challenge that requires a comprehensive and multidisciplinary solution.

The scope of this paper is to provide an overview of the current state of cyber threats with emphasis on hoaxes, phishing emails, fake generated images and videos, and fake recordings. The goal is to present effective strategies and tools that organizations can implement to increase their resilience to these threats. We analyze different approaches to detection and prevention, including the latest AI and machine learning-based technologies that enable the identification and blocking of malicious activities before they can cause significant damage. Currently, there is no one-size-fits-all or unified approach to combating cyber threats.

In this article, we also discuss the importance of cybersecurity education and awareness among employees as a key factor in preventing attacks. We focus on the strategic, technical, and human aspects of cybersecurity, provide real-world examples, and suggest best practices that organizations can adopt to become more resilient to cyber threats while protecting their assets and reputation.

II. Security threats to companies

In this chapter, we analyze the current security threats and the threats they pose to the company. We also analyze how we could help detect and address these security threats.

A. Phishing emails

In today's digital environment, phishing is becoming an increasingly sophisticated threat to organisations of all sizes. According to the authors in [1] Phishing is a security attack that aims to obtain personal information such as passwords, credit card details or other user account information through websites or emails. Phishing websites look similar to legitimate ones, making it difficult for the layperson to distinguish them. According to the authors in [2] information such as financial information, credit reports, log in details, and other sensitive and personal information is frequently shared over email. The transition time of email from sender to a receiver allows cybercriminals to exploit or breach the data shared, hence causing harm to the integrity of the data.

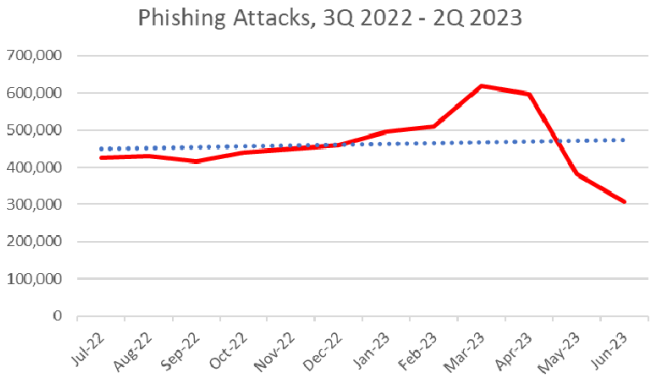

Fig. 1. Phishing attacks from 3Q 2022 to 2Q 2023 according to APWG[3]

The Anti-Phishing Working Group (APWG) claims in [3] that voice-mail phishing, or vishing, volume continues to rise. In figure 1 We can see the number of phishing attacks. In the second quarter of 2023, the APWG observed 1,286,208 phishing attacks. This was the third-highest querterly total that the APWG has ever recorded. However, phishing trended downward.

The authors in [4] claim the following interesting facts:

- 50% of phishing websites made use of SSL certificates.

- 65% increase in global losses between July 2019 to December 2021.
- Educational institutions saw a 75% increase in cyber-attacks.
- 92% of Australian organizations suffered a successful phishing attack, showing a 53% increase from the year 2021.

According to Verizon [5] 83% of breaches involved external actors with the majority being financially motivated. 74% of breaches involved the human element, which includes social engineering attacks, errors or misuse. 50% of all social engineering attacks are pretexting incidents - nearly double last year's total.

Characteristics of phishing emails:

- Deceptive Sender Addresses: Attackers often mask their sender addresses to make it appear that the email comes from a trusted source.
- Manipulative Content: Emails may contain urgent calls to action, such as fake account security alerts or offers that are too good to be true.
- Malicious Attachments or Links: Emails often contain attachments or links that can install malware or redirect victims to fake websites where they are prompted to enter sensitive information.
- Text or Design Errors: Although many phishing emails may look convincing at first glance, they often contain grammatical errors, stylistic inconsistencies, or incorrect formatting that may indicate their fraudulent nature.

According to the authors in [6] Phishing poses a significant threat to organizations, prompting the adoption of anti-phishing training, which often incurs high costs. Investing in employee training in this area is proving to be an extremely effective way to reduce the risk of successful phishing attacks and strengthen an organisation's overall cyber defences. Ultimately, an informed and vigilant employee represents the first and most important line of defense against cyber threats, making them an invaluable asset in the fight against phishing. There are also a number of tools available that can be used to train employees about phishing such as Gophish, Zphisher and Evilginx. Authors in [4] argue that 84% of US-based organizations have stated that conducting regular security awareness training has helped reduce the rate at which employees fall prey to phishing attacks.

B. JavaScript threats on websites

JavaScript is universally used to create interactive and dynamic web pages. However, despite its advantages, JavaScript also carries potential security risks, particularly in the form of JavaScript viruses. These scripts can be embedded in websites without the knowledge of their owners or be part of malicious advertising campaigns. According to the authors in [7] JavaScript is cross-platform and can be executed dynamically, it has been a major vehicle for web-based attacks. Since JavaScript is executed client-side, i.e. directly in the user's browser, attackers can use it for a variety of purposes, from simply displaying unwanted advertising to attempting to steal sensitive data such as login credentials and financial information.

Cross-Site cripting (XSS) is a common attack in which an attacker inserts malicious code into trusted websites. When a user visits such a compromised site, the code is automatically executed and can trigger unwanted actions such as stealing cookies or changing the content of the page. According to author in [8] due to healthcare institute statistics on 2017 the XSS threat got third place of most common and dangerous web security threats.

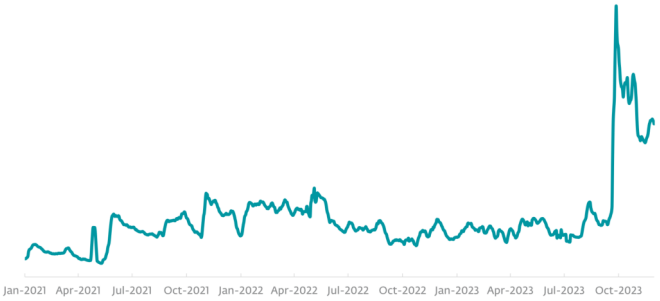

Fig. 2. JavaScript virus detection trend according to ESET [9]

According to Eset [9], the trend of JavaScript viruses has been increasing significantly in recent years as we can also see in Figure 2. For example, in 2023, the share of JavaScript attacks increased by 111%.

C. Artificial intelligence generated hoaxes, images and videos

In the era of digital technology and artificial intelligence, new methods are emerging to exploit technological advances for fraudulent purposes, including sophisticated phishing attacks. One of the latest trends in this area is the use of AI to generate fake content, such as text, images and videos, which can be a tool for more convincing and targeted attacks. These technologies open the door for the emergence of so-called deepfake videos and synthesised voices that can be used to create very convincing hoaxes. The authors in [10] argue that GenAI has significantly influenced how an organization's cybersecurity will evolve with the power and threats that LLM tools offer.

Imagine a situation where an AI-generated fake recording of a company CEO's voice is sent to an employee requesting an urgent transfer of funds or sharing sensitive information. Because the recording may sound indistinguishable from the director's real voice, the employee can easily be tricked into taking the requested action without any suspicion. According to the authors in [11] elections are also influenced by artificial intelligence-generated deepfakes. Fake videos, voice and audio clips can cause huge damage.

Such a development requires a new approach to security awareness and employee training. It is important for organizations to expand their security protocols to include training on recognizing and responding to advanced deception techniques such as deepfakes and AI-generated content. According to the authors in [12] there are various methods available for creating deep fake such as GAN (General Adversarial Network), Auto Encoders, pix2pixGAN, Cycle GAN, Style GAN, Wave Net and some of the open source digitally available tools are Deep Face Lab, Face Swap and more. In Figure 3, we can see an example of a generated deceptive image that can fool some individuals. In addition to traditional methods such as checking the sender's email address and verifying requests through secondary communication channels, employees should also be trained in the use of new technologies to detect counterfeit audio and video recordings.

Fig. 3. Generated hoax image. On the left is the original photo and on the right is the modified one.

According to the authors in [13] Generative Adversarial Networks (GANs) have rapidly risen to prominence in the sphere of deep learning. This is especially true when it comes to image generation, where GANs have displayed impressive capabilities. Since their introduction by Ian Goodfellow et al. in 2014, GANs have become a focus of research attention due to their ability to generate new, previously unseen data that is often indistinguishable from real data.

The GAN architecture includes two key components: a generator and a discriminator. The generator tries to generate data that is convincing enough to fool the discriminator, while the discriminator tries to distinguish between the real and generated data. The goal is to reach a point where the discriminator can no longer effectively distinguish between real and fake data, suggesting that the generator can produce highly realistic outputs. According to the authors in [14] there have been various types of adversarial networks present today. Among these types of networks, the most popular network is Deep Convolutional Generative Adversarial Network (DCGAN) for performing on the convolutional networks without using multilayer perceptrons.

Ensuring that employees are informed and prepared for new types of attacks is key to protecting organisations from the damaging consequences that these sophisticated phishing attacks can cause. The use of artificial intelligence and deepfake technologies in phishing attacks poses a serious threat, but with the right approach and tools it is possible to counter this threat and minimise its negative impact. The authors in [15] claim that in a deepfake, the face of a targeted person is superimposed on a source image so that this digital tampered data can be used for digital frauds, blackmailing, pornography etc. With the developments in the deep learning field, it is becoming challenging to distinguish between real and fake manually.

III. Possible solutions to security problems

Today, as cyber attacks become increasingly sophisticated, it is critically important to create an effective phishing analytics solution that can identify and prevent potential threats. In this section, we will discuss the techniques and technologies that can be applied to develop a robust system to detect phishing, fake images, videos and hoaxes. The best solution to the threats posed by artificial intelligence is to use artificial intelligence to combat them.

Several solutions are available for different problems, but not all are ideal. And even worse is the combination of these factors. For example, the use of a fake generated recording sent to an accountant. Currently, it is very difficult to combat hoaxes. In addition, new phishing threats are emerging that will be much more dangerous. That makes it all the more appropriate to devise a universal tool to combat these attacks that could help companies or public institutions. This tool should incorporate multiple layers of detection in order to be as successful as possible. For example, the first layer would verify that the messages themselves are not phishing messages. If the message is well-written and passes the filter, it would verify, for example, a recording or an image to see if it is genuine or just generated by the GAN model. In addition to this, the presence of dangerous JavaScript files on web pages, for example, can also be checked for security using artificial intelligence. Such a tool would be able to fight successfully against new security threats.

A. Integrating machine learning against phishing

The use of machine learning is key to the analysis and identification of phishing attacks. Machine learning models can be trained to recognise the distinguishing features of phishing emails and websites, such as fraudulent URLs, misleading text wording or unusual attachments. Today, there are already trained models that can currently recognize phishing emails with very high accuracy. For example, the authors in [16] claim to have achieved high success rates on their test set using the Random Forest Classifier. One of the problems with these models is that they are specialized for English. There are several solutions to this problem. The best solution is to train the model for multiple languages but this is a complicated solution. The second solution is to use a translator to translate the text into English and then compare the translated text. But this solution is worse because it reduces the detection success rate.

In order to train a good model for Phishing detection, it is essential to have large and high quality datasets containing examples of both legitimate and phishing emails and websites. Subsequently, to train the model, these texts need to be prepared into a suitable form. Begin by cleaning text data. This involves tokenization. Tokenization is breaking down the text into smaller parts like words, removing stopwords (common words that add little meaning), and vectorization (converting text into numerical format). There are several methods of vectorization like Bag of Words, TF-IDF, or using word embeddings like Word2Vec or GloVe. Techniques like TF-IDF (Term Frequency-Inverse Document Frequency) are widely used for emphasizing unique words in documents. Authors in [17] argue that text classification tasks include word preprocessing, feature advance, and classifier model training. Different from traditional text-based word processing techniques, deep text-based word processing techniques mainly use word vector techniques to extract indirect text features.

B. Detection of fake generated images audio recordings

Current solutions for detecting fake generated images focus on using advanced machine learning and artificial intelligence techniques to identify images created using generative models such as Generative Adversarial Networks (GANs), diffusion models, and other AI-based techniques. These methods seek to identify the distinguishing features that differentiate synthesized images from real ones, whether based on textures,

structures, specific artifacts, or imperfections in AI-generated images. According to the authors in [18] real-vs-fake classification, fails to detect fake images from newer breeds of generative models when trained to detect GAN fake images. The authors in [19] claim that empirical results show that fake images generated by various models can be distinguished from real ones, as there exists a common artifact shared by fake images from different models.

One approach is to develop universal fake image detectors that can generalize across different generative models. These systems are trained on large datasets containing both real and synthesized images, with the goal of teaching the models to recognize the differences between them.

Another important direction is the use of fingerprint learning, where models try to identify unique "fingerprints" associated with specific generative patterns. In this way, they can not only detect that an image has been generated, but also determine which specific model it was generated by.

The detection of fake audio recordings, particularly those generated by advanced text-to-speech and voice imitation technologies, has become a critical area of research due to the potential for misuse in generating convincing deepfakes. According to the authors in [20] current text-to-speech algorithms produce realistic fakes of human voices, making deepfake detection a much-needed area of research. The current approaches to detecting these fake audio recordings leverage a mix of machine learning and deep learning techniques, focusing on distinguishing between genuine human voices and those synthesized by algorithms.

One approach involves using various ML models, such as Logistic Regression, Support Vector Machines, and Random Forests, trained on features extracted from audio to classify them as real or fake. The only problem is that the audio recording needs to be processed into suitable data for machine learning.

IV. Conclusion

In addressing the multifaceted cyber threats of today's digital age, this analysis underscores the vital need for a layered approach to cybersecurity, blending cutting-edge technological defenses with a strong emphasis on human awareness and education. The increasing sophistication of phishing attacks, alongside the emergence of AI-generated false content, presents a formidable challenge that requires both innovative detection methods and a robust culture of security vigilance within organizations. The use of machine learning and artificial intelligence stands out as a beacon of hope, promising to enhance the accuracy and efficiency of cyber defense mechanisms against a backdrop of constantly evolving threats.

Furthermore, the discourse on cybersecurity solutions brings to light the importance of fostering an environment where continuous learning and adaptability are paramount. As cybercriminals leverage advanced technologies to create more convincing and deceptive attacks, the response from the cybersecurity community must also evolve, harnessing similar technologies for defense. The future of cybersecurity hinges on our ability to not only develop more sophisticated detection and prevention techniques but also to cultivate a widespread organizational culture that prioritizes cybersecurity awareness. This dual strategy, combining technological innovation with educated and vigilant human actors, is essential for staying ahead of cyber threats and safeguarding sensitive information in an increasingly digital world.

Acknowledgment

This work was supported by Cultural and Educational Grant Agency (KEGA) of the Ministry of Education, Science, Research and Sport of the Slovak Republic under the project No. 060TUKE-4/2022.

References

[1] S. Patil and S. Dhage, "A methodical overview on phishing detection along with an organized way to construct an anti-phishing framework," in *2019 5th International Conference on Advanced Computing & Communication Systems (ICACCS)*, 2019, pp. 588–593.

[2] P. Saraswat and M. Singh Solanki, "Phishing detection in e-mails using machine learning," in *2022 2nd International Conference on Technological Advancements in Computational Sciences (ICTACS)*, 2022, pp. 420–424.

[3] APWG, "Phishing activity trends report 2nd quarter 2023," 2023. [Online]. Available: https://docs.apwg.org/reports/apwg_trends_report_q2_2023.pdf

[4] N. J. Palatty, "81 phishing attack statistics 2024: The ultimate insight," Dec. 2023. [Online]. Available: https://www.getastra.com/blog/security-audit/phishing-attack-statistics/

[5] Verizon, "2023 data breach investigations report," 2023. [Online]. Available: https://www.verizon.com/business/en-gb/resources/reports/dbir/

[6] M. Higashino, T. Kawato, M. Ohmori, and T. Kawamura, "An anti-phishing training system for security awareness and education considering prevention of information leakage," in *2019 5th International Conference on Information Management (ICIM)*, 2019, pp. 82–86.

[7] X. He, L. Xu, and C. Cha, "Malicious javascript code detection based on hybrid analysis," in *2018 25th Asia-Pacific Software Engineering Conference (APSEC)*, 2018, pp. 365–374.

[8] T. A. Taha and M. Karabatak, "A proposed approach for preventing cross-site scripting," in *2018 6th International Symposium on Digital Forensic and Security (ISDFS)*, 2018, pp. 1–4.

[9] ESET, "Threat report h2 2023," 2023. [Online]. Available: https://bezpecnevofirme.eset.com/sk/wp-content/uploads/sites/2/2024/01/H2-2023_Threat-Report.pdf

[10] M. Gupta, C. Akiri, K. Aryal, E. Parker, and L. Praharaj, "From chatgpt to threatgpt: Impact of generative ai in cybersecurity and privacy," *IEEE Access*, vol. 11, pp. 80 218–80 245, 2023.

[11] M. Khichi and R. Kumar Yadav, "A threat of deepfakes as a weapon on digital platform and their detection methods," in *2021 12th International Conference on Computing Communication and Networking Technologies (ICCCNT)*, 2021, pp. 01–08.

[12] R. Chauhan, R. Popli, and I. Kansal, "A systematic review on fake image creation techniques," in *2023 10th International Conference on Computing for Sustainable Global Development (INDIACom)*, 2023, pp. 779–783.

[13] Z. Shi, J. Teng, S. Zheng, and K. Guo, "Exploring the effects of various generative adversarial networks techniques on image generation," in *2023 IEEE 11th Joint International Information Technology and Artificial Intelligence Conference (ITAIC)*, vol. 11, 2023, pp. 1796–1799.

[14] Prabhat, Nishant, and D. Kumar Vishwakarma, "Comparative analysis of deep convolutional generative adversarial network and conditional generative adversarial network using hand written digits," in *2020 4th International Conference on Intelligent Computing and Control Systems (ICICCS)*, 2020, pp. 1072–1075.

[15] J. John and B. V. Sherif, "Comparative analysis on different deepfake detection methods and semi supervised gan architecture for deepfake detection," in *2022 Sixth International Conference on I-SMAC (IoT in Social, Mobile, Analytics and Cloud) (I-SMAC)*, 2022, pp. 516–521.

[16] S. Uplenchwar, V. Sawant, P. Surve, S. Deshpande, and S. Kelkar, "Phishing attack detection on text messages using machine learning techniques," in *2022 IEEE Pune Section International Conference (PuneCon)*, 2022, pp. 1–5.

[17] G. Jin, "Application optimization of nlp system under deep learning technology in text semantics and text classification," in *2022 International Conference on Education, Network and Information Technology (ICENIT)*, 2022, pp. 279–283.

[18] U. Ojha, Y. Li, and Y. J. Lee, "Towards universal fake image detectors that generalize across generative models," 2023.

[19] Z. Sha, Z. Li, N. Yu, and Y. Zhang, "De-fake: Detection and attribution of fake images generated by text-to-image generation models," 2022.

[20] N. M. Müller, P. Czempin, F. Dieckmann, A. Froghyar, and K. Böttinger, "Does audio deepfake detection generalize?" 2022.

Intelligent classification of Parkinson's Disease using wearable sensor data

[1]*Stanislav HUSÁR (3rd year),*
Supervisor: [2]*Marek BUNDZEL*

[1,2]Department of Cybernetics and Artificial Intelligence, FEI TU of Košice, Slovak Republic

[1]stanislav.husar@tuke.sk, [2]marek.bundzel@tuke.sk

***Abstract*—This paper describes our most recent updates on research concerning the classification of Parkinson's disease symptoms using deep learning methods. We are developing the Rehapiano device focused on measuring hand movements. We aim to use data from the Rehapiano device to classify tremors and related movement impairments. However, the dataset acquired with the Rehapiano device is not yet available, so we have decided to start our experiments with a dataset from the Levodopa Response Study, as this dataset is from a related domain.**

***Keywords*—Parkinson's Disease, Tremor, Inertial measurements, Fourier transform, Short-time Fourier Transform, Spectrogram, CNN**

I. Introduction

Large portions of the current population suffer from various motor impairments caused by injuries or diseases. These have a significant impact on daily activities and overall quality of life.

Traditional rehabilitation is long and unadventurous. For this reason, many people give up before significant improvements arise. Clinical assessment is also a very demanding task for a physician's attention.

Modern technologies can conceal rehabilitation behind gaming goals, attracting patient's attention. Meanwhile, every movement is captured for later assessment by physicians.

Fig. 1. Rehapiano prototype CAD drawing and photograph[2]

We are currently in the late stages of development of a novel rehabilitation device, the Rehapiano (Figure 1) [3], [4], [5]. Rehapiano uses load cells to measure the flexion and extension forces of the fingers on the hands. We aim to deploy the Rehapiano prototype to a clinical environment in the near future.

This publication was made possible with support from the Michael J. Fox Foundation for Parkinson's Research (MJFF). We use the data set from the Levodopa Response Study [1] to train neural networks.

We have already started researching and developing neural networks for classifying tremors. We are currently using a data set from the Levodopa Response Study [1].

II. Problem description

Levodopa is a study of Parkinson's disease patients recruited from Boston (17) and New York (11) [1]. The Michael J. Fox Foundation supported it. They equipped all subjects with accelerometer-based sensors on the wrists of both upper limbs and at the waist. In addition, they equipped Boston subjects with additional accelerometers on each limb and lower back.

The first day of data collection commences in the hospital in a clinical ON state. It consisted of a battery of motor tasks selected from ADL activities and MDS-UPDRS Section 3. The following two days were at home, where patients performed their usual activities. Finally, the fourth day of data collection was performed in the hospital, beginning in a clinical OFF state.

Once data collection was complete, the authors resampled all data to a 50Hz sampling rate and then temporally aligned the data from various sensors.

One of the primary symptoms associated with Parkinson's disease are tremors. Tremors manifest as involuntary movements with approximately rhythmic and sinusoidal character [6]. They have regular amplitude and frequency. Other symptoms include postural instability [7].

Not all tremors indicate Parkinson's disease. The most common disorder is Essential tremor [8]. Healthy people may exhibit tremors under certain conditions, such as stress or anxiety, disrupting their fine motor functions [9].

III. Solution design

We have designed a data preparation pipeline, allowing us to load data for training quickly. As the first step, we load all the data into a hierarchical structure that preserves their relations (Figure 2). The root of this hierarchy contains data related to the patients themselves. Information related to data acquisition days, sessions, and tasks (with their repetitions where applicable) is further down the hierarchy. At the bottom of the hierarchy are the sensor readings. Finally, the dataset contains physician-provided labels at various points in the hierarchy, depending on what they relate to(including per patient, per day, per task).

After analysing the data, we performed our experiments on a subset of available data. We only use data from clinical

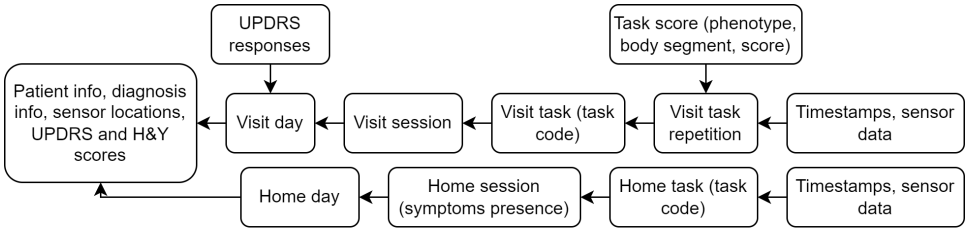

Fig. 2. Data hierarchy structure

visits because they provide individual scores for every task repetition instead of per-session scores for at-home data. Then, we decided to drop data from accelerometers only equipped by Boston subjects. Finally, we have decided to predict only upper limb scores in our experiments because lower limb scores are not available for NYC subjects.

We are conducting experiments on the classification of available labels using convolutional neural networks. We are evaluating three preprocessing strategies to present input data to convolutional neural network:

- Time series: Take a subset of data with a fixed length and present it directly to the 1D convolutional layer.
- Frequency series: Take a subset of data, transform it using Fast Fourier Transform, and then present it to the 1D convolutional layer.
- Spectrogram: Take a subset of data and transform it using the short-time Fourier transform, then present it to the 2D convolutional layer.

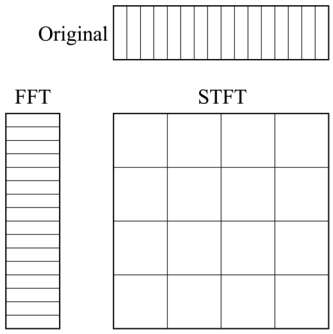

Fig. 3. Data transformations

This choice impacts the amount of temporal and spectral information entering the neural network (Figure 3). Time series without transformation have full temporal resolution but lack spectral information. Frequency series with FFT have full spectral resolution but lack temporal information. With the STFT transformation, the spectrogram images contain both temporal and spectral information. There is a trade-off between temporal and spectral resolution; the high resolution of one necessitates the low resolution of the other. However, this transformation reveals temporal changes in frequency spectrum that are invisible in pure time series or FFT spectrum.

In our experiments, we are classifying one of the following labels:

- Binary task recognition: The model classifies whether it is one specific type of task or a different one.
- Multiclass task recognition: The model classifies which type of task.
- Phenotype severity classification: The model classifies the severity of one selected phenotype. Available phenotypes are Tremor, Bradykinesia and Dyskinesia. Discrete numbers from 0(absent) to 5(severe) express the severity of the phenotype.

To help automate and visualise the experiments, we are using the Wandb platform [10]. Hyperparameter sweeps allow us to train many models sequentially with varying hyperparameters without needing to adjust the hyperparameters and re-execute training code manually. Hyperparameters can affect various training components, such as data pipelines, neural network models, and training engine behaviour.

The Wandb platform also contains extensive visualisation options. During training, we can log virtually any information into the Wandb platform, including the value of loss functions or metrics. The Wandb platform visualises these logs, utilising any configuration of several possible graph types in real-time during training and post-training.

IV. Future Work

We are currently preparing the Rehapiano device, with its associated software suite, for deployment to the clinical environment. There, we plan to acquire a dataset on control patients, and patients with stroke related disorders. This dataset will later be used in our experiments.

Meanwhile, we are conducting experiments described in Solution Design on the Levodopa dataset [1]. The experiments are still ongoing, with no preliminary results available as of writing.

References

[1] J.-F. Daneault, G. Vergara-Diaz, F. Parisi, C. Admati, C. Alfonso, M. Bertoli, E. Bonizzoni, G. F. Carvalho, G. Costante, E. E. Fabara *et al.*, "Accelerometer data collected with a minimum set of wearable sensors from subjects with parkinson's disease," *Scientific Data*, vol. 8, no. 1, p. 48, 2021.

[2] S. Husár, "Deep learning for upper limb rehabilitation," in *23rd Scientific Conference of Young Researchers*, 2023, pp. 93–94.

[3] N. Ferenčík, M. Jaščur, M. Bundzel, and F. Cavallo, "The rehapiano—detecting, measuring, and analyzing action tremor using strain gauges," *Sensors*, vol. 20, no. 3, p. 663, 2020.

[4] S. Husár, N. FERENČíK, M. Bundzel, and S. Kardoš, "Design and evaluation of the electronic sensing system of rehapiano," in *2022 IEEE 20th Jubilee World Symposium on Applied Machine Intelligence and Informatics (SAMI)*. IEEE, 2022, pp. 000 279–000 284.

[5] S. Husár, M. Bundzel, M. Hlibokỳ, S. Kardoš, and N. Ferenčík, "Advanced prototype of manus diagnostics and rehabilitation device," *Acta Electrotechnica et Informatica*, vol. 23, no. 1, pp. 32–40.

[6] R. Bhidayasiri, "Differential diagnosis of common tremor syndromes," *Postgraduate medical journal*, vol. 81, no. 962, pp. 756–762, 2005.

[7] P. F. Crawford III and E. E. Zimmerman, "Differentiation and diagnosis of tremor," *American family physician*, vol. 83, no. 6, pp. 697–702, 2011.

[8] A. Anouti and W. C. Koller, "Tremor disorders. diagnosis and management." *Western journal of medicine*, vol. 162, no. 6, p. 510, 1995.

[9] A. Puschmann and Z. K. Wszolek, "Diagnosis and treatment of common forms of tremor," in *Seminars in neurology*, vol. 31, no. 01. © Thieme Medical Publishers, 2011, pp. 065–077.

[10] L. Biewald, "Experiment tracking with weights and biases," 2020, software available from wandb.com. [Online]. Available: https://www.wandb.com/

A Comprehensive Survey of Advancements and Innovations in the field of Software-Defined Networking

[1]*Erika Abigail KATONOVÁ (1st year),*
Supervisor: [2]*Peter FECIĽAK*

[1,2]Dept. of Computers and Informatics, FEI TU of Košice, Slovak Republic

[1]erika.abigail.katonova@tuke.sk, [2]peter.fecilak@tuke.sk

***Abstract*—In today's networking world, the emergence of Software-Defined Networking (SDN) represents a key revolutionizing aspect in the way the networks are understood, designed, and managed. This paper dives into the nature of SDN, discussing its fundamental principles, architectural frameworks, and transformative potential in modern network environments. At its core, SDN separates network management from the underlying infrastructure and enables centralized programmability and orchestration through software-based controllers. By abstracting network intelligence into software layers, SDN enables dynamic adaptation to various traffic patterns, applicational and operational requirements. Furthermore, SDN allows easy integration with new, emerging technologies such as Network Functions Virtualization, Machine learning and AI, Internet of Things, fifth-generation wireless technology, and many more. Through a comprehensive review of contemporary literature and case studies from different areas of research, this work summarizes the various aspects of SDN, and establishes it as an object of innovation and efficiency in modern networks. In addition, it introduces the challenges and opportunities associated with future SDN research, including security issues as well as transmission quality challenges. By shedding light on the potential of SDN in reshaping the concept of modern networks, this paper aims to inspire further research, development and deployment, and heralds a new era of agile, intelligent and adaptive network infrastructures.**

***Keywords*—SDN, Network programmability, OpenFlow, NFV, IBN**

I. Introduction

The world of networking has witnessed a profound transformation in recent years, driven by the substantial advancements in Software-Defined Networking (SDN). This revolution of traditional networking architectures is offering remarkable levels of flexibility, scalability, and agility in managing the network resources.

The current state of research in SDN reflects a dynamic integration of theoretical insights, practical implementations, and real-world deployments, enriched by the collective efforts of academia, industry, and open-source communities. Researchers are still actively exploring the various dimensions of SDN, which is its architectural design, as well as protocol enhancements, network optimization, security mechanisms, and application-driven use cases. This diverse investigation in SDN is driven by the quest to unlock its full potential in addressing the evolving challenges of modern networking environments.

Furthermore, the broad propagation of open-source SDN platforms and frameworks has opened the access to SDN experimentation and innovation to the wide public, empowering researchers with robust tools and resources to prototype, validate, and refine their concepts in real-world settings. Open-source ecosystems such as OpenDaylight, Floodlight, and Mininet (all thoughtfully described in this article [1]) have emerged as collaborative innovation, delivering knowledge sharing, experimentation, and community-driven development in the context of SDN.

While these advancements rise, the challenges also rise along with them, starting from scalability issues and performance problems to interoperability concerns and security vulnerabilities. Addressing these challenges necessitates a concerted research effort, including the theoretical demands, evaluations, and practical insights collected from large-scale deployments and operational experiences.

In light of these developments, this paper aims to provide an overview of the current state of research in SDN, combining insights from recent literature, ongoing research effort, and possible emerging trends that shape the future path of SDN. By diving into key research themes, technological advancements, and open challenges, this paper offers a "roadmap" for navigating through the complex terrain of SDN research, by introducing few of the research areas from the quantum of available, as well as inspire future explorations of innovation in networking.

II. SDN Concepts and Architecture

Software-Defined Networking introduces an advanced network architecture that fundamentally redefines the traditional structure of networks. At its core, SDN revolutionizes network management by its ability to separate the control plane from the data plane, enabling centralized control and orchestration of network resources through software-based controllers [2] [3]. This groundbreaking and very efficient approach offers the important effects on performance and capability of the network, such as agility, scalability, and efficiency in network management and operation.

A. Architecture

As the Fig. 1 depicts, the infrastructure is separated into these key components:

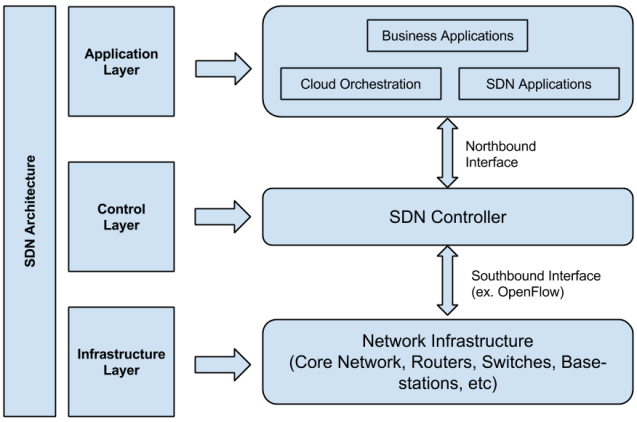

Fig. 1. The architecture of a software-defined network [4]

1) **Infrastructure Layer:** Also known as the data plane, consists of devices primarily responsible for forwarding data. These devices (in the SDN architecture) execute instructions received from the centralized controller without the need for complex decision-making processes.
2) **Control Layer (Controller):** This layer represents (in SDN networks) a software-based controller. The controller serves as the brain of the network, responsible for making decisions and distributing instructions to the data plane devices.
3) **Application Layer:** This layer contains software applications and services that use the programmable capabilities of the SDN infrastructure to implement network policies, services, and functions. It interacts with the SDN controller through northbound APIs.
4) **Southbound Interface:** The southbound interface refers to the communication protocols and interfaces used by the controller to communicate with the data plane devices. Examples of southbound interfaces include OpenFlow [5], NETCONF [6], and SNMP [7].
5) **Northbound Interface:** The northbound interface allows external applications, management systems, and network services to interact with the SDN controller. It provides an abstraction layer that enables programming and automation of network functions.

B. SDN Controller

This separation of data plane and control plane, represented by the SDN controller, allows for dynamic management and configuration of network devices, leading to increased flexibility and possible implementation of programmability in the computer networks [8]. The controller serves as the centralized decision-making device of the network. It manages the devices by distributing instructions to them, using the OpenFlow protocol for this action [9]. OpenFlow is a foundational protocol responsible for communication between the control and data plane, although alternative solutions, as discussed in these publications [10] [11], also exist and have similar outcome.

There are multiple versions or implementations of SDN controllers available, each with its own features, capabilities, and design philosophies. Some of the highly used software-based controllers in SDN environments are listed below. The selection of controllers was based on their popularity [2].

- **OpenDaylight (ODL):** OpenDaylight is one of the most widely used open-source SDN controllers. It offers a flexible platform for developing and deploying SDN applications and services. ODL supports various southbound protocols, including OpenFlow and NETCONF. [1] [12].
- **Floodlight:** Floodlight is an open-source SDN controller developed by the Open Networking Foundation (ONF). It is designed for simplicity and ease of use, making it suitable for research, education, and small deployments. Floodlight supports the OpenFlow [5] protocol and provides a RESTful API for northbound communication [1] [13].
- **Mininet:** Mininet is not a regular SDN controller itself but rather a network emulator used primarily for SDN development, testing, and education purposes. It allows users to create virtual networks with multiple hosts, switches, controllers, and links, all running within a single computer or virtual machine environment [1].
- **Open Network Operating System (ONOS):** ONOS is also an open-source SDN controller designed for large networks. It features scalability, high availability, and performance optimizations tailored to large-scale deployments. ONOS supports a range of southbound protocols and offers northbound APIs for application development and integration [14].
- **Ryu:** Ryu is a lightweight and highly modular SDN controller written in Python. It offers a simple framework for developing custom SDN applications and services. Ryu supports OpenFlow [5] and other southbound protocols and provides a straightforward API for interacting with network devices and applications [15].
- **Cisco Application Policy Infrastructure Controller (APIC):** APIC is a SDN controller developed by Cisco Systems. It is designed to work with Cisco's Application Centric Infrastructure (ACI) for policy-based automation and orchestration of network services. APIC provides centralized management and automation capabilities for multi-tenant data center environments [16].

Overall, the SDN network structure introduces a clear separation of control and data planes, centralized control and management, and standardized interfaces for programmability. This architectural paradigm enables organizations to achieve greater agility, scalability, and efficiency in deploying and managing their network infrastructures, paving the way for innovation and transformation in networking.

III. Status Quo in SDN research

Software-Defined Networking has revolutionized network management, and yet its current state still shows a dynamic progress. SDN continues to be evolving area of research, with multiple different key trends and developments shaping the current status of the topic [17]:

A. Artificial Intelligence (AI) and Machine Learning (ML)

Artificial Intelligence and Machine Learning techniques are increasingly being applied to SDN for intelligent network management, optimization, and anomaly detection. The researches in paper [18] demonstrate a significant improvement in the quality of the federated learning process through SDN. Results are explained in the Loss metric, which shows that SDN enables achieving similarly low loss values in nearly half the time compared to without SDN support. The paper

proposes a communication architecture designed to support federated learning processes while optimizing training times without sacrificing performance, therefore delivers a solution to critical issue in the next-generation network infrastructures. On the other hand, supporting the learning enhancement by ML, authors of the paper "A Survey on Machine Learning Techniques for Routing Optimization in SDN" are proposing multiple directions how to implement ML into the SDN research [19].

B. Internet of Things (IoT)

SDN provides optimized routing and traffic engineering techniques to improve the efficiency of data transmission in IoT networks. Through centralized control and programmable forwarding decisions, SDN can dynamically adjust routing paths, reroute traffic around congested areas, and balance load across network links, thereby minimizing latency, reducing packet loss, and improving overall network efficiency. All these are included in the article [20]. However, the authors are highlighting the fact that the security topic should be incorporated into more research in the future. Few years late finds the SDN significant relevance in the security research communities, particularly in the context of IoT systems. In research [21], authors offer an in-depth exploration of key SDN functionalities that can be leveraged to advance the security of IoT environments. From traffic isolation to monitoring and flow control, each identified feature is examined, deeply explained, and provided with exemplary implementations.

C. Intent-Based Networking (IBN)

Intent-Based Networking is a modern networking paradigm that focuses on the simplifying of network management and operations by focusing on "intent" of the network policies and configurations rather than the manual configuration details. The term intent is an evolved version of the term "policy". The ground for this definition is that policy management was difficult for end users without formal education in the specific field. Therefore intents abstract away implementation details, representing high-level operational and business objectives, such as security policies, performance requirements, or compliance rules. The IBN system then translates these objectives into actionable network configurations and policies, automating the provisioning, optimization, and troubleshooting of network infrastructure to align with the specified intents. For further information on this topic follow the research in the study published by turkish researchers Engin Zeydan an Yekta Turk [22].

To proceed in the topic of Software-Defined Networking, the IBN is closely connected with it, since it builds upon the capabilities of SDN by introducing a higher-level abstraction layer focused on expressing business objectives or intents in a declarative manner. Instead of dealing with low-level network configurations, administrators specify their desired network behaviors, such as security policies, performance requirements, or service-level agreements (SLAs), using natural language or domain-specific languages. The authors in research published in 2023 [23] dive into recent advancements in IBN architecture and its components.

D. Network Functions Virtualisation (NFV)

A very interesting area of research is the NFV concept. Network Function Virtualization is a networking paradigm that virtualizes and abstracts network functions traditionally performed by dedicated hardware devices. In NFV, network functions such as firewalls, load balancers, routers, and switches are implemented as software-based virtualized instances that can run on standard hardware infrastructure. NFV "detaches" network functions from proprietary hardware devices, and deploys them as virtualized software instances on commodity hardware, servers, or in the cloud. This principle of NFV usage enables greater flexibility, scalability, and agility in deploying and managing network services. Authors in this work [24] focus on the cooperation of SDN and NFV architecture while using a single framework. Also another point of view is their coexistence and mutual resource embracing in the virtualization techniques in the IoT environment, captured by several authors in paper "A survey of network virtualization techniques for internet of things using sdn and nfv." [25]. The autors introduce a problem of complex physical infrastructure of heterogeneous network systems solvable by the virtualization, softwarization and programmability offered by SDN and NFV.

E. 5G wireless technology

The approach of 5G networks and edge computing architectures presents new challenges and opportunities for SDN research. Article by researchers K. T. Selvi and R. Thamilselvan [26] deals with the challenge of the network resource allocation, where the authors propose a solution, where the centralized cloud-based SDN controller plays a crucial role in identifying the needs of necessary applications as well as provides a important forwarding regulations. Experiments of the proposed models, which predicted traffic flow found to be consistent with the actual traffic flow gathered from he measurements. Accordingly these experimental findings shed light on the predictive models' ability to effectively anticipate future traffic patterns, therefore allowing dynamic resource allocation within 5G networks.

Moreover, researchers S. Li and Q. Hu in the paper "Dynamic resource optimization allocation for 5g network slices under multiple scenarios" [27], address the limitations in network resource allocation research by proposing a dynamic scheduling scheme for bandwidth resources. The algorithm they use is built upon the classical SDN network architecture and integrates admission control and delay penalty factors to meet the performance demands of network. Simulation experiments validate the algorithm's ability to balance performance requirements across various scenarios while minimizing the cost of dynamic resource adjustment. The proposed algorithm demonstrates superior performance in terms of resource utilization and low-delay reliability.

IV. Challanges for near future

Through the complex research of SDN, there are still unopened doors leading to new discoveries in this interesting field, many of which have been dived into already. Identifying and addressing challenges is important since it drives innovation and progress in networking technologies. By firstly discovering, and secondly addressing these challenges, researchers and industry professionals can develop new solutions, algorithms, and architectures to enhance the capabilities and performance of SDN. Therefore the purpose of this section is to introduce a few of those open challenges.

A. Consistent transmission quality

Ensuring consistent quality of transmission plays a significant role as an open challenge in SDN environments. As networks become increasingly dynamic and diverse, maintaining consistent and reliable transmission quality for various types of traffic remains a critical concern. Where the factors that affect the consistency and quality are delay, data loss and load peaks.

The primary problem lies in effective managing of network congestion, due to mentioned factors, and bandwidth allocation to prevent the degradation in transmission quality. SDN controllers must dynamically adapt routing paths, prioritize traffic flows, and enforce QoS policies to ensure that the applications or devices receive the necessary bandwidth and latency guarantees while optimizing resource utilization. The possible path to solution of inconsistent and unreliable infrastructure would be in the application of the control plane of the SDN controller, where it is possible to apply various algorithms to evaluate the quality of transmission and ensure consistent end-to-end delivery with the guarantee of quality transmission parameters. Multiple of those algorithms are mentioned in this recent study from June 2022 [28], which introduces several versions and improvements of Transmission Control Protocol (TCP) ensuring the smooth data transfer.

B. Compatibility and security in a Heterogeneous networks

Heterogeneous networks consist of a variety of network devices from different vendors, each with its own proprietary protocols, configurations, and capabilities [29]. Ensuring compatibility among these devices and integrating them into an SDN environment can be challenging, as SDN controllers need to support multiple protocols and standards to communicate with diverse network elements or either within the controllers themselves. Ensuring interoperability and seamless communication therefore requires standardization efforts and protocol translation mechanisms to bridge the gap between different protocol domains. The heterogeneity of the environment can accordingly open up new areas of research to ensure the interoperability of network environments.

Security and privacy is another issue in the topic of communication in the modern heterogeneous network environments. Hence even heightened, as the presence of diverse devices introduces potential vulnerabilities and attack vectors. Ensuring the consistent security policies of heterogeneous devices requires advanced security features, including authentication, authorization, encryption, and intrusion detection systems (IDS). Additionally, the lack of standardized security mechanisms across different vendor devices complicates security management and increases the risk of security breaches. Therefore there is a room for defining support mechanisms to ensure integrity or secrecy in transmission through the network environment.

V. Conclusion

Through comprehensive analysis of the topic of SDN, following the literature review of multiple actual research papers, this work concludes the key principles and components of SDN, shedding light on their capacity to enhance network flexibility, scalability, and efficiency. The various findings in research underscore the importance of centralized control, programmability, and automation in SDN architectures, as well as their potential in future work, challenges and opportunities inherent in their deployment and management. By examining the current state of SDN architecture and exploring its potential applications in discovered emerging challenges, this study may contribute to the future discoveries and publications of this topic.

References

[1] S. Rowshanrad, V. Abdi, and M. Keshtgari, "Performance evaluation of sdn controllers: Floodlight and opendaylight," *IIUM Engineering Journal*, vol. 17, no. 2, pp. 47–57, Nov. 2016.

[2] D. Kreutz, F. M. V. Ramos, P. Esteves Verissimo, C. Esteve Rothenberg, S. Azodolmolky, and S. Uhlig, "Software-defined networking: A comprehensive survey," *Proceedings of the IEEE*, vol. 103, no. 1, pp. 14–76, Jan. 2015.

[3] N. S. B. Saeed and M. J. Alenazi, "Utilizing sdn to deliver maximum tcp flow for data centers," in *Proceedings of the 2020 The 3rd International Conference on Information Science and System*, ser. ICISS 2020. ACM, Mar. 2020.

[4] T. Wong, H. Cui, Y. Shen, W. Lin, and T. Yu, "Anonymous network communication based on sdn," in *2018 4th International Conference on Universal Village (UV)*. IEEE, Oct. 2018.

[5] A. Lara, A. Kolasani, and B. Ramamurthy, "Network innovation using openflow: A survey," *IEEE Communications Surveys amp; Tutorials*, vol. 16, no. 1, pp. 493–512, 2014.

[6] F. Izadi and H. S. Shahhoseini, "Automated formal analysis of netconf protocol for authentication properties," in *6th International Symposium on Telecommunications (IST)*. IEEE, Nov. 2012.

[7] R. Presuhn, "Version 2 of the Protocol Operations for the Simple Network Management Protocol (SNMP)," RFC 3416, Dec. 2002. [Online]. Available: https://www.rfc-editor.org/info/rfc3416

[8] W. Xia, Y. Wen, C. H. Foh, D. Niyato, and H. Xie, "A survey on software-defined networking," *IEEE Communications Surveys amp; Tutorials*, vol. 17, no. 1, pp. 27–51, 2015.

[9] B. A. A. Nunes, M. Mendonca, X.-N. Nguyen, K. Obraczka, and T. Turletti, "A survey of software-defined networking: Past, present, and future of programmable networks," *IEEE Communications Surveys amp; Tutorials*, vol. 16, no. 3, pp. 1617–1634, 2014.

[10] E. Haleplidis, J. H. Salim, J. M. Halpern, S. Hares, K. Pentikousis, K. Ogawa, W. Weiming, S. Denazis, and O. Koufopavlou, "Network programmability with forces," *IEEE Communications Surveys amp; Tutorials*, vol. 17, no. 3, pp. 1423–1440, 2015.

[11] R. Enns, M. Björklund, A. Bierman, and J. Schönwälder, "Network Configuration Protocol (NETCONF)," RFC 6241, Jun. 2011. [Online]. Available: https://www.rfc-editor.org/info/rfc6241

[12] A. Eftimie and E. Borcoci, "Sdn controller implementation using opendaylight: experiments," in *2020 13th International Conference on Communications (COMM)*. IEEE, Jun. 2020.

[13] L. Mamushiane, A. Lysko, and S. Dlamini, "A comparative evaluation of the performance of popular sdn controllers," in *2018 Wireless Days (WD)*. IEEE, Apr. 2018.

[14] A. Giorgetti, A. Sgambelluri, R. Casellas, R. Morro, A. Campanella, and P. Castoldi, "Control of open and disaggregated transport networks using the open network operating system (onos) [invited]," *Journal of Optical Communications and Networking*, vol. 12, no. 2, p. A171, Dec. 2019.

[15] S. Asadollahi, B. Goswami, and M. Sameer, "Ryu controller's scalability experiment on software defined networks," in *2018 IEEE International Conference on Current Trends in Advanced Computing (ICCTAC)*. IEEE, Feb. 2018.

[16] C.-M. Gheorghe, C.-M. Iurian, E.-F. Luchian, I.-A. Ivanciu, and V. Dobrota, "Applications of the cisco apic-em software-defined networking controller for a virtualized testbed," in *2017 16th RoEduNet Conference: Networking in Education and Research (RoEduNet)*. IEEE, Sep. 2017.

[17] G. Zhao, G. Li, P. Xie, S. Han, W. Zhang, and W. Huang, "Research on sdn network management architecture in the field of electric power communication," in *2023 IEEE 3rd International Conference on Data Science and Computer Application (ICDSCA)*. IEEE, Oct. 2023.

[18] A. Mahmod, G. Caliciuri, P. Pace, and A. Iera, "Improving the quality of federated learning processes via software defined networking," in *Proceedings of the 1st International Workshop on Networked AI Systems*, ser. NetAISys '23. ACM, Jun. 2023.

[19] R. Amin, E. Rojas, A. Aqdus, S. Ramzan, D. Casillas-Perez, and J. M. Arco, "A survey on machine learning techniques for routing optimization in sdn," *IEEE Access*, vol. 9, pp. 104 582–104 611, 2021.

[20] Y. Li, X. Su, J. Riekki, T. Kanter, and R. Rahmani, "A sdn-based architecture for horizontal internet of things services," in *2016 IEEE International Conference on Communications (ICC)*. IEEE, May 2016.

[21] I. Farris, T. Taleb, Y. Khettab, and J. Song, "A survey on emerging sdn and nfv security mechanisms for iot systems," *IEEE Communications Surveys amp; Tutorials*, vol. 21, no. 1, pp. 812–837, 2019.

[22] E. Zeydan and Y. Turk, "Recent advances in intent-based networking: A survey," in *2020 IEEE 91st Vehicular Technology Conference (VTC2020-Spring)*. IEEE, May 2020.

[23] M. Gharbaoui, B. Martini, and P. Castoldi, "Intent-based networking: Current advances, open challenges, and future directions," in *2023 23rd International Conference on Transparent Optical Networks (ICTON)*. IEEE, Jul. 2023.

[24] E. Haleplidis, D. Joachimpillai, J. H. Salim, D. Lopez, J. Martin, K. Pentikousis, S. Denazis, and O. Koufopavlou, "Forces applicability to sdn-enhanced nfv," in *2014 Third European Workshop on Software Defined Networks*. IEEE, Sep. 2014.

[25] I. Alam, K. Sharif, F. Li, Z. Latif, M. M. Karim, S. Biswas, B. Nour, and Y. Wang, "A survey of network virtualization techniques for internet of things using sdn and nfv," *ACM Computing Surveys*, vol. 53, no. 2, pp. 1–40, Apr. 2020.

[26] K. T. Selvi and R. Thamilselvan, "Dynamic resource allocation for sdn and edge computing based 5g network," in *2021 Third International Conference on Intelligent Communication Technologies and Virtual Mobile Networks (ICICV)*. IEEE, Feb. 2021.

[27] S. Li and Q. Hu, "Dynamic resource optimization allocation for 5g network slices under multiple scenarios," in *2020 Chinese Control And Decision Conference (CCDC)*. IEEE, Aug. 2020.

[28] A. Abadleh, A. Tareef, A. Btoush, A. Mahadeen, M. M. Al-Mjali, S. S. Alja'Afreh, and A. A. Alkasasbeh, "Comparative analysis of tcp congestion control methods," in *2022 13th International Conference on Information and Communication Systems (ICICS)*. IEEE, Jun. 2022.

[29] Y. Xu, G. Gui, H. Gacanin, and F. Adachi, "A survey on resource allocation for 5g heterogeneous networks: Current research, future trends, and challenges," *IEEE Communications Surveys amp; Tutorials*, vol. 23, no. 2, pp. 668–695, 2021.

Simulations and Comparison of Active Cell Balancing Based on Switched Capacitors

[1]*Daniel MARCIN (2nd year)*
Supervisor: [2]Milan LACKO

[1,2]Department of Electrical Engineering and Mechatronics, FEI TU of Košice, Slovak Republic

[1]daniel.marcin@tuke.sk, [2]milan.lacko@tuke.sk

***Abstract*—This study examines capacitor-based active cell balancing methods for enhancing electric vehicle battery systems. Through MATLAB Simulink simulations, we analyse three circuits: switched capacitors, double-tiered switched-capacitors, and an enhanced variant with an additional capacitor. Results show the double-tiered circuit achieves a 1% SOC difference in 1186 seconds, with the extra capacitor slightly extending balancing time to 1195 seconds.**

***Keywords*—Battery management system, active cell balancing, Li-ion, switched-capacitors.**

I. Introduction

The recent surge in electric vehicle (EV) adoption reflects a global push towards reducing reliance on fossil fuels and mitigating transportation-related environmental impacts. Central to the success of these EVs is the efficiency and reliability of their battery systems (BS) [1], [2]. A robust BS not only extends the vehicle's range but also enhances its overall performance and dependability.

Playing a crucial role in the functionality of EV BS is the battery management system (BMS), responsible for ensuring safe operation and optimal performance. By monitoring cell states and executing functions such as voltage and temperature regulation, fault detection and protection, the BMS safeguards the integrity of the battery pack [3].

Cell balancing, a critical aspect of BMS functionality, involves maintaining uniform charge distribution among individual cells within the battery pack. This equilibrium mitigates the risk of overloading specific cells and safeguards against performance degradation and safety hazards [4].

Active cell balancing, a non-dissipative technique, strategically transfers energy among cells to optimize their performance and longevity. Utilizing PWM signals to control switches, active cell balancing employs various components such as capacitors, inductors, transformers, or DC/DC converters to facilitate charge transfer [5]. Capacitors play a key role in many balancing circuits, facilitating charge redistribution for optimal cell equilibrium.

In this paper, we conduct a comparative analysis of three active cell balancing circuits through MATLAB simulations: switched capacitors, double-tiered switched-capacitors, and an enhanced variant incorporating an additional capacitor to the second circuit. Our aim is to provide insights into the advantages and limitations of each circuit.

II. Simulations and Results

To explore the development of a modular battery system, we conducted simulations on different capacitor-based active cell balancing circuits. Initially, we focused on the switched-capacitor balancing circuit. Subsequently, we analysed the performance of the double-tiered switched-capacitor circuit. Finally, we expanded upon the second simulation by integrating an extra capacitor between the first and last cell. The last circuit is depicted in Fig. 1. The double-tiered switched-capacitor is identical, except for the absence of the C6 capacitor. Similarly, the switched-capacitor circuit comprises only the C1 – C3 capacitors. These simulations were conducted using MATLAB and Simulink programs. These simulations are applied to the circuit only in the state, when there is no load applied to the battery pack.

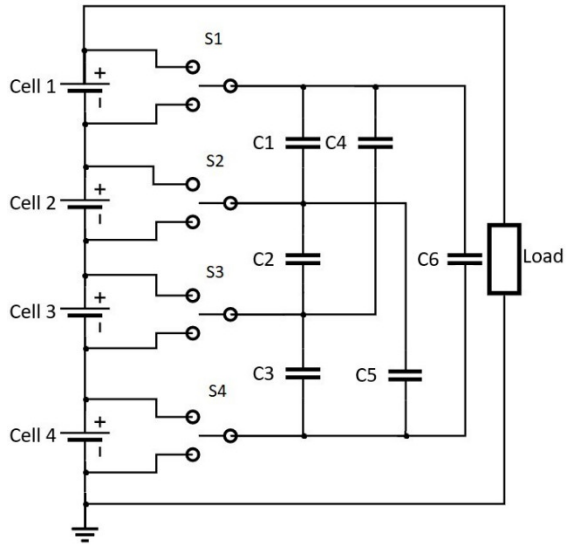

Fig. 1 Circuit of double-tiered switched-capacitors with additional capacitor

A. Modelling, parameters and simulation data

For simulation battery cell parameters were used data of manufacturer MOLICEL with model number INR18650-P26A. For our purpose we simulated on 12 cells connected in series. Simscape models of battery cell, ideal switch and capacitors were used for our purpose. Simulation parameters are shown in Table I. The switches in the circuit are connected to two PWM signals, operating at a frequency of 1 kHz.

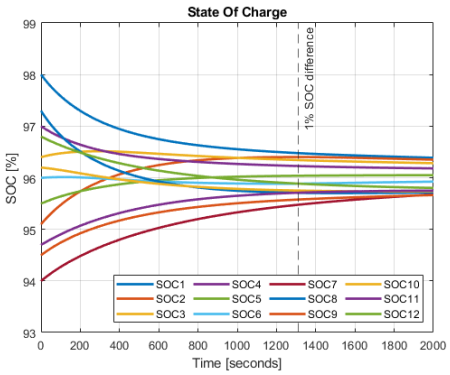

Fig. 2 SOC progress during switched-capacitor balancing simulation

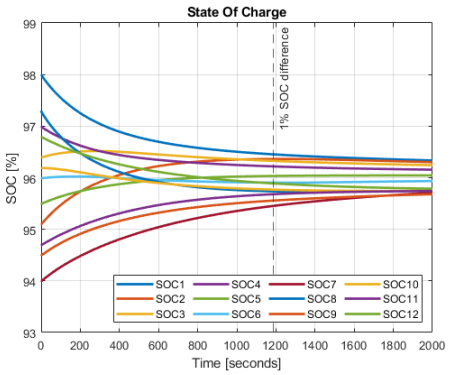

Fig. 3 SOC progress during double-tiered switched-capacitor balancing

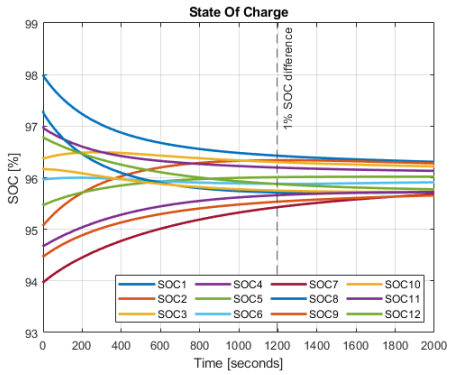

Fig. 4 SOC progress during double tiered switched-capacitor with additional capacitor balancing simulation

TABLE I
SIMULATION PARAMETERS

Parameter	*Value*	*Unit*
Battery nominal voltage	3,6	V
Battery capacity	2,6	Ah
Battery response time	0,5	s
Battery internal resistance	13,85	mΩ
Capacitor capacitance	50	mF
Switching frequency	1	kHz
Simulation time	2000	s

The simulation was initiated with cells possessing a 4 % initial imbalance, arranged randomly. To introduce greater balancing challenges, it was ensured that cells with the highest and lowest SOC were not placed adjacent to each other. These simulations were conducted over a duration of 2000 seconds.

B. Results with switched-capacitor

In the first simulation (C1 – C3 capacitors), the switched-capacitor circuit was implemented. The simulation results revealed that a 1 % imbalance was achieved in 1312 seconds. The cell with the highest SOC was Cell 1, and the cell with the lowest SOC was Cell 7. These results are depicted in Fig. 2.

C. Results with double-tiered switched-capacitor

In the second simulation (C1 – C5 capacitors), we similarly implemented the double-tiered switched-capacitor circuit in MATLAB Simulink. The simulations revealed that a 1 % imbalance was achieved in 1186 seconds, as shown in Fig. 3.As expected, this circuit, with its additional layers of capacitors, proved to be faster than the switched-capacitor circuit. The difference in balancing time was 126 seconds, and the behaviour of the cells was quite similar.

D. Results with double-tiered switched-capacitor with additional capacitor

Finally, we implemented an additional layer of capacitors into the MATLAB Simulink model (C1 – C6 capacitors). This method of balancing was expected to be the fastest due to the presence of the additional capacitor connected to the battery pack. However, the simulation results in Fig. 4. showed that with the capacitor value the same as the others, it actually made the balancing slightly slower. The balancing time to achieve a 1 % difference in SOC was 1195 seconds, which was 9 seconds slower than without the additional capacitor.

III. CONCLUSION

This paper presents the capacitor based active cell balancing methods. For construction of modular battery system which consists of multiple battery modules an active balancing method needs to be reviewed. Multiple balancing methods were discussed, and to evaluate the performance of each, they were implemented in MATLAB Simulink simulations. Switched-capacitor method is the simplest and slowest. With 12 cells in series battery module the balancing time was 1312 seconds for the 1 % SOC difference between the lowest and highest cell. Double-tiered switched capacitor method got the same 1 % difference in 1186 seconds. Interestingly, the inclusion of an additional capacitor in the double-tiered circuit resulted in a slightly longer balancing time of 1195 seconds. At the end of simulation time (2000 seconds) the SOC differences between the highest and lowest cells were 0,75 % at the switched-capacitor method. In the double-tiered method was difference at 0,68 % and with additional capacitor at 0,65 %. In the first test the additional capacitor simulation did not have the best results, but at the end of simulation comparison in was faster than without the capacitor. Interestingly, in all the simulations the Cell number 7 was the lowest charged cell for majority of the simulation time. However, at the end, Cell number 9 was the lowest charged cell in all cases. The simulation results serve as foundational research for experimental studies.

ACKNOWLEDGMENT

This work was supported by projects APVV-18-0436, VEGA 1/0363/23 and KEGA 059TUKE-4/2024.

REFERENCES

[1] M. A. Hannan, Md. M. Hoque, A. Hussain, Y. Yusof, and P. J. Ker, "State-of-the-Art and Energy Management System of Lithium-Ion Batteries in Electric Vehicle Applications: Issues and Recommendations," *IEEE Access*, vol. 6, pp. 19362–19378, 2018, doi: 10.1109/ACCESS.2018.2817655.

[2] P. Nur Halimah, S. Rahardian, and B. A. Budiman, "Battery Cells for Electric Vehicles," *International Journal of Sustainable Transportation Technology*, vol. 2, no. 2, pp. 54–57, Oct. 2019, doi: 10.31427/IJSTT.2019.2.2.3.

[3] P. Sun, R. Bisschop, H. Niu, and X. Huang, "A Review of Battery Fires in Electric Vehicles," *Fire Technol*, vol. 56, no. 4, pp. 1361–1410, Jul. 2020, doi: 10.1007/s10694-019-00944-3.

[4] G. L. Plett, *Battery management systems, Volume II: Equivalent-circuit methods*. Artech House, 2015.

[5] D. Andrea, *Battery Management Systems for Large Lithium-Ion Battery Packs*. Artech House, 2010.

Integrated Analysis of LSTM Predictive Model in Project Management

[1]*Emira Mustafa Moamer ALZEYANI (3rd year)*
Supervisor: [2]Csaba SZABÓ

[1,2]Dept. of Electrical Engineering and Informatics, FEI TU of Košice, Slovak Republic

[1]emira.mustafa.moamer.alzeyani@tuke.sk, [2]csaba.szabo@tuke.sk

***Abstract*— This paper introduces a predictive project management model using Long Short-Term Memory (LSTM). The model's features, critical technicalities, tools, and methodologies are highlighted. Based on a meticulously collected student survey dataset, the LSTM model predicts completion time, personnel needs, and estimated costs, aiding in project feasibility and resource allocation evaluation. Consistency assessments with actual team sizes and a positive correlation in predicted completion times highlight the model's effectiveness. Discrepancies between anticipated and actual results provide valuable insights for proactive decision-making in project planning. The LSTM model's iterative nature, accuracy, and reliability position it as a robust decision-support tool for operational excellence and project success.**

***Keywords*— LSTM Model, Project Management, Predictive Model.**

I. Introduction

The realm of project management has witnessed a transformative shift with the integration of advanced predictive models [1], offering unprecedented insights and foresight into project dynamics. This paper explores the profound influence of state-of-the-art predictive models, like the Long Short-Term Memory (LSTM) model, on project management [2]. Our study emphasises achieving operational excellence and project success by demonstrating the growing dependence on advanced predictive tools to forecast critical project parameters, including completion time, personnel needs, and estimated costs. The LSTM model is renowned for capturing temporal dependencies and intricate patterns in sequential data. Our research goals are twofold: first, to create a predictive project management model using LSTM to forecast completion time, personnel needs, and costs; second, to assess its effectiveness in improving project feasibility and resource allocation. We aim to empower project managers with actionable insights, promoting informed decisions and operational excellence.

II. LSTM Predictive Models in Project Management

In our pursuit of developing and implementing a predictive model, we immersed ourselves in the intricacies of the Long Short-Term Memory (LSTM) model[3], as the technicalities, tools, and methodologies that shaped the development and implementation of our LSTM model [4], the model architecture is a sequential stack comprising an input, LSTM, and dense layer. We tailored the input layer to handle diverse project features, with the LSTM layer capturing temporal dependencies and the thick layer predicting project completion time.

Our training involved curating a diverse dataset, utilising 50 epochs to balance depth without overfitting, and employing batch learning with a batch size of ten for iterative weight updates. The Adam optimiser was instrumental in ensuring efficient gradient-based optimisation [5].

In data preprocessing, we applied scaling to numerical features for a uniform learning contribution, reshaped input data into sequences suitable for LSTM, and meticulously handled missing values by replacing them with zeros.

We subjected input data to a critical transformation during the prediction stage to align with the model's requirements. Our trained LSTM model interpreted input data, extracting insights on project completion times. Post-processing included inverse scaling to obtain predictions in the original units, providing interpretable foresight and insights into the temporal horizon of the project.

III. Preparing Data

In tackling challenges within software development, we formulated a targeted questionnaire for distribution among students at the Technical University of Košice (DCI -FEI). The study aims to gather data for a model that assists students in their project development efforts, resulting in 190 responses. The analysis encompasses various stages, including data collection, verification, and classification, all aimed at ensuring the accuracy and relevance of the findings.

A. Original Dataset

The basis of our analysis is a meticulously collected dataset from surveys distributed among diverse students. This dataset contains essential project information, such as cost, team size, and expected Duration. Key columns, including project name, team experience, and dates, provide insights into project dynamics, as shown in Table 1. These curated columns form the foundation for our analysis.

TABLE 1
THE ORIGINAL DATASET

ID	Project Name	Team Experience (Years)	Team Size	Start Date	Last Date	Expected Duration (Days)
1	GPS	2	2	06/11/2023	10/12/2023	90
3	web app	4	5	26/11/2023	10/12/2023	90
4	smart clock	2	3	12/01/2022	18/03/2022	90

5	Web game	3	3	10/01/2022	21/03/2022	90
6	desktop blog app	3	2	26/11/2023	07/12/2023	90
7	Web-based game	7	3	24/01/2022	24/06/2022	180
8	Web application	6	1	11/12/2023	29/01/2024	90

B. Predictions Dataset

After training our LSTM model, we generated successful predictions for crucial project metrics, as shown in Table 2, encompassing completion time, personnel needs, and estimated project cost. These systematically compiled results provide valuable insights for project planning and management, serving as a crucial basis for evaluating feasibility and optimising resource allocation.

TABLE 2
THE PREDICTIONS DATASET

Id	Project Name	Predicted Completion Time (Days)	Persons Needed	Estimated Cost
1	GPS	87	3	169
3	web app	60	5	170
4	smart clock	70	4	166
5	Web game	66	5	166
6	desktop blog app	67	3	169
7	Web-based game	67	4	167
8	Web application	65	5	169

C. Comparison of Predicted

In assessing the alignment between LSTM model predictions and actual team sizes in project development, as shown in Fig. 2, the blue line represents original 'Team Size' values. In contrast, the orange line reflects predicted 'Persons Needed' values. Consistency between the two lines suggests the model effectively captures personnel requirements, with deviations indicating nuances influenced by project complexity outliers, displaying significant disparities and presenting opportunities for investigating and enhancing the predictive model.

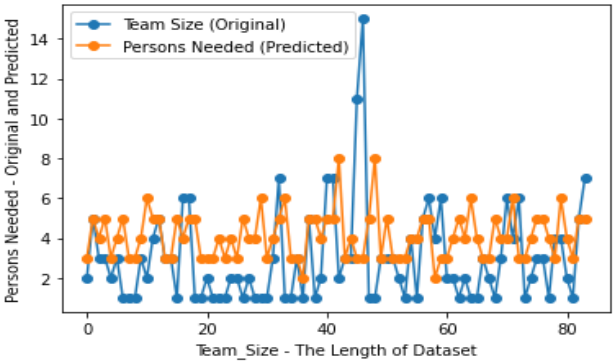

Fig. 1 The assessment between LSTM model predictions and actual team sizes in project development

D. Consistency in Predicted Completion Time

In Fig.2, comparing predicted completion time (days) from the LSTM model with expected project durations reveals essential insights. Generally, a positive correlation exists between predicted completion time and expected Duration, suggesting the LSTM model effectively captures project timelines. However, variability is observed, with some projects closely aligning with expectations while others deviate. Despite this variability, the overall trend indicates the model's capability to capture project timelines effectively.

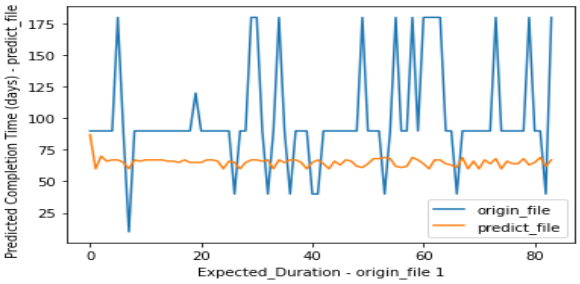

Fig. 2 Comparison of Predicted Completion Time with the Expected Duration

The disparities between the predictive model's expected timeframe and actual results stem from various factors, including student involvement in multiple projects, adherence to specific deadlines, differences in projected and actual team sizes, and the LSTM model recognising intricate project details that are not present in the original dataset. Rather than seeing these variations as discrepancies, they present opportunities for deeper insights into project dynamics. Leveraging the LSTM model's predictions and insights can proactively address challenges and optimise resource allocation for effective project planning and management decision-making.

IV. CONCLUSION

In conclusion, the LSTM-based project duration prediction model significantly enhances project management by enabling resource optimisation, improved planning, and risk mitigation. Its iterative nature supports continuous improvement, aligning well with dynamic project management needs. Serving as a transformative asset in the project manager's toolkit, it aids in planning, execution, and risk management. Optimising resource allocation and project feasibility through predictive capabilities empowers managers with actionable insights, anticipating integration into mainstream project management. Leveraging LSTM's strengths and investing in its development enables organisations to navigate modern project environments, achieving strategic objectives efficiently and confidently. Future work includes longitudinal studies to assess its long-term impact and scalability, alongside ongoing research to refine LSTM's predictive capabilities for evolving challenges.

REFERENCES

[1] Q. Wang, 'How to apply AI technology in Project Management1, 2', 2019, Accessed: Feb. 09, 2024. [Online]. Available: https://pmworldlibrary.net/wp-content/uploads/2019/03/pmwj80-Apr2019-Wang-how-to-aply-AI-in-project-management.pdf

[2] Project Group Business & Information Systems Engineering of the Fraunhofer FIT, University of Bayreuth, Bayreuth, Germany et al., 'Developing Purposeful AI Use Cases – A Structured Method and Its Application in Project Management', in WI2020 Zentrale Tracks, GITO Verlag, 2020, pp. 33–49. doi: 10.30844/wi_2020_a3-hofmann.

[3] A. Sherstinsky, 'Fundamentals of Recurrent Neural Network (RNN) and Long Short-Term Memory (LSTM) network', Phys. Nonlinear Phenom., vol. 404, p. 132306, Mar. 2020, doi: 10.1016/j.physd.2019.132306.

[4] R. E. Levitt and J. C. Kunz, 'Using artificial intelligence techniques to support project management', Artif. Intell. Eng. Des. Anal. Manuf., vol. 1, no. 1, pp. 3–24, Feb. 1987, doi: 10.1017/S0890060400000111.

[5] G. Auth, O. Jokisch, and C. Dürk, 'Revisiting automated project management in the digital age – a survey of AI approaches', Online J. Appl. Knowl. Manag., vol. 7, no. 1, pp. 27–39, May 2019, doi: 10.36965/OJAKM.2019.7(1)27-39.

[6] E. M. M. Alzeyani and C. Szabó, 'A Study on the Effectiveness of Agile Methodology Using a Dataset', Acta Electrotech. Inform., vol. 23, no. 1, pp. 3–10, Mar. 2023, doi: 10.2478/aei-2023-0001.

Advancing Capsule Neural Networks: Evolution, Challenges, and Future Directions in Interpretable AI Systems

[1]*Dominik VRANAY(3rd year),*
Supervisor: [2]*Peter SINČÁK*

[1,2]Dept. of Cybernetics and Artificial Intelligence, FEI TU of Košice, Slovak Republic

[1]dominik.vranay@tuke.sk, [2]peter.sincak@tuke.sk

***Abstract*—Capsule neural networks (CapsNets) have gained attention for their potential to enhance the interpretability of artificial intelligence (AI) systems. This paper reviews the evolution of CapsNets, addressing challenges and advancements in their development. Initial research highlighted advantages in image classification but faced issues such as high memory consumption and complex routing algorithms. Solutions, including simplified routing mechanisms and customized structures, improved practical applicability. Recent research focused on evaluating CapsNets' performance across dataset sizes, revealing their effectiveness on smaller datasets. The study also explores eXplainable AI (XAI) algorithms and delves into gradient dynamics during training. Planned work includes developing an explanation module, analyzing feature extractors, refining reconstruction processes, and visualizing the hierarchical structure of CapsNets. The overarching goal is to advance understanding and capabilities, contributing to transparent and interpretable AI systems.**

***Keywords*—Capsule Network, explainability, image classification, reconstruction, segmentation**

I. Introduction

Capsule neural networks (CapsNets) offer a promising avenue for enhancing the interpretability and transparency of artificial intelligence (AI) systems. Unlike traditional neural networks, CapsNets utilize capsules, groups of neurons, to represent features and their hierarchical relationships, thereby improving accuracy and explainability [1]. As demands for transparent AI systems grow, research into CapsNets becomes increasingly vital, given their potential to elucidate decision-making processes and foster trust [2].

However, CapsNets face challenges in capturing complex feature interactions and hierarchies. To address these obstacles, researchers are actively exploring novel techniques to optimize CapsNet architectures and training strategies [3], [4]. Despite progress, further improvements are needed to address specific sources of error, such as CapsNets' difficulty in handling variations in object shape and texture [5]. Resolving these biases will enhance the robustness and generalizability of CapsNets, thereby reinforcing the credibility and reliability of AI systems.

II. Background and Previous Findings

Initial CapsNet research yielded notable achievements, especially in image classification tasks [6]. CapsNets have shown advantages over traditional CNNs in handling object orientation and position variations. However, early CapsNet implementations faced several challenges:

- High Memory Consumption: Training CapsNets required substantial memory, posing issues for resource-limited devices [4].
- Complex Original Routing Algorithm: The original CapsNet routing mechanism was computationally intensive, leading to prolonged training times [2].
- Low Performance on Complex Datasets: CapsNets struggled to represent complex datasets, requiring exponential growth in dimensions [7].
- Difficulty in Segmentation Tasks: Initial CapsNet applications to segmentation tasks, especially in medical imagery, yielded unsatisfactory results [8].

Researchers responded to these challenges by introducing solutions that greatly improved the practical applicability of CapsNets:

- Simplification of Routing Mechanism: Developing less complicated routing algorithms between capsule layers resulted in faster training and lower computational demands [3].
- Introduction of Large Convolutional Backbones: Utilizing large convolutional backbones compressed the data and reduced the number of necessary capsules, enabling CapsNets to effectively handle more complex datasets [9].
- Development of Customized Structures: Adopting U-Net-like structures constructed using capsules and customized convolutional routing algorithms produced highly potent models suitable for segmentation tasks [10].

III. Research Highlights

Over the past year, our research extensively explored convolutional and capsule neural networks, focusing on their performance across datasets of varying sizes. We evaluated normal and pre-trained models across dataset sizes ranging from 10 to 7500 samples, with a particular emphasis on capsule networks' effectiveness in handling smaller datasets—a common challenge in real-world applications. Our comparative analysis revealed intriguing findings: while convolutional networks excel on larger datasets, capsule networks outperform them as dataset sizes decrease, albeit facing challenges with very

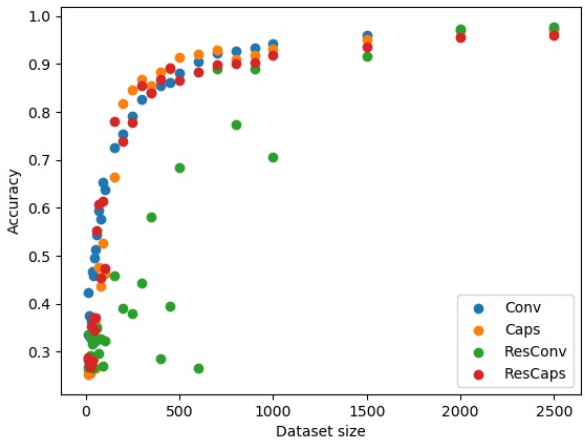

Fig. 1. Average accuracy of different models on datasets with different sizes.

small datasets. Surprisingly, pre-training has minimal impact on convolutional networks, especially for smaller datasets, whereas pre-trained CapsNet exhibits noteworthy improvements. These insights underscore capsule networks' efficacy for specific dataset sizes, with pre-training enhancing performance on smaller datasets, thus aiding in selecting suitable network architectures for diverse real-world scenarios [11]. The accuracies of the models can be seen in Fig. 1.

Our research delves into eXplainable Artificial Intelligence (XAI) algorithms, simplifying image classification and providing interpretable explanations. We explore GFNet for classification simplification through image segmentation, and the novel LIME technique for local model interpretation. Additionally, we integrate the CARE framework and Integrated Gradient method, emphasizing object detection and neural network feature visualization. With a goal to bridge technical expertise and end-user understanding, our thesis aims to develop a user-friendly interface for experimenting with convolutional neural networks, fostering broader AI system engagement. This research enhances accessibility and comprehensibility in AI, contributing to responsible and ethical AI development [12].

Furthermore, our investigation extends to dynamic gradient values during training across diverse networks. We observe consistent trends of decreasing gradients across all layers, with rising gradients in the capsule network's last routing layer. This provides valuable insights into parameter gradient dynamics during training, offering nuanced understanding of different network architectures' behavior.

Additionally, our exploration delves into analyzing shape vs texture bias exhibited by capsule neural networks, inspired by Geirhos' research [5]. This investigation aims to unravel how capsule networks prioritize shape and texture information, providing deeper insights into their decision-making processes in visual recognition tasks.

In the past year, a comprehensive review paper critically examined integrating Building Energy Management Systems (BEMSs) with Building Information Modeling (BIM) in construction and building management sectors, offering insights into BEMS-BIM integration's impact on building operations [13].

IV. Planned Work

Our research agenda comprises several pivotal components aimed at advancing capsule neural networks' understanding and capabilities.

We initially focus on developing an explanation module that utilizes capsule network outputs and segmentation masks to facilitate insightful discussions, particularly in medical scenarios [14]. Through natural language interactions, we aim to enhance the interpretability and user-friendliness of capsule network outputs.

The subsequent phase involves an in-depth analysis of feature extractors in capsule neural networks versus traditional CNNs. We systematically switch between architectures to optimize their performance and uncover insights into their complementary roles.

Concurrently, we refine the reconstruction process in capsule networks and explore various applications for explainability. By improving reconstructed image fidelity, we aim to provide clearer visualizations of network operations and enhance model transparency.

Lastly, our efforts extend to visualizing the hierarchical structure of capsule models and analyzing coupling coefficients. Through visual representations, we seek to elucidate the intricate relationships within the network and enhance understanding of object representations formed by capsules.

References

[1] G. E. Hinton, A. Krizhevsky, and S. D. Wang, "Transforming auto-encoders," in *Int. Conf. on artificial neural networks*. Springer, 2011, pp. 44–51.

[2] S. Sabour, N. Frosst, and G. E. Hinton, "Dynamic routing between capsules," *Advances in neural information processing systems*, vol. 30, 2017.

[3] V. Mazzia, F. Salvetti, and M. Chiaberge, "Efficient-capsnet: Capsule network with self-attention routing," *Scientific Reports*, vol. 11, no. 1, pp. 1–13, 2021.

[4] G. E. Hinton, S. Sabour, and N. Frosst, "Matrix capsules with em routing," in *Int. Conf. on learning representations*, 2018.

[5] R. Geirhos, P. Rubisch, C. Michaelis, M. Bethge, F. A. Wichmann, and W. Brendel, "Imagenet-trained cnns are biased towards texture; increasing shape bias improves accuracy and robustness," *arXiv preprint arXiv:1811.12231*, 2018.

[6] D. Vranay, "Capsule neural networks - future of deep learning?" in *22nd Scientific Conference of Young Researchers*, 2022, pp. 170–173.

[7] W. Wang, F. Lee, S. Yang, and Q. Chen, "An improved capsule network based on capsule filter routing," *IEEE Access*, vol. 9, pp. 109 374–109 383, 2021.

[8] R. LaLonde and U. Bagci, "Capsules for object segmentation," *arXiv preprint arXiv:1804.04241*, 2018.

[9] I. J. Jacob, "Capsule network based biometric recognition system," *Journal of Artificial Intelligence*, vol. 1, no. 02, pp. 83–94, 2019.

[10] M. Tran, L. Ly, B.-S. Hua, and N. Le, "Ss-3dcapsnet: Self-supervised 3d capsule networks for medical segmentation on less labeled data," in *2022 IEEE 19th Int. Symposium on Biomedical Imaging (ISBI)*. IEEE, 2022, pp. 1–5.

[11] D. Vranay, M. Katona, and P. Sinčák, "Comparative analysis of convolutional and capsule networks on decreasing dataset sizes: Insights for real-world applications," in *2023 World Symposium on Digital Intelligence for Systems and Machines (DISA)*. IEEE, 2023, pp. 232–238.

[12] D. Furman, M. Mach, D. Vranay, and P. Sinčák, "Exploring interpretable xai algorithms for image classification and prediction explanations," in *2023 World Symposium on Digital Intelligence for Systems and Machines (DISA)*. IEEE, 2023, pp. 66–71.

[13] M. Kozlovska, S. Petkanic, F. Vranay, and D. Vranay, "Enhancing energy efficiency and building performance through bems-bim integration," *Energies*, vol. 16, no. 17, p. 6327, 2023.

[14] D. Vranay, "Exploring capsule neural networks and the importance of explainability," in *23rd Scientific Conference of Young Researchers*, 2023, pp. 107–109.

Contribution to Experimental Identification of Nonlinear Dynamical Systems

[1]*Tomáš TKÁČIK (3rd year),*
Supervisor: [2]Anna JADLOVSKÁ, Consultant: [3]Ján JADLOVSKÝ

[1,2,3]Dept. of Cybernetics and Artificial Intelligence, FEEI TU of Košice, Slovak Republic

[1]tomas.tkacik@tuke.sk, [2]anna.jadlovska@tuke.sk, [3]jan.jadlovsky@tuke.sk

***Abstract*—This contribution presents results obtained during the last year of the author's PhD study in the field of nonlinear dynamical system identification. A brief introduction to the methodology of the experimental identification is presented with its application in the helicopter laboratory model identification. Finally, improvements to the ALFRED and DARMA applications as part of project ALICE CERN are presented.**

***Keywords*—Nonlinear Dynamical Systems, Experimental Identification Methodology, Helicopter Laboratory Model, Detector Control System**

I. Introduction

Mathematical models present a fundamental tool in various scientific and engineering disciplines. They capture important properties of the real systems in a compact form. This allows models to be useful in many tasks including analysis, prediction, diagnosis, process optimization, etc. [1]. Models are a crucial part of the model-based design paradigm that prioritizes the use of models over creating several iterations of the real system, especially when designing complex systems [2].

Two primary options exist to create the mathematical model of the real dynamical system: analytical and experimental identification [2]. Former relies on deriving a mathematical model using physics laws in the form of differential or difference equations. On the contrary, experimental identification is a data-driven paradigm that uses experimental data to infer both structure and parameters from data. The availability of relatively cheap computational power and the abundance of experimental data fueled the popularity boom of the experimental identification paradigm in recent years [3].

II. Previous analysis and achieved results

The general experimental identification methodology consists of four steps: data collection, model structure selection, choice of parameter estimation method, and approximation model validation [1], [4]. Each step is supported by the a priori knowledge gained by technical insight into the identified system and individual steps can be repeated if needed.

The data collection step requires the design of an experiment that meets multiple criteria: economical, safety, regulatory, captures target system dynamics, etc. The choice of a suitable sampling period T_s and further preprocessing algorithms are also to be considered in this step.

The amount and quality of data affect what model structures can be used. Generally, model structures derived using analytical identification methods require less data compared to data-driven techniques [1]. Conversely, self-organizing model structures (e.g., neural networks) allow to model more complex processes that would otherwise be simplified or neglected.

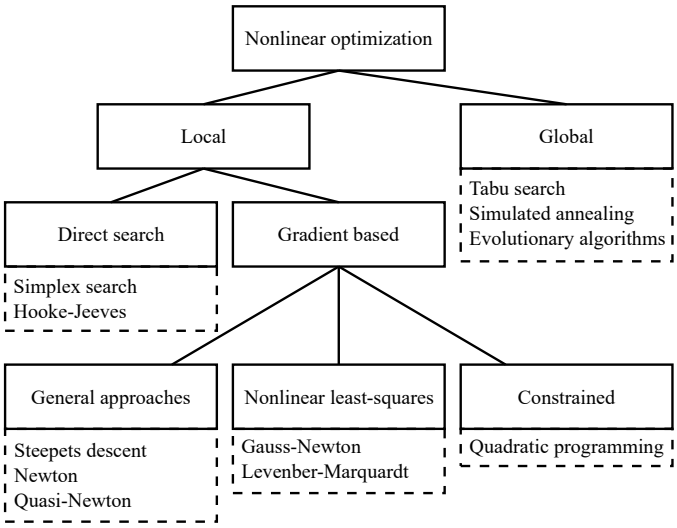

Fig. 1. Overview of nonlinear optimization methods [1].

Based on the selected model structure, a parameter approximation method is selected, see Fig. 1. Generally, all approximation methods are based on the principle of output prediction error minimization to estimate parameter values [5].

The goal of the model validation step is to gain confidence in the identified model. Both quantitative and qualitative methods are used to validate the identified model [2].

III. Solved tasks and results

During the last year, the author focused on the finalization of the case study of the CE 152 Magnetic Levitation Laboratory Model identification from Humusoft [6] and the results have been accepted for publishing in the AEEE journal [7]. This case study verified the proposed identification methodology on a single-input single-output (SISO) system with fast dynamics. However, it is necessary to verify the generality of the proposed methodology also on multiple-input multiple-output (MIMO) system. For this purpose, the CE 150 Helicopter Laboratory Model from Humusoft [8] was chosen. It is a nonlinear dynamic system with two subsystems (elevation and azimuth) with one actuator per subsystem with direct influence. Cross-coupling between both subsystems is expected [8] and is subject to experimental identification. Previously in

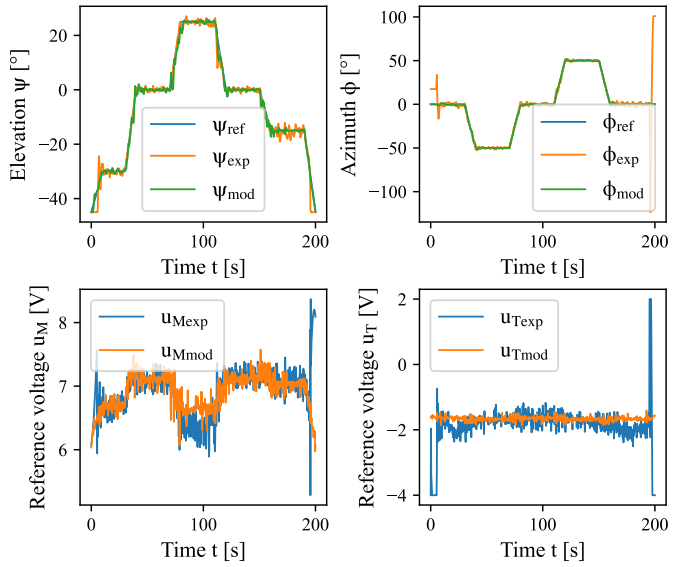

Fig. 2. Closed-loop validation of the identified helicopter model - comparison of simulation and real model output.

our research group, the Helicopter Laboratory Model was identified as a black-box model in [9]. On the contrary, the identification of a gray-box model is presented in this paper.

The data collection step relies on static and dynamic experiments. Static experiments include elevation subsystem balancing with the addition of counterweights and measuring the dependence of rotor speed and thrust using a strain gauge. Dynamic experiments capture the transient behavior of both rotors at different input voltages, the transient behavior of the elevation subsystem in a stable region, and the behavior of the azimuth subsystem with varying reference voltages. The mentioned experiments were performed for individual subsystems separately with the other subsystem locked to avoid cross-coupling. To measure interactions between subsystems, the reference voltage of both rotors was periodically varied to induce stable oscillations. Data was recorded at a sampling period $T_s = 0.01[s]$ without additional pre-processing.

The chosen structure of the model is based on the analytical model [8]. Since modeling helicopter rotors analytically is very difficult [10], a 1^{st} order linear approximation model was extended with nonlinear damping approximated by a polynomial. The dependence of the motor thrust and speed was also approximated by a polynomial.

The model parameters were initially estimated by the surrogate optimization and were later refined using the nonlinear least squares method. To reduce the complexity of the optimization problem, rotors and subsystems were identified separately. Lastly, parameter values of modeled interactions were estimated using a similar technique.

To validate the identified model, it was necessary to design a control algorithm as both subsystems are unstable in the open loop. A polynomial control algorithm with gain scheduling based on instantaneous linearization was chosen [11]. The validation results are shown in Fig. 2. The identified model correctly approximates the dynamics of the real system.

The author also contributed to the ALICE CERN project and implemented the new CERN SSO system into the DARMA information system (IS) alongside improvements in performance, graphical interface, and technological upgrades [12]. DARMA IS serves as a tool for offline access to process data from individual detectors of the ALICE experiment. At the same time, the author participated in the throughput testing of the ALFRED application using the upgraded ALF Simulator. All tests were performed on the production network at CERN. Additionally, the author has updated the database interface in the FRED framework to ensure compatibility with C++20. Results obtained by the research group were published in [13].

IV. Future Research Steps

The author is currently finalizing modifications in the identification methodology of nonlinear dynamic systems, preparing case studies on identification of Aerodynamic and Magnetic Levitation and the Helicopter Laboratory Model, exploring the possibilities of using intelligent models based on a neural networks [10] in the task of experimental identification of the Helicopter Laboratory Model, and finalizing tasks within the ALICE CERN project.

V. Conclusion

This paper summarized the identification methodology of nonlinear dynamic systems and its application in the identification of the Helicopter Laboratory Model in the form of a gray-box model. It also summarizes the progress on the DARMA and ALFRED applications in the ALICE CERN project.

Acknowledgment

This work was supported by the *Slovak Research and Development Agency* under the contract No. *APVV-19-0590* and the project *ALICE experiment at the CERN LHC: The study of strongly interacting matter under extreme conditions, ALICE TUKE 0410/2022*.

References

[1] O. Nelles, *Nonlinear system identification: from classical approaches to neural networks, fuzzy models, and gaussian processes*. Springer Nature, 2020.
[2] L. Ljung, T. Glad, and A. Hansson, *Modeling and Identification of Dynamic Systems*. Studentlitteratur AB, 2021.
[3] C. Legaard, T. Schranz, G. Schweiger, J. Drgoňa, B. Falay, C. Gomes, A. Iosifidis, M. Abkar, and P. Larsen, "Constructing neural network based models for simulating dynamical systems," *ACM Computing Surveys*, vol. 55, no. 11, pp. 1–34, 2023.
[4] T. Tkáčik, "Modeling and experimental identification of nonlinear dynamical systems," *23rd Scientific Conference of Young Researchers: proceedings from conference - Košice (Slovensko)*, pp. 103–104, 2023.
[5] T. Rogers, G. Holmes, E. Cross, and K. Worden, *On a Grey Box Modelling Framework for Nonlinear System Identification*. Springer, 03 2017, pp. 167–178.
[6] Humusoft, "Magnetic Levitation CE 152 - Educational Manual," 2008.
[7] T. Tkáčik, A. Jadlovská, and J. Jadlovský, "Modeling, identification and validation of the modified magnetic levitation model," *Advances in Electrical and Electronic Engineering*, 2024, accepted for publication on 29 January 2024.
[8] Humusoft, "Helicopter CE 150 - Educational Manual," 2012.
[9] K. Dolinský and A. Jadlovská, "Application of results of experimental identification in control of laboratory helicopter model," *Advances in electrical and electronic engineering*, vol. 9, no. 4, pp. 157–166, 2011.
[10] N. Mohajerin and S. L. Waslander, "Multistep prediction of dynamic systems with recurrent neural networks," *IEEE Transactions on Neural Networks and Learning Systems*, vol. 30, no. 11, pp. 3370–3383, 2019.
[11] K. H. McNichols and M. Fadali, "Selecting operating points for discrete-time gain scheduling," *Computers & Electrical Engineering*, vol. 29, no. 2, pp. 289–301, 2003.
[12] M. Kopecký, T. Tkáčik, and J. Jadlovský, "Modifikácia informačného systému darma pre experiment alice cern," *Electrical Engineering and Informatics 14: Proceedings of the Faculty of Electrical Engineering and Informatics of the Technical University of Košice*, pp. 267–271, 2023.
[13] M. Tkáčik, J. Jadlovský, S. Jadlovská, A. Jadlovská, and T. Tkáčik, "Modeling and analysis of distributed control systems: Proposal of a methodology," *Processes*, vol. 12, no. 1, 2024.

Artificial Intelligence in the Control of Electromechanical Systems

[1]*Tadeáš KMECIK (1st year)*
Supervisor: [2]Peter GIROVSKÝ

[1,2]Dept. of Electrical Engineering and Mechatronics, FEI TU of Košice, Slovak Republic

[1]tadeas.kmecik@tuke.sk, [2]peter.girovsky@tuke.sk

***Abstract*—In this paper, we deal with the use of artificial intelligence in the control and regulation of electromechanical systems. The article presents the advantages of using AI as well as examples of its use in electromechanical systems. At the end of the article, there is a discussion on the properties and use of AI and the possibilities of applying artificial intelligence in further research work are presented.**

***Keywords*—neural network (NN), artificial intelligence (AI), control, estimation, controller, sensor.**

I. Introduction

Artificial intelligence (AI) represents one of the most researched areas of the last decade [1],[2]. It is being implemented even in area of electromechanical systems because it allows optimal control and modelling of highly non-linear systems of higher order, as these systems are very hard to identify and mathematically describe. AI also provides an ability to identify parameters, or we can directly use it as a part of control of a specific non-linear system in form of controllers. In this article we will discuss different options for using AI in the field of electromechanical systems.

We can create artificial intelligence in different ways [3]:

- Classical symbolic AI – knowledge-based (expert) system
- Biological model-based AI – neural networks, genetic algorithms
- Model of AI – fuzzy and rough sets theory, chaotic system

Sometimes, these areas are also called "soft computing" to put an emphasis on the fact that these are only approximate models or models with limited accuracy.

In these applications, we will use the already mentioned types of AI, which are neural networks, fuzzy logic and neuro-fuzzy systems. [3]:

- Estimation of state quantity
- Estimation of system parameters
- Detection / prediction of faults
- System control
- System approximation
- System modeling
- Observation and processing of quantities

This article serves as an overview of possible usages of AI in this specific area. In other sections of this article we will introduce and describe a few practical examples including AI.

II. Methods and usages of artificial intelligence

With the increase of technology, a higher dynamics, precision, effectivity and reliability of control and regulation systems is required. These requirements are tightly connected with solution of more detailed states, which occur in that system. Because these are usually very difficult to mathematically describe, it is also very difficult to use usual methods on them. Nowadays, these states or phenomena are either ignored or simplified, what prevents us from getting desired properties and achieving a breakthrough in this area [3]. Raising interest of AI used in electromechanical systems these days is proven by significant growth of scientific publications on this topic [4].

In upcoming sections of this chapter, we will describe various usages of AI when discussing a specific topic from different parts regarding electromechanical systems.

For example, work [5] is focus on neural networks – describe principle of neural networks, their structure and methods of their training. There are metaheuristic methods mentioned in this work [6] for area of photovoltaic systems (PV). Method for monitoring capacitor's state in power electronics is also described in this work [7]. In [8][9] there are examples of application and detailed information about AI.

AI can be used in three different life cycles of electromechanical systems:

- Modelling
- Control
- Diagnostic

In these life cycles of electromechanical systems, we can use AI to fulfil these functions:

1. Optimization: serves to find the most optimal solution for given problem.
2. Classification: serves for classification and identification of various signals and signal templates. It includes processes such as sorting and categorizing.
3. Regression: serves to define dependencies between input and target variables.
4. Data Structure Exploration: it is use to examine various large-scale data structures.

Based on the Sankey diagram, shown on Fig. 1, taken from work [4], it follows that AI for the area of power electronics is

used mainly for the control and then for maintenance and design of systems.

If we are comparing the use of AI for specific functions, then it is most often used for regression and optimization, but also to a small extent for classification and data structure exploration. These methods of use are shown on the picture, which was mentioned before, for better visualisation. AI methods include: machine learning, metaheuristic methods, fuzzy logic, expert systems.

For regression, methods of machine learning and fuzzy logic are primarly used. For optimalization it's metaheuristic methods. Expert systems, unlike others, find application only in the field of regression.

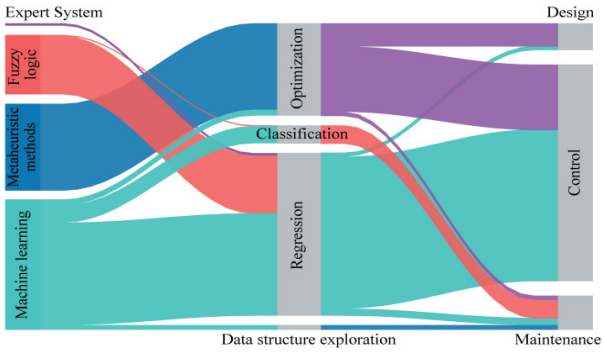

Fig. 1. Diagram of AI methods and applications [4]

Methods are usually combined to achieve better properties. In the following section, we will describe these individual methods and give specific examples of use.

A. *Expert System*

This method is usually applied in power electronics. Principially it is a database that incorporates the knowledge of various experts [10]. It uses Boolean logic. Expert knowledge is most often obtained from practical experience, facts or from simulations. The expert system makes decisions based on the IF-THEN rule, which represents the principle of human decision-making [4]. The database of expert knowledge is constantly updated and filled with new experiences.

Several practical examples of the use and detailed descriptions of the functioning of this method can be found in work [12].

B. *Fuzzy logic*

Fuzzy logic is similar to the expert system, but it works with extended multi-valued Boolean logic. This method is applied where inaccuracies and uncertainties in system processes are solved. Fuzzy logic makes it possible to create robust control systems that can also solve problems with unclear and imprecise input data [13].

As an example of use we can include control of electric powertrain, where there are many variables which significantly affect the optimal setting. Description of such controller design is in this work [14]. There, an adaptive controller is designed for solving a problem of swaying material carried by crane. The result of this work is an adaptive fuzzy controller that is able to regulate unwanted oscillations of the transported material in the required time for the range of rope length l = [1 – 12] (m) and the range of suspended material weight m = [10 – 1000] (kg).

Even though this method is currently being studied a lot, there are still unclear questions about ensuring the required stability and reliability. Therefore, it is necessary to pay attention and research the methodology of fuzzy control of nonlinear systems.

C. *Metaheuristic methods*

They are universal methods that are used in the search for approximate solutions. They are inspired by biological evolution. They are primarily used for finding optimal solutions for complex combinatorial problems, in which it is impossible to find the optimal solution by calculation [11]. When obtaining the optimal solution, they use the trial-and-error principle. Among metaheuristic methods we include, for example, genetic algorithms (GA), particle swarm optimization (PSO) and others. Their biggest advantage is that they enable obtaining an optimal solution in a short time.

Metaheuristic methods are divided into methods that are based on trajectories and populations.

Point of trajectory method is to monitor behaviour of the system over time. First, mathematical equations are formulated which describe behaviour of the system, and then these equations are solved in order to obtain information about system development as a function of time. The disadvantage is slow convergence and the possibility of being stuck in a local minimum.

Methods based on population methods generate multiple solutions at the same time and the most suitable ones are selected. Then, new solutions are created from these selected solutions by means of crossing or mutation. This process is repeated until we get the desired solution. Compared to the trajectory method, this method has faster convergence and global search capability.

It is important to note that choosing the appropriate method is not easy and sometimes the appropriateness is determined by comparison between results of different optimization variant.

Examples of the use of design optimization using heuristic methods to achieve the smallest design parameters are described in detail in work [15].

D. *Machine learning*

It is the branch of AI deals with the design of algorithms and techniques that enable computers to learn. Learning takes place based on data that can be obtained in different ways (measurement, simulation). The basic tasks of machine learning are classification and regression. Depending on the learning process, machine learning is divide to supervised learning, unsupervised learning and reinforcement learning (RL).

Supervised learning builds a system model based on a set of input and output dataset. The task is to establish clear dependencies between inputs and outputs for the model. The ability to work with data that has not been trained is called generalization. The ability to generalize is one of the most critical performance factors of this method. In order to increase robustness and dynamic performance, it is customary to include fuzzy logic into this method, resulting in an adaptive neurofuzzy interreference system (ANFIS) [16].

Unlike supervised learning, unsupervised learning has no predefined output data. The goal of this learning is to reveal patterns, structures and regularities in the supplied data.

Reinforcement learning, unlike supervised learning, does not use a pre-obtained database or clear instructions, but is managed only by feedback, where it receives a reward or a punishment depending on the action performed.

III. DEPLOYMENT OF AI IN THE LIFE CYCLES OF ELECTROMECHANICAL SYSTEMS

As we mentioned in the introduction, AI can be deploye in three main life cycles of electromechanical systems (modelling, control, diagnostic). In this chapter, we will introduce and describe practical deployment of AI in different life cycles.

A. *Modelling*

The design of electromechanical systems includes the choice of topology, dimensioning of components, circuit integration, reliability. AI performs an optimization function in this cycle of electromechanical systems [17].

As a practical example of AI usage is a design of a thermal model based on the principle of a non-linear auto regression network using exogenous inputs (NARX). This problem is solved in work [18]. Using a thermal model based on NARX, an error of less than 1 °C between the predicted and actual temperature was achieved in the mentioned work. In work [19], a thermal model of the MOSFET was designed using NN based on the nonlinear dependence of temperatures on the gate voltage, power loss, switching frequency, ambient temperature, and others.

B. *Control*

AI in the control cycle fulfils the function of regression and also optimalization. Primarily fuzzy logic, NN, RL and their combinations are used here. In this work [20], the genetic algorithm was used to optimize the PID controller. Result of the work is an optimization process that was verified on several different measurements with the result of a significant improvement in the quality of control.

In work [21], a fuzzy controller for a reluctance motor based on TSK fuzzy logic (ATSKFC) is designed. The result of the design is an adaptive controller that outperforms conventional fuzzy and PI controllers. In comparison, motor start-up using ATSKFC was 20 – 30 % faster than motor start-up using a PI controller designed by conventional methods.

NN-based controllers have the advantage of robustness, dynamics, adaptability and universal approximation. The most commonly used conventional NN controllers use feed forward multi-layer neural networks (FFNN) [22].

In addition to the FFNN structure, we also have the option of using networks with radial basis functions (RBFN). These networks have a directly connected input layer with a hidden layer.

It's also good to mention the concept of a hybrid system that combines fuzzy logic with NN [23].

C. *Diagnostic*

Currently, especially in critical applications where controlled systems are exposed to demanding conditions, there is a risk of fatal failures. Therefore, reliability and safety are critical parameters in these applications. Effective methods for reliably preventing fatal failures are condition monitoring, anomaly detection, and failure diagnostics [4]. In general, condition monitoring can be divided into model-free and model-based. The use of one or the other depends on the desired dynamics and needs of the model.

The advantage of the model-free method is that we do not need a model, which means that we do not need any preliminary knowledge about the given system. In work [24], they deal with monitoring the state of the DC intermediate circuit capacitors in a three-phase converter. Monitoring is done through the dependence between the output current and the voltage drop on the capacitors. In this way, we can reliably estimate the current capacity of the intermediate circuit. The error of the neural estimator in the mentioned work was up to 0.5 %. Model-free methods are used mainly in power electronics. Their advantage is lower hardware costs. The disadvantage is less robustness due to higher sensitivity to ambient interference.

Model-based methods require system identification. They are more robust due to higher resistance to ambient interference. For example, in work [25], method to monitor the degradation of MOSFET transistors was used, where the transition resistance is identified based on the model and measured values. Exceeding a certain resistance limit, the part is considered defective and maintenance is required.

IV. DISCUSSION

In this chapter, we will briefly list most popular AI methods. We will list their advantages and disadvantages in the form of a table.

A. *Metaheuristic methods*

Population methods find application in modelling, control and diagnostic. The trajectory method is not used in the design. From the overview above, it follows that if the simplicity of the system is an important parameter, we choose the trajectory method. When speed accuracy is required, we choose population methods. The overview is presented in the Table I.

Table I
COMPARISON METAHEURISTIC METHODS

Type (applications)	**Variants**	**Advantages and Limitations**
Population method (PM) (modeling, control, diagnostic)	Partical swarm optimization (PSO)	Compared to trajectory method: – better global of convergence – lower speed of convergence parallel capability
	Genetic algorithm (GA)	Compared to PSO: – similar features different principle
Trajectory method (TM) (control, diagnostic)	Generally	Compared to PM: – better implementation simplicity – better speed of convergence – lower global of convergence – none parallel capability

B. *Fuzzy logic*

Fuzzy logic is primarily used in control and Diagnostic. There are two types: Mamdani type is preferred due to easier analysis of the rules' additional implementation. TSK type achieves higher accuracy, but sometimes it is unnecessarily complex. TSK type also has simpler training algorithms. The overview is given in the Table II.

Table II
COMPARISON FUZZY LOGIC

Type	**Advantages and Limitations**
Mamdani type	Compared to TSK type: – flexibility in adding rules – simple interpretation – lower accuracy
Takagi-Sugeno type (TSK)	– higher accurancy – higher speed of training – sometimes unnecessary complexity

C. Machine learning

The most universal method is FFNN. RBFN is preferable to use if we require a simpler structure and higher training speed. By integrating fuzzy logic into NN, we increase the performance of the network. RNNs show better transient and dynamic capabilities. NARX is used only in the field of design and maintenance. The overview is given in the Table III.

Table III
COMPARISON MACHINE LEARNING

Type (applications)	Variants	Advantages and Limitations
Conventional NN (Design, Control, Maintenance)	Feed-forward (FFNN)	– universal application
	Radial basic functions (RBFN)	Compared to FFNN: – simple structure – higher speed of training
NN with fuzzy logic (Control, Maintenance)	Fuzzy (NN)	Compared to NN: – capability of handling uncertainty – incorporation expert system – higher speed of training
	Adaptive neuro-fuzzy(ANFIS)	Compared to FNN: – Automatic fuzzy-rule generation with less expert
NN with recurent unit (Design, Control, Maintenance)	Recurrent NN (RNN)	Compared to NN: – better transient and dynamic capability – better sensitivity – slow speed in training
	Nonlinear autoregressive(NARX)	Compared to RNN: – higher speed of training – better generalization capability – cannot be used for control

V. Conclusion

With this overview article, we have come to the conclusion that AI in the field of electromechanical systems shows great potential for use.

AI can be deployed in the three system life cycles of modeling, control and diagnostic.

AI in this area can perform the following functions: classification, regression, optimization, data structure exploration.

We have listed individual forms of AI that we can use in this area (expert systems, fuzzy logic, machine learning, metaheuristic methods). Also advantages, disadvantages and principle of operation.

For each AI method and function, practical examples of use were given with a brief explanation of the operation principle.

Acknowledgment

This work was supported by the Scientific Grant Agency of the Ministry of Education of the Slovak Republic under the project VEGA 1/0584/24 and KEGA 032TUKE-4/2024.

References

[1] C. M. Bishop, “Pattern Recognition and Machine Learning”. Berlin, Germany: Springer-Verlag, 2006.
[2] I. Goodfellow, Y. Bengio, and A. Courville, “Deep Learning”. Cambridge, MA, USA: MIT Press, 2016
[3] M. P. Kazmierkowski, R. Krishnan and F. Blaabjerg, “Control in power electronics”. California, USA, 2002
[4] S. Zhao, F. Blaabjerg and H. Wang, "An Overview of Artificial Intelligence Applications for Power Electronics," in IEEE Transactions on Power Electronics, vol. 36, no. 4, pp. 4633-4658, April 2021, doi: 10.1109/TPEL.2020.3024914.
[5] M. R. G. Meireles, P. E. M. Almeida, and M. G. Simoes, “A comprehensive review for industrial applicability of artificial neuralnetworks,”IEEE Trans. Ind. Electron., vol. 50, no. 3, pp. 585–601, Jun. 2003.
[6] M. Seyedmahmoudian et al., “State of the art artificial intelligence-based MPPT techniques for mitigating partial shading effects on PV systems—A review,” Renewable Sustain. Energy Rev., vol. 64, pp. 435–455,Oct. 2016.df
[7] H. Soliman, H. Wang, and F. Blaabjerg, “A review of the condition monitoring of capacitors in power electronic converters,” IEEE Trans.Ind. Appl., vol. 52, no. 6, pp. 4976–4989, Nov./Dec. 2016
[8] B. K. Bose, “Artificial intelligence techniques in smart grid and renew able energy systems-some example applications,” Proc. IEEE, vol. 105,no. 11, pp. 2262–2273, Nov. 2017.
[9] R. C. G. J. Pinto and B. Ozpineci, “Tutorial: Artificial intelligence applications to power electronics,” in Proc. IEEE Energy Convers. Congr.Expo., 2019, pp. 1–139.
[10] S. M. Chhaya and B. K. Bose, “Expert system aided automated design, simulation and controller tuning of AC drive system,” in Proc. 21st Annu.Conf. IEEE Ind. Electron., vol. 1, 1995, pp. 712–718.
[11] B. K. Bose, “Artificial intelligence techniques in smart grid and renewable energy systems-some example applications,” Proc. IEEE, vol. 105,no. 11, pp. 2262–2273, Nov. 2017
[12] B. K. Bose, "Expert system, fuzzy logic, and neural network applications in power electronics and motion control," in Proceedings of the IEEE, vol. 82, no. 8, pp. 1303-1323, Aug. 1994, doi: 10.1109/5.301690
[13] R. Osorio et al., “Fuzzy logic control with an improved algorithm for integrated LED drivers,” IEEE Trans. Ind. Electron., vol. 65, no. 9,pp. 6994–7003, Sep. 2018
[14] J. Smoczek and J. Szpytko, "Design of gain scheduling anti-sway crane controler using genetic fuzzy system," 2012 17th International Conference on Methods & Models in Automation & Robotics (MMAR), Miedzy zdroje, Poland, 2012, pp. 573-578, doi: 10.1109/MMAR.2012.6347822
[15] S. E. De Leon-Aldaco, H. Calleja, and J. A. Alquicira, “Metaheuristic optimization methods applied to power converters: A review,” IEEE Trans. Power Electron., vol. 30, no. 12, pp. 6791–6803, Dec. 2015.
[16] P. Z. Grabowski, M. P. Kazmierkowski, B. K. Bose, and F. Blaabjerg, “Asimple direct-torque neuro-fuzzy control of PWM-inverter-fed induction motor drive,” IEEE Trans. Ind. Electron., vol. 47, no. 4, pp. 863–870,Aug. 2000
[17] G. Bramerdorfer, J. A. Tapia, J. J. Pyrhonen, and A. Cavagnino, “Modern electrical machine design optimization: Techniques,trends, and best practices,” IEEE Trans. Ind. Electron., vol. 65, no. 10, pp. 7672–7684, Oct. 2018.
[18] Y. Zhang, Z. Wang, H. Wang, and F. Blaabjerg, “Artificial intelligence aided thermal model considering cross-coupling effects,” IEEE Trans. Power Electron., vol. 35, no. 10, pp. 9998–10002, Oct. 2020
[19] D. Chiozzi, M. Bernardoni, N. Delmonte, and P. Cova, “A neural network based approach to simulate electrothermal device interaction in SPICE environment,” IEEE Trans. Power Electron., vol. 34, no. 5, pp. 4703–4710, May 2019.
[20] L. G. Junior, J. O. P. Pinto, J. A. B. Filho, and G. Lambert-Torres, “Recursive least square and genetic algorithm based tool for PID controllers tuning,” in Proc. Int. Conf. Intell. Sys. Appl. Power Syst., 2007, pp. 1–6.
[21] C. L. Tseng, S. Y.Wang, S. C. Chien, and C. Y. Chang, “Development of a self-tuning TSK-Fuzzy speed control strategy for switched reluctance motor,” IEEE Trans. Power Electron., vol. 27, no. 4, pp. 2141–2152, Apr. 2012.
[22] B. K. Bose, “Neural network applications in power electronics and motordrives-an introduction and perspective,” IEEE Trans. Ind. Electron., vol. 54, no. 1, pp. 14–33, Feb. 2007.
[23] P. Z. Grabowski, M. P. Kazmierkowski, B. K. Bose, and F. Blaabjerg, “A simple direct-torque neuro-fuzzy control of PWM-inverter-fed induction motor drive,” IEEE Trans. Ind. Electron., vol. 47, no. 4, pp. 863–870, Aug. 2000.
[24] H. Soliman, I. Abdelsalam, H.Wang, and F. Blaabjerg, “Artificial neural network based DC-link capacitance estimation in a diode-bridge frontend inverter system,” in Proc. IEEE 3rd Int. Future Energy Electron. Conf. ECCE Asia, 2017, pp. 196–201.
[25] S. Zhao, V. Makis, S. Chen, and Y. Li, “Health assessment method for electronic components subject to condition monitoring and hard failure,” IEEE Trans. Instrum. Meas., vol. 68, no. 1, pp. 138–150, Jan. 2019.

Sparse wars: A new compression paradigm

[1]Antónia JUSKOVÁ (1st year)
Supervisor: [2]Ján ŠALIGA

[1,2]Dept. of Electronics and Multimedia Telecommunications, FEI TU of Košice, Slovak Republic

[1]antonia.juskova@tuke.sk, [2]jan.saliga@tuke.sk

Abstract— This work provides a comprehensive overview of Compressed Sensing (CS), describing its mathematical foundations, reconstruction requirements, and convex and greedy reconstruction algorithms. Additionally, it discusses the evaluation of signal sparsity, a crucial aspect of successful CS implementation. CS's stability, flexibility, and scalability have emerged with its adoption in diverse domains, including medical imaging, radar systems, signal error correction, and interference cancellation.

Keywords—compressed sensing, convex relaxation, greedy pursuits, sparsity evaluation.

I. Introduction

Data compression methods promise a compact representation of information. This is achieved by exploiting data structure or its redundant information. Those methods are divided into lossless compression and lossy compression [1]. As the name suggests, the result of reconstruction from lossless data compression is the same as the original data [2]. An example of lossless compression is entropy coding, such as Huffman codes, arithmetic codes, run-length coding, etc. [3]. Lossy compression leads to differences between original data and reconstructed compressed data. Those differences increase with multiple compressions and decompressions which can cause damage to the signal. On the other hand, the advantage of lossy methods is a higher compression rate while still meeting the requirements of the application [2].

In 2006, an article called Compressed Sensing (CS) was published by David L. Donoho [4]. CS is a lossy compression method that asserts to reconstruct a sparse signal at a lower sampling rate than the Nyquist-Shannon rate [5]. CS gained high research interest and was used in many applications for sparse data acquisition and compression. The advantages of CS are stability, flexibility, and scalability. CS method finds use in medical imagining, radars, sparse approximation, error correction, symbol detection, interference cancelation, etc. [6]. Many works of CS implications in biomedical signals were proposed, such as electrocardiograms (ECG) or magnetic resonance imaging (MRI). The ECG signal compression and reconstruction by CS was published in works [7], [8] and [9]. In the works [10], [11], CS was applied in MRI to enhance acquisition speed and image recovery.

This work is focused on the principle and thoughts behind CS, the comparison of CS with conventional compression schemes, mathematical background, reconstruction requirements, and reconstruction algorithms. Also, the signal sparsity evaluation is described, which is necessary knowledge for further application of CS.

II. Sparse Representation

A sparse vector, or matrix, can be defined as a set of data where most coefficients carry a zero or close to zero value. In signal processing, the signal can exhibit low sparsity in the time domain or transformation domain [12]. Sparsity is an important signal property for many applications in signal or image processing techniques such as compression, component separation, sampling, signal recovery, and feature extraction. Those techniques have been applied in many fields such as medical imaging, computer vision, image processing, machine learning, etc. [13]. Signal sparsity is also a crucial requirement of information recovery acquired by compressed sensing.

However, the real-world signals in the sparse domains consist of a few large values and a lot of small values that are close to, but not exactly, zero [14]. The close-to-zero coefficients are present in Fig. 1 where the signal was transformed into a multiwavelet domain with DB4 multiwavelet. In the result, the signal consists of 128 nonzero detailed coefficients in both sub-bands. Therefore, the sparsity for in d_{11} as well as d_{12} sub-band is 128.

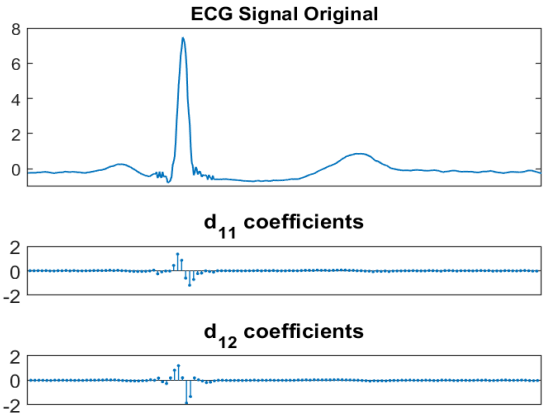

Fig. 1 ECG sparsity evaluation before threshold value filtering

Most signal energy is carried by large coefficients, so those small coefficients carry low energy [12]. Signal sparsity can be measured by energy distribution where close to zero coefficient can be removed by threshold filter. This sparsity evaluation based on the signal energy distribution was applied to ECG records in multiwavelet domains. The multiwavelet detailed coefficients were filtered based on the mean signal energy and desired signal-to-noise ratio (SNR) value or Percent Root Mean Square Difference (PRD). The result of sparsity evaluation for SNR in the range of 19 to 20 dB is shown in Fig. 2. The sparsity of multiwavelet detailed coefficients was evaluated at 6 for both d_{11} and d_{12} while still preserving the shape of original signal.

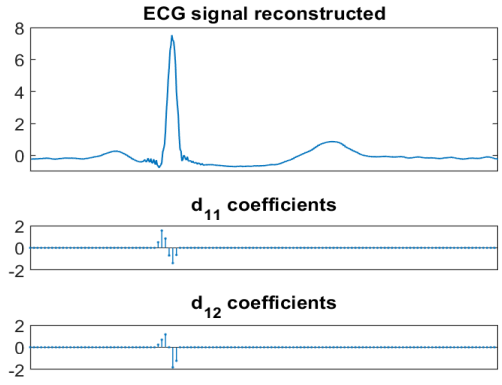

Fig. 2 ECG sparsity evaluation after threshold value filtering

Mathematically, the sparsity of the signal, represented as a vector s, can be defined by its number of non-zero elements. This can be also described as l_0 norm [14]:

$$\|s\|_0 = \sum_{i=1}^{n} |s_i|^0 \qquad (1)$$

It is obvious from the equation, that the purpose of the l_0 norm is to count a number of non-zero elements. The l_0 norm can be also described by cardinality card of a given set, which is the number of elements within the provided set:

$$\|s\|_0 := \mathrm{card}(\{i \in \{1, \cdots, n\}: s_i \neq 0\}) = k \qquad (2)$$

where $k \in \{1, \cdots, n-1\}$ is the number of non-zero elements of k-sparse signal [6]. Then, the k-sparse set of vectors is described by following equation:

$$\Sigma_k = \{s \in R^n: \|s\|_0 \leq k\} \qquad (3)$$

where Σ_k is a set of k non-zero coefficients.

III. Conventional Sampling vs. Compressed Sensing

The conventional sampling of real-world signals is based on the Shannon-Nyquist theorem. This theorem states that a signal can be exactly reconstructed if is sampled at least twice as high as the maximum signal frequency band limit [15]. Compressed sensing is an effective acquisition and effective signal reconstruction method of sparse signals [6]. In compressed sensing, signal reconstruction is based on numerical optimization methods [15]. By applying those algorithms, the acquisition rate can be below the Shannon-Nyquist sampling rate [6].

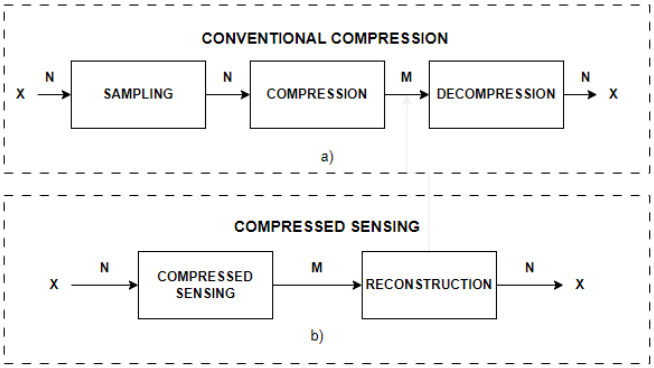

Fig. 3 Compression approach: a) conventional and b) CS block scheme

The conventional compression method uses standard Shannon-Nyquist theory (Fig. 3a). In this method, all samples need to be kept and then compressed [16]. To reduce the storage of conventionally sampled data, the compression algorithm needs to be applied to already sampled signals [15]. As a result, only samples that accurately depict the signal are kept and then transmitted or stored.

By using compressed sensing, signals are compressed during the acquisition phase (Fig. 3b). The signal can be then reconstructed by fewer samples using optimization or greedy reconstruction algorithms. The CS method is divided into compression phase and decompression phase. The phases of CS are shown in Fig. 4.

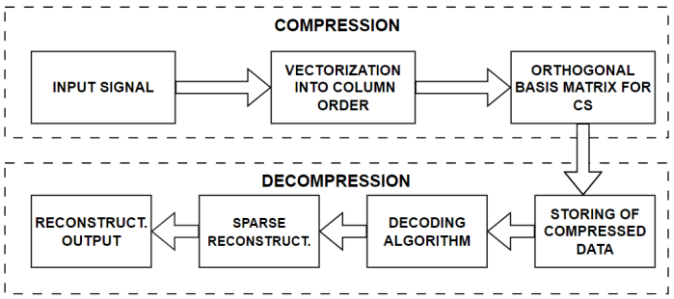

Fig. 4 The compression and decompression phases of CS

The compression phase remains of measurement of data and transformation to its sparse representation [17]. The input signal consists of measurements from real-world physical quantities, which are converted to digital samples. Those data can be acquired deterministically or randomly. The measurements are stored in measurement matrices [18].

Acquired samples are aligned into column vectors. The next step is to choose an orthogonal basis function to obtain sparse representation x of measured signal s. As a basis function, discrete orthogonal transformations can be used, such as Discrete Fourier Transform (DFT), Discrete Cosine Transform (DCT), Discrete Wavelet Transform (DWT), etc.

In the decompression phase, sparse signal x is decoded by suitable decoding algorithms. Those decoded data are further used for the reconstruction process with a sparse reconstruction algorithm. Acquired signal by CS can be reconstructed from a limited number of measurements stored in the measurement matrix ϕ.

IV. CS Reconstruction

For signal reconstruction from limited samples, there are a few requirements that need to be met [16]:

a) Sparse representation of signal.
b) Measurements stored in measurement matrix.
c) Choosing a basis for sparse representation.
d) Choosing a reconstruction algorithm.

A signal represented as vector x with size $N \times 1$ can be represented as a sparse vector in a particular domain. The discrete transformation domain needs to be orthogonal, or a dictionary can be used. The coefficients of the vector x can be computed by the orthogonal basis ψ and sparse vector x. This relationship can be expressed by the following equation:

$$x = \psi s \qquad (4)$$

where $\psi \in R^{N \times N}$ and sparsity level k of vector s is $k \ll N$.

The vector x is an unknown value and needs to be reconstructed to find a solution. Reconstruction of vector x depends on the measurements y and measurements matrix ϕ. The CS equation can be described as:

$$y = \phi x = \phi \psi s = As \tag{5}$$

where $\phi \in R^{M \times N}$ with $M \ll N$. The dimensions of the CS equation are visualized in Fig. 5.

Usually, to obtain an accurate result, the number of elements of y must be at least equal to or greater than the number of elements x. Otherwise, classical algebra classifies this problem as an underdetermined system of linear equations. The CS relies on the fact that matrix A can be designed such that the sparse signal x can be recovered exactly or approximately from the few measurements y.

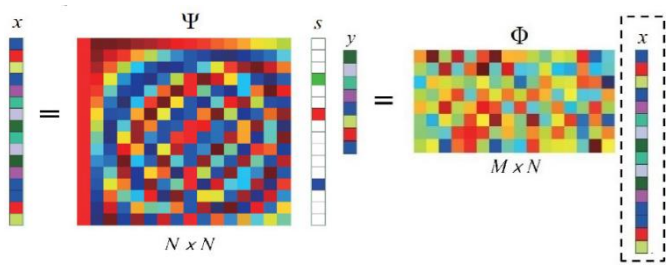

a) b)

Fig. 5 The CS visualized a) signal representation, b) CS equation.

The CS equation can be solved as an undetermined matrix system of linear equations [17]. This system has fewer equations than unknowns, so it has an infinite number of solutions. The known inputs of the equation are A and measurement vector y. The goal of CS reconstruction is to estimate sparse vector s [18]. The process involves initially obtaining a limited set of data samples, which are then utilized with suitable reconstruction algorithms to restore the original signal [17]. The reconstruction methods for CS are divided into convex relaxation and greedy pursuit reconstruction.

V. Convex Relaxation Reconstruction

The goal of this convex relaxation is to reconstruct an unknown signal from the linear system of equations by optimization algorithms to find the sparsest solution [19]. As was stated, the sparsity of the signal can be determined by its l_0-norm. The l_0 optimalization problem of the undetermined system is described by the following equation:

$$\min \|s\|_0, \qquad \text{subject to } y = As \tag{6}$$

This is s non-convex function solving problem (Fig. 6). Non-convex function means that the connection of two points may cross the course of the function at some point and it is complicated to solve it.

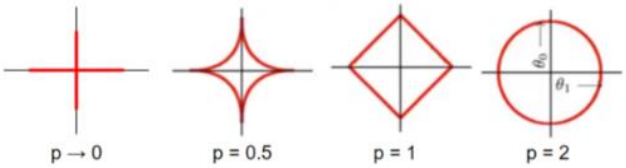

Fig. 6 L_P optimization norms.

Convex relaxation methods were the first methods used for the sparse reconstruction of CS measurements [17]. Using convex optimization, the problem of CS reconstruction can be solved more efficiently than non-convex. The result of the convex optimization solution can be considered as the result of a non-convex problem [20]. Convex relaxation algorithms are used as alternative functions to solve optimization problems by l_1 or l_2-norms visualized at Fig. 6.

A. Basis pursuit

Basis pursuit (BP) is a popular convex relaxation method and was first introduced in [21]. In algorithms based on the BP, the l_0-norm is replaced by the l_1-norm defined as [18]:

$$\|s\|_1 = \sum_{i=1}^{n} |s_i| \tag{7}$$

The problem of (6) can be rewritten by l_1-norm relaxation:

$$\min \|s\|_1, \qquad \text{subject to } y = As \tag{8}$$

Reconstruction based on BP requires a low number of measurements but is computationally expensive [17].

B. The Gradient Projection

The Gradient Projection (GP) is another group of relaxation algorithms. The GP methods use l_2-norm to smooth the l_0 non-convex problem. The l_2-norm is described as:

$$\|s\|_2 = \sqrt{\sum_{i=1}^{n} |s_i|^2} \tag{9}$$

The problem of (6) can be rewritten by l_2-norm relaxation:

$$\min \|s\|_2, \qquad \text{subject to } y = As \tag{10}$$

Several variations of l_2 relaxation methods were proposed. Many of the convex relaxation solutions use hybrid methods with greedy pursuits.

VI. Greedy Algorithms Reconstruction

Greedy algorithms solve a problem by progressively building solutions for the approximation of more optimal solutions at each stage [22]. The problems are solved by iteration procedures based on conditions to find the sparsest solution [18]. The process continues until the error decreases to less than a certain level [23]. In general, greedy algorithms cannot find a global optimal solution, but they may produce good locally optimal solutions in a shorter time, than convex methods, and with less computational effort.

A. Matching Pursuit

Greedy pursuits are based on selecting matching elements and storing them in a support set [22]. Matching Pursuit (MP) is considered as the “purest greedy algorithm”. The procedure consists of one column selection from A. In each iteration, the elements of vector s are updated based on the selected column [23]. The new element of s is calculated using the previous element, which can reduce computational time.

B. Orthogonal Matching Pursuit

The Orthogonal Matching Pursuit (OMP) is more complicated than MP. It also selects columns from A, but is based on maximum correlation with measurements y [23]. Through the iteration process, the column of A is selected based on the correlation with the current residual element. The index of the chosen column is added to the set used for re-arranging the columns of A to obtain the maximum desired value and minimum error [18].

C. Iterative Hard Thresholding

Iterative Hard Thresholding (ITH) is more directive in updating the signal vector estimation than OMP. The methodology of ITH starts from the zero initial value of the vector x. then in a very straightforward manner, it updates the signal vector by a gradient descent algorithm [18]. The key idea behind IHT is to iteratively update an estimation of the signal by a thresholding operator after each update step [24]. This thresholding operation ensures that only the significant components are retained while discarding the insignificant ones.

VII. Conclusion

Compression Sensing (CS) emerges as a promising approach to data compression, offering distinct advantages over traditional methods. This paper provided a comprehensive overview of CS, including its mathematical foundations, reconstruction requirements, and algorithms. This work aims to equip researchers and practitioners with the necessary knowledge for further research and implications. The discussion on signal sparsity evaluation highlights the importance of understanding the underlying data structure for successful CS implementation. Looking ahead, continued research and development in CS hold promise for further advancements in data compression and signal processing.

VIII. Past, Present, and Future

Last year, the author proposed and presented in the poster section The Design of Vehicle Surround View Monitor at the 26th IMEKO TC4 conference in Pordenone, Italy. The author cooperated on the article ECG Sparsity Evaluation on a Multiwavelet Basis where the sparsity of ECG signals in the multiwavelet domain was evaluated and compressed with emphasis on the energy distribution. Currently, the author is working and cooperating on an article oriented to the evaluation of the run-length encoding algorithm “Quite OK Encoding”, shortly QOE, for publication in Measurement. Also, the author processes the experiments of cross-correlation analysis of 12-lead ECG records in multiple domains. The future work of the author is oriented toward the evaluation of 12-lead ECG signals and shaping knowledge about the structure of those signals. This evaluation can lead to 2D compression sensing of 12-lead signals.

References

[1] Sayood K. "Data Compression", Encyclopedia of Information Systems, Elsevier, 2003, Pages 423-444, ISBN 9780122272400, https://doi.org/10.1016/B0-12-227240-4/00029-0.

[2] Zhang P. "Data Communications in Distributed Control System", Industrial Control Technology, William Andrew Publishing, 2008, Pages 675-774, ISBN 9780815515715, https://doi.org/10.1016/B978-081551571-5.50007-4.

[3] Pearlman WA, Said A., "Entropy coding techniques", In: Digital Signal Compression: Principles and Practice. Cambridge University Press; 2011:41-76.

[4] Fornasier, M., Rauhut, H., "Compressive Sensing", In: Handbook of Mathematical Methods in Imaging, 2011 Springer, New York, NY. https://doi.org/10.1007/978-0-387-92920-0_6.

[5] Erkoc, M.E., Karaboga, N., "A comparative study of multi-objective optimization algorithms for sparse signal reconstruction", Artif Intell Rev 55, Pages 3153–3181 (2022). https://doi.org/10.1007/s10462-021-10073-5

[6] Maroua T., "Compressed sensing", In: Computing in Communication Networks, Academic Press, 2020, Pages 197-215, ISBN 9780128204887, https://doi.org/10.1016/B978-0-12-820488-7.00023-2.

[7] P. Dolinský, I. Andráš, J. Šaliga, "Reconstruction for ECG Compressed Sensing Using a Time-Normalized PCA Dictionary," 2019 12th International Conference on Measurement, Smolenice, Slovakia, 2019, pp. 30-33, doi: 10.23919/MEASUREMENT47340.2019.8779960

[8] Ondrej Kováč, Jozef Kromka, "Multiwavelet-based ECG compressed sensing", Measurement, Volume 220, 2023, 113393, ISSN 0263-2241, https://doi.org/10.1016/j.measurement.2023.113393.

[9] J. Šaliga, I. Andráš, "ECG compressed sensing method with high compression ratio and dynamic model reconstruction Measurement", 183 (2021), p. 109803, 10.1016/j.measurement.2021.109803

[10] T. Minh-Chinh, N. Linh-Trung, "On the implementation of chaotic compressed sensing for MRI", in: International Conference on Advanced Technologies for Communications, ATC, Hanoi, Vietnam, 2016, pp. 103–107.

[11] J. Song, Z. Liao, "A new fast and parallel MRI framework based on contourlet and compressed sensing sensitivity encoding", in: International Conference on Machine Learning and Cybernetics, ICMLC, Jeju, South Korea, 2016, pp. 750–755.

[12] Mahmoudian E., Amindavar H., Ahadi S. M., "New sparsity measure based on energy distribution", Displays, Vol. 80, 2023, ISSN 0141-9382, https://doi.org/10.1016/j.displa.2023.102542.

[13] J. Huang, Y. Li, "Chapter 7 - Advanced sparsity techniques in magnetic resonance imaging", In: The Elsevier and MICCAI Society Book Series, Machine Learning and Medical Imaging, Academic Press, 2016, Pages 183-236, ISBN 9780128040768, https://doi.org/10.1016/B978-0-12-804076-8.00007-4.

[14] V. Behravan, N. E. Glover, "Rate-adaptive compressed-sensing and sparsity variance of biomedical signals," 2015 IEEE 12th International Conference on Wearable and Implantable Body Sensor Networks (BSN), Cambridge, MA, USA, 2015, pp. 1-6, doi: 10.1109/BSN.2015.7299419.

[15] Srinivas, K., Srinivas, N., "Performance Comparison of Measurement Matrices in Compressive Sensing", In: ICACDS 2018. Communications in Computer and Information Science, vol 905. Springer, Singapore. https://doi.org/10.1007/978-981-13-1810-8_34

[16] Saumya P., Ankita V., "An efficient optimization of measurement matrix for compressive sensing", In: Journal of Visual Communication and Image Representation, Vol.95, 2023, 103904, ISSN 1047-3203, https://doi.org/10.1016/j.jvcir.2023.103904.

[17] Belgaonkar S. M., Singh V., "Image compression and reconstruction in compressive sensing paradigm", In: Global Transitions Proceedings, 2022, Pages 220-224, https://doi.org/10.1016/j.gltp.2022.03.026.

[18] Hosny S., Abdel-Hamid A. T., "Survey on compressed sensing over the past two decades", In: Memories - Materials, Devices, Circuits and Systems, Vol. 4, 2023, ISSN 2773-0646.

[19] M. Rudelson, R. Vershynin, "Sparse reconstruction by convex relaxation: Fourier and Gaussian measurements," 2006 40th Annual Conference on Information Sciences and Systems, Princeton, NJ, USA, 2006, pp. 207-212, doi: 10.1109/CISS.2006.286463.

[20] S.P. Boyd and L. Vandenberghe. "Convex optimization", Cambridge University Press, United Kingdom, 2004.

[21] Chen S.S., Donoho D.L., Saunders M.A., "Atomic decomposition by basis pursuit", In: Soc. Ind. Appl. Math., 43 (1) (2001), pp. 129-159

[22] D. Sundman, "Greedy algorithms for distributed compressed sensing", Stockholm: Electrical Engineering, KTH Royal Institute of Technology, 2014.

[23] Khosravy M., Gupta N., "Chapter 2 - Recovery in compressive sensing: a review", In: Advances in ubiquitous sensing applications for healthcare, Compressive Sensing in Healthcare, Academic Press, 2020, Pages 25-42, ISBN 9780128212479, https://doi.org/10.1016/B978-0-12-821247-9.00007-X.

[24] Blumensath T., Davies M. E., "Iterative hard thresholding for compressed sensing", In: Applied and Computational Harmonic Analysis, Volume 27, Issue 3, 2009, Pages 265-274, ISSN 1063-5203, https://doi.org/10.1016/j.acha.2009.04.002.

Phase-shift full-bridge converter, decades ago and now

[1]*Daniel Gordan (1st year)*
Supervisor: [2]Marek Pástor

[1,2]Dept. of Electrical Engineering and Mechatronics, FEI TU of Košice, Slovak Republic

[1]daniel.gordan@tuke.sk, [2]marek.pastor@tuke.sk

***Abstract*— The paper describes a DC-DC full-bridge converter which has been used for years due to high efficiency, large ratio, and galvanic isolation. New wide bandgap semiconductors allow to improve the performance of the original PSFB converter. However, the question is how much and what this change means for the PSFB.**

***Keywords*— dc-dc converter, efficiency, full-bridge, GaN, phase-shift,**

I. INTRODUCTION

The past has shown us how much power electronics can change the world we live in. Since their invention, converters have been installed in almost every aspect of life, changing industry as well as homes and consumer electronics.

Nowadays, we need high-efficiency dc-dc converters used for example in the automotive industry in mild hybrids, electric cars [1], in MPPT converters for photovoltaic systems [2], or battery storage systems [3]. For almost all fields the criteria are similar, namely high-power density, high efficiency, high voltage and current range and galvanic isolation. All these aspects can be achieved by using a phase-shift full-bridge (PSFB) converter, which was first used decades ago [4]. While the main converter topology is the same as it was decades ago, auxiliary circuits [5], change in control [6] and the use of more advanced semiconductor components [7] allow for improved efficiency and power density.

In addition to the above general advantages, PSFB converter also has the advantage of naturally achieving zero-voltage switching (ZVS) for the primary transistors and low voltage and current stress on the primary side. ZVS is caused by the utilization of the leakage inductance and output capacitances of primary transistors. On the other hand, the ZVS is dependent on the load current and is harder to achieve at lights load.[8] The mentioned paper [8] describes an additional network on the primary side that solves this problem and the problem with the circulating current. The circulating current is the current reflected from the filter inductance which increases the losses on the primary transistors. Another way how to limit the circulating current is to use a controlled rectifier on the secondary side, which interrupts the current flow at the time of a change of the switching pair on the primary side. In the case of a controlled rectifier, there is hard switching and increasing losses on the secondary side, so it is necessary to use auxiliary snubbers to provide soft switching.[9] It is worth noting that auxiliary networks on the secondary side suppress the occurrence of over-voltage spikes on the rectifier, even in the case of a diode-uncontrolled rectifier. Voltage ringing is caused due to the resonance between the leakage inductance and the parasitic capacitance of the rectifier. It occurs when the primary current reaches the value of the reflected current after diode commutation.[10]

At the department of Electrical Engineering and Mechatronics, FEI TU of Košice several concepts have been proposed which tried to eliminate the disadvantages of PSFB converter, they are presented in [9] and in [11]-[14], the best result was reached in [9].

In recent years, modern semiconductors such as GaNs (Gallium Nitride) have allowed higher efficiency to be achieved on the primary side without additional networks. Lower parasitic capacitance (C_{oss}) of GAN transistors reduces switching losses on the primary side and increases the ZVS area [7]. Today, in order to achieve high efficiency, concepts with a GaN inverter and a current doubler [15] or centre tap rectifier [16]-[17] are used. In these concepts, power is controlled on the primary side, so they do not need complicated auxiliary networks to guarantee soft switching on the secondary transistors.

The paper describes the functionality of several types of converters, highlights their advantages and disadvantages, and compares newer concepts with the years-tuned converter described in [9].

II. ORIGINAL CONCEPT

The schematic of the years improved 2 kW converter [9], is shown in Fig. 1, parameters in Tab. 1, and parts in Tab. 2.

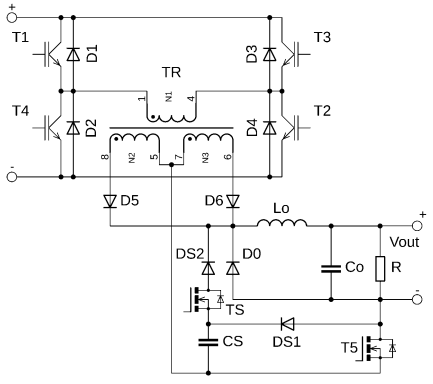

Fig. 1. The schematic of the original converter [9]

TABLE I
PARAMETERS OF ORIGINAL CONVERTER

Parameter	Value
Supply voltage V_{IN}	300 V
Output current I_O	50 A
Output no-load voltage V_O	50 V
Output power P_2	2 kW
Switching frequency fs	50 kHz

TABLE II
COMPONENTS OF ORIGINAL CONVERTER

Component	Value
Primary transistors $T_1 – T_4$ with antiparallel diodes $D_1 – D_4$	G4PSC71UD
Rectifier diodes D_5 and D_6	150EBU04
Secondary transistor T_5	IRFP4668
Snubber transistor T_S	IRFP4668
Snubber diodes D_{S1} and D_{S2}	150EBU04
Smoothing choke L_O	5 µH
Output capacitor C_O	150 µF
Snubber capacitor C_S	100 nF

Primary transistors T_1 - T_4 form an inverter that operates with a fixed phase shift and a fixed duty cycle of 50%. On the secondary side there is an uncontrolled rectifier formed by diodes D_5 and D_6. The output is regulated by transistor T_5, whose duty cycle sets the duration of connection of the load to the rectifier. Another function of transistor T_5 is to interrupt the circulating current before the switching pair on the primary side is changed, which leads to ZC switching on the primary side, because only a small magnetizing current flows through the transistors at the time of switching. So, this converter is ZVZCS (Zero Voltage and Zero Current Switching). Transistor T_5 is hard switching, which is solved by a snubber formed by T_S, D_{S1}, D_{S2}, C_S. Diode D_0 is conducting a current of inductance L_0 at the time of transistor T_5 switching off. The converter efficiency which was measured in [14] is shown in Fig. 2. Table III shows the Pros and Cons of the original converter.

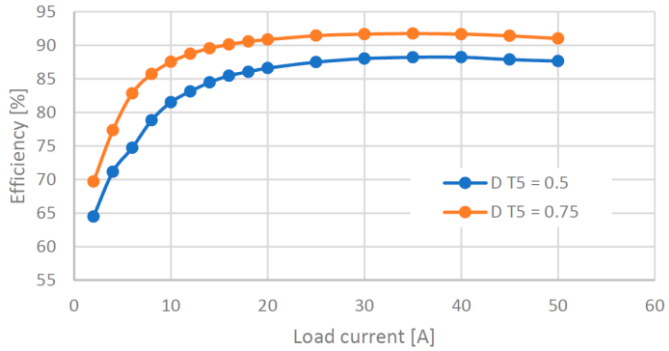

Fig. 2. Efficiency of original converter [14]

TABLE III
PROS AND CONS OF ORIGINAL CONVERTER

Pros	Cons
ZVZCS for primary side, T_1 - T_4 have low losses even with IGBT	The Cs capacitor cannot be properly selected for the entire load range
High eff. in comparison with older concepts	More semiconductors on the secondary side increases losses
Simple control of output power by duty cycle of T_5	The problem of the primary side is shifted to the secondary

III. MODERN CONCEPTS

GaN Inverter

GaN transistors find application in modern converter concepts because some of their properties are unmatched compared to Si transistors. They have no reverse recovery loss, lower switching energy, enable faster switching, achieve lower switching losses, and lower dead time losses [18],[19]. Fig. 3 shows the use of semiconductors as a function of power and frequency.

Lower switching losses, smaller heat sinks and the possibility of increasing the frequency will be reflected in the smaller magnetic cores of the transformers and filter inductances, so that a higher power density will be achieved. Infineon's presentation [20] shows a PFC (Power Factor Corrector) converter where the application of GaN transistors resulted in a three times increase in power density.

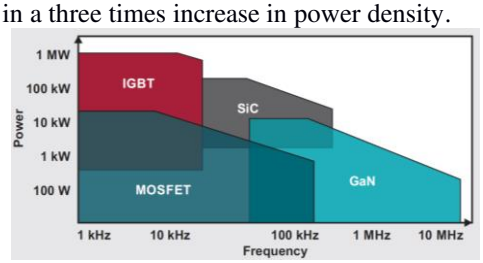

Fig. 3. Semiconductor selection due to frequency and power [18]

The reason for the ZVS of the PSFB converter is the resonance between the output capacitance (C_{oss}) and the leakage inductance. If the resonance is not completed, partial ZVS or loss of ZVS occurs, which means that soft switching is very dependent on the C_{oss} of the transistor. Low C_{oss} and low crossover losses results in extensive soft switching region and low loss during hard switching [7],[21]. The paper [21] also describes the sensitivity of the PCB design with GaNs with respect to parasitic inductances.

Due to their advantages, GaN transistors are favored for PSFB converters and can be found in almost every modern concept on the primary side. Lower losses on the inverter allow regulation on the primary side, which greatly simplifies the secondary side and leads to fewer semiconductors.

PSFB with Current Doubler Rectifier

For high output currents and using a transformer with one secondary winding, a current doubler rectifier achieves high efficiency [15],[22],[23]. The schematic is shown in Fig. 4.

The current doubler rectifier divides the output current between two inductances. The primary transistors Q_1 – Q_4 switch with a duty cycle of 50% and a small safety gap to avoid short circuits in the branch and to achieve ZVS. Output regulation is achieved by changing the switching phase-shift on the primary side. The synchronous rectifier formed by SR_1 and SR_2 naturally switches at zero current, which has a significant effect on the resulting converter efficiency. [15]

An additional active clamp circuit can be used on the secondary side, which increases the efficiency[15].

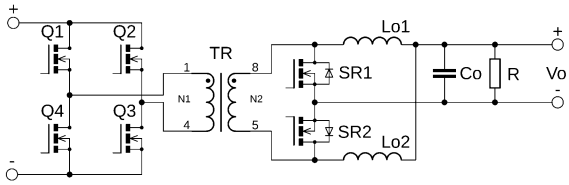

Fig. 4. Schematic of Gan inverter and rectifier with current doubler [23]

The parameters of the converter [23] are shown in Table IV and the list of components is given in Table V. The efficiency of the converter is shown in Fig. 5. Pros and cons are shown in Table VI.

TABLE IV
PARAMETERS OF PSFB WITH CURRENT DOUBLER

Parameter	Value
Supply voltage V_{IN}	380 V
Output current I_O	84 A
Output voltage V_O	12 V
Output power P_2	1 kW
Switching frequency fs	350 kHz

TABLE V
COMPONENTS OF PSFB WITH CURRENT DOUBLER

Component	Value
Primary CoolGAN $Q_1 – Q_4$	IGT60R070D1
SR_1 and SR_2	BSC028N06NS
Smoothing choke Lo_1	1,8 µH
Smoothing choke Lo_2	1,8 µH
Output capacitor C_O	940 uF

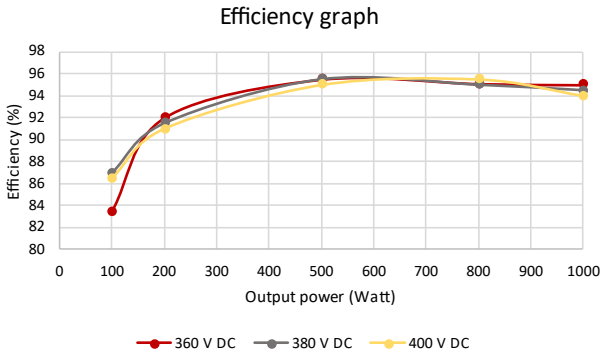

Fig. 5. Eff. of converter with current doubler rectifier [23]

TABLE VI
PROS AND CONS OF PSFB WITH CURRENT DOUBLER

Pros	Cons
ZVS for a large range of output current	More complex output power regulation compared to the original converter
Only two MOSFETs on the secondary side, lower losses	Requires two filter inductances
Simple transformer	

PSFB with Center-Tapped Rectifier

The topology in Fig. 6 is used when a center-tapped transformer is selected. Compared to the previous rectifier, only one filter inductance is used at the cost of a more complex transformer.

A real-world application for the data center is shown in [24]. The Texas Instruments (TI) company in [17] gives an engineering guide for designing this topology. In [17] TI shows a reference design for a 3kW converter.

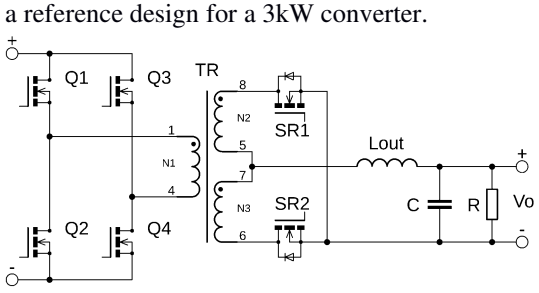

Fig. 6. PSFB with center tap rectifier [24]

Primary side switching and regulation is the same as in the previous rectifier. synchronous rectifier is formed by transistors SR_1 and SR_2, output filter by inductance L_{OUT} and capacitor C. If the primary side of the transformer is polarized positively, transistor SR_2 conducts on the secondary side, if negatively so does SR_1. Current flows through only one semiconductor component in one direction and the synchronous rectifier switches at ZC (Zero Current). Thus, no large losses are produced on the secondary side, although the occurrence of overvoltages increases these losses. Overvoltage makes it necessary to use the MOSFET at higher voltages, which will also increase losses because such MOSFETs have higher RDS_{on}. As in the previous case, the rectifier can be supplemented with an active clamp circuit, which suppresses the occurrence of overvoltage. Such a circuit is presented in [26]. The converter [17] parameters are shown in Table VII, and the component list in Table VIII. Achieved efficiency in Fig. 7. Pros and cons in Table IX.

TABLEVII
PARAMETERS OF PSFB WITH CENTER TAPPED RECTIFIER

Parameter	Value
Supply voltage V_{IN}	385 V
Output current I_O	250 A
Output voltage V_O	12 V
Output power P_2	3 kW
Switching frequency fs	100 kHz

TABLE VIII
COMPONENTS OF PSFB WITH CENTER TAPPED RECTIFIER

Component	Value
Primary GAN $Q_1 – Q_4$	LMG3522
SR_1 and SR_2	PMP23126
Smoothing choke L_{out}	not specified
Output capacitor C	not specified

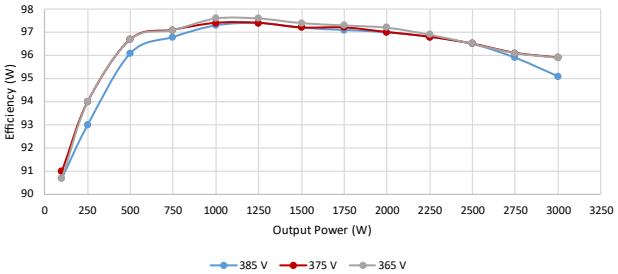

Fig. 7. Eff. of converter with center tapped rectifier [17]

TABLE IX
PROS AND CONS OF PSFB WITH CURRENT DOUBLER

Pros	Cons
ZVS for a large range of output current	More complex output power regulation compared to the original converter
Only two MOSFETs on the secondary side, lower losses	Compared to current doubler it is necessary to use more complex transformer
only one filter inductance	

PSFB with Full-Bridge rectifier

The Full bridge topology [26],[27] requires a simple transformer and one filter inductance, but the current in one direction flows through two rectifier components and is therefore not used if a high output current is required. Schematic is shown in Fig. 8.

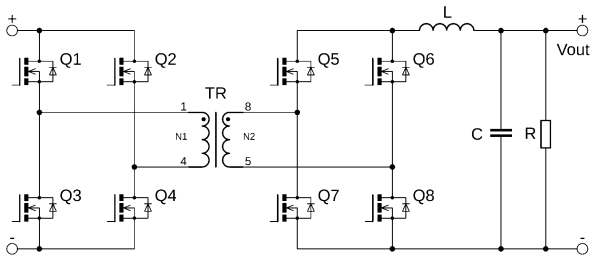

Fig. 8. PSFB with full bridge rectifier [26]

IV. Conclusion

The paper describes the principle of functionality, components used, efficiency achieved for three PSFB converter topologies. The first older topology used regulation on the secondary side and nowadays also older semiconductor components. Nevertheless, it is possible to achieve relatively high efficiency even with this topology. Modern concepts achieve high efficiency mainly due to the use of modern Gan transistors on the primary side, where the output power is also regulated. The secondary side thus contains far fewer semiconductors, which also translates into lower losses.

The paper also describes two modern concepts, the current doubler, and the center-tap rectifier, which achieve high efficiency even without the use of additional circuits, although the addition of an active clamp can increase the efficiency even further.

GaN transistor allowed simplification while maintaining even higher efficiency in the PSFB converter. On the other hand, if we want to push the limits of efficiency even further, we still can't do without auxiliary circuits on the secondary side. The next step is to verify these topologies by simulation and then measure them under laboratory conditions.

Acknowledgment

This work was supported by the Scientific Grant Agency of the Ministry of Education of the Slovak Republic under the project VEGA 1/0363/23.

References

[1] S. Telrandhe, J. Sabnis, M. Rajne, “Design considerations for a on-board charger based on PSFB converter with ZVS,” in 2020 IEEE First International Conference on Smart Technologies for Power, Energy and Control (STPEC), 2020, pp. 1-5, DOI: 10.1109/STPEC49749.2020.9297715

[2] S. Mukherjee, S. Sankar Saha, S. Chowdhury, “Battery Integrated Three-Port Soft-Switched DC–DC PSFB Converter for SPV Applications,” in IEEE Access, 2023, pp. 62472-62483, DOI: 10.1109/ACCESS.2023.3287149

[3] A. Brandis, K. Knol, D. Pelin, D. Topić, “Prototype Proposal of an 18 kW Non-Isolated Bidirectional Converter for Battery Energy Storage System,” in 2023 22nd International Symposium on Power Electronics (Ee), 2023, pp. 01-06, DOI: 10.1109/Ee59906.2023.10346198

[4] L.H. Mweene, C.A. Wright, M.F. Schlecht, “A 1 kW, 500 kHz front-end converter for a distributed power supply system,” in Proceedings, Fourth Annual IEEE Applied Power Electronics Conference and Exposition, 1989, pp. 423-432, DOI: 10.1109/APEC.1989.36994

[5] Dai-Duong Tran, Hai-Nam Vu, S.Yu, W. Choi, “A Novel Soft-Switching Full-Bridge Converter With a Combination of a Secondary Switch and a Nondissipative Snubber,” in IEEE Transactions on Power Electronics. 2017, vol. 33, no. 2, pp. 1440-1452, DOI: 10.1109/TPEL.2017.2688580

[6] H. Liu, Y. Zhao, M. Al Shurafa, J. Chen, J. Wu; Y. Cheng, “A Novel PID Control Strategy Based on PSO-BP Neural Network for Phase-Shifted Full-Bridge Current-Doubler Synchronous Rectifying Converter,” in 2021 IEEE 4th Advanced Information Management, Communicates, Electronic and Automation Control Conference (IMCEC), 2021, pp. 1241-1245,

[7] F. Qi, Z. Wang, Y. Wu, P. Zuk, “Advantage of GaN in Phase Shift Full Bridges,” in 2019 IEEE 7th Workshop on Wide Bandgap Power Devices and Applications (WiPDA), 2019, pp. 384-387, DOI: 10.1109/WiPDA46397.2019.8998838

[8] Young-Do Kim, Kyu-Min Cho, Duk-You Kim, Gun-Woo Moon, “Wide-Range ZVS Phase-Shift Full-Bridge Converter With Reduced Conduction Loss Caused by Circulating Current,” in IEEE Transactions on Power Electronics 2013, vol. 28, no. 7, pp. 3308-3316, DOI: 10.1109/TPEL.2012.2227280

[9] M. Pastor, J. Dudrik, R. Michal, “High-Frequency Soft-Switching DC-DC Converter with Simple Secondary Turn-Off Snubber,” in 2022 IEEE 20th International Power Electronics and Motion Control Conference (PEMC), 2022, pp. 42-47, DOI: 10.1109/PEMC51159.2022.9962897

[10] Song-Yi Lin, Chern-Lin Chen, “Analysis and design for RCD clamped snubber used in output rectifier of phase-shift full-bridge ZVS converters,” in IEEE Transactions on Industrial Electronics, 1998, vol. 45, no. 2, pp. 358-359, DOI: 10.1109/41.681236

[11] J. Dudrik, M. Pástor, M. Lacko, R. Žatkovič, “Zero-Voltage and Zero-Current Switching PWM DC–DC Converter Using Controlled Secondary Rectifier With One Active Switch and Nondissipative Turn-Off Snubber,” in IEEE Transactions on Power Electronics, 2018, vol. 33, no. 7, pp. 6012-6023, DOI: 10.1109/TPEL.2017.2748569

[12] M. Pastor, J. Dudrik, M. Lacko, “High-Frequency Soft-Switching DC-DC Converter with Non-Dissipative Turn-Off Snubber,” in 2018 IEEE 18th International Power Electronics and Motion Control Conference (PEMC), 2018, pp. 127-132, DOI: 10.1109/EPEPEMC.2018.8521863

[13] M. Pástor, J. Dudrik, A. Vitkovská, “Soft-Switching DC-DC Converter with SiC Full-Bridge Rectifier,” in 2019 International Conference on Electrical Drives & Power Electronics (EDPE), 2019, pp. 347-352, DOI: 10.1109/EDPE.2019.8883908

[14] M. Pastor, M. Lacko, J. Dudrik, A. Marcinek, “Soft-Switching Full-Bridge DC-DC Converter with Energy Recovery Capacitor Snubber,” in Energies, 2023, pp. 42–47, DOI: 10.3390/en16041591

[15] M. Heintze, S. Butzmann, “A GaN 500 kHz High Current Active Clamp Phase-Shifted Full-Bridge Converter With Zero-Voltage Switching Over the Entire Line and Load Range,” in 2018 20th European Conference on Power Electronics and Applications (EPE'18 ECCE Europe), 2018, pp. P.1-P.9.

[16] R. Ramachandran, M. Nymand, “Switching losses in a 1.7 kW GaN based full-bridge DC-DC converter with synchronous rectification,” in 2015 17th European Conference on Power Electronics and Applications (EPE'15 ECCE-Europe), 2015, pp. 1-10, DOI: 10.1109/EPE.2015.7311754

[17] Texas Instruments, “3-kW Phase-Shifted Full Bridge With Active Clamp Reference Design With > 270 W/in3 Power Density,” April 2022, Texas Instruments

[18] M. Beheshti, “Wide-bandgap semiconductors: Performance and benefits of GaN versus SiC,” in Analog Design Journal, 2021, Texas Instruments

[19] N. Keshmiri, D. Wang, B. Agrawal, R. Hou; A. Emadi, “Current Status and Future Trends of GaN HEMTs in Electrified Transportation,” in IEEE Access, 2020, vol. 8, pp. 70553-70571, doi: 10.1109/ACCESS.2020.2986972

[20] T. McDonald, “GaN in a Silicon world: competition or coexistence?”, APEC 2016, 2016, Infineon

[21] Dong-Myoung Joo, Byoung-Kuk Lee, Dong-Sik Kim, Jong-Soo Kim, Hee-Jun Kim, “Analysis of GaN HEMT-based phase shifted full bridge dc-dc converter,” in 2015 IEEE International Telecommunications Energy Conference (INTELEC), 2015, pp. 1-5, DOI: 10.1109/INTLEC.2015.7572352

[22] S. Abdel-Rahman, “Design of Phase Shifted Full-Bridge Converter with Current Doubler Rectifier,” Design Note, 2013, Infineon Technologies North America

[23] Infineon Technologies AG, “1000 W 400 V phase-shifted full-bridge currentdoubler with XDPP1100 and CoolGaN™,” Application note, 2020, Infineon Technologies AG

[24] Y. Cui, W. Zhang, L. M. Tolbert, F. Wang, B. J. Blalock, “Direct 400 V to 1 V converter for data center power supplies using GaN FETs,” in 2014 IEEE Applied Power Electronics Conference and Exposition - APEC 2014, 2014, pp. 3460-3464, DOI: 10.1109/APEC.2014.6803806

[25] Texas Instruments, “Phase-Shifted Full Bridge DC/DC Power Converter Design Guide,” Application Note, 2014, Texas Instruments

[26] Texas Instruments, “Achieving high converter efficiency with an active clamp in a PSFB converter,” in Analog Design Journal, 203, Texas Instruments

[27] S. Chothe, Rajaram. T. Ugale, A. Gambhir, “Design and modeling of Phase Shifted Full Bridge DC-DC Converter with ZVS,” in 2021 National Power Electronics Conference (NPEC), 2021, pp. 01-06, DOI: 10.1109/NPEC52100.2021.967

Multimodal detection of antisocial behaviour in social media

[1]*Viliam Balara (1st year),*
Supervisor: [2]*Kristína Machová*

[1,2]Dept. of Cybernetics and Artificial Intelligence, FEI TU of Košice, Slovak Republic

[1]viliam.balara@tuke.sk, [2]kristina.machova@tuke.sk

***Abstract*—Social media are currently the most widely used tool of communication. Apart from serving beneficial purposes to the general public, a significant portion of transferred content bears malicious intent that aims to harm, deceive, or spread hateful news across the community of users. The malicious content is being spread in a textual, visual, or even audio form. This work aims to provide insight into the multimodal detection of antisocial behavior present on online platforms. In this article, we will focus on the basic categorization of such behavior, the forms in which it appears, and the description of current machine learning and deep learning methods associated with this detection.**

***Keywords*—antisocial behavior detection, deep-learning, machine learning, transformers**

I. Introduction

In recent years, the increasing presence of social media in everyday life significantly altered the way of communication. With the rapid multiplication of social media platforms, which comes along with available anonymity, ease of access, and creation of online groups or communities that actively participate in the online exchange of opinions and information, the issue of the early detection of antisocial behavior gains significant importance regarding participating individuals, affected societies as well as policy-makers and research community. While bearing beneficial attributes to the affected groups, social media may serve as a tool of intentional detriment. Early detection and prevention of the spread of this harmful content is of high importance for social, financial, and individual purposes. Despite the differing definitions of antisocial behavior in terms of legislation from one country to another, generally, the definition includes the communication that conveys messages of animosity towards other individuals or groups, which can be transferred in multimodal interpretations, often hidden under the pretense of satirical content [1]. The problem of hate speech is rather serious, as it escapes the virtual boundaries of social media platforms. Paper [2] reports that the observed increase in antisocial behavior observed on social media platforms bears a correlation with real-life hate crimes. The article is structured in the following manner. The following section concentrates on the importance of the detection of antisocial behavior in online platforms. The third section describes the possible approaches to multimodal antisocial behavior detection. The following two sections describe machine learning and deep learning approaches and the final section describes our approach to this topic.

II. Approaches for multimodal antisocial behaviour detection

Paper [3] describes antisocial behavior as acts that encompass various forms of harmful online behavior: from trolling, hate speech, spamming, or cyberbullying to acts of impoliteness, rudeness, or incivility. In the case of social media platforms, antisocial offenses include posting content that collides with particular community standards. The categorization of antisocial behavior is depicted in Table I. Manual detection and monitoring of online content is resource intensive, thus rendering automatic systems for the screening of user-generated text content for traces of antisocial online behavior a key attention point. Multimodal machine learning aims at integrating and the ability to process multiple communicative modalities, including linguistic, acoustic, and visual messages [4]. The recent advances in the field of Deep Learning have enabled the combination of multiple modalities in a single learning framework in an intuitive and efficient manner [5]. There are two major approaches to handling multimodality, the first one being the early-fusion and the second late-fusion approach [6]. In the case of the early-fusion approach, individual modalities are combined before the content classification. On the other hand, late-fusion first processes each particular modality and afterward combines the achieved results that contribute to the final decision.

TABLE I: Types of online antisocial behaviour [3]

Type of antisocial behavior	Antisocial behaviour actions
Personal	Actions against a specific person or group
Nuisance	Actions that cause trouble for a certain community
Environmental	Actions that affect the environment

Currently [7], two prominent approaches are being employed in the task of antisocial behavior detection - classical machine learning classifiers approaches and deep learning. Classifiers belonging to the first group are support vector machines(SVM), logistic regression, naive Bayes, or extreme gradient boosting. Classical machine learning methods are commonly accompanied by methods to convert textual representation into vector ones, such as Bag of Words or TF-IDF (term frequency-inverse document frequency) [8]. A multitude of works have employed machine learning classifiers [9], deep

learning classifiers [10] as well as the combination of both approaches [11]. In recent years, deep learning methods have revolutionized the fields of computer vision and NLP, in which they now have achieved a benchmark status [12]. A significant step forward was the transformer architecture introduced by [13], which achieved state-of-the-art results in terms of natural language understanding. Another improvement in this regard is the use of fine-tuning existing models for the use of new tasks [14]. Fine-tuning of existing models is often put to use as a part of transfer learning [15].

III. Traditional Machine Learning Approaches

Traditional machine learning methods, also called shallow detection methods, are methods that utilize traditional word representation methods to encode words and apply shallow classifiers to conduct classification [7]. To identify or classify user-generated content, text features indicating antisocial behavior have to be extracted. Naive Bayes, Support Vector Machine, and Logistic Regression models are commonly used in text classification [16]. Another important variant is ensemble learning, which aims to overcome the limitations of several individual machine learning algorithms while combining their advantages [17]. Every model possesses certain limitations, however, ensemble approaches aim to harness the benefits of multiple models to attain improved performance in comparison to individual constituent models. Bagging methodology, Random Forest (RF) [18] and boosting method [18] are examples of the ensemble approach.

IV. Deep Learning approaches

Deep learning introduces a multilayer structure in the neural network's hidden layers, thus providing the network with the ability to attain more intricate outcomes. Contrary to the conventional machine learning methods where features have to be set manually or obtained through feature selection techniques, deep learning models are able to learn and extract information without human intervention. Furthermore, these frameworks can learn hidden representations from complex inputs, both in terms of context and content, which play an advantageous role in the detection of antisocial behavior tasks.

A. Long short-term memory

Long Short-Term Memory (LSTM) is a type of recurrent neural network (RNN) that addresses the vanishing gradient problem, making it more effective in capturing long-range dependencies in sequential data. LSTM [19] can be used for sentiment analysis and hate speech detection like standard RNNs but with the advantage of handling longer texts and preserving context over longer sequences. LSTM can effectively capture the sequential dependencies between words, allowing it to understand the context and sentiment expressed in the sentence. The LSTM processes the input text word after word and continually updates the hidden state, thus preserving the captured contextual information and dependencies between individual words. To improve the efficiency of antisocial behavior detection with LSTM, additional techniques such as attention mechanisms are put to use. Attention mechanisms provide the model with the ability to focus on individual segments of text that may bear indicative signs of antisocial behavior.

B. Autoencoder

An autoencoder is a feed-forward neural network that regenerates the input and creates a compressed latent space representation. The main benefit of autoencoders is that they do not need labels for input data. The structure of an autoencoder consists of an encoder that transforms the data into dimensionally reduced representation, followed by a decoder that rebuilds the input as output. A variation of the autoencoder is used in [20] for multidomain and multilingual Hate speech detection.

C. Generative adversarial networks

GAN is a class of unsupervised DL techniques presented by [21]. The GAN model architecture involves two sub-models: a generator that learns to create new sample data that are similar to the training data and a discriminator that classifies the generated data as real or fake. Therefore, the generator and discriminator play a two-player game in which one tries to outperform the other. Both models are updated after every epoch, the discriminator gets better at classifying the produced samples, and the generator efficiently generates samples that are closer to the real ones.

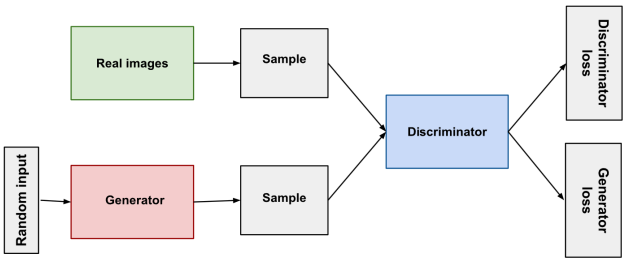

Fig. 1: Basic principle of GAN

D. Transformer

The past few years have witnessed the tremendous success of pre-trained Transformer-based models [13] on a wide variety of NLP tasks. This is mainly caused by the ability to employ pre-training with a large corpus that enables Transformer-based models to gain rich universal language representations that are transferable to vast downstream tasks. It aims to solve sequence-to-sequence tasks and handles long-range dependencies. To compute representations of its input and output, it relies on self-attention without using sequence-aligned RNNs or convolutional neural networks (CNNs). A transformer network consists of the encoder stack and the decoder stack that have the same number of units, depicted on Figure 2. In addition to the self-attention and feed-forward layers that are present in both the encoder as well as decoder, the decoders also have one additional layer of Encoder-Decoder Attention layer to focus on the appropriate parts of the input sequence. Some examples of transformer-based models used in the classification of social media posts are BERT [22], RoBERTa, and DistilBERT.One of the main advantages of available transformer-based models is that they are pre-trained and can be fine-tuned for a wide variety of tasks tasks.

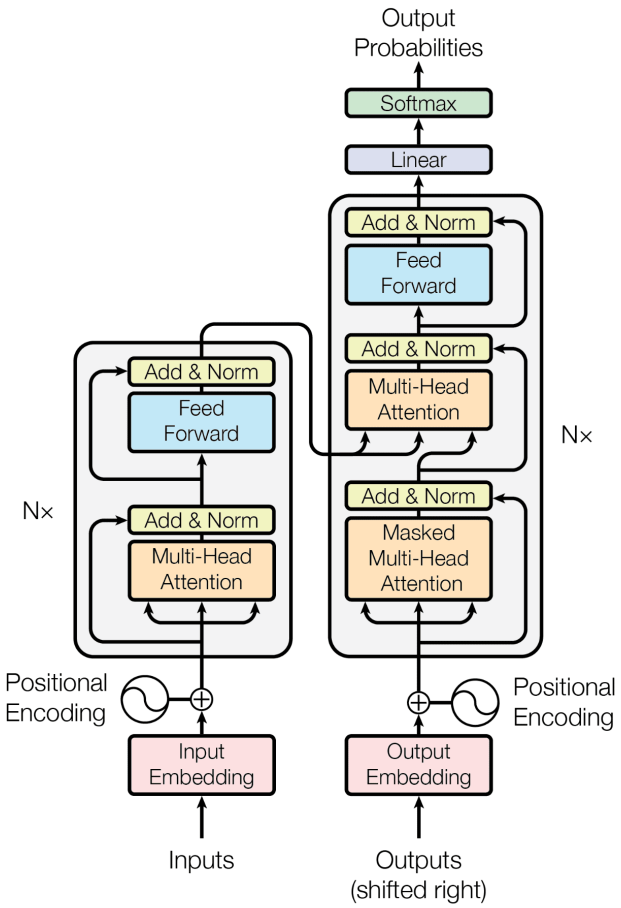

Fig. 2: Transformer architecture [13]

V. Deepfake

A combination of terms deep-learning and fake, deepfake is a synthetic media that was created with the aim to deceive, manipulate, or otherwise provide non-existing visual or audio content. Today, with the use of advanced DL techniques such as GANs, Deepfakes are created with realistic features that can be incorporated into images, video, and audio making them hardly discernible by humans [23]. The majority of people may be inadequately adept at spotting whether they are being deceived by deepfakes. [24] found that people correctly identify fakes in only about 50% of cases. Which, statistically speaking is as good as random guessing. Detection proved to be especially unsatisfactory in the cases when the users had to evaluate videos with artifacts that are caused by the compression which is commonly used on social media or website versions for mobile devices.Since the scope of our work is aimed at mainly text and image data, we will focus on models aimed at processing these modalities.

A. Image-to-text

Text-to-image models have been built using a variety of architectures. The text encoding step may be performed with a RNN, for example, an LSTM network, however, today transformer models are generally considered as a more popular option. For the image generation step, conditional generative adversarial networks have been commonly used, with diffusion models gaining increased popularity in recent years. Instead of directly training a model to create a high-resolution image conditioned on a text embedding, a widely used method is to train a model to generate low-resolution images, and subsequently upscale it with the use of one or more auxiliary deep learning models, adding finer details.

B. Stable Diffusion

Stable Diffusion is a text-to-image model, released in 2022, that uses a deep learning technique known as latent diffusion [25] to generate images based on text prompts. Unlike some previous Text-to-Image models, Stable Diffusion's code and model weights are publicly available and can be run on commonly available consumer hardware. To generate images, Stable Diffusion uses CLIP [26] to project a text prompt into a joint text-image embedding space and select a rough, noisy image that is semantically close to the input prompt. This image is subsequently subjected to a denoising method based on the latent diffusion model to produce the final image. In addition to a text prompt, the text-toiImage generation script within Stable Diffusion provides users with the ability to select various parameters such as sampling type, output image dimensions, and seed value. The seed value is typically set randomly, but a constant number enables reproducibility and the conservation of certain image features across different prompts. An example of image produced by with the use of Stable Diffusion can be seen on Figure 3.

Fig. 3: Image of a dog generated by Stable Diffusion

VI. Our ongoing and future research

Based on the current results of the mentioned research papers, the goal of our future research will be to propose a specific architecture that will put to use transformer-based models, employing further fine-tuning for particular multimodal tasks. In our case, we would like to focus on visual data, particularly computer-generated images that are misleading or aim to mislead the user, specifically those that contain depictions of humans. The created methodology should include the ability to process textual and visual information gathered from social media and be robust enough to successfully classify social media content. Due to underlying differences in the content,

the resulting methodology will be tested on data from multiple social media outlets. We aim to utilize existing text-to-image models, such as stable diffusion to generate content, in our case containing human faces (pretending to be existing users) and depictions of human actors during potentially controversial activity that could be misused (e.g. photo of a driver speeding). Our next step, after generating content hardly discernible by the human eye will be to train deep learning models for the classification into real and computer-generated content. Our methodology of testing our generated content and trained classification models will be divided into two steps - the first one being a classical survey for participants to judge whether the provided content is "fake" or real. The second one will be conducted with the trained classification model, after which we will compare the achieved results of human and computer classification in order to assess the efficiency of the trained model and identify its possible shortcomings. Subsequently, we will focus on fine-tuning image-to-text models to extract auxiliary data found written or otherwise depicted on images present on social media. Additionally, depending on the availability of user-associated metadata in relation to the particular social network, we would like to focus on the behavioral characteristics of a user in order to support classification accuracy.

Acknowledgment

This work was supported by the Scientific Grant Agency of the Ministry of Education, Science, Research and Sport of the Slovak Republic, and the Slovak Academy of Sciences under grant no. 1/0685/21 and by the Slovak Research and Development Agency under Contract no. APVV–22–0414.

References

[1] D. Kiela, H. Firooz, A. Mohan, V. Goswami, A. Singh, P. Ringshia, and D. Testuggine, "The hateful memes challenge: Detecting hate speech in multimodal memes," 2021.

[2] M. L. Williams, P. Burnap, A. Javed, H. Liu, and S. Ozalp, "Hate in the machine: Anti-black and anti-muslim social media posts as predictors of offline racially and religiously aggravated crime," *The British Journal of Criminology*, vol. 60, no. 1, pp. 93–117, 2020.

[3] C. Haythornthwaite, "Moderation, networks, and anti-social behavior online," *Social Media + Society*, vol. 9, no. 3, 2023.

[4] L.-P. Morency and T. Baltrušaitis, "Multimodal machine learning: Integrating language, vision and speech," in *Proceedings of the 55th Annual Meeting of the Association for Computational Linguistics: Tutorial Abstracts*, M. Popović and J. Boyd-Graber, Eds. Vancouver, Canada: Association for Computational Linguistics, Jul. 2017, pp. 3–5.

[5] P. Lippe, N. Holla, S. Chandra, S. Rajamanickam, G. Antoniou, E. Shutova, and H. Yannakoudakis, "A multimodal framework for the detection of hateful memes," *CoRR*, vol. abs/2012.12871, 2020.

[6] K. Perifanos and D. Goutsos, "Multimodal hate speech detection in greek social media," *Multimodal Technologies and Interaction*, vol. 5, no. 7, 2021.

[7] J. S. Malik, H. Qiao, G. Pang, and A. van den Hengel, "Deep learning for hate speech detection: A comparative study," 2023.

[8] M. Liang and T. Niu, "Research on text classification techniques based on improved tf-idf algorithm and lstm inputs," *Procedia Computer Science*, vol. 208, pp. 460–470, 2022, 7th International Conference on Intelligent, Interactive Systems and Applications.

[9] T. Davidson, D. Warmsley, M. Macy, and I. Weber, "Automated hate speech detection and the problem of offensive language," *Proceedings of the International AAAI Conference on Web and Social Media*, vol. 11, no. 1, pp. 512–515, May 2017.

[10] S. Raza, "Automatic fake news detection in political platforms - a transformer-based approach," in *Proceedings of the 4th Workshop on Challenges and Applications of Automated Extraction of Socio-political Events from Text (CASE 2021)*, A. Hürriyetoğlu, Ed., Aug. 2021, pp. 68–78.

[11] P. Badjatiya, S. Gupta, M. Gupta, and V. Varma, "Deep learning for hate speech detection in tweets," in *Proceedings of the 26th International Conference on World Wide Web Companion - WWW '17 Companion*. ACM Press, 2017.

[12] Y. LeCun, Y. Bengio, and G. Hinton, "Deep learning," *nature*, vol. 521, no. 7553, p. 436, 2015.

[13] A. Vaswani, N. Shazeer, N. Parmar, J. Uszkoreit, L. Jones, A. N. Gomez, L. Kaiser, and I. Polosukhin, "Attention is all you need," 2023.

[14] Q. Pham, N. Viet Anh, L. Doan, N. Tran, and T. Thanh, "From universal language model to downstream task: Improving roberta-based vietnamese hate speech detection," 11 2020.

[15] G. Kovács, P. Alonso, and R. Saini, "Challenges of hate speech detection in social media," *SN Computer Science*, vol. 2, no. 2, p. 95, Feb 2021.

[16] S. MacAvaney, H.-R. Yao, E. Yang, K. Russell, N. Goharian, and O. Frieder, "Hate speech detection: Challenges and solutions," *PLOS ONE*, vol. 14, no. 8, pp. 1–16, 08 2019.

[17] W. Liao, B. Zeng, X. Yin, and P. Wei, "An improved aspect-category sentiment analysis model for text sentiment analysis based on roberta," *Applied Intelligence*, vol. 51, pp. 3522–3533, 2021.

[18] M. Wiegand, M. Siegel, and J. Ruppenhofer, "Overview of the germeval 2018 shared task on the identification of offensive language," 2018.

[19] F. Alkomah and X. Ma, "A literature review of textual hate speech detection methods and datasets," *Information*, vol. 13, no. 6, 2022.

[20] G. L. De la Peña Sarracén and P. Rosso, "Unsupervised embeddings with graph auto-encoders for multi-domain and multilingual hate speech detection," in *Proceedings of the Thirteenth Language Resources and Evaluation Conference*, 2022, pp. 2196–2204.

[21] I. J. Goodfellow, J. Pouget-Abadie, M. Mirza, B. Xu, D. Warde-Farley, S. Ozair, A. Courville, and Y. Bengio, "Generative adversarial networks," 2014.

[22] T. Tiţa and A. Zubiaga, "Cross-lingual hate speech detection using transformer models," 2021.

[23] N. C. Köbis, B. Doležalová, and I. Soraperra, "Fooled twice: People cannot detect deepfakes but think they can," *iScience*, vol. 24, no. 11, p. 103364, Nov. 2021.

[24] A. Rössler, D. Cozzolino, L. Verdoliva, C. Riess, J. Thies, and M. Nießner, "Faceforensics: A large-scale video dataset for forgery detection in human faces," *arXiv preprint arXiv:1803.09179*, 2018.

[25] R. Rombach, A. Blattmann, D. Lorenz, P. Esser, and B. Ommer, "High-resolution image synthesis with latent diffusion models," in *Proceedings of the IEEE/CVF conference on computer vision and pattern recognition*, 2022, pp. 10 684–10 695.

[26] N. Dehouche and K. Dehouche, "What's in a text-to-image prompt? the potential of stable diffusion in visual arts education," *Heliyon*, vol. 9, no. 6, p. e16757, 2023.

Logical Modeling of Agent Systems – The Symbolic Aproach

[1]*Samuel NOVOTNÝ (1st year),*
Supervisor: [2]*William STEINGARTNER*

[1,2]Dept. of Computers and Informatics, FEI TU of Košice, Slovak Republic

[1]samuel.novotny@tuke.sk, [2]william.steingartner@tuke.sk

***Abstract*—The anthropomorphic nature of the concept of agent systems attests to its high level of complexity. However, from the perspective of their implementation, this level of abstraction is unbearable, and it is necessary to proceed with its formalization, in which the use of exact logical frameworks has a long tradition. Therefore, in this work, we will focus on the analysis of fundamental logical models of agent systems, emphasizing their relevance.**

***Keywords*—agent systems, formal modeling, logic, symbolic AI**

I. Introduction

Agent system (AS) can be considered one of the most complex concepts of the fifth generation of computing systems development, known as artificial intelligence (AI). Since this stage of the development of computing systems is mainly associated with the process of their anthropomorphization [1], it should be clear that the complexity of this concept lies precisely in the complexity of the human approach to solving certain problems, which AS tries to reproduce.

An essential role in the smooth transition from such a concept to its specific implementation is played by its formal – mathematical model, behaviorally and compositionally equivalent to the modeled object. The purpose of such a model is generally to:

- Enable a deep understanding of complex concepts by using mathematically precise terms and a reasonable degree of abstraction, e.g. from implementation details that are irrelevant to formal models.
- To provide space for examination and verification of various properties of the modeled object.
- Assist in the process of implementation (model-driven development), which is clearly confirmed by the work of d'Inverno et al. [2], which presents this purpose of the model as key.

These facts are illustrated by the diagram in Figure 1, capturing the gradual increase in abstraction from the level of concrete implementations to the level of highly abstract concepts.

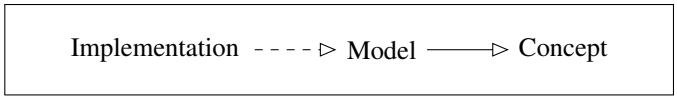

Fig. 1: Levels of abstractions[1]

From the above, it is clear that formal models provide several benefits with both practical (implementation) and theoretical (academic or pedagogical) significance, based on which, in the following section, we will focus on the analysis of the current state in the field of formal AS modeling.

II. Formal modeling of AS

At the beginning of this section, we briefly and informally outline the concept of AS. Furthermore, we will introduce a method of classification of its models, to restrict our subsequent analysis to models exhibiting logical characteristics.

A. AS concept

As seen in Figure 2, the concept of AS includes two entities:

- environment, and
- agent.

While the environment, with its internal characteristic – state, represents a passive element of this concept, the agent plays an active role within it through actions autonomously performed to achieve a specific change in the environment's state. An indispensable part of this concept is also the realization of interactive processes (communication and coordination) among individual agents in the case of multi-agent systems (MAS).

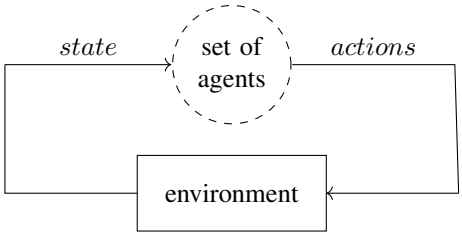

Fig. 2: Simple model of AS

It is evident that the fundamental formal requirement for an AS model, respecting the previously mentioned compositional equivalence of the model and the modeled object, lies in its composition of:

- environment model, and
- agent model.

[1]Within this diagram, the standard UML notation of relationships between individual entities was deliberately used, to capture the difference between these two relationships of this diagram

B. Clasification

The exposure of the topic of classification of specific AS implementations based on various criteria, in contrast to the absence of an explicit division of their formal models within the standard literature dedicated to AS such as Russel's work [3], forces us to consider how to approach the second of the above-mentioned classifications as professionally as possible. So let's first look at the principle of the first one.

In the case of classifying AS, i.e., their specific implementations, we typically proceed one level higher and, based on the corresponding formal model, establish specific classification criteria. This is supported by the following formulation from the work of d'Iverno et al. [2]: "*The properties identified by using a formalism serve to measure and evaluate implementations of agent systems.*" By adhering to this principle, in the classification of formal models of AS, we should once again move one level higher and determine this criterion based on the concept.

The previously mentioned absence of an explicit division of formal models of AS also clearly implies the absence of classification criteria for this concept. However, if we were to choose a much broader concept like AI, which has an incomparably greater number of classification criteria, we could comfortably base the division of these models on a suitable existing classification of AI. We would then reinterpret it for the purposes of classifying AS models. From this perspective, the most useful criterion for dividing AI seems to be the level at which anthropomorphization takes place, specifically the reproduction of cognitive processes. Based on this, we distinguish three fundamental types of AI:

- symbolic or classical,
- subsymbolic, and
- neuro-symbolic.

The following Table I is partially inspired by the one within Kuhnberger's work [4] and presents selected basic differences of the aforementioned types of AI except the last one. This omission is because it represents a combination of the previous two types.

TABLE I: Comparation of symbolic and subsymbolic AI

Criteria	Symbolic	Subsymbolic
methods	logical, algebraic	statistical, numerical
biologically inspired	no	yes
reproduction target	higher cognitive processes	lower cognitive processes
explainability of results	*transparent-box* design	*black-box* design

Now we delve into a closer description of these types of AI. In the case of symbolic AI, the implementation of (higher) cognitive processes, as generalizations, occurs at the level of symbol manipulation, so it can be argued that this approach is largely inspired by formal logic. However, it also includes other areas such as knowledge representation, search, and methods used in logical programming, the emergence of which was stimulated by research in this field. Since this logic-based approach results in the explainability of its outcomes, it can also be referred to as transparent box design, unlike the subsymbolic approach, which, as the name implies, goes beyond these symbolic representations. Inspired by the neurobiological nature of cognitive processes (primarily lower cognitive processes like classifications), it approaches their implementation at a statistical, numerical level. As a consequence, it loses the important property of explainability of its results and is therefore often referred to as black-box design.

The first difference between symbolic and subsymbolic approaches listed in Table I is the reason why we chose this division of AI as a starting point for designing the classification of AS models. This distinction will concern the nature of formal models of AS, allowing us to accept this classification as one distinguishing between models:

- logical or algebraic,
- statistical or numerical, and
- combined.

In the following subsections, we will focus on the basic formal models of individual components of AS, placing emphasis exclusively on the group of logical models, as they constitute the foundational basis of our dissertation research.

C. Logical models of environment

From the very beginning, it was clear that logical frameworks built on classical logic do not provide sufficient expressive power for the compositional and behavioral description of AS. As a result, modal logic systems were primarily utilized for their characterization. The intensional nature of these systems offered a relatively good apparatus for describing the basic structure and simple functionality of AS. In this section, we will provide a brief overview of this area.

1) Models of modal logic: The formalization of the AS environment can be realized based on existing logical models, primarily modal logic systems such as alethic, linear temporal, and branching temporal logic. All corresponding models exhibit an analogous structure, allowing us to define a general form for these models as follows.

Definition 2.1: Let $Prop$ be the set of all elementary propositions. Modal logical models have the form (A, R, l), where:

- A is the carrier set of the given modal logical model,[2]
- R is an order relation on the carrier set A, $R \subset A \times A$, the so-called accessibility relation,
- l is a labeling function $l : A \to 2^{Prop}$, which assigns to each element of the carrier set A a set of elementary propositions that are valid in it.

In tuple, (A, R, l) a subtuple – pair (A, R) is called a frame of certain modal logic.

Although these models are analogous, their usage and interpretation are diametrically different. The modal logic model, also known as Kripke's model [6], can be utilized in a special case of strongly static single-state environments, where we model not so much the actual environment but rather the agent's mental image of this environment. The carrier set of this model consists of so-called possible (epistemic) worlds, which can be understood as states of the agent's knowledge. A typical example of using this model is solving epistemic multi-agent problems such as the *Muddy Children Puzzle* [7]. An interesting categorical perspective on the use of Kripke's model in MAS was presented in Porter's work [8].

Unlike the aforementioned Kripke model, temporal logic models are used to describe actual dynamic environments. Their carrier sets consist of time instances, and the order

[2]This carrier set consists of elements that can be characterized as truth-relativizing elements based on Stalnaker's work [5].

relation on this set can be interpreted based on the incrementation of time. These models represent a very effective tool for logical modeling of the AS environment, as demonstrated by Wooldridge in his dissertation [9].

2) Wooldridge's model: While modal logic models were originally defined for the semantics of modal logic systems, we will now continue with an environment model constructed by Wooldridge in his work [10], directly tailored for the AS concept. Since this model is based on the non-standard concept of *run*, we will first approach the formal definition of this term as follows.

Definition 2.2: Let S be the set of states, s_0 be the initial state of the environment, and Ac be the set of agent actions. Then,

- R is the set of all possible runs, i.e., finite alternating sequences of states and actions starting with the initial state s_0,
- R^S is the set of all possible runs ending in a state, $R^S \subseteq (S \times Ac)^n \times S$, where $n \in \mathbb{N}_0$,
- R^{AC} is the set of all possible runs ending in an action, $R^{Ac} \subseteq (S \times Ac)^n$, where $n \in \mathbb{N}$. [3]

Now, we can finally proceed to the definition of the formal model of the AS environment according to Wooldridge.

Definition 2.3: Let S be the set of states, s_0 be the initial state of the environment, R be the set of all possible runs, and R^{Ac} be the set of runs ending with an agent's action. Then, the task environment model $TEnv$ is (S, s_0, τ, Ψ), where:

- τ is the state transformation function

$$\tau : R^{Ac} \to 2^S, \tag{1}$$

- Ψ is the task specification predicate, evaluating the success of a run

$$\Psi : R \to \{0, 1\}. \tag{2}$$

From the way the state transformation function (2.3) is declared, which describes the principle of modifying the state of the environment, it can be concluded that Wooldridge tried to construct this model as general as possible, as evidenced by the following facts:

- By choosing the set R^{Ac} as the domain of this function, he expressed the dependence of the new environment state not only on the action performed by the agent but also on the entire history of the environment.[3]
- By choosing the power set of the set S as the codomain of this function, he ensured implementability of both stochastic and deterministic environments, limiting it only to single-element subsets of the set S.
- He also captured the specific case, when the environment cannot assume any state. This is achieved by exploiting the fact that the empty set is also an element of the set 2^S.

It should also be evident that the model presented in Definition 2.3 exhibits the characteristics of a standard mathematical model – a state machine. It can be considered as its historically explicitly dependent variant.[3] However, based on this fact, one can observe some drawbacks in this model:

- As Kaelbling points out [11]: "*State machines are a method of modeling systems whose output [implicitly] depends on the entire history of their inputs, and not just on the most recent input. Compared to purely functional systems...*" Is Wooldridge's declaration of the state transformation function based on runs unnecessary, then? It seems so, and it could be just declared in the standard way of declaring the transition function of a nondeterministic state machine as follows:

$$\tau : \underbrace{S \times Ac}_{\text{current}} \to 2^S. \tag{3}$$

- While Wooldridge's approach to declaring the state transformation function considered both possibilities of characterizing stochasticity, in the case of characterizing dynamicity, this approach describes only static environments. This problem can be addressed by further modification of the state transformation function declaration, as follows using dummy action ε:

$$\tau : S \times (Ac \cup \varepsilon) \to 2^S. \tag{4}$$

Based on the above, it is possible to state the possibility of formalizing the AS environment based on a nondeterministic state machine, modifying this state dynamically or by consuming the actions of agents.

D. Logical models of agent

Among the most significant and simultaneously most complex processes related to this component of AS are the decision-making process of agents, as a consequence of the considerable autonomy that AS possess, and their mutual communication, as a consequence of the strong decentralization of MAS. For this reason, in the following presentation of formal logical models of agents, we will focus precisely on these processes.

1) Wooldridge's general model of agent: Similarly to the model of the environment, Wooldridge also constructed the agent model in his work [10] based on the concept of runs, as follows.

Definition 2.4: Let Ac be the set of agent actions, and R^S be the set of runs ending with a state. Then, the agent model is a selection function Ag with the following declaration:

$$Ag : R^S \to Ac. \tag{5}$$

As implied by the above definition 2.4 of the agent model, its basic functionality is the autonomous selection of an action to perform. By choosing the set R^S as the domain of this function, Wooldridge expressed the dependence of this selection not only on the current state but on the entire history of the environment. In this case, however, this approach cannot be objected to since the agent model is constructed as a purely functional model. By choosing the set S as the domain of this function, we would lose any dependence on the history of the environment.

However, certain drawbacks are emerging, such as the fact that, in terms of the observability characteristics of the environment, this agent model describes only fully observable environments – environments about which the agent has all the information. Based on this, it can be argued that this approach is not sufficiently general, leading us to another agent model.

[3]The fact $R^{Ac} \subseteq (S \times Ac)^n$, where $n \in \mathbb{N}$ can also be expressed in an expanded form as follows, $R^{Ac} \subseteq \underbrace{(S \times Ac)^n}_{\text{history}} \times \underbrace{S \times Ac}_{\text{current}}$, where $n \in \mathbb{N}_0$.

2) Deduction model of agent: Deductive models of agents rely on the decision-making process based on proof. Their foundational model, the so-called belief subsystem, was conceived by Konolige in his dissertation thesis [12]. As seen in Figure 3, this model is composed of the belief base $\mathcal{B}$ – any deductively and logically consistent subset of the set of all possible beliefs, the set of inference rules ρ, and a control strategy that manages the application of inference rules to the belief base.

If we denote the set of all belief bases as Bel, based on the above, we can proceed to redefine the selection function of the agent model Ag as follows:

$$Ag : Bel \rightarrow Ac. \tag{6}$$

This agent model (6) has addressed the issue of the previous model (5), which described only fully observable environments. In this case, the input to the selection function now includes only information mediated by the agent's model through its perceptions, i.e., a specific belief base $\mathcal{B}$.

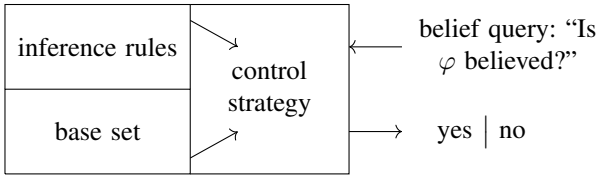

Fig. 3: A Schematic Belief Subsystem form Konolige's work [12]

3) Logical formalization of communication within MAS: Most works addressing communication within MAS focus on one of two relatively distinct aspects of communication:

- syntactic standardization (e.g., Singh's work [13] based on the theory of speech acts),
- description of its realization (e.g., McBurney's work using game theory [14]).

In our work [15], however, we constructed the TIL-message formalization system, exhibiting both the properties of a syntactic standard based on Transparent Intensional Logic (TIL) and an abstract description of communication realization based on the procedural nature of the semantics of this logical system, captured by a certain variation of typed λ-calculus.

III. Summary and Future Research

Since this work focuses on the logical modeling of AS, right from the beginning, we attempted a general definition of the term model. We stated that it represents a middle level of abstraction between the too concrete notion of implementation and the highly abstract notion of a concept, suitable for the formulation of a mathematical specification.

Subsequently, to narrow down the analysis of AS formal models exclusively to *logical* one, we focused on their classification. Based on this, we could finally proceed to the main part of this paper, the analysis of specific logical models of AS which discovered facts that stimulate and require further research.

Despite the analogous nature of modal and temporal logic models, we noted their completely different applications within AS. From that perspective, the use of the semantic model of TIL, which combines a modal and temporal approach into a unique logical formalism, would be a fascinating direction for further research providing the more general model of AS.

IV. Conclusion

Although the current era, with its incredible computing capacity, seems destined for the unrivaled dominance of subsymbolic AI, several factors indicate that the actual dominance lies in the integration of symbolic and subsymbolic approaches within the means of neuro-symbolic AI [16]. The most known and currently increasingly discussed example of this is large language models [17] such as GPT-3. Based on this, it is evident that the development in the field of symbolic AI and thus logical models of AI is still alive and, as Chomsky states in the interview with Katz [18], necessary for achieving so-called general intelligence.

Acknowledgment

This work was supported by the project project 030TUKE-4/2023 "Application of new principles in the education of IT specialists in the field of formal languages and compilers", granted by Cultural and Education Grant Agency of the Slovak Ministry of Education.

References

[1] T. Mauch, *Artificial Intelligence and Anthropomorphism. Does Alan Turings Imitation Game Enhance Anthropomorphism in AI Research?* United Kingdom: GRIN Verlag, 2021.

[2] M. d'Inverno, M. Fisher, A. Lomuscio, M. Luck, M. De Rijke, M. Ryan, and M. Wooldridge, "Formalisms for multi-agent systems," *The Knowledge Engineering Review*, vol. 12, no. 3, pp. 315–321, 1997.

[3] S. Russell and P. Norvig, *Artificial Intelligence: A Modern Approach*, 3rd ed. Prentice Hall, 2010.

[4] K.-U. Kühnberger, H. Gust, and P. Geibel, "Perspectives of neuro–symbolic integration–extended abstract–," in *Dagstuhl Seminar Proceedings*. Schloss Dagstuhl-Leibniz-Zentrum für Informatik, 2008.

[5] R. Stalnaker, "Possible worlds and situations," *Journal of Philosophical Logic*, vol. 15, no. 1, pp. 109–123, 1986.

[6] S. A. Kripke, "Semantical considerations on modal logic," *Acta Philosophica Fennica*, vol. 16, pp. 83–94, 1963. [Online]. Available: http://saulkripkecenter.org/wp-content/uploads/2019/03/Semantical-Considerations-on-Modal-Logic-PUBLIC.pdf

[7] A. Baltag and B. Renne, "Dynamic epistemic logic," in *The Stanford Encyclopedia of Philosophy*, E. N. Zalta, Ed. Metaphysics Research Lab, Stanford University, 2016. [Online]. Available: https://plato.stanford.edu/archives/win2016/entries/dynamic-epistemic/

[8] T. Porter, "Interpreted systems and kripke models for multiagent systems from a categorical perspective," *Theoretical Computer Science*, vol. 323, no. 1, pp. 235–266, 2004.

[9] M. J. Wooldridge, "The logical modelling of computational multi-agent systems," Ph.D. dissertation, The University of Manchester, 1992.

[10] M. J. Wooldridge, *An Introduction to MultiAgent Systems*, 2nd ed. Chichester, United Kingdom: Wiley, 2009.

[11] L. Kaelbling, "Introduction to electrical engineering and computer science i," 2011. [Online]. Available: https://ocw.mit.edu/courses/6-01sc-introduction-to-electrical-engineering-and-computer-science-i-spring-2011/resources/mit6_01scs11_textbook/

[12] K. Konolige, *A deduction model of belief and its logics*. Stanford University, 1984.

[13] M. P. Singh, "Towards a formal theory of communication for multiagent systems," in *IJCAI'91: Proceedings of the 12th international joint conference on Artificial intelligence*, J. Mylopoulos and R. Reiter, Eds. Morgan Kaufmann Publishers Inc., 1991, pp. 69–74. [Online]. Available: https://www.ijcai.org/Proceedings/91-1/Papers/012.pdf

[14] P. McBurney and S. Parsons, "Dialogue games in multi-agent systems," *Informal Logic*, vol. 22, 2001. [Online]. Available: https://api.semanticscholar.org/CorpusID:53330823

[15] S. Novotný, M. Michalko, J. Perháč, V. Novitzká, and F. Jakab, "Formalization and modeling of communication within multi-agent systems based on transparent intensional logic," *Symmetry*, vol. 14, no. 3, 2022. [Online]. Available: https://www.mdpi.com/2073-8994/14/3/588

[16] A. d. Garcez and L. C. Lamb, "Neurosymbolic ai: The 3 rd wave," *Artificial Intelligence Review*, pp. 1–20, 2023.

[17] K. Hammond and D. Leake, "Large language models need symbolic ai," in *Proceedings of the 17th International Workshop on Neural-Symbolic Learning and Reasoning, La Certosa di Pontignano, Siena, Italy*, vol. 3432, 2023, pp. 204–209.

[18] Y. Katz, "Noam chomsky on where artificial intelligence went wrong," *The Atlantic*, 2012.

Computer Vision in Smart Transportation System

[1]*Kristián MIČKO (3rd year),*
Supervisor: [2]*Peter PAPCUN*

[1,2]Dept. of Cybernetics and Artificial Intelligence, FEI TU of Košice, Slovak Republic

[1]kristian.micko@tuke.sk, [2]peter.papcun@tuke.sk

***Abstract*—Amidst the global push for smarter, more sustainable cities, smart transportation systems emerge as critical components in enhancing urban mobility, safety, and environmental health. The relentless pursuit of efficiency and reliability in these systems fuels the need for innovative approaches that can adapt to the dynamic urban landscape. Smart transportation systems are one of the most researched industries in the world, with many approaches existing that utilize various sensor systems and data mining techniques. Our research focuses on using Computer Vision (CV) techniques deployed on the edge computing layer. The research challenge is using computer vision methods that require significant computational resources, especially for real-time conditions. The requirements are directly proportional to the frame's resolution. This paper describes the survey of the most successful computer vision methods usable for edge computing, focusing on motion detection and object tracking in the smart transportation system. These methods are adopted and developed by our research. Our research focuses on improving the quality of computer vision methods by fusion of the volumetric data. Volumetric data can be obtained from neural network depth estimation, lidars, time-of-flight, or stereo vision cameras.**

***Keywords*—computer vision, edge computing, single-board computers, volumetric data, key points descriptor, motion detection, object tracking, smart transportation system**

I. Introduction

Computer Vision (CV) approaches solve many tasks in various companies. These approaches can be applied to image or video datasets, as well as datasets generated by other sensors, such as light detection and ranging (lidar) or ultrasound scanners. Numerous sensor systems are suitable for tasks in smart transportation systems.

The fusion of lidar sensors with camera systems can reconstruct image data that has been distorted by weather impacts. Many intelligent digital camera systems utilize pre-trained neural network (NN) models to preprocess and reconstruct images with noise. These features enable us to develop specific-purpose CV methods that are suitable for deployment on single-board computers (SBCs), capable of operating under various weather conditions.

This paper will summarize methods suitable for motion detection and object tracking within the observed traffic surveillance system. These methods leverage advanced intelligent digital camera systems that employ embedded NN models for preprocessing and reconstructing digital images. Improving the quality of preprocessed images can facilitate the use of simpler and computationally more efficient methods that are adaptable to various conditions in smart transportation systems.

II. The initial status

In the previous analysis, we identified numerous sensor systems frequently used to monitor road infrastructure. This included a comparison of the difficulty of installation, purchasing and maintenance costs, and the types of data that could be processed [1].

The data from sensor systems can be divided into several categories. One category includes sensors whose data are processable by CV methods. Another comprises sensors generating data that CV methods cannot process. Beyond cameras, there are sensors that produce 2D heatmaps/rangemaps or volumetric data. 2D heatmaps can be interpreted as types of images with observable patterns [2]. Volumetric data can be represented by depth maps (a kind of heatmap) or generated point clouds.

The most recent research has focused on connecting or generating data using various techniques. Point clouds generated from lidars can reconstruct the shape of objects observed in dark conditions for digital cameras, and faint color information from softly reflected light can be utilized for color reconstruction of the observed object [3].

Conversely, monocular or stereo cameras can generate depth maps or point clouds given sufficient light sources, such as sunny weather or strong torches [4]. Last year, our focus was on classifying moving objects in traffic surveillance systems.

We decided to improve the classification metric's success by using volumetric data. This data provides additional third-dimension information, allowing for the extraction of new features to aid in object classification without the need for training complex NN models. Large NN models are unsuitable for edge computing architectures, and it is challenging to acquire, annotate, and train complex datasets (different weather, daytime, and angle views) [1].

Last year also summarized the potential for distributing CV methods into independent services [5]. Depending on the computational power of edge devices and the complexity of CV methods, these services enable scalable solutions. The following section discusses the research progress in this area over the recent period and the success of its implementation.

III. The tasks solved in previous year

The research paper focuses on utilizing traditional CV methods that enable us to distribute computational power across many computational nodes [5]. The challenge was addressed by employing simple mathematical operations, such as calculating the mean pixel value in a binary image obtained from edge detectors [6], [7], [8]. Our research is dedicated to

using only image data and generating volumetric data derived solely from CV methods (photogrammetry).

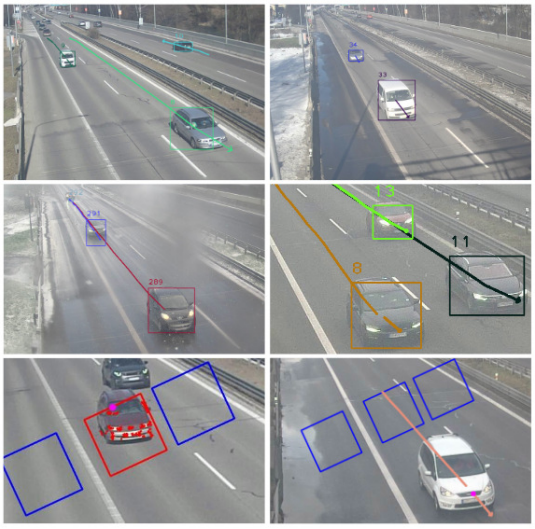

Fig. 1. Algorithms detection output [6]

The calculation was applied in specific regions of interest (ROIs), significantly reducing computational complexity. Thresholding the mean pixel value can classify the presence of a new object in the observed region of interest.

Classifying the presence of a new object in specific ROIs helps us detect motion within a video frame. These ROIs are also used for triggering the MOSSE object tracker (Fig. 1).

The MOSSE object tracker [9] assists in determining the geometrical centroids' positions of detected objects. These geometrical centroids trace the trajectory of the object's motion vector, which defines the motion's direction. This is beneficial for various applications in intelligent traffic surveillance systems (Fig. 1) (TABLE I).

TABLE I
EVALUATION OF VEHICLE COUNTING [6].

Data acquisition method	**Video 1**	**Video 2**	**Video 3**	**Video 4**
Real value	53	72	120	61
Foreground modeling	60	80	127	82
YOLOv4	111	181	240	132
Template matching	42	44	86	20

In Fig. 2, we employed the aforementioned strategy to mitigate errors caused by shadows overlapping vehicles. The strategy was enhanced by utilizing key point descriptors [7] and features obtained through the histogram of oriented gradients (HoG) [10]. These descriptors facilitated the development of oriented object detectors [11], which can indicate the direction of moving objects and prevent shadow overlap with vehicles.

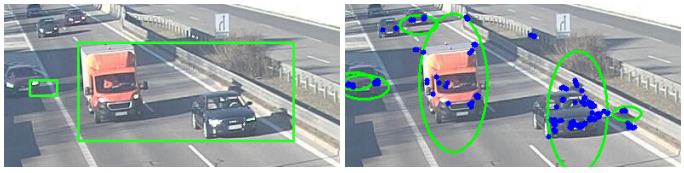

Fig. 2. The implemented oriented object detectors in our research.

Key point descriptors, marked with blue dots, identify significant candidate areas and eliminate areas affected by shadows (Fig. 2). A clustering algorithm connects the key points into a single geometric centroid [12]. This algorithm draws oriented ellipsoids at these centroids based on the HoG dominance angle.

The CV methods described are suitable for most edge devices based on SBCs and have been deployed on devices such as the Raspberry Pi 3b+ model, Raspberry Pi 4 model, NVidia Jetson Nano, and ARM Cortex M7-based SBCs. The NVidia Jetson Nano SBC has the advantage of utilizing CUDA cores to parallelize computation, making CV methods and algorithms more efficient than relying solely on CPU power.

IV. Future work

This paper describes the tested CV methods and algorithms for motion detection and object tracking, deployed on edge devices connected to the camera surveillance system. Our research supports the assertion that NNs are not necessary for detecting motion and tracking detected objects. Traditional CV methods prove efficient for this purpose. We have identified optimal methods for processing 2D images, which are also suitable for the edge computing layer using SBCs.

We have demonstrated that combining SBCs, CV methods, and a connection to a live-stream camera surveillance system allows us to replace some intrusive sensors.

The final task involves developing a vehicle classification method based on calculated volumetric data obtained from 2D images. These images can be generated using the MiDaS NN model from RGB pictures or produced by a new generation of ToF camera sensors with VGA resolution.

Acknowledgment

This publication is the result of the APVV grant ENISaC - Edge-eNabled Intelligent Sensing and Computing (APVV-20-0247).

References

[1] K. Micko, P. Papcun, and I. Zolotova, "Review of iot sensor systems used for monitoring the road infrastructure," *Sensors*, 2023.
[2] R. M. Haralick and L. G. Shapiro, "Glossary of computer vision terms." *Pattern Recognit.*, vol. 24, no. 1, pp. 69–93, 1991.
[3] T. Tian and B. Zhang, "A haze removal method based on additional depth information and image fusion," in *Sensor Networks and Signal Processing*. Springer Singapore, 2021, pp. 423–433.
[4] R. Birkl, D. Wofk, and M. Müller, "Midas v3. 1–a model zoo for robust monocular relative depth estimation," *arXiv preprint arXiv:2307.14460*, 2023.
[5] K. Micko, "Computer vision services in transportation," in *23nd Scientific Conference of Young Researchers : proceedings from conference.* TUKE, 2023.
[6] K. Mičko, T. Vank, J. Maciak, and P. Papcun, "Movement vector computing of vehicles on mast-mounted camera systems," in *2023 DISA*. IEEE, 2023.
[7] K. Mičko and P. Papcun, "Parking management system based on key points detection," *Acta Electrotechnica et Informatica*, vol. 23, no. 3, pp. 33–39.
[8] K. Micko, M. Kocurekova, A. Maciakova, and I. Zolotova, "Motion detection methods for automatic number plate recognition," in *2023 DISA*. IEEE, 2023.
[9] K. Han, "Image object tracking based on temporal context and mosse," *Cluster Computing*, vol. 20, pp. 1259–1269, 2017.
[10] K. Lee and M. Mokji, "Automatic target detection in gpr images using histogram of oriented gradients (hog)," in *2014 2nd international conference on electronic design (ICED)*. IEEE, 2014, pp. 181–186.
[11] S. Ha, L. Pham, H. Phan, and P. Ho, "A robust algorithm for vehicle detection and classification in intelligent traffic system," 12 2015.
[12] R. Grycuk, "Novel visual object descriptor using surf and clustering algorithms," *Journal of Applied Mathematics and Computational Mechanics*, vol. 15, no. 3, pp. 37–46, 2016.

Training Deep Learning Models for Grammatical Error Correction in Slovak Texts

[1]*Maroš HARAHUS (3^{rd} year),*
Supervisor: [2]*Matúš PLEVA*

[1,2]Department of Electronics and Multimedia Communications, Faculty of Electrical Engineering and Informatics
Technical University of Kosice, Letná 9, 042 00 Košice, Slovak Republic, Tel. +421 55 602 2298

[1]maros.harahus@tuke.sk, [2]matus.pleva@tuke.sk

***Abstract*—This article explores the improvement of grammatical error correction (GEC) capabilities for the Slovak language using the latest natural language processing (NLP) technologies. Our research includes a wide range of methodologies, including fine-tuning the "ApoTro/slovak-t5-small" model, etc. In a series of experiments using different levels of data corruption, we evaluate the performance of the models in correcting grammatical inaccuracies. The results show the significant potential of these models, especially the T5 model fine-tuned for minimally corrupted data, which has demonstrated accuracy. Additionally, we propose expanding our dataset and exploring advanced Fairseq architectures for further optimization. As an application of our findings, we outline the development of a web interface aimed at providing real-time grammar correction services to users. Our work not only contributes to academia by filling the gap in GEC resources for Slovak, but also suggests practical applications that improve language teaching and text correction tools.**

***Keywords*—Deep Learning Models, Fairseq, Grammatical Error Correction, Model Fine-Tuning, OpenNMT, Slovak Texts, T5 Model**

I. Introduction

The development of computational models for grammatical error correction (GEC) represents a significant frontier in the field of natural language processing (NLP). While substantial progress has been made in creating effective GEC models for widely spoken languages, there exists a noticeable gap in resources tailored to less common languages, such as Slovak. This research endeavor aims to bridge this gap by developing a GEC model specifically designed for the Slovak language. The motivation for this task stems from the observed limitations of existing tools, which, while capable of identifying and correcting isolated lexical errors, often fail to account for the broader linguistic context within which these errors occur. Unlike these tools, our model seeks to incorporate a deeper understanding of Slovak syntax and grammar, taking into consideration the contextual relationship between words in a sentence. This approach not only promises to enhance the accuracy of grammatical correction but also contributes to the broader goal of advancing language technology for underrepresented languages.

II. Related work

The field of grammar correction within machine translation has witnessed significant advancements over the past decades. Early research primarily centered around integrating rule-based and statistical systems into Statistical Machine Translation (SMT) workflows to address grammatical errors [1], [2]. While these approaches yielded some improvement, the rise of Neural Machine Translation (NMT) opened new avenues for enhancing grammatical fluency. NMT models, due to their ability to better model long-range dependencies and generate more natural language, have implicitly improved the grammatical quality of machine-translated output [3], [4].

More recently, the development of large-scale pretrained language models like T5 (Text-to-Text Transfer Transformer) has revolutionized grammar correction [5]. By framing grammar correction as a text-to-text problem, T5-based models can be fine-tuned on datasets with explicitly labeled grammatical errors. This approach, exemplified by the GECTOR model, has led to substantial progress in automated grammar correction [6].

III. Metrics

Bilingual Evaluation Understudy (BLEU) [7] measures how well the machine translation aligns with human translations, focusing on the precision of word sequences. It calculates matching n-grams (word sequences) between the machine translation and reference translations, applying a penalty for too short translations.

Google-BLEU (GLEU), developed by Google, is similar to BLEU but also includes a recall component, assessing both how many words from the reference are included in the translation and how many are accurately captured from the source text. GLEU aims to provide a more comprehensive evaluation by balancing precision and recall.

IV. Datasets and experiments

A. Automated Generation of Grammatical Error Datasets for Slovak

In the initial phase of dataset preparation, a wide-ranging effort was made to gather various types of textual content from multiple online sources. This effort included collecting comments from social media, excerpts from books, titles of news articles, and other similar textual forms. The objective was to create a dataset that represents a wide range of text types and writing styles.

We created a Python script to create a dataset with grammatically incorrect sentences derived from correct Slovak sentences. It randomly applies character substitutions and transformations (e.g. changing "yi" to "iy", modifying diacritics) to

simulate common grammatical errors. The goal is to create a dataset that reflects the types of errors made by native speakers, which is crucial for training models to correct grammatical errors in Slovak. The input is a text file of correct sentences and the output is a CSV file containing pairs of incorrect and correct sentences. This dataset facilitates the development of NLP applications for Slovak by providing material for machine learning models to learn error identification and correction, thus contributing significantly to the advancement of automatic proofreading and language learning tools for languages with fewer resources.

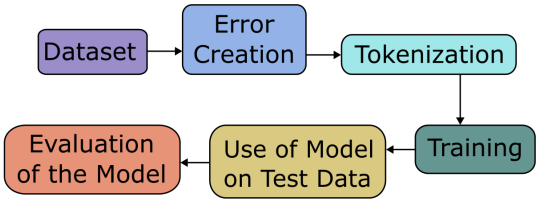

Fig. 1. Process Flow: From Dataset to Model Evaluation

B. Training Slovak GEC Models with OpenNMT

A dataset containing 1 million sentences was run through varying training intensities using the OpenNMT [8] and SentencePiece [9] framework for tokenization, yielding insightful performance metrics. Training percentages ranging from 1% to 30% of the dataset were investigated, each consistently set to 50,000 Unigram models and a vocabulary size of 10,000. The performance metrics, represented by precision, recall, and F1 scores, showed a fluctuating trend, with 10% training resulting in the highest F1 score of 70.60, indicating a peak in model performance. Conversely, lower training cuts, such as 5% and 15%, showed lower F1 scores, suggesting a correlation between the amount of training data and the model's ability to accurately correct grammatical errors. These results highlight the differential impact of the amount of training data on model accuracy and suggest an optimal data threshold for maximizing grammar correction performance.

C. Fairseq GEC Model Insights for Slovak

Leveraging Fairseq [10] for Slovak grammatical error correction, we used MosesDecoder [11] and Subword-NMT [12] for tokenization, focusing on optimizing training with a 1 million sentence dataset. Training percentages varied from 1% to 30%, employing 10,000 BPE units for vocabulary. Evaluation through BLEU scores revealed a high of 68.81 for the 1% training dataset, indicating an effective grasp of grammatical nuances with minimal data. However, as training data increased, BLEU scores showed fluctuating trends, peaking at 66.23 for 25% training volume before a slight decline. This underscores the complexity of balancing training data volume and model accuracy, highlighting Fairseq's adaptability in processing linguistic data efficiently.

D. Correcting Grammatical Errors in Slovak by Retraining the T5 Model

In an effort to correct grammatical errors in Slovak texts, the "ApoTro/slovak-t5-small" [13] model was fine-tuned across different levels of input corruption, ranging from 1% to 30%. The results of this fine-tuning process are quantified through training and validation losses, BLEU, and GLEU scores. Notably, as the corruption level decreased, the model's performance improved significantly, with the highest GLEU score (0.4557) and the lowest validation loss (0.0120) observed at the 1% corruption level. This pattern suggests that the model is highly effective in correcting grammatical errors when dealing with minimally corrupted inputs. Conversely, at a 30% corruption level, there was an expected increase in both training and validation losses, alongside a decrease in BLEU and GLEU scores, indicating a challenge in error correction with more heavily corrupted inputs. Overall, these outcomes demonstrate the model's potential to enhance the grammatical quality of Slovak texts, particularly when fine-tuned with carefully curated data sets.

Model/Approach	Metric	Best Value
OpenNMT	F1 Score	70.60
Fairseq	BLEU Score	68.81
T5-small	GLEU Score	0.4557

TABLE I
BRIEF COMPARISON OF MODEL RESULTS

V. Future work

In the upcoming period, the research focus will shift towards broadening the scope of techniques and models for enhancing grammatical error correction capabilities in Slovak texts. This endeavor will explore the integration of the BERT model, capitalizing on its advanced language comprehension to tailor a solution specifically for grammatical inaccuracies. Additionally, the investigation will extend into the realms of LSTM networks and encoder-decoder architectures, examining their potential in the nuanced task of grammatical correction through their proven efficacy in sequential data processing.

Further exploration within the Fairseq platform will delve into a variety of architectural innovations and modifications offered beyond the conventional transformer model, aiming to identify more effective or efficient grammatical error correction methodologies. Given the promising outcomes associated with OpenNMT, particularly concerning dataset size and model performance, an expansion of the training corpus is anticipated to refine the model's understanding and correction of grammatical patterns.

A significant advancement towards making this technology accessible and practical will be the development of a web interface. This interface will allow users to input sentences and receive corrections, thereby not only serving as a direct application of the research findings but also facilitating broader testing and iterative feedback. This comprehensive approach, encompassing model exploration, dataset expansion, and application development, is poised to significantly contribute to the advancement of natural language processing tools for the Slovak language, enhancing both academic research and practical language learning applications.

Acknowledgment

The research in this paper was supported partially by the Ministry of Education, Research, Development and Youth of the Slovak Republic under project VEGA 2/0165/21, the Cultural and Educational Grant Agency of the Slovak Republic

project KEGA 049TUKE-4/2024, and by the Slovak Research and Development Agency under the projects APVV-22-0414 & APVV-22-0261.

References

[1] A. Rozovskaya and D. Roth, "Grammatical error correction: Machine translation and classifiers," in *Proc. of the 54th Annual Meeting of the ACL*, 2016, pp. 2205–2215.

[2] D. Xiong and M. Zhang, *Linguistically Motivated Statistical Machine Translation*. Springer, 2015.

[3] M.-T. Luong and C. D. Manning, "Achieving open vocabulary neural machine translation with hybrid word-character models," in *Proc. of 54th Annual Meeting of the ACL*. Berlin, Germany: Association for Computational Linguistics, Aug. 2016, pp. 1054–1063. [Online]. Available: https://aclanthology.org/P16-1100

[4] M. Rowshan, A. Burg, and E. Viterbo, "Polarization-adjusted convolutional (PAC) codes: Fano decoding vs list decoding," *CoRR*, vol. abs/2002.06805, 2020. [Online]. Available: https://arxiv.org/abs/2002.06805

[5] C. Raffel, N. Shazeer, A. Roberts, K. Lee, S. Narang, M. Matena, Y. Zhou, W. Li, and P. J. Liu, "Exploring the limits of transfer learning with a unified text-to-text transformer," *CoRR*, vol. abs/1910.10683, 2019. [Online]. Available: http://arxiv.org/abs/1910.10683

[6] Z. Han, Z. Ding, Y. Ma, Y. Gu, and V. Tresp, "Learning neural ordinary equations for forecasting future links on temporal knowledge graphs," in *Proceedings of the 2021 Conference on Empirical Methods in Natural Language Processing*. Online and Punta Cana, Dominican Republic: Association for Computational Linguistics, Nov. 2021, pp. 8352–8364. [Online]. Available: https://aclanthology.org/2021.emnlp-main.658

[7] K. Papineni, S. Roukos, T. Ward, and W.-J. Zhu, "Bleu: a method for automatic evaluation of machine translation," in *Proceedings of the 40th annual meeting of the Association for Computational Linguistics*, 2002, pp. 311–318.

[8] G. Klein, Y. Kim, Y. Deng, J. Senellart, and A. Rush, "OpenNMT: Open-source toolkit for neural machine translation," in *Proceedings of ACL 2017, System Demonstrations*, M. Bansal and H. Ji, Eds. Vancouver, Canada: Association for Computational Linguistics, Jul. 2017, pp. 67–72. [Online]. Available: https://aclanthology.org/P17-4012

[9] T. Kudo and J. Richardson, "Sentencepiece: A simple and language independent subword tokenizer and detokenizer for neural text processing," 2018.

[10] M. Ott, S. Edunov, A. Baevski, A. Fan, S. Gross, N. Ng, D. Grangier, and M. Auli, "fairseq: A fast, extensible toolkit for sequence modeling," in *Proc. of the 2019 Conf. of the North American Chapter of the ACL*. Minneapolis, Minnesota: Association for Computational Linguistics, Jun. 2019, pp. 48–53. [Online]. Available: https://aclanthology.org/N19-4009

[11] H. Hoang and P. Koehn, "Design of the moses decoder for statistical machine translation," in *Software Engineering, Testing, and Quality Assurance for Natural Language Processing*, 2008, pp. 58–65.

[12] R. Sennrich, B. Haddow, and A. Birch, "Neural machine translation of rare words with subword units," *arXiv preprint arXiv:1508.07909*, 2015.

[13] R. A. Cepka, "Slovak t5-small," https://huggingface.co/ApoTro/slovak-t5-small, 06 2022, accessed: February 21, 2024.

Cosmic Ray Modulation Analysis: Solution Uniqueness and Employing Neural Networks

[1]*Martin NGUYEN (2nd year),*
Supervisor: [2]*Ján GENČI, Consultant:* [3]*Pavol BOBÍK*

[1,2]Dept. of Computers and Informatics, FEI TU of Košice, Slovak Republic
[3]Department of Cosmic Physics, Institute of Experimental Physics SAS Kosice, Slovak Republic

[1]martin.nguyen@student.tuke.sk, [2]jan.genci@tuke.sk, [3]bobik@saske.sk

***Abstract*—The domain of cosmic ray modulation within the heliosphere is still a subject of ongoing study at UEF SAV and TUKE. This study addresses two primary challenges: the estimation of statistical errors in cosmic ray modulation models and the examination of solution uniqueness. By using the numerical Stochastic Differential Equation (SDE) method in our research, we aim to improve the accuracy and reliability of cosmic ray propagation models. These models are crucial for the astrophysical theories and space weather forecasting. We developed and introduced the tool called CudaHelioCommander to efficiently explore the uniqueness of solutions in cosmic ray modulation models. Using the tool, we conducted the uniqueness test and formulated the research findings in a publication in the Computer Physics Communications journal where we emphasized the non-uniqueness of solutions derived from the Parker's equation. Our future research plans aims to further improve the prediction accuracy and efficiency of these models by employing neural networks to navigate the vast parametric space of cosmic ray modulation models.**

***Keywords*—Cosmic Ray Modulation, Parker Equation, Neural Networks, AMS-02 Data Analysis**

I. Introduction

The exploration of cosmic ray modulation within the heliosphere is a critical area of research for understanding the dynamic processes affecting cosmic ray transport and distribution in space. In our two main studies [1] [2], we looked into the statistical analysis of cosmic ray modulation models and employed a sophisticated SDE method to assess statistical errors and solution uniqueness. The motivation lies in refining our models to better predict and analyze cosmic ray data which is considered as the main pillar for both theoretical astrophysics and practical space weather forecasting.

II. Challenges that needed to be solved

In the previous year, the research focused on addressing two primary challenges within the field of cosmic ray modulation in the heliosphere: the estimation of statistical errors in modeling results and the examination of solution uniqueness. The study utilized the numerical stochastic differential equation (SDE) method, which is a widely recognized approach for solving Parker's equation and used in the cosmic ray modulation studies. The tasks involved a detailed analysis of statistical errors for models utilizing the SDE method and a comprehensive investigation into the uniqueness of solutions offered by these models.

A. Statistical Error Estimation for Cosmic Ray Modulation Models

A core focus of the research was the development of a methodology to evaluate statistical errors within the numerical models employing the Stochastic Differential Equation (SDE) method. The task required an analysis of error propagation in these models which led to a clearer understanding of the reliability of model outputs.

B. Analysis of Solution Uniqueness in Heliospheric Modulation Models

Another significant task was the examination of solution uniqueness for 1D and 2D models of heliospheric modulation, particularly for the SOLARPROP [3] and Geliosphere 2D [4] models. This task involved an extensive parametric space scan, which was crucial for understanding how different combinations of input parameters could lead to similar modeling outcomes. This analysis was crucial in challenging the prevailing assumptions about the uniqueness of solutions in cosmic ray modulation models.

III. CudaHelioCommander and the Parker Equation Uniqueness

For studying the uniqueness of the Parker Equation Solution, we developed the tool called CudaHelioCommander [5] to address the uniqueness of solutions in cosmic ray modulation within the heliosphere. This desktop application was designed and developed using C#, Windows Presentation Foundation (WPF) and .NET 6.0, and licensed under GPLv3. The tool is also accessible and adaptable for further research and made publicly available in the GitHub repository for the broader scientific audience. It was specifically developed to manage the creation and analysis of models' results libraries. By implementing an easy graphical user interface, CudaHelioCommander also facilitated the execution of simulations which allows efficient interaction with heliospheric computations.

This tool also enabled precise estimation of statistical errors and facilitated the examination of solution uniqueness for 1D B-p model and two publicly available models: SOLARPROP [3] and Geliosphere 2D [4]. The study provided valuable insights into the reliability and accuracy of these models by conducting parametric space scans and comparing results with experimental data from the PAMELA and AMS-02 experiments.

In the context of advancing informatics within cosmic ray research, CudaHelioCommander represents a very good innovation for the scientists in UEF SAV. The tool's development was motivated by the need to enhance the efficiency of handling vast datasets generated by cosmic ray modulation models and to address the challenge of solution uniqueness directly. By enabling researchers to easily manipulate simulation parameters, visualize data through both graphs and heatmaps, and to compare results from different models, CudaHelioCommander has become a great and helpful tool in the exploration of cosmic ray behavior and the validation of theoretical models against observational data. The usefuleness of the tool was acknowledged at the rapporteur talk [6] during the 38th International Cosmic Ray Conference in Nagoya, Japan. This supports the broader goal of refining our understanding of cosmic ray modulation processes and their implications for space weather forecasting and fundamental astrophysics.

IV. Publication and Dissemination

The culmination of these tasks was the preparation and publication of the research findings in a Q1 article in the Computer Physics Communications journal with the impact factor 6.20. This task involved not just the writing of the article but also the synthesis of the research findings into a coherent narrative that could be understood and appreciated by the broader scientific community. The publication of the article contributed to the valuable knowledge to the field and served to share the advancements made in the understanding of cosmic ray modulation in the heliosphere.

V. Next Steps in Cosmic Ray Research

The previous research phase made significant progress in understanding cosmic ray modulation in the heliosphere, particularly highlighting the non-uniqueness of solutions derived from Parker's equation. This finding underscores the complexity of cosmic ray modulation and the need for sophisticated analytical techniques to better navigate and understand the vast parametric space associated with these models. The next phase aims to use the power of neural networks to improve the exploration of this parametric space which offers a more efficient and accurate method for predicting model parameters based on given input conditions.

We formulated following objectives:

- Develop a Neural Network Model: Design and train a neural network capable of predicting cosmic ray intensities and model input parameters within the cosmic ray modulation models that will likely yield results closest to observed data or desired outcomes.
- Select appropriate data to train the model: The labels, in this case, cosmic ray intensities measurements, with the most probable candidate in AMS-02 daily spectra published in [7]. Select appropriate features, in this case, physical parameters of space where modulation takes place, such as solar tilt angle, solar wind velocity, the pressure of solar wind, the intensity of interplanetary magnetic field at 1AU, solar sunspot number, and possibly others, from sources like OMNIweb [8].
- Improve Efficiency of Parametric Space Exploration: Utilize the neural network to navigate the parametric space more efficiently than traditional scanning methods, reducing computational time and resources.
- Validation Against Experimental Data: Validate the neural network's predictions using experimental data from cosmic ray detection experiments like PAMELA or AMS-02.

We will employ following methodology:

- Data Collection and Preprocessing: Compile a comprehensive dataset from existing cosmic ray modulation models and experimental results. This dataset will serve as the training and validation set for the neural network.
- Neural Network Design and Training: Design a neural network architecture suitable for regression analysis of cosmic ray model parameters. The network will be trained using the prepared dataset, with a focus on minimizing prediction error.
- Integration with Cosmic Ray Modulation Models: Develop an interface between the trained neural network and existing cosmic ray modulation models (e.g., SOLARPROP, Geliosphere 2D) to allow for smooth prediction and parameter selection.
- Experimental Validation: Compare the neural network's parameter predictions with actual experimental data to assess accuracy and reliability. Adjustments and retraining will be conducted as necessary based on validation results.

As an expected outcome, we want a fully functional neural network capable of accurately predicting cosmic ray intensities and modulation model parameters. We expect a significant reduction in the time and computational resources required to explore the parametric space of these models. Therefore, we aim to enhance the understanding of cosmic ray modulation predictions and to contribute to the broader field of heliospheric physics.

VI. Conclusion

The preliminary research shows the importance of addressing the uniqueness of the solution and statistical error for models of cosmic ray modulation in the heliosphere. Further research should focus on the evaluation of the ability and precision of machine learning models to predict cosmic ray intensities at 1AU.

References

[1] M. Nguyen, P. Bobik, and J. Genci, "The uniqueness of the parker equation solution," *Proceedings of 38th International Cosmic Ray Conference — PoS(ICRC2023)*, Aug 2023.

[2] V. Mykhailenko, M. Nguyen, M. Solanik, J. Genči, Y. Kolesnyk, and P. Bobik, "Sde method for cosmic rays modulation in the heliosphere statistical error and solution uniqueness," *Computer Physics Communications*, vol. 296, p. 109026, Mar 2024.

[3] R. Kappl, "Solarprop: Charge-sign dependent solar modulation for everyone," *Computer Physics Communications*, vol. 207, p. 386–399, 2016.

[4] M. Solanik, P. Bobík, and J. Genči, "Geliosphere - parallel cpu and gpu based models of cosmic ray modulation in the heliosphere," *Computer Physics Communications*, vol. 291, p. 108847, 2023.

[5] V. Mykhailenko, M. Nguyen, M. Solanik, J. Genči, Y. Kolesnyk, and P. Bobik, "SDE method for cosmic rays modulation in the heliosphere statistical error and solution uniqueness," 2023. [Online]. Available: https://doi.org/10.17632/cptpkwphn4.1

[6] A. Gil, "Rapporteur talk: Sh," *Proceedings of 38th International Cosmic Ray Conference — PoS(ICRC2023)*, Oct 2023.

[7] M. Aguilar, L. A. Cavasonza, G. Ambrosi, L. Arruda, N. Attig, F. Barao, L. Barrin, A. Bartoloni, S. Başeğmez-du Pree, R. Battiston, and et al., "Periodicities in the daily proton fluxes from 2011 to 2019 measured by the alpha magnetic spectrometer on the international space station from 1 to 100gv," *Physical Review Letters*, vol. 127, no. 27, 2021.

[8] NASA, "Interface to produce plots, listings or output files from omni 2." [Online]. Available: https://omniweb.gsfc.nasa.gov/form/dx1.html

Developing Knowledge Graphs

[1]*Jakub Ivan VANKO (3rd year)*
Supervisor: [2]Peter BEDNÁR

[1,2]Dept. of Cybernetics and Artificial Intelligence, FEEI TU of Košice, Slovak Republic

[1]jakub.ivan.vanko@tuke.sk, [2]peter.bednar@tuke.sk

***Abstract*—This article presents a theoretical overview of knowledge graphs and their significance, focusing on the description of general methodology used in their development. The study describes the application of this methodology combined with top-bottom and bottom-up approaches in two main domains - agriculture and collaboration environment.**

***Keywords*— Knowledge graph development, machine learning, ontologies**

I. Introduction

In this age of information abundance, leveraging the immense expanse of data to extract valuable insights and promote efficient knowledge representation has become an urgent quest. Knowledge graphs (KG), which are organized representations of interrelated entities and their relationships, have emerged as effective tools for organizing, retrieving, and analyzing knowledge across multiple domains [1]. The significance of knowledge graphs extends beyond traditional databases, offering a semantic layer that facilitates a more nuanced understanding of information. As the volume and diversity of data continue to grow, the construction of high-quality knowledge graphs becomes a pivotal task, enabling enhanced search capabilities, improved question-answering systems, and more sophisticated recommendation engines. Knowledge graphs are used for a variety of purposes, including search and querying, functioning as a semantic database, and big data analytics.

II. Knowledge graph development

Knowledge graph development has a substantial impact on the performance of AI and ML systems. These structured representations serve as a foundation for algorithms, allowing them to better understand relationships between entities. The end effect is that AI systems make more accurate predictions, classifications, and decisions. Knowledge graph development can be broadly classified into two main types: top-down and bottom-up approaches [2]. The top-down method involves defining the ontology or data schema first and then extracting knowledge based on this predefined structure. In contrast, the bottom-up approach entails extracting knowledge from data and subsequently defining the ontology of the knowledge graph based on the extracted information.

While most researchers focused on state-of-the-art techniques that can be used in the development of knowledge graphs, Tamašauskaitundefined and Groth [3] described a general process that consists of 6 main steps:

1. Data identification – identify a domain of interest, a data source, and a way of data acquisition.
2. Knowledge graph ontology construction – provide a top-level structure for the knowledge graph; this step is needed when the top-down approach is used.
3. Knowledge extraction – extract entities, relations, and attributes from the data. Extraction from semi-structured and unstructured data requires more effort and more complex techniques, such as natural language processing [4].
4. Knowledge processing – ensuring the knowledge is of high quality as expected.
5. Knowledge graph construction – ensuring the accessibility and availability of the graph for use.
6. Knowledge graph maintenance – the knowledge is constantly changing and evolving, it is necessary to monitor and update the knowledge graph as needed.

This process is also shown in Fig. 1.

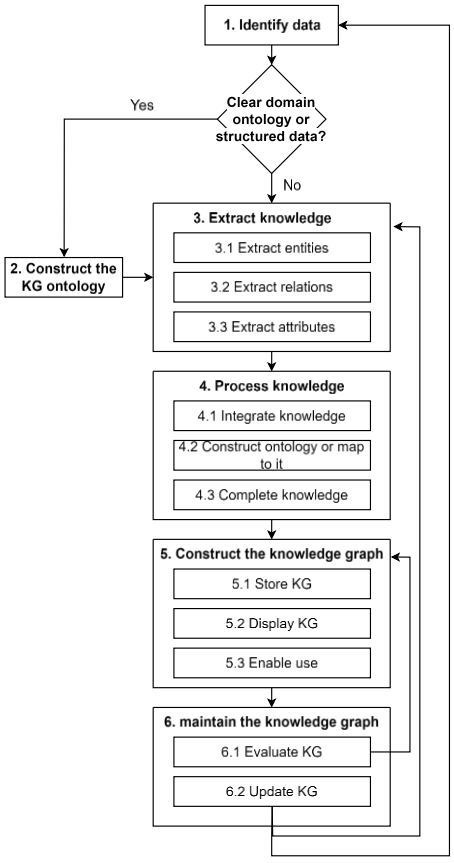

Fig. 1. Knowledge graph development process

III. Current progress

This section provides how we applied the described general methodology for building knowledge graphs in various domains, specifically agriculture and collaborative management.

A. Agriculture knowledge graph

In the past year, we have been participating in a project with the Slovenian company Tomappo [5], which focuses on agriculture and gardening on both a commercial and research level. The main goal was to create a large knowledge graph of plants with crucial information about the process of planting and growing them, including all of the activities that have to be done with the tools needed. This final graph will be used for garden and agriculture planning and for the recommendation system in the application developed by the company. The creation of the knowledge graph was an iterative process of data collection, knowledge extraction, and knowledge processing. At first, we started with the data containing various plants Tomappo provided us, which we used as a base for the taxonomy extraction from the known European and Mediterranean Plant Protection Organization (EPPO) database [6] and Wikidata [7]. In this phase, we also extracted various pests and basic information for each plant, such as names, descriptions, and definitions in different languages. After getting the taxonomy done, we started to collect the data describing planting and caring activities for each plant, including recommended tools for each activity. Most of the relations we extracted were described by the Simple Knowledge Organization System (skos) [8], and the final graph is stored on the SPARQL server. The simplified meta graph describing relations for activities and plants is displayed in Fig. 2.

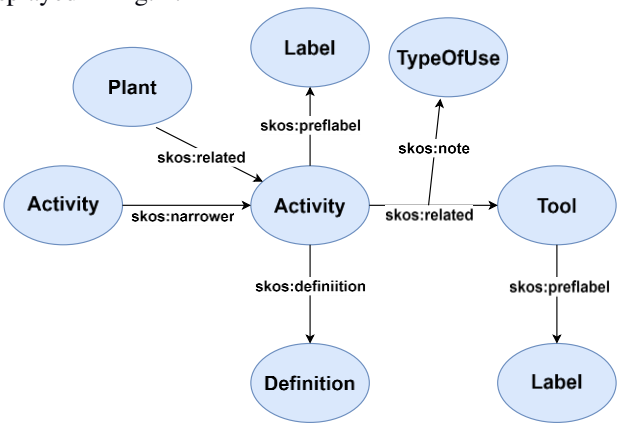

Fig. 2. Meta graph of agricultural KG

B. Collaboration knowledge graph

During the development of the second knowledge graph, we collaborated with the company Ayanza Inc. [9]. They developed an application where teams can design their workflows, organize tasks transparently, and schedule their meeting cycles in a useful way. Ayanza provides us with the data from the beta version of their application. Their goal is to recommend user a document that would be relevant for his work and increase their effectivity. For example, it could show the user the most relevant documents for him depending on the tasks on which he works or suggest a workspace or user to assign for a particular document. These documents contain a lot of important information, usually in text form, so we will need to use natural language processing techniques for their extraction. After investigating the data, we chose to extract 5 types of entities that would help us achieve our goal. These extracted entities reflect ownership of documents, comments, and user affiliation to various important parts of the organization. Since this graph reflects the collaboration of the companies, the time factor is very important, so we also extracted the times of creation of each entity and used it as an attribute, so the recommendation system would recommend only relevant and up-to-date documents and workspaces.

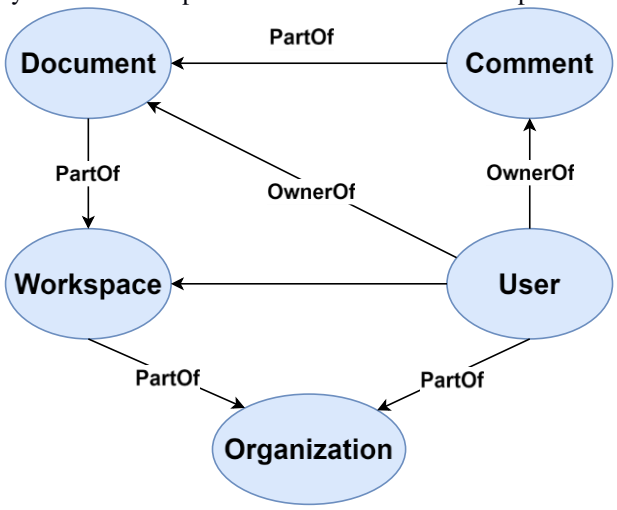

Fig. 3. Meta graph of collaboration KG

IV. Future work

Our focus in the near future is to finish the collaborative knowledge graph by extracting important information from the unstructured text contained in each document. After finishing it, we would like to look at the topic of synthetic knowledge graphs and use them in future experiments since we touched on that topic in one of our research papers already on tabular data [10]. Our main focus in future research will be graph prediction experiments using graph representation learning [11], mostly focusing on link prediction problem [12] in various domains. Due to the popularity of large language models and the fact that our collaborative knowledge graph contains many unstructured natural language data, we would also like to experiment with combining text modality with graph representation for predictive tasks on knowledge graphs. This approach should help us to gain more contextual information in knowledge graphs, which is very important in our research. In the last part, we will evaluate the predictive methods with text modality in various domains of the data we have prepared.

Acknowledgment

This work was supported by the Slovak Research and Development Agency under the contract No. APVV-22-0414 and contract No. APVV-20-0232, and by the Scientific Grant Agency of the Ministry of Education, Research, Development and Youth of the Slovak Republic and the Slovak Academy of Sciences under grant No. 1/0685/21.

References

[1] Yan, J. et al. (2018) ‘A retrospective of knowledge graphs’, Frontiers of Computer Science, 12(1), pp. 55–74. doi: 10.1007/s11704-016-5228-9.

[2] Li, F. et al. (2020) ‘Research on Optimization of Knowledge Graph Construction Flow Chart’, in 2020 IEEE 9th Joint International

Information Technology and Artificial Intelligence Conference (ITAIC), pp. 1386–1390. doi: 10.1109/ITAIC49862.2020.9338900.
[3] Tamašauskaitundefined, G. and Groth, P. (2023) 'Defining a Knowledge Graph Development Process Through a Systematic
[4] Chen, Y., Kuang, J., Cheng, D., Zheng, J., Gao, M., Zhou, A. (2019). AgriKG: An Agricultural Knowledge Graph and Its Applications. In: Li, G., Yang, J., Gama, J., Natwichai, J., Tong, Y. (eds) Database Systems for Advanced Applications. DASFAA 2019. Lecture Notes in Computer Science()
[5] "Tomappo." [Online]. Available: https://tomappo.com/
[6] "European and Mediterranean Plant Protection Organisation." [Online]. Available: https://www.eppo.int/
[7] Vrandečić, D. and Krötzsch, M. (2014) 'Wikidata: a free collaborative knowledgebase', Commun. ACM. New York, NY, USA: Association for Computing Machinery, 57(10), pp. 78–85. doi: 10.1145/2629489.
[8] Introduction to SKOS. W3C. SKOS Simple Knowledge Organization System [online]. 2004, 1.1.2012 [cit. 2013-05-26]. Available: http://www.w3.org/2004/02/skos/intro#main
[9] "Ayanza." [Online]. Available: https://ayanza.com/
[10] Lohaj, O., Paralič, J., Kushnir, D., Vanko, J. I.: Usability of a synthetically generated dataset for decision support. 2024 IEEE 22nd World Symposium on Applied Machine Intelligence and Informatics (SAMI), Stará Lesná, Slovakia, 2024, pp. 000435-000440, doi: 10.1109/SAMI60510.2024.10432913.
[11] Graph Representation Learning / Jakub Ivan Vanko Spôsob prístupu: http://scyr.kpi.fei.tuke.sk/wp-content/scyr-files/proceedings/SCYR_2023_Proceedings.pdf... - 2023. In: 23rd Scientific Conference of Young Researchers : proceedings from conference. - Košice (Slovensko) : Technická univerzita v Košiciach s. 90-92 . - ISBN 978-80-553-4377-8
[12] Link prediction in knowledge graphs / Jakub Ivan Vanko Spôsob prístupu: http://scyr.kpi.fei.tuke.sk/wp-content/scyr-files/proceedings/SCYR_2022_Proceedings.pdf... - 2022. In: 22nd Scientific Conference of Young Researchers : proceedings from conference. - Košice (Slovensko) : Technická univerzita v Košiciach s. 52-55 [CD-ROM, print]. - ISBN 978-80-553-4061-6

Biometric-Enhanced Authentication using OPAQUE Protocol: Keystroke Dynamics and EMG Signals

[1]*Eva Kupcová (1st year),*
Supervisor: [2]*Matúš Pleva*

[1,2]Dept. of Electronics and Multimedia Telecommunications, FEI TU of Košice, Slovak Republic

[1]eva.kupcova@tuke.sk, [2]matus.pleva@tuke.sk

***Abstract*—In today's rapidly evolving digital security landscape, robust authentication methods are crucial for safeguarding sensitive information. The Oblivious Password Authenticated Key Exchange (OPAQUE) protocol stands out as a reliable solution, offering strong protection against diverse cyber threats. Yet, the integration of biometric factors has become a focus for enhanced security and user convenience. This study delves into combining keystroke dynamics and electromyography (EMG) biometrics with the OPAQUE protocol, creating a robust biometric-enhanced authentication framework. Keystroke dynamics capture unique typing patterns, while EMG signals detect muscle movements, enriching user identification. In this article, we describe a theoretical analysis that underscores the benefits of merging the OPAQUE protocol with biometrics and provide a current overview of the issue of OPAQUE protocol and biometric authentication, aiming to advance secure and user-friendly authentication in digital domains.**

***Keywords*—authentication, biometric, EMG signals, keystroke dynamics, OPAQUE protocol**

I. Introduction

The privacy and security of personal data is currently a challenge, as it is still more of our data is stored online. Authentication is one of the fundamental methods to ensure the confidentiality and availability of data to the legitimate user. For this reason, care must be taken to securely authenticate and encrypt all communications forwarded between client and server. Traditional authentication methods reliant solely on passwords have proven susceptible to various security threats, including brute-force attacks, dictionary attacks [1], and rainbow table attacks [2]. Consequently, there has been a growing emphasis on developing more secure and user-friendly authentication solutions.

The OPAQUE (Oblivious Password Authenticated Key Exchange) protocol [3] has emerged as a promising cryptographic primitive for password-based authentication (PBA) [4], offering strong security guarantees without revealing users' passwords to the server or adversaries. By leveraging secure cryptographic techniques, the OPAQUE protocol ensures that user authentication occurs securely even in the presence of a compromised server. However, as the threat landscape continues to evolve, there is a recognized need to augment PBA with additional factors to enhance security and user experience [3].

Biometric authentication (BA) [5], which utilizes unique physiological or behavioral characteristics of individuals, presents a compelling approach to address the limitations of traditional password-based systems. Keystroke dynamics (KD), which captures users' unique typing patterns, and electromyography (EMG) biometrics [6], which senses muscle movements, are two promising biometric modalities for authentication. Integrating these biometric features with the OPAQUE protocol offers the potential to create a robust authentication system.

In our research, we emphasize the advantages of integrating the OPAQUE protocol with biometrics, providing an overview of both the OPAQUE protocol itself and the existing biometric systems and authentication methods. Specifically, we delve into the advantages of utilizing KD and EMG signals for authentication. Additionally, we review related work that addresses the KD and EMG signals for authentication process and the integration of BA into authentication protocols. Finally, we elucidate the rationale behind integrating BA into the OPAQUE protocol and articulate its intended purpose.

II. OPAQUE protocol

The name of the OPAQUE protocol originated from the combination of OPRF (Oblivious Pseudorandom Function) [7] and PAKE [8]. The protocol is relatively new, with the first proposal being published in October 2018 [3].

The OPAQUE protocol belongs to the Password Authenticated Key Exchange (PAKE) protocol family [8], which means that the user is authenticated based on a password, and after successful authentication, a shared cryptographic key is established between the client and server. OPAQUE is the first PAKE protocol that allows the addition of salt to the hashed password value without disclosing the salt to the client. This property makes the OPAQUE protocol secure against attacks with precomputed tables. The protocol hides the password from the server even during the registration phase, ensuring that the password remains safe on the client side, while the randomly generated salt added to the hashed password value remains only on the server side. The use of the protocol increases the difficulty of offline dictionary attacks by implementing iterated password hashing. The protocol allows the transformation of any suitable authenticated key exchange (AKE) protocol into a secure aPAKE protocol. The protocol is designed to be modular, allowing integration with other AKE protocols such as TLS or protocols based on post-quantum principles. In addition to the fact that OPAQUE can be built on top of different AKE protocols, it works with any password hashing function. Another advantage is that password hashing is performed on the client, thus reducing the load on the server [3].

III. Biometric Authentication

BA has gained considerable traction in recent years, spurred by advancements in sensor technology, machine learning algorithms, and the growing need for secure yet user-friendly authentication solutions. BA is divided into two main categories based on the characteristics of the user: physiological properties, which cover the visible parts of the human body such as the fingerprint, retina, and iris, and behavioural properties, which analyze the behaviour of a user through user profiling, gait, mouse dynamics, KD, EMG, and more [9].

Traditional biometric characteristics such as fingerprints, iris scans, and facial recognition have seen widespread adoption in various applications, from smartphone unlocking to border control or airport control. However, these modalities are not without their limitations because are bodily information without liveness that can be forged raising security concerns. Fingerprint scanners can be susceptible to spoofing attacks using artificial replicas (using 3D printers), while facial recognition systems may struggle with accuracy in varying lighting conditions or with individuals wearing masks. Furthermore, due to worries regarding privacy and data security, there is a growing demand for alternative authentication methods that reduce the gathering and retention of sensitive biometric data [10].

KD and biosignals, offer a compelling alternative, leveraging the unique characteristics of human behaviour and physiology to enhance security while addressing some of the limitations of traditional biometric modalities. Examples of biosignals include EMG, electrocardiogram (ECG), and electroencephalogram (EEG) signals but in this article, our attention will remain solely on EMG signals. In addition, KD and EMG are liveness, thereby having strong security advantages as they cannot be forged and falsified. KD, for example, are inherently tied to an individual's typing habits, making them difficult to replicate or impersonate. Similarly, EMG signal represents a signal obtained in the form of a voltage value by measuring a microcurrent generated whenever there is a muscle contraction. Advantage is that EMG signal is distinctive and cannot be reproduced externally.

A. Keystroke dynamics

Typing biometrics, also known as KD, is the field of biometrics that studies the way a user interacts with a keyboard. This is a relatively new area of interest in terms of security, especially in user authentication, due to its various advantages. The first advantage is that KD have a low implementation cost, and no additional hardware is required in the authentication process. The second advantage is that it has a simpler implementation compared to other BA methods, as the collection of typing data is relatively simple and does not require special permission from the user [11].

KD is an authentication method that verifies the rhythm of a user's typing to grant access to a system. It relies entirely on timing information of key presses and releases. When a keystroke is pressed, three timing atomic events occur: the key down event, key up event, and key press event. The key down event occurs when the key is depressed, the key up event occurs when it is released, and the key press event is fired when an actual character is being inserted. These events are used to extract characters divided into two groups: global and individual [12].

1) Global Character Extraction: Global character extraction involves analyzing typing patterns across a large user population or dataset. In this approach, characters are extracted and analyzed in aggregate, considering common trends and patterns observed among multiple users. It aims to identify general characteristics and statistical measures of typing behavior that apply widely across a population of users. Global character extraction is useful for developing generalized models for KD authentication applicable to a wide range of users. Some examples of global characteristics in KD analysis are: Error Rate, Letter Deletion, Shift Key usage, Control Key Usage, Alt Key Usage and General Typing Speed [13].

2) Individual Character Extraction: Individual character extraction focuses on analyzing the typing patterns of specific users on an individual basis. Characters are extracted and analyzed for each user separately, considering their unique typing behaviors and characteristics which can be extracted. The aim is to create personalized typing profiles for individual users based on their distinct KD. Individual character extraction enables the development of personalized authentication models tailored to the specific typing patterns of each user [13].

KD are captured through various features extracted from the user's typing rhythm, including latency between consecutive keystroke, flight time, and dwell time based on the key down, press, and up events. Other features such as overall typing speed, frequency of errors, and control key usage are also considered. Features are extracted based on di-graph, tri-graph, or n-graph segments of the entire text. In these segments, latencies, intervals, and flight times are measured for each sequence of keystroke [12].

B. EMG signals

EMG signals, which measure the electrical activity of muscles, have emerged as a promising tool for authentication purposes. EMG signals offer a unique approach to authentication by harnessing the distinct muscle activation patterns of individuals. This biological uniqueness provides a robust foundation for identity verification, potentially surpassing traditional authentication methods in reliability and security [14].

One significant advantage of EMG authentication lies in its non-intrusive nature. Unlike other biometric modalities that may require specialized hardware or physical contact, EMG signals can be seamlessly integrated into existing systems without disrupting user experience. This inherent ease of implementation makes EMG authentication an attractive option for a wide range of applications, from mobile devices and computers to wearable technology and Internet of Things (IoT) devices [14].

Furthermore, EMG authentication offers the potential for continuous verification. By continuously monitoring and analyzing the user's muscle activity patterns in real-time, systems can dynamically verify the user's identity throughout their interaction. This continuous authentication approach enhances security by adapting to changes in user behavior and detecting unauthorized access attempts promptly [15].

As research in EMG-based authentication continues to advance, the potential for its integration into various security-critical applications becomes increasingly apparent. With its combination of reliability, security, and versatility, EMG authentication is poised to play a significant role in shaping the future of BA technologies.

C. Advantages of Biometric Authentication

BA offers several advantages over traditional password-based methods. It provides a more secure and convenient way to verify user identity, eliminating the need for users to remember complex passwords or carry physical tokens. Biometrics are inherently tied to the individual and are difficult to replicate, reducing the risk of unauthorized access and identity theft. Additionally, BA enhances user experience by streamlining the authentication process and reducing friction in accessing digital resources. The table I provides several comparisons between BA and PBA [16].

TABLE I
COMPARISON OF BIOMETRIC AUTHENTICATION AND PASSWORD-BASED AUTHENTICATION

Biometric Authentication
• High Security: Biometric traits are unique to individuals. • Convenience: Eliminates the need for complex passwords. • Reduced Fraud: Difficult to forge or replicate biometric traits. • Improved User Experience: Streamlines authentication process. • Reliability: Tied to individual and difficult to forget. • Scalability: Can accommodate large user populations.
Password-Based Authentication
• Vulnerable to Theft: Passwords can be stolen or forgotten. • Management Burden: Users must remember and update passwords. • Susceptible to Guessing: Weak passwords can be easily guessed. • Lack of Uniqueness: Users may reuse passwords across accounts. • Increased Friction: Authentication process may be cumbersome. • Limited Scalability: Complex passwords can be challenging to manage at scale.

IV. RELATED WORK

This section is dedicated to related work in biometric security research, specifically focusing on authentication using KD and EMG signals. Below is a compilation of works that address, at least in part, the topics discussed in this article.

- *Developing a Keystroke Biometric System for Continual Authentication of Computer Users* [17] - The focus of this work is on fast intruder detection, the authentication process works on short bursts of about a minute of keystroke, while the training process can be extensive and take hours of input. The biometric system consists of components for data capture, feature extraction, authentication classification, and receiver operating characteristic curve generation. They were able to extract the statistical properties of keystroke durations and digraph transition times and achieve very high verification accuracy based on distance measurement (99% on 14 subjects, 96% on 30 subjects).
- *Biometric User Identification by Forearm EMG Analysis* [18] - This research underscores the effectiveness of EMG sensor-based devices for user authentication, highlighting their potential in cybersecurity. The results presented in this article show the potential of EMG based controllers, in particular the Myo armband, to identify a computer system user. In the first scenario, training classifiers with 25 keyboard typing movements and testing with 75, a 1-dimnesional convolutional neural network achieves 93% accuracy using only Myo armband EMG data. With 75 movements for training and cross-validation, accuracy improves to 96.45%. However, concerns over their availability and the need for user feedback integration remain significant considerations for future research.
- *EMG Data Collection for Multimodal Keystroke Analysis* [19] - This work introduce a data collection procedure and accompanying software tool, known as Myo record, designed to gather multimodal data during keyboard typing. This encompasses EMG and inertial measurement unit data captured from Myo armbands, along with keyboard timing, audio, and video recordings.
- *Electromyograph and Keystroke Dynamics for Spoof-Resistant Biometric Authentication* [20] - This work introduces the use of EMG signals and key press timings as novel biometric signatures, proposing them as alternatives to conventional biometric modalities like face, iris, and fingerprint recognition. Through experiments utilizing subspace modeling and Bayesian classifiers, promising verification rates are achieved, highlighting the potential of EMG signals and key press timings for user-specific BA.
- *Personal Authentication and Hand Motion Recognition based on Wrist EMG Analysis by a Convolutional Neural Network* [21] - This work presents a system utilizing wrist EMG for simultaneous hand motion recognition and personal authentication. Using eight dry sensors, EMG signals were measured during Japanese Janken motions, preprocessed to remove noise, and features extracted using CNN before identification via a full connection layer. Achieving 94.6% accuracy in hand motion recognition and 95.0% accuracy in personal authentication, the proposed method demonstrates promising performance in dual-function biometric systems.
- *Comparing Natural and Strong Typing Behavior for Keystroke Dynamics Multimodal Database Collection* [22] - The paper indicates no significant advantage in incorporating strong typing behavior in Multimodal KD Analysis, though EMG sensory identification demonstrates benefits with natural typing behavior. Consequently, resource allocation for future research will focus exclusively on natural typing behavior, informing methodology for recording Multimodal KD in subsequent studies involving 50–100 subjects.
- *A study of an EMG-based authentication algorithm using an Artificial Neural Network* [15] - This work proposes a user authentication method based on EMG signals, with analysis revealing an 81.6% accuracy rate using artificial neural networks (ANN) for individual authentication. The findings suggest the potential commercialization of this high-security personal certification technology, enabled by wearable EMG detection devices and the ANN algorithm for simplified personal authentication.
- *Biometric Knowledge Extraction for Multi-factor Authentication and Key Exchange* [23] - This work presents a robust biometrics-based protocol for authenticated key exchange (B-AKE) that ensures strong, multi-factor, and mutual authentication. The protocol utilizes the Diffie-Hellman key agreement to establish a symmetric encryption key, derived from shared knowledge extracted

from biometric sensors, providing forward secrecy and safeguarding user credentials without revealing sensitive information to potential imposters or observers.

V. Potential for Enhancing Digital Security

The integration of BA with the OPAQUE protocol presents a promising avenue for enhancing digital security and usability. By incorporating KD and EMG biometrics alongside PBA, the protocol offers an additional security layer while ensuring user privacy and streamlining the authentication process.

By merging these three technologies, we aim to achieve enhanced user authentication security and also improve resilience against various types of attacks. Additionally, we want to leverage the property of the OPAQUE protocol, which ensures that authentication data is not sent in plain text over the network. This feature is crucial for biometric data, as each individual has a finite amount of such data, and they remain almost unchanged throughout life.

For the reasons mentioned, we would like to explore possibilities for expanding the implementation of the OPAQUE protocol, a cryptographic protocol for PAKE, enhanced with additional biometric verification. We plan to investigate the integration of KD and EMG signal scanning to reinforce the protocol against potential security breaches. Subsequently, we intend to conduct real-world tests to validate the effectiveness of the proposed implementation. Our overarching goal is to enhance the security of user authentication and mitigate unauthorized access to sensitive data. We aspire to design a novel authentication method more resilient to evolving cyber threats.

VI. Conclusion

This article has illuminated the potential of combining KD and EMG biometrics with the OPAQUE protocol to create a robust biometric-enhanced authentication framework. Our theoretical analysis underscores the advantages of merging these technologies, showcasing the promise of enhanced security and user convenience in digital authentication.

As we traverse the rapidly evolving digital security landscape, the integration of biometric factors has proven to be a pivotal step towards fortifying authentication methods. The synergy of OPAQUE with KD and EMG signals presents a formidable defence against cyber threats, offering a multifaceted approach to user identification.

Acknowledgment

The research in this paper was partially supported by the Ministry of Education, Research, Development and Youth of the Slovak Republic under the research project VEGA 2/0165/21, the Cultural and Educational Grant Agency of the Slovak Republic project number KEGA 049TUKE-4/2024, and by the Slovak Research and Development Agency under the projects APVV-22-0414 & APVV-22-0261.

References

[1] L. Bošnjak, J. Sreš, and B. Brumen, "Brute-force and dictionary attack on hashed real-world passwords," in *2018 41st international convention on information and communication technology, electronics and microelectronics (mipro)*. IEEE, 2018, pp. 1161–1166.

[2] L. Zhang, C. Tan, and F. Yu, "An improved rainbow table attack for long passwords," *Procedia Computer Science*, vol. 107, pp. 47–52, 2017. [Online]. Available: https://www.sciencedirect.com/science/article/pii/S1877050917303290

[3] S. Jarecki, H. Krawczyk, and J. Xu, "Opaque: an asymmetric pake protocol secure against pre-computation attacks," in *Advances in Cryptology–EUROCRYPT 2018: 37th Annual International Conference on the Theory and Applications of Cryptographic Techniques, Tel Aviv, Israel, April 29-May 3, 2018 Proceedings, Part III 37*. Springer, 2018, pp. 456–486.

[4] A. Conklin, G. Dietrich, and D. Walz, "Password-based authentication: a system perspective," in *37th Annual Hawaii International Conference on System Sciences, 2004. Proceedings of the*, 2004, pp. 10 pp.–.

[5] K. Dharavath, F. A. Talukdar, and R. H. Laskar, "Study on biometric authentication systems, challenges and future trends: A review," in *2013 IEEE International Conference on Computational Intelligence and Computing Research*, 2013, pp. 1–7.

[6] Y.-H. Byeon, S.-B. Pan, and K.-C. Kwak, "Biometrics and healthcare system using emg and ecg signals," in *2022 7th International Conference on Mechanical Engineering and Robotics Research (ICMERR)*. IEEE, 2022, pp. 196–200.

[7] A. Davidson, A. Faz-Hernandez, N. Sullivan, and C. A. Wood, "Oblivious Pseudorandom Functions (OPRFs) Using Prime-Order Groups," RFC 9497, Dec. 2023. [Online]. Available: https://www.rfc-editor.org/info/rfc9497

[8] J.-M. Schmidt, "Requirements for Password-Authenticated Key Agreement (PAKE) Schemes," RFC 8125, Apr. 2017. [Online]. Available: https://www.rfc-editor.org/info/rfc8125

[9] I. Alsaadi, "Physiological biometric authentication systems, advantages, disadvantages and future development: A review," *International Journal of Scientific Technology Research*, vol. Volume 4, 12 2015.

[10] M. Pleva, *Biometric security systems*. University Textbooks, Technical University of Košice, 2021. [Online]. Available: http://biometria.web.tuke.sk/BSB-ucebnica.pdf

[11] N. Raul, R. Shankarmani, and P. Joshi, "A comprehensive review of keystroke dynamics-based authentication mechanism," in *International Conference on Innovative Computing and Communications*. Singapore: Springer Singapore, 2020, pp. 149–162.

[12] P. R. Dholi and K. P. Chaudhari, *Typing Pattern Recognition Using Keystroke Dynamics*. Berlin, Heidelberg: Springer Berlin Heidelberg, 2013.

[13] H. K. Kasprowski P, Borowska Z, "Biometric identification based on keystroke dynamics," *Sensors (Basel)*, 2022. [Online]. Available: https://www.ncbi.nlm.nih.gov/pmc/articles/PMC9105156/

[14] A. N.-A. Noureddine Belgacem, Régis Fournier and F. Bereksi-Reguig, "A novel biometric authentication approach using ecg and emg signals," *Journal of Medical Engineering & Technology*, vol. 39, no. 4, pp. 226–238, 2015. [Online]. Available: https://doi.org/10.3109/03091902.2015.1021429

[15] S. Shin, J. Jung, and Y. T. Kim, "A study of an emg-based authentication algorithm using an artificial neural network," in *2017 IEEE SENSORS*, 2017, pp. 1–3.

[16] A. Ezugwu, E. Ukwandu, C. Ugwu, M. Ezema, C. Olebara, J. Ndunagu, L. Ofusori, and U. Ome, "Password-based authentication and the experiences of end users," in *Scientific African*, vol. 21. Elsevier, 2023, p. e01743.

[17] J. V. Monaco, N. Bakelman, S.-H. Cha, and C. C. Tappert, "Developing a keystroke biometric system for continual authentication of computer users," in *2012 European Intelligence and Security Informatics Conference*, 2012, pp. 210–216.

[18] M. Pleva, S. Korecko, D. Hladek, P. Bours, M. H. Skudal, and Y.-F. Liao, "Biometric user identification by forearm emg analysis," in *2022 IEEE International Conference on Consumer Electronics - Taiwan*, 2022, pp. 607–608.

[19] S. Korecko, M. Haluska, M. Pleva, M. H. Skudal, and P. Bours, "Emg data collection for multimodal keystroke analysis," in *2022 12th International Conference on Advanced Computer Information Technologies (ACIT)*, 2022, pp. 351–355.

[20] S. Venugopalan, F. Juefei-Xu, B. Cowley, and M. Savvides, "Electromyograph and keystroke dynamics for spoof-resistant biometric authentication," in *2015 IEEE Conference on Computer Vision and Pattern Recognition Workshops (CVPRW)*, 2015, pp. 109–118.

[21] R. Shioji, S.-i. Ito, M. Ito, and M. Fukumi, "Personal authentication and hand motion recognition based on wrist emg analysis by a convolutional neural network," in *2018 IEEE International Conference on Internet of Things and Intelligence System (IOTAIS)*, 2018, pp. 184–188.

[22] M. H. Skudal, M. Pleva, S. Korecko, P. Bours, and D. Hladek, "Comparing natural and strong typing behavior for keystroke dynamics multimodal database collection: Poster," in *Norsk IKT-konferanse for forskning og utdanning*, no. 3, 2021.

[23] P. H. Griffin, "Biometric knowledge extraction for multi-factor authentication and key exchange," *Procedia Computer Science*, vol. 61, pp. 66–71, 2015, complex Adaptive Systems San Jose, CA November 2-4, 2015. [Online]. Available: https://www.sciencedirect.com/science/article/pii/S1877050915029804

Use of WAM systems to determine the ampacity of overhead transmission lines

[1]*František MARGITA(1st year)*
Supervisor: [2]Ľubomír BEŇA

[1,2]Dept. of Electric Power Engineering, FEI TU of Košice, Slovak Republic

[1]frantisek.margita@tuke.sk, [2]lubomir.bena@tuke.sk

***Abstract*—The growing demand for electrical energy requires increased capacities not only in the installed power of energy sources but also in the transmission capabilities of electrical grids. Expanding the transmission capacities of electrical grids through the construction of new lines is a time-consuming and financially costly process. Grid operators strive to utilize existing transmission capacities of lines as efficiently as possible. The growing trend in WAMS (Wide-Area Measurement Systems) technology enables achieving the maximum potential ampacity of lines. The publication provides a brief overview of the thermal evaluation of overhead transmission lines. The article describes the methodologies of CIGRE 601 (International Council on Large Electrical Systems) and IEEE-738 (Institute of Electrical and Electronics Engineers), which deal with standards and algorithms for estimating ampacity and conductor temperature. The paper summarizes the resolved steady-state ampacity and offers a perspective on transient dynamic ampacity.**

***Keywords*—ampacity, CIGRE 601, PMU, thermal rating, WAMS.**

I. Introduction

The ampacity of overhead transmission lines is defined as the maximum electrical current that the line can carry without causing a reduction in its electrical and mechanical properties. The most used conductors for overhead transmission lines are ACSR (Aluminum Conductor Steel Reinforced), where the conducting layer is made of aluminum. Manufacturers of these wires specify their maximum operating temperature in the range of 90 to 110 °C. If this temperature is exceeded for an extended period, the material becomes more brittle, leading to a reduction in its lifespan [1], [2].

The ampacity of overhead transmission lines must also not exceed its elongation or maximum sag, which, if exceeded, would violate the minimum safe distances from the ground, objects, or other conductors under the overhead lines. To ensure in practice that the material strength of the electrical conductor is not compromised, nominal values are assigned to transmission lines during the design process, i.e., limits for energy transmission. The minimum safe height of the conductors is determined by standards for various types of environments, which are designed for the most critical circumstances and with a high level of reliability [2]. The factors influencing the ampacity of the conductor are described in Fig. 1. [3].

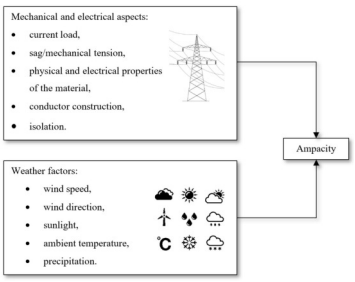

Fig. 1. Factors affecting conductor ampacity

II. Thermal evaluation of overhead electrical conductors

A. Categorization of thermal rating

Ampacity determination is carried out through thermal evaluation, which is categorized as follows [4]:

- static ampacity (probabilistic approach, static thermal rating, STR)
- dynamic ampacity (deterministic approach, dynamic thermal rating, DTR):
  - direct methods,
  - indirect methods.

The ampacity of long lines is often defined by stability limits or voltage constraints, whereas the ampacity of short lines is determined by temperature limitations [4].

B. Static thermal rating

In STR, electrical grids are operated under the assumption that their conductors have a constant ampacity, which remains the same for every hour of the day, any day of the year, or season. Regions with numerous overhead lines are considered to have uniform meteorological conditions. STR provides a conservative estimate based on assumptions of weak convective cooling due to wind, high air temperatures, and solar radiation, where the calculation is theoretical rather than based on actual ampacity [5].

STR is calculated using a thermal model of the bare conductor's heat balance, low perpendicular wind speed (e.g., 0.5 m/s), seasonal air temperature close to the peak (e.g., 35 °C or higher in summer), and full solar heating (e.g., 1000 W/m2), as described in CIGRE Technical Brochure 299 [6].

Meteorological conditions used for STR assessment vary depending on the environmental characteristics of the region

and the risk tolerance of energy systems. Each transmission line may have several types of STR assessment, including normal rating (or continuous), long-term emergency rating, and short-term emergency rating [7].

C. Dynamic line rating

DTR is the ability to dynamically adjust ampacity in real-time in response to changing environmental conditions. The goal is to maximize current loading at any given moment. The thermal ampacity of overhead lines can be influenced by both heating and cooling, resulting in fluctuations in performance either upward or downward. The ampacity of the conductor increases when it is cooled by the wind or when the ambient temperature decreases, allowing for greater power transmission through the line [3].

In most situations, a very small increase in thermal rating (5% to 20%) above the static rating is sufficient to rectify operational problems in the system. As a result, DTR provides system operators with a rapidly deployable and cost-effective technique for increasing line ratings, which can be applied without the need for additional physical equipment or the shutdown of critical lines [3].

D. Dynamic ampacity with indirect methods

DTR considers that the ampacity of transmission lines dynamically changes depending on environmental conditions. Environmental conditions include all climatic factors such as [1], [3], [4]:

- ambient temperature,
- wind speed and direction,
- solar radiation intensity,
- precipitation.

The rating of the line is calculated indirectly using meteorological data recorded or forecasted along the transmission line. This method is also known as weather-dependent line rating. Meteorological data, whether measured or predicted, are considered primary inputs into weather-dependent line rating systems. Weather sensors can be placed along the transmission line to gather weather data for implementing DTR. Evaluating the conductor's thermal balance equation is the primary basis for weather-dependent line rating calculations [4].

E. Dynamic ampacity with direct methods

Calculation of line ampacity in real-time can be assessed similarly through line attributes, such as [3]:

- line loading,
- conductor sag,
- conductor-to-ground clearance,
- spacing between conductors,
- mechanical tension of the line,
- conductor temperature.

The direct method of DTR is based on directly measuring properties of the electrical conductor, such as conductor temperature, mechanical tension of the line, and conductor sag. Line assessment is typically calculated using additional data from a weather monitoring system. Concurrently, several approaches have been discussed for estimating DTR of overhead transmission lines [4].

F. Potential utilization of dynamic ampacity

There are various commercial methods available for determining dynamic ratings of electrical conductors. These methods may be based on [2]:

- weather monitoring,
- phasor measurements of voltage and current,
- conductor temperature measurements.

The use of dynamic ratings for electrical conductors can bring benefits such as time and cost savings, as existing electrical lines would be utilized more efficiently. Additionally, it can help avoid the need for new construction of electrical lines and unnecessary over-sizing. [2]. Furthermore, it offers opportunities to reduce transmission line overload, enable the integration of wind energy, and enhance the reliability of the power system [4], [8], [9]. DTR can predict energy transmission ampacity, which can assist with overall system planning [3].

Limited ampacity of transmission lines causes numerous negative impacts on the power system as well as on end consumers. This includes delayed integration of renewable energy sources and operation of the system in a less economical or less reliable manner [9].

There are several grid reconstruction solutions aimed at increasing the ampacity of overhead lines. These may include [9]:

1. reconstruction of overhead lines to higher voltage,
2. replacement of existing conductors with larger cross-sectional area conductors and special conductors (compact conductors, high-temperature conductors),
3. increasing the grid voltage level with reduced phase-to-phase distances (compact lines),
4. installation of compensation devices,
5. construction of new substations,
6. utilization of control devices.

All these enhancements and modernizations of transmission lines involve lengthy processes and significant investments, as summarized in Fig. 2. Utilizing load current optimization considering climatic conditions is a cost-effective solution for increasing line ampacity [9].

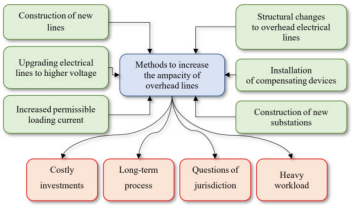

Fig. 2. The schematic diagram of possible measures for optimizing the permissible load current

III. THERMAL BALANCES OF OVERHEAD ELECTRICAL TRANSMISSION LINES AS SUGGESTED BY STANDARDS

CIGRE and IEEE address standards that explain algorithms for estimating conductor ampacity and temperature [11].

IEEE created the IEEE-738 standards for DTR, and CIGRE developed various recommendations and approaches for DTR, such as Technical Brochure 601. Additionally, research communities have made efforts not only to improve DTR technology but also to address regulatory problems to effectively utilize the ampacity of existing overhead transmission lines [12].

Both techniques (CIGRE and IEEE) are based on the thermal balance of heat gained and lost in the conductor, according to the load and environmental factors [11].

The first CIGRE method calculates the conductor temperature using steady-state conditions according to equation (1), whereas the second method estimates its temperature using dynamic equilibrium (equation (2)), which considers the thermal inertia of the conductor. In steady-state conditions, the basic thermal balance is defined as [11]:

$$P_t + P_r = P_S + P_j + P_m, \tag{1}$$

where

- P_c represents cooling due to convection (W/m),
- P_r represents cooling due to radiation to the surroundings (W/m),
- P_S represents heating due to solar radiation (W/m),
- P_j represents heating due to Joule effect (W/m),
- P_m represents heating due to magnetic effect (W/m).

If the thermal inertia of the conductor is considered, the following dynamic thermal balance is applied instead of equation (1) [11]:

$$m \cdot c \cdot \frac{\mathrm{d}T_c}{\mathrm{d}t} = P_s + P_j + P_m - P_c - P_r, \tag{2}$$

where

- m is the mass per unit length of the conductor (kg/m),
- c is the specific heat capacity of the conductor (J/(kg·K)),
- T_c is the temperature of the conductor (°C).

The equation for the steady-state thermal balance in IEEE 738 standard is represented by [13]:

$$P_r + P_c = P_S + P_J, \tag{3}$$

where [13]

- P_r represents cooling due to radiation to the surroundings (W/m),
- P_c represents cooling due to convection (W/m),
- P_S represents heating due to solar radiation (W/m),
- P_J represents heating due to Joule effect (W/m).

Accordingly, the thermal balance equation (3) of the IEEE 738 manual can be graphically depicted as shown in Fig. 3. [13].

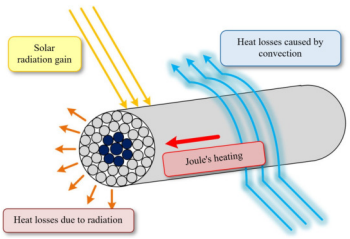

Fig. 3. Thermal balance of an overhead conductor according to IEEE 738

IV. Monitoring Operational Parameters Using WAMS

The increase in electricity consumption and the restructuring of the energy system have brought new challenges for the operation, management, and monitoring of energy systems. The Supervisory Control and Data Acquisition (SCADA) system alone is insufficient to ensure the security and stability of the energy system. SCADA often cannot measure data from all buses simultaneously. Additionally, the sampling frequency in this system is not sufficient for some energy system applications. Therefore, the information obtained from SCADA does not accurately represent the dynamics of the energy system [14], [15].

Developing measurement system technologies enable energy systems to independently analyze their transmission capabilities. This suggests a perspective in which these elements can dynamically adapt to meet the desired energy transfer, possibly utilizing WAMS for optimal performance. Consequently, these advancements affect overhead transmission lines, particularly in regulating conductor temperatures or line ampacity, thereby facilitating the development of more flexible and efficient energy transmission methods [16].

To enhance energy system monitoring, the development of WAMS has addressed the limitations of SCADA systems. Phasor measurement units (PMUs) constitute the core of WAMS, encompassing three essential processes: data acquisition, transmission, and analysis. WAMS receives data through high-speed communication channels, facilitating decision-making processes aimed at improving system performance subsequent to data processing and extraction of pertinent information [14].

PMUs constitute the primary components of WAMS, capable of measuring voltage and current phasors with high precision (error less than 0.1%) and at high speeds (up to 60 samples per second). PMUs employ GPS (Global Positioning System) for synchronizing measured data. With a sufficient number of PMUs installed across different buses, the system becomes observable, enabling the system operator to estimate the real-time state of the system. Consequently, one of the strategic challenges is to determine the optimal quantity and placement of PMUs to reflect a fully observable system whereas being economically viable and practically deployable [17].

V. Summary of Solved and Unsolved Problems

Currently, the steady-state dynamic approach to ampacity is being examined through PMU units in real-time, utilizing additional weather data.

This methodology was applied to study real transmission lines. The conductor examined in this study is the widely used 352-AL1/59-ST1A conductor in Slovakia. The data analyzed in this study were provided by the transmission system operator SEPS (Slovenská elektrizačná prenosová sústava). The data were obtained from two phasor measurement units (PMUs) - PMU No. 1 was located at the RSOB-V427-PMU1 substation (Rimavská Sobota), and PMU No. 2 at the MOLD-V427-PMU1 substation (Moldava nad Bodvou). These PMUs were synchronized with GPS and sampled phase voltages and currents at a frequency of 1 sample per second. The data were obtained on November 25, 2021. The conductor temperature was monitored using knowledge from the electrical model of the overhead transmission line.

The steady-state dynamic ampacity of the conductor was calculated in accordance with the standards outlined in the CIGRE 601 manual [18], [19], [20].

Whereas

1. Fig. 4. depicts the dynamics of conductor temperature in response to changes in weather conditions,
2. Fig. 5. shows the ampacity of the conductor over time considering changing meteorological conditions,

3. Fig. 6. illustrates the current percentage of line loading under present meteorological conditions.

The upcoming research will focus on a method of transient dynamic thermal rating in real-time, which will adapt to the changing parameters of the conductor. This research directly relates to the significance and utilization of HTLS (High Temperature Low Sag) conductors. Given their ability to withstand high operating temperatures of up to 210 °C, it is expected that these HTLS conductors will enable the efficient transmission of higher amounts of electrical energy compared to traditional conductors.

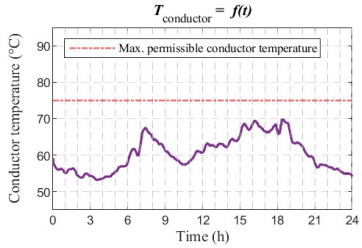

Fig. 4. The dynamics of conductor temperature in response to changes in weather conditions

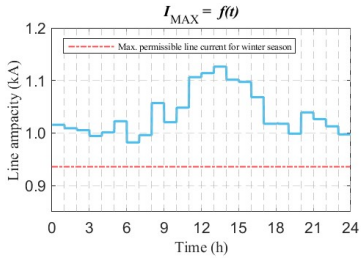

Fig. 5. Line ampacity over time with respect to changing weather conditions

Fig. 6. Current line loading under present meteorological conditions

VI. References

[1] Beňa Ľ., Kolcun M., Medveď D., Pavlík M., Čonka Z., Király J., *The influence of climatic conditions on the dynamic ampacity of external lines*, Elektroenergetika, vol. 15, no. 2, pp. 47 (2022).

[2] D. Kladar, *Dynamic Line Rating in the world – Overview* (2014).

[3] IRENA, *System Operation: Innovation Landscape Briefs*, pp. 1-20 (2020).

[4] Karimi S., Musilek P., Knight A. M., *Dynamic thermal rating of transmission lines: A review*, Renewable and Sustainable Energy Reviews, vol. 91, pp. 600-612 (2018), DOI: 10.1016/j.rser.2018.04.001.

[5] Simms M., Meegahapola L., *Comparative analysis of dynamic line rating models and feasibility to minimise energy losses in wind rich power networks*, Energy Conversion and Management, vol. 75, pp. 11-20 (2013), DOI: 10.1016/j.enconman.2013.06.003.

[6] Alberdi R., Fernandez E., Albizu I., Bedialauneta M. T., Fernandez R., *Overhead line ampacity forecasting and a methodology for assessing risk and line capacity utilization*, International Journal of Electrical Power & Energy Systems, vol. 133, pp. 107305 (2021), DOI: 10.1016/j.ijepes.2021.107305.

[7] Douglass D. A., et al., *A Review of Dynamic Thermal Line Rating Methods With Forecasting*, IEEE Transactions on Power Delivery, vol. 34, no. 6, pp. 2100-2109 (2019), DOI: 10.1109/TPWRD.2019.2932054.

[8] Čonka Z., Kolcun M., Vojtek M., Kosterec M., Suleymenov A., *Proposal of WAMS Controlled TCSC for Improvement of Transfer Capacity in Power System,* Proceedings of the 9th International Scientific Symposium on Electrical Power Engineering, Stará Lesná, Slovakia, pp. 146-150 (2017), DOI: 10.1051/e3sconf/20198401002.

[9] Kumar B., Szepesi G., Čonka Z., Kolcun M., Péter Z., Berényi L., Szamosi Z., *Trendline Assessment of Solar Energy Potential in Hungary and Current Scenario of Renewable Energy in the Visegrád Countries for Future Sustainability*, Sustainability, vol. 13, pp. 5462 (2021), DOI: 10.3390/su13105462.

[10] Beryozkina S., Sauhats A., Vanzovichs E., *Climate conditions impact on the permissible load current of the transmission line*, IEEE Trondheim PowerTech, Trondheim, Norway, pp. 1-6 (2011), DOI: 10.1109/PTC.2011.6019252.

[11] Arroyo A., Castro P., Martinez R., Manana M., Madrazo A., Lecuna R., Gonzalez A., *Comparison between IEEE and CIGRE Thermal Behaviour Standards and Measured Temperature on a 132-kV Overhead Power Line*, Energies, vol. 8, no. 12, pp. 13660-13671 (2015), DOI: 10.3390/en81212391.

[12] Rácz L., Németh B., *Dynamic Line rating — an effective method to increase the safety of power lines*, Applied Sciences, vol. 11, no. 2, pp. 492 (2021), DOI: 10.3390/app11020492.

[13] Karunarathne E., Wijethunge A., Ekanayake J., *Enhancing PV Hosting Capacity Using Voltage Control and Employing Dynamic Line Rating*, Energies, vol. 15, pp. 134 (2022), DOI: 10.3390/en15010134.

[14] Alhelou H., Abdelaziz A., Siano P., *Wide Area Power Systems Stability, Protection, and Security*, Springer (2020).

[15] Čonka Z., Kolcun M., Vojtek M., Kosterec M., Suleymenov A., *Proposal of WAMS Controlled TCSC for Improvement of Transfer Capacity in Power System*, in Proceedings of the 9th International Scientific Symposium on Electrical Power Engineering, Stará Lesná, Slovakia, pp. 146-150 (2017).

[16] Kacejko P., Pijarski P., *Dynamic fitting of generation level to thermal capacity of overhead lines*, Przeglad Elektrotechniczny, vol. 84, pp. 80-83 (2008).

[17] Bashian A., Assili M., Anvari-Moghaddam A., Catalão J.P.S., *Optimal Design of a Wide Area Measurement System Using Hybrid Wireless Sensors and Phasor Measurement Units*, Electronics, vol. 8, pp. 1085 (2019), DOI: 10.3390/electronics8101085.

[18] Kanálik M., Tomčík J., *Transmission and distribution of electricity*, TUKE, 2019.

[19] Štieberová N., Beňa L., Margitová A., Kanálik M., *Calculation of parameters related to the dynamic ampacity of external lines*, Electrical Engineering and Informatics XI, vol. 11, no. 1, pp. 380-385 (2020).

[20] Margitová A., *Increasing the transmission capacity of external power lines by calculating the dynamic ampacity*, PhD Thesis, TUKE, Košice, 2021.

Enhancing Heart Arrhythmia Classification Through Ensemble Learning: A Comparative Study

[1]*Dávid Vaľko (3rd year)*
Supervisor: [2]Norbert Ádám

[1,2]Dept. of Computers and informatics, FEI TU of Košice, Slovak Republic

[1]david.valko@tuke.sk, [2]norbert.adam@tuke.sk

***Abstract* — This paper explores the intersection of heart arrhythmia classification and ensemble learning techniques. It highlights the innovative strategies and benefits of combining these fields. Through a comprehensive review of current works we aim to demonstrate the potential of ensemble learning in advancing the accuracy of heart arrhythmia classification, thus paving the way for more effective and personalized patient medical care. In our research, we have achieved 93,2 % accuracy in ECG classification using ensemble learning.**

***Keywords* — ensemble learning, ECG classification, medical data, personalized medicine**

I. Introduction

Heart arrhythmias pose significant diagnostic and treatment challenges within the field of cardiology. These conditions range from benign to life-threatening and require accurate detection and classification for appropriate treatment. Traditional diagnostic methods rely heavily on the analysis of ECG signals. While this approach is effective, it demands significant expertise in given field and can be subject to interpretation variability by doctors. The advantage of machine learning in healthcare offers a big potential for enhancing the precision and efficiency of heart arrhythmia diagnosis.

The integration of ensemble learning into heart arrhythmia classification presents a significant expansion of diagnostic methodologies. The „combined effort" of various classifiers offers numerous benefits, including improved diagnostic accuracy, reduced variability in interpretation, and the potential for real-time analysis and prediction [1]. Using the collective power of multiple learning algorithms, researchers and doctors can overcome some of the limitations of traditional ECG analysis and diagnosis techniques.

Furthermore, ensemble learning approaches are particularly well-suited to address the challenges posed by imbalanced datasets, a common issue in medical data where certain arrhythmia classes are minimized [2]. Ensemble learning benefits from the diversity of the models it combines. By combining these models, we can capture both linear and non-linear patterns in the data more effectively than any single model could [3]. Additionally, researches are showing that categorization of specific heart diseases by ensemble learning showed significant potential [4].

II. Prerequisites for experiment

In this paper, we wanted to experiment with the use of ensemble learning in field of ECG classification. Researches also suggest that ensemble learning is a good solution for signal recognition [5]. We will be using MIT-BIH Arrhythmia database for this experiment. This database, which contains ECG signal values, is one of the most widely used datasets for the development and evaluation of algorithms for heart arrhythmia detection. During the preprocessing phase, we have eliminated 50/60 Hz noise from the ECG leads using signal filtration techniques.

After obtaining preprocessed and valid data, we will train three classifiers separately namely:

- Logistic regression
- Random forest
- Gradient boosting

These classifiers were chosen because they represent a diverse range of algorithm types suitable for classification tasks. Logistic regression is a simple linear model, random forest is an ensemble method known for handling complex data and outliers, and Gradient Boosting is powerful for capturing complex relationships in data and reducing bias.

A. Logistic regression

Logistic regression is a statistical method used for analyzing a dataset in which there are one or more independent variables that determine an outcome. Compared to more complex models, logistic regression offers greater interpretability. It allows clinicians and researchers to understand the influence of each feature (e.g., specific aspects of the ECG signal) on the classification outcome. However, standalone logistic regression may not be the best choice for this problem especially when the relationship between the features and the outcome is highly non-linear [6].

B. Random forest

Random forest combines the predictions of multiple decision trees, which generally leads to higher accuracy than individual decision trees. This is particularly useful in ECG classification, where accurate identification of different heart conditions based on ECG signals is crucial [7].

C. Gradient boosting

Gradient boosting is known for its high accuracy in predictive tasks. By iteratively correcting errors made by previous models and adding new models that address these errors, gradient boosting can often achieve high levels of accuracy [8]. We have to keep in mind that gradient boosting can sometimes overfit to the training data, especially if the dataset is not large enough or if there is a lot of noise present.

III. Methodology and acquired results

This section aims to explore the complexity of each algorithm separately, followed by an example of how these algorithms can be combined into an ensemble model to achieve superior predictive performance.

At this point, we conduct feature extraction, where we define the features from the labels in our used dataset [9][10]. We now have training and testing data ready for our subsequent model training and evaluation. Each classifier undergoes a training phase on the training data. To evaluate these models, we define an evaluation function that computes accuracy, precision, recall, and the F1 score.

A. The voting strategy for ensemble learning

To construct a more robust predictive model, we initialize an ensemble classifier using the „hard" voting strategy. When constructing a voting classifier, there are typically two main voting strategies: „hard" and „soft" voting. The choice between these two strategies depends on the nature of the problem, the behavior of the individual classifiers, and the desired outcome of the ensemble model [11]. Hard voting makes its decision based on the majority vote of the classifiers. Each classifier in the ensemble predicts the class label. The class label receiving the majority votes is chosen as the final prediction. This method is straightforward and effective, especially when the classifiers are diverse and each has different areas of strength across the input data. Hard voting does not require the classifiers to estimate probabilities for each class, making it suitable for classifiers that can only provide class labels. Through this approach, we aim to capitalize on the diverse strengths of the individual models, while minimizing their respective weaknesses.

B. Acquired results

Our results in heart arrhythmia classification shows competitive performance compared to existing literature. In Table I. we can see acquired results from above mentioned classifiers. The training of all three models took roughly 20 minutes to complete.

TABLE I
ACHIEVED RESULTS FROM SEPARATE CLASSIFIERS

Classifier	Accuracy	Precision	Recall	F1 score
Logistic regression	67,78%	44,46%	76,30%	56,18%
Random forest	90,11%	85,73%	82,66%	84,16%
Gradient boosting	88,14%	60,83%	88,05%	71,95%

After receiving these results, we conducted the approach of using ensemble learning technique, which combined the above-mentioned classifiers. The process of training was also around 20 minutes time. The achieved results are presented in Table II.

TABLE II
RESULTS FROM ENSEMBLE LEARNING MODEL

Classifier	Accuracy	Precision	Recall	F1 Score
Ensemble learning	93,20%	72,26%	87,85%	79,29%

IV. Future research

Future research in the field of ensemble learning for ECG classification should focus on exploring the integration of more diverse and advanced machine learning models to further enhance predictive accuracy. Investigating the use of deep learning algorithms, such as convolutional neural networks and recurrent neural networks, within ensemble learning could provide valuable knowledge into capturing specific patterns in ECG data more effectively. Additionally, examining the impact of data augmentation techniques and the use of unsupervised learning methods for feature extraction could reveal new ways of data representation. There is also the possibility of developing an accurate and real-time ECG diagnosis machine that will non-invasively measure and classify patient's heart status using ensemble learning models. In future, we will explore more combinations to see which offers best results.

V. Conclusion

In exploration of ensemble learning, we have combined logistic regression, gradient boosting, and random forest classifiers. The idea was to bring together different models that can work better than using just one by itself. By using these classifiers together, we get the best parts of each one. This combination created a system that not only predicts better, but also gives us insights that we might not get if we stuck with just one approach. The overall accuracy of our ensemble learning model was 93,2%, which is significantly higher than results achieved by any of the individual classifiers used in isolation. Thus, we highlight the effectiveness of combining multiple learning algorithms to improve diagnostic precision in ECG classification.

References

[1] N. Ramteke and P. Maidamwar, "Cardiac Patient Data Classification Using Ensemble Machine Learning Technique," 2023 14th International Conference on Computing Communication and Networking Technologies (ICCCNT), Delhi, India, 2023, pp. 1-6, doi: 10.1109/ICCCNT56998.2023.10307702.

[2] X. -Y. Liu, J. Wu and Z. -H. Zhou, "Exploratory Undersampling for Class-Imbalance Learning," in IEEE Transactions on Systems, Man, and Cybernetics, Part B (Cybernetics), vol. 39, no. 2, pp. 539-550, April 2009, doi: 10.1109/TSMCB.2008.2007853.

[3] Dietterich, Thomas G. "Ensemble methods in machine learning." International workshop on multiple classifier systems. Berlin, Heidelberg: Springer Berlin Heidelberg, 2000.

[4] D. Chakravarty, A. M. Thomas and V. Vivek, "A Survey on Decentralization and Virtualization of Medical Trials: An approach through Ensemble learning models and Convolutional Neural Networks," 2023 International Conference on Computer Science and Emerging Technologies (CSET), Bangalore, India, 2023, pp. 1-7, doi: 10.1109/CSET58993.2023.10346978.

[5] Y. Yang, M. Zhang and H. Pei, "A Comparative Study of Signal Recognition Based on Ensemble Learning and Deep Learning," 2023 International Seminar on Computer Science and Engineering Technology (SCSET), New York, NY, USA, 2023, pp. 340-343, doi: 10.1109/SCSET58950.2023.00081.

[6] Aspuru, Javier, et al. "Segmentation of the ECG signal by means of a linear regression algorithm." Sensors 19.4 (2019): 775.

[7] Kumar, R. Ganesh, and Y. S. Kumaraswamy. "Investigating cardiac arrhythmia in ECG using random forest classification." Int. J. Comput. Appl 37.4 (2012): 31-34.

[8] Goodfellow, Sebastian D., et al. "Classification of atrial fibrillation using multidisciplinary features and gradient boosting." 2017 Computing in Cardiology (CinC). IEEE, 2017.
[9] Moody GB, Mark RG. The impact of the MIT-BIH Arrhythmia Database. IEEE Eng in Med and Biol 20(3):45-50 (May-June 2001). (PMID: 11446209)
[10] Goldberger, A., et al. "PhysioBank, PhysioToolkit, and PhysioNet: Components of a new research resource for complex physiologic signals. Circulation [Online]. 101 (23), pp. e215–e220." (2000).
[11] Kuncheva, Ludmila I. Combining pattern classifiers: methods and algorithms. John Wiley & Sons, 201

Drone Swarm Simulation: A Real-Time Control and Dynamic Interaction

[1]*Dušan Herich (3rd year),*
Supervisor: [2]*Ján Vaščák*

[1,2]Dept. of Cybernetics and Artificial Intelligence, FEI TU of Košice, Slovak Republic

[1]dusan.herich@tuke.sk, [2]jan.vascak@tuke.sk

***Abstract*—This paper presents a drone swarm simulation system using Blender for 3D modeling and Python for controls. It offers scalable, realistic simulations with an intuitive interface, accurately mimicking drone swarm behaviors. Future efforts will focus on autonomous control integration and increased environmental complexity, advancing swarm robotics research by linking theory with practical applications.**

***Keywords*—drones, IoV, simulation, swarm**

I. Introduction

The rise of drone technology and its use, in swarm robotics has brought advancements in research and operational capabilities. Swarm robotics, which draws inspiration from behaviors observed in nature such as bird flocks, fish schools and ant colonies explores how multiple robots can work together in environments to achieve common objectives. The potential applications are extensive spanning from monitoring and disaster response to surveillance and environmental mapping [1]. Before deploying drones in real world scenarios, simulating their behaviors within controlled environments offers benefits. It enables to test coordination algorithms, collision avoidance strategies and task allocation methods among swarm members without the risk of equipment damage [2]. Furthermore simulations can be conducted under conditions that may be challenging or impossible to replicate in reality providing insights into how swarms adapt to different challenges. However developing swarm robotics systems comes with challenges. These include ensuring communication, among swarm members, thus designing algorithms for decentralized decision making processes and creating physically robust robots capable of operating across diverse environments. Additionally, the dynamic nature of swarms—where collective behavior emerges from robot interactions—requires modeling and simulation capabilities.

II. System design

The creation of a simulation system, for swarm robotics involves integrating algorithms, physical models and real time interaction capabilities. In this section we will discuss the foundations, technological integration and practical considerations that form the basis of our simulation systems design and functionality.

Ensuring the fidelity of drone models is pivotal to achieving useful simulation results [3]. Drone models was meticulously crafted to replicate the characteristics and flight dynamics observed in real world drones. We paid attention to factors like size, weight and propulsion mechanisms when designing components such as rotors, bodies and sensors using Blender [4]. This enabled us to mimic their interactions within the simulation environment mirroring those found in the realm.

To ensure real-world like behaviors within our simulation framework we integrated Blender Game Engine physics engine. This allowed us to apply principles, like gravity, momentum and aerodynamic drag to our drone models accurately. The engine also helped us simulate collisions, between drones and obstacles in the environment [5]. Developing this simulation system required finding a balance between realism and computational limitations. To overcome this obstacle we utilized optimization techniques such as polygon reduction for models and level of detail rendering (LOD). These strategies ensured that the simulation could run smoothly in time without compromising its quality too much [6].

Through the creation of drone models and a thorough understanding of their surroundings, coupled with the integration of a reliable physics engine and the successful resolution of considerable design obstacles we have created a platform that provides insights, into the dynamics of drone swarms [7].This system serves as a valuable testing ground for real world applications, across diverse fields.

The communication module (Figure. 1) of the simulation system comprises a server and several clients. After it is started a socket is created with predefined parameters (addressing type and socket type). The socket then needs to be bound to a specific address and port. In the next step the server listens for incoming connections from clients. Next, the server must accept the incoming connection. In this step, the server is looped until a defined number of clients connect. Once a client is connected, the server returns a socket to the client that represents their connection and allows communication. When controlling a drone, the client always sends a message first and the server then replies with a confirmation message with the drone's current position in space. The sending and receiving of messages is done in an infinite cycle until the termination condition is met.

In the client part, in the beginning, the socket initialization takes place, when the client connects to the server in order to send control commands via the keyboard. The cycle begins waiting for input from the user. Once the keyboard is pressed, validation takes place and a key from the list of allowed keys is detected. If so, the server a message containing that key is sent.

In the server part, it starts with initialization, which consists

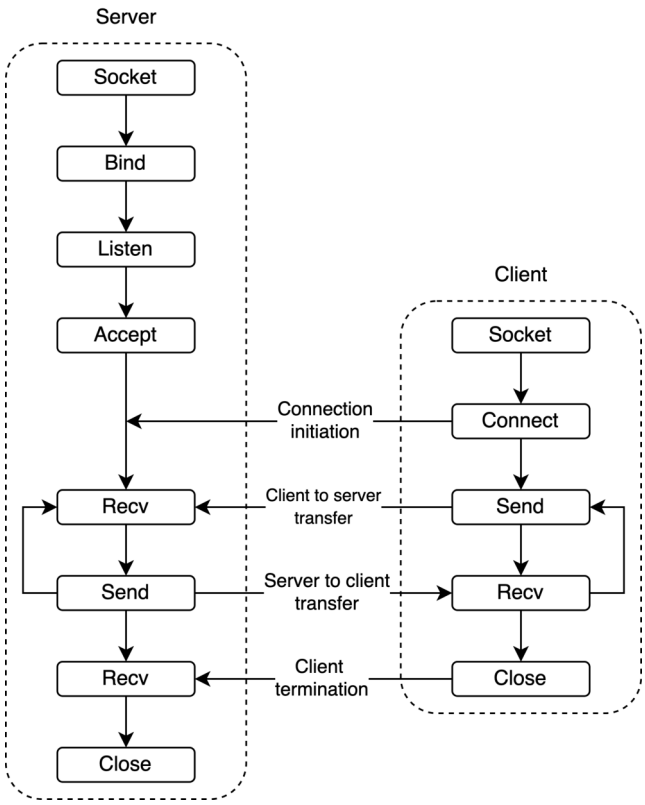

Fig. 1. Client-server communication.

of finding the drone and camera objects to work on next and creating two threads running alongside the main thread. The main thread takes care of running Blender, and thus for other work would it should not be used for any other work - if it were used, it would most likely halt the program and terminate it. The first thread created takes care of receives messages from the client. The second one in turn handles the processing and execution of the received commands. The thread for receiving messages initializes the socket at the very beginning and waits for the client to connect. After a successful connection, it listens for incoming messages on the designated port. When a message is received, it validates it and queues it sends it to the other thread. The given thread, which is also running a loop reads the message and performs the necessary action based on the key. This can be e.g. moving forward, turning left, changing the camera, restarting, ending the simulation, etc. After a successful command from the user is executed, it is returned to the client The current position of the drone is sent back to the client.

III. Evaluation

In this section we will discuss the methods employed to assess the simulations performance evaluate the authenticity of drone behaviors and determine the systems usefulness as a research tool.The performance of the system was assessed based on metrics, like frame rate and responsiveness to real time control inputs. We aimed for a frame rate of 60 frames per second (FPS) in ensuring a smooth and uninterrupted user experience (Table I. To gauge real time responsiveness we measured the delay between command inputs and observable reactions from the drones.

We also tested the scalability of the system by increasing the number of drones and complexity of the environment. These tests showcased that our system could handle swarms and dynamic scenarios without performance deterioration. This was made possible through optimization techniques such as model simplification and level of detail (LOD) (Table II, Table III) rendering. Additionally we monitored resource efficiency metrics, like CPU and memory usage, which confirmed that our system utilized resources efficiently.

TABLE I
Applying the Un-Subdivide method to a drone

Experiment	No. objects	No. polygons	FPS
joined objects	44	97 607	50-60
parent-child	187	97 607	< 5
dec. modifier	44	30 566	80-100
materials	44	30 566	85-100

TABLE II
Performance with applied Collapse method to a model of drone

Rate	No. polygons	No. vertices	No. tris
0.4	25 695	16 512	33 099
0.3	19 133	12 333	24 825
0.2	12 796	8 158	16 549
0.1	6 921	3962	8 274

TABLE III
Performance with apllied Un-Subdivide method to a model of drone

Rate	No. polygons	No. vertices	No. tris
1	21 908	21 293	42 736
2	15 468	12 907	25 962
4	11 315	8 072	16 323
5	10 813	7 436	15 053

A future research should prioritize improving simulations of drone swarms in differing settings by advancing real time decision making and machine learning algorithms to enhance adaptability and efficiency. Investigating how different types of drones can work together within swarms offers opportunities to broaden their capabilities for uses.

Acknowledgment

This publication was supported by the VEGA grant EDEN: EDge-Enabled intelligeNt systems (1/0480/22)

References

[1] W. Chen, J. Liu, H. Guo, and N. Kato, "Toward robust and intelligent drone swarm: Challenges and future directions," *IEEE Network*, vol. 34, no. 4, pp. 278–283, 2020.

[2] R. Casado and A. Bermúdez, "A simulation framework for developing autonomous drone navigation systems," *Electronics*, vol. 10, no. 1, p. 7, 2020.

[3] E. Soria, F. Schiano, and D. Floreano, "Swarmlab: A matlab drone swarm simulator," in *2020 IEEE/RSJ International Conference on Intelligent Robots and Systems (IROS)*. IEEE, 2020, pp. 8005–8011.

[4] N. Grigoropoulos and S. Lalis, "Simulation and digital twin support for managed drone applications," in *2020 IEEE/ACM 24th International Symposium on Distributed Simulation and Real Time Applications (DS-RT)*. IEEE, 2020, pp. 1–8.

[5] R. Rocca, "Fault animation with 3d model integrating drone and satellite images," in *EGU General Assembly Conference, 2021. Proceedings. doi*, vol. 10, 2021.

[6] M. Wisniewski, Z. A. Rana, and I. Petrunin, "Drone model classification using convolutional neural network trained on synthetic data," *Journal of Imaging*, vol. 8, no. 8, p. 218, 2022.

[7] V. Hassija, V. Chamola, A. Agrawal, A. Goyal, N. C. Luong, D. Niyato, F. R. Yu, and M. Guizani, "Fast, reliable, and secure drone communication: A comprehensive survey," *IEEE Communications Surveys & Tutorials*, vol. 23, no. 4, pp. 2802–2832, 2021.

Improvement of routing techniques using KNN and fitness function in Cloud MANET

[1]*Natalia KURKINA (3rd year),*
Supervisor: [2]*Ján PAPAJ*

[1,2]Dept. of Electronics and Multimedia Telecommunications, FEI TU of Košice, Slovak Republic

[1]natalia.kurkina@tuke.sk, [2]jan.papaj@tuke.sk

***Abstract*—This study introduces the Cloud Mobile Ad Hoc Network, a hybrid architecture that integrates MANET with the cloud. In this network, the selection of the cluster head node is crucial, as it significantly impacts the overall efficiency of the routing process. To solve this challenge, the paper suggests an algorithm that combines the k-nearest neighbor method and a fitness function for optimal cluster head selection and clustering. The simulation results demonstrate improved packet delivery, reduced service packets, and increased network throughput.**

***Keywords*—MANET, Cloud MANET, routing protocols, KNN, AODV.**

I. Introduction

MANET (Mobile Ad Hoc Network) networks are self-organizing networks consisting of mobile nodes. These nodes can move in arbitrary directions, and each node in this network acts as a router [1]. Thus, the information is transmitted from the source node to the destination node through intermediate nodes. Such networks are used most frequently in areas where standard infrastructure is not available, such as in earthquake rescue operations.

The primary challenge in such networks is routing and determining the optimal path for fast and trusty delivery of data from the source node to the destination node [2].

With the propagation of cloud technologies in the modern world, a new concept of Cloud MANET has emerged in recent years. Cloud MANET (C-MANET) combines two approaches, traditional MANET networks and cloud infrastructure [3]. The general diagram of a C-MANET is presented in Figure 1. As can be seen from the figure, several mobile networks can co-exist in an area. The cloud serves to connect these networks. Each network can have one or more nodes connected to the cloud. Additionally, each MANET network can be divided into one or several clusters. Each cluster head has a connection to the cloud. The cloud not only serves the function of connecting several networks into one network, but also participates in the routing process [4], [5]. When the source node wants to send data, these data are first sent to the selected cluster head. This cluster head forwards the data to the cloud. The cloud sends them to another cluster head, which will transfer the data to the destination node.

Cluster formation and cluster head selection are crucial components in C-MANET, as they significantly influence the overall efficiency and performance of the network routing process [6].

This paper introduces an algorithm designed for the optimal selection of a cluster head and clustering in C-MANET.

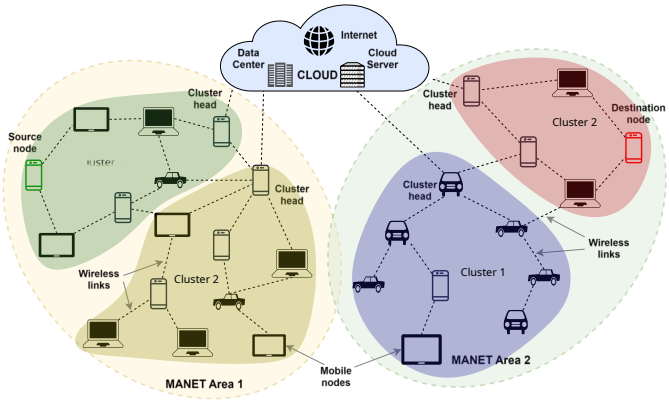

Fig. 1. The basic clustering scheme for Cloud MANET.

The presented method combines utilisation of the k-nearest neighbor (KNN) technique and a fitness function, and it is employed in combination with the AODV reactive routing protocol. The proposed algorithm is named AODV+KNN. The selection of the cluster head is not only based on the count of connected mobile nodes; it also considers parameters such as the hop count from the node to the cluster head, the occurrence of transmission errors, and the availability of free buffer space on the cluster head.

II. Proposed work

In C-MANET, the nodes are randomly distributed within the network, incorporating various gateway nodes connected to the cloud. Following the establishment of the network, nodes engage in information exchange to create a neighbourhood and compute parameters for each neighbour. Consequently, each node has a list of directly or indirectly linked gateways, enabling it to precisely select one of them.

The presented scheme introduces the following terms::

1) The set of all MANET nodes provided by $M = \{m_1,\ m_2,\ m_3, ...,\ m_n\}$.
2) The set of gateway nodes denoted by $GW = \{gw_1,\ gw_2,\ gw_3, ...,\ gw_l\}$, where $l \leq n$.
3) Node m_j $(j \leq n)$ could be connected to some gateways $GW_j = \{gw_{j1}, gw_{j2}, ..., gw_{ji}\}$, where $i \leq l$.

So, the main problem is to choose an optimal cluster head for node m_j from GW_j. The process of selecting a suitable node must be performed on the node itself. For this purpose, a scheme was proposed using the KNN algorithm and the fitness function, which is calculated using the formula below:

$$FF = min(\alpha * hc_{ji} + \beta * txErr_{ji} + \gamma * fS_{ji}) \quad (1)$$

where hc_{ji} is the number of hop count from node m_j to gateway gw_{ji}. $txErr_{ji}$ represent the number of transmission errors, fS_{ji} is the number of free buffer space on gateway gw_{ji}. α, β, γ coefficients were chosen as follows $\alpha = 0.4$, $\beta = 0.4$, $\gamma = 0.2$ and $\alpha + \beta + \gamma = 1$. The algorithm to select an optimal node in the proposed scheme can be divided into two cases: when a node has directly connected some gateways and when a node selects a suitable gateway through its neighbors. In the first case, the node uses the fitness function, and in the second case, the node uses the KNN algorithm and chooses the gateway as the cluster head that has the maximum number of neighbors in the neighbor table. If some gateways have an equal number of neighbours, the fitness function will be used to choose the optimal.

III. Performance Evaluation

The NS-3 simulator was chosen for the simulated C-MANET. The Table I contains the simulated parameters. Simulation software was used to compare AODV and AODV+KNN, evaluating parameters such as packet delivery ratio, number of routing packets, and throughput.

TABLE I
Simulation Parameters

Simulation Area [m^2]	800 × 800
Simulation Time [s]	100
The number simulation for each scenario	10
Number of MANET nodes	50, 100, 150
Max. transmission range of MANET node [m]	200
Transmission Technology	IEEE 802.11b
Mobility Model	Random WayPoint
Moving Speed [m/s]	2 – 4, 4 – 6, 6 – 8

A. Experimental results

Figures 2-4 present the simulation results for varying numbers of mobile nodes and different node speeds. Figure 2 illustrates that, on average, the AODV+KNN protocol delivers 9.4% more packets compared to the AODV protocol. Figure 3 reveals that the AODV+KNN protocol results in a 9.5% reduction in the average number of service packets compared to the AODV protocol. In Figure 4, the network throughput for the AODV+KNN protocol is, on average, 8.5% higher than that of AODV. The most advantageous results were observed with 50 nodes and a node speed of 6-8 m/s. In summary, using the proposed cluster head selection and clustering algorithm provides positive results in C-MANET.

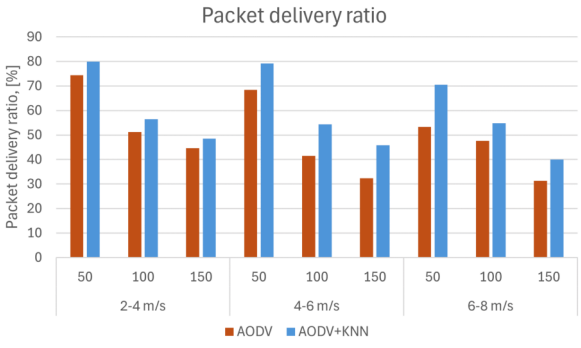

Fig. 2. Packet Delivery Ratio for AODV and AODV+KNN routing protocols (number of nodes - 50, 100, 150, speed of nodes - 2-4, 4-6, 6-8 m/s).

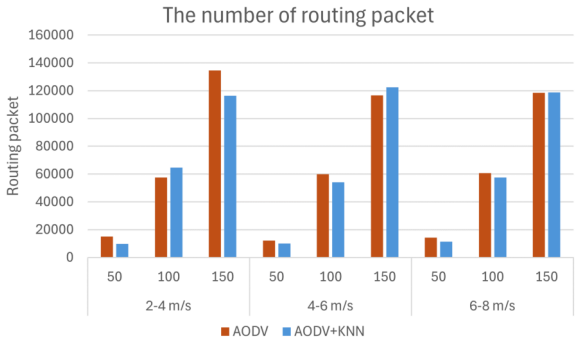

Fig. 3. The number of routing packets for AODV and AODV+KNN routing protocols (number of nodes - 50, 100, 150, speed of nodes - 2-4, 4-6, 6-8 m/s)

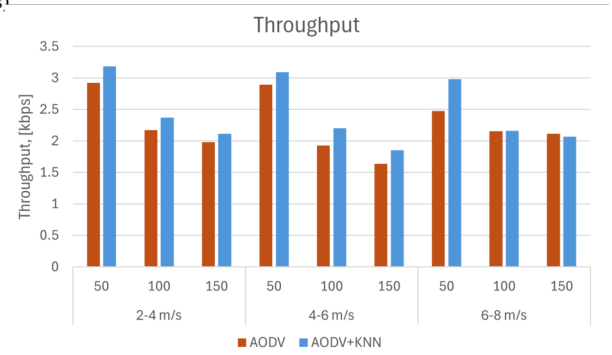

Fig. 4. Throughput for AODV and AODV+KNN routing protocols (number of nodes - 50, 100, 150, speed of nodes - 2-4, 4-6, 6-8 m/s).

IV. Conclusion

This paper introduces the AODV+KNN algorithm, a dynamic method for selecting optimal gateways and clustering in C-MANET. Simulation results highlight the effectiveness of the proposed algorithm, showing enhancements in packet delivery, reduced service packets, and increased network throughput compared to the conventional AODV protocol. These outcomes suggest that the AODV+KNN algorithm positively influences C-MANET, improving routing efficiency and overall network performance.

Acknowledgment

This research was funded by the Slovak research and Development Agency, research grant no. APVV-17-0208 and VEGA 1/0260/23.

References

[1] V. Krishnamoorthy, I. Izonin, S. Subramaian, S. K. Shandilya, S. Velayutham, T. R. Munichamy, and M. Havryliuk, "Energy saving optimization technique-based routing protocol in mobile ad-hoc network with iot environment," *Energies*, p. 1385, 2023.

[2] S. Dalal, N. Dahiya, B. Seth, V. Jaglan, M. Malik, S. Surbhi, U. Rani, D.-N. Le, and Y.-C. Hu, "An adaptive traffic routing approach toward load balancing and congestion control in cloud–manet ad hoc networks," *Soft Computing*, vol. 26, pp. 1–12, 2022.

[3] H. Tao, J. Zhou, Y. Lu, D. Jawawi, D. Wang, E. Onyema, and C. Biamba, "Enhanced security using multiple paths routine scheme in cloud-manets," *Cloud Comp*, vol. 12, p. 68, 2023.

[4] B. V. S. U. Prathyusha and K. R. Babu, "Eabrt-topsis: An enhanced aodv routing protocol with topsis-based backup routing table for energy-efficient communication in ca-manet," *2023 ACCTHPA*, pp. 1–6, 2023.

[5] A. Bajulunisha, M. Surya, and T. Azhagesvaran, "Energy efficient data routing protocol in cloud assisted manet," *2023 ACCTHPA*, pp. 1–6, 2023.

[6] F. Hamza and S. Vigila, "Cluster head selection algorithm for manets using hybrid particle swarm optimization-genetic algorithm," *International Journal of Computer Networks and Applications*, vol. 8, p. 119, 2021.

Leveraging Gumbel Softmax to Optimize Split Computing and Early Exiting for Autonomous Driving Applications in Vehicular Edge Computing

[1]*Róbert RAUCH (3rd year),*
Supervisor: [2]*Juraj GAZDA*

[1,2]Dept. of Computers and Informatics, FEI TU of Košice, Slovak Republic

[1]robert.rauch@tuke.sk, [2]juraj.gazda@tuke.sk

***Abstract*—Computer vision is a key technique for processing high-dimensional data such as images from camera sensors. However, it typically involves a long processing time. Therefore, achieving low latency without compromising the high accuracy of existing algorithms is essential for such applications, especially for autonomous driving. In this work, we present a novel approach for determining the split point and the exit point using DDPG with Gumbel softmax. We show that our approach outperforms other baselines by achieving a better accuracy-latency trade-off.**

***Keywords*—autonomous driving, early exiting, Gumbel softmax, split computing**

I. Introduction

Autonomous driving is an emerging field that enables connected autonomous vehicles (CAVs) to make driving decisions without human intervention. These CAVs typically communicate with the road-side infrastructure to enhance their situational awareness and performance. As [1] reported, autonomous driving applications have already been deployed for consumers, despite the ongoing research challenges in developing algorithms that can process sensor data with high accuracy. One of the most promising fields for processing visual data from sensors (e.g., cameras, LiDARs) is computer vision (CV) [2], which often employs deep learning (DL) techniques, especially convolutional neural networks (CNNs), to extract meaningful information from such data [3]. To ensure the safety of CAVs passengers and other road users, as well as the efficiency of the traffic system, CAVs need to make real-time predictions based on the CV tasks [4]. These tasks are often offloaded to a nearby computationally powerful server [5], called an edge server, which is often co-located at the base station. This paradigm is known as vehicular edge computing (VEC). Therefore, there is a demand for highly accurate and fast CNNs that can support the VEC framework.

CNNs are computationally demanding and may overload the edge server if all tasks are offloaded. Hence, Kang *et al.* [6] devised a novel split computing method that collaborates between the mobile device and the edge server. This method gains up to 6.7 times higher server throughput, enabling more task processing and device accommodation. However, CNNs generate high data volume between layers, making some offloading points suboptimal [6]. Yet, [7] demonstrated that autoencoders can compress data to create better splitting points. Another way to reduce CNN latency is to use mobile-friendly architectures, such as [8], [9]. However, these networks may sacrifice accuracy for CAVs, unlike deeper CNNs, such as [10], [11]. Thus, deeper networks are preferable. However, they may not meet CAVs' real-time requirement in harsh conditions [12]. This can be addressed by introducing branches into the CNN and dynamically selecting the exit branch based on traffic conditions [13], [12].

Autoencoders and early exiting may degrade the model accuracy significantly. This is because autoencoders perform a lossy compression and early exiting bypasses deeper network layers. Therefore, it is preferable to have a dynamic CNN execution that adapts to the environmental conditions and the latency and accuracy requirements of CAVs. Li *et. al.* [12] used a heuristic-based approach to find the optimal split and exit, whereas Zhao *et. al.* [14] employed a reinforcement learning (RL) approach, specifically a deep deterministic policy gradient (DDPG), to choose the split point and confidence thresholds for exit branches optimally, where confidence indicates the level of certainty of the CNN prediction as in [13]. This implies that [14] evaluates every branch before exiting, which may incur additional computational overhead.

We present an RL approach to determine the optimal strategy for splitting and exiting. Our approach predicts the optimal split point and exit branch before the CNN execution. We use the Gumbel softmax to predict the splits and exits as discrete actions, rather than continuous values as in [14]. The Gumbel softmax [15] is more suitable for RL problems with discrete and finite action spaces. We also use autoencoders, as in [7], to reduce the dimensionality of the intermediate data and improve the latency when offloading this data. We compare our approach with [14] and a baseline that uses softmax for split and exit prediction.

II. System Model

We model our system with a set of CAVs, denoted as $V = \{v_1, v_2, ..., v_{N^V}\}$. These CAVs are connected to the edge server denoted as b. Each CAV generates a set of CNN tasks $C_{t,v} = \{c_1, c_2, ..., c_{N^C}\}$, within a time interval t. Tasks are generated periodically to simulate a camera sensor with a static frames per second (FPS). Each task has a strategy under which CNN is being executed in a time interval t. This strategy is denoted as $a_t = \{s, e\}$, where $s \in S$ is a set of splits within a CNN and $e \in E$ is a set of exit branches. Note, that each split

$s \in S$ has autoencoder for data compression, implemented as in [7].

We estimate the data that needs to be sent to the edge server. We use 3D tensors and therefore we can easily estimate the data size by multiplying the tensor width D_s^{width}, tensor height D_s^{height} and tensor channel size D_s^{ch}. Furthermore, we need to multiply this by the bit size D_s^{bit} of a single unit in a tensor, which depends on the computer format used, e.g., float32 [16]. Our final formula is:

$$D_{c,s} = D_s^{\text{width}} D_s^{\text{height}} D_s^{\text{ch}} D_s^{\text{bit}}. \tag{1}$$

Because we train autoencoders before simulation, we can measure each of these values beforehand.

To get the latency for offloading the task c to the edge server we can therefore use the following equation:

$$t_c^{\text{comm}} = \frac{D_{c,s}}{r_{t,v}}, \tag{2}$$

where $r_{t,v}$ is the current data rate for CAV v, which can be estimated as in [17].

To get the latency for computational processing on device and on server we can use the following equation [17]:

$$t_c^{\text{comp}} = \frac{I_{c,v}}{\eta_v} + \frac{I_{c,b}}{\eta_b}, \tag{3}$$

where $I_{c,v}$ and $I_{c,b}$ are the computational demand for task c, that needs to be inferred on CAV v and edge server, respectively. η_v and η_b correspond to the computational power of CAV and edge server, respectively. Note that $I_{c,v}$ and $I_{c,b}$ can be estimated based on the parameters of each layer, similarly to [18].

Our final execution latency for task c can be calculated as follows:

$$t_c = t_c^{\text{comp}} + t_c^{\text{comm}} + t_{w,c}, \tag{4}$$

where $t_{w,c}$ is the waiting time incurred due to network dynamics, queues etc., as in [19].

III. Gumbel Softmax-based strategy selection

Our goal is to design a system that can balance the accuracy and latency of a CNN using splits and early exits. Our CNN performs a classification task, following the approach of other works such as [12], [14]. To this end, we propose a utility function that can measure the performance of our system for a CAV. This utility function is defined as:

$$u_{t,v} = \Phi(\mu_{t,v}) w_\mu + \Phi(t_t) w_t, \tag{5}$$

where $\mu_{t,v}$ is the accuracy of classification tasks executed within a time interval t for a CAV v. t_t represents the execution time shown in (4) averaged over all tasks within a time interval t. Note that by all tasks we mean all tasks that belong to a set $Z_{t,v}$. w_μ and w_t are weights that determine the importance of meeting the latency $\psi_{\mu,v}$ and accuracy $\psi_{t,v}$ requirements. Φ is a normalizing function that maps our accuracy and latency into a [0, 1] range as follows:

$$\Phi(\mu_{t,v}) = \frac{\mu_{t,v} - \psi_{\mu,v}}{1 - \psi_{\mu,v}}, \tag{6a}$$

$$\Phi(t_t) = (1 - \frac{t_{t,v}}{\psi_{t,v}}). \tag{6b}$$

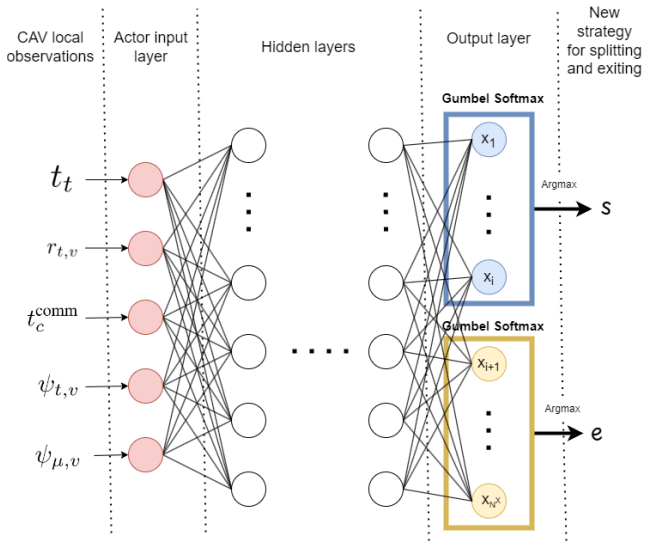

Fig. 1. Actor network with Gumbel softmax

We formulate our system as a Markov decision process (MDP) in the following way. The state of the system is represented by the local observations of a CAV. These observations consist of five values as follows:

$$o_{t,v} = \{t_t, r_{t,v}, t_c^{\text{comm}}, \psi_{t,v}, \psi_{\mu,v}\}. \tag{7}$$

The reward function for our agent is defined by our utility function in (5). The action space of the system is modeled as a set $X = \{x_1, x_2, ..., x_i, x_{i+1}, ...x_{N^X}\}$, which is the output layer of our actor network, as shown in Fig. 1. We divide the set of actions into two subsets: $X_1 = \{x_1, x_2, ..., x_i\}$, where x_i is the number of splits, and X_1 contains the logit values for each split; and $X_2 = \{x_{i+1}, ..., x_{N^X}\}$, where X_2 contains the logit values for each exit. We apply the Gumbel softmax function on both of these subsets, as shown in Fig. 1. To perform the Gumbel softmax function, we use the following equation [15]:

$$y_i = \frac{\exp\left(\log(\pi_i) + g_i\right)/\tau}{\sum_{j=1}^{k} \exp\left(\log(\pi_j) + g_j\right)/\tau}, \tag{8}$$

where y_i is the probability of choosing category i (e.g., split index), π_i are the prior probabilities, g_i are the Gumbel noise samples, and τ is the temperature parameter, which controls the smoothness of the distribution.

This gives us a differentiable approximation of our subsets. Then, we can perform the Argmax operation, to determine the index of the split and exit that we want to set as our new strategy, as shown in Fig. 1.

IV. Numerical Results

We evaluate the performance of our approach using the Monte Carlo method, where we average over 3 CAVs and 5 simulations. We simulate the movement of our CAVs using the Manhattan mobility model [20]. We assign the weights as $w_t = 1$ and $w_\mu = 0.15$. For our requirements, we set $\psi_{t,v} = 0.1$ and $\psi_{\mu,v} = 0.81$. These settings indicate that we prefer lower latency over higher accuracy. We train our DDPG agent for 10 thousand steps and test its performance for 1.5 thousand steps.

We show the achieved latency in Fig. 2(a). The graphs demonstrate that we obtained significantly lower latency, more

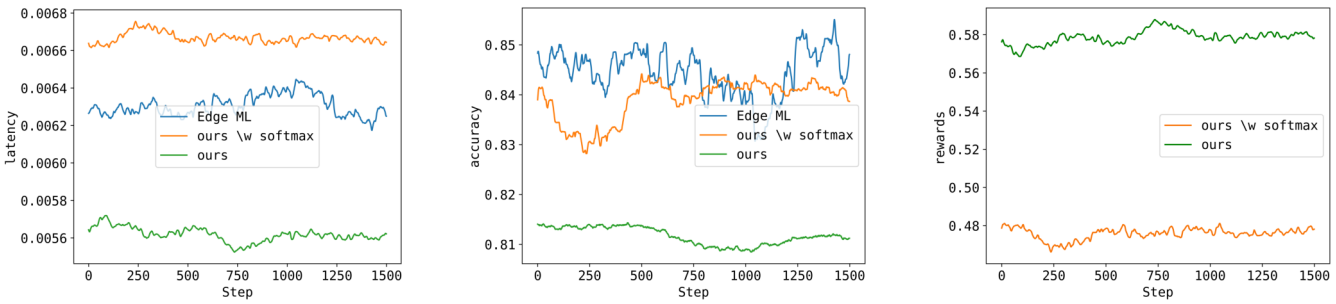

(a) Graph comparing latency between our approach, our approach with softmax and Edge ML

(b) Graph comparing accuracy between our approach, our approach with softmax and Edge ML

(c) Graph comparing rewards between our approach and our approach with softmax

Fig. 2. Graphs showing performance of our approach to baselines

precisely, we improved the latency by 12.24% on average compared to our approach with softmax and by 18.31% compared to Edge ML.

This improvement in latency reduced the accuracy, but only by 3.98% on average compared to our approach with softmax and by 3.31% compared to Edge ML. This can be observed in Fig. 2(b).

It is important to note that we prioritized latency over accuracy and our approach still satisfied the accuracy requirements. Therefore, we achieved a better accuracy-latency trade-off, as evidenced by our rewards in Fig. 2(c), where we increased the rewards by 21.18% on average. We do not include Edge ML reward function in Fig. 2(c), as Edge ML has a different reward function and is not comparable.

V. Conclusion

In this paper, we proposed the use of Gumbel softmax in DDPG for split point and exit selection. We compared our results with the state-of-the-art baseline Edge ML and our approach that used softmax instead of Gumbel softmax. We achieved lower latencies on average, while maintaining accuracy within acceptable ranges and only losing a small amount of accuracy compared to the baselines. We also obtained higher rewards than our approach with softmax. For future work, we plan to evaluate our approach in a more realistic environment by varying different parameters of our simulation. We can also enhance our actor network with long short-term memory (LSTM). Since we are dealing with offloading, LSTM can be used to forecast future states, such as data rate.

Acknowledgment

This work was supported by The Slovak Research and Development Agency project no. APVV-18-0214, no. APVV SK-CZ-RD-21-0028, and the Slovak Academy of Sciences under Grant VEGA 1/0685/23.

References

[1] E. Yurtsever, J. Lambert, A. Carballo, and K. Takeda, "A survey of autonomous driving: Common practices and emerging technologies," *IEEE access*, vol. 8, pp. 58 443–58 469, 2020.

[2] B. Kanchana, R. Peiris, D. Perera, D. Jayasinghe, and D. Kasthurirathna, "Computer vision for autonomous driving," in *2021 3rd International Conference on Advancements in Computing (ICAC)*. IEEE, 2021, pp. 175–180.

[3] É. Zablocki, H. Ben-Younes, P. Pérez, and M. Cord, "Explainability of deep vision-based autonomous driving systems: Review and challenges," *International Journal of Computer Vision*, vol. 130, no. 10, pp. 2425–2452, 2022.

[4] S. Raza, S. Wang, M. Ahmed, M. R. Anwar *et al.*, "A survey on vehicular edge computing: architecture, applications, technical issues, and future directions," *Wireless Communications and Mobile Computing*, vol. 2019, 2019.

[5] L. Liu, C. Chen, Q. Pei, S. Maharjan, and Y. Zhang, "Vehicular edge computing and networking: A survey," *Mobile networks and applications*, vol. 26, pp. 1145–1168, 2021.

[6] Y. Kang, J. Hauswald, C. Gao, A. Rovinski, T. Mudge, J. Mars, and L. Tang, "Neurosurgeon: Collaborative intelligence between the cloud and mobile edge," *ACM SIGARCH Computer Architecture News*, vol. 45, no. 1, pp. 615–629, 2017.

[7] A. E. Eshratifar, A. Esmaili, and M. Pedram, "Bottlenet: A deep learning architecture for intelligent mobile cloud computing services," in *2019 IEEE/ACM International Symposium on Low Power Electronics and Design (ISLPED)*, 2019, pp. 1–6.

[8] D. Sinha and M. El-Sharkawy, "Thin mobilenet: An enhanced mobilenet architecture," in *2019 IEEE 10th annual ubiquitous computing, electronics & mobile communication conference (UEMCON)*. IEEE, 2019, pp. 0280–0285.

[9] F. N. Iandola, S. Han, M. W. Moskewicz, K. Ashraf, W. J. Dally, and K. Keutzer, "Squeezenet: Alexnet-level accuracy with 50x fewer parameters and< 0.5 mb model size," *arXiv preprint arXiv:1602.07360*, 2016.

[10] K. Simonyan and A. Zisserman, "Very deep convolutional networks for large-scale image recognition," *arXiv preprint arXiv:1409.1556*, 2014.

[11] K. He, X. Zhang, S. Ren, and J. Sun, "Deep residual learning for image recognition," in *Proceedings of the IEEE conference on computer vision and pattern recognition*, 2016, pp. 770–778.

[12] E. Li, L. Zeng, Z. Zhou, and X. Chen, "Edge ai: On-demand accelerating deep neural network inference via edge computing," *IEEE Transactions on Wireless Communications*, vol. 19, no. 1, pp. 447–457, 2020.

[13] S. Teerapittayanon, B. McDanel, and H. Kung, "Branchynet: Fast inference via early exiting from deep neural networks," in *2016 23rd International Conference on Pattern Recognition (ICPR)*, 2016, pp. 2464–2469.

[14] Z. Zhao, K. Wang, N. Ling, and G. Xing, "Edgeml: An automl framework for real-time deep learning on the edge," ser. IoTDI '21. New York, NY, USA: Association for Computing Machinery, 2021, p. 133âĂŞ144. [Online]. Available: https://doi.org/10.1145/3450268.3453520

[15] E. Jang, S. Gu, and B. Poole, "Categorical reparameterization with gumbel-softmax," *arXiv preprint arXiv:1611.01144*, 2016.

[16] M. Imani, S. Gupta, Y. Kim, and T. Rosing, "Floatpim: In-memory acceleration of deep neural network training with high precision," in *Proceedings of the 46th International Symposium on Computer Architecture*, 2019, pp. 802–815.

[17] M. Vološin, E. Šlapak, Z. Becvar, T. Maksymyuk, A. Petik, M. Liyanage, and J. Gazda, "Blockchain-based route selection with allocation of radio and computing resources for connected autonomous vehicles," *IEEE Transactions on Intelligent Transportation Systems*, 2023.

[18] L. K. Muller, "Overparametrization of hypernetworks at fixed flop-count enables fast neural image enhancement," in *Proceedings of the IEEE/CVF Conference on Computer Vision and Pattern Recognition*, 2021, pp. 284–293.

[19] A. B. de Souza, P. A. L. Rego, T. Carneiro, P. H. G. Rocha, and J. N. de Souza, "A context-oriented framework for computation offloading in vehicular edge computing using wave and 5g networks," *Vehicular Communications*, vol. 32, p. 100389, 2021.

[20] B. Ramakrishnan, "Analysis of manhattan mobility model without rsus," *IOSR Journal of Computer Engineering (IOSR-JCE)*, vol. 9, no. 5, pp. 82–90, 2013.

Ambient Software Solutions

[1]*Tomáš KORMANÍK (1st year),*
Supervisor: [2]*Jaroslav PORUBÄN*

[1,2]Dept. of Computers and Informatics, FEI TU of Košice, Slovak Republic

[1]tomas.kormanik@tuke.sk, [2]jaroslav.poruban@tuke.sk

***Abstract*—This article aims to present current and possible future advances in ambient applications. To effectively use all available biometric and multimedia data in this day and age, it is required to pay attention to the software engineering aspect as well. We aim to summarize all current and related knowledge while outlining the direction of our future research, which will standardize ambient applications. Possible use cases will be explored, including use in software engineering, which is close to our expertise. However, we will focus on use cases for the general public as well.**

***Keywords*—ambient software, pervasive computing, interaction, Internet of Things**

I. Introduction

In the past decade, we have observed the skyrocketing popularity of Internet of Things (IoT) devices. Their implementation in industry and general use can be considered seamless since they have made a multitude of tasks simpler and easier to perform. Environments that utilise such devices mostly rely on user input or simple algorithms to determine their current and future behaviour. Such behaviour makes everything more comfortable, but on the contrary, it is not more seamless or ambient.

The definition of ambience or ambient environment slightly varies in all fields; however, the key meaning remains. We personally consider the closest definition as *pertaining to the surrounding environment* as is specified in one of the Oxford Dictionaries [1]. In the case of software engineering, we are looking at the development of applications that can leverage the environment to their advantage, adapt to it, and, as a result, mitigate negative factors that are present. It can be argued that *user experience*-related research targets this goal, but at a closer look, we can see that the goal of ambience is not to improve interaction in the same way but to actually completely remove it if possible. Ideally, ambient applications perform in a way that does not interfere with the surrounding world, causing the user to fully forget the presence of any interface at all. Naturally, the ideal result is only theoretical and cannot be achieved.

Due to the desired characteristics of ideal ambient applications, seamlessness is closely tied to this topic. Being able to start, stop, interrupt, or adjust the usage of an application without the user needing to even think about it is a goal that is far-fetched for the near future. Making all operations with the application as seamless as possible further solidifies and improves its ambience.

II. Related research

The general scientific and professional community commonly uses several collocations for similar topics, such as *Ambient Intelligence*, *Ambient Applications*, or *Ambience-oriented Software*. Every now and then, some unique modifications of these collocations pop up, but they generally refer to similar concepts. Sadly, this area is not particularly leading the research around the world, so the availability of relevant scientific papers is rather low. Thankfully, we can still find usable information on the topic of pervasive computing, which covers all of our subtopics.

A. Development in time

To broaden our knowledge and pinpoint the state of the art in this field, we considered it relevant to gather statistics about keywords that are related to this field. We identified ten keywords that influence our research. All keywords were searched using their abbreviations, full form, singular, and plural, in order to include all possible variants of them. Relevant sources of our information were online databases and portals, which are generally popular among the scientific community.

Keywords *user interfaces* and *human computer interaction* are broad, but they are included in significant portions of relevant articles, so we mention them as references. *Ubiquitous computing* is a topic that appeared in the 2000's. It's popularity is currently past its peak and is steadily declining, but we consider it the root topic of related research in our field.

While searching for related topics, *pervasive computing* popped up, which matched our research field and was widely popular. *Ambient intelligence* is often mentioned together with pervasive computing in keywords. *Smart space* and *ambient space* can both be used to develop and use ambient software, so we consider them our main topics of research. *Intelligent space*, *ambient user experience*, and *ambient software* are specific, and contributions are appearing only sporadically. Putting all relevant information into a graph (Fig. 1) made it easily readable.

B. Article analysis

The *International Symposium on Ambient Intelligence* (ISAmI) is especially dedicated to this field, which makes further research in this area significantly easier. Generally, articles included in such conferences are primarily targeted at specific solutions that are considered 'ambient' by their authors, but they sometimes misinterpret or misjudge the nature of their research or implementation. Most interesting were the 2012[2] and 2013[3] editions, which presented possible implementations of various experimental and real-life use cases and scenarios. We found article [4] that directly affects our research by explaining the process of implementation of

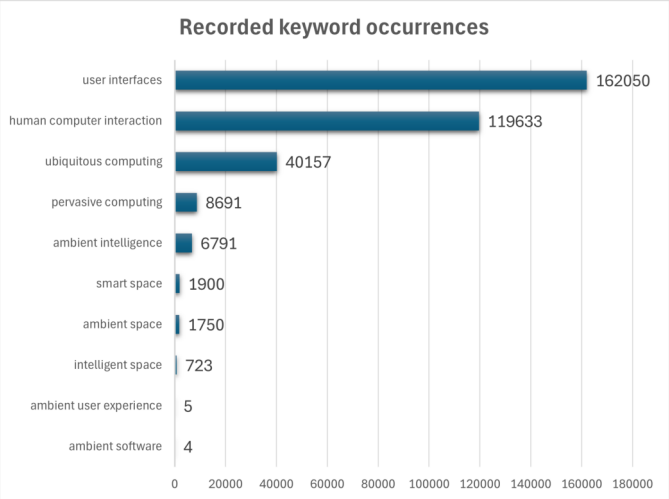

Fig. 1. Graph of recorded keyword occurrences (data from Scopus as of 1.4.2024)

ambient applications. Another interesting piece of reading was the work by García et al.[5], which explored the use of this technology in collaborative learning and education. On the contrary, we considered recent additions to the proceedings of this conference not so beneficial. The main influential factor is most likely the local nature of this conference without any major involvement of researchers from other research-oriented institutions.

Quite popular is also *Journal of Ambient Intelligence and Smart Environments*[6] of Dutch origin. This journal contains more theoretical and investigative articles, which can provide a good foundation for our future research in terms of knowledge. We personally liked the survey conducted by Preuveneers and Novais [7], which outlined the opinions of people on ambient software and systems. The survey included examples of code snippets and potential usages stated by respondents, which can come in handy in the future.

Alternatively, a survey by Díaz-Oreiro et al. [8] was also available, which provided a look from a different perspective. A more broad survey by Sadri [9] provides a general look into ambient intelligence. Linked to this is the survey by Dunne et al. [10], which addresses progress and changes during the 10-year period since the survey by Sadri. These surveys provide information mainly on possible and present issues in usability, privacy, and ethics. The survey by Dunne is focused on potential researchers by laying out viable opportunities and paths of research.

Some articles, such as one written about *Agent Factory Micro*[11] grasp this concept in a slightly different approach but still correctly. Their work tracks the progress of software creation in detail. Observing the work they documented and presented is vital for gaining experience for our future experiments.

Personally, we considered work by Kordts et al. to be most influential and informative in this subject. Article named *Towards Self-Explaining Ambient Applications*[12] contained proper explanation of this topic with addition of their thoughts and opinions on various approaches. This article helped us greatly in shaping our opinion and future work. The extended talk about goal of creating common software development framework, which is specifically made to help develop ambient software is innovative and it promotes accessibility of ambient technologies in future. Creation of such framework can also create foundation and common ground for all future IoT products.

Multiple scientific articles use desired keywords only as buzzwords. Some actually work with the goal of ambience, but their understanding of it is vague. Thanks to these factors, relevant statistics about the number of relevant papers in this field can be somewhat inaccurate. We can safely state that further development in this area is possible, as the technology and its availability are progressing rapidly, thanks to higher accessibility in terms of technical and software assets.

Thankfully, many fields of research have direct or indirect intersections with ambient software thematic. Intelligent spaces are most likely to be used during our research in order to gather the required data and perform scientific experiments. Viable for us might be the work of Japanese researchers who have looked into the detection of object interaction [13]. A multitude of recent studies have also looked into object detection in intelligent spaces [14]. Even simpler papers, for example, one that contained an experiment using a tool to assist with home office tasks ([15]), outline the simple possibility of utilizing intelligent space for non-scientific purposes.

Field of psychology has also close ties to ambient software. Precise determination of persons cognitive type or psychological predispositions can enhance future decision making of such software. Recently published article about analysis of user cognitive types [16] provides good resource. In our case, ideally we would determine this information even before person begins or takes part in the interaction with ambient software. This practice would however severely impact privacy. Each space which is using such approach would require prior notice of users and their consent, as is required by General Data Protection Regulation (GDPR). Additionally, it can be beneficial to determine current emotions of users. Electroencephalograms (EEG) are quite useful, since they can be used to determine emotions of users, as is demonstrated by Jayaweera et al. [17]. This solution utilizes machine learning. Current peak of popularity in machine learning research can be leveraged and utilized in ambient software solutions quite easily, if properly planned and trained on correct data.

III. Research infrastructure

Thanks to the available scientific materials, we have a solid foundation for future research activities. In order to perform experiments, measure user experience, and gather metrics, we need a suitable environment. Luckily, at our department, we have several spaces equipped with appropriate architecture. In general, our desired architecture ideally consists of *analog sensors* (e.g., light, humidity, pressure, temperature, motion), *multimedia devices* (e.g., IP cameras, speakers, microphones, monitors, projectors), and *smart devices* (e.g., blinds, lights, curtains, ventilation).

Naturally, not all of our available environments have all of these desired elements, but as we mentioned before, an ideal ambient application uses everything at its disposal (if possible and allowed by the user or maintainer). Missing elements might cause minor inaccuracies, which can be addressed and resolved accordingly. Also, thanks to technological progress, it's possible that more advanced sensors and software frameworks will appear, which might make parts of our research obsolete or irrelevant. Due to this fact, we need to perform frequent updates and analyse current trends on the go.

Fig. 2. Laboratory *OpenLAB* (left) and *Caprica* (right) at Department of Computers and Informatics

Sensors	Caprica	OpenLAB
Light	No	Yes
Humidity	No	Yes
Pressure	No	Yes
Temperature	Yes	Yes
Motion	No	Yes
IP cameras	Yes	Yes
Speakers	Yes	Yes
Microphones	Yes	Yes
Monitors	No	Yes
Projectors	Yes	Yes
Blinds	Yes	Yes
Lights	Yes	Yes
Curtains	Yes	Yes
Ventilation	No	No

Fig. 3. Available architecture at *OpenLAB* and *Caprica* laboratories

Many researchers in the Department of Computers and Informatics have already conducted research in the field of intelligent spaces and smart environments. So far, research aimed, for example, to improve education[18] or to help elderly people[19]. Naturally, there are more works available, but we have picked the ones that we found the most interesting and relevant.

Environments used in previous experiments are at our disposal, which allows us to conduct experiments. Laboratory *Caprica* (Fig. 2) is created from a former classroom on the premises of our department. It is ideal for controlled experiments and testing unfinished solutions. There are several IoT appliances and features at our disposal that can be utilised to gather data and change the overall ambience of the whole room. Thanks to these features, we can easily prepare the environment for the specific type of experiment we desire and observe the progress.

Located in the lobby of the Department of Computers and Informatics, *OpenLAB* provides a significant amount of depersonalised data on a daily basis. Equipped with more appliances and sensors than *Caprica*, it is ideal for mass data gathering campaigns. To conduct experiments at the production level, it is necessary to create a solution that is specifically tailored to this environment. This creates a slight drawback, as having such a unique environment means that our solutions will most likely not work on different systems. However, if we desire only passive gathering of data and interaction with this space, its location is a huge advantage, as can be seen in the picture (Fig. 2). To summarise both environments, we created a colourful table (Fig. 3), which displays the available architecture in both environments. Of course, additional sensors can be connected with minimal effort.

Additionally, we also have EEG measuring tool kits at our disposal, but they are bulky, which limits our possibilities of experiments on scenarios that are supposed to simulate the highest possible ambiance. More practical are smart watches or smart rings, which are quite commonly owned by people. Using these to gather biometric data is almost unnoticeable to people who wear them regularly. A more invasive approach can be achieved by utilising data available in health monitoring apps. This can be considered a significant invasion of privacy, but it can be quite useful in analysing and predicting the behavioural patterns of each individual.

IV. Upcoming research

In the upcoming scientific work, we are looking forward to several potentially viable experiments. Most ideas are initially scrapped or redesigned. Huge help can be provided during regular discussions of our results and plans with colleagues and researchers from different departments. In our case, we are eager to use common methods, such as "Devil's Advocate," which we consider useful in our environment. Our heavily technical thinking can negatively impact our decisions and influence our goal of an open-minded approach. As we researched studies[20], this approach is well known and effective.

Our current primary goal is to measure the influence of displayed information on people and determine if their focus can be positively affected by a specific ambient feature. If possible, we would like to measure the impacts of such features and outline clear recommendations for each of them. We would like to avoid inaccuracies caused by psychological disposition, health conditions, and environmental extremes. For example, it would be impractical to measure how well people can observe images displayed in their ambient space if some of them have impaired eyesight and can't even interpret the information.

To conclude our reconnaissance of scientific materials, we created a simple diagram that presents the flow of data in an ideal ambient software solution (Fig. 4). As we can see, such software has a significant number of inputs and outputs, which can influence each other in a seamless and infinite cycle. We would like to emphasise the possibility of utilising wearable devices such as smart watches, EEG analyzers, and motion sensors. Thanks to current technology, a simple device like a smart watch can measure several biometrics at once, creating the opportunity to utilise it for our software (with user consent).

The first experiment would utilise available monitors in *OpenLAB*, showcasing the main information screen and a duo or trio of secondary screens. *We would like to measure the effects of different ambience-oriented display methods on groups of individuals.* We are hoping to find clear indicators for the best method to display ambient information for software engineers. In case of success, we are hoping to expand the testing sample to a larger group of individuals in order to determine the best method in general, not only for software engineers. Since multiple monitors are used by a larger number of software engineers than other professions, they might be more accustomed to this environment, and they might respond more positively.

Alternatively, we are planning to look into the possibility of normalising all available data from the ambient environment,

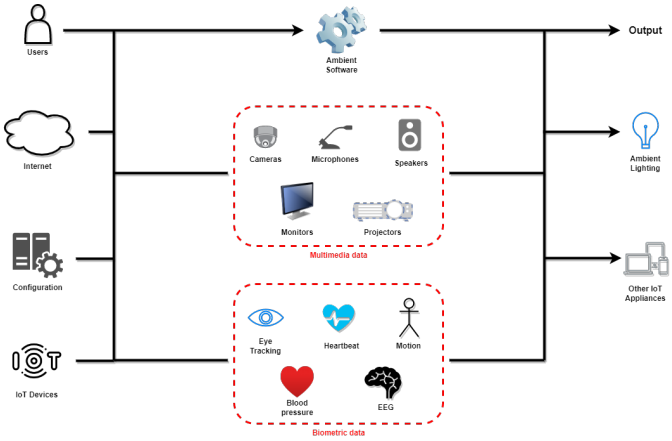

Fig. 4. Diagram of ambient software data flow

biometric smart devices, and applications in order to create a universal framework for ambient software. This can help in future experiments, which should contain a multitude of smart devices. *Aggregating and formatting all of this information into one chunk of data in the shortest amount of time is critical as the number of smart devices in the environment rises.* Naturally, a multitude of related experiments and issues might pop up during further development.

V. Conclusion

We have determined that further research and improvement in this field are possible. With that in mind, our main goal is to gather as much relevant and objective data as possible in order to provide finite and straightforward results. The overall availability of research oriented towards ambient software is below average; however, close concepts such as intelligent spaces and IoT have a significant amount of viable and resourceful data available. Many topics intersect with ambient software, which gives us the possibility of finding needed information reliably.

Acknowledgment

This work was supported by project VEGA No. 1/0630/22 “Lowering Programmers’ Cognitive Load Using Context-Dependent Dialogs”.

References

[1] M. Kent, *The Oxford Dictionary of Sports Science & Medicine*, ser. Oxford medical publications. Oxford University Press, 2006, no. zv. 10. [Online]. Available: https://books.google.sk/books?id=pO45AQAAIAAJ

[2] P. Novais, K. Hallenborg, D. Tapia, and J. Corchado Rodríguez, *Ambient Intelligence - Software and Applications: 3rd International Symposium on Ambient Intelligence (ISAmI 2012)*. Springer, 01 2012, vol. 153.

[3] A. van Berlo, K. Hallenborg, J. M. Corchado Rodríguez, D. I. Tapia, P. Novais *et al.*, *Ambient Intelligence-Software and Applications*. Springer, 2013.

[4] J. van Diggelen, M. Grootjen, E. M. Ubink, M. van Zomeren, and N. J. J. M. Smets, “Content-based design and implementation of ambient intelligence applications,” in *Ambient Intelligence - Software and Applications*, A. van Berlo, K. Hallenborg, J. M. C. Rodríguez, D. I. Tapia, and P. Novais, Eds. Heidelberg: Springer International Publishing, 2013, pp. 1–8.

[5] Ó. García, R. S. Alonso, D. I. Tapia, and J. M. Corchado, “Cafcla: An ami-based framework to design and develop context-aware collaborative learning activities,” in *Ambient Intelligence - Software and Applications*, A. van Berlo, K. Hallenborg, J. M. C. Rodríguez, D. I. Tapia, and P. Novais, Eds. Heidelberg: Springer International Publishing, 2013, pp. 41–48.

[6] “Journal of ambient intelligence and smart environments,” https://www.iospress.com/catalog/journals/journal-of-ambient-intelligence-and-smart-environments, accessed: 2024-02-25.

[7] D. Preuveneers and P. Novais, “A survey of software engineering best practices for the development of smart applications in ambient intelligence,” *Journal of Ambient Intelligence and Smart Environments*, vol. 4, pp. 149–162, 08 2012.

[8] I. Díaz-Oreiro, G. López, L. Quesada, and L. A. Guerrero, “Ux evaluation with standardized questionnaires in ubiquitous computing and ambient intelligence: a systematic literature review,” *Advances in Human-Computer Interaction*, vol. 2021, pp. 1–22, 2021.

[9] F. Sadri, “Ambient intelligence: A survey,” *ACM Comput. Surv.*, vol. 43, no. 4, oct 2011. [Online]. Available: https://doi.org/10.1145/1978802.1978815

[10] R. Dunne, T. Morris, and S. Harper, “A survey of ambient intelligence,” *ACM Comput. Surv.*, vol. 54, no. 4, may 2021. [Online]. Available: https://doi.org/10.1145/3447242

[11] C. Muldoon, G. M. P. O’Hare, R. Collier, and M. J. O’Grady, “Agent factory micro edition: A framework for ambient applications,” in *Computational Science – ICCS 2006*, V. N. Alexandrov, G. D. van Albada, P. M. A. Sloot, and J. Dongarra, Eds. Berlin, Heidelberg: Springer Berlin Heidelberg, 2006, pp. 727–734.

[12] B. Kordts, B. Gerlach, and A. Schrader, “Towards self-explaining ambient applications,” in *Proceedings of the 14th PErvasive Technologies Related to Assistive Environments Conference*, ser. PETRA ’21. New York, NY, USA: Association for Computing Machinery, 2021, p. 383–390. [Online]. Available: https://doi.org/10.1145/3453892.3461325

[13] D. T. T. Haruhiro Ozaki and J.-H. Lee, “Effective human–object interaction recognition for edge devices in intelligent space,” *SICE Journal of Control, Measurement, and System Integration*, vol. 17, no. 1, pp. 1–9, 2024. [Online]. Available: https://doi.org/10.1080/18824889.2023.2292353

[14] Q. Tang, X. Li, M. Xie, and J. Zhen, “Intelligent space object detect driven by space object data,” 2023, not reviewed.

[15] B. Tusor, S. Gubo, and A. R. Várkonyi-Kóoczy, “A personal home office helper,” in *2023 IEEE International Symposium on Medical Measurements and Applications (MeMeA)*, 2023, pp. 1–6.

[16] N. Zhang, S. Wang, and H. Li, “Improving user satisfaction by analysing users’ subjective cognitive types in smart home systems,” *Universal Access in the Information Society*, pp. 1–15, 2024.

[17] D. Jayaweera, L. Wijesinghe, A. Gallage, R. Ragel, I. Nawinne, M. Wickrmasinghe, and V. Thambawita, “Human emotion detection with ecg and eeg signals using ml techniques,” 2023.

[18] J. Porubän, “Challenging the education in the open laboratory,” in *2018 16th International Conference on Emerging eLearning Technologies and Applications (ICETA)*, 2018, pp. 439–444.

[19] M. Novák, M. Biňas, and F. Jakab, “Unobtrusive anomaly detection in presence of elderly in a smart-home environment,” in *2012 ELEKTRO*, 2012, pp. 341–344.

[20] J. Brohinsky, G. Sonnert, and P. Sadler, “The devil’s advocate: Dynamics of dissent in science education,” *Science & Education*, vol. 31, no. 3, pp. 575–596, 2022.

Post-process sealing of plasma sprayed alumina coating

[1]*Tomáš KMEC (4th year)*
Supervisor: [2]Juraj ĎURIŠIN

[1,2]Dept. of Technologies in Electronics, FEI TU of Košice, Slovak Republic

[1]tomas.kmec@student.tuke.sk, [2]juraj.durisin@tuke.sk

***Abstract*—Plasma sprayed Al_2O_3 coatings of steel surfaces are susceptible to porosity and cracking, but $AlPO_4$ sealing can eliminate these defects by filling them with a crystalline phosphate phase. In this study, an $AlPO_4$ nanocomposite slurry was prepared and applied on Al_2O_3 surfaces, but it was found that the Al_2O_3 nanopowder tended to form agglomerates that limited its ability to fill small pores and cracks. Acoustic mixing was not sufficient to break up these agglomerates, but alternative mixing techniques may be more effective. Firing the slurry in the oven helps to promote thermochemical reactions of the crystalline phosphate phase that improves the tenacity of the coating, but care must be taken to avoid bending the steel substrate. Further research is needed to optimize the slurry composition and application process for $AlPO_4$ sealing of plasma-sprayed Al_2O_3 coatings.**

***Keywords*—Al_2O_3, $AlPO_4$, plasma spray, coating, impregnation.**

I. Introduction

Thermal spraying is a commonly utilized technology for creating coated layers on various surfaces. Plasma spraying is a type of thermal spray coating process that uses a high-energy plasma jet (with a temperature up to 15000 °C) to melt and propel material onto a substrate to form a dense, well-adhered coating with desirable properties such as wear resistance, corrosion resistance, thermal insulation, and electrical conductivity. One particular application of plasma spraying is the formation of an Al_2O_3 insulation layer on steel surfaces for the company BSH drives and pumps s.r.o. (BSH). However, thermally sprayed coatings can suffer from a lack of homogeneity. They often contain defects generated by unmelted particles, pores, cracks, and delaminations (~ 1-10 µm). [1]

Thermally sprayed Al_2O_3 coatings differ in their mechanical, technical or electrical parameters from their substrate material. [2]

To reduce the impact of defects and to improve the properties of these coatings, post-processing techniques are employed. In the past, various post-processing techniques like sealing, isostatic pressing (100-700 MPa), laser and spark sintering, and annealing (500-1000 °C) have been used to improve thermally sprayed coatings. Al_2O_3 coatings are used as an electrical insulation layer between steel substrates and electrically conductive heating layers in the heating elements of the company BSH. However, the Al_2O_3 insulation layer exhibits electrical resistance changes (up to 100 kΩ) based on air humidity levels. Post-processing techniques can strengthen the weak points of thermally sprayed coatings by filling pores and cracks on the surface and by reducing humidity distribution, thus improving resistance. Further studies are being conducted on the application of post-processing sealing to plasma-sprayed Al_2O_3 coatings in order to enhance their resistance. [2]

II. Production and analysis

According to current knowledge, $AlPO_4$ sealing is an effective method for enhancing the durability of plasma-sprayed Al_2O_3 coatings. The sealing process improves dry abrasion wear resistance, erosion wear resistance, and corrosion resistance by forming a crystalline phosphate phase with the coating. This reaction is also expected to increase the electrical resistance (up to 100 kΩ). Overall, $AlPO_4$ sealing is a promising technique for improving the performance of Al_2O_3 coatings in various applications. [3]

A. Samples preparation

Experiments were conducted using commercially available steel plates that were laser cut into small samples measuring 20 mm x 30 mm with a thickness of 1.2 mm. The samples underwent abrasive grit blasting to remove the surface oxidation layer mechanically with final surface roughness (Ra 2,5 µm). On the clean steel surface, a NiCr adhesive layer (~10 µm) was applied by plasma spraying, which was directly followed by the application of an Al_2O_3 insulation layer (thickness ~300 µm) from a second plasma torch. The prepared samples were then used for the experimental application of prepared $AlPO_4$ sealing. Fig. 1 shows a cross-section of the prepared initial sample.

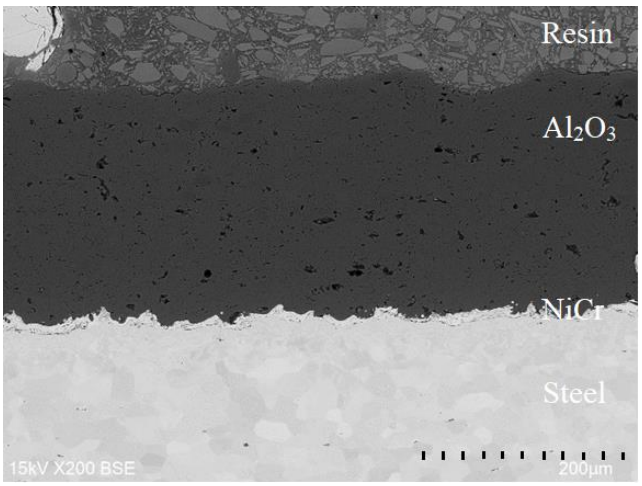

Fig. 1. Cross section of initial sample without $AlPO_4$ sealing

B. Slurry preparation

Experiments have been conducted on an $AlPO_4$ nanocomposite slurry used for sealing of plasma-sprayed Al_2O_3 coatings. The slurry was produced by mixing Al_2O_3 nanopowder, H_3PO_4, and $Al(OH)_3$ in a Resodyn lebram acoustic mixer (30 minutes with acceleration 21 Gs). The prepared slurry was then applied on the Al_2O_3 surface of the investigated samples using a brushing technique and the slurry was then fired in an oven (~ 1000 °C). The focus of the experiments was to analyze the penetration of the composite into the Al_2O_3 layer, specifically in terms of filling the pores and cracks and creating a homogeneous surface. Fig. 2 shows a cross section of the applied slurry. [4]

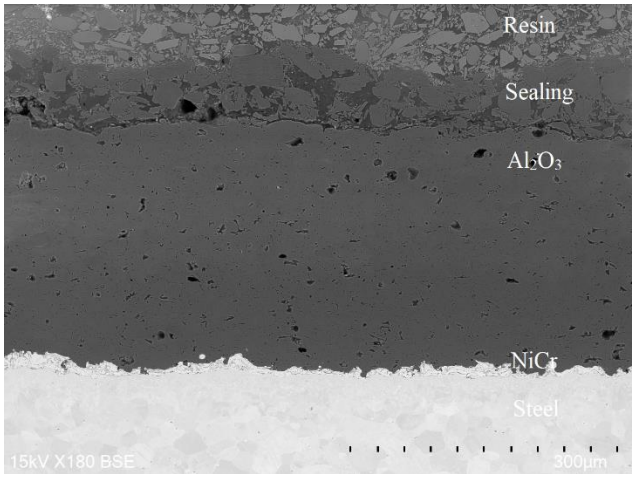

Fig. 2. Cross section of initial sample with $AlPO_4$ sealing

C. Sample analysis

The Al_2O_3 nanopowder used to produce the slurry has a tendency to form agglomerates (~10 times than the pores and cracks), which can limit its ability to fill the pores and cracks in the plasma-sprayed Al_2O_3 coatings. Typical agglomerates in the initial 20 nm Al_2O_3 nanopowder with more than 100 µm diameter are shown in Fig. 3. Acoustic mixing was used to break up these agglomerates, but it was not energetic enough to achieve a complete deagglomeration. As a result, some of the agglomerates remain in the slurry and cannot fill the pores and cracks that are several times smaller than the agglomerates themselves. In the follow-up analysis, the 20 nm Al_2O_3 nanopowder was used as an input, and it was found that there were already large agglomerates present even before the slurry mixing process.

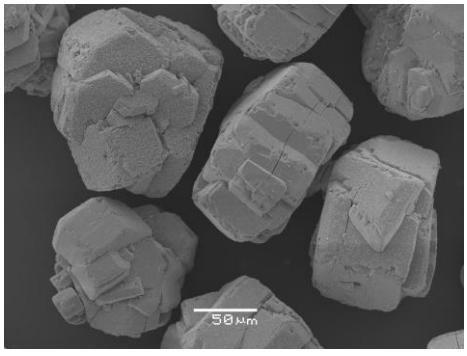

Fig. 3. Microscopic view of agglomerates inside initial 20 nm Al_2O_3 nanopowder

Firing the slurry in the oven helps to promote thermochemical reactions of the crystalline phosphate phase that improve the tenacity of the coating. However, the different thermal expansion coefficients of steel and Al_2O_3 (Al_2O_3 is about half of steel) can cause the steel substrate to bend during the firing, which can have a negative effect on the coating and lead to delamination. Overall, the $AlPO_4$ nanocomposite slurry shows to be a promising sealing material for plasma-sprayed Al_2O_3 coatings. Further research is needed to optimize the slurry composition and application process to improve its effectiveness and reliability.

III. Future work

Manual slurry application with a brush seems to be easy and cost-effective, although it is not possible to apply a homogeneous layer. The currently produced slurry is weakly compacted and contains large agglomerates (with a size of tens of µm). The agglomerated structure demonstrates poor penetration into the Al_2O_3 layer and predominantly remains on the surface.

Before initiating a new round of sampling, it appears necessary to remove agglomerates from the Al_2O_3 nanopowder. Ultrasonic or acoustic mixing alone is insufficient to produce a nanostructured slurry without agglomerates. Planetary ball milling is a dry grinding technique that uses high-energy collisions between grinding balls and the powder to break up the agglomerates and thus produces uniform nanoparticles. Hence, the ball milled Al_2O_3 nanopowder is presumed to have higher efficiency in disintegrating the agglomerates, followed by acoustic mixing of the slurry. For the next sampling, it is preferable to use a semi-automatic application by an electrostatic spray gun. [5]. The samples and slurry currently used are compatible with the mentioned spray technique. The third improvement step could include laser sintering of the applied slurry as an alternative to regular oven firing. Heating the entire sample in an oven can cause deformation of the steel substrate and delamination of the Al_2O_3 layer due to the different temperature expansion coefficients of the substrate and coating.

References

[1] P.L. Fauchais; J.V.R. Heberlein; M.I. Boulos, *Thermal spray fundamentals*. New York: Springer, 2014, ch. 2, 17.

[2] R.B. Heimann, *Plasma spray coating*. New York: Wiley-VCH, 1996, ch.4, 5, 6.

[3] M. Vippola; J. Vuorinen; P. Vuoristo; T. Lepisto; T. Mantyla, "Thermal analysis of plasma sprayed oxide coatings sealed with aluminium phosphate," *Journal of the European ceramic society 22*, 2002, pp 1937-1946

[4] H. Li; Z. Ke; J. Li; L. Xue; Y. Yan, "An effective low-temperature strategy for sealing plasma sprayed Al2O3-based coatings," ," *Journal of the European ceramic society 38*, 2018, pp 1871-1877

[5] A.G. Bailey, "The science and technology of electrostatic powder spraying, transport and coating," *Journal of the electrostatic 45*, 1995, pp 85-120

Stylistic Patterns in Source Code as Behavioral Biometric Markers for Programmer Identification

[1]*Marek HORVÁTH (1st year),*
Supervisor: [2]*Emília PIETRIKOVÁ*

[1,2]Department of Computers and Informatics, FEI TU of Košice, Slovak Republic

[1]marek.horvath@tuke.sk, [2]emilia.pietrikova@tuke.sk

***Abstract*—This study explores the integration of behavioral biometrics with programming styles to improve programmer identification methods. By utilizing stylometric analysis machine learning techniques, it identifies coding habits that serve as unique biometric markers. The research examines the role of programming style in improving cybersecurity, verifying authorship, and reducing plagiarism, while also considering the accuracy of algorithms and privacy issues. The findings contribute to the review of the most recent digital authentication techniques directions, highlighting opportunities for research in digital identity security.**

***Keywords*—Behavioral Biometrics, Intellectual Property Protection, Programmer Identification, Programming Style Analysis, Software Security, Source Code Stylometry**

I. Introduction

The addition of behavioral biometrics to the digital authentication and cybersecurity areas introduces a practical approach to security. By analyzing the unique programming styles and behaviors, this method offers a complementary alternative to traditional biometric systems. It focuses on understanding the problem-solving patterns and distinct coding habits of users, contributing to the development of new identity verification techniques.

Behavioral biometrics have several practical advantages [1]:

- *Continuous Verification:* They offer the ability to constantly check who is using the system, maintaining security beyond the initial login.
- *Subtle Data Gathering:* Data can be collected in a way that doesn't interrupt or inconvenience the user.
- *Standard Equipment:* They can often use existing devices, like standard cameras and microphones, for data collection, eliminating the need for special hardware.
- *Reliable Authentication:* These biometrics are valuable for ongoing verification processes, reinforcing security defenses without being the sole security measure.

Adding to the discussion on the benefits of behavioral biometrics, keystroke dynamics, alongside mouse movements and GUI interaction patterns, form a trio of behavioral biometrics that enhance user authentication methods. Keystroke dynamics, in particular, capture the unique patterns of how a user types, similar to a personal signature. Machine learning leverages these patterns to differentiate users [2]. These methods contribute to security by:

- Establishing a system for continuous verification, which is crucial in maintaining the integrity of software development environments.
- Providing cost-effective and subtle security enhancements that strengthen both login procedures and the surveillance of sensitive areas without being invasive [3].

The conversation also extends to *code stylometry*, which analyzes the textual and structural features of source code for authorship determination. Evidence suggests that aspects such as code structure, naming conventions, and formatting choices are markers for distinguishing programmers [4]. Looking at code on sites like GitHub helps us see the challenges of staying anonymous while still taking responsibility for the work. This kind of review not only shows who's contributing what but also helps in figuring out who might be behind controversial projects. It points out how important it is to find the right mix of keeping things private and being open in software development [5].

The use of both static and dynamic analysis techniques provides a way to document a programmer's style. This mix of looking at how people code in real-time and checking their source code offers a clear insight into different programming styles [6]. It is key to developing effective models that can rightfully associate code with its creators, improving integrity and security.

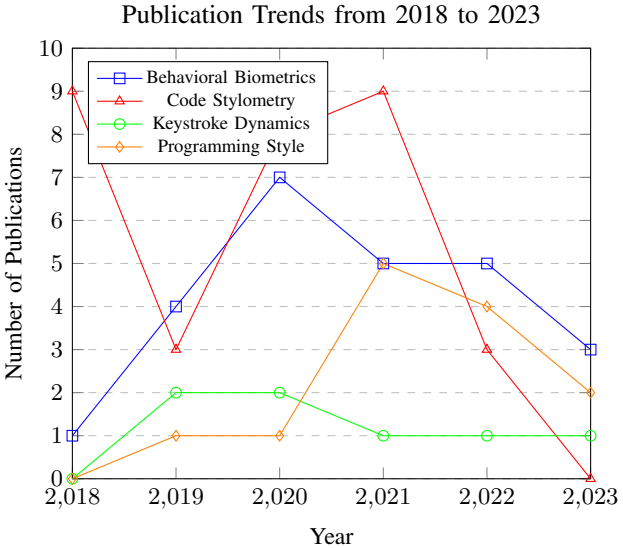

Figure I illustrates the publication trends within behavioral biometrics from 2018 to 2023. This summary, retrieved from Scopus database searches, reflects consistent scholarly engagement with four central themes: Behavioral Biometrics, Code Stylometry, Keystroke Dynamics, and Programming Style. The trends indicate a variable yet ongoing interest in these

subjects. The data shows more people are studying Behavioral Biometrics, hinting at a growing interest that might be leading to more agreement among researchers. In the case of Code Stylometry, the fluctuating number of publications may be influenced by the recurring patterns of research interests or external factors impacting cybersecurity. Keystroke Dynamics maintains a constant presence in the literature. Meanwhile, the rise in research related to Programming Style could point to its increasing relevance and the community's rising interest in the use of coding as a unique identifier.

II. Current Status of Behavioral Biometrics in Programmer Identification

Combining behavioral biometrics with identifying programmers is a practical step forward in cybersecurity, software forensics, and digital authentication. This emerging area connects computer science with behavioral analysis, aiming to use unique coding patterns and styles to recognize programmers. More and more studies are using detailed computer analysis to understand these coding styles better, which could help in accurately figuring out who wrote a piece of code and in keeping digital information safe.

A. Current research directions

Identifying programmers now involves an integrated analysis of various elements, as shown in Figure 1. This includes methods of user authentication through GUI interaction, keystroke, and mouse dynamics, along with task interaction patterns like scrolling, task switching, and text searching. Further, it involves a detailed look at programming style, version control habits, and problem-solving techniques, each contributing unique insights into an individual's coding approach.

- *Keystroke and Mouse Dynamics:* The detailed analysis of how programmers interact with their keyboards and mice provides patterns that are valuable for behavioral biometric systems. This method is getting better at noticing the unique ways people use their keyboards and mice, which helps tell users apart [7], [2].
- *Graphical User Interface (GUI) Interaction Analysis:* Studying how users navigate and interact with GUI elements offers additional behavioral data, enriching the biometric profile of users and complementing keyboard and mouse dynamics for a complete behavioral biometric system [7].
- *Task Interaction Patterns:* Studying how people switch tasks, search for text, and scroll could improve the way we understand and use behavioral biometrics. These interactions have not yet been fully explored and thus present an opportunity for contributions to the field [7].
- *Cognitive Biometrics from Problem-Solving:* EEG variations during problem-solving tasks in different programming environments suggest the presence of unique cognitive biometric markers. These markers could provide insights into a programmer's thought process and offer an additional layer of identification [8].
- *Version Control Commit Analysis:* Investigating the patterns within version control commits, particularly from repositories like Git, can bring valuable biometric data. Looking at version control logs can offer clues about who wrote certain pieces of code by examining the record of their changes [5].
- *Programming Style Analysis:* Specifics of programming styles, such as naming conventions, indentation, and error handling, provide the basis of source code stylometry. This analysis uses a broad set of features to build a profile that can be used for authorship attribution with high precision [9].
- *Comment Analysis for Biometric Identification:* Analytical tools that can process syntactic and semantic patterns, such as Code2Vec and CodeBERT, indicate that personal coding styles reflected in comments can be used for biometric identification. [10]

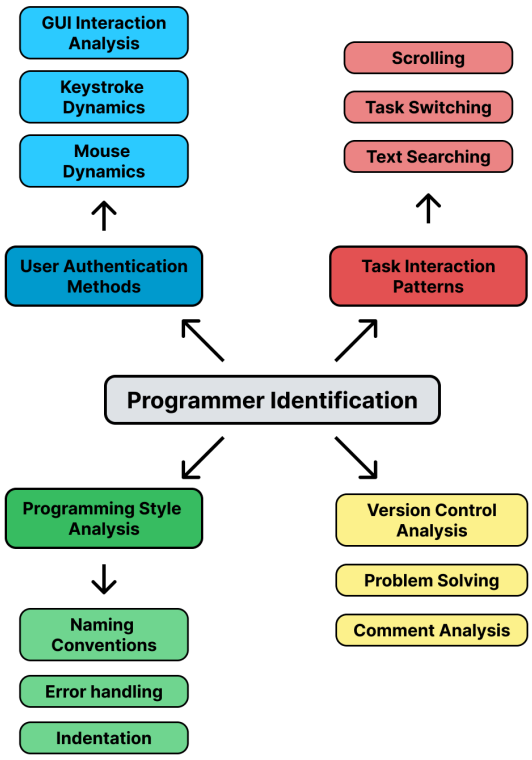

Fig. 1. Conceptual Framework of Behavioral Biometrics in Programmer Identification

B. Research opportunities and new directions

Research into *programming styles* as a way to identify coders has been making steady progress, with different areas working together more. This research aims to improve how we confirm a programmer's identity, providing useful tools for digital security and protecting creative work. Regularly reviewing coding styles is practical for confirming identities online. Knowing who wrote the code is helpful, especially when many people contribute to a project or in schools, where you need to be sure students are turning in their own work. Looking closely at how code is written can help identify the writer and prevent copying, while also encouraging students to be original [7]. Focusing on honest work helps prepare them for professional expectations. We've described this approach in Table I, which includes the characteristics that help match coders with their styles.

TABLE I
KEY FEATURES FOR CODE STYLE ANALYSIS [11]

Feature	*Explanation*
Keyword Usage	Frequency of keywords typical to the programming language.
Operator Use	Distribution of arithmetic and logical operators.
Code Tokens	Variety and frequency of language-specific tokens.
Literal Values	Use of numbers, strings, and characters as constants.
Function Definitions	Quantity and average length of functions in the code.
Comment Style	Frequency and length of comments used for documentation.
Indentation Pattern	Style and consistency of indentation in code blocks.
Line Formatting	Use of whitespace and character alignment in lines.
Code Organization	Structuring and arrangement of code sections and blocks.
Syntax Complexity	Depth and intricacy of the code's syntax structure.
Variable Naming	Convention and consistency in naming variables.
Error Handling	Methods and frequency of error-checking routines.

Using *stylometric methods* for forensic analysis shows how flexible this research can be. In situations involving security breaches or the spread of malicious code, being able to trace code back to its author is crucial for cybersecurity measures. Developments like the *"SnapCode"* method, which uses snapshots to automatically pull out code features, go further than old-school manual ways of doing extraction. This progress helps a lot with figuring out who wrote the code and finding copied work, giving us a clearer picture of different ways to write code [12]. Continuously developing scalable and precise models for programmer identification is a consistent research focus. New methods are being developed to make models more scalable and accurate, making them useful for various programming situations and addressing problems like copyright disputes, plagiarism, and maintaining the trustworthiness of collaborative platforms [13].

The investigation of stylistic analysis for author identification reveals that programmers have unique coding styles, similar to how everyone has distinct handwriting [14]. As we use behavioral biometrics in programming, it's important to think about privacy and be careful. Making sure we protect people's privacy and use clear, safe methods is crucial as we improve how we identify programmers [6].

III. ANALYSIS OF SOLVED AND UNSOLVED CHALLENGES IN PROGRAMMING STYLE RECOGNITION

In this section, we're looking at how other researchers have used programming styles to recognize the authors of code. The focus is on studies that apply machine learning to identify the unique signatures in coding styles. These efforts reveal the potential of this approach, but they also bring several challenges. From privacy concerns to ensuring these methods can be used in real-world applications.

A. Achievements in behavioral biometrics

Machine learning successes: Recent advancements in *machine learning* have enhanced our ability to analyze coding behavior, enabling us to detect unique patterns that are specific to individual programmers. This has led to the development of models that can effectively distinguish between programmers by examining various aspects of their coding habits. These models have demonstrated their utility in *authorship verification*, providing a mechanism for countering *plagiarism* [6].

The research [15] has explored various methodologies for attributing authorship to source code. While *abstract syntax trees* (ASTs) offer an initial approach to identifying stylistic elements, the limited set of features analyzed may not capture the full spectrum of an author's style, particularly in shorter code samples. In contrast, *n-gram analysis* provided a more detailed and consistently accurate identification, possibly due to its expansive feature set. The fusion of AST and n-gram features resulted in the most accurate authorship prediction, benefiting from a richer array of coding characteristics. This integrated approach points to the future direction of using machine learning to improve recognition techniques, with potential applications in verifying code authorship in both educational and legal settings.

Research by Caliskan-Islam et al. and Dauber et al. [5] demonstrates the effectiveness of machine learning techniques in *de-anonymizing programmers* through a hybrid lexical-syntactic analysis of source code. Their work analyzed a dataset of source code from 1,600 programmers, all participants in the Google Code Jam, an annual international programming competition. This dataset includes a broad range of programming tasks and was subjected to analysis with a *random forest classifier* to accurately link programmers with their specific snippets of code [4].

In the process of this machine learning study, attributes such as comment naming conventions, the use of variables and functions, and structural elements like program formatting were taken into account. Out of over 120,000 features, the most impactful 928 were identified, with a significant portion being syntactic, while others were related to layout and lexical choices. These features were found to be resilient against class changes, maintaining the distinctiveness of a programmer's coding style even when faced with a variety of tasks, from simple to complex. It was noted that programmers with more extensive skill sets were more easily identifiable, indicating that the proficiency of a programmer can be reflected in their coding style [8].

Researchers also observed that the coding style becomes more obvious during the implementation of more challenging tasks, offering a clearer biometric marker for identification purposes [9]. A subset of the features that demonstrated information gain in a smaller 250 programmer dataset was extracted and applied to this larger dataset, helping to confirm the scalability of the approach. The use of a random forest with fewer trees than might be expected did not significantly affect accuracy, highlighting the effectiveness of the chosen features. This approach could de-anonymize programmers using limited computational resources, demonstrating the potential for practical application on a large scale.

In summarizing the dataset and methodology, the characteristics of the 1,600 programmers in the dataset, including the types of programming tasks and the specific features

used for machine learning, were crucial in achieving a high level of accuracy in programmer identification. This data underscores the importance of selecting appropriate features and the potential for machine learning to scale effectively for large datasets.

B. Unresolved challenges and ethical considerations

In the area of behavioral biometrics, there are also several challenges and ethical considerations to be mindful of:

- *Algorithmic refinement:* The diversity of coding styles and programming languages poses a challenge in developing algorithms that can universally capture the programming style. The quest for a model adaptable across various environments points to the need for further research into flexible and versatile algorithms [16].
- *Privacy versus security:* This ethical dilemma involves balancing the need for security with the protection of privacy rights. The process of monitoring and analyzing programming behavior for identification must be conducted ethically, with respect for individual privacy [7].
- *Real-world application integration:* Applying programming style analysis in areas like digital forensics and cybersecurity raises questions about its practicality [13].

IV. Conclusion

Research into the current state of *programming style as a behavioral biometric marker* has brought us several insights that we'll use in further research. Behavioral analysis offers practical applications such as user authentication and subsequent content verification, using biometrics to uncover plagiarism, or ensuring software integrity. The combination of behavioral biometric data represents a link between computer science and other fields, which could lead to a wide range of applications.

The most crucial part was finding and analyzing different ways to identify a programmer. Based on the literature, we've categorized these methods into several groups:

- *User authentication methods:* This includes mouse and keystroke dynamics as well as GUI interaction.
- *Task interaction patterns:* Such as text searching, task switching, scrolling.
- *Programming style analysis:* Including naming conventions, error handling, indentation.
- *Other types* like version control analysis, problem-solving, comment analysis.

Another focus of our review was the application of *machine learning techniques* in processing source code, leading to successful de-anonymization of programmers. These techniques, particularly through the analysis of large datasets have highlighted the power of machine learning in distinguishing programmers based on their unique coding styles. Notable methods, such as the use of *abstract syntax trees* (ASTs) and *n-gram analysis*, have improved the precision of identifying programmers. These machine learning models showing a high level of accuracy in recognizing individual programmers' signatures.

In our future research, we will investigate these categories and explore their application in practical tasks, such as datasets from school assignments in various languages, where we will test their effectiveness in the clear identification of a programmer. The issues of multiple types of architectures, programming languages, or approaches remain an unresolved challenge in this area. Moreover, it's important to consider *privacy and security*. The last recognized challenge is integrating these findings into real-world systems.

Acknowledgment

This work was supported by project VEGA No. 1/0630/22 "Lowering Programmers' Cognitive Load Using Context-Dependent Dialogs"

References

[1] M. Sharma and H. Elmiligi, *Recent Advances in Biometrics*. IntechOpen, 2022. [Online]. Available: http://dx.doi.org/10.5772/intechopen.102841

[2] S. Krishnamoorthy, L. Rueda, S. Saad, and H. Elmiligi, "Identification of user behavioral biometrics for authentication using keystroke dynamics and machine learning," 05 2018, pp. 50–57.

[3] D. D. Alves, G. Cruz, and C. Vinhal, "Authentication system using behavioral biometrics through keystroke dynamics," in *2014 IEEE Symposium on Computational Intelligence in Biometrics and Identity Management (CIBIM)*, 2014, pp. 181–184.

[4] A. Caliskan-Islam, R. Harang, A. Liu, A. Narayanan, C. Voss, F. Yamaguchi, and R. Greenstadt, "De-anonymizing programmers via code stylometry," in *24th USENIX Security Symposium (USENIX Security 15)*. Washington, D.C.: USENIX Association, aug 2015, pp. 255–270. [Online]. Available: https://www.usenix.org/conference/usenixsecurity15/technical-sessions/presentation/caliskan-islam

[5] D. Watson, "Source code stylometry and authorship attribution for open source," Master's thesis, 2019. [Online]. Available: http://hdl.handle.net/10012/15134

[6] N. Wang, S. Ji, and T. Wang, "Integration of static and dynamic code stylometry analysis for programmer de-anonymization," in *Proceedings of the 11th ACM Workshop on Artificial Intelligence and Security*, ser. AISec '18. New York, NY, USA: Association for Computing Machinery, 2018, p. 74–84. [Online]. Available: https://doi.org/10.1145/3270101.3270110

[7] K. O. Bailey, J. S. Okolica, and G. L. Peterson, "User identification and authentication using multi-modal behavioral biometrics," *Computers and Security*, vol. 43, pp. 77–89, 2014. [Online]. Available: https://www.sciencedirect.com/science/article/pii/S0167404814000340

[8] D. Watson, "Source code stylometry and authorship attribution for open source," Master's thesis, University of Waterloo, Waterloo, Ontario, Canada, 2019, c Daniel Watson 2019.

[9] I. Krsul and E. H. Spafford, "Authorship analysis: Identifying the author of a program," *Computers & Security*, vol. 16, no. 3, pp. 233–257, 1997.

[10] W. Ou, S. H. H. Ding, Y. Tian, and L. Song, "Scs-gan: Learning functionality-agnostic stylometric representations for source code authorship verification," *IEEE Transactions on Software Engineering*, vol. 49, no. 4, pp. 1426–1442, 2023.

[11] W. Dong, Z. Feng, H. Wei, and H. Luo, "A novel code stylometry-based code clone detection strategy," in *2020 International Wireless Communications and Mobile Computing (IWCMC)*, 2020, pp. 1516–1521.

[12] S. A. P. Sarnot, S. Rinke, R. Raimalwalla, R. Joshi, R. Khengare, and P. Goel, "Snapcode - a snapshot based approach to code stylometry," in *2019 International Conference on Information Technology (ICIT)*, 2019, pp. 337–341.

[13] C. Aguilera Gonzalez, L. Albors Zumel, J. Antonanzas Acero, V. Lenarduzzi, S. Martinez-Fernandez, and S. Rabanaque Rodriguez, "A preliminary investigation of developer profiles based on their activities and code quality: Who does what?" in *2021 IEEE 21st International Conference on Software Quality, Reliability and Security (QRS)*, 2021, pp. 938–945.

[14] R. R. Joshi and R. V. Argiddi, "Author identification: an approach based on style feature metrics of software source codes," *International Journal of Computer Science and Information Technologies*, vol. 4, no. 4, 2013.

[15] S. F. Frankel and K. Ghosh, "Machine learning approaches for authorship attribution using source code stylometry," in *2021 IEEE International Conference on Big Data (Big Data)*, 2021, pp. 3298–3304.

[16] M. Iqbal, A. Raza, M. Aslam, M. Farhan, and S. Yaseen, "A stylometric fingerprinting method for author identification using machine learning," *Technical Journal*, vol. 28, no. 01, pp. 28–35, Mar 2023.

Containerization in Edge Intelligence

[1]*Ľubomír URBLÍK (2nd year),*
Supervisor: [2]*Peter PAPCUN*

[1,2]Dept. of Cybernetics and Artificial Intelligence, FEEI TU of Košice, Slovak Republic

[1]lubomir.urblik@tuke.sk, [2]peter.papcun@tuke.sk

***Abstract*—The onset of cloud computing brought with it an adoption of containerization – a lightweight form of virtualization, which provides an easy way of developing and deploying solutions across multiple environments and platforms. Certain applications run into obstacles when deployed on the cloud due to the latency it introduces or the amount of data that needs to be processed. These issues are addressed by edge intelligence. This paper describes our approach to data processing and artificial intelligence at the network's edge. We describe the creation of a custom framework to support development and deployment of edge intelligence solutions.**

***Keywords*—containerization, edge computing, edge intelligence, data processing**

I. Introduction

Clive Humby stated that "data is the new oil" in 2006 [1]. Like oil, the value of data is primarily found in its many applications, but in its raw form, it is essentially useless [2]. Cloud computing has become incredibly popular in the last ten years. However, there are disadvantages to this strategy as well. According to Berisha et al. [3], each person generates approximately 1.7 MB of data per day, or 44 zettabytes total. A ZepDo analysis [4] states that approximately 4 zettabytes of data are transmitted over the internet annually worldwide. By comparing these numbers, we can observe that a vast quantity of data is never sent to the cloud, where it may be squandered without yielding valuable insights.

II. The Initial Status

At last year's conference, we discussed the load distribution between edge and cloud environments in the Internet of Things (IoT). The main idea was to intelligently distribute the tasks between the cloud and the edge to achieve ideal performance in terms of latency. We looked at various approaches to load balancing, task distribution, and task offloading and their specific advantages and disadvantages. These ranged from simple random algorithms to swarm intelligence-based algorithms.

When working on our solution, we ran into a problem with existing approaches to data processing on the edge – the granularity of the software used. The solutions were often created as monoliths, and all of the data processing took place inside a single application. Distributing such solutions is not ideal, as certain steps in the processing may be too demanding for an edge device.

During our research, we came across Directed Acyclic Graphs (DAGs) and their use in data processing [5]. This approach splits the entire process into a series of steps called nodes and manages the data flow from one node to the next. These steps can be concurrent or sequential. The utilization of DAGs allows for an easy visualization of the entire process. Splitting the data processing into steps is more similar to the microservice architecture (MSA), which is heavily used in current software development. In MSA the services are connected via Application Programming Interfaces (APIs) which exchange data using common protocols and data formats, such as HTTP or MQTT and JSON or XML. The main advantage of this approach is the ability to change the inner workings of a service without affecting any other parts of the application.

III. Objectives Solved in Previous Year

In order to be able to distribute the data processing tasks between the edge and the cloud, the entire process must be able to be split into a series of steps [6]. We drew inspiration from a pipeline approach to data processing, where the output from one step is an input to the next step [7].

We use containers to make our solution portable – to be able to deploy it in both edge and cloud environments without the need to modify the solution. Docker containers are OCI compliant [8] and can be used with other container platforms and tools, which makes them suitable for this use case. We have split the processing pipeline into a series of steps, where each step is deployed as its own container, together with all the relevant libraries and data needed to run the task correctly. The full architecture of our solution is shown in Fig. 1. We employ environmental variables during deployment to change the parameters as needed [9].

The communication between containers is done using ZeroMQ, an asynchronous messaging library fit for use in distributed solutions. We have also selected this library because of its compatibility with many programming languages. We want our framework to be modular and for users to be able to create their own tasks and seamlessly integrate them with existing parts. ZeroMQ allows us to do this as the parts are independent from each other, and the only thing that matters is the data sent between them. We have developed a few example processing tasks, which we call services. The first is the transformation of the input data. Data can arrive in various formats, but most often in JSON or as a raw value. The data must, therefore, be transformed to a unified format so other parts of the pipeline can process it. The data is loaded using the MQTT broker, where the transformation container is subscribed to the topic named after the data source. The other approach uses HTTP or MQTT to query the device for new data in predefined intervals. We are also currently implementing a database connector, where the transformation container can connect to a wide array

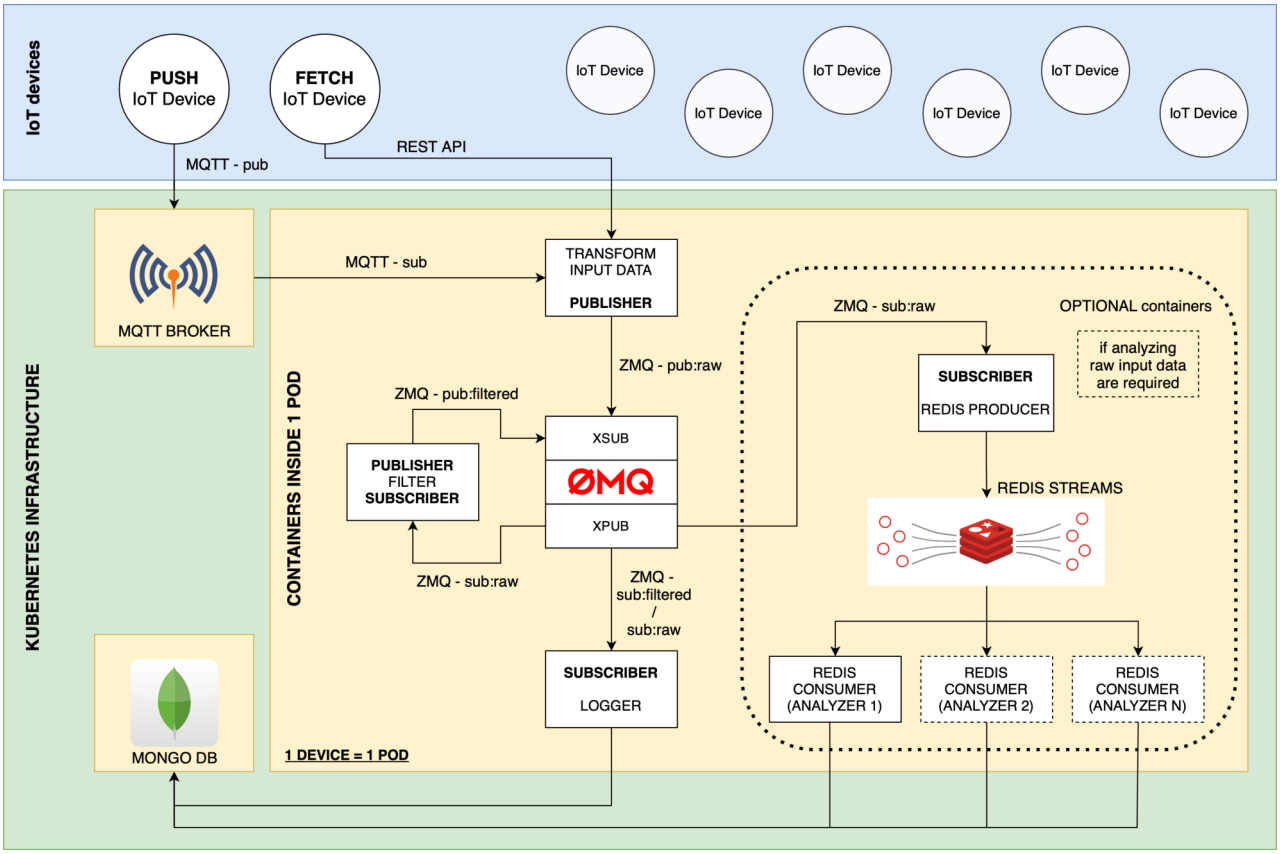

Fig. 1: The architecture of our solution [9]

of relational databases and load the data whenever a new value appears or in predefined intervals. The second is the filtering service. The data can be filtered either by defining threshold values or by the rate of change. To be able to measure the rate of change, we use the Redis Streams database as a temporary storage. The data is then saved into a MongoDB database for long-term storage.

We use Kubernetes (K8s), a container orchestration platform, to manage the entire pipeline. Each device is added as a worker node to the K8s cluster, where it can be easily managed from the manager node. The nodes can be labeled to allow tasks to be assigned to a specific node. We can select nodes based on the distance from the data source, their processing capabilities, or connected devices. We can also monitor the entire cluster using existing tools, for example, OpenLens. Each data source is deployed as a pod containing all the selected services, which are represented as containers inside the pod.

IV. Future work

As previously mentioned, we are working on expanding our framework to include more predefined services. We want to include artificial intelligence and machine learning capable services, both for training and inference, to enable edge intelligence. We are currently transforming existing edge solutions to containers while preserving full functionality. The setup of such solutions is difficult as libraries are very dependent on versions of other libraries, and to ensure compatibility across heterogeneous edge environments, all the versions must be correct and inter-compatible.

The end goal of our research is the proposal and development of a modular data processing framework inspired by DAGs and capable of a wide array of tasks. The framework should also provide a no-code or low-code way of creating a data processing pipeline. After the pipeline is created, the framework should distribute the tasks across devices on both edge and cloud to achieve ideal performance in terms of latency.

Acknowledgment

This publication was supported by the APVV grant ENISaC - Edge-eNabled Intelligent Sensing and Computing (APVV-20-0247).

References

[1] C. Arthur, “Tech giants may be huge, but nothing matches big data,” *The Guardian*, 8 2013. [Online]. Available: https://www.theguardian.com/technology/2013/aug/23/tech-giants-data

[2] D. D. Hirsch, “The glass house effect: Big data, the new oil, and the power of analogy,” *Me. L. Rev.*, vol. 66, p. 373, 2013.

[3] B. Berisha, E. Mëziu, and I. Shabani, “Big data analytics in cloud computing: an overview,” *Journal of Cloud Computing*, vol. 11, no. 1, p. 24, aug 2022.

[4] E. Alexander, “Essential internet traffic statistics in 2024 • zipdo,” jun 2023. [Online]. Available: https://zipdo.co/statistics/internet-traffic/

[5] T. Malaska and S. Babu, *Rebuilding reliable data pipelines through modern tools*, first edition. ed. Sebastopol, CA: O’Reilly Media, 2019.

[6] P. Pääkkönen and D. Pakkala, “Extending reference architecture of big data systems towards machine learning in edge computing environments,” *Journal of Big Data*, vol. 7, no. 1, Apr 2020.

[7] G. Rong, Y. Xu, X. Tong, and H. Fan, “An edge-cloud collaborative computing platform for building aiot applications efficiently,” *Journal of Cloud Computing*, vol. 10, no. 1, Jul 2021.

[8] “About the open container initiative.” [Online]. Available: https://opencontainers.org/about/overview/

[9] L. Urblik, E. Kajati, P. Papcun, and I. Zolotova, “A modular framework for data processing at the edge: Design and implementation,” *Sensors*, vol. 23, no. 17, 2023. [Online]. Available: https://www.mdpi.com/1424-8220/23/17/7662

Adaptive Edge-Based Computing in Autonomous Vehicle Mobility

[1]*Matúš Čavojský (1st year),*
Supervisor: [2]*Gabriel Bugár*

[1,2]Dept. of Electronics and Multimedia Communications, FEI TU of Košice, Slovak Republic

[1]matus.cavojsky@tuke.sk, [2]gabriel.bugar@tuke.sk

***Abstract*—This paper explores the challenges and opportunities of applying split computing techniques to semantic segmentation models for autonomous vehicles. Semantic segmentation is a critical function for autonomous vehicles to understand and navigate the environment, but it requires substantial computational resources. Model pruning combined with edge computing emerges as a promising strategy for handling computational demands, entailing offloading some processing load to the edge server while maintaining a streamlined model on the device, thus enabling efficient image segmentation in autonomous vehicles without sacrificing speed or accuracy, motivating the focus of this work on developing efficient network architectures for on-device segmentation. The paper evaluates the performance and efficiency of different U-Net architectures, a popular model for image segmentation. The paper also proposes future research directions to enhance semantic segmentation for autonomous vehicles, such as early exiting, sensor fusion, and federated learning.**

***Keywords*—Autonomous Vehicles, Convolutional Neural Networks, Semantic Segmentation, Multi-Access Edge Computing**

I. Introduction

Mobile devices, autonomous vehicles, and drones are increasingly harnessing the power of artificial neural networks (ANNs) for a variety of complex inference tasks, including the critical function of image segmentation. Image segmentation, particularly essential in autonomous vehicles for understanding and navigating the environment, demands substantial computational resources. The continuous operation of complete neural networks for tasks like image segmentation on a mobile device can rapidly exhaust battery life and overwhelm the processor [1]. While offloading tasks to edge servers can alleviate the computational burden on the mobile device, factors such as unpredictable channel quality and varying loads on the network and edge servers can introduce significant delays [2].

In response to these challenges, recent innovations in split computing [3] (SC) offer a promising solution by dividing the ANN into two segments: a head model that operates on the mobile device and a tail model that runs on the edge server, enhancing efficiency by potentially reducing bandwidth usage and energy consumption. This approach is particularly relevant to autonomous vehicles, where real-time image segmentation is crucial for safety and navigation. Furthermore, the concept of early exiting [4] (EE) introduces multiple "exits" within the network architecture, allowing for a balance between model accuracy and execution time, adaptable to current needs or specific application demands. Matsubara et al. [5] suggests the research to focus on expanding the application domain of SC and EE to include more types of ANNs such as image segmentation.

II. Related Work

Image segmentation allows for the precise identification and localization of various objects within the driving environment, such as vehicles, pedestrians, and road markers. Semantic segmentation, a subset of image segmentation, assigns a semantic label to each pixel in an image, enabling precise identification and understanding of objects and their boundaries within the scene, enhancing situational awareness and perception accuracy, which are vital for navigating complex traffic scenarios and adapting to dynamic environmental conditions such as rain or fog [6]. This capability is crucial for making informed decisions and ensuring safety on the road.

Among the architectures developed for this purpose, SegNet and U-Net stand out due to their distinct approaches to segmentation. SegNet [7], recognized for its memory-efficient encoder-decoder architecture, emphasizes context capture and pixel-wise classification with minimal computational overhead by storing only max-pooling indices. Conversely, U-Net [8] introduces skip connections between encoder and decoder components, enhancing spatial information preservation and facilitating precise localization, thus showing particular efficacy in medical and complex urban environment segmentations.

Recent advances have led to innovative U-Net modifications to handle various semantic segmentation difficulties. Attention-Based U-Net [9] refines emphasis on key picture regions with attention gates, boosting segmentation accuracy without increasing model complexity. Recurrent neural network elements in the Recurrent U-Net [10] can use temporal information in video sequences to improve scene interpretation in dynamic driving situations.

III. Description of the tasks solved

Applying split computing techniques to networks like U-Net [8], which are one of the most common models for image segmentation due to their sophisticated layer interdependencies, presents unique challenges. The architecture of U-Net, which requires the integration of information from previous layers into subsequent ones, complicates the straightforward application of split computing. As a result, model pruning, a technique that involves reducing the size of a neural network by

removing unnecessary parameters and connections, together with edge computing, emerges as a promising approach for managing computational requirements, thereby enabling faster inference times and efficient inference on resource-constrained devices. The proposed approach involves splitting some of the processing load to a powerful edge server while maintaining a streamlined model on the device, ensuring that autonomous vehicles can efficiently perform image segmentation without compromising on inference speed or accuracy. With a larger, more resource-intensive model available at the edge (for example, an Attention U-Net with 31 million parameters), the resource-constrained device can offload the computation to the edge server, load-balance the computation, or perform segmentation on its own in the event that the edge server becomes unavailable. For this reason, the work was focused on creating an efficient network architectures for on-device segmentation. The goal was to design and evaluate compact neural network architectures that are capable of performing semantic segmentation directly on autonomous vehicles' on-board systems while maintaining high levels of accuracy and minimizing computational and memory requirements.

The study utilizes the Cambridge-driving Labeled Video Database (CamVid) [11], [12] to benchmark various image segmentation models, allowing for both the creation and comparison between various approaches. CamVid's real-scene data not only supports the training and testing of models but also enhances the understanding of the complexities inherent in image segmentation tasks. A key objective of this research was to evaluate the computational demands and network efficiency of the original U-Net architecture against its advanced variants, Attention U-Net and Recurrent U-Net, under the constraints of increased network size. Previously in our comparative analysis [13] the complexity of two models that utilized long-short term memory layers was compared to the two feed-forward dense models. The study highlighted the need for efficient usage of recurrent layers due to their complexity. To address the escalated computational requirements, especially noted in the Recurrent U-Net due to its substantial increase in GFLOPs, model pruning techniques such as structured pruning and channel reductions were employed.

The subjective evaluation method is widely acknowledged as the most reliable approach for evaluating the quality of image segmentation [14]. However, it's execution is impractical due to the significant amount of time it requires. These metrics are commonly classified as either region-based or boundary-based. Region-based metrics utilize overlapping manually labeled ground truth and segmentation results to differentiate between matching and mismatching pixels. Examples of such metrics are the Jaccard Index and F1-score. In situations such as autonomous driving, when important objects are only a small part of the image, the learning process may get trapped in local minima of the loss function. This might result in network predictions that are biased towards the background and therefore a Jaccard distance was used as a loss function with mean intersection over union as an evaluation metric. Mean intersection over Union (mIoU) measures the ratio of the intersecting area between the predicted and ground truth masks to the union of their respective areas, providing an evaluation of segmentation accuracy across all classes.

The initial assessments found that the difference between U-Net and Attention U-Net was minor in terms of both parameter count and computational complexity measured in GFLOPs, as shown in Table I. This observation suggested a relatively minor modification in Attention U-Net's design that did not dramatically increase resource requirements and/or training time. In sharp contrast, Recurrent U-Net showed a substantial increase in GFLOPs, demanding greater memory allocation and significantly longer training times. Despite attempts to prune the model, Recurrent U-Net's computational cost remained unreasonably high, prompting the decision to focus following evaluations on U-Net and Attention U-Net due to their relative efficiency.

TABLE I
COMPLEXITY OF PROPOSED U-NET MODIFICATIONS.

Network	Parameters	GFLOP	mIoU
U-Net	31.0M	510.2	81.3
Attention U-Net	31.4M	522.2	83.3
Attention U-Net (small)	2.0M	33.4	78.9
Recurrent U-Net	39.1M	1614.4	-
Recurrent U-Net (small)	2.4M	102.0	51.8

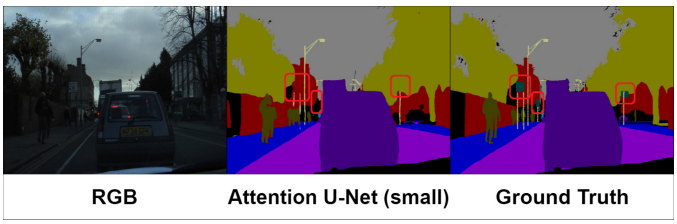

Fig. 1. Attention U-Net had tendency to disregard road signs.

Performance-wise, the baseline U-Net architecture established a mean Intersection over Union (mIoU) of 81.3%, serving as a benchmark for subsequent comparisons. The Attention U-Net, with a slight increase in parameters and GFLOPs, achieved an mIoU of 83.3%, marking a 2% improvement over the baseline. This enhancement underscores the efficiency of integrating attention mechanisms, albeit with a modest increase in model complexity. However, the application of model pruning on Attention U-Net resulted in a reduced mIoU of 78.9%, alongside challenges in accurately segmenting smaller objects such as traffic signs and cyclists, as depicted in Figure 1. This reduction in performance highlights a potential drawback of the attention mechanism, which tends to favor larger objects over smaller, yet crucial, elements in a scene.

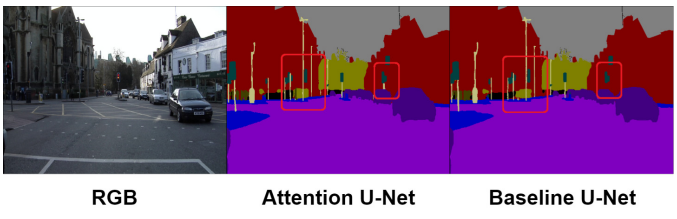

Fig. 2. Enhanced segmentation of small, distant objects by Attention U-Net.

On the other hand, a notable enhancement of around 5% mIoU was observed when comparing the precision of baseline U-Net with Attention U-Net particularly when it came to identifying smaller objects such as vulnerable road users and traffic signs, as illustrated in Figure 2 and Table II. This finding emphasizes the potential benefits of incorporating attention mechanisms into bigger models, indicating an approach to improve the balance between model complexity and segmenta-

tion accuracy, particularly for essential small-object detection in autonomous vehicle mobility scenarios.

TABLE II
PERFORMANCE COMPARISON OF SELECTED MODIFICATIONS.

	U-Net	Att U-Net	Att U-Net (s)	Rec U-Net (s)
mIoU	81.3	83.3	78.9	51.8
std	10.5	9.4	10.4	14.6
max	96.6	96.9	95.3	82.9
min	52.1	56.8	52.0	22.5
Empty	43.9	47.5	41.2	13.0
Sky	93.9	93.9	93.6	86.6
Building	78.7	81.4	75.3	60.2
Pillar	34.7	38.4	30.9	9.3
Road	94.4	95.2	94.2	65.1
Sidewalk	78.1	80.6	76.9	10.4
Vegetation	75.5	77.9	73.0	40.6
Sign	41.4	45.8	0.0	19.0
Fence	55.0	63.0	52.6	26.2
Vehicles	68.6	73.9	65.8	24.5
Pedestrians	40.8	49.1	36.0	8.6
Cyclists	44.0	48.8	42.4	4.3

The analysis underscores the nuanced trade-offs between computational efficiency, model complexity, and segmentation performance across different U-Net architectures. While Attention U-Net modification presents an advantageous improvement in segmentation accuracy, particularly for small objects, it necessitates a careful balance between computational demands and the strategic application of model pruning techniques.

IV. Conclusion and Future Work

Future research directions present a multitude of opportunities to further the capabilities of semantic segmentation models within the realm of autonomous vehicle mobility. One promising area of exploration involves the development of semantic segmentation models that leverage early exits to specifically prioritize the detection and understanding of vulnerable road users, such as pedestrians and cyclists, across a variety of environmental conditions. This proposal attempts to improve autonomous vehicle safety in densely populated urban areas. Urban traffic safety can be greatly improved by fine-tuning models to recognize and respond to vulnerable road users in various situations. Research in this area by [15] focuses on identifying specific features for urban safety and multi-sensor data driven pedestrian detection by [16].

The integration of data from LiDAR, RADAR, and cameras into semantic segmentation procedures in multi-access edge computing frameworks provides further research opportunities. Such research would focus on improving sensor fusion [6], [16] to improve segmentation accuracy and reliability. In complex driving settings, autonomous cars' decision-making relies on near-object detection precision and inference speed. Improved sensor fusion could help vehicles traverse difficult situations safely and effectively. Typically, a KITTI dataset [17] is employed for the segmentation of multi-sensor data. Nevertheless, modern datasets like the A2D2 dataset [18] or the Carla autonomous car simulator frequently get overlooked.

The idea and implementation of a federated learning framework for early semantic segmentation model exits is a unique approach to autonomous vehicle collaborative learning. This platform would allow several vehicles to share segmentation findings without transferring raw data, preserving privacy. Such a collaborative strategy could create more robust and generalized semantic segmentation models using a variety of data sources and real-world driving experiences. Federated learning allows vehicles to share knowledge and develop segmentation models for novel environments and scenarios. For instance, a car may face a rare scenario when it encounters an overturned vehicle, which the neural network was not exposed to during its training as stated in [19] CODA dataset. By employing on-device training, the weight updates of a neural network can be distributed over multiple automobiles during the nighttime when the self-driving vehicle is receiving electricity from the power grid.

Together, these future research tasks aim to advance the field of semantic segmentation for autonomous vehicles, focusing on enhancing road safety, model accuracy, inference time, and data privacy. By addressing these critical areas, the next generation of autonomous vehicle technologies can enhance reliability and performance, paving the way for safer and more intelligent mobility solutions.

Acknowledgment

This work was supported by the Ministry of Education, Science, Research and Sport of the Slovak Republic, and the Slovak Academy of Sciences under Grant VEGA 1/0685/23; by the Slovak Research and Development Agency under Grant APVV SK-CZ-RD-21-0028 and from the Operational program Integrated infrastructure project ITMS 313011V422, co-financed by the European Regional Development Found.

References

[1] O. Durmaz Incel and S. Ö. Bursa, "On-device deep learning for mobile and wearable sensing applications: A review," *IEEE Sensors Journal*, vol. 23, no. 6, pp. 5501–5512, 2023.

[2] M. Raeisi-Varzaneh, O. Dakkak, A. Habbal, and B.-S. Kim, "Resource scheduling in edge computing: Architecture, taxonomy, open issues and future research directions," *IEEE Access*, vol. 11, pp. 25 329–25 350, 2023.

[3] Y. Kang, J. Hauswald, C. Gao, A. Rovinski, T. Mudge, J. Mars, and L. Tang, "Neurosurgeon: Collaborative intelligence between the cloud and mobile edge," *SIGARCH Comput. Archit. News*, vol. 45, no. 1, p. 615–629, 4 2017. [Online]. Available: https://doi.org/10.1145/3093337.3037698

[4] S. Teerapittayanon, B. McDanel, and H. T. Kung, "Branchynet: Fast inference via early exiting from deep neural networks," *2016 23rd International Conference on Pattern Recognition (ICPR)*, pp. 2464–2469, 2016. [Online]. Available: https://api.semanticscholar.org/CorpusID:2916466

[5] Y. Matsubara, M. Levorato, and F. Restuccia, "Split computing and early exiting for deep learning applications: Survey and research challenges," 2021. [Online]. Available: https://arxiv.org/abs/2103.04505

[6] S. Yao, R. Guan, X. Huang, Z. Li, X. Sha, Y. Yue, E. G. Lim, H. Seo, K. L. Man, X. Zhu, and Y. Yue, "Radar-camera fusion for object detection and semantic segmentation in autonomous driving: A comprehensive review," *IEEE Transactions on Intelligent Vehicles*, pp. 1–40, 2023.

[7] V. Badrinarayanan, A. Kendall, and R. Cipolla, "Segnet: A deep convolutional encoder-decoder architecture for image segmentation," *IEEE transactions on pattern analysis and machine intelligence*, vol. 39, no. 12, pp. 2481–2495, 2017.

[8] O. Ronneberger, P. Fischer, and T. Brox, "U-Net: Convolutional networks for biomedical image segmentation," in *Medical Image Computing and Computer-Assisted Intervention – MICCAI 2015*. Cham: Springer International Publishing, 2015, pp. 234–241.

[9] O. Oktay, J. Schlemper, L. L. Folgoc, M. Lee, M. Heinrich, K. Misawa, K. Mori, S. McDonagh, N. Y. Hammerla, B. Kainz *et al.*, "Attention U-Net: Learning where to look for the pancreas," *arXiv preprint arXiv:1804.03999*, 2018.

[10] M. Z. Alom, M. Hasan, C. Yakopcic, T. M. Taha, and V. K. Asari, "Recurrent residual convolutional neural network based on U-Net (R2U-Net) for medical image segmentation," *arXiv preprint arXiv:1802.06955*, 2018.

[11] G. J. Brostow, J. Shotton, J. Fauqueur, and R. Cipolla, "Segmentation and recognition using structure from motion point clouds," in *Computer Vision – ECCV 2008*. Berlin, Heidelberg: Springer Berlin Heidelberg, 2008, pp. 44–57.

[12] G. J. Brostow, J. Fauqueur, and R. Cipolla, "Semantic object classes in video: A high-definition ground truth database," *Pattern Recognition Letters*, vol. 30, no. 2, pp. 88–97, 2009, video-based Object and Event Analysis. [Online]. Available: https://www.sciencedirect.com/science/article/pii/S0167865508001220

[13] M. Čavojský, G. Bugár, and D. Levický, "Comparative analysis of feed-forward and RNN models for intrusion detection in data network security with UNSW-NB15 dataset," in *2023 33rd International Conference Radioelektronika (RADIOELEKTRONIKA)*, 2023, pp. 1–6.

[14] R. Shi, K. N. Ngan, and S. Li, "Jaccard index compensation for object segmentation evaluation," in *2014 IEEE International Conference on Image Processing (ICIP)*, 2014, pp. 4457–4461.

[15] M. Klanjčić, L. Gauvin, M. Tizzoni, and M. Szell, "Identifying urban features for vulnerable road user safety in europe," *EPJ data science*, vol. 11, no. 1, pp. 1–15, 2022.

[16] M. Dimitrievski, I. Shopovska, D. Van Hamme, P. Veelaert, and W. Philips, "Automatic labeling of vulnerable road users in multi-sensor data," in *2021 IEEE International Intelligent Transportation Systems Conference (ITSC)*, 2021, pp. 2623–2630.

[17] A. Geiger, P. Lenz, C. Stiller, and R. Urtasun, "Vision meets robotics: The KITTI dataset," *International Journal of Robotics Research (IJRR)*, vol. 32, no. 11, pp. 1231–1237, 2013.

[18] J. Geyer, Y. Kassahun, M. Mahmudi, X. Ricou, R. Durgesh, A. S. Chung, L. Hauswald, V. H. Pham, M. Mühlegg, S. Dorn *et al.*, "A2d2: Audi autonomous driving dataset," *arXiv preprint arXiv:2004.06320*, 2020.

[19] K. Li, K. Chen, H. Wang, L. Hong, C. Ye, J. Han, Y. Chen, W. Zhang, C. Xu, D.-Y. Yeung, X. Liang, Z. Li, and H. Xu, "CODA: A real-world road corner case dataset for object detection in autonomous driving," in *Computer Vision – ECCV 2022*. Cham: Springer Nature Switzerland, 2022, pp. 406–423.

Non-metallic Turnbuckle Diamond Anvil Cell for Magnetisation Measurement

[1]*Július BAČKAI (4th year)*
Supervisor: [2]Slavomír GABÁNI

[1]Department of Physics, FEI TU Košice, Slovak Republic
[1,2]Centre of Low Temperature Physics, IEP SAS Košice, Slovak Republic

[1]julius.backai@tuke.sk, [2]gabani@saske.sk

Abstract— **Magnetisation (*M*) is a fundamental physical property characterising the response of a material to applied magnetic field. The temperature (*T*), magnetic field (*B*), and pressure (*p*) dependencies of *M* could reveals the nature of magnetic interactions, the critical *T*, *B*, and *p* of magnetic phase transitions. As the modern magnetometers [1, 2] can provide precise control in temperature and magnetic field change, high pressure instrumentation for the magnetometer became an important field of magnetisation study over past decades. The main target of this paper is to show development of plastic high-pressure diamond anvil cell for the Magnetic Property Measurement System (MPMS) from Quantum Design [2], which is the one of the most popular commercial magnetometers as the sensitivity of this magnetometer reaches 10^{-7} emu over a wide range of temperature and magnetic fields.**

***Keywords*— low temperature, high-pressure, magnetization, diamond anvil cell**

I. Introduction

Despite the ability of most magnetometers to perform magnetic measurements in both direct current (dc) or alternating current (ac) modes [1, 2], high-pressure magnetic studies with these setups have been primarily limited to dc measurements. The reason for this is that traditional diamond anvil cells (DAC) are constructed using metals and alloys, creating issues involving eddy currents and sample screening when coupled with high-frequency ac techniques. At present, the high-pressure ac measurements are only available in cells with built-in pick-up coils [3-8]. In comparison with use of the commercial magnetometer, fabrication of pick-up coils is complicated, time consuming, and can be expensive. Nonetheless, ac measurements can yield information about magnetisation dynamics which cannot be obtained in dc measurement. Thus, the motivation for this study was to address challenges presented by designing an entirely non-metallic high-pressure cell which can be used to perform such measurements in both dc and ac modes.

The presented work describes the development of a non-metallic pressure cell from the concept and design to experimental testing for which a Magnetic Property Measurement System (MPMS) from Quantum Design [2] is used. The design adapted for the pressure cell is based on the turnbuckle principle which has been pioneered by S. Tozer [9–11]. In this paper, we design and construct diamond anvil cell, investigate magnetic properties of advanced composite material and analyze test measurements with superconductors and magnetic systems. The name of the cell presented in this article is abbreviated as PTM-DAC for plastic turnbuckle magnetic diamond anvil cell.

II. Material and Design

The material used in previously reported plastic cells [11, 12] is a high strength polymer referred to as Parmax 1200 in the US. It is the strongest non-reinforced material to date which exhibits excellent cryogenic performance [13, 14]. Unfortunately, manufacturing of this material stopped several years ago. It is hoped that the material will be reintroduced as Tecamax SRP by Ensigner shortly. As both Parmax 1200 and Tecamax SRP are not currently available, we focused on finding an alternative material. We found suitable candidate in carbon-fibre reinforced SustaPEEK (PolyetherEtherKetone) coded as SustaPEEK CM CF 30 [15]. It is a high-performance thermoplastic made with up to 30% carbon fibre and 70% PEEK, manufactured using the compression method (CM stands for Compression Moulding)

Our starting point was modifying the existing turnbuckle magnetic DAC (TM-DAC) [16] which is made from CuBe alloy and designed for dc measurement in MPMS system. For ac measurement, the metallic material in this design needs to be replaced by non-metallic material. Moreover, the dimensions of PTM-DAC need to be as large as possible to provide sufficient support to diamond anvils. Which is mainly in the view of the SustaPeek CM CF 30 plastic which is far weaker than CuBe alloy. As shown in Fig. 1, the original design was revised to achieve the maximum allowable dimensions in order to compensate for lower material strength.

The external diameter of the cell is approximately 8.5 mm and the cell body 9 mm long. The end-nut with a hexagonal head and M5x0.5 fine thread is used for this cell with the fit between the internal and external threads made as tight as possible. In addition, because the brittle material is much more sensitive to the stress concentration, side holes for observing anvil alignment in the TM-DAC were removed in this design. Standard-cut 16 facet 4 mm diameter diamonds with 800 μm culet from Almax easyLab [17] were used. The anvil alignment is achieved through precision machining of the end-nuts and

the cell body. The operation of the cell is as in the case of TM-DAC [16].

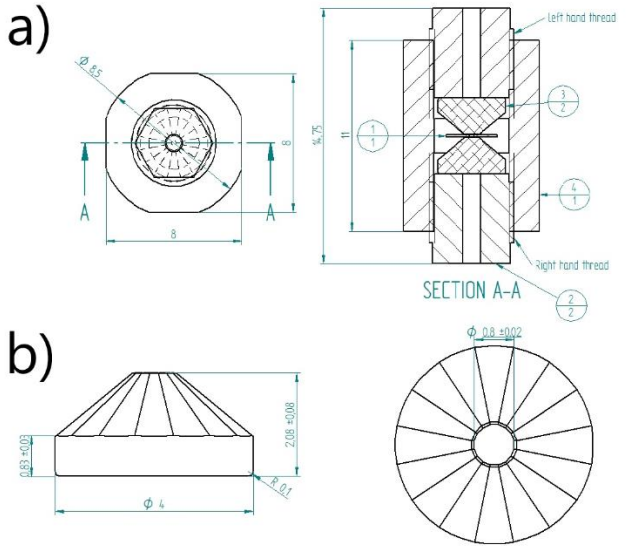

Fig. 1. a) desing of PTM DAC body and end nuts with a key dimension b) 4 mm custom-designed diamond, the culet is 800 µm and bevels up to 900 µm at 9° girdle ground round with 0.10 mm radius.

III. Measurements

After successful assembling of PTM DAC (Fig. 2a) pressurization process could start. The following step involved the design and implementation of pressurization clamps. While existing clamps were utilized, minor adjustments were made to ensure proper fitting of our cell and to minimalize potential damage during pressurization (Fig. 2b). After completing the pressurization clamp, test measurements were initiated.

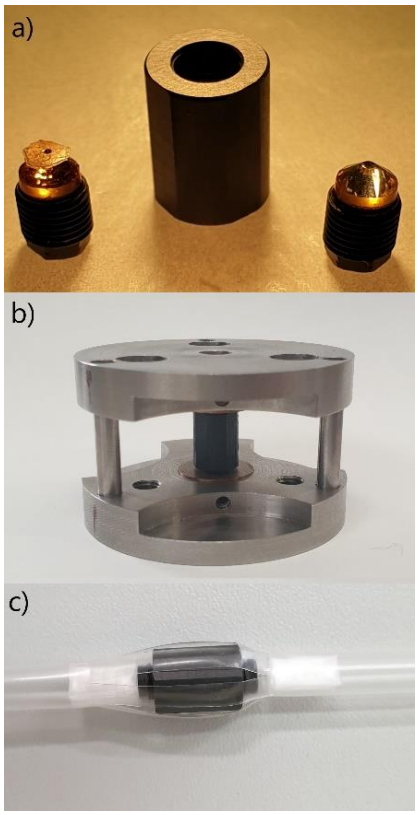

Fig. 2. a) PTM DAC body and end nuts with glued diamonds and CuBe gasket b) pressurization clamps with PTM DAC c) pressurized PTM DAC in standard plastic straw for measurements in MPMS magnetometer.

At first, measurements were taken on an empty pressure cell at different magnetic fields to obtain background information about the cell. Next, a pure Pb sample was tested to determine if the superconducting phase transition (at the well-known temperature T_c = 7.19 K) could be observed (as shown in Fig. 3a). Finally, measurements were conducted on a TmB_4 sample, which is a magnetic system with a complex phase diagram that has distinct antiferromagnetic phases. The magnetic transitions within this system were successfully detected at ambient pressure as well as at highest reached pressure p = 18 kbar at temperatures T_{N1} (0 kbar) = 11.33 K, T_{N2} (0 kbar) = 9.6 K and T_{N1} (18 kbar) = 11.82 K, T_{N2} (18 kbar) = 10.2 K respectively (Fig. 3b). Also, a fractional magnetization plateau that is characteristic for this frustrated metallic system was observed (Fig. 3c). The pressure in PTM DAC was estimated by ruby spectra analysis.

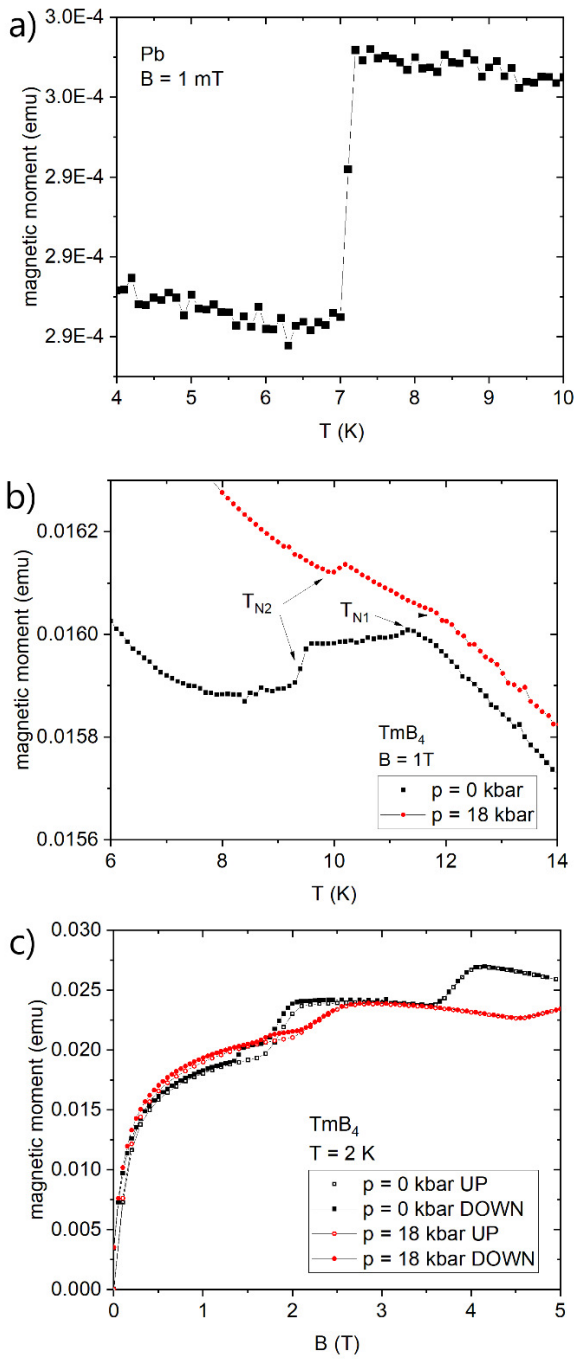

Fig. 3. a) Superconducting phase transition of Pb sample in PTM DAC b) magnetization of TmB_4 as a function of temperature c) magnetization of TmB_4 as a function of magnetic field.

IV. Conclusion

Diamond anvil cell made of plastic for magnetic measurements was successfully developed and tested. PTM DAC is suitable for measuring both superconducting transition as well as magnetic ones. Maximum pressure applied in PTM DAC was 18kbar. Pressurization is a crucial step in high-pressure experiments conducted in PTM-DAC, even though it is considered safe to apply pressure up to 60 kbar. However, we need to re-evaluate and optimize the pressurization process to have better control over the process and prevent any potential damage. Once we have improved the process, we can proceed with the experiment.

Acknowledgment

This work was supported by projects VA SR ITMS2014+ 313011W856, H2020-824109 by the European Microkelvin Platform and by Doktogrand APP0396. Liquid nitrogen for experiments was sponsored by U.S. Steel Košice, s.r.o.

References

[1] http://www.qdusa.com

[2] https://qdusa.com/products/mpms3.html

[3] T. C. Kobayashi, H. Hidaka, H. Kotegawa, K. Fujiwara, and M. I. Eremets, "Nonmagnetic indenter-type high-pressure cell for magnetic measurements," Review of Scientific Instruments, vol. 78, no. 2, p.023909, 2007.

[4] N. Moulton, S. Wolf, E. Skelton, D. Liebenberg, T. Vanderah, A. Hermann, and H. Duan, "Pressure dependence of TC in Tl2Ba2CaCu2O8 at hydrostatic pressures to 6 GPa," Physical Review B, vol. 44, pp. 12632–12634, Dec. 1991.

[5] J. Schilling, J. Diederichs, S. Klotz, and R. Sieburger, "Ac Susceptibility Studies of Superconducting Properties Under High Hydrostatic Pressure," Magnetic Susceptibility of Superconductors and Other Spin Systems, pp. 107–128, 1991.

[6] C. C. Kim, M. E. Reeves, M. S. Osofsky, E. F. Skelton, and D. H. Liebenberg, "A system for in-situ pressure and ac susceptibility measurements using the diamond anvil cell: Tc(P) for HgBa2CuO4+δ," Review of Scientific Instruments, vol. 65, no. 4, p. 992, 1994.

[7] D. D. Jackson, C. Aracne-Ruddle, V. Malba, S. T. Weir, S. A. Catledge, and Y. K. Vohra, "Magnetic susceptibility measurements at high pressure using designer diamond anvils," Review of Scientific Instruments, vol. 74, no. 4, p. 2467, 2003.

[8] Y. A. Timofeev, V. V. Struzhkin, R. J. Hemley, H.-k. Mao, and E. A. Gregoryanz, "Improved techniques for measurement of superconductivity in diamond anvil cells by magnetic susceptibility," Review of Scientific Instruments, vol. 73, no. 2, p. 371, 2002.

[9] C. Martin, C. C. Agosta, S. W. Tozer, H. A. Radovan, T. Kinoshota, and M. Tokumoto, "Critical Field and Shubnikov-de Haas Oscillations of κ-(BEDT-TTF)2Cu(NCS)2 under Pressure," Journal of Low Temperature Physics, vol. 138, pp. 1025–1037, Mar. 2005.

[10] M. Kano, N. Kurita, M. Hedo, Y. Uwatoko, S. W. Tozer, H. Suzuku, T. Onimaru, and T. Sakakibara, "Electrical Resistivity Measurements on PrPb3 under High Pressures," Journal of the Physical Society of Japan suppl. A, vol. 76, pp. 56–57, 2007.

[11] D. E. Graf, R. L. Stillwell, K. M. Purcell, and S. W. Tozer, "Nonmetallic gasket and miniature plastic turnbuckle diamond anvil cell for pulsed magnetic field studies at cryogenic temperatures," High Pressure Research, vol. 31, pp. 533–543, Dec. 2011.

[12] W. A. Coniglio, D. E. Graf, and S. W. Tozer, "Small plastic piston-cylinder cell for pulsed magnetic field studies at cryogenic temperatures," High Pressure Research, vol. 33, pp. 425–431, June 2013.

[13] V. Toplosky, R. Walsh, S. W. Tozer, and F. Motamedi, Advances in Cryogenic Engineering Materials, vol. 46. Boston, MA: Springer US, 2000.

[14] A. L. Woodcraft, V. Martelli, and G. Ventura, "Thermal conductivity of Tecamax SRP from millikelvin temperatures to room temperature," Cryogenics, vol. 50, pp. 66–70, Feb. 2010.

[15] https://www.roechling.com/industrial/materials/thermoplastics/high-performance-plastics/peek/sustapeek-cm-cf-30-black-591258

[16] G. Giriat, W. Wang, J. P. Attfield, A. D. Huxley, and K. V. Kamenev, "Turnbuckle diamond anvil cell for high-pressure measurements in a superconducting quantum interference device magnetometer.," The Review of scientific instruments, vol. 81, p. 073905, July 2010.

[17] https://almax-easylab.com

Synergizing Composite AI and Industry 5.0 to Tackle Energy Quadrilemma Challenge

[1,2]*Nikola HRABOVSKÁ (2nd year),*

Supervisor: [2]*Ivana BUDINSKÁ, Consultants:* [1]*Iveta ZOLOTOVÁ,*[1]*Erik KAJÁTI*

[1]Dept. of Cybernetics and Artificial Intelligence, FEEI TU of Košice, Slovak Republic
[2]Institute of Informatics, Slovak Academy of Sciences, Bratislava, Slovak Republic

nikola.hrabovska@tuke.sk, ivana.budinska@savba.sk, iveta.zolotova@tuke.sk, erik.kajati@tuke.sk

***Abstract*—The global quest for a balanced energy future is an enormous task in an era characterized by growing concerns about sustainability, security, affordability, and societal impact. As the complexity of the power system is rapidly increasing at a time when the possibilities of AI applications are rapidly developing, we see this as a challenge to explore the synergy between the two topics. Through our comprehensive exploration of potential technologies, including energy management systems, edge computing, blockchain technology, digital twin, and composite AI, we have identified composite AI as a pivotal tool in effectively navigating the complexities of this transition. Subsequently, we describe our results, where we use composite artificial intelligence to investigate various energy problems.**

***Index Terms*—Energy Quadrilemma, Industry 5.0, Sustainability, Data mining, Composite AI, Artificial Intelligence**

I. Introduction

Finding efficient and sustainable energy sources is a major challenge in today's rapidly evolving world. We need reliable energy that doesn't harm the environment, and is affordable for everyone. This balancing act is known as the energy trilemma [1]. However, there's an even bigger challenge called the energy quadrilemma. This new dimension introduces the social aspect, emphasizing the critical importance of social acceptability alongside the established pillars of security, sustainability, and affordability [2]. Fundamentally, Industry 5.0's emphasis on efficiency, technology integration, and human-machine cooperation is in line with the ideas needed to resolve the energy quadrilemma. In order to achieve a more sustainable and inclusive future for companies and energy systems alike, these concepts place a strong emphasis on technical innovation, collaborative approaches, and sustainable behaviors. As societies evolve, the role of community engagement, equitable access, and ethical considerations in energy transitions have come to the forefront, reshaping the discourse around energy decision-making. As the complexity of the power system is rapidly increasing at a time when the possibilities of AI applications are rapidly developing, we see this as a challenge to explore the synergy between the two topics [3], [4].

II. The Initial Status

In a recent article [5], I delved into the significant disruption faced by the European and global natural gas markets due to restrictions imposed on gas supplies by Russia. This abrupt change brought about rough conditions and volatile prices, leading to complications for households, industries, and gas-importing countries across the globe heavily reliant on natural gas. We began by explaining the concept of the energy trilemma, detailing energy security, energy sustainability, and affordability. The Global Energy Trilemma emphasizes how crucial it is for nations to strike a balance between these three elements. For instance, diversifying energy sources may come at a higher cost for nations looking to improve energy security [6]. Nevertheless, nations aiming to attain energy sustainability may encounter limitations concerning the accessibility of particular energy resources.

Next, we gave a brief overview of Industry 5.0 to explore possible links with the energy trilemma, as both concepts aim to ensure a stable and sustainable future [5], [7].

III. The Tasks Solved in the Previous Year

We explored possible technologies that could be used in the framework design to adapt to new conditions and keep production running effectively. As part of the research, we describe technologies such as energy management systems, edge computing, blockchain technology, digital twin, and composite AI, based on the latest studies, which address the possibilities of how they can help in the transition to sustainable energy, with which the energy quadrilemma and Industry 5.0. We have included our results and the overview of this topic in an article that we will soon publish [8]. The energy quadrilemma necessitates balancing energy security, environmental sustainability, economic affordability, and social inclusivity. Based on our research, we can say that composite AI is proving to be the architect of this balance, optimizing energy consumption, predicting maintenance needs, enhancing quality control, and fostering inclusivity through human-machine collaboration. Composite AI, with its adaptive learning algorithms and real-time data processing capabilities, stands as a technological chameleon, capable of evolving alongside the changing needs of smart factories and energy systems [9].

As part of the research, we first needed to cover some of the statistical analysis to have a better overview of the potential

challenges of applying composite AI. First, we examined the effects of weather on natural gas demand, and based on this analysis, we quantified the extent to which weather influences natural gas demand as an external factor. The research relied on various data sources, including historical weather data, natural gas price data for previous years, and historical natural gas demand data. We analyzed the link between weather variables, such as precipitation or temperature, and natural gas demand using statistical analytical techniques. At the core of the work were graphical and numerical results from the analysis of historical weather and gas demand data. By analyzing the correlations between demand and weather at the same time, we concluded how much influence weather has on gas demand.

In further work, we investigated the impact of external factors on the gas distribution network in Europe and used data analysis to confirm or refute the chosen hypotheses. We chose crises, namely the COVID-19 pandemic and the Russian military invasion of Ukraine, as external factors. The work has provided new insights into the functioning of the natural gas market in times of crisis. The analysis is based on data on the state of the natural gas market in Germany, France, the UK, and the Netherlands, obtained from open sources and in the framework of the EPIC – International research and development workplace of TUKE and EPH/EPC project. The core of the work is the graphical outputs of the market data analysis, where we used the Python programming language. Based on the demand analysis, we cannot confirm that there is a correlation between the change in gross domestic product and the change in demand for natural gas. Using the data, we can confirm that price has a low impact on demand in contrast to season. Using data on natural gas production, we can confirm that Europe is experiencing a decline in its own production, with an associated increase in dependence on external suppliers. Europe's desire to reduce its carbon footprint is also contributing to the changes in the market, which is increasing the demand for gas for electricity generation.

Further, we are mainly focusing on renewable energies. We have started to develop a theoretical part, where we discuss the electricity market and renewable energies in the EU electricity market and describe in more detail the Integration of solar and wind energy. The aim of this thesis will be to develop a detailed overview of renewable energies, their advantages and disadvantages, and to develop possible solutions for the scenarios we have proposed to contribute to a better and faster adaptation to the different changes.

Further work will cover the performance-driven AI Day-Ahead Model price projection. As part of the work, we would like to split the data into time frames, create a prediction model, test different prediction methods, automate the evaluation process for standard spreadsheets, and create a Microsoft Excel interface for analysts. So far, we have done the time frames and the basic model, which can be seen in the following figure (Fig. 1). In the picture, we see two curves, where one shows the real values and the other represents the predicted values, where as a result we reached up to 6079.52 in Mean Square Error (MSE).

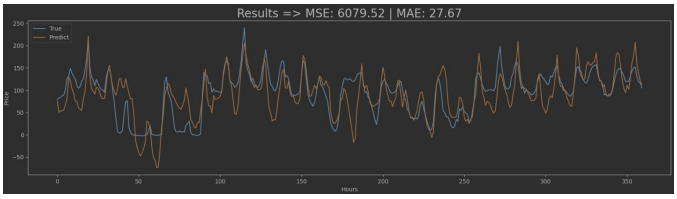

Fig. 1. First results for Day-Ahead Model price projection

IV. Future Work

In our forthcoming endeavors, our primary objective will revolve around delving deeper into the realm of advanced machine learning techniques within the Composite AI framework. This entails a comprehensive exploration and implementation of cutting-edge methodologies to further augment our model's capabilities. We will delve into the realm of deep learning architectures, seeking to design and deploy sophisticated neural network structures capable of processing and analyzing complex energy data with unprecedented accuracy and efficiency. Moreover, our future work will entail an in-depth exploration of reinforcement learning methods, focusing on leveraging these techniques to optimize decision-making processes within the Composite AI framework. By integrating reinforcement learning algorithms, we aim to imbue our model with the ability to adapt and refine its predictive capabilities over time, thus ensuring continuous improvement and adaptability in the face of evolving energy challenges. Overall, our future endeavors will be dedicated to pushing the boundaries of machine learning innovation within the context of sustainable energy transition, with the ultimate goal of developing a robust and agile Composite AI framework capable of driving meaningful advancements in Industry 5.0.

Acknowledgment

This work was supported by the Ministry of Education, Science, Research and Sport of the Slovak Republic and the Slovak Academy of Sciences VEGA 2/0135/23.

References

[1] W. E. Council, "World energy trilemma index," *World Energy Council*, 2022. [Online]. Available: https://www.worldenergy.org/transition-toolkit/world-energy-trilemma-index

[2] A. Foley and A. G. Olabi, "Renewable energy technology developments, trends and policy implications that can underpin the drive for global climate change," *Renewable and Sustainable Energy Reviews*, vol. 68, pp. 1112–1114, 2017.

[3] W. Lyu and J. Liu, "Artificial intelligence and emerging digital technologies in the energy sector," *Applied energy*, vol. 303, p. 117615, 2021.

[4] R. Singh, S. V. Akram, A. Gehlot, D. Buddhi, N. Priyadarshi, and B. Twala, "Energy system 4.0: Digitalization of the energy sector with inclination towards sustainability," *Sensors*, vol. 22, no. 17, p. 6619, 2022.

[5] N. Hrabovska, "Overview of energy trilemma for commodity trading," pp. 141–144, 2023. [Online]. Available: http://scyr.kpi.fei.tuke.sk/wp-content/scyr-files/proceedings/SCYR_2023_Proceedings.pdf

[6] L. M. Grigoryev and D. D. Medzhidova, "Global energy trilemma," *Russian Journal of Economics*, vol. 6, no. 4, pp. 437–462, 2020.

[7] "Industry 5.0. research and innovation." 2023. [Online]. Available: https://research-and-innovation.ec.europa.eu/research-area/industrial-research-and-innovation/industry-50_en

[8] N. Hrabovska, I. Budinska, E. Kajati, and I. Zolotova, "Sustainable energy for industry 5.0: A review," 2024. [work in progress].

[9] *AIMultiple*. [Online]. Available: https://research.aimultiple.com/composite-ai/

The impact of technological process modulations on structural and colloidal stability of Magnetoferritin

[1]*Kristina ZOLOCHEVSKA (3rd year)*
Supervisor: [2]Peter KOPČANSKÝ

[1]Dept. of Physics, FEI TU of Košice, Slovak Republic
[1,2]Institute of Experimental Physics of the Slovak Academy of Sciences, Košice, Slovak Republic

[1]kristina.zolochevska@tuke.sk, [2]kopcan@saske.sk

***Abstract*—Structural changes in the iron storage protein (ferritin) are linked to various pathological phenomena in the body, including the formation of magnetite in people with neurodegenerative, cardiovascular, and oncological diseases. The new tasks are geared towards gaining a deeper comprehension of magnetite's interaction with biological macromolecules, with the intention of expanding its utility in diagnostic and therapeutic modalities within the field of medicine. Ferritin's cavity can be used to make a material known as magnetoferritin (MFer). The iron-based magnetic nanoparticles present in magnetoferritin give a stronger sensitivity to the applied magnetic field, making it possible to develop further applications in diagnostic and treatment methods in medicine. So, there are presented structural studies of magnetoferritin samples obtained by controlled physicochemical synthesis in vitro. Significant structural and dimensional changes were observed by increasing post-synthesis treatment and the iron content. It has been experimentally proven that colloidal stability can be successfully modulated using suitable solvents. The presented results helped to improve the efficiency of various applications of magnetoferritin according to specific industrial requirements.**

***Keywords*—Colloidal stability, dynamic light scattering, magnetic nanoparticles, ferritin.**

I. INTRODUCTION

Iron is the one of essential elements for every living organism. It generally occurring in two different oxidation states: the first one is a relatively soluble but highly toxic ferrous form (Fe^{2+}), and the second one is a very insoluble but nontoxic ferric state (Fe^{3+}). Both iron deficiency and excessive iron levels can be harmful, and thus, it is stored in the interior of a spherical protein called ferritin, which is becoming increasingly significant in biomedicine.

Ferritin is a spherical protein that is composed of an of 24 subunits and an iron core, which surrounds ferrihydrite (FeOOH) nanocrystals. It was discovered in bacteria, plants and humans. The core of native ferritin might turn from ferrihydrite to magnetite, thereby forming biogenic magnetoferritin (MFer) [1]. Magnetoferritin is a superparamagnetic protein composed of an apoferritin shell and iron-based magnetic nanoparticles, which results in increased sensitivity to an applied magnetic field [2].

Magnetic nanoparticles are well-regarded for their low toxicity, biocompatibility, and high surface area, as well as their intrinsic magnetic properties. An effective surface engineering of magnetic nanoparticles can be used as a strategy to precisely adjust its ability to target specific cells and enhance its intrinsic properties and other crucial features for biomedical applications such as colloidal stability [3]. In this context, numerous surface engineering methods for magnetic nanoparticles have been employed to improve modern therapeutic approaches, such as in drug delivery systems, magnetic resonance imaging (MRI), and hyperthermia.

The objectives of the work are:

1. Making synthesis of magnetoferritin (MFer) with different loading factors (LF);
2. Investigating structural studies of magnetoferritin samples using controlled in vitro physicochemical synthesis conditions and post-synthesis modifications (freeze-drying, ultrasonic wave, different solvents, dynamic light scattering, colloidal stability measurements, infrared spectroscopy).

II. ANALYSIS OF THE TOPIC

Under laboratory conditions, small molecular components are reorganized into higher structures in specific constrained environments. And apoferritin is known as a well-described material that is suited for clarifying the structural arrangements of the components dependent on the environment [4]. Apoferritin can store free iron from the surrounding medium to form ferritin metalloprotein with a size up to 12 nm. Ferritin's structure and function vary depending on the ratio of H (heavy) and L (light) protein chains, leading to specific roles in specific organs. For example, brain ferritin structure demands higher oxygen consumption; liver ferritin provides catalysis for xenobiotic transformation; heart ferritin needs regular rhythms and easy iron entry and release; placental ferritin provides energy storage; and muscular ferritin needs rapid iron output for muscle growth and formation [5]. The main task of researchers over the past few decades has been the search for magnetite-based materials which must simultaneously be highly stable and biocompatible for biomedical applications. The problem is in side effects elimination, such as protein activity loss, immunological reaction, or blood clogging with aggregates [6]. The optimal selection of technology processes

and apparatus design is necessary for each material application. Therefore, the creation of physicochemical conditions before, during and after synthesis makes it possible to obtain various types of bio-ferrofluids. The primary advantages of similar Fe-based nanocrystals in liquid include efficiency, the potential for magnetic separation, degradability, simplicity, and the rate of chemical preparation [5]. Magnetite formation has been observed in people with neurodegenerative, cardiovascular, and oncological diseases. The cause has not yet been fully elucidated, and detailed factors influencing this transformation have not been described. And a temperature above 65 (◦C) and strongly alkaline pH, necessary for magnetite mineralization, cannot be achieved in living tissues. We used the iron ferritin core as a suitable sample, which is composed of ferrihydrite-like minerals combined with an iron-overloading effect with the help of various additives. So in this work, in vitro-prepared magnetoferritin (MFer) samples were studied using different methods. The results show that the inorganic part of materials directly affects the structure of the protein.

III. Materials and Methods

Preparation

1. Synthesis of magnetoferritin with different loading factors was prepared by an in vitro laboratory procedure using controlled thermo-oxidation conditions adapted to the formation of magnetite, temperature 65 (°C), alkaline pH 8.6, constant stirring and controlled addition of Fe-oxidant into the apoferritin nanocage. Loading factor is the number of iron atoms added to the reaction. It affected the size of the iron core, the formation of aggregates, and the chemical composition.

2. Loading factors levels were determined using the quantitative method on a UV–VIS spectrophotometer.

3. The hydrodynamic diameter of magnetoferritin (MFer) colloidal solution was measured using dynamic light scattering (DLS). This method allowed for the analysis of the intensity fluctuations of scattered light from magnetoferritin particles in solution, which perform Brownian motion.

IV. Results

We first examined the physicochemical properties of the prepared magnetoferritin samples. Specifically, the technological setup of the synthesis (temperature, solution pH, and freeze-drying process) and loading factor (Fe^{2+} solution amount) contributed to all measured parameter variations.

The dynamic light scattering (DLS) method was used for particle size determination. The first dynamic light scattering output indicated the same hydrodynamic friction as an ideal solid sphere would exhibit. The size distribution curves, displayed with maximum peaks between 11 and 75 nm for the samples, were plotted as the relative particle population (% of particle number) versus diameter (Figure 1). The hydrodynamics diameter growth for MFer04, MFer05, and MFer07 led to the conclusion that the loading factor ~ 400 can be a limit above which the structure of magnetoferritin becomes strongly affected by loading factor. On the other hand, the "hydrodynamic region" between 0 and 50 nm can be more influenced by liquid characteristics, such as concentration, solvent type, or pH. Moreover, hydrodynamic size depends on the ionic double-layer thickness around the particle, particle concentration, type, and viscosity of the solvent. While the iron loading caused larger hydrodynamics diameter for MFer07, the large hydrodynamics diameter of MFer04 and MFer05 prepared at increased synthesis temperature up to 69 (◦C) (near the protein denaturation point) was the result of the thermal decomposition of the protein [7]. However, the high synthesis temperature increases the preference for Fe_3O_4 nanocrystal mineralization, necessarily accompanied by protein unfolding.

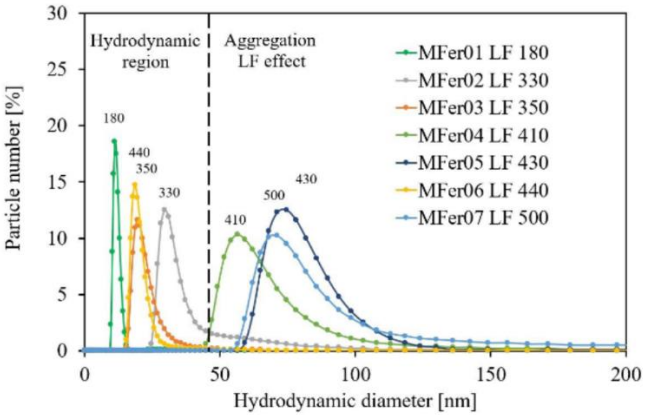

Figure 1. Hydrodynamic size distribution curves for MFer01–MFer07 samples. All protein samples were diluted in AMSPO buffer 1:10 for dynamic light scattering (DLS) measurements.

V. Conclusions

This work describes the effect of the physicochemical conditions of aqueous environment and preparation procedures on the size and protein structure of magnetoferritin. Results indicate that the magnetoferritin sample structure, disrupted by extreme synthesis technological conditions (temperature or pH), may be restored through suitable adjustments to solvent viscosity. Different physicochemical synthesis conditions and post-synthesis modifications can lead to the preparation of the most effective material with specific requirements for applied research.

References

[1] L. Xue, D. Deng and J. Sun, "Magnetoferritin: Process, Prospects, and Their Biomedical Applications," International Journal of Molecular Sciences, vol. 20, no. 10, p. 2426, 2019.

[2] L. Balejcikova, M. Molcan, J. Kovac, M. Kubovcikova, K. Saksl, Z. Mitroova, M. Timko, P. Kopcansky, "Hyperthermic effect in magnetoferritin aqueous colloidal solution," Journal of Molecular Liquids, vol. 283, pp. 39-44, 2019.

[3] S. M. Silva, R. Tavallaie, L. Sandiford, R. D. Tilley, J. J. Gooding, "Gold coated magnetic nanoparticles: from preparation to surface modification for analytical and biomedical applications," Chemical Communications, vol. 52, pp. 7528-7540, 2016.

[4] Jurado, R.; Adamcik, J.; Sánchez-Ferrer, A.; Bolisetty, S.; Mezzenga, R.; Gálvez, N. Understanding the Formation of ApoferritinAmyloid Fibrils. Biomacromolecules vol. 22, pp. 2057–2066, 2021.

[5] Balejcikova, L.;Zolochevska, K.; Tomasovicova, N.;Nagornyi, A.; Tomchuk, O.; Petrenko,V.I.; Garamus, V.M.; Almásy, L.;Timko, M.; Kopcansky, P. Variationsin the Structural and ColloidalStability of Magnetoferritin under theImpact of Technological ProcessModulations. Crystals vol. 13, p. 1493, 2023.

[6] Kim, M.; Rho, Y.; Jin, K.S.; Ahn, B.; Jung, S.; Kim, H.; Ree, M. pH-dependent structures of ferritin and apoferritin in solution: Disassembly and reassembly. Biomacromolecules, vol. 12, p. 1629, 2011.

[7] Balejcíková, L.; Kovác, J.; Garamus, V.M.; Avdeev, M.V.; Petrenko, V.I.; Almásy, L.; Kopcanský, P. Influence of synthesis temperature on structural and magnetic properties of magnetoferritin. Mendeleev. Commun. 2019, 29, 279–281.

Cloud-Based Wizard of Oz: Towards Task Autonomy

[1]*Lukáš Hruška (5th year),*
Supervisor: [2]*Peter Sinčák*

[1,2]dept. of Cybernetics and Artificial Intelligence, FEI TU of Košice, Slovak Republic

[1]lukas.hruska@tuke.sk, [2]peter.sincak@tuke.sk

***Abstract*—The sheer complexity of human-robot interaction poses an impressive challenge in the field of social robotics. To study the interaction, many researchers rely on teleoperation in place of autonomous systems. This led to the development of several teleoperation systems over the years. In this paper, we explore the possibility of improving one such system by integrating an agent able to learn from the interaction.**

***Keywords*—Deep reinforcement learning, graph convolutional network, learning from demonstration, wizard of Oz**

I. Introduction

The field of robotics is continually advancing towards greater levels of autonomy. A key aspect of this evolution involves the gradual replacement of human operators in robot teleoperation with artificial intelligence (AI) systems and supervisory control structures. Initially, human operators directly control robots' actions, as seen in traditional teleoperation or Wizard-of-Oz setups. However, as AI technology improves, many of these controlled tasks are being delegated to machine learning algorithms, allowing robots to perform complex tasks independently. As AI takes over more functions, the human operator transitions into a supervisor's role, overseeing the robot's operations and intervening only when necessary. This transition introduces semi-autonomous systems where humans and AI work collaboratively. The operator maintains the ability to override or instruct the AI, ensuring safety and control when required. This approach combines the strengths of both AI (precision, speed, and tirelessness) and human operators (adaptability, nuanced understanding, and ethical judgement) to create more effective and efficient robotic systems.

The Wizard of Oz provides a simple means to conduct HRI experiments. From a long-term viewpoint, however, it is not feasible to keep an operator at hand the whole time, plus it oftentimes even turns repetitive, thus putting further strain on the wizard and negatively impacting the interaction as a whole. It is expected that the wizard should be replaced by an autonomous agent.

Reinforcement learning (RL) is a type of machine learning where an agent learns to make decisions by performing certain actions in an environment to maximise some notion of cumulative reward, thus learning the relationship between an action and its consequences. This makes it ideal for (physical) real world interactions, such as robotics. Unlike supervised learning, where models are trained with explicit answers (i.e., labelled data), in RL, agents learn from trial and error, using feedback from their actions to improve over time. At first, the agent has to explore its environment (the exploration phase) through trial and error, after which, in the exploitation phase, it is able to utilise the knowledge gained to efficiently solve the task at hand.

II. Presented work

A. CoWoOZ

CoWoOZ is a cloud-based teleoperation system we previously developed and serves as a basis for further adaptations. It was designed as an alternative to other teleoperation systems, such as RMS[1] and OpenWOZ[2], with the mind to address issues of the aforementioned ones. It is lightweight with its core hosted in the cloud and does not heavily rely on any specific robotic platform (thus it can be used on a wide variety of platforms regardless of their support for ROS or proprietary frameworks), with one condition: the platform has to support the execution of user-supplied code.

The use of modern application stacks allows for modular solutions with interchangeable parts (except for the back-end). This modularity allows for modification of the system to suit various use cases, not just its original HRI purpose. Consequently, the user interface is not strictly tied to the system and can be replaced by another one (conforming to the API and communication protocols). The original interface, however, focuses on so called "scenarios" - sets of parametrized scripts that are meant to be run in a sequence, which is especially helpful in guided interactions, such as cognitive exercises for elderly people. Moreover, it is also possible for multiple operators to cooperatively control a single platform as well as share their scripts and even whole scenarios.

The robot-side logic works as a client; therefore, it has to initialise the connection to the server on its own. This allows it to be hidden behind a router (NAT or firewall) without any prior configuration on the network. The logic is split into two layers: a universal, codenamed Wrapper, which has to connect to the server, handle communication, and pass down commands to a platform-specific layer, which is responsible for their execution (either directly or by passing them further to frameworks or services, such as NAOqi or ROS).

Normally, if a designer wanted to achieve intelligent behaviour, they would need to manually formulate the problem as a learning task solvable by reinforcement learning. In real-world scenarios, this task may prove more challenging than the solution itself. Therefore, instead of defining the way feedback is given to the learning agent (the reward function), we may

demonstrate the necessary action and let the agent assume our behaviour is optimal. This learning from demonstration (LfD) allows the operator (trainer) to quickly transfer the knowledge to the learning agent.

B. Reinforcement learning

Basic reinforcement learning algorithms usually suffer from poor sample efficiency and thus require a significant number of iterations during the learning process. This may be offset in several ways, such as by introducing the domain model. This can be done by using model-based algorithms that learn an explicit model of the system alongside the value function and policy [3]. Alternatively, we can also use domain knowledge directly to specify a suitable spatial representation or relations between states [4]. There are multiple ways to achieve this, including: experience reuse across similar parts of the state space [5], relational policies [6], and neighbourhood relations [7]. Alternatively, we have opted to use deictic representation. Deixis, a term only recently borrowed from ancient Greek, means "demonstration" or "reference". Hence, a deictic expression would be one that points to something relative to the one speaking or demonstrating. Examples in terms of natural language would include "the table that I am pointing at" or "the window he is looking through".

Our algorithm, GDDRL [8], uses domain experts' knowledge to transform the state representation into a form of node graph where each relevant object is represented by a node and their relations are expressed with edges. This representation is then processed by a graph convolutional network based on the DQN algorithm to output the predicted Q-values of each action for the current state of the environment.

In our testing (described in [8]), GDDRL required significantly fewer games, was comparable in the reward gained with other state representations (such as raw memory, images, and various forms of deixis) in simple Gridworld environments, and was the best-performing one once the complexity increased. For example see 1, where four enemies try to catch the agent - 1000 randomly generated environments are used, and each agent plays any given environment only once, but each agent is presented with the same sequence of environments.

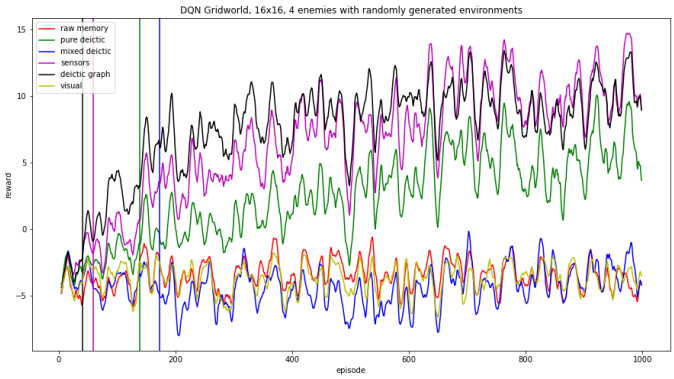

Fig. 1. Comparison of the performance of conventional and deictic state representations in a scenario, where four enemies try to catch the agent in a set of 1000 randomly generated environments

As a proof-of-concept, we are currently testing CoWoOZ's ability to utilise LfD in a simulated environment – a Gridworld-based game. We have opted out of HRI for this experiment due to the high complexity, repetitiveness, and tediousness of such interactions. This proof-of-concept is based on the experiments mentioned in the paragraph above, where the agent (player/robot) has to navigate through a 2-dimensional grid minefield in order to reach the goal. CoWoOZ's wrapper is used to interface with the game engine. This allows the operator to "play" the game and demonstrate near-optimal behaviour, and the data (an observation in the form of a screenshot, corresponding action) is stored in the database for later use. It would be impractical to continuously query the database during the learning process; hence, after the demonstration is done, the desired interaction is downloaded so the learning algorithm can use it locally.

Our goal in this experiment is threefold. Firstly, compare the performance of the GDDRL algorithm with that of human players on a large enough sample of users. Secondly, we want to explore the possibilities of several learning methods for GDDRL, namely LfD, inverse reinforcement learning, and their combinations. Finally, we want to utilise the gathered data to extend the capabilities of CoWoOZ by integrating these learning methods into the system. Moreover, recent developments in speech recognition and language models allow for quickly integrating chatbots into HRI. We would like to explore the possibility of integrating such systems with our platform to further enhance the social aspect of the interaction.

III. Conclusion

We consider integration of the aforementioned systems as the next step towards supervised mission autonomy. By integrating learning agents into the teleoperation system, we can gradually shift the role of the human operator into that of a supervisor. Furthermore, we want to integrate external services to improve the capabilities of our system.

Acknowledgment

This work was supported by the Slovak National Science Foundation project "Basic Research of Deep Learning for Image processing - DL4VISION" supported during 2022-2025 under registration code 1/0394/22.

References

[1] R. Toris, D. Kent, and S. Chernova, "The robot management system: A framework for conducting human-robot interaction studies through crowdsourcing," *Journal of Human-Robot Interaction*, vol. 3, no. 2, pp. 25–49, 2014.

[2] G. Hoffman, "Openwoz: A runtime-configurable wizard-of-oz framework for human-robot interaction," in *2016 AAAI Spring Symposium Series*, 2016.

[3] C. G. Atkeson and J. C. Santamaria, "A comparison of direct and model-based reinforcement learning," in *Proceedings of International Conference on Robotics and Automation*, vol. 4. IEEE, 1997, pp. 3557–3564.

[4] L. Frommberger, *Qualitative Spatial Abstraction in Reinforcement Learning*. Springer Science & Business Media, 2010.

[5] R. Glaubius and W. Smart, "Manifold representations for value-function approximation in reinforcement learning," Technical Report 05-19, Department of Computer Science and Engineering ..., Tech. Rep., 2005.

[6] T. Lane and A. Wilson, "Toward a topological theory of relational reinforcement learning for navigation tasks." in *FLAIRS Conference*, 2005, pp. 461–467.

[7] A. P. Braga and A. F. Araújo, "A topological reinforcement learning agent for navigation," *Neural Computing & Applications*, vol. 12, no. 3-4, pp. 220–236, 2003.

[8] L. Hruska and P. Sincak, "Graph-based deictic deep reinforcement learning with a priori information," in *2023 World Symposium on Digital Intelligence for Systems and Machines (DISA)*, 2023.

Benchmark of convolutional neural models for lung ultrasound sign classification

[1]*Maroš HLIBOKÝ (3rd year),*
Supervisor: [2]*Marek BUNDZEL*

[1,2]Dept. of Cybernetic and Artificial Intelligence, FEI TU of Košice, Slovak Republic

[1]maros.hliboky@tuke.sk, [2]marek.bundzel@tuke.sk

***Abstract*—Our research concentrates on automating the identification of lung artifacts, such as A- and B-lines, using deep learning and CNN architectures. Additionally, we conduct a model comparison to evaluate the effectiveness of different CNN architectures in this task.**

***Keywords*—medical image classification, cnn, lung ultrasound, pathology detection**

I. Introduction

Lung diseases represent a significant global health challenge, necessitating precise diagnosis and continuous monitoring. With the onset of the COVID-19 pandemic, there has been a surge in efforts to gather clinical data and leverage artificial intelligence, particularly through machine learning techniques. Among the diagnostic modalities gaining traction is lung ultrasound (LUS), renowned for its safety, portability, and cost-effectiveness.

In contrast to conventional diagnostic tools such as chest X-rays, CT scans, and MRI scans, LUS offers a radiation-free alternative. This attribute not only prioritizes patient safety but also contributes to its widespread adoption. Additionally, ultrasound devices are more accessible and economical, enabling healthcare providers to reach a larger patient population efficiently [1].

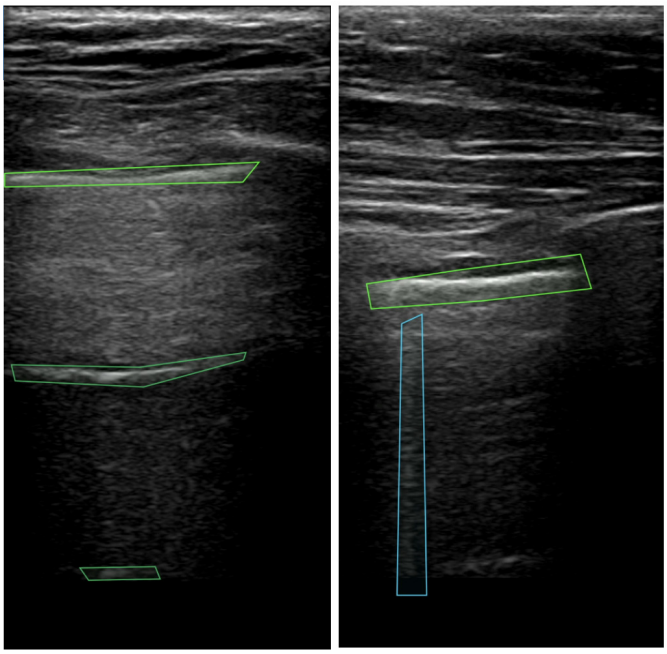

Fig. 1. Example of LUS dataset and areas of labeled signs. The left image represents Alines signs. The right image represents Bline sign. The pleural line is represented as the first horizontal sign from the top of USG image

II. Lung signs

A-lines appear as horizontal lines parallel to the pleural line, generated by ultrasonic waves reflecting between the pleura and the transducer. These lines indicate healthy lungs, with the most prominent one representing the pleura. Detecting the pleura is crucial, and the spacing between A-lines should correspond to the probe's distance from the pleura.

B-lines are vertical artifacts originating from the pleural line and extending downwards, perpendicular to it. These lines synchronize with the patient's breathing and provide crucial diagnostic insights into pulmonary conditions. Automated classification of A- and B-lines enhances diagnostic accuracy, facilitating timely medical intervention.

III. Dataset

Our experiments using ultrasound data from lung area have been conducted in collaboration with the Thoracic Surgery and the Clinic of Radiology at Jessenius Faculty of Medicine in Martin [2]. The dataset was acquired through the collaboration of doctors from this institute, ensuring that the images were captured by medical professionals with expertise in the field. Our project is focusing on detecting lung ultrasound signs for identifying final diseases, following the Blue Protocol treatment procedure. One of the crucial steps in this procedure is the detection of A- and B- lines within the lung ultrasound images. These lines serve as essential indicators for evaluating pulmonary health and identifying potential abnormalities.

We have a dataset comprising 39 A-line videos, 33 B-line videos, and 86 without any sign videos. Each video in the dataset is recorded at 30 frames per second (FPS) and is labeled every 10 frames. On average, the duration of each video is 10 seconds.

We employ cross-validation techniques to validate the performance of our models, utilizing a 5-fold approach. This methodology ensures robustness and reliability by systematically partitioning the dataset into five subsets, with each subset serving as a validation set once while the remaining four subsets are used for training.

IV. Research Contribution

We examine the models employed in our experiments, specifically ResNet-18, ResNet-34, ResNet-50, and Inception-v3. Our exploration centers on understanding the architectural characteristics and design principles inherent in these models, highlighting their unique attributes and contributions to the field of deep learning.

A. Residual Blocks in ResNet Architectures

Residual blocks constitute a pivotal component of ResNet architectures, enabling the training of very deep neural networks. These blocks address the vanishing gradient problem by introducing skip connections or shortcuts that bypass one or more layers. By doing so, they facilitate the flow of gradients during backpropagation, thereby easing the optimization process. The residual connections allow information to propagate more efficiently through the network, enabling the training of deeper models without encountering degradation in performance [3].

B. Inception Blocks in Inception-v3

Inception-v3 utilizes inception blocks as its fundamental building blocks, which are designed to capture multi-scale features efficiently. These blocks consist of parallel convolutional pathways with different kernel sizes, allowing the network to simultaneously capture features at various scales. By aggregating information from different receptive fields, inception blocks enable the model to learn rich hierarchical representations, enhancing its discriminative power and generalization performance [4], [5].

V. Results

A. A lines

ResNet-18 emerges as the top performer among the models evaluated for A lines. It achieves the highest mean F1 score of 0.825, indicating strong overall performance. With a low standard deviation of 0.091, ResNet-18 demonstrates consistent performance across various experimental conditions. Its robustness is evident from its high minimum value of 0.733 and relatively high maximum value of 0.928, highlighting its effectiveness across different scenarios. ResNet-18's superior performance across different percentiles further reinforces its reliability and versatility. Overall, ResNet-18 presents a compelling choice for tasks within A lines datasets, offering high average performance, consistency, and robustness. These findings validate ResNet-18's effectiveness and provide valuable insights for future research.

B. B lines

ResNet-34 stands out with the highest mean F1 score of 0.876 among all models evaluated for B lines. This indicates robust overall performance across the experiments conducted within the context of B lines. Its relatively low standard deviation of 0.060 underscores consistent performance across different experimental conditions compared to other models.

Additionally, ResNet-34 demonstrates effectiveness in handling diverse experimental scenarios, as evidenced by its notable minimum value of 0.777 and high maximum value of 0.935. The consistently superior quartile values further emphasize its performance across different percentiles.

In conclusion, ResNet-34 emerges as the most suitable model for tasks within the context of B lines, offering a compelling combination of high average performance, consistency, and robustness across varying experimental conditions. These findings validate ResNet-34's efficacy and provide valuable insights for future research and applications in similar domains, positioning it as a promising solution for addressing challenges in B lines datasets.

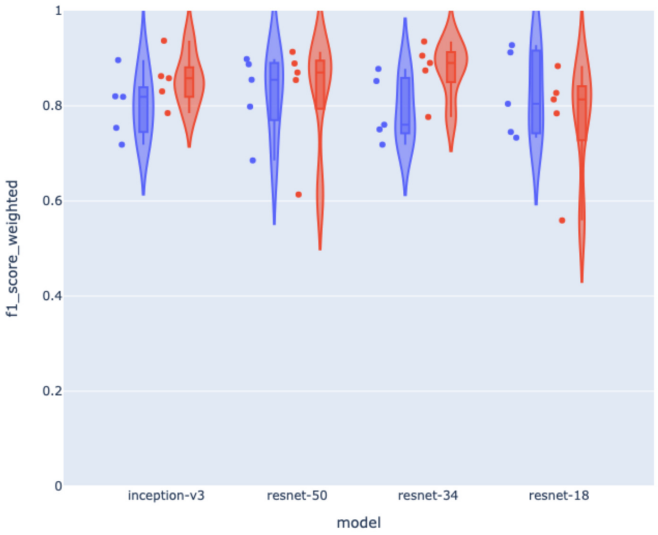

Fig. 2. Model performance comparison for A (blue) and B (red) lines model separately with cross validation

VI. Conclusion

ResNet-18 excels in handling A lines datasets, showcasing superior performance with the highest mean F1 score of 0.825. Its consistency and reliability make it an optimal choice for tasks within A lines datasets.

For B lines datasets, ResNet-34 emerges as the most suitable model, demonstrating the highest mean F1 score of 0.876 and consistent performance across diverse experimental settings.

These findings highlight the effectiveness of ResNet-18 and ResNet-34 in addressing the challenges posed by A and B lines datasets, respectively, underscoring their potential for medical applicationsand contributing to the advancement of the application of deep learning in lung ultrasound.

Acknowledgment

This work was supported by the Slovak Research and Development Agency under Grant No. APVV-20-0232.

References

[1] M. E. Bernardino, B.-S. Jing, J. L. Thomas, M. M. Lindell Jr, and J. Zornoza, "The extremity soft-tissue lesion: a comparative study of ultrasound, computed tomography, and xeroradiography." *Radiology*, vol. 139, no. 1, pp. 53–59, 1981.

[2] M. Hlibokỳ, J. Magyar, M. Bundzel, M. Malík, M. Števík, Š. Vetešková, A. Dzian, M. Szabóová, and F. Babič, "Artifact detection in lung ultrasound: An analytical approach," *Electronics*, vol. 12, no. 7, p. 1551, 2023.

[3] S. Targ, D. Almeida, and K. Lyman, "Resnet in resnet: Generalizing residual architectures," *arXiv preprint arXiv:1603.08029*, 2016.

[4] X. Ding, X. Zhang, J. Han, and G. Ding, "Diverse branch block: Building a convolution as an inception-like unit," in *Proceedings of the IEEE/CVF Conference on Computer Vision and Pattern Recognition*, 2021, pp. 10 886–10 895.

[5] N. Dong, L. Zhao, C.-H. Wu, and J.-F. Chang, "Inception v3 based cervical cell classification combined with artificially extracted features," *Applied Soft Computing*, vol. 93, p. 106311, 2020.

Comparison of different steganographic techniques for writing QR codes into images

[1]*Samuel ANDREJČÍK (3rd year)*
Supervisor: [2]Ľuboš OVSENÍK

[1,2]Dept. of Electronics and Multimedia Communications, FEI TU of Košice, Slovak Republic

[1]samuel.andrejcik@tuke.sk, [2]lubos.ovsenik@tuke.sk

***Abstract*— The main reason for investigation of this topic is the constant demand for more secure communications and transmitted data. Concepts such as authenticity, data integrity and copyright have become an everyday necessity. Every day this issue is advancing, which is a direct motivation for us to design more and more secure systems that meet strict requirements and criteria. The solutions proposed in this article describe the ways in which a QR code carrying information of 1000 characters length is written into the cover image, while this writing is carried out at the Least Significant Bit plate. Subsequently, individual methods, specifically XOR, LSB replacement and LSB matching, are subjected to mathematical testing with parameters PSNR, NCC and SSIM.**

***Keywords*—Image processing, information hiding, LSB, security, QR code, steganography**

I. INTRODUCTION

Steganography, as a branch of cryptography, deals with hiding information in various carriers so that their presence is difficult to detect. This technique was originally used for secret messaging between armies or spies [1]. Currently, steganography is used in the digital environment to protect and transmit sensitive data [2].

This paper describes image processing in steganography using the LSB (Least Significant Bit) method, in which information is written by a logical XOR bit operation into the LSB plane (Fig. 1) and then the quality of the proposed solution between the cover image and the stego image is evaluated using mathematical evaluations. LSB replacement and LSB matching methods are also used, which uses an algorithm that replaces the least significant bits of the cover image with bits of the secret message[3].

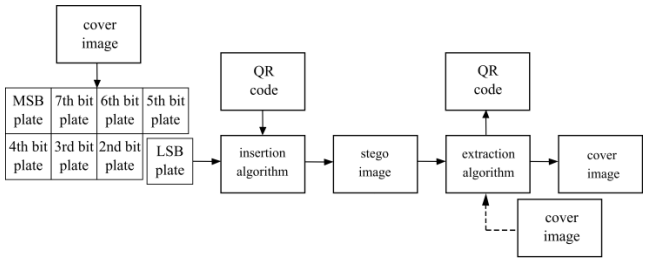

Figure 1 Block diagram showing a steganographic design for hiding data in an image

II. METHODS OF COMPARING THE QUALITY OF PROPOSED SOLUTIONS

Several indicators can be used to compare the proposed solutions. Subjective methods include those that are based on human perception [4], however, for the needs of evaluating our proposed solution, mathematical parameters were used in the evaluation of this proposal. We use the parameters PSNR (Peak signal-to-noise ratio), MSE (Mean squared error), NCC (Normalized cross-correlation) and SSIM (Structural similarity index).

PSNR is a quantity that expresses the difference between two images in decibels. The higher this value is, the better the quality of the stego image [5]. We calculate the PSNR according to the equation:

$$PSNR = 10 \cdot \log_{10}\left(\frac{MAX^2}{MSE}\right) \tag{1}$$

where the *MAX* variable represents the maximum possible pixel intensity of the image, which means that in an eight bit representation this value is equal to 255. The PSNR value approaches infinity when the MSE approaches zero; this shows that a higher PSNR value provides higher image quality.

MSE is a quantity that measures the root mean square difference between the actual and ideal pixel values. It is true that the lower this quantity is, or close to zero, the smaller the error/difference between these values is. It is calculated as follows:

$$MSE = \frac{1}{WH} \cdot \sum_{y=0}^{W-1} \cdot \sum_{x=0}^{H-1} [E(x,y)]^2 \tag{2}$$

where x and y denote the pixel positions and W and H are the width and height values of the image, respectively, and $E(x,y)$ is the difference between the cover and stego images. Although the *MSE* quality assessment will not be used directly in the evaluation of the results of this work, the PSNR parameter, which is based on the *MSE*, will be used, so it is important to define which quantity it is.

The NCC value can range from <-1;1> and can be calculated using the following formula:

$$NCC = \frac{\sum_{x=0}^{H-1}\sum_{y=0}^{W-1}(I(x,y)-\bar{I})(K(x,y)-\bar{K})}{\sqrt{\sum_{x=0}^{H-1}\sum_{y=0}^{W-1}(I(x,y)-\bar{I})^2 \cdot \sum_{x=0}^{H-1}\sum_{y=0}^{W-1}(K(x,y)-\bar{K})^2}} \tag{3}$$

where x and y are the coordinates of the rows and columns in the images, H and W are the height and width of images. I and K represent the original image and $\bar{I}$ and $\bar{K}$ are the arithmetic means of their intensities [6].

SSIM is a well-known quality metric used to measure the similarity between two images [7]. Instead of using traditional error summation methods, SSIM is designed by modeling any image distortion as a combination of three factors, which are correlation loss, luminance distortion, and contrast distortion. We calculate the SSIM according to the equation:

$$SSIM(x,y) = [l(x,y)]^{\alpha} \cdot [c(x,y)]^{\beta} \cdot [s(x,y)]^{\gamma} \quad (4)$$

where:

$$l(x,y) = \frac{2\mu_x\mu_y + C_1}{\mu_x^2 + \mu_y^2 + C_1} \quad (5)$$

$$c(x,y) = \frac{2\sigma_x\sigma_y + C_2}{\sigma_x^2 + \sigma_x^2 + C_2} \quad (6)$$

$$s(x,y) = \frac{\sigma_{xy} + C_3}{\sigma_x\sigma_y + C_3} \quad (7)$$

The first term (5) is the luminance comparison function, which measures the closeness of the mean luminance of two images (μ_x and μ_y). This factor is maximal and equal to 1 only if $\mu_x = \mu_y$. The second term (6) is the contrast comparison function, which measures the closeness of the contrast of two images. Here the contrast is measured by the standard deviation $\sigma_x$and σ_y. This term is maximal and equal to 1 if and only if $\sigma_x = \sigma_y$. The third term (7) is the texture comparison function, which measures the correlation coefficient between two images x and y. It should be noted that σ_{xy} is the covariance between x and y. Positive values of the SSIM index are in the range [0,1]. A value of 0 means no correlation between the images and 1 means that $x = y$. The positive constants C_1, C_2 and C_3 are used to avoid a zero denominator.

III. Proposed solution

The solution can be applied to both colour and greyscale images. The solution is also not limited by the resolution of the cover image. Since the images are not square, i.e. they are oriented either horizontally or vertically, there is a part of the code in the algorithm that detects the orientation of the image and ensures an even distribution of the QR code over the entire image (Fig. 2), so that there is no unnecessary loss of transmitted information. The data that is still lost after the attacks is subsequently recovered thanks to the self-correcting Reed-Solomon coding that ensures redundant writing of the QR code data.

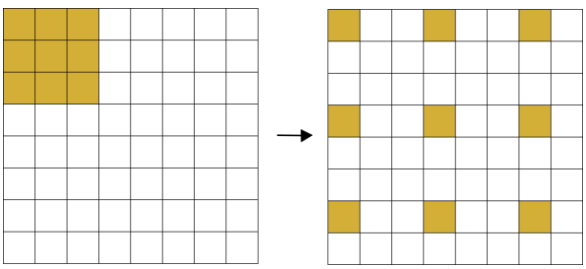

Figure 2 Distribution of the QR code within secret message into the LSB plane of the cover image

After the information is successfully written into the LSB plane of the cover image, all the bit planes can be combined again to form a stego image, that is, an image that consists of the original cover image and now the transmitted information.

Table 1 Assessing the quality of the stego image after inserting a QR code with information about the length of 1000 characters using an XOR method

Image name	PSNR (dB)	SSIM	NCC
baboon.bmp	64.9239	0.925466	0.91622
baboonG.bmp	60.1526	0.916545	0.91511
barbaraG.bmp	60.1526	0.925636	0.90583
cameramanG.bmp	60.1526	0.914225	0.90674
f16.bmp	64.9239	0.915452	0.91595
lena.bmp	64.9239	0.926331	0.92531
lenaG.bmp	60.1527	0.935624	0.91851
pentagonG.bmp	60.1273	0.916526	0.93461
peppers.bmp	64.9239	0.925416	0.92672
sailboat.bmp	64.9239	0.946515	0.91541
Average	62.5357	0.924774	0.91804

As we can see, the results of the XOR method are not very flattering, so we implement the LSB replacement method instead.

Table 2 Assessing the quality of the stego image after inserting a QR code with information about the length of 1000 characters using an LSB replacement

Image name	PSNR (dB)	SSIM	NCC
baboon.bmp	75.8413	0.945416	0.94652
baboonG.bmp	72.5432	0.936545	0.94561
barbaraG.bmp	73.6345	0.945616	0.93523
cameramanG.bmp	74.4236	0.944255	0.93654
f16.bmp	72.5224	0.955492	0.92565
lena.bmp	73.6445	0.946301	0.94561
lenaG.bmp	75.7356	0.925654	0.91861
pentagonG.bmp	74.7248	0.946526	0.94451
peppers.bmp	75.8413	0.945416	0.94652
sailboat.bmp	72.5432	0.936545	0.94561
Average	74.1454	0.942777	0.93904

As the last method of writing the QR code into the LSB plane of the cover image, we use the LSB matching method. After writing the secret information into the LSB plane of the cover image, the next part of the algorithm mathematically evaluates the proposed solution by comparing the cover image and the newly created stego image.

Table 3 Assessing the quality of the stego image after inserting a QR code with information about the length of 1000 characters using an LSB matching

Image name	PSNR (dB)	SSIM	NCC
baboon.bmp	81.8413	0.964516	0.96642
baboonG.bmp	82.5432	0.956454	0.96511
barbaraG.bmp	82.6345	0.965126	0.95523
cameramanG.bmp	74.4236	0.984225	0.94644
f16.bmp	81.5224	0.965962	0.94565
lena.bmp	83.6445	0.956371	0.95541
lenaG.bmp	84.7356	0.975624	0.93841
pentagonG.bmp	82.7248	0.965226	0.95421
peppers.bmp	81.8413	0.964516	0.96642
sailboat.bmp	82.5432	0.956454	0.96511
Average	81.8454	0.965447	0.95584

IV. Future Work

In the continuation of this work, we are heading for the implementation of various types of attacks. Currently, we have tested cutting attacks, where we cut out the corner of the image, but also the image across its entire width. We also attack the image with noise, using Salt&Pepper noise, and we also plan to blur and rotate the image.

Currently, we are considering testing other ways of writing a QR code into a cover image.

V. Conclusion

In this work, the main task was to design and implement new ways of writing a QR code carrying a secret message into a cover medium, in our case a cover image. The QR code carried a secret information that contained 1000 characters and testing was done on a sample of images that are commonly known in testing steganographic techniques.

All experiments used the same secret message. Message was generated within matlab algorithm, thanks to string generator of length of 1000 characters and QR code generator which was developed within proposed solution.

LSB replacement and LSB matching methods were added to the original XOR method notation, which have been shown to improve the observed results, especially in the PSNR domain, by up to 18,5%, respectively 30% on average.

The proposed solution is also suitable to be applied to all types of images, it has no limitation on the image resolution and can be applied to both color images and also greyscale images.

Acknowledgment

This work was supported by following research grants: APVV-22-0400 - Extension of the autonomous applications of monitoring through multi-band UWB sensors and VEGA 1/0260/23 - Artificial intelligence, robust MANET and multi-hop D2D networks integrated into 6G network.

References

[1] J. Fridrich, M. Goljan, R. Du, “Reliable Detection of LSB Steganography in Color and Grayscale Images,” in *Proc. of the 2001 Workshop on Multimedia and Security*, 2001.

[2] J. Fridrich, Steganography in Digital Media. Binghamton, NY: Cambridge University Press, 2014.

[3] J. Kodovský, J. Fridrich, V. Holub, “Ensemble classifiers for steganalysis of digital media, in *IEEE Transactions on Information Forensics and Security*, vol. 7(2), pp. 432-444, 2012.

[4] T. Mahmood, Z. Mehmood, M. Shah, T. Saba, “A robust technique for copy-move forgery detection and localization in digital images via stationary wavelet and discrete cosine transform.” in *J. of Vis. Commun. and Image Represent.*, Pakistan, 2018.

[5] A. Pradhan, et al. “Performance evaluation parameters of image steganography techniques,” in. *Int. Conf. on Research Advances in Integrated Navigation Systems*, 2016.

[6] A. Rehman, T. Saba, T. Mahmood, Z. Mehmood, M. Shah, A. Anjum, “Data hiding technique in steganography for information security using number theory,” in. *J. of Information Science,* Saudi Arabia, 2018.

[7] W. S. Bhaya, A Habbal, “A comprehensive survey on steganography and steganalysis techniques and tools“, in *Int. J. of Computer Science and Information Security*, vol. 14(5), pp. 287, 2016.

Identifying Illicit Activities in Blockchain Transaction Graph Networks

[1]*Tomáš ADAM (3rd year)*
Supervisor: [2]František BABIČ

[1,2]Department of Cybernetics and Artificial Intelligence, FEI TU of Košice, Slovak Republic

[1]tomas.adam@tuke.sk, [2]frantisek.babic@tuke.sk

***Abstract*— This paper explores the application of machine learning and graph neural networks to detect phishing fraud within blockchain networks, focusing on Ethereum transactions. By leveraging dynamic subgraph generation and contrastive learning, the study identifies anomalous behaviors indicative of fraudulent activity. The methodology was tested on a labeled, publicly available transaction dataset and showed promising results in distinguishing between legitimate and fraudulent activities. The core innovation lies in the creation of dynamic subgraphs that encapsulate transactions within specific temporal windows, addressing the computational challenges of large-scale blockchain transaction graphs.**

***Keywords*—blockchain, transaction graph, phishing detection, supervised learning.**

I. Introduction

In recent years, the ascent of blockchain technology and its applications in digital currencies, trading platforms, and payment systems has captured the attention of both the financial industry and the overseeing regulatory entities. The allure of blockchain lies in its promises of transparency, security, and decentralization, making it a revolutionary technology that also opens avenues for its misuse. Illegal activities such as money laundering, terrorism financing, and multiple forms of fraud becoming a significant concern [1]. Among these, phishing fraud has emerged as a prevalent form of cybercrime [2], exploiting the system's anonymity and decentralized nature to execute sophisticated fraud schemes. The challenge of detecting and mitigating such activities is compounded by the significant imbalance between legitimate transactions and suspicious activities, further exacerbated by the lack of general knowledge and labeled data [3].

II. Initial Status in the Solving of the Research Task

The foundational research presented in paper [3] leveraged unsupervised machine learning algorithms to identify and rank accounts based on anomaly scores. This approach highlighted the potential of machine learning in unveiling patterns indicative of suspicious activities, such as botnets, arbitrage, or phishing patterns. The core achievement of this initial phase was the successful identification of suspicious addresses that demonstrated atypical transaction frequencies or patterns, signaling the potential for illicit activities. This groundwork laid the foundation for deeper investigation of the specific behavioral patterns validated within the Ethereum blockchain.

Building upon these initial insights, the present research focuses on the significant influence of temporal dynamics on transaction patterns (Fig. 1) suggesting that the timing and sequence of transactions could be instrumental in identifying illicit activities. This approach is based on the observation that certain accounts exhibit specific transactional behaviors in temporal windows, which may potentially indicate suspicious or fraudulent operations. By conducting a comprehensive cross-chain examination of the selected transaction datasets, the objective of the proposed approach, is to effectively detect these temporal behavioral patterns.

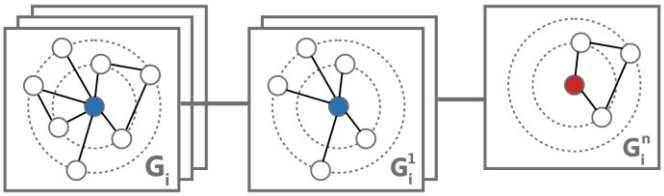

Fig. 1. Temporal dynamics of fraudulent activities.

III. Phishing Accounts Detection

The presented methodology constitutes a concept approach toward understanding and identifying fraudulent activities within the Ethereum blockchain, with a specific emphasis on phishing activities detection within the WAX blockchain transactions. Leveraging a dataset comprising 987 phishing nodes and 239,000 randomly selected normal nodes sourced from a well-documented public dataset[1] for validation.

The initial step involved processing Ethereum transactions through a multi-dimensional directed graph representation. This representation was crucial in capturing the complex interactions within the network, allowing for a nuanced analysis beyond simple transactional data. By focusing on nodes that exhibit moderate levels of connectivity, we eliminated outliers that could potentially negatively impact the analysis. This filtration ensured that the focus remained on the most relevant entities without smart contracts, to understand the network's fraudulent and non-fraudulent behaviors.

A. Dynamic Subgraph Generation and Feature Calculation

The main aspect of the research is the generation of dynamic subgraphs centered around selected nodes, capturing transaction activities within specific time frames. This approach is essential given the large scale of the transaction graph, rendering direct analysis computationally infeasible.

[1] Chen, L., Peng, J., Liu, Y., Li, J., Xie, F., & Zheng, Z. (2019). XBLOCK Blockchain Datasets: InPlusLab Ethereum Phishing Detection Datasets. Retrieved from http://xblock.pro/ethereum/

By segmenting the transaction history into time-sliced subgraphs, we obtain a granular view into the transaction activities of specific nodes, providing valuable insights into potential anomalous behavior. For every generated transaction subgraph, an in-depth feature calculation process recalculates various node features within the context of each time slice, including the number and total value of incoming and outgoing transactions or unique sender/receiver counts.

B. Behavior Pattern Differentiation

The application of Graph Neural Networks (GNNs), including Graph Attention Networks (GAT) and Long Short-Term Memory (LSTM) layers, is instrumental in processing the dynamic subgraphs [4]. These networks allow capturing the structural and temporal characteristics of the transaction network while modeling the complex dependencies that exist between nodes. The embeddings generated from this process provide a multi-dimensional representation of observed node behavior over time, encapsulating address-specific transaction contexts and broader interaction patterns.

The integration of contrastive learning [5] represents a significant advancement in the model's capability to discern between different types of transaction behaviors (Fig. 2). By contrasting embeddings from known fraudulent transactions against those from non-fraudulent ones, the model fine-tunes its ability to distinguish differences in transaction patterns. This contrastive approach improves the accuracy of anomaly detection and enriches the model's understanding of what constitutes normal versus potentially suspicious behavior within the transaction network.

Through the optimization of a contrastive loss function, the model undergoes a self-improvement process, enhancing its discriminative capabilities to cluster embeddings representing similar node behaviors closer together, while embeddings of dissimilar behaviors farther apart.

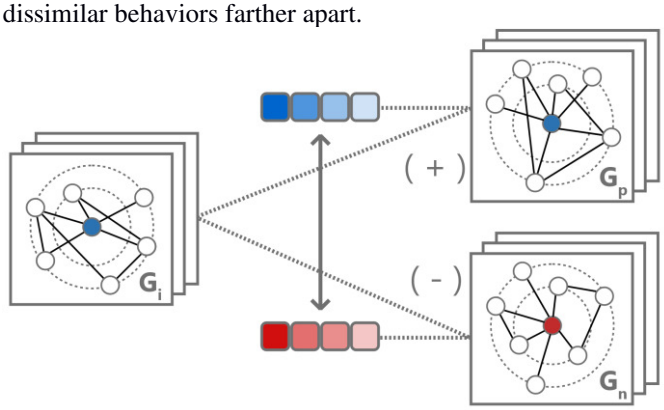

Fig. 2. Embedding generation and contrast learning process.

C. Model Evaluation and Results

In the evaluation of various machine learning models for classifying Ethereum transactions, the focus has been primarily on their performance in accurately identifying fraudulent (minority class) transactions. The models were assessed based on their accuracy and, more critically, their F1 scores for the minority class, providing a balanced measure of their precision and recall capabilities.

The results from the extensive evaluation of various machine learning models on the Ethereum transaction dataset provide insightful conclusions about the effectiveness of each approach in distinguishing between fraudulent and non-fraudulent transactions. These models were rigorously trained and tested across multiple folds to ensure the reliability and robustness of the results (Table 1).

TABLE I
MODEL PERFORMANCE COMPARISON

Method	F1	Recall	Precision
Baseline Model [7]	63%	56%	72%
Ada Boost	85%	83%	86%
Random Forest	89%	87%	89%

FUTURE WORK

A promising direction for future research involves the exploration of ego network embeddings, aimed at defining the contextual position of a node within its local subgraph. This innovative approach seeks to capture not just the behavioral patterns of individual accounts but also their roles and relationships within the broader network structure. By analyzing the ego network embeddings, we can gain deeper insights into the contextual relevance of each node, enhancing our ability to detect more sophisticated fraud schemes that exploit the complex topology of blockchain networks.

Building on the foundation laid by the proposed approach, the next phase will extend the methodology to the WAX blockchain, with a particular focus on quantifying NFT (Non-Fungible Token) transfers and detecting NFT-related phishing activities. The WAX blockchain, characterized by its active trading and unique transaction patterns, offers a fertile ground for applying and testing the fraud detection approach. NFT phishing transactions, with their clear pattern of acquiring and subsequently selling NFTs followed by the transfer of funds, should theoretically present even more pronounced behavioral embeddings for fraud detection. This distinct pattern provides a potential advantage in identifying fraudulent activities within NFT markets, as fraudulent accounts may exhibit anomalous behaviors compared to typical user transactions.

An integral part of this future work involves the verification of identified suspicious nodes against blacklisted accounts obtained from smart contract crawls [4]. This validation step is essential for assessing the accuracy and reliability of our detection methodology in real-world scenarios. By comparing our findings with officially blacklisted accounts, we can refine our models to improve precision and recall, ensuring that the approach remains robust in identifying fraudulent activities.

ACKNOWLEDGMENT

The work was supported by The Slovak Research and Development Agency under grant no. APVV-20-0232 and The Scientific Grant Agency of the Ministry of Education, Science, Research and Sport of the Slovak Republic under grant no. VEGA 1/0685/21.

REFERENCES

[1] Kayikci, S., Khoshgoftaar, T.M. Blockchain meets machine learning: a survey. J Big Data 11, 9 (2024), doi: /10.1186/s40537-023-00852-y

[2] R. Zieni, L. Massari and M. C. Calzarossa, "Phishing or Not Phishing? A Survey on the Detection of Phishing Websites," in *IEEE Access*, vol. 11, pp. 18499-18519, 2023, doi: 10.1109/ACCESS.2023.3247135.

[3] T. Adam, F. Babič, "Anomaly Detection on Distributed Ledger Using Unsupervised Machine Learning," *2023 IEEE International Conference on Omni-layer Intelligent Systems (COINS)*, Berlin, Germany, 2023, pp. 1-4, doi: 10.1109/COINS57856.2023.10189278

[4] Motie, S., & Raahemi, B. (2024). Financial fraud detection using graph neural networks: A systematic review. *Expert Systems with Applications*, *240*, 122156. https://doi.org/10.1016/j.eswa.2023.122156

[5] Deng, Z., Xin, G., Liu, Y., Wang, W., & Wang, B. (2022). Contrastive graph neural network-based camouflaged fraud detector. *Information Sciences*, *618*, 39–52. https://doi.org/10.1016/j.ins.2022.10.072

Detection of toxic Slovak comments on social media based on sentiment analysis

[1]*Zuzana SOKOLOVÁ (3rd year),*
Supervisor: [2]*Jozef JUHÁR*

[1,2]Department of Electronics and Multimedia Communications, FEI TU of Košice, Slovak Republic

[1]zuzana.sokolova@tuke.sk, [2]jozef.juhar@tuke.sk

***Abstract*—Sentiment analysis, a powerful tool in the realm of natural language processing, serves to interpret the emotions conveyed within textual content, distinguishing between positive, negative, or neutral sentiments. This analysis not only offers valuable insights into social networks, aiding businesses and researchers in making informed decisions, but it also plays a crucial role in detecting and addressing the alarming prevalence of online hate speech. In the paper, we presented and summarized all the studies to which we have dedicated ourselves, focusing on the nuanced analysis of sentiment and the vigilant detection of hate speech within the expansive online environment. Through our research endeavors, we have successfully achieved remarkable results, shedding light on the effectiveness and importance of these methodologies in the digital landscape.**

***Keywords*—detection, hate speech, offensive language, sentiment analysis, Slovak language, text processing, toxicity**

I. Introduction

Sentiment analysis (SA), a critical aspect of natural language processing, pertains to the detection of hate speech and offensive language. According to Pang et al. [1], SA involves the identification and evaluation of emotional tones in the text to comprehend opinions and attitudes. SA has become increasingly vital with the rise of digital communication, assisting businesses, researchers, and organizations in understanding public opinions, customer feedback, and societal trends. It detects and assesses sentiment in text, seeking to recognize and categorize opinions and emotions. On a sentence level, SA determines whether a sentence expresses positive or negative sentiments. A simple principle of sentiment analysis is shown in Figure 1. Various studies in sentiment analysis were examined, highlighting trends in algorithms and applications. Medhat et al. [2] categorized and summarized fifty-four recent articles, showing ongoing interest in sentiment classification and feature selection algorithms. Naïve Bayes and Support Vector Machines were identified as commonly used in SA, with a growing focus on languages beyond English. Di et al. [3] introduced an improved version of PASTA for automatically organizing crisis tweets into clusters. Wankhade et al. [4] explored sentiment analysis techniques, emphasizing classification methods and their advantages. Supervised learning methods like Naïve Bayes and Support Vector Machines were noted for their simplicity and accuracy, particularly in data collection and feature selection. Jiang et al. [5] innovated by comparing methods with different data ratios, demonstrating machine learning's effectiveness with limited data and deep learning's superior results with larger datasets. Bidirectional Recurrent Neural Networks stood out for their performance. Del et al. [6] addressed hate speech on Italian public pages, creating hate categories and designing classifiers for detecting Italian hate speech, using a manually annotated corpus. In marketing, sentiment analysis is often utilized for prediction. Studies like [7] linked sentiment analysis to predicting book sales, product sales from blogs, and movie success. This approach helps companies understand customer feedback for product improvement. Similarly, politicians analyze social media comments to gauge public sentiment and preferences [8].

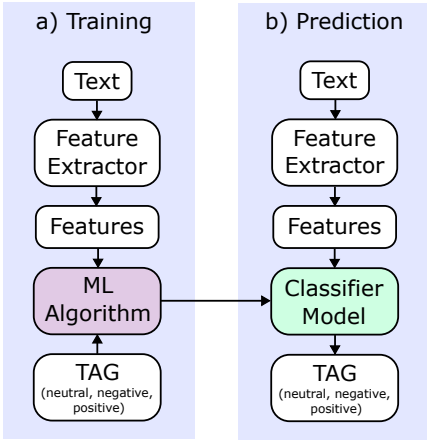

Fig. 1. A simple principle of sentiment analysis

II. Related work

In this section, we offer an overview of our achieved results and published works focusing on sentiment analysis, hate speech, and offensive language. Our research has resulted in impactful publications that explore sentiment intricacies and address the prevalence of hate speech online. Through our work, we contribute to understanding digital emotion expression and enhancing detection methods for a safer online environment.

In paper [9], we have provided an overview of the most recent advancements and findings in the realm of hate speech and offensive language detection. We discussed the application of transfer learning and elaborated on its functioning. Additionally, we described the methodology for employing transfer learning in training language models, with a specific emphasis on hate speech and sentiment analysis. We proposed guidelines

for annotating the corpus and identified key textual cues to consider. Furthermore, we provided a comparative analysis by citing several significant studies, including [10] and [11].

In the following paper [12], we presented the creation of our own corpus of texts focused on hate speech and offensive language. The corpus comprised comments from the social network Facebook, which were annotated and categorized into three groups: positive, neutral, and negative. It encompassed a total of 34,528 comments, with 55% classified as negative, 30% as neutral, and 15% as positive. The neural network-based model utilized achieved an accuracy of 52.83%. Subsequently, we endeavored to construct a smaller dataset comprising 581 comments, ensuring balanced representation across classes. This smaller dataset yielded an accuracy of 61.32%. Our findings underscore the importance of creating balanced corpora for model training. Concurrently, we developed a hate word detector based on a dictionary of offensive terms that we curated.

In the study [13], we delved into various approaches centered around transformers, including BERT, DistilBERT, AlBERT, and mBERT. Our exploration encompassed a comprehensive review of studies that focused on leveraging these transformer models to tackle the complex challenges of hate speech detection and sentiment analysis. Through our examination, we elucidated the nuanced methodologies employed in these studies and highlighted their contributions to advancing the field. Moreover, alongside our analysis of transformer-based approaches, we dedicated a significant portion of our discussion to elucidating foundational techniques such as Word Embedding. By elucidating the intricacies of Word Embedding, we aimed to provide readers with a comprehensive understanding of the underlying principles that underpin many contemporary natural language processing tasks. Additionally, we explained the architecture of GPT-2, a language model renowned for its exceptional performance in various language understanding tasks.

In the paper [14], we offered an overview of trends in the detection of hate speech and offensive language on social networks. We described the most commonly utilized methods from recent scientific studies in this area. Additionally, we outlined the future direction of our research.

Subsequently, in the paper [15], we proceeded to outline the process of constructing a corpus of texts tailored for tasks involving the detection of hate speech, offensive language, and sentiment analysis. Drawing from a broad perspective, we established the fundamental criteria for assembling a corpus of Slovak-language texts.

In our paper [16], we effectively evaluated the performance of classifiers using Slovak datasets, uncovering notable variances between the original and translated models. While the translated datasets yielded reasonably satisfactory outcomes, the native Slovak datasets enabled the models to achieve superior predictive accuracy. This observation underscores the critical significance of developing and utilizing authentic datasets tailored to individual languages. Nonetheless, translated datasets serve a valuable purpose in instances where access to original data is limited or unavailable.

In the latest paper [17], we compared machine learning approaches for sentiment analysis in Slovak. As part of our experimental approach, we evaluated three Slovak datasets containing social network comments. In the initial task, which involved three classes (positive/neutral/negative), the SlovakBERT model achieved F1 scores between 67.68% and 71.53% on the "SentiSK" and "Sentigrade" [18] datasets. In the second task, with two classes (positive/negative), both mBERT and SlovakBERT models achieved F1 scores ranging from 75.35% to 95.04% across the "SentiSK," "Sentigrade," and "Slovak dataset for SA [19]." We utilized eight algorithms or models for this evaluation: RFC, MLP, LR, SVC, KNN, Multinomial NB, mBERT, and SlovakBERT.

III. Conclusion

In the paper, we presented seven studies in which we addressed the issue of sentiment analysis and the detection of hate speech and offensive language on social networks. Overall, outstanding results were achieved for the Slovak language. We have released a new dataset specifically tailored for sentiment analysis tasks. Additionally, we have curated a dataset focused on binary classification (toxic/non-toxic). We conducted tests using various deep learning models and compared the results.

In future work, we want to focus on completing the benchmark dataset focused on toxic language according to the newly proposed annotation scheme. At the same time, we are dedicated to deep learning models for correcting grammatical errors and detecting stereotypical biases.

Acknowledgment

The research in this paper was partially supported by the Ministry of Education, Science, Research and Sport of the Slovak Republic under the research project VEGA 2/0165/21, the Cultural and Educational Grant Agency of the Slovak Republic project number KEGA 049TUKE-4/2024, and by the Slovak Research and Development Agency under the projects APVV-22-0414 - Modermed & APVV-22-0261. Also by the projects FBR-PDI-019 - FakeDetect (EHP & Norway funds) and European Online Hate Lab (EOHL).

References

[1] B. Pang, L. Lee *et al.*, "Opinion mining and sentiment analysis," *Foundations and Trends® in information retrieval*, vol. 2, no. 1–2, pp. 1–135, 2008.

[2] W. Medhat, A. Hassan, and H. Korashy, "Sentiment analysis algorithms and applications: A survey," *Ain Shams engineering journal*, vol. 5, no. 4, pp. 1093–1113, 2014.

[3] E. Di Corso, F. Ventura, and T. Cerquitelli, "All in a twitter: Self-tuning strategies for a deeper understanding of a crisis tweet collection," in *2017 IEEE International Conference on Big Data (Big Data)*. IEEE, 2017, pp. 3722–3726.

[4] M. Wankhade, A. C. S. Rao, and C. Kulkarni, "A survey on sentiment analysis methods, applications, and challenges," *Artificial Intelligence Review*, vol. 55, no. 7, pp. 5731–5780, 2022.

[5] L. Jiang and Y. Suzuki, "Detecting hate speech from tweets for sentiment analysis," in *2019 6th International conference on systems and informatics (ICSAI)*. IEEE, 2019, pp. 671–676.

[6] F. Del Vigna12, A. Cimino23, F. Dell'Orletta, M. Petrocchi, and M. Tesconi, "Hate me, hate me not: Hate speech detection on facebook," in *Proceedings of the first Italian conference on cybersecurity (ITASEC17)*, 2017, pp. 86–95.

[7] Y. Liu, X. Huang, A. An, and X. Yu, "Arsa: a sentiment-aware model for predicting sales performance using blogs," in *Proceedings of the 30th annual international ACM SIGIR conference on Research and development in information retrieval*, 2007, pp. 607–614.

[8] A. Ceron, L. Curini, S. M. Iacus, and G. Porro, "Every tweet counts? how sentiment analysis of social media can improve our knowledge of citizens' political preferences with an application to italy and france," *New media & society*, vol. 16, no. 2, pp. 340–358, 2014.

[9] Z. Sokolová, "Recent trends in detection of hate speech and offensive language on social media," *22nd Scientific Conference of Young Researchers*, vol. 2022, pp. 211–214, 2022.

[10] I. Mollas, Z. Chrysopoulou, S. Karlos, and G. Tsoumakas, "Ethos: a multi-label hate speech detection dataset," *Complex & Intelligent Systems*, vol. 8, no. 6, pp. 4663–4678, 2022.
[11] G. Kovács, P. Alonso, and R. Saini, "Challenges of hate speech detection in social media: Data scarcity, and leveraging external resources," *SN Computer Science*, vol. 2, pp. 1–15, 2021.
[12] Z. Sokolová, J. Staš, and D. Hládek, "An introduction to detection of hate speech and offensive language in slovak," in *2022 12th International Conference on Advanced Computer Information Technologies (ACIT)*. IEEE, 2022, pp. 497–501.
[13] Z. Sokolová, J. Staš, and J. Juhár, "Review of recent trends in the detection of hate speech and offensive language on social media," *Acta Electrotechnica et Informatica*, vol. 22, no. 4, pp. 18–24, 2022.
[14] Z. Sokolová, "Overview of trends in the field of detection of hate speech and offensive language on social media," *23rd Scientific Conference of Young Researchers*, vol. 2023, pp. 174–175, 2023.
[15] Z. Sokolová, H. Maroš, J. Staš, and J. Juhár, "Tvorba korpusu textov pre úlohy detekcie nenávistných prejavov, ofenzívneho jazyka a analýzy sentimentu," *Electrical Engineering and Informatics 14*, vol. 2023, pp. 399–402, 2023.
[16] Z. Sokolová, M. Harahus, J. Juhár, M. Pleva, D. Hládek, and J. Staš, "Comparison of sentiment classifiers on slovak datasets: Original versus machine translated," in *2023 21st International Conference on Emerging eLearning Technologies and Applications (ICETA)*. IEEE, 2023, pp. 485–492.
[17] Z. Sokolová, M. Harahus, J. Juhár, M. Pleva, J. Staš, and D. Hládek, "Comparison of machine learning approaches for sentiment analysis in slovak," *Electronics*, vol. 13, no. 4, p. 703, 2024.
[18] R. Krchnavy and M. Simko, "Sentiment analysis of social network posts in slovak language," in *2017 12th International Workshop on Semantic and Social Media Adaptation and Personalization (SMAP)*. IEEE, 2017, pp. 20–25.
[19] K. Machová, "Slovak dataset for sentimet analysis," https://kristina.machova.website.tuke.sk/useful/, Accessed 2024.

Overview of machine learning methods in astrophysics

[1]*Lenka Kališková (2nd year),*
Supervisor: [2]*Peter Butka*

[1,2]Dept. of Cybernetics and Artificial Intelligence, FEI TU of Košice, Slovak Republic

[1]lenka.kaliskova@tuke.sk, [2]peter.butka@tuke.sk

***Abstract*—This paper provides an overview of multiple machine learning approaches and assesses their application significance in astrophysics. Various approaches such as convolutional neural network or YOLO are considered to address three main tasks, which are object classification, detection and segmentation of small objects. Additionally, the possibility of additional potential enhancement via the use of advanced data augmentation and optimization of model hyperparameters is considered.**

***Keywords*—Convolutional Neural Network, Generative Adversarial Network, Optimization of Hyperparameters, Image Segmentation, Object Detection, YOLO**

I. Introduction

Using machine learning for analysis of observational data is crucial in the fields of astronomy and geophysics, particularly in image data processing. Our focus is aimed on tasks like object classification, detection, and segmentation, which could provide a valuable contribution to a better understanding of various phenomena [1].

Object classification focuses on class identification of a phenomenon in an image, such as stars or galaxies, while object detection locates entities in images, employing deep learning models like convolutional neural networks [2]. Object segmentation divides images into distinct regions, which is a crucial step in the analysis of structures like solar eruptions or coronal holes [3].

These processes automate the analysis of extensive astronomical datasets, providing essential insights into cosmic structures and dynamics. To enhance classification, detection, and segmentation, various approaches are explored, often influenced by challenges in astronomical data.

Insufficient data availability in astronomy may lead to challenges, which could be addressed by generating new data from existing sets. Another option is to use specialized algorithm adjustments and search approaches for optimal model learning.

Our motivation is to propose and leverage these approaches to improve output model quality.

II. Preliminary results

As already mentioned, multiple machine learning approaches were considered, therefore following section is dedicated to approaches and data, which we already covered and which are foundation for the future research.

A. Detection of TLE events

In collaboration with the Department of Astronomy and Astrophysics at Comenius University, a model for detecting Transient Luminous Events (TLE) [4] using data from Slovak AMOS cameras was trained [5]. The dataset comprised images from 2014 to 2021, capturing not only TLE but also other objects such as meteors. In the first two years, only 27 images with TLE occurrences were obtained. Subsequent years averaged around 44 500 images annually, with approximately 60 unique images each year featuring at least one TLE event. The Fig. 1 shows different types of TLE.

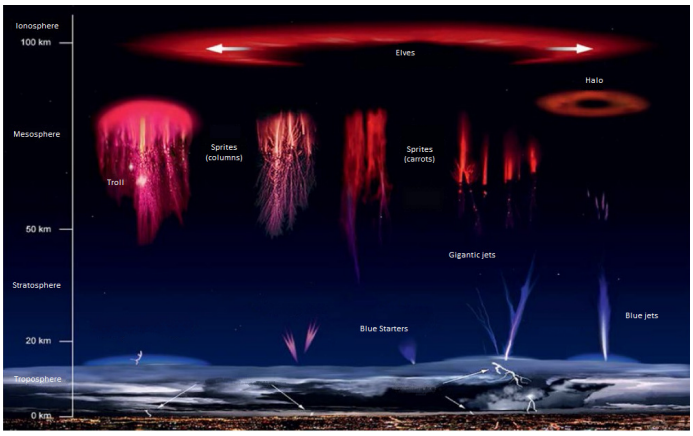

Fig. 1. Transient Luminous Events

We employed the YOLOv5 and YOLOv8 models [6] for TLE detection, but it suffered from a significant number of false detections. Annually, the model could identify over a thousand images presumed to contain TLE events, yet only about 50 of them actually did. To enhance the model, we opted for artificial data augmentation. Our technique included inversion, rotation, TLE object segmentation, and removal of false detections. Experiments with YOLOv5 [7] and YOLOv8 [8] showed that both correctly identified the majority of TLE events, but YOLOv8 exhibited fewer false detections. Training new models with augmented data yielded improvements. YOLOv5 correctly identified all TLE events without false detections, while YOLOv8 mislabeled two images.

The overall contribution lies in increasing data diversity and improving the accuracy of models for TLE detection.

B. Detection of meteors

Detection of meteors using AMOS cameras in Slovakia, utilizing video recordings, differs from the typical radio spectrogram [9]. The project's motivation was to explore the use of deep learning for automating the sorting and labelling of meteors from AMOS cameras. The goal was to reduce these images and facilitate manual sorting of meteors. The YOLOv5 network was applied to these data for meteor localization, labelling, and distinguishing from satellites and other phenomena.

In terms of qualitative evaluation, the actual number of meteors on detected images reached 248, of which the algorithm detected 247. Only one meteor was missing for 100% recall. Regarding false positives, the detection count stopped at 7, most of which were satellites. Although the original dataset did not contain truly negative images, 4 phenomena were incorrectly labelled as meteors in the test set. The algorithm failed to detect these phenomena, except for one satellite correctly classified in the satellite class, marking them as truly negative. Moreover, detection frames were more accurate than annotations in the dataset in a large number of cases.

C. Detection of meteoric echoes

The work focuses on meteoric echoes, recorded by radio scattering. This effective technique for monitoring meteors utilizes reflections of radio waves from their trails upon entry into the atmosphere. Collaboration with Comenius University addressed issues with echoes and aimed to create a neural network model, specifically YOLO for their automatic detection.

The proposed YOLOv5 model identified 392 out of 408 cases with minimal false detections. In total, there were 512 positive and 22 negative events, with the model predicting 508 positives and 26 negatives.

D. Segmentation of coronal holes and active regions

The coronal hole is a dark area on the solar disk in the shape of an irregular circle or oval, reaching several times the size of the Earth [10]. Active regions are temporary areas with a stronger magnetic field than their surroundings, affecting life on Earth [11].

The SOHO satellite, a collaboration between ESA and NASA, has been studying the Sun since 1995 with 12 instruments for observing the solar corona, helioseismology, and solar wind. To improve the segmentation of coronal holes and active phenomena, a SCSS-Net model was created using images from the SOHO spacecraft since 1996. Hyperparameters were tuned with respect to previous work [12].

The model achieved satisfactory results with Dice and IoU metrics on the test set for the segmentation of coronal holes and active regions. In comparison with SPoCA annotations, it achieved lower values by 7% for the segmentation of active regions. Limitations of SPoCA annotations may have contributed to a higher occurrence of false-positive pixels, affecting metrics even when the segmentation was correct.

III. Conclusion

We focus on analyzing image observational data, particularly from the astronomical domain and we successfully applied detection and segmentation architectures to various image datasets. The aim is to develop suitable methods, often in collaboration with specific partners from the physical domain, to improve the processing and analysis of scientific data.

Among machine learning methods, convolutional neural networks are indispensable for analyzing observational data in our work. These networks, along with GANs [13], effectively detect and segment objects in astronomical images, crucial for identifying and categorizing astronomical objects. The rarity of some phenomena and their characteristics present interesting challenges not only from a domain perspective but also in terms of applying deep learning methods, such as detecting small objects or employing advanced augmentation techniques. Hyperparameter optimization is another important aspect of our research, ensuring that our models achieve maximum performance and accuracy.

Hence, our main motivation is to apply these approaches to address challenges arising in the processing of astronomical image data within the tasks undertaken in our research group. Therefore, emphasis will be placed on the mentioned methods to improve model quality through specialized methods for detecting small objects, addressing issues with a low number of target detections, and optimizing model configuration and learning. We are also interested in exploring not only individual aspects but also the combination of the mentioned approaches. The fundamental premise for verifying the proposed approaches is their ability to improve the output models.

Acknowledgment

This work was supported by the Slovak VEGA grant no. 1/0685/21.

References

[1] L. Kališková and P. Butka, "Overview of machine learning methods in the analysis of observation data," *SCYR 2023: 23rd Scientific Conference of Young Researchers*, pp. 127–131, 2023.

[2] A. Dhillon and G. Verma, "Convolutional neural network: a review of models, methodologies and applications to object detection," *Progress in Artificial Intelligence*, vol. 9, 12 2019.

[3] E. A. Illarionov and A. G. Tlatov, "Segmentation of coronal holes in solar disc images with a convolutional neural network," *Monthly Notices of the Royal Astronomical Society*, vol. 481, no. 4, pp. 5014–5021, 2018.

[4] E. Blanc, "Space observations of transient luminous events and associated emissions in the upper atmosphere above thunderstorm areas," *Comptes Rendus Geoscience*, vol. 342, no. 4-5, pp. 312–322, 2010.

[5] J. Tóth, J. Šilha, P. Matlovič, L. Kornoš, P. Zigo, J. Világi, D. Kalmančok, J. Šimon, and P. Vereš, "Amos—the slovak worldwide all-sky meteor detection system," in *Proc. 1st NEO and Debris Detection Conference*, vol. 1, 2019.

[6] J. Redmon, S. Divvala, R. Girshick, and A. Farhadi, "You only look once: Unified, real-time object detection," in *Proceedings of the IEEE conference on computer vision and pattern recognition*, 2016, pp. 779–788.

[7] G. Jocher, A. Stoken, J. Borovec, L. Changyu, A. Hogan, L. Diaconu, J. Poznanski, L. Yu, P. Rai, R. Ferriday *et al.*, "ultralytics/yolov5: v3. 0," *Zenodo*, 2020.

[8] J. Glenn, "Ultralytics yolov8 official documentation," 2023. [Online]. Available: https://docs.ultralytics.com/

[9] J. Tóth, L. Kornoš, P. Zigo, Š. Gajdoš, D. Kalmančok, J. Világi, J. Šimon, P. Vereš, J. Šilha, M. Buček *et al.*, "All-sky meteor orbit system amos and preliminary analysis of three unusual meteor showers," *Planetary and space science*, vol. 118, pp. 102–106, 2015.

[10] S. R. Cranmer, "Coronal holes," *Living Reviews in Solar Physics*, vol. 6, pp. 1–66, 2009.

[11] L. van Driel-Gesztelyi and L. M. Green, "Evolution of active regions," *Living Reviews in Solar Physics*, vol. 12, pp. 1–98, 2015.

[12] Š. Mackovjak, M. Harman, V. Maslej-Krešňáková, and P. Butka, "Scss-net: solar corona structures segmentation by deep learning," *Monthly Notices of the Royal Astronomical Society*, vol. 508, no. 3, pp. 3111–3124, 2021.

[13] I. J. Goodfellow, J. Pouget-Abadie, M. Mirza, B. Xu, D. Warde-Farley, S. Ozair, A. Courville, and Y. Bengio, "Generative adversarial networks," 2014.

Lease Contract Named Entity Recognition

[1]*Tatiana KUCHČÁKOVÁ (3rd year),*
Supervisor: [2]*Jaroslav PORUBÄN*

[1,2]Dept. of Computers and Informatics, FEI TU of Košice, Slovak Republic

[1]tatiana.kuchcakova@tuke.sk, [2]jaroslav.poruban@tuke.sk

***Abstract*—This paper presents a new dataset and approach for recognizing specific information in legal documents, focusing on lease contracts. Named entity recognition (NER) is a crucial step in analyzing legal texts, especially given the variety of contract types and their unique characteristics. Our project leverages a rich source of data from the Central Register of Contracts in Slovakia. Using this dataset, we trained a new legal NER model by adapting the SlovakBert model. This fine-tuning process is designed to capture the specific nuances of lease contracts.**

***Keywords*—named entity ecognition, legal processing, lease contract analysis**

I. Introduction

The legal domain introduces a unique set of challenges that extend beyond general language processing. Most of the NLP tasks created over legal documents require an information extraction process. One of the main parts of information extraction is named entity recognition (NER), which is also specific within the legal domain according to the current solving task. When dealing with contract analysis tasks, entity recognition also depends on the contract type.

In classical NER, the task might simply involve identifying a person, organizaton or dates mentioned within a contract. This process is generally straightforward and relies on relatively clear rules or patterns. However, in the context of legal contracts, simply identifying a person or organization is insufficient. Legal NER systems must discern the specific role that the person plays within the contract, for instance, whether the person is a lessor or a lessee. This requirement significantly complicates the entity recognition process, as it necessitates a deep understanding of the contract's context and the relationships between parties. Moreover, the term for lessor or lessee in the context of a legal contract can refer to a broader range of entities besides persons. It can denotate also organizations or even cities and locations. In addressing the complexities in legal NER, incorporating additional information beyond plain text may affect entity detection accuracy. As a preliminary step to validate this assumption, we need to create a legal NER model.

In this paper, we present our dataset created from a central registry of contracts, labeled for the lease contract named entity recognition task, based on which a new legal NER model is trained by finetuning the *SlovakBERT*[1] model. This model can serve as a baseline for comparison with models that incorporate additional, emphasized text.

II. Corpus of Central Register of Contracts of the Slovak Republic

Central Register of Contracts (Centrálny register zmlúv (CRZ)) [1] of Slovakia is an official platform where contracts related to public procurement, government, and public sector agreements are published for transparency. The site lists various types of contracts, including those that have been supplemented or canceled, and allows for detailed searches based on specific criteria. This initiative is part of Slovakia's government efforts to enhance transparency and public oversight of government spending and contracting practices. In order to create a corpus for lease-named entity recognition, we filtered and web-scraped non-scanned PDF files of lease contracts from this registry that we converted to plain text. For our purposes, a small set (approximately 400 leases) of this database is used. Our corpus contains the following two columns:

- id - Represents the unique identification number of the data element. It is number of contract web-scraped from registry
- text - Contains text extracted from PDF file of lease contracts

III. preprocessing and annotation

To effectively train a deep neural network, it's crucial to convert our data into a structure that fits statistical models of supervised learning method. Initially, we will cleanse the data by eliminating unnecessary whitespace. Following this preliminary step, we will proceed to separate the sentences into individual tokens.

The preprocessing data task is followed by the annotation process. In our annotation process, we used a combination of techniques to annotate our dataset effectively. We were able to get additional data from the CRZ registry, which was web-scraped alongside PDF files like information about customers and suppliers. We used a script to detect this data in contract text and labeled the customer as *Lessee* and the supplier as *Lessor*. After applying the script to the data, it was manually reviewed by two annotators. Since the additional contract data on the web is manually input by workers who upload the contracts, this data was often inaccurately stated in comparison to the information in the actual contracts. In approximately 30% of all scraped contracts, the additional data for lessor and lessee were reversed. Other errors included incorrect spelling and failure to state the correct parties involved.

[1]Centrálny register zmlúv https://www.crz.gov.sk/

In cases where additional data were not provided correctly, we used automatic annotation with a pre-trained *'crabz/slovakbert-ner'* [2] model available on the Hugging Face Hub. This model is a finetuned NER model that is able to detect three basic character entities, namely: *Person*, *Organization*, and *Location*. The model is trained on the *WikiANN* dataset[3] dataset, which was created for multilingual named entity tagging. *WikiANN* dataset consists of data from Wikipedia articles in multiple language configurations. The Slovak configuration of this dataset was used to train the *SlovakBERT-NER* model. The dataset is annotated by standard *IOB* format labels since the entities that represent *Person*, *Organization*, or *Location* are usually made of more than one token.

Considering the lease contract, two main entities, *Lessor* and *Lessee*, are usually in one of the categories mentioned above. We manually corrected these detected entities on our dataset and renamed them with *Lessor* or *Lessee* labels, respectively, preserving the *IOB* format. In cases where none of these techniques was successful enough, we manually corrected tags. In the first stages [2], [3], we also used labeling with regular expressions and manual labeling. In the final step, all labeled data were concatenated together and manually checked by two annotators.

IV. MODELING

After dataset preparation data was sampled randomly and divided into three spilts. In our case, we first divided the training and test data in a ratio of 80:20. Subsequently, we further divided the training data with a similar ratio into training and validation data.

An important part of the finetuning model is a *tokenizer*. Since we are finetuning the *SlovakBERT* model, we need to use a tokenizer that works on the same principle. The *SlovakBERT* model uses a *RoBERTa* tokenizer, which we also used. Transformers models like *SlovakBERT* use special types of *subword* tokenizers. These tokenizers not only divide sentences into words but even divide words into smaller tokens and add special tokens like *[CLS]* at the beginning and *[SEP]* at the end [4]. Applying this type of tokenizer to our data creates inconsistency in the number of tags, annotated in a dataset with the word-per-token technique. In order to ensure that these special tokens in our input data do not contribute to the loss calculation during training, we labeled these tokens with a pecial value. The reason for choosing specific value [5] is to inform the loss function to exclude these tokens from the loss calculation.

RoBERTa is special type of subword tokenizer using Byte-Pair Encoding (BPE) [6]. Initially, BPE operates by breaking down the training data into words using a preliminary tokenizer that splits the text into a sequence of words. Following this initial tokenization, a unique set of words is compiled along with the frequency of occurrence of each word within the training dataset. Every word in the text is treated as a sequence of characters plus a special end-of-word symbol to distinguish between the same sequence of characters within different word boundaries. BPE then counts the frequency of each symbol and every possible adjacent pair of symbols in the text. In each iteration, it identifies the most frequent pair of adjacent symbols and merges them to form a new symbol. This new symbol is added to the vocabulary, and its frequency is updated in the context of the entire text. This process is repeated for a predefined number of iterations or until a desired vocabulary size is reached.

After configuring the tokenizer, we chose automatic token classification on the *'gerulata/slovakbert'*[4] model tailored for the Slovak language, available through a Hugging face library for natural language processing. In the process of configuring our model for training, we set specific training arguments and used standardized metrics for the model against validation data.

Precision	Recall	F1	Accuracy
0.8740	0.8938	0.88384	0.9635

TABLE I
EVALUATION RESULTS OF FINETUNED MODEL

V. CONCLUSION

In this paper, we introduced a novel annotated dataset derived from the Central Register of Contracts of Slovakia, specifically tailored for the task of lease contract analysis. This dataset serves as a foundation for addressing the complex challenge of Named Entity Recognition (NER) within Slovak legal documents. Through preprocessing and annotation, we adapted and fine-tuned the SlovakBERT model to better understand and categorize legal terminology and entities present in lease agreements. Results can be seen in table I. The model can be beneficial in analyzing contracts. Given that the only source for identifying contracts associated with physical persons or organizations (often inaccurately recorded) working with state institutions is the additional data about contract parties manually provided on the CRZ website, our model has the potential to improve transparency and assist in detecting corruption.

ACKNOWLEDGMENT

This work was supported by project VEGA No. 1/0630/22 "Lowering Programmers' Cognitive Load Using Context-Dependent Dialogs".

REFERENCES

[1] M. Pikuliak, Š. Grivalskỳ, M. Konôpka, M. Blšták, M. Tamajka, V. Bachratỳ, M. Šimko, P. Balážik, M. Trnka, and F. Uhlárik, "Slovakbert: Slovak masked language model," *arXiv preprint arXiv:2109.15254*, 2021.
[2] T. Kuchčáková and J. Porubän, "Processing legal contracts using natural language processing techniques," in *Proceedings of the 22nd Scientific Conference of Young Researchers*, 2022, pp. 226–229.
[3] T. Kuchčáková, "Incorporating visual features of documents for improved information extraction in the legal domain," in *23rd Scientific Conference of Young Researchers: Proceedings from Conference*. Košice, Slovensko: Technická univerzita v Košiciach, 2023, pp. 189–190.
[4] Hugging Face, "Preprocessing - transformers documentation," 2023. [Online]. Available: https://huggingface.co/docs/transformers/en/preprocessing
[5] PyTorch, "PyTorch Documentation: torch.nn.NLLLoss," https://pytorch.org/docs/stable/generated/torch.nn.NLLLoss.html, 2023, accessed: 2024-02-23.
[6] Hugging Face, "Byte pair encoding tokenization - chapter 6.5 of nlp course," 2023. [Online]. Available: https://huggingface.co/learn/nlp-course/en/chapter6/5#byte-pair-encoding-tokenization

[2] SlovakBERT-NER model - https://huggingface.co/crabz/slovakbert-ner
[3] WikiANN dataset - https://huggingface.co/datasets/wikiann
[4] SlovakBERT model -https://huggingface.co/gerulata/slovakbert

Isolated bidirectional power converters for microgrids – A Review

[1]*Tomáš BASARIK (1st year),*
Supervisor: [2]*Milan LACKO*

[1,2]Dept. of Electrical Engineering and Mechatronics, FEI TU of Košice, Slovak Republic

[1]tomas.basarik@tuke.sk, [2]milan.lacko@tuke.sk

***Abstract*—DC-DC converters are essential for efficient power conversion over a wide range of voltage levels. This article reviews current control methods and modelling techniques for dual active bridge (DAB) and multi active bridge (MAB) converters. The types of modulation used to drive the full H-bridges used in these types of converters are also discussed.**

***Keywords*—DC-DC converter, multi-active-bridge converter, power redistribution, power flow control**

I. Introduction

Much of the world's emissions today come from industry, the heating of buildings, and global transport, where trucks and cars also play a major role. There are several ways to reduce these emissions. One is the use of renewable energy sources such as fuel cells, photovoltaics or battery energy storage. The main requirement for all these sources is reliable conversion of motive energy into electrical energy. However, the problem with this conversion is that, in practice, there are countless devices with different voltage levels that cannot function without electricity. As a result, DC-DC or DC-AC converters with a DC link or DC bus have become the most widely used method for connecting devices or sources and devices with different voltage levels. The main disadvantage of this topology is the higher number of conversion steps, which contributes to lower efficiency. As a result, the use of a large number of DC-DC converters increases the system overhead, increases the system size and reduces the power density of the overall system [1].

The disadvantages of DC bus topologies can be overcome by using multiport converters. These converters are capable of transferring power between ports in a single conversion step. They are structurally based on basic DC-DC converter topologies, where the ports of the multiport converter are interconnected by magnetic or capacitive coupling. In the case of magnetic coupling, there are also nonisolated and isolated ports. The ports in multiport converters are already largely designed for bidirectional power flow. It is therefore possible to both supply and extract electrical energy through a bidirectional inverter port. These inverters are characterised by a low number of conversion steps, smaller overall system size, high power density and high inverter modularity. Such a multiport inverter, with all its advantages, can then be used for interconnecting renewable energy sources, but also in electromobility for energy spillover between different sources/appliances [1].

II. DAB Converter

The Dual Active Bridge (DAB), introduced in [2], is a power converter topology used for isolated bidirectional power conversion. It consists of two full H-bridges, each with its own set of switches and a planar transformer. It is used for its ability to efficiently transfer power between two separate voltage levels while maintaining isolation between them. A simplified circuit is used for the analysis, see Fig. 1. In the simplified circuit, the full H-bridges are replaced by a pulse voltage source. The primary and secondary winding resistances and the magnetising inductance are neglected. The complete circuit of the DAB converter is shown in Fig. 2

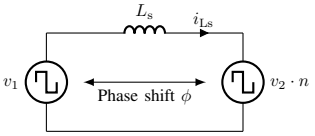

Fig. 1. Simplified circuit of DAB converter [3], [4]

A. Types of modulations

The most commonly used modulations for DAB converters are listed in [4]. The literature lists three modulation techniques. These are the phase shift modulation, trapezoidal and the triangular current mode modulation.

1) Phase shift modulation: The principle of the phase shift modulation is very simple. Square-wave voltages v_1 and v_2, which do not have any clamping invtervals, are applied to the planar transformer. The power transmitted from the primary to the secondary side depends on the phase shift ϕ between the AC voltages v_1 and v_2. The relationship between the transmitted power and the phase shift is given by [4]:

$$P_{12} = -\frac{V_1 n V_2 \phi \left(\pi - |\phi|\right)}{\pi \omega_s L_\mathrm{s}}, \tag{1}$$

where V_1 and V_2 is DC voltages of the sources, n is trasformer ratio, ω_s is angular frequency and L_s is branch inductance. The maximum power that can be transmitted with this type of modulation can be calculated as [4]:

$$P_{12\max} = \pm\frac{\pi V_1 n V_2}{4\omega_s L_\mathrm{s}} \tag{2}$$

The waveforms of the voltages v_1, v_2 and current i_{Ls} corresponding to the phase shift modulation are shown in Fig. 3.

Phase shift modulation has the advantage of simplicity, with only one degree of freedom, making it relatively easy to

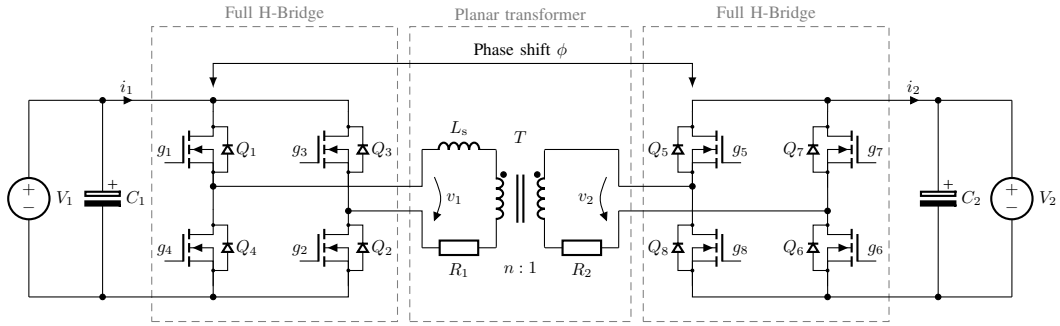

Fig. 2. Dual active bridge converter [5], [4]

implement. It also allows the highest achievable power flow, but at the cost of higher RMS transformer current and a limited operating range, especially in terms of low switching losses.

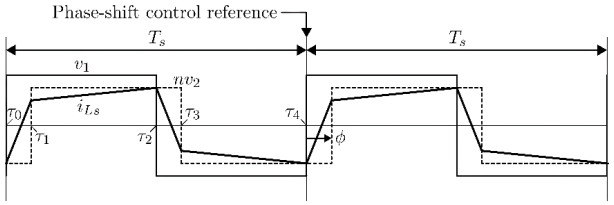

Fig. 3. Phase shift modulation [4]

2) Trapezoidal current mode modulation: The square-wave voltages v_1 and v_2, with clamping intervals, are applied to the planar transformer. The power transmitted from the primary to the secondary side depends on the phase shift ϕ between the voltages v_1 and v_2. The transmitted power is given by [4]:

$$P_{12} = -\text{sign}\left(\phi\right) \frac{V_1 n V_2 \left(\pi \left|\phi\right| - 2\phi^2 + 2\delta_1\delta_2\right)}{\pi\omega_s L_\text{s}} \tag{3}$$

with $\delta_1 = f(\phi) \in [0, \pi/2]$, $\delta_2 = f(\phi) \in [0, \pi/2]$ and $\phi \in [-\pi, \pi]$. The maximum power that can be transmitted with this type of modulation can be calculated from the following equation [4]:

$$P_{12\text{max}} = \pm \frac{\pi V_1^2 n^2 V_2^2}{2\omega_s L_\text{s} \left(V_1^2 + n^2 V_2^2 + V_1 n V_2\right)} \tag{4}$$

The waveforms of the voltages v_1, v_2 and current i_{Ls} corresponding to the trapezoidal current mode modulation are shown in Fig. 4.

Trapezoidal modulation offers higher achievable power compared to triangular modulation and still achieves zero current switching (ZCS) on some switching instances. However, it cannot be used efficiently for low power transfer scenarios and does not consistently achieve ZCS on the secondary, limiting its practicality.

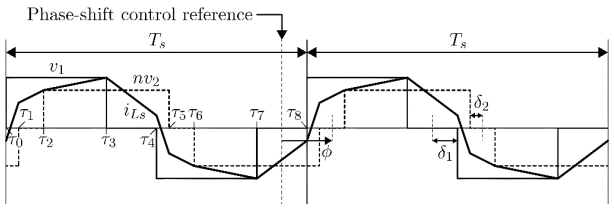

Fig. 4. Trapezoidal current mode modulation [4]

3) Triangular current mode modulation: The square-wave voltages v_1 and v_2, with clamping intervals, are also applied to the planar transformer. The power transmitted from the primary to the secondary side depends on the phase shift ϕ between the voltages v_1 and v_2. The transmitted power is determined by [4]:

$$P_{12} = -\frac{V_1 n V_2 \phi \left(\pi - 2\delta_1\right)}{\pi\omega_s L_\text{s}} \tag{5}$$

with $\delta_1 = f(\phi) \in [0, \pi/2]$, $\delta_2 = f(\phi) \in [0, \pi/2]$ and $\phi \in [-\pi, \pi]$. The maximum power that can be transmitted with this type of modulation can be calculated as [4]:

$$P_{12\text{max}} = \pm \frac{\pi n^2 V_2^2 \left(V_1 - n V_2\right)}{2\omega_s L_\text{s} V_1} \tag{6}$$

The waveforms of the voltages v_1, v_2 and current i_{Ls} corresponding to the triangular current mode modulation are shown in Fig. 5.

Triangular modulation offers advantages such as ensuring that the secondary always switches at zero current, reducing the RMS transformer current and improving converter efficiency. However, it introduces increased complexity and defines the power transfer direction based on voltage differences, which limits the achievable power flow, especially near $V_1 = nV_2$.

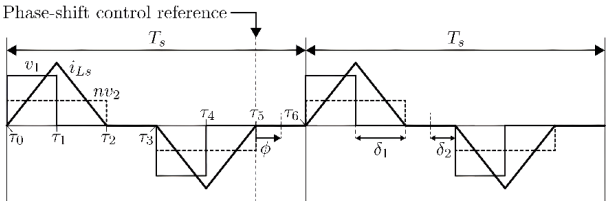

Fig. 5. Triangular current mode modulation [4]

B. Modelling of DAB

Modelling a DAB converter is not easy. The problem is to describe the current flowing through the inductance i_{Ls}, whose mean value is zero. In the literature [6], other types of DAB converter modelling are presented, such as:

- *Reduced-Order Model* – which ignores the dynamics of current i_Ls and is based on the mean values of input current i_1 and output current i_2.
- *Generalized Average Model* – which includes the dynamics of the current i_Ls but considers only the first harmonic component of the current.
- *Discrete-Time model* – which describes state changes variables in defined time steps. In the case of a DAB

converter with phase shift modulation, four states can be defined during the switching cycle.

Satisfactory results are provided by the Reduced-Order Model and the Discrete-Time Model. The Generalized Average Model method achieves a small deviation.

C. Control of DAB converters

When controlling a DAB converter, it is necessary to choose a controlled variable. The control can be focused on output voltage, output current or output power. The literature [5] describes the available output voltage control methods, including conventional feedback control, linearisation control, feedforward plus feedback control, etc. The control of the output current is described in the literature [7].

III. MAB Converter

The name multi active bridge is derived from the name dual active bridge. The name implies that it is an inverter that has multiple active bridges and therefore multiple inputs and outputs. Several such multi-active or multi-port active bridges derived from DAB are given in [8], [9], [10], [11], [12], [13]. This type of converter has also been analyzed and presented in [3]. The use of independent two-input transformers is referred to as the so-called multitransformer approach. The presented topology is also electrically equivalent to other multiport active bridges such as the "quad-active-bridge" (QAB) [14] or other topologies with a single multi-input transformer [15]. In this paper will be described multiport active bridge with multiple dual winding transformers whose secondary windings are electrically interconnected, such an inverter is shown in Fig. 6.

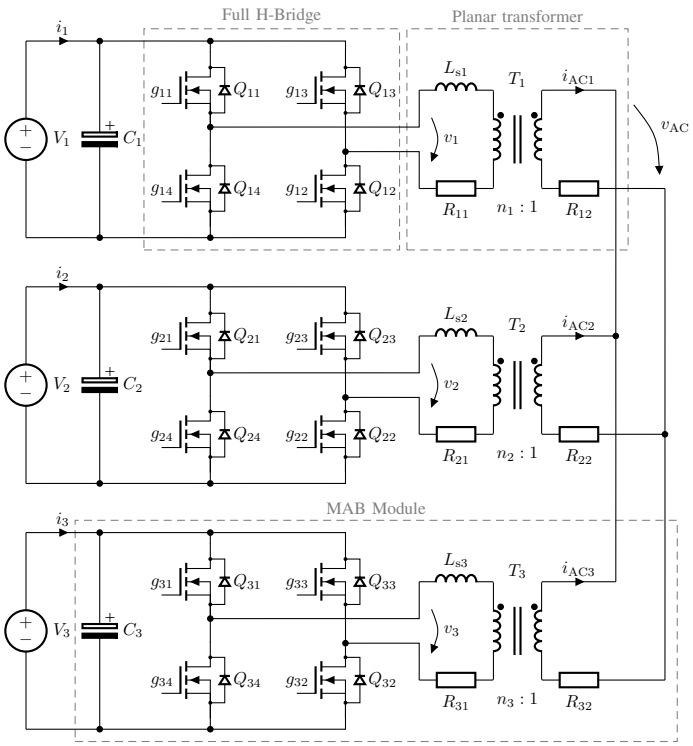

Fig. 6. Three port multi active bridge converter [3]

For the analysis of the MAB converter, a simplified circuit can be used, which is shown in Fig. 7.

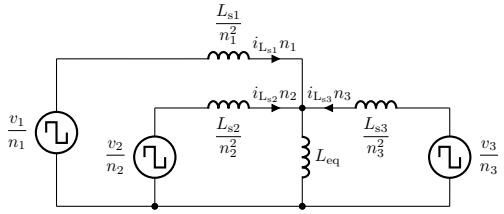

Fig. 7. Simplified circuit of MAB converter [17]

A. Types of modulations

Different types of modulation can be used to control the full H-bridge of the MAB converter, similar to the DAB converter. However, the most commonly used is Phase shift modulation.

B. Intermediate circuit voltage

The power transferred between ports is then determined by the interaction of the voltage of a particular bridge v_{k} and the intermediate circuit voltage v_{AC} across the branch inductance L_{sk}. The steady state intermediate circuit voltage can be calculated as [1]:

$$v_{\mathrm{AC}} = \frac{\sum_{k=1}^{M} v_{\mathrm{k}} \dfrac{n_{\mathrm{k}}}{L_{\mathrm{sk}}}}{\dfrac{1}{L_{\mathrm{eq}}}} \tag{7}$$

where

$$L_{\mathrm{eq}} = \left(\sum_{k=1}^{M} \frac{n_{\mathrm{k}}^2}{L_{\mathrm{sk}}} \right)^{-1} \tag{8}$$

The voltages and phase shifts of the individual bridges as well as the intermediate circuit voltage are shown in Fig. 8.

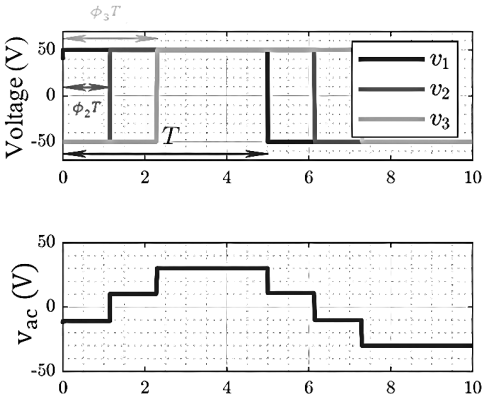

Fig. 8. Phase shift between bridges (upper) and intermediate circuit voltage (lower) [1]

C. Control of MAB converters

The difficulty of controlling such multiport active bridges is described in [16], [17], [18], [19], [20]. The basic control principle of multiport active bridges is to change the phase shift between the individual bridges. However, it is difficult to precisely define the calculation of the phase shifts according to the desired power distribution, since the performance of each port depends on all the other phase shifts. However, the situation is complicated by the fact that the relationship between the currents and phase shifts of the bridges is not linear in the case of the MAB converter. In the literature [1], two main groups of methods for removing nonlinearity are given by numerical methods and hardware methods.

IV. Applications of DAB and MAB converters

Dual active bridge and multi active bridge are suitable converter topologies for creating microgrids. Both inverters achieve high efficiency, but despite their similar structure they work differently. A microgrid formed from a MAB converter has a smaller component count requirement than that of a DAB converter, thus achieving a higher power density. On the other hand, the MAB converter has more complex control than the DAB converter. Microgrids consist of DAB converters is shown in Fig. 9 and microgrids consist of MAB converters is shown in Fig. 10.

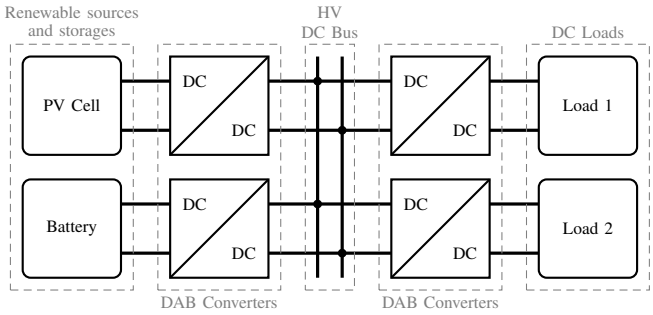

Fig. 9. Microgrids consist of DAB converters

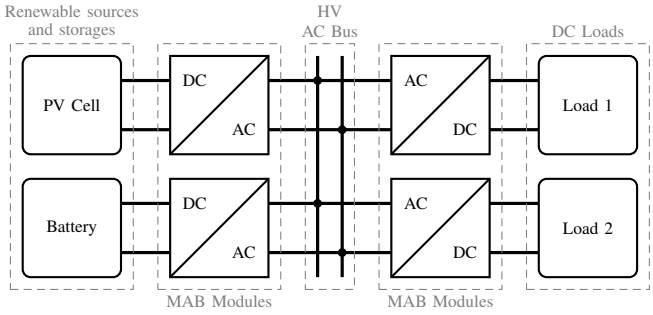

Fig. 10. Microgrids consist of MAB converters

Tab. I shows a comparison of DAB and MAB converters. Power density, circuit and control complexity and efficiency are compared.

TABLE I
Comparison of DAB and MAB converters

	DAB Converter	MAB Converter
Power density	++	+++
Circuit complexity	+++	++
Control complexity	+	+++
Efficiency	+++	+++
Note: +++ High; ++ Medium; + Low		

V. Conclusion

This article discusses two types of DC-DC converters that are applicable to microgrids. The first inverter is the dual active bridge and the other one is multi active bridge. The possible modulation types and also the modelling types of each converter have been mentioned in the article. The control types of these converters are also mentioned. For further investigation, it is useful to focus on solving the multi active bridge control problem which is caused by the nonlinearities between the performances of the individual modules and their phase shifts with each other.

Acknowledgment

This work was supported under projects APVV-18-0436 and VEGA 1/0363/23.

References

[1] A. Marcinek and M. Pastor, "Power control of three port mab converter," in *2023 International Conference on Electrical Drives and Power Electronics (EDPE)*, 2023, pp. 1–8.

[2] M. Kheraluwala, R. W. Gascoigne, D. M. Divan, and E. D. Baumann, "Performance characterization of a high-power dual active bridge dc-to-dc converter," *IEEE Transactions on industry applications*, vol. 28, no. 6, pp. 1294–1301, 1992.

[3] P. Zumel, C. Fernandez, A. Lazaro, M. Sanz, and A. Barrado, "Overall analysis of a modular multi active bridge converter," in *2014 IEEE 15th Workshop on Control and Modeling for Power Electronics (COMPEL)*, 2014, pp. 1–9.

[4] F. Jauch and J. Biela, "Generalized modeling and optimization of a bidirectional dual active bridge dc-dc converter including frequency variation," *IEEJ Journal of Industry Applications*, vol. 4, no. 5, pp. 593–601, 2015.

[5] S. Shao, L. Chen, Z. Shan, F. Gao, H. Chen, D. Sha, and T. Dragičević, "Modeling and advanced control of dual-active-bridge dc–dc converters: A review," *IEEE Transactions on Power Electronics*, vol. 37, no. 2, pp. 1524–1547, 2022.

[6] P. Zumel, L. Ortega, A. Lázaro, C. Fernández, A. Barrado, A. Rodríguez, and M. M. Hernando, "Modular dual-active bridge converter architecture," *IEEE Transactions on Industry Applications*, vol. 52, no. 3, pp. 2444–2455, 2016.

[7] M. Neubert, "Modeling, synthesis and operation of multiport-active bridge converters," Ph.D. dissertation, Dissertation, Rheinisch-Westfälische Technische Hochschule Aachen, 2020, 2020.

[8] S. Falcones, R. Ayyanar, and X. Mao, "A dc–dc multiport-converter-based solid-state transformer integrating distributed generation and storage," *IEEE Transactions on Power Electronics*, vol. 28, no. 5, pp. 2192–2203, 2013.

[9] B. J. Vermulst, J. L. Duarte, E. A. Lomonova, and K. G. Wijnands, "Scalable multi-port active-bridge converters: modelling and optimised control," *IET Power Electronics*, vol. 10, no. 1, pp. 80–91, 2017.

[10] A. M. Ari, L. Li, and O. Wasynczuk, "Control and optimization of n-port dc–dc converters," *IEEE Transactions on Control Systems Technology*, vol. 24, no. 4, pp. 1521–1528, 2015.

[11] S. Falcones and R. Ayyanar, "Lqr control of a quad-active-bridge converter for renewable integration," in *2016 IEEE Ecuador Technical Chapters Meeting (ETCM)*. IEEE, 2016, pp. 1–6.

[12] Y. Chen, P. Wang, H. Li, and M. Chen, "Power flow control in multi-active-bridge converters: Theories and applications," in *2019 IEEE Applied Power Electronics Conference and Exposition (APEC)*. IEEE, 2019, pp. 1500–1507.

[13] P. Wang, Y. Chen, P. Kushima, Y. Elasser, M. Liu, and M. Chen, "A 99.7% efficient 300 w hard disk drive storage server with multiport ac-coupled differential power processing (mac-dpp) architecture," in *2019 IEEE Energy Conversion Congress and Exposition (ECCE)*. IEEE, 2019, pp. 5124–5131.

[14] S. Falcones, R. Ayyanar, and X. Mao, "A dc–dc multiport-converter-based solid-state transformer integrating distributed generation and storage," *IEEE Transactions on Power electronics*, vol. 28, no. 5, pp. 2192–2203, 2012.

[15] P. Wang, Y. Chen, Y. Elasser, and M. Chen, "Small signal model for very-large-scale multi-active-bridge differential power processing (mab-dpp) architecture," in *2019 20th Workshop on Control and Modeling for Power Electronics (COMPEL)*. IEEE, 2019, pp. 1–8.

[16] Y. Chen, P. Wang, H. Li, and M. Chen, "Power flow control in multi-active-bridge converters: Theories and applications," in *2019 IEEE Applied Power Electronics Conference and Exposition (APEC)*, 2019, pp. 1500–1507.

[17] S. Bandyopadhyay, P. Purgat, Z. Qin, and P. Bauer, "A multiactive bridge converter with inherently decoupled power flows," *IEEE Transactions on Power Electronics*, vol. 36, no. 2, pp. 2231–2245, 2021.

[18] X. Ruan, W. Chen, L. Cheng, K. T. Chi, H. Yan, and T. Zhang, "Control strategy for input-series–output-parallel converters," *IEEE Transactions on Industrial Electronics*, vol. 56, no. 4, pp. 1174–1185, 2008.

[19] P. Zumel, L. Ortega, A. Lázaro, C. Fernández, A. Barrado, A. Rodríguez, and M. M. Hernando, "Modular dual-active bridge converter architecture," *IEEE Transactions on Industry Applications*, vol. 52, no. 3, pp. 2444–2455, 2016.

[20] K. Filsoof and P. W. Lehn, "A bidirectional multiple-input multiple-output modular multilevel dc–dc converter and its control design," *IEEE Transactions on Power Electronics*, vol. 31, no. 4, pp. 2767–2779, 2015.

Optimizing Clock Generators for Ultra-Wideband Sensor Systems: VCOs, PLLs, and DROs

[1]*Patrik Jurík (3rd year),*
Supervisor: [2]*Pavol Galajda*

[1,2]Dept. of Electronics and Multimedia Communications, FEI TU of Košice, Slovak Republic

[1]patrik.jurik@tuke.sk, [2]pavol.galajda@tuke.sk

***Abstract*—This paper summarizes the design and implementation of the clock generator circuits for Ultra-Wideband (UWB) sensor systems. Several voltage-controlled oscillators were fabricated as application-specific integrated circuits (ASICs), and a few oscillators were created from discrete components with microstrip dielectric resonator coupling. Furthermore, the article discusses the integration of a Phase-Locked Loop (PLL) ADF4002 to address limitations in voltage-controlled oscillators (VCOs), ensuring enhanced phase noise performance and stability crucial for radar applications. Finally, the article touches upon the design and tuning of a tunable dielectric resonator oscillator (DRO) for high-frequency applications, underscoring the importance of precise tuning methods for optimal performance.**

***Keywords*—Oscillator, ASIC, PLL, DRO, UWB**

I. Introduction

Today's ultra-wideband (UWB) sensor systems represent a significant advance over their predecessors, facilitating their widespread deployment and utilization in the 21st century. These advancements stem from notable improvements in the miniaturization of electronic components, resulting in UWB sensors characterized by enhanced quality, affordability, and reduced size. These new generations of sensors lead the way for a wider range of applications and new innovations in various industries, contributing to increased efficiency and accuracy in many fields such as: medicine [1], industry [2], [3], [4], or security [5].

These systems include different topologies and types of emitted signals, which include impulse radars [6], random noise radars [7], and FMCW [8] radars. UWB sensor systems are a promising technology in many fields and form part of sensors capable of non-invasive measurements. Our research is directed towards the design and development of UWB sensors utilizing M-sequence technology. Over the past two decades, various types of M-sequence UWB sensors have been created for different applications. Depending on the specific application and semiconductor technology employed, as well as on the operational frequency ranges from a few hundred megahertz to tens of gigahertz.

The sensor system consists of a number of sub-circuits. For each application, the specific hardware is required with a specially designed front-end ASCI circuits. One of the key circuits is the clock pulse generator. As part of development, a voltage-controlled oscillator (VCO) was designed and implemented, in 0.25 µm semiconductor technology [9]. In contrast to other technologies [10], this particular technology is comparatively affordable. The maximum transit frequency of the utilized technology is f_t = 110 GHz, which allows designs up to 60 GHz. The designed VCO has a resonant frequency of 22 GHz, with the possibility of tuning the output frequency using a varicap and a capacitive bank. However, the phase noise and overall stability of the circuit is not sufficient for use with a radar system so it was necessary to consider other options.

II. Phase Locked Loop circuits

In light of this, we turned our attention to the Phase-Locked Loop (PLL) ADF4002. This sophisticated PLL offered the potential to address the shortcomings observed in the VCO, promising enhanced phase noise performance and improved stability crucial for radar applications. The integration of the PLL ADF4002 marked a pivotal moment in our development process, underscoring our commitment to delivering a robust and reliable sensor system. To test our phase-locked VCO with phase locked loop, an evaluation board was designed (Fig. 1a), the board contains a low-noise low-dropout regulator (LDO) for powering the VCO and the ADF4002 (Fig. 1b), it also contains trimmers for the ability to adjust and tune the operating points of the oscillator transistors. The ADF4002 circuit needs an external low frequency clock generator on the order of tens of megahertz for functionality. In practice, a commercial crystal with very low phase noise is used, in our case we used an external Keysight N5183B generator. Phase locked-loop ADF4002 offers a variety of settings such as adjusting the reference frequency and oscillator frequency division ratio, charge pump current level, and more. For proper functionality of VCO and PLL with sensor system it is necessary to achieve frequency 21.75 GHz,however our VCO works at higher frequency after tuning bias voltage and PLL settings we were able to lock oscillator frequency to 21.94 GHz, when changing frequency it was necessary to change reference frequency to 50 MHz and after recalculation we achieved desired oscillator stability at frequency 21.94 GHz by using divisor ratio R=7, N=6, we were able to achieve oscillator stability at frequency 21.94 GHz. With our VCO and PLL configuration we reduce the overall power consumption of system by 1 W.

The previous results have been incorporated into the design of a new ASIC circuit using 130 nm SG13G2 technology, with a maximum transit frequency (f_t/f_{max}) = 350/450 GHz. The circuit comprises three different voltage-controlled oscillators. Additionally, the ASIC will feature a basic Phase-Locked

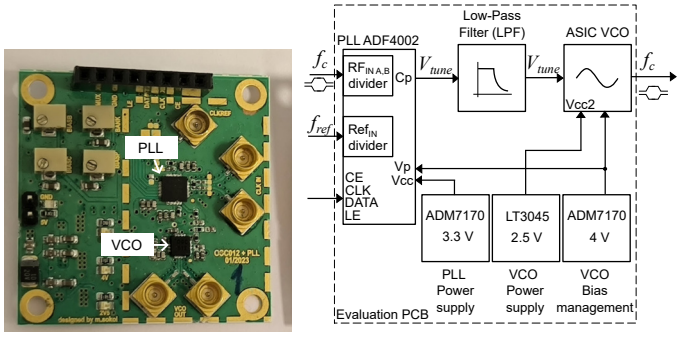

(a) (b)

Fig. 1: Evaluation board with PLL ADF4002 and VCO (a.). Block diagram of evaluation board (b.).

Loop (PLL) implementation, equipped with a serial register for setting the dividers ratio, charge pump current, phase polarity and output multiplexer. Through simulations, the designed voltage-controlled oscillators have demonstrated the capability to achieve low phase noise and improved stability compared to previous ASICs. With a custom PLL integrated onto a single chip, this ASIC offers a comprehensive solution for clock signal generation in UWB sensor systems. Furthermore, placing all components onto a single ASIC chip facilitates enhanced circuit integration within the System-in-Package.

III. Tunable Oscillator with Dielectric Resonator

In the past, oscillators based on discrete components using a dielectric resonator and a high-frequency transistor have also been designed and implemented. In this type of oscillators, the dielectric puck is coupled with microstrip lines, and the puck is adhered to a specific location. For tuning this type of oscillator, two methods are commonly used: electrical and mechanical. We have acquired tuning screws with micro-threading designed for tuning High-frequency filters and other microwave circuits. With the correct position above the resonator, we are able to ensure tuning of the oscillator in the range of 400 MHz around the resonant frequency of 21.74 GHz. The designed oscillator is encapsulated in a custom-made metal enclosure with an output high-frequency SMA connector (32K724-600S5) (see Fig. 2). The main advantage of this oscillator is its low power consumption and low manufacturing cost compared to commercial solutions.

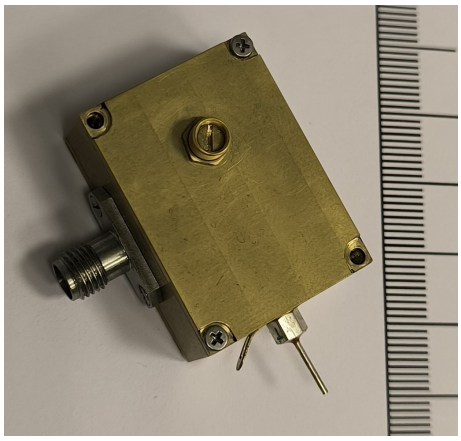

Fig. 2: A manufactured oscillator with dielectric resonator in a brass box with microwave tuning screw on top.

IV. Conclusion

Overall, this study deals with the design and implementation of clock generator circuits for Ultra-Wideband (UWB) sensor systems, containing various methodologies such as ASIC fabrication and discrete component integration with microstrip dielectric resonators. Notably, the integration of a Phase-Locked Loop (PLL) ADF4002 with our VCOs was explored. Based on our findings, new oscillators integrated on ASICs were designed together with a simple configurable phase-locked loop on a single chip. In the near future, the circuit could be integrated as a system in a package together with transceivers and a receiver. This is expected to reduce costs, decrease overall power consumption, and improve the performance of the UWB sensor system. Another possibility for the future is to test an oscillator with a dielectric resonator in a radar system. The DRO provides low phase noise, however, it does not offer the same configuration possibilities as VCOs with a PLL circuit. Nonetheless, the total power consumption of the given solution (35 mW) is 10 times lower compared to VCOs and PLL circuits, which allows the use of UWB sensors in large sensor networks intended for, for example, localisation or environmental monitoring.

Acknowledgment

This work was supported by the Slovak Research and Development Agency under the Contract No. APVV-22-0400 and Scientific Grant Agency (VEGA) under the Contract No. 1/0584/20. We would like to acknowledge the research team at Ilmsens, GmbH. in Ilmenau, Germany for participating and supporting this research.

References

[1] M. Helbig, B. Faenger, S. Ley, and I. Hilger, "Multistatic m-sequence uwb radar system for microwave breast imaging," in *2021 IEEE Conference on Antenna Measurements & Applications (CAMA)*. IEEE, 2021, pp. 540–545.

[2] C. Smeenk, T. E. Wegner, G. Kropp, J. Trabert, and G. Del Galdo, "Localization and navigation of service robots by means of m-sequence uwb radars," in *2021 18th European Radar Conference (EuRAD)*. IEEE, 2022, pp. 189–192.

[3] T. E. Wegner, S. Gebhardt, and G. Del Galdo, "Fill level measurements using an m-sequence uwb radar," *International Journal of Microwave and Wireless Technologies*, vol. 15, no. 1, pp. 74–81, 2023.

[4] B. Sewiolo, B. Laemmle, and R. Weigel, "Ultra-wideband transmitters based on m-sequences for high resolution radar and sensing applications," in *6th Conference on Ph.D. Research in Microelectronics & Electronics*, 2010, pp. 1–4.

[5] R. Zetik and G. Del Galdo, "Uwb m-sequence based radar technology for localization of first responders," in *2017 18th International Radar Symposium (IRS)*. IEEE, 2017, pp. 1–9.

[6] L. Liu, Z. Liu, and B. E. Barrowes, "Through-wall bio-radiolocation with uwb impulse radar: Observation, simulation and signal extraction," *IEEE Journal of Selected Topics in Applied Earth Observations and Remote Sensing*, vol. 4, no. 4, pp. 791–798, 2011.

[7] H. Wang, R. M. Narayanan, and Z. O. Zhou, "Through-wall imaging of moving targets using uwb random noise radar," *IEEE Antennas and Wireless Propagation Letters*, vol. 8, pp. 802–805, 2009.

[8] D. Wang, S. Yoo, and S. H. Cho, "Experimental comparison of ir-uwb radar and fmcw radar for vital signs," *Sensors*, vol. 20, no. 22, p. 6695, 2020.

[9] P. Jurik, M. Sokol, and P. Galajda, "Design of high frequency oscillators for ultra-wideband systems," in *2021 31st International Conference Radioelektronika (RADIOELEKTRONIKA)*. IEEE, 2021, pp. 1–5.

[10] "Europractice ihp overview." [Online]. Available: https://europractice-ic.com/technologies/asics/ihp/

Spatio-Temporal Sparse Voxel Octrees: a Hierarchical Data Structure for Geometry Representation of Time Varying Voxelized 3D scenes

[1]*Heidar KHORSHIDIYEH (3rd year)*
Supervisor: [2]*Branislav MADOŠ*

[1,2]Dept. of Computers and Informatics, FEI TU of Košice, Slovak Republic

[1]heidar.khorshidiyeh@tuke.sk, [2]branislav.mados@tuke.sk

***Abstract*—The paper deals with the problematics of the representation of the geometry of voxelized 3D scenes using hierarchical data structures. The paper continues in the efforts to more compactly represent this geometry, and moves this topic away from the realm of static voxelized 3D scenes to dynamic scenes. Spatio-temporal sparse voxel octrees data structure is designed and tested within this research. It was empirically found that the new data structure made it possible to reduce storage space requirements to less than half (49.03%) within the tests.**

***Keywords*— hierarchical data structures, voxelized 3D scenes, sparse voxel octrees, spatio-temporal sparse voxel octrees**

I. Introduction

Representation of scientific data using regular grids of voxels along with the use of this approach in computer graphics is gaining more and more attention. In this approach, the 3D scene is represented as the regular grid of voxels. One of the basic attributes of the scene is its geometry, as the formal representation of the information about which parts of the scene are transparent (passive) to rays of light (rays can travel across these parts of the scene) and which are not transparent (active) to rays of light (rays are bouncing from these parts of the scene). Activity of voxels can be represented as the three dimensional grid of bits. If voxel is passive, bit is set to 0 and if voxel is active, the bit is set to 1. This straight forward approach is very space consuming, when for example static scene of the size of $1024 \times 1024 \times 1024$ voxels, consumes 1Gb (128MB) of the space. In case of time varying scene, of the same size, with 1024 time steps, grid that represents geometry consumes 1Tb (128GB). That is why big attention is paid to the more compact representation of this information. Useful solution for static 3D scenes are hierarchical data structures (HDSs) based on sparse voxel octrees (SVOs) or directed acyclic graphs (DAGs). This paper continues in this effort and investigates the possibility of the use of HDSs within the field of geometry representation of the time varying 3D voxelized scenes. The paper suggests the use of in this paper proposed HDS called Spatio-Temporal Sparse Voxel Octrees (STSVO).

II. Related Works

In attempt to represent multi-dimensional grid of data in linearized form, linearization functions [1] are used. Morton order [2] and Hilbert curve [3] are the most popular (Fig. 1).

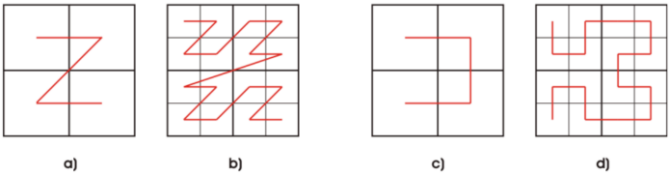

Fig. 1 Linearization of the two-dimensional space using Morton order and Hilbert curve to the first and second level.

The most basic HDS within this field is Sparse Voxel Octrees (SVOs). It is based on the decomposition of the three-dimensional voxelized scene into octants. Internal nodes of the data structure are incorporating pointers to the child nodes. When those pointers are not present, the data structure is called Pointerless Sparse Voxel Octrees (PSVOs). Baert introduced in 2013 algorithm [4] for SVOs building. Another approach was introduced by Pätzold and Kolb in 2013 in [5]. Madoš et al designed in 2022 hierarchical data structure based on SVOs principle, called Clustered Sparse Voxel Octrees (CSVOs) [6]. Contribution of this work was is in compression gains.

Kämpe et al invented Sparse Voxel Directed Acyclic Graphs (SVDAGs) data structure [7] in 2013. Crucial, modification, when compared to the SVOs, is the use of the Common Subtrees Merge (CSM). In the data structure PSVDAGs, that was designed in 2020 by Vokorokos et al [8], pointerless data structure that can use CSM was introduced. All data structure is pointerless and when CSM must be applied, labels and callers are used for the labeling of the template subDAGs. Algorithm for quick transformation of the PSVDAG into the to SVDAG was introduced by Madoš and Ádám in 2021 in [9].

Villanueva et al introduced Symmetry-aware Sparse Voxel Directed Acyclic Graphs (SSVDAGs) hierarchical data structure [10] in 2016. CSM can be applied also to suboctants that are similar when reflective symmetry is applied.

Approaches to representation of the time varying voxelized data were examined in [11][12].

III. Designed Solution

Basic SVO HDS can be used for the representation of the geometry of voxelized 3D scene. If one wants to represent time varying scene, that is formed from the set of time frames, he can use series of discrete SVOs, one for each time frame. For example, scene with the size of $1K^3$ voxels, where set of 1024 time frames is needed, can be represented as the 1024 discrete SVOs. Data structure Spatio-Temporal Sparse Voxel Octrees (STSVO), proposed in this paper, is describing another approach, where each voxel has four coordinates. Three of them are spatial x, y, z and fourth coordinate t is temporal. So we can constitute 4D grid of voxels and related $1K^4$ grid of 1b per voxel geometry information. Modified Baert's algorithm is able to transform information about active voxels of this grid into STSVO data structure. Simple modification of this algorithm is in its transformation from 3D to 4D.

STSVO, in its first iteration, decomposes scene into 16 hexadecants. In x, y and z axis, it decomposes space in halfs in all three axis and in t axis decomposes time range into halfs. If there is no active voxel in hexadecant (within space and also within time), this hexadecant is considered empty. There will be no child node then and no pointer to this child. If there is at least one active voxel in this hexadecant, there will be bit 1 present within the Child Node Mask (CHNM) and there will be 32b pointer (PT) as the address where the child node is located. Hexadecant is then recursively decomposed.

While in SVO there are just 8 octants, and that is why only 8b CHNM is needed, in STSVO there are 16 hexadecants and thus 16b CHNM is needed. The first 8 hexadecants and thus first 8 bits in CHNM are for the first half of time range, second 8 hexadecants and thus second 8 bits of CHNM are for the second half of the time range. Number of pointers (in both data structures 32b long) is varying and in SVO is from the range 1 to 8, in STSVO is from the range of 1 to 16. Details of examples of the internal node construction can be found on Fig. 2.

Leaf nodes are in both data structures representing just voxels, 8 of them in SVO and 16 of them in STSVO.

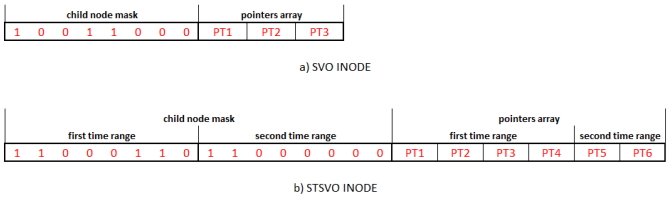

Fig. 2 Construction of the internal node of a) SVO and b) STSVO.

IV. Results

Tests were made to validate empirically if the STSVO data structure has advantages over the solution, in which each time frame is separately encoded using SVO HDS.

Voxelized scene had the spatial resolution of 128^3 voxels and 128 time frames have been generated, when the voxelized model of Angel Lucy statue (Fig. 3) was moving up from the scene. Overall number of voxels was 128^4 and not compressed version of the related grid consumed 32MB of the space.

Simple SVO encoding geometry was generated for each time frames of the scene. Then STSVO was created for this space and all time frames. Size of 128 SVOs was then compared to the size of STSVO. While SVOs needed 3,61MB, STSVO needed just 1,77MB (49% when compared to STSVO).

Fig 3 Visualization of the Angel Lucy model.

V. Conclusion

The paper dealt with the problem of HDSs intended for representation of the geometry of voxelized 3D scenes. Design of the Spatio-Temporal Sparse Voxel Octrees (STSVO) HDS was introduced. Empirically determined results showed that STSVO capturing n time frames for a 3D scene with a resolution of n^3 voxels is more compact than n discrete 3D scenes stored in a total of n SVO hierarchical data structures. Tests mentioned in this paper are showing that there was significant gain in compression when STSVO was used.

Future research in this area will be focused on further optimization of the proposed HDS. There is potential to use features that are similar to those HDSs based on DAGs, like CSM, or frequency based compaction. Another potential is in the use of multiple lengths of pointers to child nodes and in the equivalent of inter-frame difference information known from the storage of video sequences.

References

[1] Sagan, H. Space-Filling Curves; Springer-Science+Business Media, LLC: New York, NY, USA, 1994; p. 194.

[2] Morton, G.M. A Computer Oriented Geodetic Data Base and a New Technique in File Sequencing; Research Report; International Business Machines Corporation (IBM): Ottawa, Canada, 1966; p. 20. Available online: dominoweb.draco.res.ibm.com/reports/Morton1966. pdf

[3] Hilbert, D. Via the Continuous Mapping of a Line onto a Patch of Area (Über die stetige Abbildung einer Linie auf ein Flächenstück). Dritter Band: Analysis Grundlagen der Mathematik Physik Verschiedenes; Springer: Berlin/Heidelberg, Germany, 1935.

[4] Baert, J.; Lagae, A.; Dutré, P. Out-of-Core Construction of Sparse Voxel Octrees. In Proceedings of the 5th High-Performance Graphics Conference (HPG '13), Anaheim, USA, 19–21 July 2013; pp. 27–32.

[5] Pätzold, M.; Kolb, A. Grid-free out-of-core voxelization to sparse voxel octrees on GPU. In Proceedings of the 7th Conference on High-Performance Graphics (HPG '15),USA, 7–9 August 2015; pp. 95–103.

[6] Madoš, B.; Chovancová, E.; Chovanec, M.; Ádám, N. CSVO: Clustered Sparse Voxel Octrees—A Hierarchical Data Structure for Geometry Representation of Voxelized 3D Scenes. Symmetry 2022, 14, 2114. https://doi.org/10.3390/sym14102114

[7] Kämpe, V.; Sintorn, E.; Assarson, U. High Resolution Sparse Voxel DAGs. ACM Trans. Graph. 2013, 32, 1–13.

[8] Vokorokos, L.; Madoš, B.; Bilanová, Z. PSVDAG: Compact Voxelized Representation of 3D Scenes Using Pointerless Sparse Voxel Directed Acyclic Graphs. Comput. Inform. 2020, 39, 587–616.

[9] Madoš, B.; Ádám, N. Transforming Hierarchical Data Structures—A PSVDAG—SVDAG Conversion Algorithm. APH. 2021, 18, 47–66.

[10] Villanueva, A.J.; Marton, F.; Gobetti, E. Symmetry-aware Sparse Voxel DAGs. In Proceedings of the 20th ACM SIGGRAPH Symposium on Interactive 3D Graphics and Games (I3D '16), Redmond, Washington, USA, 27–28 February 2016; pp. 7–14.

[11] Kämpe, V.; Rasmuson, S.; Billeter, M.; Sintorn, E.; Assarsson, U. Exploiting Coherence in Time-Varying Voxel Data. In Proceedings of the 20th ACM SIGGRAPH Symposium on Interactive 3D Graphics and Games, Redmond, WA, USA, 27–28 February 2016; pp. 15–21.

[12] Martinek, M.; Thiemann, P.; Stamminger, M. Spatio-temporal filtered motion DAGs for path-tracing. Comput. Graph. 2021, 99, 224–233

Bridging the Understanding Gap between Tester's Domain and Programmer's Domain

[1]*Filip GURBÁL' (4th year),*
Supervisor: [2]*Jaroslav PORUBÄN*

[1,2]Dept. of Computers and Informatics, FEI TU of Košice, Slovak Republic

[1]filip.gurbal@tuke.sk, [2]jaroslav.poruban@tuke.sk

***Abstract*—We describe a method to interpret the connection between test cases and source code in a way that both testers and programmers can understand. This method allows testers to gain some insight into the source code structure without needing any programming skills, and it can serve as a common ground in communication with programmers. The method uses code coverage analysis and two clustering methods to show similarities between test cases. The similarity of test cases shows when the test case starts to be redundant or if there is a part of source code that is hard to cover. The method also helps with estimations and prioritization.**

***Keywords*—Code Coverage, Density-Based Spatial Clustering, Hierarchical Clustering, Manual Testing**

I. Introduction

Manual testing is often performed by testers without a technological background because it usually requires only understanding of the application domain. They simulate various actions that real users can perform within the application trying to find software faults. The possibilities of the application are defined by the specification, which can be understood by any user. Testing without knowledge of the implementation domain is called specification-based testing.

However, the specification may describe features that have not yet been implemented or some of the specification may be missing. Relying only on the specification may seem convenient for the manual testers to ensure the quality of the software, but in reality it results in big gaps between the test case and the source code. According to Richardson, O'Malley and Tittle [1] there are two significant problems with this approach:

- significant redundancies may be introduced into test cases,
- test cases based only on specification can create big portions of untested software.

Redundancies can be caused by testing seemingly different parts of the software that in reality use the same implementation. Implementation can also cover functionalities that were discovered implicitly and are not covered by specification. These are nearly impossible to find by specification-based testing.

The tester can minimize these problems by understanding the structure of the source code and adjusting the test cases accordingly. But this is not an easy task, even for a tester with some programming skills. Even communication with a programmer will be difficult if the developer is not familiar with the test cases. There is an understanding gap between the tester's domain and the programmer's domain. This gap is demonstrated in figure 1.

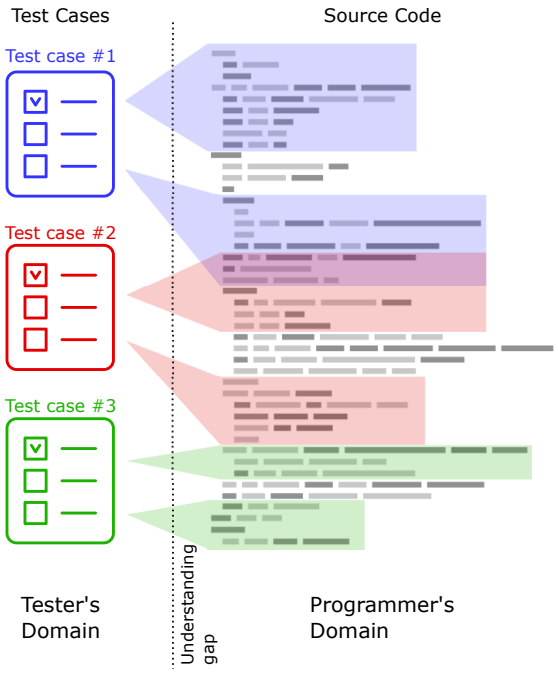

Fig. 1. Connection between test cases and source code and the gap in tester's and programmer's understanding

In this paper, we describe our method of interpreting the connection between test cases and source code in a way that both testers and programmers can understand. Using this method, testers will gain some insight into the source code structure without needing any programming skills and it can serve as a common ground in communication with programmers.

II. Previous Research

A simple way to find a connection between a test case and the source code is to see which part of the code was executed during the testing. Our previous research led to the observation that we can compare test cases based on their individual code coverage data and determine the amount of similarity [2].

We created a tool that gathers code coverage data from UI testing [3]. We used these data for hierarchical clustering based on test case similarity. Clustering gave us a visual

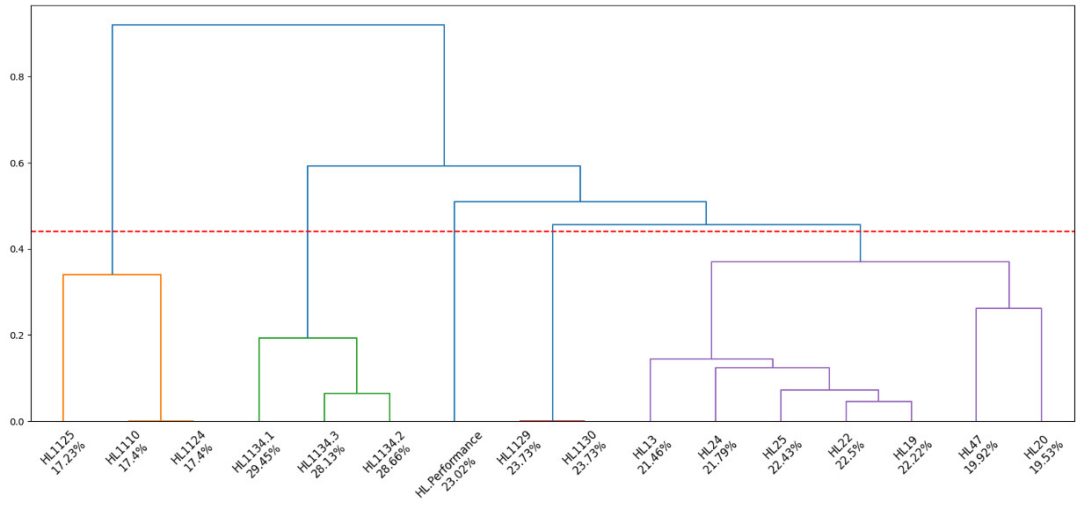

Fig. 2. Dendrogram of hierarchical clustering of test cases.

representation of similarities between test cases, as shown in figure 2 [4].

Using this tool, we gathered data from a commercial project that is fully deployed for public use. The application provides a wide range of tools for hiring new employees, from handling interviews to evaluating candidates.

III. The Experiment

We presented our method to testers to see if they can benefit from the information. To evaluate our experiment, we decided to conduct interviews with experienced testers from six different companies.

A. The Presentation

For presentation we picked a few test cases from a project we applied our method to and prepared a simple description of what functionality they cover. Then we provide the outputs of our method. In addition to the dendrogram, we added some additional information to our presentation for testers.

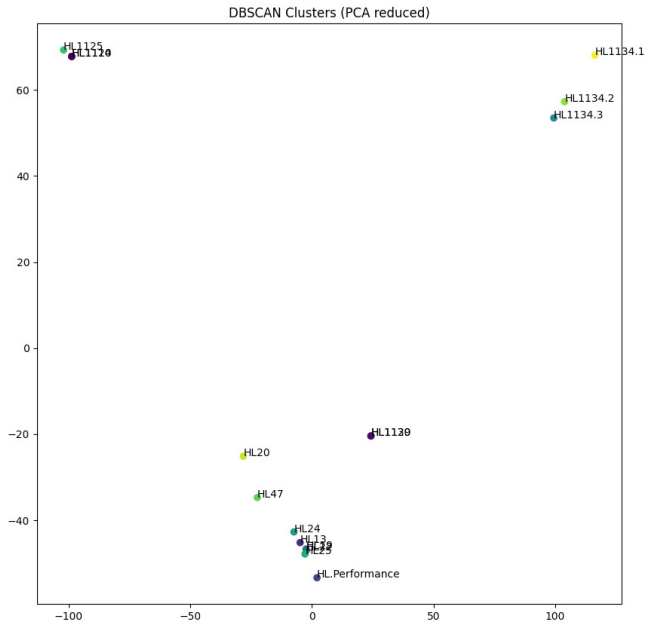

Fig. 3. Density-based spatial clustering of test cases reduced to 2 dimensions.

Our final presentation contained the following items:

- Brief description of test cases
- Percentage value of code coverage of each individual test case (also displayed in the dendrogram in figure 2)
- Dendrogram
- 2D interpretation of test case similarities using density-based spatial clustering (figure 3)

B. The Interview

Most of the interview was informal discussion. We can categorize topics into categories:

1) Programming experience
2) Communication with programmers
3) Presenting data
4) Gather feedback

The feedback from the testers to our method differed depending on their skills and the way they work in the company. However, we made some observations.

Testers frequently communicate with programmers, but never about the implementation. They were more interested in our method when they had some programming skills and would try to figure out the structure of the source code themselves. However, no tester would initiate the communication about the structure with the programmer, because they do not want to bother them.

Otherwise, we see the benefits of our method in manual testing. The similarity of test cases clearly shows where the test cases start to be redundant or if there is some source code that is hard to cover. Repeated application of the method can also indicate the tester's progression in coverage, which can help with estimations. Another side effect is help with prioritization in case of regression testing.

References

[1] D. Richardson, O. O'Malley, and C. Tittle, "Approaches to specification-based testing," in *Proceedings of the ACM SIGSOFT'89 third symposium on Software testing, analysis, and verification*, 1989, pp. 86–96.

[2] F. Gurbál' and J. Porubän, "Using coverage metrics to improve system testing processes," *SCYR 2022: Nonconference Proceedings of Young Researchers*, pp. 215–216, 2022.

[3] ——, "Collecting code coverage from ui testing," *IPSI Transactions on Internet Research*, vol. 19, pp. 55–58, 2023.

[4] ——, "Clustering ui test cases for effective prioritization and selection," *SCYR 2023: Nonconference Proceedings of Young Researchers*, pp. 164–165, 2023.

Author's index

SCYR 2024: 24rd Scientific Conference of Young Researchers

Proceedings from Conference

Published: Faculty of Electrical Engineering and Informatics
Technical University of Košice
Edition I, 182 pages
Number of CD Proceedings: 50 pieces

Editors: Assoc. Prof. Ing. Karol Kyslan, CSc.
Assoc. Prof. Ing. Emília Pietriková, PhD.
Ing. Lukáš Pancurák

ISBN 978-80-553-3474-5